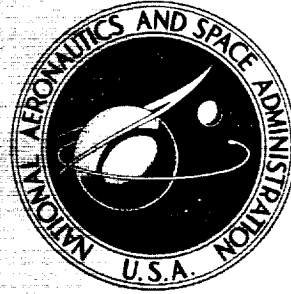


**CONTRACTOR
REPORT**



NASA CR-912

FACILITY FORM 602

N68-24802
(ACCESSION NUMBER)
849
(PAGES)
CR 912
(NASA CR OR TMX OR AD NUMBER)

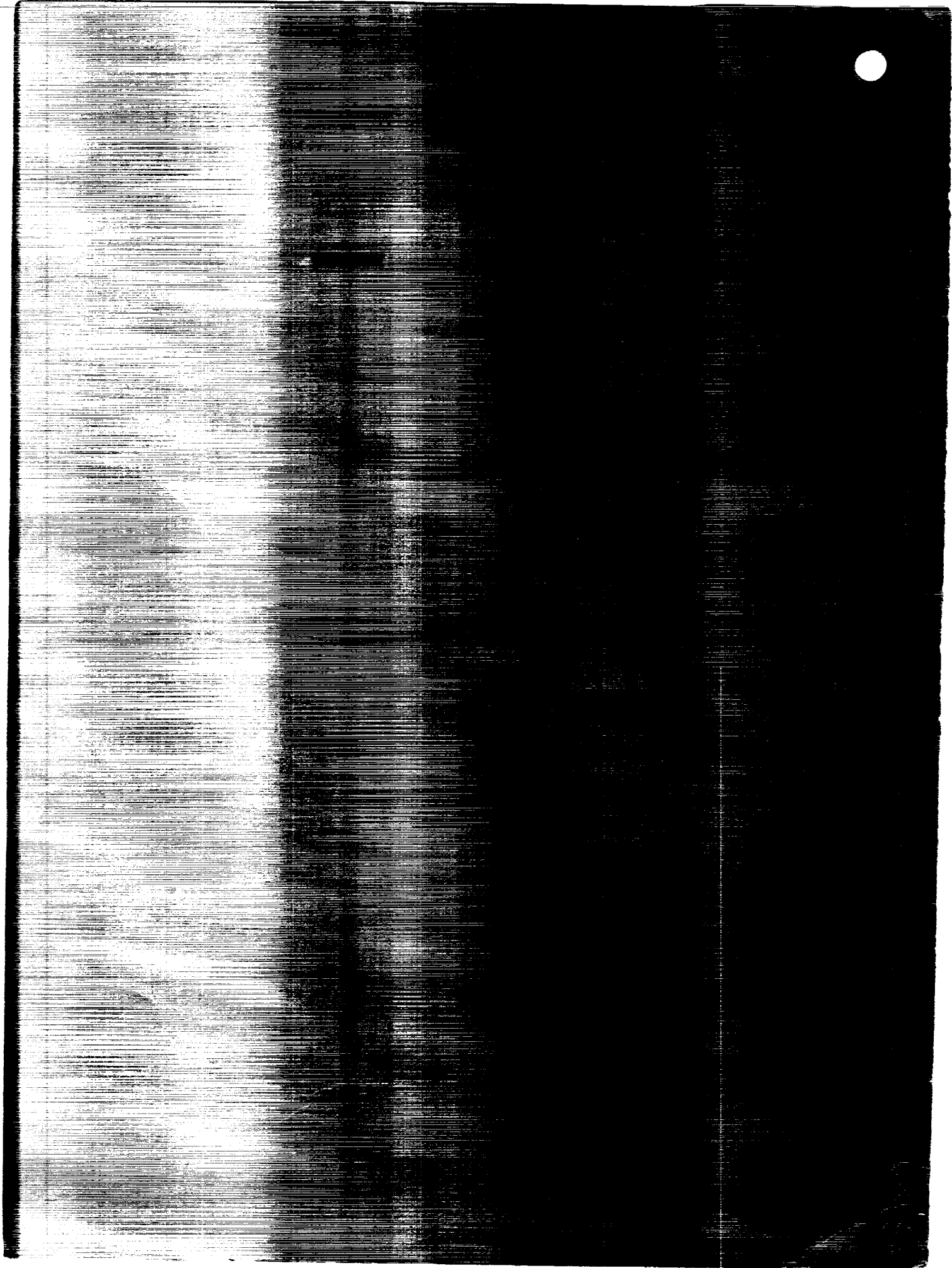
(THRU)
1

(CODE)
32

(CATEGORY)

ky,

WASHINGTON, D. C. • APRIL 1968



FOREWORD

The intent of this Shell Analysis Manual is to provide specific instructions, procedures, basic solutions, and recommendations to facilitate the expedient static structural analysis of shell-type spacecraft structures, and to provide an introduction to and reference for the practical static structural analysis of shells.

This document was prepared by the Structures and Dynamics Department of North American Aviation, Inc., Space and Information Systems Division, Downey, California, under Contract NAS9-4387 for the National Aeronautics and Space Administration, Manned Spacecraft Center, Houston, Texas. Mr. Herbert C. Kavanaugh, Jr., was the NASA Technical Representative for the program. Mr. F. L. Rish of the NAA Space and Information Systems Division was the Program Manager. The program was performed between May 1965 and June 1966.

Generally, the information contained in this document is a condensation of material published by U. S. Government agencies, universities, scientific and technical journals, text books, aerospace industries, including North American Aviation, Inc., and foreign

publications. Particular credit is given to the following publishers who granted NAA permission to use their publications:

American Concrete Institute

American Institute of Aeronautics and Astronautics

American Society of Civil Engineers

Leibniz-Verlag, West Germany

Springer-Verlag, West Germany

This manual was authored by Drs. E.H. Baker, A.P. Cappelli, L. Kovalevsky, and R.M. Verette under the direction of F.L. Rish. The authors are indebted to Messrs. R.M. Bereznak, R.W. Johnson, A.H. McHugh, K.E. Pauley, D. Salinas, and A.E. Zagorski for technical assistance.

NOTE

Comments and suggestions for revisions and editions to this Manual will be appreciated and should be sent to: Chief, Structures and Mechanics Division, Code ES, NASA Manned Spacecraft Center, Houston, Texas 77058.

ABSTRACT

This Shell Analysis Manual provides specific instructions, procedures, basic solutions, and recommendations to facilitate the expedient static structural analysis of shell-type spacecraft structures. It also provides an introduction to and reference for the practical static structural analysis of shells.

The manual comprises the following chapters:

- 1.00 Introduction to Shell Theory
- 2.00 Procedures for Static Analysis of Shell Structures
- 3.00 Procedures for Stability Analysis of Shell Structures
- 4.00 Minimum Weight Shell Design
- 5.00 Optimum Use of Computer Programs

Chapter 1.00 presents a derivation of general shell theory from concepts of the linear theory of elasticity and includes the basic relationships of shell geometry, geometry of strain, stress-strain, and equilibrium. The various shell theories are classified according to the simplifications made to a higher-order theory. Approximate theories and simplifications that have made the solution to these theories possible are delineated. A presentation of nonlinear shell theory to be used for large deflection analysis of shells is included. This

development is based on variational principles and the concept of stationary potential energy. Structural stability shell theory is discussed. The shell stability equations are presented and techniques for determining buckling loads using variational procedures are outlined. A discussion of the discrepancies between the theoretical and experimental results is included.

In Chapter 2.00, instructions, procedures, basic solutions, and recommendations are presented to determine static deflections and internal load and stress distributions in shells under various loading conditions. This chapter also includes membrane solutions for various loading conditions, unit edge loading solutions, and combined solutions for various shell geometries and constructions, loadings, and boundary conditions. Factor of safety concepts, failure criteria, and margin of safety calculation under uniaxial and biaxial loading conditions are also presented.

Methods of analysis for the static instability (buckling) of shell structures are presented in Chapter 3.00. This chapter presents methods for obtaining the design allowable buckling loads for unstiffened cylinders, cones, spherical caps, and curved panels under various loading conditions. Also included are procedures for the stability analysis of orthotropic shells, stiffened cylinders, and sandwich shells. Analyses for inelastic buckling and combined loading conditions are also presented.

Chapter 4.00 presents methods of analysis to be used in preliminary design to determine the lightest shell wall for various constructions subjected to specific loading conditions. A survey of pertinent literature is also included in this chapter.

An introduction to the fundamentals of computer utilization is presented in Chapter 5.00. The basic computer characteristics are described. An introduction to matrix algebra is included in this chapter, in addition to a description of the techniques used in solving shell problems and discussions of the use of computers in conjunction with these techniques.



CONTENTS

| | Page |
|---|-------------|
| NOMENCLATURE | xxv |
| 1.00 INTRODUCTION TO THE THEORY OF SHELLS | 1 |
| 1.01 GENERAL | 1 |
| 1.10 LINEAR SHELL THEORY | 3 |
| 1.11 Introduction | 3 |
| 1.12 Basic Relationships for the Theory of | |
| Thin Shells | 6 |
| 1.12.1 Geometry of Shells | 6 |
| 1.12.2 Geometry of Strain | 17 |
| 1.12.3 Stress and Stress Resultants | 20 |
| 1.12.4 Equilibrium Equations for a | |
| Shell | 25 |
| 1.12.5 Stress-Strain Relations | 31 |
| 1.13 Classification of Shell Theories | 35 |
| 1.13.1 First-Order Approximation Shell | |
| Theory | 37 |
| 1.13.2 Second-Order Approximate Shell | |
| Theories | 54 |
| 1.13.3 Shear Deformation Shell Theories | 60 |

| | Page |
|---|------|
| 1.13.4 Specialized Theories for Shells of Revolution | 63 |
| 1.13.5 Membrane Theory of Shells | 83 |
| 1.13.6 Summary | 92 |
| 1.20 NONLINEAR SHELL THEORY | 93 |
| 1.21 Introduction | 93 |
| 1.22 General Strain-Displacement Relations | 95 |
| 1.23 Stress-Strain Relations and Stress Resultants | 100 |
| 1.24 Principle of Potential Energy | 102 |
| 1.25 Nonlinear Equilibrium Equations | 107 |
| 1.26 Nonlinear Equations for Cylindrical Shells | 114 |
| 1.27 Summary | 118 |
| 1.30 STABILITY THEORY OF SHELLS | 119 |
| 1.31 Introduction | 119 |
| 1.32 Concept of Stability | 122 |
| 1.33 Adjacent Equilibrium Method | 125 |
| 1.34 Energy Method | 133 |
| 1.35 "Classical" Buckling Analysis | 138 |

| | Page |
|--|-------------|
| 1.36 Discrepancy Between Theoretical and Experimental Results | 142 |
| 1.37 Summary and Conclusions | 155 |
| REFERENCES | 157 |
| 2.00 PROCEDURES FOR STATIC ANALYSIS OF SHELL STRUCTURES . | 166 |
| 2.10 INTRODUCTION | 166 |
| General | 166 |
| Geometrical Considerations of Shell Segments . | 167 |
| Membrane Solution | 169 |
| Bending Forces and Their Interaction with Membrane Forces | 169 |
| Unit Edge Loading Method of Solution | 172 |
| 2.20 GENERAL APPROACH OF UNIT-LOADING | |
| METHOD | 173 |
| 2.21 Introduction | 174 |
| 2.21.1 Nature of Statically Indeterminate Structures | 174 |
| 2.22 Membrane and Bending Theories | 176 |
| 2.22.1 Membrane Theory | 176 |
| 2.22.2 Bending Theory | 177 |
| 2.22.3 Comparison of Membrane and Bending Theories for Nonshallow Shells | 178 |

| | Page |
|---|-------------|
| 2.22.4 Combined Bending and Membrane Theory | 179 |
| 2.22.5 Unit-Loading Method Applied to the Combined Theory | 179 |
| 2.23 Interaction Between Shells of Various Geometries | 182 |
| 2.23.1 Breakdown for Complicated Shell Geometry | 182 |
| 2.23.2 Interaction Between Two Shell Elements | 183 |
| 2.23.3 Interaction Between Three or More Shell Elements | 188 |
| 2.23.4 Summary | 192 |
| 2.24 Conclusion | 193 |
| 2.30 MONOCOQUE SHELLS | 194 |
| 2.31 Introduction | 194 |
| 2.32 Primary Solutions | 195 |
| 2.32.1 Determination of Membrane Internal Forces | 195 |
| 2.32.2 Determination of Membrane Displacements | 198 |

| | Page |
|--|-------------|
| 2.32.3 Any Shape of Meridian | 200 |
| 2.32.4 Spherical Shells | 202 |
| 2.32.5 Conical Shells | 208 |
| 2.32.6 Cylindrical Shells | 216 |
| 2.32.7 Elliptical Shell | 222 |
| 2.32.8 Cassini Shells | 227 |
| 2.32.9 Toroidal Shells | 233 |
| 2.32.10 Other Geometries of Shells . . | 237 |
| 2.32.11 Irregular Shell | 240 |
| 2.32.12 Conclusion | 245 |
| 2.33 Secondary Solutions | 246 |
| 2.33.1 Introduction and General Discussion | 246 |
| 2.33.2 Spherical Shells (Open, Closed) . | 252 |
| 2.33.3 Conical Shells | 265 |
| 2.33.4 Cylindrical Shell | 275 |
| 2.33.5 Salvadori's Approximate Method for Irregular Shell | 289 |
| 2.33.6 Conclusion | 293 |
| 2.34 Summary | 294 |

| | Page |
|--|------|
| 2.40 SPECIAL SOLUTIONS | 296 |
| 2.41 Introduction | 296 |
| 2.42 Hampe Method | 298 |
| 2.42.1 Stresses | 299 |
| 2.42.2 Distortions | 301 |
| 2.42.3 Coefficients and Tables | 301 |
| 2.42.4 Analysis of Cylinders With Rotationally Symmetrical Dis- continuities in Geometry or Loading | 321 |
| 2.42.5 Spherical Shell, Any Fixity at the Lower Boundary | 327 |
| 2.42.6 Definition of F-Factors | 331 |
| 2.43 Approximate Method for Determination of Location and Maximum Stresses in Cylinders | 343 |
| 2.44 Circular Plates | 353 |
| 2.44.1 Primary Solutions | 354 |
| 2.44.2 Secondary Solutions | 359 |
| 2.44.3 Special Cases | 361 |

| | Page |
|--|-------------|
| 2.45 Circular Rings | 367 |
| 2.46 Conclusion | 369 |
| 2.50 MULTISHELL STRUCTURES | 370 |
| 2.51 Introduction | 370 |
| 2.52 Force Method | 372 |
| 2.52.1 Introduction | 372 |
| 2.52.2 Analysis | 372 |
| 2.52.3 System Combined From Statically Determinate Elements | 374 |
| 2.52.4 Structural System Combined From Statically Indeterminate | 376 |
| 2.52.5 Conclusion | 379 |
| 2.53 Deflection Method | 380 |
| 2.53.1 Introduction | 380 |
| 2.53.2 Analysis | 380 |
| 2.53.3 Conclusion | 384 |
| 2.54 Tables for Multishell Analysis | 385 |
| 2.55 Summary | 402 |
| 2.60 COMPOSITE SHELLS | 404 |
| 2.61 Introduction | 404 |

| | Page |
|--|-------------|
| 2.62 Stiffened Shells | 407 |
| 2.62.1 General | 407 |
| 2.62.2 Cylindrical Shell | 408 |
| 2.62.3 Spherical Shell | 408 |
| 2.62.4 Conical Shell | 408 |
| 2.62.5 Approach for Analysis | 408 |
| 2.62.6 Method of Transformed Section | 411 |
| 2.63 Sandwich Shells | 415 |
| 2.63.1 Introduction | 415 |
| 2.63.2 Modes of Failure of Sandwich Elements | 415 |
| 2.63.3 Structural Function of Sandwich | 418 |
| 2.63.4 Types of Sandwich Cores | 421 |
| 2.63.5 Design Requirements for Inspection and Structural Test | 423 |
| 2.63.6 Analysis of Sandwich Shells | 424 |
| 2.63.7 Conclusion | 425 |
| 2.64 Orthotropic Shells | 427 |
| 2.64.1 Introduction | 427 |
| 2.64.2 Extensional and Bending Rigidities in Shells Theory | 427 |

| | Page |
|--|-------------|
| 2.64.3 Orthotropic Characteristics . . . | 430 |
| 2.64.4 Orthotropic Analysis, If Shear Distortions are Neglected . . . | 431 |
| 2.64.5 Orthotropic Analysis, If Shear Distortions are Included . . . | 443 |
| 2.64.6 Influence of Axial Forces on Bending in Cylinder . . . | 447 |
| 2.65 Conclusion | 449 |
| 2.70 UMSYMMETRICALLY LOADED SHELLS . . . | 450 |
| 2.71 Introduction | 450 |
| 2.72 Shells of Revolution | 451 |
| 2.73 Shells of Beam Systems | 454 |
| 2.73.1 Cantilever Cylindrical Shell . . . | 454 |
| 2.73.2 Cantilevered Conical Shell . . . | 457 |
| 2.73.3 Simple and Fixed Beam Cylindrical Shell | 469 |
| 2.73.4 Continuous Cylindrical Shell Under Dead Weight | 472 |
| 2.73.5 Curved Panels (Barrel Vaults) . . | 475 |
| 2.74 Summary | 482 |

| | Page |
|--|-------------|
| 2.80 MARGIN OF SAFETY | 483 |
| 2.81 General | 483 |
| 2.82 Definitions | 485 |
| 2.83 Three-Dimensional Field of Stresses | 487 |
| 2.83.1 Maximum Stress Theory | 487 |
| 2.83.2 Maximum Strain Theory (Mariotte) | 487 |
| 2.83.3 Maximum Shear Theory (Kulon) | 488 |
| 2.83.4 Maximum Strain Energy Theory (Beltrami) | 489 |
| 2.83.5 Mohr's Theory | 490 |
| 2.84 Conditions of Plasticity (Hencky, Meses, and Tresca) | 492 |
| 2.85 Two-Dimensional Field of Stresses | 495 |
| 2.86 Comparison of Results | 497 |
| 2.87 Failure | 498 |
| 2.88 Conclusion | 501 |
| 2.90 SUMMARY AND CONCLUSION | 503 |
| REFERENCES | 505 |

- 3.00 PROCEDURES FOR STABILITY ANALYSIS 508
 - 3.10 GENERAL 508
 - 3.20 UNSTIFFENED SHELLS 513
 - 3.21 General 513
 - 3.22 Curved Panels 514
 - 3.22.1 Axial Compression, Curved Panels 514
 - 3.22.2 Shear, Curved Panels 519
 - 3.22.3 Bending, Curved Panels 524
 - 3.22.4 External Pressure, Curved Panels 526
 - 3.22.5 Combined Loading, Curved Panels 526
 - 3.23 Cylinders 528
 - 3.23.1 Axial Compression, Unstiffened Cylinders 528
 - 3.23.2 Shear or Torsion, Unstiffened Cylinders 532
 - 3.23.3 Bending, Unstiffened Cylinders 536
 - 3.23.4 External Pressure, Unstiffened Cylinders 540
 - 3.23.5 Combined Loading, Unstiffened Cylinders 544

| | Page |
|--|-------------|
| 3.24 Cones | 550 |
| 3.24.1 Axial Compression, Unstiffened Cones | 550 |
| 3.24.2 Shear or Torsion, Unstiffened Cones | 555 |
| 3.24.3 Bending, Unstiffened Cones | 557 |
| 3.24.4 Lateral and Axial External Pressure, Unstiffened Cones | 561 |
| 3.24.5 Combined Loading, Unstiffened Cones | 564 |
| 3.25 Spherical Caps | 565 |
| 3.25.1 External Pressure, Shallow Spherical Caps | 565 |
| 3.25.2 External Pressure, Spherical Caps | 567 |
| 3.30 ORTHOTROPIC SHELLS | 569 |
| 3.31 General | 569 |
| 3.32 Elastic Constants | 571 |
| 3.32.1 Definitions | 571 |
| 3.32.2 Orthotropic Layered Shells | 573 |
| 3.32.3 Sandwich Shells | 578 |
| 3.32.4 Integrally Stiffened Waffle Shells | 581 |
| 3.33 Cylinders | 588 |

| | Page |
|---|-------------|
| 3.33.1 Axial Compression, Orthotropic Cylinders | 588 |
| 3.33.2 Torsion, Orthotropic Cylinders. | 599 |
| 3.33.3 Bending, Orthotropic Cylinders. | 603 |
| 3.33.4 Lateral External Pressure, Orthotropic Cylinders. | 605 |
| 3.34 Cones | 610 |
| 3.34.1 Axial Compression, Orthotropic Cones | 610 |
| 3.34.2 Torsion, Orthotropic Cones | 612 |
| 3.34.3 Bending, Orthotropic Cones | 612 |
| 3.34.4 Lateral External Pressure, Orthotropic Cones | 613 |
| 3.40 STIFFENED SHELLS | 614 |
| 3.41 General | 614 |
| 3.42 Frame and Stringer Stiffened Cylinders | 615 |
| 3.42.1 Axial Compression, Frame and Stringer Stiffened Cylinders | 615 |
| 3.42.2 Bending, Frame and Stringer Stiffened Cylinders | 615 |
| 3.43 Frame-Stiffened Cylinders | 637 |

| | | |
|--------|--|-----|
| 3.43.1 | Lateral and Axial External Pressure, Frame-Stiffened Cylinders | 637 |
| 3.50 | SANDWICH SHELLS | 647 |
| 3.51 | General | 647 |
| 3.52 | Local Instability | 649 |
| 3.52.1 | Intracell Buckling | 649 |
| 3.52.2 | Face Sheet Wrinkling | 653 |
| 3.53 | Cylinders | 657 |
| 3.53.1 | Axial Compression, Sandwich Cylinders | 657 |
| 3.53.2 | Torsion of Shear, Sandwich Cylinders | 661 |
| 3.53.3 | Bending, Sandwich Cylinders | 669 |
| 3.53.4 | Lateral External Pressure, Sandwich Cylinders | 669 |
| 3.54 | Cones | 689 |
| 3.54.1 | Axial Compression, Sandwich Cones | 689 |
| 3.54.2 | Torsion, Sandwich Cones | 689 |
| 3.54.3 | Bending, Sandwich Cones | 690 |
| 3.54.4 | Lateral External Pressure, Sandwich Cones | 691 |

| | Page |
|--|------|
| 3.60 INELASTIC BUCKLING | 692 |
| 3.61 General | 692 |
| 3.62 Plasticity Correction Factor | 692 |
| 3.63 Combined Loadings | 724 |
| REFERENCES | 727 |
| 4.00 MINIMUM WEIGHT SHELL DESIGN | 736 |
| 4.10 INTRODUCTION | 736 |
| 4.20 STIFFENED SHELLS | 738 |
| 4.21 General | 738 |
| 4.22 Stiffened Cylindrical Shells in Pure Bending | 743 |
| 4.30 SANDWICH SHELLS | 745 |
| 4.31 General | 745 |
| 4.32 Buckling of Sandwich Cylinders Under Axial Compression | 748 |
| REFERENCES | 750 |
| 5.00 OPTIMUM USE OF COMPUTER PROGRAMS | 755 |
| 5.10 INTRODUCTION | 755 |
| 5.20 FUNDAMENTALS OF COMPUTER UTILIZATION | 757 |
| 5.30 INTRODUCTION TO MATRIX ALGEBRA | 760 |

| | Page |
|--|------|
| 5.40 TECHNIQUES FOR SOLVING SHELL PROBLEMS AND THE USE OF THE COMPUTER IN THESE TECHNIQUES | 768 |
| 5.41 The Finite Difference Method | 769 |
| 5.42 The Numerical Integration Method | 776 |
| 5.43 The Budiansky-Radkowski Method | 783 |
| 5.44 The Finite Element Method | 786 |
| 5.50 ASSOCIATED PROBLEMS AND FEATURES RELATED TO COMPUTER USAGE | 793 |
| 5.51 Accuracy | 794 |
| 5.52 Time | 795 |
| 5.53 Compatibility Problems | 796 |
| 5.54 The Dynamic Nature of the Computer | 798 |
| 5.60 A TYPICAL COMPUTER PROGRAM | 799 |
| 5.70 CONCLUSION | 803 |
| REFERENCES | 804 |

NOMENCLATURE

| | |
|---|---|
| A_f | Frame area |
| A_i | Cross-sectional area; Lamé parameters |
| A_{ij} | Generalized Hooke's law coefficients |
| A_{st} | Stringer cross-sectional area |
| $A_s, A_{w_s}, A_x,$ $A_{x\theta}, A_\theta$ | Waffle constants (Paragraph 3.32.4) |
| a | Panel width or length |
| a_{ij} | Coefficients in assumed displacement function |
| B | Extensional stiffness (rigidity), $\frac{Et}{1-\mu^2}$ for homogeneous isotropic shells; plasticity curve |
| B_x, B_θ | Extensional stiffnesses (rigidities) for orthotropic shells (Section 3.32) |
| b | Stringer spacing; panel length; flange length |
| b_f | Stringer flange width |
| b_w | Web depth |

| | |
|--------------------------------------|---|
| C | Rigidity $\frac{Et}{4(1 - \mu^2)}$; buckling coefficient for stiffened cylinder; plasticity curve |
| C_b, C_c, C_s | Buckling coefficients for circular cylinders and cones subjected to bending, axial compression, and torsion, respectively |
| $\Delta C_b, \Delta C_c, \Delta C_s$ | Increase in the buckling coefficients due to internal pressure for the loading cases of bending, axial compression, and torsion, respectively |
| C_e | Material and shape parameter for crippling |
| C_p | Buckling coefficient for spheres or cylinders subjected to external pressure |
| $C_{x_i}, C_{\theta_i}, C_{\mu_i}$ | Layered construction material constants (Section 3.32) |
| c | Sandwich core depth; column fixity coefficient |
| C_f | Frame stiffness parameter for stiffened shell (Paragraph 3.42.2) |
| D | Bending stiffness (rigidity) $\frac{Et^3}{12(1 - \mu^2)}$ for homogeneous isotropic shells; plasticity curve |

| | |
|---|---|
| \bar{D} | $D_{x\theta}/D_x + \mu_\theta$ |
| $D_x, D_\theta, D_{x\theta},$ D_{Q_x}, D_{Q_y} | Stiffness rigidities for orthotropic shells (Paragraph 3.32.1) |
| d | Frame spacing for stiffened cylinders |
| d_e | Effective width of sheet acting with frame |
| E | Modulus of elasticity; plasticity curve |
| E_c | Flatwise compression modulus of core |
| E_{x_i}, E_{θ_i} | Modulus of elasticity for orthotropic material (Section 3.32) |
| $(EI)_f$ | Flexural stiffness of frame |
| e_{11}, e_{22}, e_{12} | Non-linear in-plane strains |
| e_1^o, e_2^o, e_{12}^o | Components of nonlinear in-plane middle surface strains; also, strains corresponding to equilibrium configuration |
| $\bar{e}_1, \bar{e}_2, \bar{e}_{12},$ $\bar{\bar{e}}_1, \bar{\bar{e}}_2, \bar{\bar{e}}_{12}$ | Admissible variations of the strains from equilibrium position |

| | |
|-----------------------------|--|
| e_{1z}, e_{2z} | Non-linear transverse shear strains (Eq. 1.22-1b) |
| F | Functions: $F_i(\xi) = F_i(kL\xi)$ and $F_i = F_i(kL)$; |
| G | Shear modulus; shear stress functions; plasticity curve |
| \bar{G} | $\frac{B_\theta (1 - \mu'_x \mu'_\theta)}{2 G_{x\theta}} - \mu'_\theta$ |
| $G_{xz}, G_{\theta z}, G_c$ | Transverse shear moduli of the sandwich core (Section 3.50) |
| $G_{x\theta_i}$ | In-plane shear modulus of material (Section 3.32) |
| $G_{x\theta}$ | In-plane shear stiffness of the wall of an orthotropic shell (Paragraph 3.32.1) |
| H | Overall depth of waffle |
| H_p | Height of shallow spherical cap |
| h | Distance between the centroids of the facing sheets for a sandwich element |
| I | Moment of inertia |

| | |
|---|--|
| I_e | Effective moment of inertia |
| I_f | Moment of inertia of frame |
| I_p | Polar moment of inertia of stringer |
| $I_s, I_{w_s}, I_x,$ $I_{x\theta}, I_\theta$ | Waffle constants (Paragraph 3.32.4) |
| i | Designation of the edge of the cone or lower edge of the spherical segment; part number, layer number |
| J | Torsion constant for stringer cross section |
| K_b, K_c, K_p, K_s | Buckling coefficient |
| K_L | Buckling coefficient for intracell buckling |
| k | Designation of the edge of the cone or upper edge of the spherical segment; spring constant for torsional instability; $\frac{\sqrt[4]{3(1-\mu^2)}}{\sqrt{t_{x_m} \cot \alpha_o}}$; $\frac{\sqrt[4]{3(1-\mu^2)}}{\sqrt{Rt}}$ |

| | |
|--|--|
| k_2 | Negative of slope of C_c versus V_c curve |
| $k_{\text{sheet}}, k_{\text{web}}$ | Spring constant for torsional instability of stringer |
| $\bar{k}_s, \bar{k}_x, \bar{k}_{x\theta}, \bar{k}_\theta,$ \bar{k}_{ws} | Waffle constants (Paragraph 3.32.4) |
| L | Length of cylinder; slant height of cone |
| \bar{L} | Distance between bulkheads along the meridian |
| L | Effective length of column |
| L_e | Equivalent length (cones) |
| l | Height of cone |
| M | Body bending moment |
| M_{ik} | Bending moment at edge i |
| M_{ki} | Bending moment at edge k |
| M_x | Bending moment per unit length acting at section $x = \text{constant for cone and cylinder}$ |
| M_θ | Bending moment per unit length acting at section $\theta = \text{constant for cone and cylinder}$ |

| | |
|------------------|--|
| M_ϕ | Bending moment per unit length acting at section $\phi = \text{constant for sphere}$ |
| $M_{x\theta}$ | Twisting moment per unit length acting at section $x = \text{constant for cone and cylinder}$ |
| $M_{\theta x}$ | Twisting moment per unit length acting at section $\theta = \text{constant for cone and cylinder}$ |
| $M_{\theta\phi}$ | Twisting moment per unit length acting at section $\theta = \text{constant for sphere}$ |
| $M_{\phi\theta}$ | Twisting moment per unit length acting at section $\phi = \text{constant for sphere}$ |
| M_1 | Bending moment per unit length acting in meridional coordinate direction |
| M_2 | Bending moment per unit length acting in circum- ferential coordinate direction |
| M_{12} | Twisting moment per unit length acting on coordinate line parallel to ξ_2 and acting about the coordinate line ξ_1 ($M_{12} = M_{21}$) |

| | |
|------------------|---|
| m | Number of layers or parts |
| N_x | Longitudinal inplane force per unit length acting at section $x = \text{constant}$ for cone and cylinder |
| N_θ | Circumferential inplane force per unit length acting at section $\theta = \text{constant}$ |
| N_ϕ | Meridional inplane force per unit length acting at section $\phi = \text{constant}$ for sphere |
| $N_{x\theta}$ | Shear per unit length acting at section $x = \text{constant}$ for cylinder and cone |
| $N_{\theta x}$ | Shear per unit length acting at section $\theta = \text{constant}$ for cylinder and cone |
| $N_{\theta\phi}$ | Shear per unit length acting at section $\theta = \text{constant}$ for sphere |
| $N_{\phi\theta}$ | Shear per unit length at section $\phi = \text{constant}$ for sphere |
| N_1 | Inplane force per unit length acting in meridional coordinate direction (Fig. 1. 12-14) |

| | |
|------------|---|
| N_2 | Inplane force per unit length acting in circumferential coordinate direction (Fig. 1.12-14) |
| N_{12} | Shear per unit length acting perpendicular to ξ_1 coordinate in a direction of ξ_2 ($N_{12} = N_{21}$) (Fig. 1.12-14) |
| n | Number of buckles |
| P_{cr} | Total axial compressive load for a cylinder, cone, or sheet stringer panel |
| P_1 | Loading component in meridional direction |
| P_2 | Loading component in circumferential direction |
| P_{cr} | Design-allowable external buckling pressure |
| P_f, P_s | Pressure parameters (Paragraph 3.43.1) |
| Q_1 | Transverse shear per unit length acting on coordinate line parallel to ξ_2 acting in Z direction (Fig. 1.12-14) |
| Q_2 | Transverse shear per unit length acting on coordinate line parallel to ξ_1 acting in Z direction (Fig. 1.12-14) |

| | |
|------------|--|
| Q_b | Dimensionless parameter for buckling analysis of frame and stringer stiffened cylinders subjected to bending |
| Q_{ik} | Horizontal load at edge i sphere, cone, and cylinder |
| Q_{ki} | Horizontal load at edge k sphere, cone, and cylinder |
| Q_x | Transverse shear at section $x = \text{constant}$ for cone and cylinder |
| Q_θ | Transverse shear at section $\theta = \text{constant}$ for cone, sphere, and cylinder. |
| Q_ϕ | Transverse shear at section $\phi = \text{constant}$ for sphere |
| q | Loading component in the normal direction to the surface |
| R | Radius of cylinder measured from the axis of rotation to the centroidal surface of the cylinder wall; radius of sphere measured from the center of the sphere to the middle surface of sphere wall |

| | |
|----------------------|--|
| R_i | Radii of curvature ($i = 1, 2$ for ξ_1 and ξ_2 , respectively; $i = 0$ means initial value) |
| R_1, R_2 | Radii for cones (Fig. 3.34-1) |
| R_b, R_c, R_s, R_p | Stress ratios |
| R_e | Equivalent radius |
| r | Radius of circumferential circle; coordinate in polar coordinates; local radius of curvature of stringer. |
| r_o | Base radius of spherical cap |
| r_{ws} | Local radius for waffle type construction |
| S | Ratio of principal stresses (Section 3.52) |
| S_i | Factors for the degree of fixity on boundaries of cylindrical or spherical shell. |
| S_1, S_2 | $\frac{(1 - \omega_2)}{2\bar{G}(\omega_2 - \omega_3)}, \frac{B_x}{B_\theta} \frac{(1 - \omega_3)}{(\omega_2 - \omega_3)}$, respectively |

| | |
|-----------------------------|---|
| S_3, S_4, S_5 | $(D_x B_\theta)/(D_\theta B_x), \bar{D} D_x^{1/2}/D_\theta^{1/2}, \bar{G} B_x^{1/2}/B_\theta^{1/2}$ respectively |
| s | Arc length |
| T | Torque |
| t | Shell thickness |
| t_s | Sheet thickness for stiffened cylinders |
| t_w | Web thickness of stiffener |
| t_{ws} | Stiffener width for integrally stiffened waffle construction |
| t_1, t_2 | Facing sheet thickness for sandwich construction |
| $\bar{u}, \bar{v}, \bar{w}$ | An admissible variation of displacements from the equilibrium configuration |
| u^0, v^0, w^0 | Displacements corresponding to equilibrium configurations |
| \bar{U} | Potential energy (internal strain energy) |

| | |
|------------------------------|--|
| $U, U_M, U_1,$ U_2, U_3 | Orthotropic cylinder parameters (Paragraph 3.33.1) |
| u | Displacement in direction of x ; displacement in direction of meridional coordinate |
| \bar{V} | $= \bar{U} - \bar{W} =$ total potential energy |
| V_c, V_p, V_s | Sandwich cylinder shear stiffness parameters (Section 3.53) |
| v | Displacement in direction of circumferential coordinate |
| W_b, W_c | Weight of sandwich bond and core, respectively |
| \bar{W} | Potential energy (external work due to applied loads) |
| W | Weight of sandwich |
| w | Displacement in direction of normal coordinate (perpendicular to u and v displacements) |
| w_e | Effective sheet width |
| w^* | Assumed initial imperfection displacement function |

| | |
|------------------------------------|---|
| X | Loading component in meridional direction |
| x | Coordinate along the length of the cylinder; coordinate measured along the generator of a cone surface |
| x or $\xi = \frac{x}{L_i}$ | For the upper portion of cylinder from discontinuity |
| \bar{x} | Coordinate along the cone-meridian, measured from the upper bulkhead k for segment of the cone |
| \bar{x} or $\xi = \frac{x}{L_i}$ | For the lower portion of cylinder from discontinuity |
| x_m | Distance between the apex and a point on the cone- meridian that corresponds to half of the distance between the upper and lower bulkheads |
| x_1 | Coordinate that locates the upper edge of the cone with respect to the apex, along the meridian |
| x_2 | Coordinate that locates the lower edge of the cone with respect to the apex, along the meridian |

- Y Loading component in tangent-direction to the circumference (psi)
- y Coordinate of any circumferential surface with respect to the apex
- Z $\left[B_{\theta} (1 - \mu'_x \mu'_{\theta}) \right]^{1/2} L^2 / \left[R (12D_x)^{1/2} \right]$, for unstiffened isotropic shell $Z = L^2 (1 - \mu^2) / (Rt)$ or loading component in the normal direction to the surface
- Z_p, Z_s Orthotropic cylinder parameter (Paragraphs 3.33.4 and 3.33.2, respectively)
- z Coordinate in direction of surface normal
- α Cone angle (Fig. 3.34-1); reduced Lamé parameter $\left(\frac{A_1}{1 + Z/R_1} \right)$
- α_0 Angle between the radius on the circumferential surface and the meridian of the cone
- β Rotation meridional angle; rotation angle of tangents on meridional line

| | |
|---|--|
| β_{ik} | Forced rotation of tangent on meridian at edge i for sphere and cone |
| β_{ki} | Forced rotation of tangent on meridian at edge k for sphere and cone |
| β_1, β_2 | Rotation of middle surface in ξ_1 and ξ_2 directions, respectively (Eq. 1.13-24) |
| $\beta^\circ, \bar{\beta}$ | Rotation of middle surface for equilibrium and admissible variation, from equilibrium position respectively |
| Γ | Torsional bending constant |
| $\gamma, \gamma_1, \gamma_2$ | Correction factors for stability analysis; shape parameter |
| $\gamma_{12}, \gamma_{13}, \gamma_{23}$ | Linear shear strains ($\gamma_{13} = \gamma_{1z}$ and $\gamma_{23} = \gamma_{2z}$ are usually called traverse shear strains) |
| $\gamma_1^\circ, \gamma_2^\circ, \gamma_{12}^\circ$ | Components of middle surface in-plane shear strains |
| Δr | Change of radius |

| | |
|---|---|
| Δr_{ik} | Forced change of radius at upper bulkhead i for sphere and cone |
| r_{ki} | Forced change of radius at lower bulkhead k for sphere and cone |
| $\Delta_x, \Delta_\theta, \Delta_\mu, \Delta_{x\theta}$ | Parameters for layered shells (Paragraph 3.32.2) |
| ξ_i | Parameter for layered shells (Fig. 3.32-1) |
| ξ_1, ξ_2 | Contribution to the middle surface twist (Eq. 1.13-22c) |
| ϵ_1, ϵ_2 | Linear extensional shear strains (normally $\epsilon_3 = 0$ for thin shells) (See Eq. 1.12-6a-c) |
| $\epsilon_1^0, \epsilon_2^0$ | Components of the middle surface extensional (in-plane) strains in ξ_1, ξ_2 directions, respectively |
| η, η_A, η_G | Plasticity correction factor |
| θ | Angle defining the location of the point under consideration on the circumference of the sphere or cone; angle for locating meridians for cylinder ($0 \leq \theta \leq 2\pi$); polar coordinate |

| | |
|--|--|
| $\kappa_1, \kappa_2, \kappa_{12}$ | Change in curvature and twist of the middle surfaces and bending distortions |
| λ | Parameter for shallow spherical caps (Paragraph 3.25.1) |
| λ | Arbitrarily small parameter used in non-linear and stability analysis |
| $\lambda, (\mu = G)$ | Lame parameters (engineering technical constants) ($G =$ modulus of shear) |
| λ_1 | Torsional buckling parameter (Paragraph 3.42.2) |
| λ_2, λ_3 | Parameters used for frame stiffened cylinders (Fig. 3.43-5) |
| μ | Poisson's ratio, amplitude of imperfection as a fraction of shell thickness |
| $\mu_x, \mu_\theta, \mu'_x, \mu'_\theta$ | Poisson's ratios for an orthotropic shell (Paragraph 3.32.1) |
| $\mu_{x_i}, \mu_{\theta_i}$ | Poisson's ratios for an orthotropic layer (Section 3.32) |

| | |
|-------------------------|--|
| ξ | x/L ($0 \leq \xi \leq 1$), meridional coordinate |
| ξ_1, ξ_2 | Curvilinear coordinates |
| ξ_3 | Coordinate in direction of normal surface |
| ρ | Radius of gyration; wavelength parameter |
| ρ_f, ρ_s | Radii of gyration of frame sheet combination and stringer sheet combination, respectively |
| σ_{cc} | Stringer crippling stress |
| σ_{cl} | "Classical" buckling stress |
| σ_{cp} | Sheet stringer lateral buckling stress |
| σ_{cr} | Design allowable buckling stress |
| σ_{cs} | Buckling stress of sheets between stringers |
| σ_{ct} | Stringer torsion instability stress |
| σ_{cy} | Compressive yield stress |
| σ_i, σ_{ii} | Normal stresses (for $i = 1, 2, 3$) in ξ_1, ξ_2, ξ_3 coordinate directions, respectively ($\sigma_{33} = 0$ for thin shells) |

| | |
|---|--|
| $\sigma_i^\circ, \sigma_2^\circ, \tau_{12}^\circ$ | Components of stress corresponding to the equilibrium configuration |
| $\sigma_{ij}, \tau_{ij} (i \neq j)$ | In-plane shear stresses (i, j = 1, 2, 3) |
| $\bar{\sigma}_1, \bar{\sigma}_2, \bar{\tau}_{12},$ $\bar{\bar{\sigma}}_1, \bar{\bar{\sigma}}_2, \bar{\bar{\tau}}_{12}$ | Associated stress of admissible variations from the equilibrium position stresses ($\sigma_1^\circ, \sigma_2^\circ, \tau_{12}^\circ$) (Eq. 1.25-21) |
| σ_0 | Stress level at which initial dimpling occurs for sandwich construction with cellular core |
| τ_{cr} | Design allowable shear buckling stress |
| T | Waffle angle |
| ϕ | Angle defining the location of the point under consideration on the meridian |
| ϕ_1 | ϕ at edge i |
| ϕ_2 | ϕ at edge k |
| χ | Angle between tangents to curvilinear coordinate lines (for orthogonal coordinates $\chi = 90^\circ$); ratio of different values as shown in the text |

$$\downarrow \quad \frac{nL}{2\pi R}$$

$\omega_1, \omega_2, \omega_3$ Parameters for orthotropic cylinders
(Paragraph 3.33.1)

Superscripted ()[°] or barred (-) notations used on the internal loads represent equilibrium and incremental variation from the equilibrium configurations, respectively

1.00 INTRODUCTION TO THE THEORY OF SHELLS

1.01 GENERAL

The theory of shells constitutes that part of the theory of elasticity concerned with the study of deformations of thin elastic bodies under the influence of loads. Theories of thin shells may be broadly classified according to the fundamental theories of elasticity which they approximate: (classical) linear or nonlinear elasticity. Shells in the inelastic range will not be discussed in this chapter.

The most common shell theories are those based on linear elasticity concepts. Linear shell theories adequately predict stresses and deformations for shells exhibiting small elastic deformations. By small deformations, it is assumed that the equilibrium equation conditions for deformed elements are the same as if they were not deformed.

The nonlinear theory of elasticity forms the basis for the finite deflection and stability theories of shells. Large deflection theories are often required when dealing with shallow shells, highly elastic membranes, and buckling problems. The nonlinear shell equations are considerably more difficult to solve and for this reason are more limited in use.

An essential problem in the analysis of shells is that of shell stability. The buckling analysis of shells requires the determination of the stability of the equilibrium states obtained from nonlinear elasticity theories. The

stability of shells will be treated in a unified manner with linearized and nonlinear shell theories in such a manner as to indicate the essential unity of shell theory.

This chapter is divided into three sections. The first is concerned with the shell theories based on linear elasticity. The linear theory of shells is presented starting from basic relationships of three-dimensional elasticity. The basic assumptions necessary in the development of linear shell theory from elasticity considerations are outlined along with a variety of simplifications.

The second section considers the problem of shells when displacements or, to be more precise, displacement gradients can no longer be considered negligible. In this case, the shell theory developed must be based on concepts of nonlinear elasticity. A presentation of nonlinear shell theory follows from minimum potential energy considerations as derived from calculus of variations.

The third section is devoted to the theory of shell stability or buckling. A discussion of the concept of stability together with the stability equations is included.

This chapter presents a brief review and summary of shell theories; the intent is to supply the analyst with the theoretical background necessary for use of subsequent chapters of the manual.

1.10 LINEAR SHELL THEORY

1.11 INTRODUCTION

The theory of small deflections of thin elastic shells is now considered. The relationships governing the behavior of thin elastic shells are based upon the equations of the mathematical theory of linear elasticity.

The geometry of shells (i. e. , one dimension much smaller than the other dimensions) does not warrant, in general, the consideration of the complete three-dimensional elasticity field equations. In fact, the consideration of the complete elasticity equations leads to expressions and equations which are so complicated that it becomes impossible to obtain solutions for shell problems of practical interest.

Fortunately, sufficiently accurate analyses of thin plates and shells can be obtained using simplified versions of the general elasticity equations. In the development of thin shell theories, this is accomplished by attempting to reduce the shell problem to the study of the deformations of the middle (or reference) surface of the shell. In all cases, one begins with the governing equations in the three-dimensional theory of elasticity and attempts to reduce the system of equations, involving three independent space variables, to a new system involving only two space variables. These two variables are more conveniently taken as coordinates on the middle (or reference) surface of the shell.

Shell theories of varying degrees of accuracy may be derived depending upon the degree to which the elasticity equations are simplified. The approximations necessary for the development of an adequate theory of shells have been the subject of considerable controversy among the investigators in the field.

Historically, the first attempt to formulate a general bending theory for elastic shells from the general equations of elasticity is credited to Aron (Ref. 1-1). The first apparently successful approximate theory was presented by Love (Ref. 1-2) in 1888. Love applied an analogy to the Navier hypothesis (elementary beam theory) or Kirchhoff assumption (plates) in the treatment of shell problems. This theory, often referred to as Love's first approximation, has since occupied a position of prominence. In spite of its popularity, the development given by Love is not free from inadequacies in that it is inconsistent with regard to small terms. Many investigators, including Love (Ref. 1-3) himself, have attempted to improve on the approximations to arrive at a consistent linear shell theory. (See Ref. 1-4.) However, Novozhilov (Ref. 1-5) has indicated that the inconsistencies obtained using Love's approximations are, in general, not of great importance in the practical analysis of most shell problems. The simplicity and complete analogy with the corresponding formulas of the theory of plates, makes Love's first approximation an important tool in the development of shell theory.

To better understand the theory of shells, the subsequent development of the theory will start from consideration of the general elasticity equations. The various shell theories will be classified and the assumptions and simplifications necessary in the development of each shell theory will be specified and their effects assessed. A linear shell theory based on Love's first approximations will be completely developed from elasticity considerations. The limitations or range of applicability of Love's assumptions will be pointed out. Other approximate or specialized theories will be discussed as they appear.

1.12 BASIC RELATIONSHIPS FOR THE THEORY OF THIN SHELLS

In this section the basic formulas pertaining to the analysis of stress and strain in terms of orthogonal curvilinear coordinates are presented. These are given for reference and serve as a basis for the subsequent developments of linear shell theory.

1.12.1 Geometry of Shells

A. Arbitrary Shell

Before discussing shell theory, the geometry of a shell in three-dimensional space is defined. The geometry of a shell is entirely defined by specifying the form of the middle surface and the thickness of the shell at each point. To describe the form of the middle surface it is necessary to present some of the important geometrical properties of a surface. A more detailed presentation of the theory of surfaces can be found in books on tensor analysis and differential geometry (Refs. 1-6, 1-7, and 1-8).

The position of points on any smooth surface can be described in terms of two independent parameters (ξ_1, ξ_2). If the range of these parameters is restricted so that every point on the surface corresponds to one and only one pair of values (ξ_1, ξ_2); then the parameters (ξ_1, ξ_2) constitute a curvilinear coordinate system for points on the surface.

Equations $\xi_1 = \text{constant}$ and $\xi_2 = \text{constant}$ represent families of curves on the surface (Fig. 1.12-1). These parametric curves are called

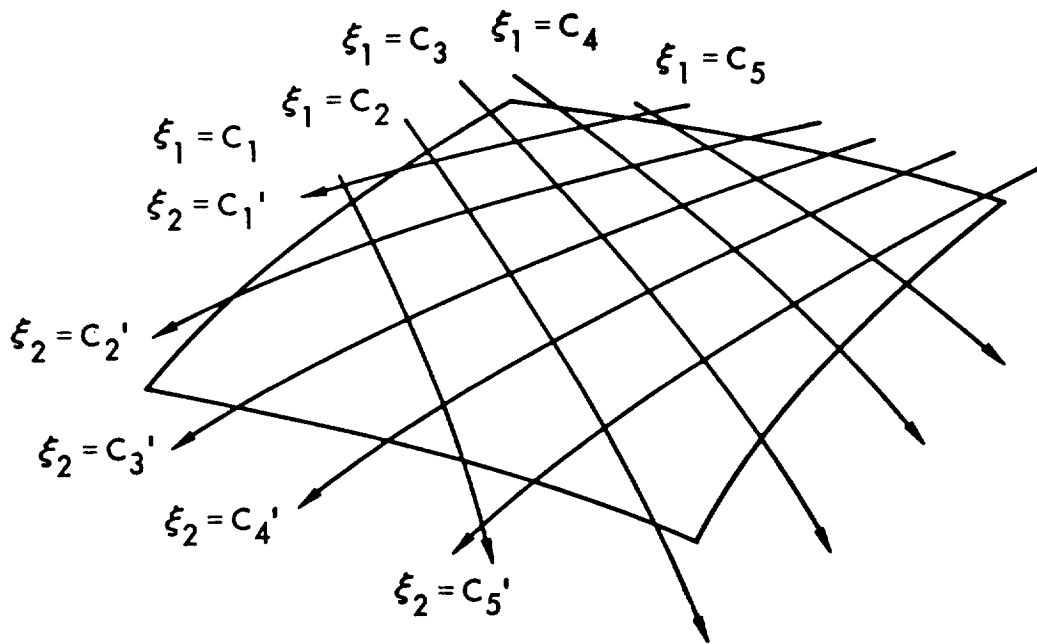


FIG. 1.12-1. Families of Curves on a Surface

coordinate lines of the surface. Thus, a surface can be completely described by a doubly infinite set of such parametric curves where the position of any point on the surface is determined by the values of ξ_1 and ξ_2 . (A simple illustration of this concept is the lines of latitude and longitude on a world globe. Geographical locations are given by latitude and longitude. These lines can be thought of as coordinate lines.) The distance between two neighboring points on a surface can be related by the differential distance (ds).

The square of the linear element (ds) of any curve traced on the surface is given by an expression of the form:

$$ds^2 = \alpha_1^2 d\xi_1^2 + \alpha_2^2 d\xi_2^2 + 2\alpha_1\alpha_2 \cos\chi d\xi_1 d\xi_2 \quad (1.12 - 1)$$

where χ is the angle between the tangents to the coordinate lines ξ_1 and ξ_2 at any point. Eq. 1.12.1-1 is called the first quadratic form of arc length in the theory of surfaces. For orthogonal coordinate systems, the angle χ is equal to 90° and Eq. 1.12.1-1 is considerably simpler because the last term vanishes. The coefficients α_1 and α_2 are, in general, functions of ξ_1 and ξ_2 and represent the first fundamental magnitudes of the surface (for orthogonal systems). The quantities α_1 , α_2 are sometimes called Lamé parameters or coefficients.

Lamé parameters can be interpreted geometrically as lengths of linear elements along constant coordinate lines of the surface when the increment (differential) of one of the two independent variables has a unit value (Fig. 1.12-2).

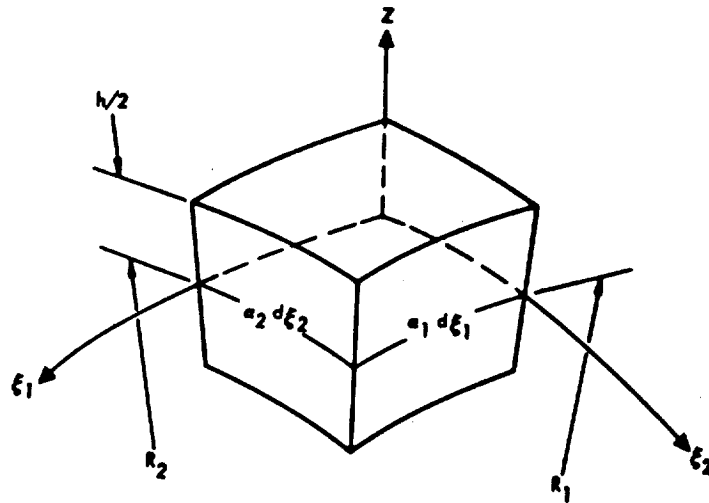
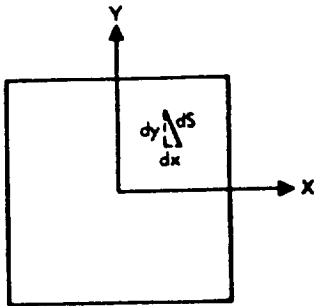


FIG. 1.12-2. Length of Linear Elements Along Constant Coordinate Lines

The quadratic form for a given surface will have different expressions in different systems of curvilinear orthogonal coordinates (ξ_1, ξ_2) . In other words, for particularly selected coordinates (ξ_1, ξ_2) there will correspond specific expressions for α_1 and α_2 . To illustrate, consider the specialized curvilinear coordinate systems: Cartesian and polar coordinates. In Cartesian coordinates (two dimensions), the quadratic form (Eq. 1.12-1) is given by

$$ds^2 = dx^2 + dy^2$$

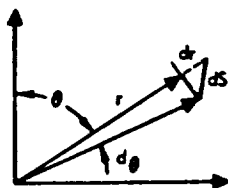
where, in this case, $\xi_1 = x, \xi_2 = y$ and the Lamé parameters become $\alpha_1 = \alpha_2 = 1$



Consider now a system of polar coordinates. The quadratic form in this case becomes

$$ds^2 = dr^2 + r^2 d\theta^2$$

and noting that $\xi_1 = r, \xi_2 = \theta$ the Lamé parameters are given by $\alpha_1 = 1, \alpha_2 = r$



For convenience, the orthogonal curvilinear system of coordinates is chosen to simplify the formulas for the surface. Such a system is that

in which the two families of coordinate curves are simultaneously lines of principal curvature of the surface. A line of curvature is a curve in the surface which possesses the property that normals to the surface at consecutive points on the curve intersect. In the general case, the curvature of this line varies with its orientation on the surface. The directions at which the curvature reaches extremes are the directions of the lines of principal curvature. The direction of the lines of principal curvature can be shown to be orthogonal (Fig. 1.12-3). Quantities R_1 , R_2 denote principal radii

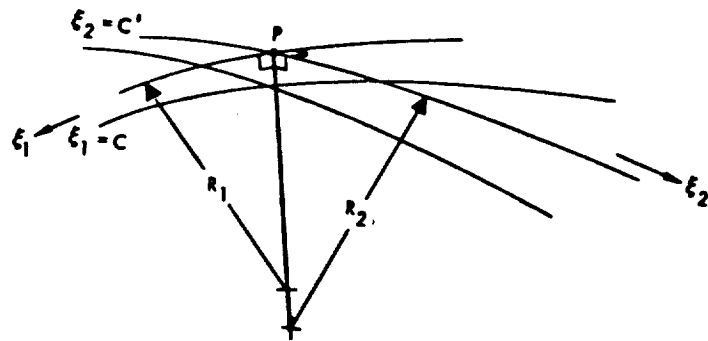


FIG. 1.12-3. Principal Radii of Curvatures

of curvature of the surface at a point (P), R_1 being the radius of curvature at that section drawn through the normal at the point (P) which contains the tangent to the curve of the family ξ_1 .

The position points in a surface have been shown to be related by the curvilinear coordinates ξ_1 and ξ_2 . The location of a point on a shell with

thickness, t , can be related by three parameters. Two (ξ_1, ξ_2) vary on the middle surface of the shell, and the third (z) varies along the normal to the middle surface.

The position of an arbitrary point, M , in space is fixed by three parameters; the coordinates $\xi_1 = c_1, \xi_2 = c_2$ of the base of the perpendicular, and the length of the perpendicular $z = c_3$ (Fig. 1.12-4).

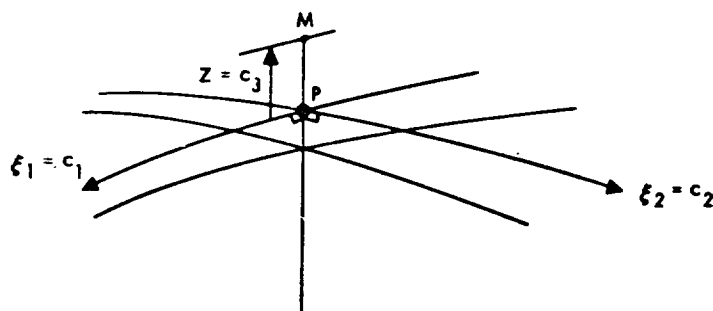


FIG. 1.12-4. Position at an Arbitrary Point in Space

In such a triorthogonal system of curvilinear coordinates, the square of a linear element in space would have the form

$$dS^2 = A_1^2 d\xi_1^2 + A_2^2 d\xi_2^2 + A_3 dz^2 \quad (1.12-2)$$

where the Lamé parameters are now written as

$$A_1 = \alpha_1 \left(1 + \frac{z}{R_1} \right)$$

$$A_2 = \alpha_2 \left(1 + \frac{z}{R_2} \right) \quad (1.12-3)$$

$$A_3 = 1$$

The geometrical significance of Eq. 1.12-3 can be seen by examination of Fig. 1.12-5 which shows the cross section of a shell element cut along a coordinate axis.

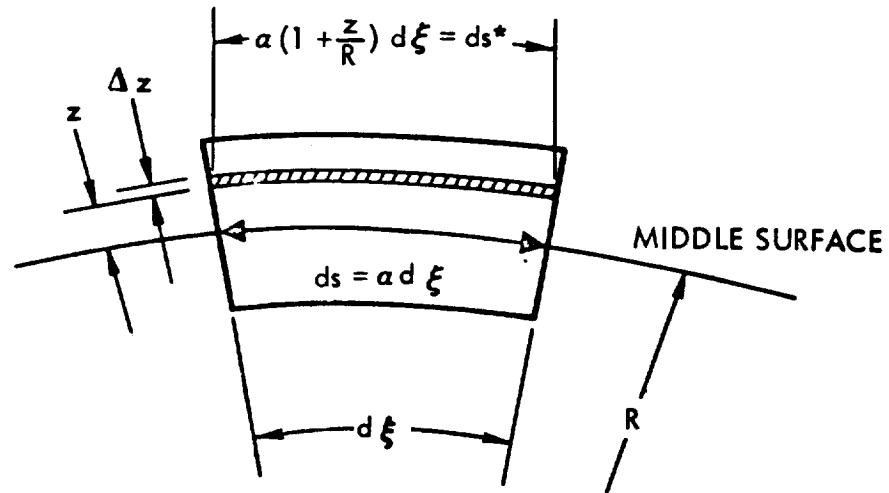


FIG. 1.12-5. Geometrical Significance of Lamé' Parameters

α_1 , α_2 , R_1 , R_2 in Eq. 1.12-3 are functions of ξ_1 and ξ_2 and must satisfy the three relationships from the theory of surfaces. Two of these relationships, known as the condition of Codazzi, are given by

$$\frac{1}{R_2} \frac{\partial \alpha_1}{\partial \xi_2} = \frac{\partial}{\partial \xi_2} \left(\frac{\alpha_1}{R_1} \right)$$

$$\frac{1}{R_1} \frac{\partial \alpha_2}{\partial \xi_1} = \frac{\partial}{\partial \xi_1} \left(\frac{\alpha_2}{R_2} \right)$$

(1.12-4a)

The other relation, called the condition of Gauss, is

$$\frac{\partial}{\partial \xi_1} \left(\frac{1}{\alpha_1} \frac{\partial \alpha_2}{\partial \xi_1} \right) + \frac{\partial}{\partial \xi_2} \left(\frac{1}{\alpha_2} \frac{\partial \alpha_1}{\partial \xi_2} \right) = - \frac{\alpha_1 \alpha_2}{R_1 R_2} \quad (1.12-4b)$$

Equations 1.12-4a and -4b are presented for reference. For a more complete description of the Gauss-Codazzi relationships, see Ref. 1-5.

B. Shells of Revolution

In the engineering application of thin shells, a shell whose reference surface is in the form of a surface of revolution has extensive usage. The previous section considered the differential geometry of any surface. This discussion will now be restricted to surfaces of revolution. A surface of revolution is obtained by rotation of a plane curve about an axis lying in the plane of the curve. This curve is called the meridian, and its plane is the meridian plane. The intersection of the surface with planes perpendicular to the axis of rotation are parallel circles and are called parallels.

For such shells the lines of principal curvature are its meridians and parallels. Accordingly, a convenient selection of coordinates of the middle surface are the angle ϕ (between the normal to the middle surface and the axis of rotation) and the angle θ , determining the position of a point on the corresponding parallel circle (Figs. 1.12-6 and 7).

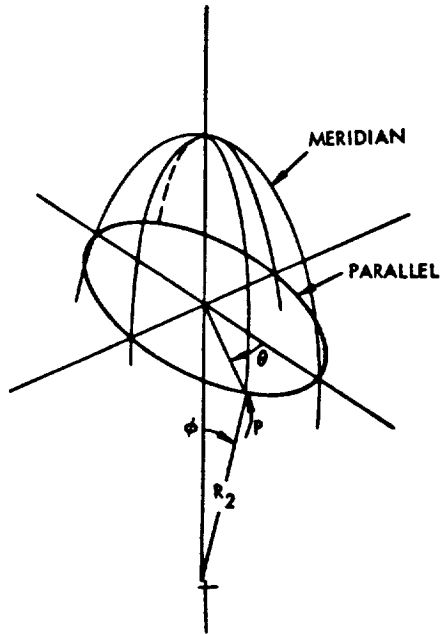


FIG. 1.12-6. Coordinates on a Surface of Revolution

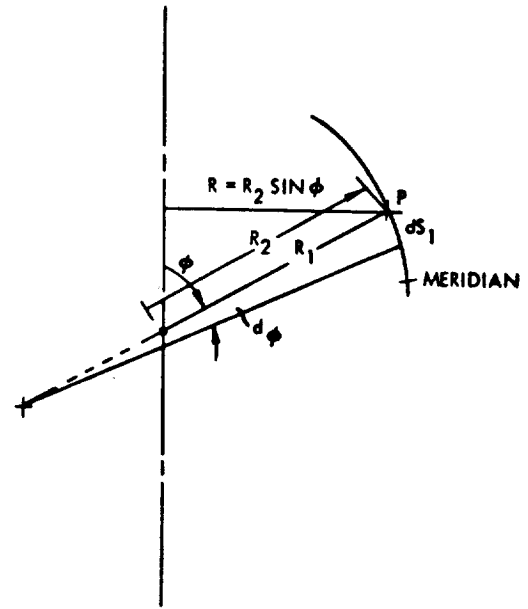


FIG. 1.12-7. Coordinates on a Surface of Revolution

Let R_1 be the radius of curvature of the meridian. The second radius of curvature R_2 will always be the length of the intercept of the normal to the middle surface between the surface and the axis of the shell since, considering two adjacent points on the same circle, the normal from these points intersect on the axis of the shell.

The element of arc of a meridian will be given by

$$ds_1 = R_1 d\phi$$

Correspondingly, the element of arc of a parallel circle is given by

$$ds_2 = R_2 \sin\phi d\theta$$

In this case, the Lamé parameters are

$$\alpha_1 = R_1$$

$$\alpha_2 = R_2 \sin \phi \quad (1.12-5)$$

where

$$\xi_1 = \phi$$

$$\xi_2 = \theta$$

Thus, the middle surface of a shell of revolution is completely determined by knowledge of its principal radii of curvature R_1 , R_2 , which will be functions of only one of the curvilinear coordinates, namely ϕ .

Table 1.12-1 presents the radii of curvature expressions generated by the rotation of second order curves about their axes of symmetry.

TABLE 1.12-1. GEOMETRY OF SHELLS OF REVOLUTION

| <p>Increment of Arc</p> $ds^2 = \alpha_1^2 d\phi^2 + \alpha_2^2 d\theta^2$ <p>where Lamé parameters are of the form:</p> $\alpha_1 = R_1$ $\alpha_2 = R_2 \sin \phi = R$ | | | |
|--|---------------|--|--|
| Shell Shape | | R_1 | R_2 |
| Sphere | $\gamma = 0$ | $\frac{R_0}{(1 + \gamma \sin^2 \phi)^{3/2}}$ <p>$R_0 =$ Radius of curvature at $\phi = 0$ $\gamma =$ Shell shape parameter</p> | $\frac{R_0}{(1 + \gamma \sin^2 \phi)^{1/2}}$ |
| Paraboloid | $\gamma = 1$ | | |
| Ellipsoid | $\gamma > -1$ | | |
| Hyperboloid | $\gamma < -1$ | | |
| <p>Degenerate Cases</p> <p>Increment of Arc</p> $ds^2 = \alpha_1^2 dx^2 + \alpha_2^2 d\theta^2$ <p>Lamé parameters of form:</p> $\alpha_1 = 1$ $\alpha_2 = R_2$ | | | |
| | | R_1 | R_2 |
| Cylinder | | ∞ | R |
| Cone | | ∞ | $\frac{R}{\sin(90^\circ - \alpha)}$ |

1. 12. 2 Geometry of Strain

As stated previously, the theory of shells is concerned, among other things, with the determination of small deformations due to load. Some of the basic geometrical properties of deformation (strain) will be examined in this section.

The basic problem of the determination of strain at a point in the shell requires relating the position of points in the shell before deformation with their location after deformation.

The deformation condition in an elastic body can be described, in general, by three displacement quantities or by six strain quantities. The three displacements must be independent of each other to uniquely define the deformed condition of the body. Since both deformation quantities (displacements or strain) describe the same state of affairs, three relationships relating the six dependent components of strain must exist. These relationships are the compatibility conditions of the state of strain (Ref. 1-5).

As previously stated, the displacement components and the components of strain describe the same state of deformations in the shell; therefore, they can be linked by virtue of this state. The relating of strains to displacements is purely a geometrical problem requiring the consideration of shell geometry before and after deformation. A detailed development of the strain equations based on geometrical considerations can be found in many of the books on elasticity (Refs. 1-3, 1-9, and 1-10).

The strain displacement relationships appropriate for linear shell analysis can be readily obtained in terms of a system of orthogonal curvilinear coordinates from the corresponding relations for a general elastic body. The general strain equations of three dimensional elasticity are introduced to illustrate the assumptions inherent in the development of a linear shell theory from elasticity considerations.

For small deformation theory, the components of normal strain ($\epsilon_1, \epsilon_2, \epsilon_3$) and of shear strain ($\gamma_{12}, \gamma_{13}, \gamma_{23}$) are related to displacement components (U, V, W) measured along tangents to the coordinates lines of the orthogonal coordinate system (ξ_1, ξ_2, ξ_3) as follows:

$$\epsilon_1 = \frac{1}{A_1} \frac{\partial U}{\partial \xi_1} + \frac{V}{A_1 A_2} \frac{\partial A_1}{\partial \xi_2} + \frac{W}{A_1 A_3} \frac{\partial A_1}{\partial \xi_3} \quad (1.12-6a)$$

$$\epsilon_2 = \frac{1}{A_2} \frac{\partial V}{\partial \xi_2} + \frac{U}{A_1 A_2} \frac{\partial A_2}{\partial \xi_1} + \frac{W}{A_2 A_3} \frac{\partial A_2}{\partial \xi_3} \quad (1.12-6b)$$

$$\epsilon_3 = \frac{1}{A_3} \frac{\partial W}{\partial \xi_3} + \frac{V}{A_3 A_2} \frac{\partial A_3}{\partial \xi_2} + \frac{U}{A_1 A_3} \frac{\partial A_3}{\partial \xi_1} \quad (1.12-6c)$$

$$\gamma_{12} = \frac{A_2}{A_1} \frac{\partial}{\partial \xi_1} \left(\frac{V}{A_2} \right) + \frac{A_1}{A_2} \frac{\partial}{\partial \xi_2} \left(\frac{U}{A_1} \right) \quad (1.12-6d)$$

$$\gamma_{13} = \frac{A_1}{A_3} \frac{\partial}{\partial \xi_3} \left(\frac{U}{A_1} \right) + \frac{A_3}{A_1} \frac{\partial}{\partial \xi_1} \left(\frac{W}{A_3} \right) \quad (1.12-6e)$$

$$\gamma_{23} = \frac{A_3}{A_2} \frac{\partial}{\partial \xi_2} \left(\frac{W}{A_3} \right) + \frac{A_2}{A_3} \frac{\partial}{\partial \xi_3} \left(\frac{V}{A_2} \right) \quad (1.12-6f)$$

where (A_1, A_2, A_3) are the Lamé parameters which are basic quantities in the characterization of the coordinate system, ξ_1, ξ_2, ξ_3 , (see Section 1.12.1-A.).

In describing the geometry of shells, in Sec. 1.12.1, the coordinates (ξ_1, ξ_2) were specialized to correspond to the parametric curves consisting of lines of curvature $\xi_1 = \text{constant}$, $\xi_2 = \text{constant}$ of a reference surface within the shell wall, and z was taken to correspond to ξ_3 , where z is a coordinate measured along the normal to this surface such that (ξ_1, ξ_2, z) form a right-hand coordinate system. (See Fig. 1.12-8.)

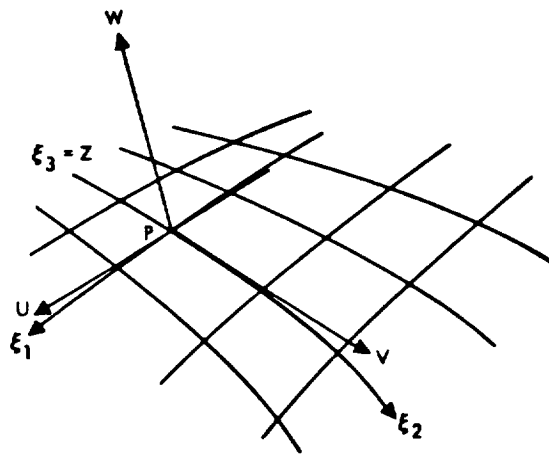


FIG. 1.12-8. Surface Coordinates for a Right-Hand Curvilinear Coordinate System

The Lamé parameters when specialized for a shell coordinate system are described by Eq. 1.12-3.

In the development of the small deformation strain displacement equations (Eq. 1.12-6), the assumptions consistent with classical elasticity have been introduced. These assumptions are as follows:

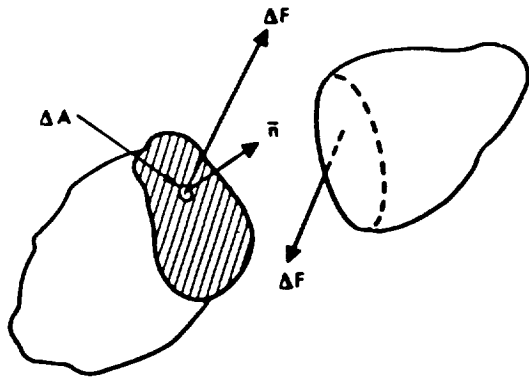
1. Strains are small in comparison with unity, i. e., $\epsilon \ll 1$
2. Displacement gradients are of the order of magnitude of strain and assumed small in comparison with unity, i. e., terms such as $\frac{\partial W}{\partial \xi_1}$, $\frac{\partial U}{\partial \xi_2}$, etc... $\ll 1$
3. Displacements are small (compared with linear dimensions of the shell), i. e., in a shell of thickness t , $\frac{W}{t} \ll 1$

Assumptions 2 and 3 imply that rotation expressions are small in comparison with unity. These assumptions permit higher order terms in the strain displacement equations to be neglected. The more complicated strain equations of nonlinear elasticity will be discussed in Sec. 1.20.

1.12.3 Stress and Stress Resultants

In the next two subsections, the basic relationships for shells obtained from the law of statics are presented. The concept of stress resultants will be introduced together with relationships for static equilibrium.

When a shell is under the action of external forces, it undergoes distortion, and the effect of the forces is transmitted throughout the body. Across any small internal plane area of the body, forces are exerted by the part of the body on one side of the area upon the part of the body on the other side. The term "stress" denotes this internal force per unit area. (See Fig. 1.12-9).



$$\text{Stress} = \sigma = \lim_{\Delta A \rightarrow 0} \left(\frac{\Delta F}{\Delta A} \right) \quad (1.12-7)$$

FIG. 1.12-9

Consider a stressed element of shell of thickness t , cut along coordinate lines ξ_1 , $\xi_1 + d\xi_1$, ξ_2 and $\xi_2 + d\xi_2$ (Fig. 1.12-10).

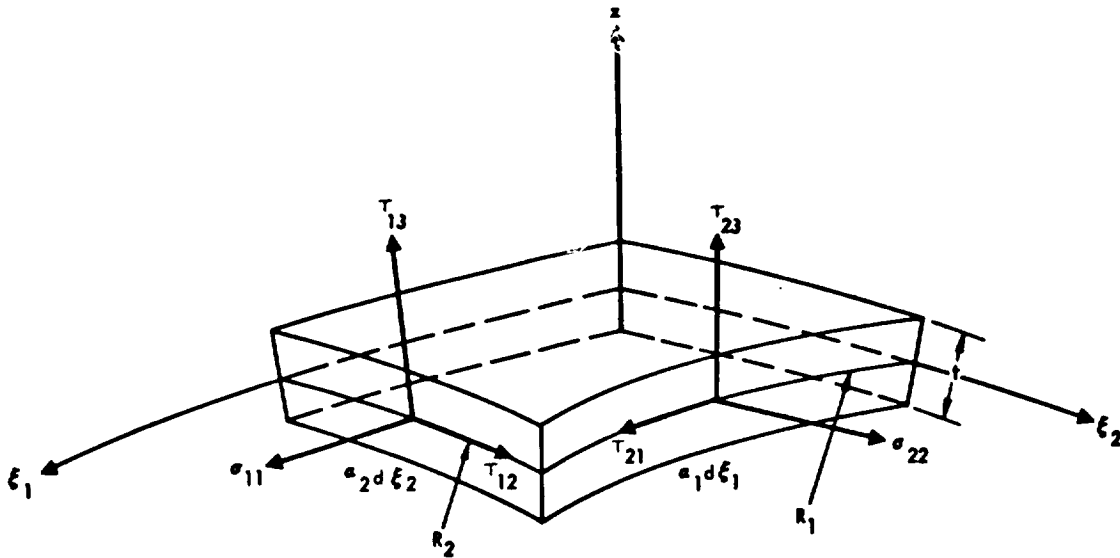


FIG. 1.12-10. Internal Stresses on a Shell Element

The internal stresses shown in this figure are described as follows:

σ_{11} , σ_{22} are normal stresses, acting on the faces of the element.

τ_{12} , τ_{21} are in-plane shear stresses acting parallel to the middle surface.

τ_{13} , τ_{23} are transverse shear stresses acting normal to the middle surface.

The positive directions of stresses are as shown in Fig. 1.12-10, i.e., normal stresses acting on the faces which coincide with positive directions are positive.

For purposes of obtaining a two-dimensional theory of shells, it will be convenient to introduce statically equivalent forces and bending moments instead of these stresses. The introduction of stress resultants and couples permits the elimination of the z coordinate in the equilibrium equations.

As an example, consider a simple linearly varying stress distribution acting on a face of an element of shell; this stress, which will be called σ_{11} , can be considered a combination of a uniform and bending type of stress distribution (Fig. 1.12-11).

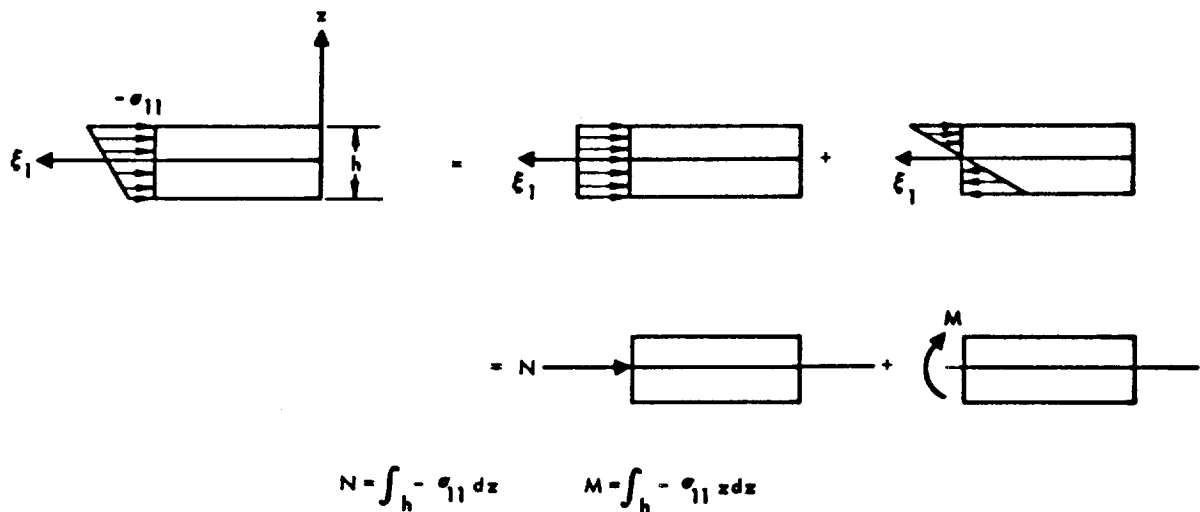


FIG. 1.12-11. Statically Equivalent Force System

The resultants (forces per unit length of given arc length) acting on a shell element with arc lengths on their principal lines of curvature,

($ds_1 = A_1 d\xi_1$ and $ds_2 = A_2 d\xi_2$), are for stresses σ_{11} , τ_{12} , τ_{13} , ... etc.,

$$\begin{aligned}
 N_1 &= \int_{-t/2}^{t/2} \sigma_{11} \left(1 + \frac{z}{R_2}\right) dz \\
 N_{12} &= \int_{-t/2}^{t/2} \tau_{12} \left(1 + \frac{z}{R_2}\right) dz \\
 Q_1 &= \int_{-t/2}^{t/2} \tau_{13} \left(1 + \frac{z}{R_2}\right) dz \\
 N_2 &= \int_{-t/2}^{t/2} \sigma_{22} \left(1 + \frac{z}{R_1}\right) dz \\
 N_{21} &= \int_{-t/2}^{t/2} \tau_{21} \left(1 + \frac{z}{R_1}\right) dz \\
 Q_2 &= \int_{-t/2}^{t/2} \tau_{23} \left(1 + \frac{z}{R_1}\right) dz
 \end{aligned}
 \tag{1. 12-8a}$$

and for the stress resultants for moments,

$$\begin{aligned}
 M_1 &= \int_{-t/2}^{t/2} z \sigma_{11} \left(1 + \frac{z}{R_2}\right) dz \\
 M_{12} &= \int_{-t/2}^{t/2} z \tau_{12} \left(1 + \frac{z}{R_2}\right) dz \\
 M_2 &= \int_{-t/2}^{t/2} z \sigma_{22} \left(1 + \frac{z}{R_1}\right) dz \\
 M_{21} &= \int_{-t/2}^{t/2} z \tau_{21} \left(1 + \frac{z}{R_1}\right) dz
 \end{aligned}
 \tag{1. 12-8b}$$

In the above expression, the term $\left(1 + \frac{z}{R}\right)$ is present to account for the trapezoidal shape of the shell element resulting from the curvature of the shell. Fig. 1.12-5 illustrates how an incremental portion of shell a distance z from the middle surface is augmented by an amount $\frac{z}{R}$.

By replacing the stresses by their equivalent forces and moments, one may, in the future, consider instead of the space element cut from the shell the corresponding element of the middle surface on the sides of which act these resultant forces and moments (Fig. 1.12-12).

The significance of the ten resultants so defined is suggested simply by the laws of statics, irrespective of material or of the state of deformation of elements in the shell.

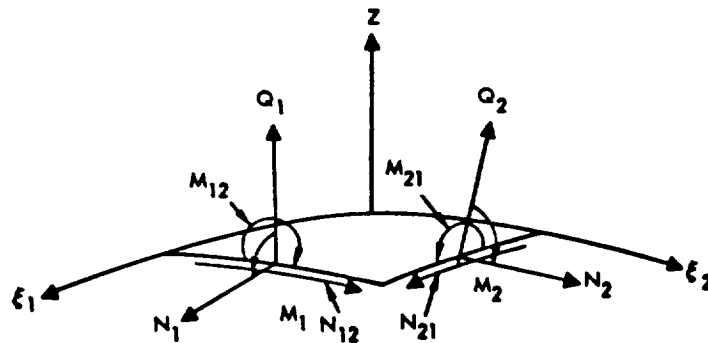


FIG. 1.12-12. Resultant Forces on a Typical Shell Element

1. 12. 4 Equilibrium Equations for a Shell

The shell element in the state of stress described in the previous section will now be considered and the conditions for its equilibrium under the influence of all external and internal loads will be determined. The equations arising by virtue of the demands of equilibrium and the compatibility of deformations will be derived by considering an individual differential element. These equations, therefore, are relations between differential quantities or between differential changes in the internal forces and, therefore, are called differential equations.

The external loads are comprised of body forces that act on the element and surface forces (stresses) that act on the upper and lower boundaries of the element, which are sections of the curved surfaces bounding the shell. The internal forces will be stress resultants acting on the faces of the shell element.

In the preceding section, all the internal stresses were transferred to the boundaries of the section of the middle surface corresponding to the considered element of the shell and they were replaced by statically equivalent forces and moments. An analogous operation for reducing the shell problem to a two-dimensional one can be executed for the external forces by replacing them by statically equivalent stresses distributed at the middle surfaces. The middle surface is thus loaded by forces as well as moments.

Now, instead of considering the equilibrium of an element of a shell one may study the equilibrium of the corresponding element of the middle surface. The stresses, in general, vary from point to point in the shell and as a result the stress resultants will also vary.

Consider now the stress resultants of concern applied to the middle surface of the shell as shown in Figs. 1.12-13 and 14.

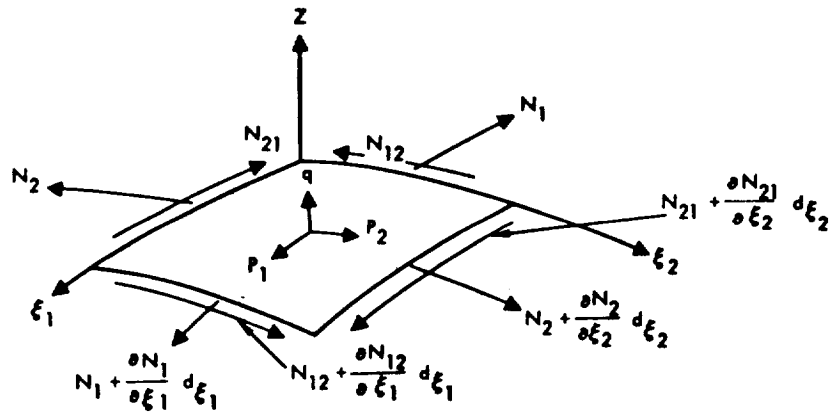


FIG. 1.12-13. Typical Shell Reference Element With Axial and In-Plane Shear Forces

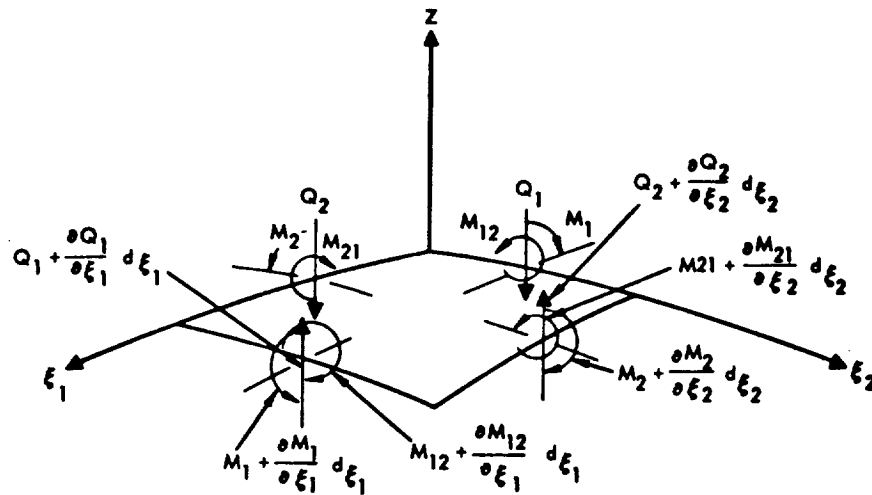


FIG. 1.12-14. Typical Shell Reference Element With Transverse Shear, Bending, and Twisting Elements

The equilibrium of the shell in the ξ_1 , ξ_2 , and z coordinate directions respectively are given by the following equations:

$$\begin{aligned} \frac{\partial \alpha_2 N_1}{\partial \xi_1} + \frac{\partial \alpha_1 N_{21}}{\partial \xi_2} + N_{12} \frac{\partial \alpha_1}{\partial \xi_2} - N_2 \frac{\partial \alpha_2}{\partial \xi_1} + Q_1 \frac{\alpha_1 \alpha_2}{R_1} + \alpha_1 \alpha_2 p_1 &= 0 \\ \frac{\partial \alpha_1 N_2}{\partial \xi_2} + \frac{\partial \alpha_2 N_{12}}{\partial \xi_1} + N_{21} \frac{\partial \alpha_2}{\partial \xi_1} - N_1 \frac{\partial \alpha_1}{\partial \xi_2} + Q_2 \frac{\alpha_1 \alpha_2}{R_2} + \alpha_1 \alpha_2 p_2 &= 0 \quad (1.12-9a) \\ \frac{\partial \alpha_2 Q_1}{\partial \xi_1} + \frac{\partial \alpha_1 Q_2}{\partial \xi_2} - \alpha_1 \alpha_2 \left(\frac{N_1}{R_1} + \frac{N_2}{R_2} \right) + \alpha_1 \alpha_2 q &= 0 \end{aligned}$$

where p_1 , p_2 , and q are components of the effective external force per unit area applied to the middle surface of the shell. (The details of obtaining the expressions for curvilinear coordinate systems can be found in Refs. 1-5, 1-9, and 1-11.)

The equilibrium of moments about the ξ_1 , ξ_2 , and z coordinates result in the following moment equilibrium expressions.

$$\begin{aligned} \frac{\partial \alpha_2}{\partial \xi_1} M_{12} + \frac{\partial \alpha_1}{\partial \xi_2} M_2 - M_1 \frac{\partial \alpha_1}{\partial \xi_2} + M_{21} \frac{\partial \alpha_2}{\partial \xi_1} - Q_2 \alpha_1 \alpha_2 &= 0 \\ \frac{\partial \alpha_1}{\partial \xi_2} M_{21} + \frac{\partial \alpha_2}{\partial \xi_1} M_1 - M_2 \frac{\partial \alpha_2}{\partial \xi_1} + M_{12} \frac{\partial \alpha_1}{\partial \xi_2} - Q_1 \alpha_1 \alpha_2 &= 0 \quad (1.12-9b) \\ N_{12} - N_{21} + \frac{M_{12}}{R_1} - \frac{M_{21}}{R_2} &= 0 \end{aligned}$$

The force components of the last equilibrium expression are due to warping of the faces and result from in-plane shears and twisting moments.

In the equilibrium equations presented here, changes in the dimensions and in the shape of the element of the middle surface arising from its deformation have been neglected. This simplification arises from the assumption of small deformations.

The form of the equilibrium equations is simplified when shells of revolution are considered. Examples of conical and spherical shells follow:

Example 1: Equilibrium Equations for a Cone

Noting Fig. 1.12-15, if the coordinate axes are expressed as

$$\xi_1 = x \quad \text{distance along generatrix}$$

$$\xi_2 = \theta \quad \text{angle between two meridians in the plane of a parallel}$$

$$z = z \quad \text{a direction normal to the middle surface formed by the other two coordinates}$$

and the Lamé parameters become

$$\alpha_1 = 1, \alpha_2 = R = R_0 + x \sin \alpha$$

the principal radii of curvatures of a cone are then expressed as

$$R_1 = R_\phi = \infty, R_2 = \frac{R}{\cos \alpha} = \frac{R_0}{\cos \alpha} + x \tan \alpha$$

where

$$\alpha = 1/2 \text{ apex angle and is constant}$$

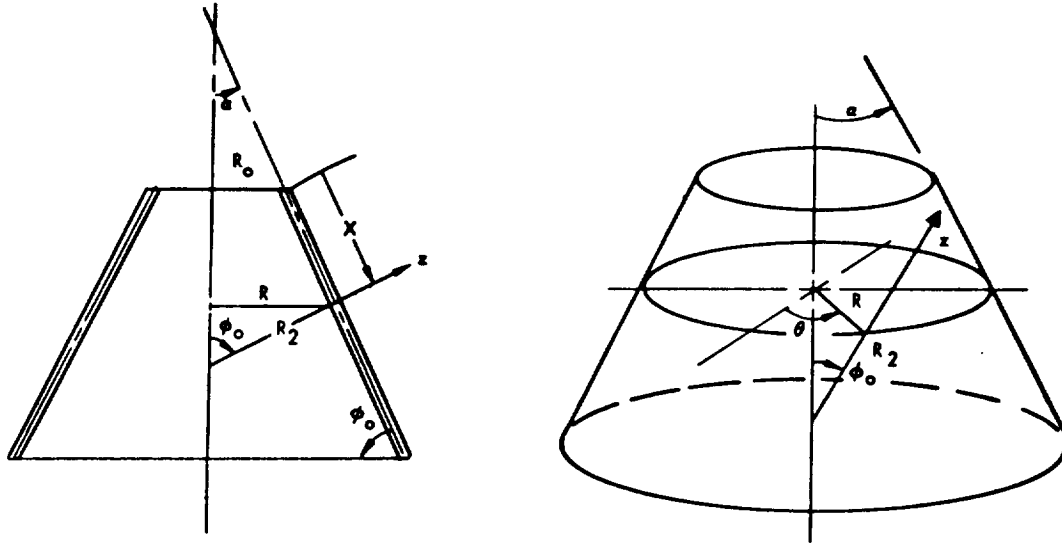


FIG. 1.12-15. Shell Coordinates for a Cone (or Cylinder with $\alpha = 0$)

By inserting the above coefficients into the general equilibrium equations we arrive at the equilibrium equations for a cone, namely

$$\begin{aligned} \frac{\partial}{\partial x} (N_{xx}) \sin \alpha + R_0 \frac{\partial}{\partial x} (N_x) - N_\theta \sin \alpha + \frac{\partial N_{\theta x}}{\partial \theta} + p_x R &= 0 \\ \frac{\partial N_\theta}{\partial \theta} + \frac{\partial}{\partial x} (N_{x\theta x}) \sin \alpha + R_0 \frac{\partial}{\partial x} (N_{x\theta}) + N_{\theta x} \sin \alpha + Q_\theta \cos \alpha + p_\theta R &= 0 \\ - N_\theta \cos \alpha + \frac{\partial Q_\theta}{\partial \theta} + \frac{\partial}{\partial x} (Q_{xx}) \sin \alpha + R_0 \frac{\partial}{\partial x} (Q_x) + q R &= 0 \end{aligned} \quad (1.12-10)$$

$$\frac{\partial M_\theta}{\partial \theta} + \frac{\partial}{\partial x} (M_{x\theta x}) \sin \alpha + R_0 \frac{\partial}{\partial x} (M_{x\theta}) + M_{\theta x} \sin \alpha - Q_\theta R = 0$$

$$\frac{\partial}{\partial x} (M_{xx}) \sin \alpha + R_0 \frac{\partial}{\partial x} (M_x) - M_\theta \sin \alpha + \frac{\partial M_{\theta x}}{\partial \theta} - Q_x R = 0$$

$$N_{x\theta} - N_{\theta x} - \frac{M_{\theta x}}{R} = 0$$

Eqs. 1.12-10 become the equilibrium equations for a cylindrical shell when the angle α is set equal to zero. In this case, R_0 represents the radius of curvature of the cylinder ($R_0 = R = R_2$).

Example 2. Equilibrium Equations for a Spherical Shell

If the coordinate axes were to be specified as

$\xi_1 = \phi$ an angle along a meridian of the shell

$\xi_2 = \theta$ an angle along the parallel of the shell

$z =$ a direction along the normal to the surface formed by the above two coordinates

the Lamé parameters become

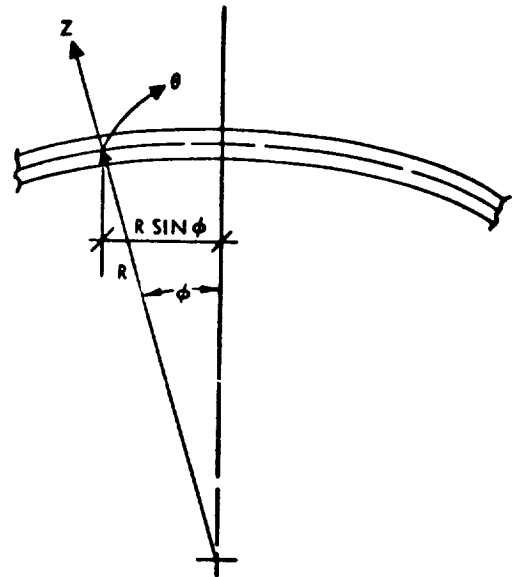
$$\alpha_1 = R, \quad \alpha_2 = R \sin \phi$$

where R is the radius of a sphere and the principal radii of curvature are

$$R_\phi = R_\theta = R = \text{const.}$$

then these coefficients may be inserted into the general thin shell equilibrium equations

(Eqs. 1.12-9a, b) and the differential equations for a sphere become:



$$\frac{\partial}{\partial \phi} (N_{\phi} \sin \phi) - N_{\theta} \cos \phi + \frac{\partial N_{\theta \phi}}{\partial \theta} + Q_{\phi} \sin \phi + R p_{\phi} \sin \phi = 0$$

$$\frac{\partial N_{\theta}}{\partial \theta} + \frac{\partial}{\partial \phi} (N_{\phi \theta} \sin \phi) + N_{\theta \phi} \cos \phi + Q_{\theta} \sin \phi + R p_{\theta} \sin \phi = 0$$

$$N_{\phi} \sin \phi + N_{\theta} \sin \phi - \frac{\partial Q_{\theta}}{\partial \theta} - \frac{\partial}{\partial \phi} (Q_{\phi} \sin \phi) - R q \sin \phi = 0 \quad (1.12-11)$$

$$\frac{\partial M_{\theta}}{\partial \theta} + \frac{\partial}{\partial \phi} (M_{\phi \theta} \sin \phi) + M_{\theta \phi} \cos \phi - Q_{\theta} R \sin \phi = 0$$

$$\frac{\partial}{\partial \phi} (M_{\phi} \sin \phi) - M_{\theta} \cos \phi + \frac{\partial M_{\phi \theta}}{\partial \phi} - Q_{\phi} R \sin \phi = 0$$

$$M_{\theta \phi} - M_{\phi \theta} + N_{\theta \phi} R - N_{\phi \theta} R = 0$$

1.12.5 Stress-Strain Relations

The relations derived in preceding sections were based upon purely geometrical or static considerations. The two concepts are tied together by consideration of material properties of the shell. For a complete description of the problem of analyzing thin shells, the relations between components of stress and components of strain as the shell is subjected to its history of applied loads is required. It will be assumed that a continuous body satisfies the generalized Hooke's Law, that is that stresses are linear functions of strains and thus the proportionality coefficients are constant for the range of materials under consideration. Materials which do not possess this linear law should be treated by a nonlinear theory of stress versus strain.

This section is devoted to a brief description of the basic ideas governing the relationships between stress and strain when considering anisotropic, orthotropic, and isotropic materials.

A. Anisotropic Bodies

In the general case of a uniform anisotropic body, i. e., a material body whose physical properties may vary in any direction, the generalized Hooke's Law expressed for a differential element in a curvilinear system of coordinates ξ_1, ξ_2, ξ_3 takes the form (Fig. 1.12-16):

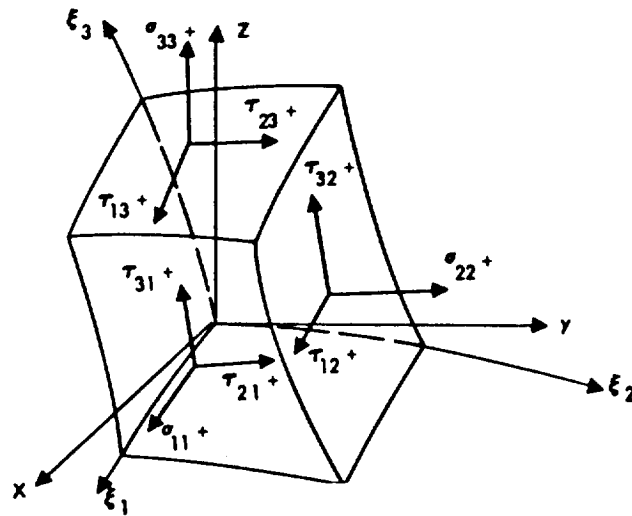


FIG. 1.12-16. Differential Element in a General Curvilinear Coordinate System

$$\begin{aligned}
 \sigma_{11} &= A_{11} \epsilon_1 + A_{12} \epsilon_2 + A_{13} \epsilon_3 + A_{14} \gamma_{23} + A_{15} \gamma_{13} + A_{16} \gamma_{12} \\
 \sigma_{22} &= A_{21} \epsilon_1 + A_{22} \epsilon_2 + A_{23} \epsilon_3 + A_{24} \gamma_{23} + A_{25} \gamma_{13} + A_{26} \gamma_{12} \\
 \sigma_{33} &= A_{31} \epsilon_1 + A_{32} \epsilon_2 + A_{33} \epsilon_3 + A_{34} \gamma_{23} + A_{35} \gamma_{13} + A_{36} \gamma_{12} \\
 \tau_{23} &= A_{41} \epsilon_1 + A_{42} \epsilon_2 + A_{43} \epsilon_3 + A_{44} \gamma_{23} + A_{45} \gamma_{13} + A_{46} \gamma_{12} \\
 \tau_{31} &= A_{51} \epsilon_1 + A_{52} \epsilon_2 + A_{53} \epsilon_3 + A_{54} \gamma_{23} + A_{55} \gamma_{13} + A_{56} \gamma_{12} \\
 \tau_{12} &= A_{61} \epsilon_1 + A_{62} \epsilon_2 + A_{63} \epsilon_3 + A_{64} \gamma_{23} + A_{65} \gamma_{13} + A_{66} \gamma_{12}
 \end{aligned}
 \tag{1.12-12}$$

As shown in Ref. 1-12, the 36 coefficients reduce to 21 when symmetry is noted; i. e., $A_{ij} = A_{ji}$ ($i, j = 1, 2, 3 \dots, 6$).

The inverse of Eq. 1.12-12 is possible if strains as a function of stresses are desired. The A_{ij} 's are material constants. Space and the very limited usefulness of such a general system prohibits enclosure of the coefficient definitions here. Of much more practical usage and applicability to the majority of shell problems is the consideration of materials where certain planes of elastic symmetry are present. For the more important cases, the generalized Hooke's relations of Eq. 1.12-12 or its inverse reduce to forms which are considerably simplified.

B. Orthotropic Bodies

If a solid body with three mutually perpendicular planes of symmetry is considered, then the body is said to be orthotropic. Materials such as wood and synthetic fiberboard possess this property. For this case, the generalized Hooke's Law reduces to

$$\begin{aligned}
 \sigma_{11} &= E_1 \epsilon_1 + E_2 \mu_{21} \epsilon_2 + E_3 \mu_{31} \epsilon_3 \\
 \sigma_{22} &= E_1 \mu_{12} \epsilon_1 + E_2 \epsilon_2 + E_3 \mu_{32} \epsilon_3 \\
 \sigma_{33} &= E_1 \mu_{13} \epsilon_1 + E_2 \mu_{23} \epsilon_2 + E_3 \epsilon_3 \\
 \tau_{23} &= G_{23} \gamma_{23}, \tau_{31} = G_{31} \gamma_{31}, \tau_{12} = G_{12} \gamma_{12}
 \end{aligned}
 \tag{1.12-13}$$

By virtue of symmetry, the coefficients are reduced to nine independent constants. The symmetry conditions are

$$E_2 \mu_{21} = E_1 \mu_{12}, E_3 \mu_{32} = E_2 \mu_{23}, E_1 \mu_{13} = E_3 \mu_{31}
 \tag{1.12-14}$$

C. Isotropic Bodies

Many bodies have elastic properties which do not vary with respect to orientation in the body. Metals such as steel and aluminum very closely resemble this property. Hooke's Law for this class of material is

$$\begin{aligned}\sigma_{11} &= 2 \bar{\mu} \epsilon_1 + \lambda e \\ \sigma_{22} &= 2 \bar{\mu} \epsilon_2 + \lambda e \\ \sigma_{33} &= 2 \bar{\mu} \epsilon_3 + \lambda e \\ \tau_{12} &= 2 \bar{\mu} \gamma_{12}, \quad \tau_{13} = 2 \bar{\mu} \gamma_{13}, \quad \tau_{23} = 2 \bar{\mu} \gamma_{23}\end{aligned}\tag{1.12-15}$$

where

$$\begin{aligned}\lambda &= \frac{\mu E}{(1 + \mu)(1 - 2\mu)} \\ \bar{\mu} &= \frac{E}{2(1 + \mu)} = G\end{aligned}\tag{1.12-16}$$

$$e = \epsilon_1 + \epsilon_2 + \epsilon_3$$

and E, G and μ are called the engineering technical constants. The number of independent elastic constants has been reduced to two.

For a plane stress problem, the stress-strain relations are given as follows:

$$\begin{aligned}\sigma_1 &= \frac{E}{1 - \mu^2} (\epsilon_1 + \mu \epsilon_2) \\ \sigma_2 &= \frac{E}{1 - \mu^2} (\epsilon_2 + \mu \epsilon_1) \\ \tau_{12} &= G \gamma_{12} = \frac{E}{2(1 + \mu)} \gamma_{12}\end{aligned}\tag{1.12-17}$$

for convenience, these simplified stress-strain relationships will be utilized freely in the subsequent developments.

1.13 CLASSIFICATION OF SHELL THEORIES

In the preceding sections the basic relations for shells were developed either from the law of statics or from purely geometrical considerations. As in the theory of elasticity, a relationship for connecting the geometric and static phenomena is presented by the introduction of a generalized Hooke's Law.

The physical hypothesis expressed by these relations is sufficient for the description of the state of deformation or stress in the shell. To be able to establish a connection between forces, moments, and deformation components of the middle surface it is necessary to know how either the stresses or strains vary across the shell thickness. This situation arises from attempts to reduce the shell problem from a three-dimensional elasticity problem to a two-dimensional one.

The essential problem in the development of a theory of shells; i. e., the formulation of appropriate constitutive relationships or stress-strain relationships, has now been determined. The problem can now be resolved to one of arbitrarily choosing quantities to represent the state of deformation in the shell. The introduction of certain assumptions permit the evaluation of stress resultant equations (Eqs. 1.12-8) in order that approximate relationships between force and deformations can be established.

The selection of the proper form of these approximations has been the subject of considerable controversy among the many investigators in the field. As a result, there is a large number of general and specialized thin shell theories in existence, developed within the framework of linear elasticity. It will be desirable in the subsequent discussion to discuss the most commonly encountered theories and classify them according to the assumptions for which they are based.

For the purpose of discussion, the various linear shell theories will be classified into five basic categories:

1. First-Order Approximation Shell Theory
2. Second-Order Approximation Shell Theory
3. Shear Deformation Shell Theory
4. Specialized Theories for Shells of Revolution
5. Membrane Shell Theory

The order of a particular approximate theory will be established by the order of the terms in the thickness coordinate that are retained in the strain and constitutive equations.

In the case of thin shells, the simplified bending theories of shells are (in general) based on Love's first-approximation and second-approximation shell theories. Although some theories do not adhere strictly to Love's original approximations, they can be considered as

modifications thereof and as either first- or second-order approximate theories. Theories which neglect transverse shear deformations may be distinguished from those which include the shear effect. Linear membrane theory is understood to be the limiting case corresponding to a zero-order approximation or momentless state. Under specialized shell theories are included several engineering theories that are usually restricted to particular shell shapes or types of loading (e. g. , shallow shell theory, Geckeler's approximation for symmetrically loaded shells, etc.)

Although the Shear Deformation and Specialized Shell Theories presented are based on Love's first-approximation; they are classified separately because of their particular physical significance.

1.13.1 First-Order Approximation Shell Theory

Love was the first investigator to present a successful approximate shell theory based on classical elasticity. To simplify the strain-displacement relationships and, consequently, the constitutive relations, Love (Ref. 1-3) introduced the following assumptions, known as first approximations and commonly termed the Kirchhoff-Love hypothesis:

1. The shell thickness, t , is negligibly small in comparison to the least radius of curvature, R_{\min} , of the middle surface;

i. e. $\frac{t}{R_{\min}} \ll 1$ (therefore, terms $\frac{z}{R} \ll 1$).

2. Linear elements normal to the unstrained middle surface remain straight during deformation and suffer no extensions.
3. Normals to the undeformed middle surface remain normal to the deformed middle surface.
4. The component of stress normal to the middle surface is small compared to other components of stress, and may be neglected in the stress-strain relationships.
5. Strains and displacements are small so that quantities containing second- and higher-order terms are neglected in comparison to first-order terms in the strain equations.

The last assumption is consistent with the formulation of the classical theory of linear elasticity. The other assumptions will be used to simplify the elasticity relations.

A. Strain-Displacement Relations

The Kirchhoff-Love assumptions outlined will now be used to simplify the strain Eq. 1.12-6 of linear elasticity presented earlier.

The inextensibility of normals from assumption (2) implies that the normal strain vanishes (i. e., from Eq. 1.12-6).

$$\epsilon_z = \frac{\partial W}{\partial z} = 0 \quad (1.13-18)$$

Utilizing this requirement, the deflection, W , is independent of the z coordinate.

Assumption (2) of Love's first approximation is analogous to Navier's hypothesis in elementary beam theory which requires that plane sections remain plane. Thus, displacements of a point on the shell can be expressed, as a first approximation, by relationships of the form

$$\begin{aligned}
 U &= u + z\beta_1 \\
 V &= v + z\beta_2 \\
 W &= w
 \end{aligned}
 \tag{1.13-19}$$

where u , v , and w are displacements of the middle (or reference) surface (i. e., $z = 0$) and β_1 , β_2 are rotations that represent changes of slope of the normal to the middle surface. It should be noted that terms u , v , w , β_1 , and β_2 are functions of coordinates ξ_1 , ξ_2 only. It can be seen that the displacement functions at any point in the shell can be described in terms of middle surface displacements, utilizing the linear relationships in the coordinate z previously described. Substituting the displacement relationships (Eq. 1.13-19) and Lamé parameter expressions (Eq. 1.12-3) into the general strain expressions (Eqs. 1.12-6 a, b, d) yields relationships for the shell in the form (Ref. 1-13):

$$\epsilon_1 = \frac{1}{1 + \frac{z}{R_1}} (\epsilon_1^0 + z \kappa_1)$$

$$\epsilon_2 = \frac{1}{1 + \frac{z}{R_2}} (\epsilon_2^0 + z \kappa_2) \quad (1.13-20)$$

$$\gamma_{12} = \frac{\gamma_1^0 + z \delta_1}{1 + \frac{z}{R_1}} + \frac{\gamma_2^0 + z \delta_2}{1 + \frac{z}{R_2}}$$

where

$$\epsilon_1^0 = \frac{1}{\alpha_1} \left(\frac{\partial u}{\partial \xi_1} + \frac{v}{\alpha_2} \frac{\partial \alpha_1}{\partial \xi_2} \right) + \frac{w}{R_1}; \quad \epsilon_2^0 = \frac{1}{\alpha_2} \left(\frac{\partial v}{\partial \xi_2} + \frac{u}{\alpha_1} \frac{\partial \alpha_2}{\partial \xi_1} \right) + \frac{w}{R_2} \quad (1.13-21)$$

are extensional strains at the middle surface and

$$\kappa_1 = \frac{1}{\alpha_1} \frac{\partial \beta_1}{\partial \xi_1} + \frac{\beta_2}{\alpha_1 \alpha_2} \frac{\partial \alpha_1}{\partial \xi_2}$$

$$\kappa_2 = \frac{1}{\alpha_2} \frac{\partial \beta_2}{\partial \xi_2} + \frac{\beta_1}{\alpha_1 \alpha_2} \frac{\partial \alpha_2}{\partial \xi_1}$$

(1.13-22a)

are changes in curvature of the middle surface directions ξ_1 , and ξ_2 , respectively.

Contributions γ_1^0 and γ_2^0 to the inplane shear strain and δ_1 , δ_2 to the rotation of the middle surface are given by

$$\gamma_1^o = \frac{1}{\alpha_1} \left(\frac{\partial v}{\partial \xi_1} - \frac{u}{\alpha_2} \frac{\partial \alpha_1}{\partial \xi_2} \right); \quad \gamma_2^o = \frac{1}{\alpha_2} \left(\frac{\partial u}{\partial \xi_2} - \frac{v}{\alpha_1} \frac{\partial \alpha_2}{\partial \xi_1} \right) \quad (1.13-22b)$$

$$\delta_1 = \frac{1}{\alpha_1} \left(\frac{\partial \beta_2}{\partial \xi_1} - \frac{\beta_1}{\alpha_2} \frac{\partial \alpha_1}{\partial \xi_2} \right); \quad \delta_2 = \frac{1}{\alpha_2} \left(\frac{\partial \beta_1}{\partial \xi_2} - \frac{\beta_2}{\alpha_1} \frac{\partial \alpha_2}{\partial \xi_1} \right) \quad (1.13-22c)$$

The validity of the second assumption in the case of thin shells follows from the small strain assumption. By this assumption is meant, any possible secondary displacements, over and above those derivable from a translation and a rotation of the original normal line, must have infinitesimal gradients which vanish at $z = 0$. The thinness condition requires that such secondary displacements cannot build up to noticeable values away from $z = 0$. (See Fig. 1-13-1.)

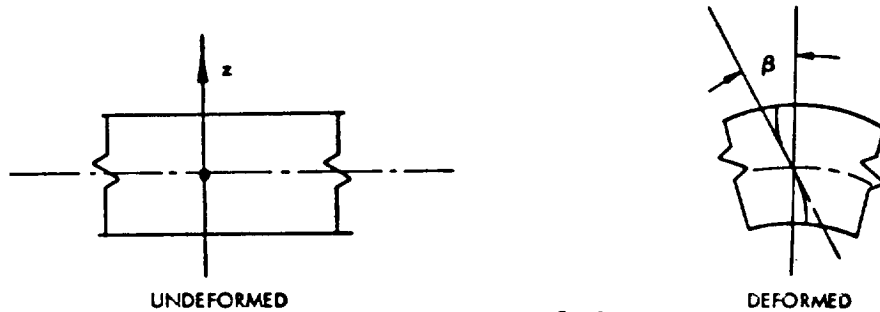


FIG. 1.13-1.

The strain equations (Eq. 1-12-6) are further simplified by assumption (3) which implies that transverse shear deformations are neglected. Consequently, normals to the middle plane not only remain straight but remain normal and suffer the same rotation as the middle surface. The angle change between the middle surface and normal is

given by the transverse shear strains, γ_{1z} , γ_{2z} (evaluated at $z = 0$). Since the angle between normal and middle surface does not change, the transverse shear deformations vanishes; therefore,

$$\gamma_{1z} = \frac{1}{1 + \frac{z}{R_1}} \left(\frac{1}{\alpha_1} \frac{\partial w}{\partial \xi_1} - \frac{u}{R_1} + \beta_1 \right) = 0 \quad (1.13-23)$$

$$\gamma_{2z} = \frac{1}{1 + \frac{z}{R_2}} \left(\frac{1}{\alpha_2} \frac{\partial w}{\partial \xi_2} - \frac{v}{R_2} + \beta_2 \right) = 0.$$

With this requirement, the rotation terms, β_1 , β_2 are now determinate and can be expressed in terms of displacement u , v , and w of the middle surface. These rotation expressions, upon evaluation of Eq 1.13-23 become

$$\beta_1 = \frac{u}{R_1} - \frac{1}{\alpha_1} \frac{\partial w}{\partial \xi_1} \quad (1.13-24)$$

$$\beta_2 = \frac{v}{R_2} - \frac{1}{\alpha_2} \frac{\partial w}{\partial \xi_2}$$

The degree of error introduced by this assumption naturally depends on the magnitude of the transverse shearing forces. For discontinuous loads and local areas around a shells edge, shear deformations may be comparable to bending and axial deformation, and cannot be ignored. Generally, however, shells with continuously distributed

surface forces, having flexibly supported edges, are usually assumed to have negligible transverse shear deformation.

When shear deformations cannot be neglected, the rotation terms cannot be expressed strictly in terms of displacements and the transverse shear strains must be included in the shell analysis. See Paragraph 1.13.3.

From the thinness assumption (1), terms $\frac{z}{R}$ are small in comparison with unity, and can be neglected in the strain and stress resultant expressions. Utilizing this assumption, the strains are distributed linearly across the thickness of the shell. For this case, from Eq. 1.13-20, the in-plane strain expressions reduce to

$$\begin{aligned}\epsilon_1 &= \epsilon_1^0 + z \kappa_1 \\ \epsilon_2 &= \epsilon_2^0 + z \kappa_2\end{aligned}\tag{1.13-25}$$

$$\gamma_{12} = \gamma_{12}^0 + z \kappa_{12}$$

where the shear strain, γ_{12}^0 , of the middle surface from Eq. 1.13-22b is given by

$$\gamma_{12}^0 = \gamma_1^0 + \gamma_2^0 = \frac{1}{\alpha_1} \left(\frac{\partial v}{\partial \xi_1} - \frac{u}{\alpha_2} \frac{\partial \alpha_1}{\partial \xi_2} \right) + \frac{1}{\alpha_2} \left(\frac{\partial u}{\partial \xi_2} - \frac{v}{\alpha_1} \frac{\partial \alpha_2}{\partial \xi_1} \right)\tag{1.13-26a}$$

and the twisting distortion, κ_{12} , is described by

$$\kappa_{12} = \delta_1 + \delta_2 = \frac{1}{\alpha_1} \left(\frac{\partial \beta_2}{\partial \xi_1} - \frac{\beta_1}{\alpha_2} \frac{\partial \alpha_1}{\partial \xi_2} \right) + \frac{1}{\alpha_2} \left(\frac{\partial \beta_1}{\partial \xi_2} - \frac{\beta_2}{\alpha_1} \frac{\partial \alpha_2}{\partial \xi_1} \right) \quad (1.13-26b)$$

The above are the kinematical relationships for Love's first approximation, where middle surface strains (ϵ_1^0 , ϵ_2^0 , γ_{12}^0) and measures of bending distortion (κ_1 , κ_2 , κ_{12}) are given by Eqs. 1.13-21, 22a, and 26.

Love's equation for (κ_{12}) leads to inconsistencies in that strains do not vanish for small rigid body rotations. Other versions of these equations have been proposed by Novozhilov, (Ref. 1-5) Sanders, (Ref. 1-14), and others. This inconsistency vanishes for axisymmetrically loaded shells of revolution. It should be pointed out that from Love's first approximation, the strain equations include terms up to the first order in the thickness coordinate. Thus, the distribution of strains is linear across the thickness.

B. Constitutive Relationships (Stress—Strain Equations)

Utilizing the strain equations developed in the previous section together with the fourth assumption, it is now possible to describe the constitutive or stress—strain relations of Love's first approximation theory.

Assumption (4) is based not on geometry but on the statics of the problem. An order of magnitude consideration of the equilibrium equations for stresses shows that, unless the surface loads are highly

concentrated, the traverse normal stress, σ_z , is generally of smaller order of magnitude than the in-plane stresses σ_1 , and σ_2 . Consequently, it is conventional to neglect the term involving σ_z in the general stress strain relationships. For simplicity, consider isotropic material behavior. In this case, the stress-strain relationships corresponding to a plane stress condition are given by (Eq. 1.13-27),

$$\begin{aligned}\sigma_1 &= \frac{E}{1-\mu^2} [\epsilon_1 + \mu \epsilon_2] \\ \sigma_2 &= \frac{E}{1-\mu^2} [\epsilon_2 + \mu \epsilon_1] \\ \tau_{12} &= \frac{E}{2(1+\mu)} \gamma_{12}\end{aligned}\tag{1.13-27}$$

From assumption (2) it is assumed that $\epsilon_z = 0$. A theory which includes the two hypotheses $\sigma_z = 0$ and $\epsilon_z = 0$ would lead to a contradiction (as pointed out in Ref. 1-15).

This difficulty is usually avoided by neglecting σ_z in the stress strain relationships and then determining ϵ_z from the resulting expressions. To remove the resultant inconsistency, it would be necessary to correct the original assumption for W by the addition of terms which are linear and quadratic in z . (See Naghdi Ref. 1-13.) If no boundary layers, of width on the order of thickness t , are present these additional terms are small in comparison with the leading term, W .

Thus, to obtain a first approximation theory the additional terms may be neglected in introducing W into the expressions for strains ϵ_1 , ϵ_2 , and γ_{12} .

Utilizing these assumptions, the appropriate stress strain or constitutive relations can be determined. The thinness assumption that terms $\frac{z}{R}$ can be neglected in comparison with unity permits simplification of the stress resultants note (Eq. 1.12-8a, b)

$$N_1 = \int_{-t/2}^{t/2} \sigma_1 dz, \quad N_2 = \int_{-t/2}^{t/2} \sigma_2 dz, \quad \dots \text{etc.} \quad (1.13-28)$$

In this case, $N_{12} = N_{21}$ and $M_{12} = M_{21}$. Thus, the number of resultants reduce to eight.

For an isotropic shell, utilizing Eqs. 1.13-25, 27, and 28, the following constitutive equations are obtained relating stress resultants and couples to components of strain

$$N_1 = \frac{Et}{1 - \mu^2} \left[\epsilon_1^0 + \mu \epsilon_2^0 \right]$$

$$N_2 = \frac{Et}{1 - \mu^2} \left[\epsilon_2^0 + \mu \epsilon_1^0 \right]$$

$$N_{12} = N_{21} = \frac{Et}{2(1 + \mu)} \gamma_{12}^0$$

$$M_1 = D \left[\kappa_1 + \mu \kappa_2 \right] \quad (1.13-29)$$

$$M_2 = D \left[\kappa_2 + \mu \kappa_1 \right] \quad (1.13-29 \text{ cont})$$

$$M_{12} = M_{21} = \frac{1 - \mu}{2} D \kappa_{12}$$

where

$$D = \frac{Et^3}{12(1 - \mu^2)}$$

and where (middle surface) strains $(\epsilon_1^0, \epsilon_2^0, \gamma_{12}^0)$ are given in equations 1.13-21 and 26a and change in curvature and twist terms $(\kappa_1, \kappa_2, \kappa_{12})$ are given in Eqs. 1.13-22a and 1.13-26b.

C. Shell Equilibrium Equations

The constitutive relations described in the previous section together with the shell equilibrium equations define the state of deformation of thin walls. The number of equilibrium equations necessary for consideration in Love's theory can be reduced from six to three by the assumption that shear deformations are to be neglected. The reasoning for this is described in statements that follow.

It is essential to note that in assuming normals remain normal the shear displacements corresponding to the stresses τ_{13}, τ_{23} are

neglected. Thus it might be thought that one should neglect shear forces Q_1 , Q_2 , and consequently assume that the shearing forces are zero. However, this is not correct, since the shear forces play an essential role in the equilibrium equations. The hypothesis which requires normals to remain normal is one applied to determine the law of deformation of a shell parallel to the middle surface. In the development of the equilibrium equations this condition is not used. In this case, the shear forces Q_1 , Q_2 cannot be determined from stress resultant expressions but are instead determined from consideration of the equilibrium Eq. 1.12-9b. Substituting the resulting expressions for Q_1 and Q_2 into the first three equilibrium equations (Eq. 1.13-9a) yields:

$$\begin{aligned} & \frac{\partial \alpha_2 N_1}{\partial \xi_1} + \frac{\partial \alpha_1 N_{21}}{\partial \xi_2} + N_{12} \frac{\partial \alpha_1}{\partial \xi_2} - N_2 \frac{\partial \alpha_2}{\partial \xi_1} + \frac{\partial \alpha_2 M_1}{R_1 \partial \xi_1} + \\ & \frac{\partial \alpha_1 M_{21}}{R_1 \partial \xi_1} - \frac{M_1}{R_1} \frac{\partial \alpha_2}{\partial \xi_2} + \frac{M_{12}}{R_1} \frac{\partial \alpha_1}{\partial \xi_2} + \alpha_1 \alpha_2 P_1 = 0 \\ & \frac{\partial \alpha_1 N_2}{\partial \xi_2} + \frac{\partial \alpha_2}{\partial \xi_1} N_{12} + N_{21} \frac{\partial \alpha_2}{\partial \xi_1} - N_1 \frac{\partial \alpha_1}{\partial \xi_2} + \frac{\partial \alpha_2 M_{12}}{R_2 \partial \xi_1} + \\ & \frac{\partial \alpha_1 M_2}{R_2 \partial \xi_2} - \frac{M_1}{R_2} \frac{\partial \alpha_1}{\partial \xi_2} + \frac{M_{21}}{R_2} \frac{\partial \alpha_2}{\partial \xi_1} + \alpha_1 \alpha_2 P_2 = 0 \end{aligned} \tag{1.13-30}$$

$$\begin{aligned}
& \frac{\partial}{\partial \xi_1} \left[\frac{1}{\alpha_1} \left(\frac{\partial \alpha_1 M_{21}}{\partial \xi_2} + \frac{\partial \alpha_2 M_{12}}{\partial \xi_1} - M_2 \frac{\partial \alpha_2}{\partial \xi_1} + M_{12} \frac{\partial \alpha_1}{\partial \xi_2} \right) \right] + \\
& \frac{\partial}{\partial \xi_2} \left[\frac{1}{\alpha_2} \left(\frac{\partial \alpha_2 M_{12}}{\partial \xi_1} + \frac{\partial \alpha_1 M_{21}}{\partial \xi_2} - M_1 \frac{\partial \alpha_1}{\partial \xi_2} + \right. \right. \\
& \left. \left. M_{21} \frac{\partial \alpha_2}{\partial \xi_1} \right) \right] - N_1 \frac{\alpha_1 \alpha_2}{R_1} - N_2 \frac{\alpha_1 \alpha_2}{R_2} + \alpha_1 \alpha_2 q = 0
\end{aligned} \tag{1.13-30 cont}$$

It is worthwhile to note that the substitution of Eq. 1.13-29 into the general equilibrium equations (Eq. 1.12-9) do not identically satisfy these relationships. In the usual derivation of the equations of Love's first approximation theory, the distinction between N_{12} and N_{21} and between M_{12} and M_{21} is dropped and the last of equation (Eq. 1.12-9b) is suppressed. (See Ref. 1-16.)

In a straightforward manner, the substitution of the force-displacement relations (Eqs. 1.13-21, 22, 24, and 29) into the equilibrium Eq. 1.13-30 transforms these equations into three simultaneous partial differential equations for the three middle surface displacements u , v , w . Hence, the solution of these equations determines the deformed position of the shell from which repeated use of the elastic relations also determines the internal forces.

D. Boundary Conditions

The equations describing Love's first approximation theory naturally, as yet, do not completely determine the state of stress in a shell and, hence, do not have solutions as long as they are subject to boundary conditions (i. e., until a certain number of relations between forces, moments, displacements or functions of these quantities at the supporting edge of the shell are specified).

In prescribing boundary conditions for approximate theories, consideration must be given to the interdependence of the assumed force and moment resultants.

On each edge of a shell element (Fig. 1. 12-12) five different resultants have been defined. However, for theories which assume zero transverse shear strains, only four conditions are required to be prescribed on a boundary in order to ensure a solution. This requirement comes about due to the fact that in neglecting shear strains the first approximation theory yields an eight order set of field equations which requires four boundary conditions at each boundary.

The five resultants are reduced to four by noting that the distribution of twisting moments across an edge is statically equivalent to a

distribution of shear forces. This leads to shell boundary conditions corresponding to the Kirchhoff boundary conditions for a flat plate. Love has derived the required shell edge conditions for an arbitrary boundary curve. For an edge $\xi_1 = \text{a constant}$, the conditions that must be specified are that either

$$\begin{aligned}
 & N_\phi \text{ or } u \\
 & Q_1 - \frac{M_{12}}{R_2} \text{ or } v \\
 & Q_2 - \frac{\partial M_{21}}{A_2 \partial \xi_2} \text{ or } w
 \end{aligned}
 \tag{1.13-31}$$

$$M_2 \text{ or } \frac{\partial w}{\partial \phi} \text{ are prescribed.}$$

(Note the restrictions, i. e., N and u for instance cannot be used simultaneously.)

The above boundary conditions apply to Love's approximation theories. The modification of these when considering shear deformation will be discussed later.

E. Remarks on First-Order Shell Theory

The theory presented was first given by Love (Ref. 1-2) and is referred to as Love's first approximation theory. It will be classified as a first order theory because the strain Eq. 1.13-25 and constitutive relationships,

Eq. 1.13-29, include terms up to the first order in the thickness coordinate z . This approach will offer a convenient way for classification of shell theories.

Reissner in Ref. 1-11 presented a straightforward derivation of Love's theory. Since then Sanders (Ref. 1-14) has developed an improved form of the first approximation theory. Sanders selected a more realistic set of strain displacement relations in that all strains vanish for small rigid body rotations of the shell whereas for Love's theory they do not. The equilibrium equations of Sanders are similar to Eq. 1.12-9 with modified forms for the in-plane force and twisting moment expressions. A tensor formulation of Sanders first order linear shell theory is given in Ref. 1-17. Sander's modified theory has removed some of the inconsistencies in Love's theory. However, it is generally believed (Ref. 1-5) that Love's formulation of the problem contains all the essential facts necessary for the treatment of practical problems in their shells, as long as special conditions do not require inclusion of the effect of transverse shear and normal stresses.

Practically speaking, the solution of the simultaneous differential equations of Love's theory is possible only in rare cases or with additional approximations. In the case of a loaded structure, the general solution of

the nonhomogeneous differential equations consists of a particular solution of the nonhomogeneous differential equation and the general solution of the homogeneous differential equations. In the case of an unloaded structure the solution consists of only the general solution of the homogeneous differential equation.

The nonhomogeneous solution of Love's equation, to a first approximation, equals the solution of the corresponding extensional (pure membrane) problem. The homogeneous solution is a self equilibrating system of stress resultants which satisfy compatibility conditions at the edges of the shell ("edge effect") and in other regions of discontinuity. The general solution is generally of the mixed type, involving both boundary and middle plane stresses, but for some problems, such as a shell under concentrated loads, the homogeneous solution may be assumed to be of the inextensional type.

Thus, there are two extreme cases possible within the first approximation; (1) the inextensional or pure bending case in which middle plane strains are neglected compared to flexural strains and (2) the extensional or membrane case in which only middle plane strains are considered. The general or mixed case lies between these two extremes. The significance of this is discussed in Chapter 2.00 on practical analysis of shells.

1.13.2 Second-Order Approximation Shell Theories

Several writers (Flügge, Ref. 1-18; Bryne, Ref. 1-19; Biezeno, Ref. 1-20, etc.) have attempted to improve on Love's first approximation theory by retaining $\frac{z}{R}$ terms in the strains and stresses resultants (Eqs. 1.13-20 and 1.12-8).

The basic procedure used by these investigators has been to expand the denominators in the strain equations (Eq. 1.13-20) in terms of power series expansions. For example,

$$\frac{1}{1 + \frac{z}{R_1}} = 1 - \frac{z}{R_1} + \frac{z^2}{R_1^2}$$

Utilizing these expansions, the strain equations can be expressed in power series of z , retaining second-order terms in z ; the in-plane strains can be written as

$$\begin{aligned} \epsilon_1 &= \epsilon_1^0 + z \left(\kappa_1 - \frac{\epsilon_1^0}{R_1} \right) + \frac{z^2}{R_1} \left(\kappa_1 - \frac{\epsilon_1^0}{R_1} \right) \\ \epsilon_2 &= \epsilon_2^0 + z \left(\kappa_2 - \frac{\epsilon_2^0}{R_2} \right) + \frac{z^2}{R_2} \left(\kappa_2 - \frac{\epsilon_2^0}{R_2} \right) \\ \gamma_{12} &= \gamma_1^0 + z (\delta_1 - \gamma_1^0) + \frac{z^2}{R_1} \left(\frac{\gamma_1^0}{R_1} - \delta_1 \right) + \gamma_2^0 \\ &\quad + z \left(\delta_2 - \frac{\gamma_2^0}{R_2} \right) + \frac{z^2}{R_2} \left(\frac{\gamma_2^0}{R_2} - \delta_2 \right) \end{aligned} \tag{1.13-32}$$

If these expressions are substituted into the stress resultant expressions, retaining second-order terms in z , the constitutive equations (Eq. 1.13-29) are replaced by

$$\begin{aligned}
 N_{11} &= \frac{Et}{1-\mu^2} \left[(\epsilon_1^o + \mu\epsilon_2^o) - \frac{t^2}{12} \left(\frac{1}{R_1} - \frac{1}{R_2} \right) \left(\kappa_1 - \frac{\epsilon_1^o}{R_1} \right) \right] \\
 N_{22} &= \frac{Et}{1-\mu^2} \left[(\epsilon_2^o + \mu\epsilon_1^o) - \frac{t^2}{12} \left(\frac{1}{R_2} - \frac{1}{R_1} \right) \left(\kappa_2 - \frac{\epsilon_2^o}{R_2} \right) \right] \\
 N_{12} &= Gt \left[\gamma_{12}^o - \frac{t^2}{12} \left(\frac{1}{R_1} - \frac{1}{R_2} \right) \left(\kappa_{12} - \frac{\gamma_{12}^o}{R_1} \right) \right] \\
 N_{21} &= Gt \left[\gamma_{12}^o - \frac{t^2}{12} \left(\frac{1}{R_2} - \frac{1}{R_1} \right) \left(\kappa_{12} - \frac{\gamma_{12}^o}{R_2} \right) \right] \quad (1.13-33) \\
 M_{11} &= \frac{Et^3}{12(1-\mu^2)} \left[(\kappa_1 + \mu\kappa_2) - \left(\frac{1}{R_1} - \frac{1}{R_2} \right) \epsilon_1^o \right] \\
 M_{22} &= \frac{Et^3}{12(1-\mu^2)} \left[(\kappa_2 + \mu\kappa_1) - \left(\frac{1}{R_2} - \frac{1}{R_1} \right) \epsilon_2^o \right] \\
 M_{12} &= \frac{Gt^3}{12} \left[\tau - \left(\frac{1}{R_1} - \frac{1}{R_2} \right) \gamma_1^o \right] \\
 M_{21} &= \frac{Gt^3}{12} \left[\tau - \left(\frac{1}{R_2} - \frac{1}{R_1} \right) \gamma_2^o \right]
 \end{aligned}$$

where

$$2\kappa_{12} = \tau + \frac{\gamma_2^o}{R_1} + \frac{\gamma_1^o}{R_2}$$

The preceding equations are characteristic of the Flügge-Byrne theory. They are identical in form to the results obtained by Luré (Ref. 1-21) as described by Novozhilov (Ref. 1-5). The form of the stress resultants in this case identically satisfies the sixth equilibrium equation. (See Novozhilov, Ref. 1-5.)

Application of the Flügge-Byrne equations has generally been restricted to circular cylindrical shapes for which solutions have been obtained by Flügge (Ref. 1-18) and Kempner (Ref. 1-22).

It is important to note that although explicit use was not made of the assumption $\frac{z}{R} \ll 1$, such an assumption is implicit in these equations inasmuch as Eq. 1.13-32 are reasonable approximations only if $z \ll R$, since they can be considered as truncations of the Taylor series expansions. In addition, although the results are elegant, the retention of small terms in the wall thickness leads to relations that contain terms of the same order of magnitude as would also be obtained if less basic restrictive assumptions were made (e. g., if normal stress effects were included, see Ref 1-13, 15).

Comparing these formulas with Eq. 1.13-29, it is seen that they are considerably more cumbersome, and it is clear from the preceding discussion that these additional terms introduce corrections into the theory which do not exceed the accuracy of the initial assumptions.

Hence, these formulas are regarded as inconsistent and, for shells of arbitrary form, introduce quite unnecessary complications.

From this discussion, it is apparent that although this theory contains second-order terms in the thickness coordinate, it essentially offers a first-order approximate theory. However, because in the strain and constitutive relationships, second-order terms in z are retained, this theory, according to our classification, is a second approximation.

Love attempted to improve on his first approximation by introducing three types of corrections. In his second approximation, Love states that such modifications are unnecessary unless flexural strains ($z\kappa_1, z\kappa_2, z\kappa_{12}$) are large in comparison with extensional strains ($\epsilon_1^0, \epsilon_2^0, \gamma_{12}^0$). In the problem of highly curved shells the shell thickness can no longer be considered small in relation to the radius of curvature. Thus, higher-order terms are required in the strain equations. Love attempted to improve his first approximation by retaining second-order terms in the strain equations in a manner as previously described in this section. However, in relaxing restrictions on $\frac{t}{R}$ ratios, Love realized that the corresponding displacements are no longer negligible. By considering the second-order effects of such normal displacements, the strain components parallel to the middle surface are nonlinearly

distributed or, as before, terms up to and including the second power in the thickness coordinate are retained. This description essentially gives the characteristic difference between Love's first and second approximate theories. This classification can be used to categorize many of the various shell theories.

In his second approximation, Love considered, as a first modification, the transverse displacement (Eq. 1.13-19) to be expressed in a more flexible form

$$W = w + \tilde{w}(\xi_1, \xi_2, z) \quad (1.13-34)$$

The second modification consists in not neglecting $\frac{z}{R}$ with respect to unity but assuming

$$\frac{1}{1 + \frac{z}{R_1}} \approx 1 - \frac{z}{R_1} \quad (1.13-35)$$

These modifications, together with additional approximations as described in Ref. 1-15, were used by Love to obtain the following expressions for strains

$$\begin{aligned} \epsilon_1 &= \epsilon_1^0 + \left(z - \frac{z^2}{R_1} \right) \kappa_1 + \frac{\tilde{w}}{R_1} \\ \epsilon_2 &= \epsilon_2^0 + \left(z - \frac{z^2}{R_2} \right) \kappa_2 + \frac{\tilde{w}}{R_2} \end{aligned} \quad (1.13-36)$$

and

$$\bar{w} = \frac{\mu_z E}{(1 - \mu) E_z} \left[z (\epsilon_1^0 + \epsilon_2^0) + \frac{1}{2} z^2 (\kappa_1 + \kappa_2) \right] \quad (1.13-37)$$

From a third modification, the stress σ_z is not neglected in the stress strain equations. Using these approximations, the constitutive equations become

$$\begin{aligned} N_{11} = & \frac{Et}{1 - \mu^2} \left\{ (\epsilon_1^0 + \mu \epsilon_2^0) - \frac{t^2}{12} \left(\frac{1}{R_1} - \frac{1}{R_2} \right) \kappa_1 \right. \\ & - \frac{t^2}{12} \frac{\mu_z E}{(1 - \mu) E_z} \left[\left(\frac{1}{R_1} + \frac{\mu}{R_2} \right) (\kappa_1 + \kappa_2) \right. \\ & \left. \left. + \frac{\kappa_1 + \mu \kappa_2}{R_1} + \frac{\kappa_2 + \mu \kappa_1}{R_2} \right] \right\} \quad (1.13-38) \end{aligned}$$

together with an analogous expression for N_{22} .

A comparison of Eq. 1.13-38 with the first equation of Eq. 1.13-33 shows that similar terms are present in both (except that $\frac{\epsilon_1^0}{R_1}$ terms are neglected). More important, however, is the fact that new terms are introduced as a result of including the partial effect of normal stress. Furthermore, these terms do not vanish when $R_1 = R_2$. It also should be noted that no consideration has been given the possible effects of transverse shear strains.

As can be seen, Love's second approximation contains some degree of refinements over the first approximation.

It is characteristic of second approximation theories that strains and constitutive relations contain second-order terms in the thickness coordinate, z . Another second approximate theory of significance was developed by Vlasov (Ref. 1-16) in considering a thick shell.

Other refinements to shell theories have been presented by Bassett (Ref. 1-23), Trefftz (Ref. 1-24), and others (e. g., Ref. 1-15).

1. 13. 3 Shear Deformation Shell Theories

In the development of Love's first and second approximation theories in the previous paragraphs, the effects of transverse shear deformations were neglected. This neglect resulted because of the geometrical assumptions that normals remain normal. It is possible that for some loads or shell configurations, the transverse shear strains can no longer be neglected and, therefore, these effects must be included in the theory. A shear deformation theory for shells will be developed in the following paragraphs.

It will be necessary in the subsequent development to refer to equations presented in Paragraph 1. 12. 4. Paragraph 1. 13. 1 A, Strain-Displacement Relations, indicates that, from the assumption of normals remaining normal, the rotations could be expressed in terms of

displacements u , v , w , and their derivatives. When the effects of shear deformations are included, the shear strains (Eq. 1.13-23) no longer vanish and, as a result, the rotation expressions are no longer determinate. The rotation expressions must be considered as unknown variables. Since the shear stresses are no longer considered negligible, the shear forces are expressed by

$$Q_1 = \int_{-\frac{t}{2}}^{\frac{t}{2}} \tau_{1z} dz$$

$$Q_2 = \int_{-\frac{t}{2}}^{\frac{t}{2}} \tau_{2z} dz$$

(1.13-39)

where, for simplicity, the terms $(1 + \frac{z}{R})$ have been approximated by unity. This assumption is not necessary for the inclusion of shear deformation effects. Therefore, shear deformation theories can be classified as first- or second-order approximations, depending on whether terms are neglected or retained in the strain and constitutive equations.

Since the shear forces are now related to deformations, they cannot be eliminated from equilibrium equations as was

done in Paragraph 1.12.4. Thus, when shear effects are included, the following five equilibrium equations must be considered

$$\frac{\partial \alpha_2 N_1}{\partial \xi_1} + \frac{\partial \alpha_1 N_{21}}{\partial \xi_2} + N_{12} \frac{\partial \alpha_1}{\partial \xi_2} - N_2 \frac{\partial \alpha_2}{\partial \xi_1} + Q_1 \frac{\alpha_1 \alpha_2}{R_1} + \alpha_1 \alpha_2 P_1 = 0$$

$$\frac{\partial \alpha_1 N_2}{\partial \xi_2} + \frac{\partial \alpha_2 N_{12}}{\partial \xi_1} + N_{21} \frac{\partial \alpha_2}{\partial \xi_1} - N_1 \frac{\partial \alpha_1}{\partial \xi_2} + Q_2 \frac{\alpha_1 \alpha_2}{R_2} + \alpha_1 \alpha_2 P_2 = 0$$

$$\frac{\partial \alpha_2 Q_1}{\partial \xi_1} + \frac{\partial \alpha_1 Q_2}{\partial \xi_2} - N_1 \frac{\alpha_1 \alpha_2}{R_1} - N_2 \frac{\alpha_1 \alpha_2}{R_2} + \alpha_1 \alpha_2 q = 0 \quad (1.13-40)$$

$$\frac{\partial \alpha_2 M_{12}}{\partial \xi_1} + \frac{\partial \alpha_1 M_2}{\partial \xi_2} - M_1 \frac{\partial \alpha_1}{\partial \xi_2} + M_{21} \frac{\partial \alpha_2}{\partial \xi_1} - Q_2 \alpha_1 \alpha_2 = 0$$

$$\frac{\partial \alpha_1 M_{21}}{\partial \xi_2} + \frac{\partial \alpha_2 M_1}{\partial \xi_1} - M_2 \frac{\partial \alpha_2}{\partial \xi_2} + M_{12} \frac{\partial \alpha_1}{\partial \xi_2} - Q_1 \alpha_1 \alpha_2 = 0$$

For these equations, five boundary conditions are necessary at each boundary. It is not necessary to use the Kirchhoff hypothesis to obtain an equivalent shear condition as was done previously. The boundary conditions in this case become:

N_1 or u

U_2 or v

M_1 or β_1

M_2 or β_2

Q or w

Reissner (Ref. 1-25) was one of the first investigators to incorporate the effects of shear deformation in plate theory. The extension to shells is presented by Hildebrand, et al. (Ref. 1-15). Many investigators have attempted to improve upon shear deformation described in Ref. 1-15. For example, Naghdi (Ref. 1-13).

1.13.4 Specialized Theories for Shells of Revolution

The bending shell theories previously presented can be simplified considerably for specialized conditions of geometry and loading. In this section, some of the simplified shell theories resulting from consideration of shells of revolution of specific geometry will be presented. These theories are based on Love's first approximation; however, for purposes of illustration they are classified separately to better illustrate the assumptions introduced.

In this section, the simplified shell equations are presented for shells of particular interest. Included are the Reissner-Meissner equations, Geckeler's approximations, shallow-shell theory, Donnell's theory, and others.

A. General Shells of Revolution Axisymmetrically Loaded

Love's first approximation equations for a general shell of revolution are obtained by inserting the geometric parameters from

Eq. 1.12-5 into relationships developed in section 1.13. For the particular case of axisymmetric deformations, the displacement V is zero, and all derivatives of displacement components with respect to θ vanish. In this case, middle surface strain-displacement Eqs. 1.13-21 and 1.13-26a reduce to

$$\epsilon_1^o = \epsilon_\phi^o = \frac{1}{R_1} \frac{du}{d\phi} + \frac{w}{R_1} \quad (1.13-41a)$$

$$\epsilon_2^o = \epsilon_\theta^o = \frac{u \cot\phi}{R_1} + \frac{u dR_2}{R_1 R_2 d\phi} + \frac{w}{R_2}$$

$$\gamma_{12}^o = \gamma_{\phi\theta}^o = 0$$

and the curvature (Eq. 1.13-22a) and twist (Eq. 1.13-26b) expressions become

$$\kappa_1 = \kappa_\phi = -\frac{1}{R_1} \frac{d}{d\phi} \left(\frac{1}{R_1} \frac{dw}{d\phi} - \frac{u}{R_1} \right)$$

$$\kappa_2 = \kappa_\theta = -\frac{1}{R_1^2} \left[\cot\phi + \frac{1}{R_2} \frac{dR_2}{d\phi} \right] \left[\frac{dw}{d\phi} - u \right] \quad (1.13-41b)$$

$$\kappa_{12} = \kappa_{\phi\theta} = 0$$

For a general surface of revolution, the expressions $\frac{dR}{d\phi}$ and $\frac{dR_2}{d\phi}$ are as follows for $R = R_2 \sin \phi$

$$\frac{dR}{d\phi} = R_1 \cos \phi \quad (1.13-42)$$

$$\frac{dR_2}{d\phi} = (R_1 - R_2) \cot \phi$$

Inserting the above values of derivatives into Eq. 1.13-41 yields

$$\epsilon_2 = \frac{u \cot \phi}{R_2} + \frac{w}{R_2} \quad (1.13-43)$$

$$\kappa_2 = - \frac{\cot \phi}{R_1 R_2} \left[\frac{dw}{d\phi} - u \right]$$

while the remaining strain-displacement equations of 1.13-41 are unchanged. Consequently, the resultant forces $N_{\phi\theta}$, Q_θ , and moments $M_{\phi\theta}$ vanish and the equilibrium relations from Eq. 1.12-9 become

$$\frac{d(N_\phi R)}{d\phi} - N_\theta R_1 \cos \phi + Q_\phi R + R_1 R p = 0$$

$$\frac{d(Q_\phi R)}{d\phi} - N_\phi R_1 - N_\theta R_1 \sin \phi + R_1 R q = 0 \quad (1.13-44)$$

$$\frac{d(M_\phi R)}{d\phi} - M_\theta R_1 \cos \phi - R_1 R Q_\phi = 0$$

where the second, fourth, and sixth equations of Eq. 1.12-9 have been identically satisfied.

The above relations are identical with those shown by Timoshenko (Ref. 1-26). By eliminating Q_ϕ between the first and last equilibrium equations and determining the force resultants from Eq. 1.13-29, -42 and -43, two second order ordinary differential equations in the two unknown displacement components u and w are obtained. Rather than obtain equations in this manner, however, a transformation of dependent variables can be performed leading to a more manageable pair of equations which, for shells of constant meridional curvature and constant thickness, combine into a single fourth order equation solvable in terms of a hypergeometric series. Historically (Ref. 1-4), transformation of variables was first introduced by H. Reissner (Ref. 1-27) for spherical shells and then generalized to all shells of constant thickness and constant meridional curvature by E. Meissner (Ref. 1-28). Meissner (Ref. 1-29) shows that the equations for a general shell of revolution are transformable to Reissner-Meissner type equations provided the thickness t and the radius R_1 both vary in a way to satisfy a certain relationship for all values of ϕ , (the "Meissner condition.")

The transformation to the Reissner-Meissner equations is accomplished by introducing, as new variables, the angular rotation

$$\tilde{V} = \frac{1}{R_1} \left(u - \frac{dw}{d\phi} \right) \quad (1.13-45)$$

and the quantity

$$\tilde{U} = R_2 \Omega_\phi$$

This substitution of variables leads to two second order differential equations in \tilde{U} and \tilde{V} replacing the corresponding two equations in u and w . The details of this transformation are illustrated in Ref. 1-26.

For shells of constant thickness and constant meridional curvature or, in fact, for any shell of revolution satisfying the Meissner condition, the transformed pair of equations can be combined into a single fourth order equation, the solution of which is determined from the solution of a second order complex equation. For shells of the above description, the shell equations can be represented in the simplified form

$$L \left(\tilde{U} + \frac{\mu}{R_1} \tilde{U} \right) = Et\tilde{V} \quad (1.13-46)$$

$$L(\tilde{V}) - \frac{\mu}{R_1} \tilde{V} = -\frac{\tilde{U}}{D}$$

where the operator

$$L(\) = \frac{R_2}{R_1^2} \frac{d^2(\)}{d\phi^2} + \frac{1}{R_1} \left[\frac{d}{d\phi} \left(\frac{R_2}{R_1} \right) + \frac{R_2}{R_1} \cot\phi \right] \frac{d(\)}{d\phi} - \frac{R_1 \cot^2\phi}{R_2 R_1} \quad (1.13-47)$$

From the above system of two simultaneous differential equations of second order an equation of fourth order is obtained for each unknown. Following operations described in Ref. 1-26 yields an equation of the form

$$LL(U) + \Gamma^4 U = 0 \quad (1.13-48)$$

where

$$\Gamma^4 = \frac{Et}{D} - \frac{\mu^2}{R_1^2} \quad (1.13-49)$$

The solution of the fourth order equation can be considered the solution of two second order complex equations of the form

$$L(\tilde{U}) \pm i\Gamma^2 \tilde{U} = 0 \quad (1.13-50)$$

Reissner-Meissner type equations are the most convenient and widely employed forms of the first approximation theory for axisymmetrically loaded shells of revolution. They follow exactly from the relations of Love's first approximation when the meridional curvature and thickness are constant, as they are for cylindrical, conical,

spherical, and toroidal shells of uniform thickness. Furthermore, they follow directly from Love's equations in the more general case, provided special restraints on the variation of thickness and geometry are satisfied.

Using the modified Reissner-Meissner equations (Ref. 1-30), toroidal shells of constant thickness were investigated by Clark (Ref. 1-31) and ellipsoidal shells of constant thickness by Naghdi and DeSilva (Ref. 1-32). In the latter case, the Meissner-type condition, which would require the radius R_1 to be constant, is obviously not satisfied. However, it was shown that assuming the Meissner condition to be satisfied was indeed a justifiable approximation for ellipsoidal shells. A version of the Reissner-Meissner equations including the effects of transverse shear distortion has been presented by Naghdi (Ref. 1-33).

B. Spherical Shells

The general case of an arbitrarily loaded spherical shell is considered by Love in the classical manner, employing expansions of the displacement components into Fourier series (Ref. 1-3). Novozhilov (Ref. 1-5) introduces complex force resultants into the equilibrium equations of the shell to solve the problem.

For axisymmetrically loaded spherical shells of constant thickness, the variable \bar{U} becomes equal to RQ_ϕ and the Reissner-Meissner equations reduce to form (Ref. 1-26)

$$\frac{d^2 Q_\phi}{d\phi^2} + \cot\phi \frac{dQ_\phi}{d\phi} - (\cot^2\phi - \mu) Q_\phi - Et\bar{V} = 0 \quad (1.13-51)$$

$$\frac{d^2 \bar{V}}{d\phi^2} + \cot\phi \frac{d\bar{V}}{d\phi} - (\cot^2\phi + \mu) \bar{V} + \frac{R^2 Q_\phi}{D} = 0$$

The homogeneous form of the equations, omitting all surface forces, is given above. It is assumed that the nonhomogeneous solution corresponds to the pure membrane case for the first approximation.

Eq. 1.13-51 can be reduced to a single fourth order equation in Q_ϕ and it leads to the solution of a second order hypergeometric equation (Ref. 1-26). Eq. 1.13-51 can also be solved by methods of asymptotic integration (Ref. 1-34).

Two simplified versions of the Reissner-Meissner equations are of engineering interest, namely Geckeler's approximation (Ref. 1-35) for nonshallow spherical shells and the Esslinger approximation for shallow shells (Ref. 1-36).

As described in Ref. 1-37, the fourth order equation obtained by the elimination of \bar{V} between Eq. 1.13-51 is

$$\frac{d^4 Q_\phi}{d\phi^4} + A_3 \frac{d^3 Q_\phi}{d\phi^3} + A_2 \frac{d^2 Q_\phi}{d\phi^2} + A_1 \frac{dQ_\phi}{d\phi} + A_0 Q_\phi + 4\lambda^4 Q_\phi = 0 \quad (1.13-52)$$

where

$$A_0 = 1 - 3 \csc^4 \phi - \mu^2$$

$$A_1 = \cot \phi (2 + 3 \csc^2 \phi)$$

$$A_2 = 1 - 3 \csc^2 \phi$$

$$A_3 = 2 \cot \phi$$

and $\lambda^4 = 3(1 - \mu^2) \frac{R^2}{t}$

In the Geckeler approximation, all terms except the first and last in Eq. 1.13-52 are neglected, leaving

$$\frac{d^4 Q_\phi}{d\phi^4} + 4\lambda^4 Q_\phi = 0 \quad (1.13-53)$$

Geckeler's Eq. 1.13-53 is seen to be the same form of equation as for the beam on an elastic foundation.

This approximation is valid for large values of λ and high angles ϕ ; that is, for thin, nonshallow spherical shells. This can be seen from the fact that Q_ϕ is a rapidly damped function of the form $e^{-\lambda\phi}$, so that its fourth derivative is of the order $\lambda^4 Q_\phi$, while the lesser derivatives are of correspondingly lower order. Since the

coefficients A_0, \dots, A_3 are small for high angles ϕ , all the terms involving these coefficients are lower than order $\lambda^3 Q_\phi$ and therefore, for large λ , are negligible compared to the λ^4 terms. The approximation is particularly good in the vicinity of $\phi = 90^\circ$, for at that value $A_3 = 0$ and only terms of order $\lambda^2 Q_\phi$ are neglected relative to $\lambda^4 Q_\phi$. The Geckeler approximation is, however, considered to be sufficiently accurate down to angles as low as $\phi = 20^\circ$ (Ref. 1-38).

A slightly more accurate approximation for nonshallow shells presented by Blumenthal (Ref. 1-39) is based on the introduction of the transformation

$$\bar{Q}_\phi = Q_\phi \sqrt{\sin \phi} \quad (1.13-54)$$

into Eq. 1.13-52. Following similar order of magnitude approximations, an equation of form similar to Eq. 1.13-53 results by replacing Q_ϕ by \bar{Q}_ϕ (Eq. 1.13-54). Complete solutions of the approximate equations were given by Hetenyi (Ref. 1-40).

For small angles ϕ , Reissner-Meissner Eqs. 1.13-51 or 52 can be approximated by making the usual small angle assumption that $\sin \phi \approx \phi$ and $\cos \phi \approx 1$, a simplification considered in detail by Esslinger (Ref. 1-36). The angle being small, only the highest power of $(1/\phi)$ is retained in each coefficient of Eq. 1.13-52, i. e.,

$$A_0 \approx -\frac{3}{\phi^4}$$

$$A_1 \approx -\frac{3}{\phi^3}$$

$$A_2 \approx -\frac{3}{\phi^2}$$

$$A_3 \approx \frac{2}{\phi}$$

and Eq. 1.13-52 becomes

$$\frac{d^4 Q_\phi}{d\phi^4} + \frac{2}{\phi} \frac{d^3 Q_\phi}{d\phi^3} - \frac{3}{\phi^2} \frac{d^2 Q_\phi}{d\phi^2} + \frac{3}{\phi^3} \frac{dQ_\phi}{d\phi} - \frac{3}{\phi^4} Q_\phi + 4\lambda^4 Q_\phi = 0 \quad (1.13-55)$$

which may be rewritten as

$$\left[\frac{d^2(\)}{d\phi^2} + \frac{1}{\phi} \frac{d(\)}{d\phi} - \frac{1}{\phi^2} \right] \left[\frac{d^2 Q_\phi}{d\phi^2} + \frac{1}{\phi} \frac{dQ_\phi}{d\phi} - \frac{1}{\phi^2} Q_\phi \right] + 4\lambda^4 Q_\phi = 0 \quad (1.13-56)$$

This equation can be solved by solving the following second-order equation:

$$\frac{d^2 Q_\phi}{d\phi^2} + \frac{1}{\phi} \frac{dQ_\phi}{d\phi} - \frac{1}{\phi^2} Q_\phi \pm 2i\lambda^2 Q_\phi = 0 \quad (1.13-57)$$

The general solution of Eq. 1.13-57 can be found in Ref. 1-26.

Particular applications of both the Geckeler and Esslinger approximations are considered in Chapter 2.00. Since each approximation is a limiting version of the Reissner-Meissner equations, a

measure of their relative accuracy at a particular angle ϕ can be obtained by inserting solutions of approximate Eqs. 1.13-53 and -57 into true Eq. 1.13-51.

The approximate versions of the Reissner-Meissner equations considered above for spherical shells can be generalized for arbitrary shell shapes by returning to the variables $U = R_2 Q_\phi$ and writing λ in its general form

$$\lambda^4 = 3(1 - \mu^2) \frac{R_1^4}{R_2^2 t^2} \quad (1.13-58)$$

Solutions of the approximate equations can be obtained by considering λ to be constant over short segments of the shell (Refs. 1-26 and 1-41).

C. Shallow Spherical Caps

An approximate form of the Reissner-Meissner equations were presented in the previous section for the analysis of shallow spherical

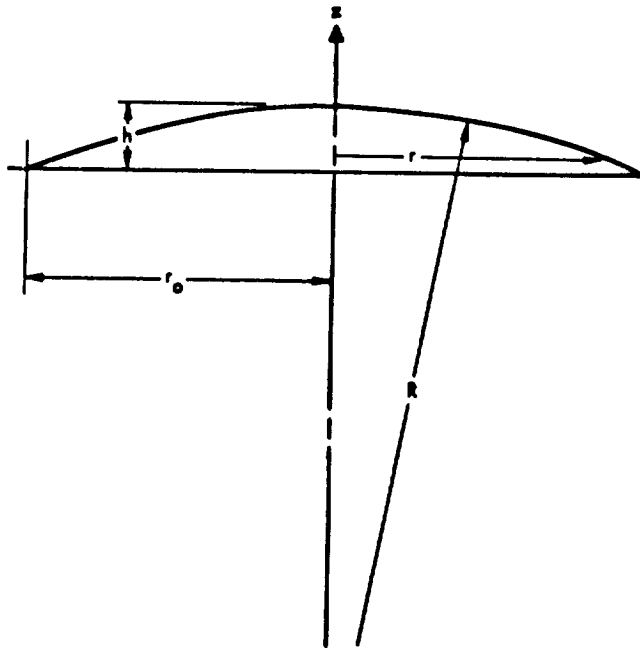


FIG. 1.13-2

segments. Reissner (Ref. 1-42) derived and obtained solutions for a more exact set of equations for spherical caps. The criteria for shallowness of a spherical shell segment used by Reissner is that if the ratio of height to base diameter is less than say 1/8. The

analysis is applicable to shells that are not shallow when the stresses are effectively restricted to a shallow zone.

The differential equations can be obtained from Eq. 1.13-40 by substitution of the quantities

$$\begin{aligned}
 \xi_1 &= r \\
 \xi_2 &= \theta \\
 \alpha_1 &= 1 \\
 \alpha_2 &= r \\
 R_1 &= R_2 = R = \text{Const.}
 \end{aligned}
 \tag{1.13-59}$$

The strains of the middle surface are obtained from Eqs. 1.13-21, -22, and -26 by the appropriate substitution of the above identities. If the effects of transverse shear distortion are neglected and, from the geometry of shallow shells it is assumed that $\frac{U}{R}, \frac{V}{R} \ll 1$, then the bending strains are given by

$$\begin{aligned}
 \kappa_r &= -\frac{\partial^2 w}{\partial r^2} \\
 \kappa_\theta &= -\frac{1}{r^2} \frac{\partial^2 w}{\partial \theta^2} - \frac{1}{r} \frac{\partial w}{\partial r} \\
 \kappa_{r\theta} &= -2 \frac{\partial}{\partial r} \left(\frac{1}{r} \frac{\partial w}{\partial \theta} \right)
 \end{aligned}
 \tag{1.13-60}$$

The bending distortion expressions are the same as in the theory of plates.

The observation can be made that for shallow shells the effect of transverse shear terms Q_1, Q_2 in the two equations of force

equilibrium (Eq. 1.13-40) in the meridional and circumferential directions are negligible. Proceeding on this assumption, these two equations reduce to the equilibrium equations of plane stress.

As in the theory of plane stress from elasticity, these equations may be satisfied by means of a stress function F which is obtained by setting

$$N_{\theta} = \frac{\partial^2 F}{\partial r^2}$$

$$N_r = \frac{1}{r} \frac{\partial F}{\partial r} + \frac{1}{r^2} \frac{\partial^2 F}{\partial \theta^2} \quad (1.13-61)$$

$$N_{r\theta} = - \frac{\partial}{\partial r} \left(\frac{1}{r} \frac{\partial F}{\partial \theta} \right)$$

For convenience, the load potential has been neglected. The complete expressions are given in Ref. 1-42.

As in the theory of plane stress, a differential equation for F can be obtained by utilizing the appropriate compatibility condition, which results in an expression of the form

$$\nabla^2 \nabla^2 F - \frac{tE}{R} \nabla^2 w = 0 \quad (1.13-62)$$

where

$$\nabla^2 = \frac{\partial^2}{\partial r^2} + \frac{1}{r} \frac{\partial}{\partial r} + \frac{1}{r^2} \frac{\partial^2}{\partial \theta^2}$$

The second differential equation involving F and w is obtained by substitution of the moment equilibrium equations (Eq. 1.12-9b) into the transverse force equilibrium equation. This gives a second fundamental equation

$$D \nabla^2 \nabla^2 w + \frac{1}{R} \nabla^2 F = 0 \quad (1.13-63)$$

For the case of rotationally symmetric bending of shells, exact solutions for the above equations can be obtained in terms of Thomson-Kelvin functions (Ref. 1-42). Naghdi (Ref. 1-33) presented a similar set of shallow spherical shell equations for the case when the effects of transverse shear deformations are included.

D. Circular Cylindrical Shells

For the case of circular cylindrical shells arbitrarily loaded, two first approximate theories are of prime importance; Love's first approximation theory and its simplified version due to Donnell.

For cylindrical shells, $\alpha_1 = 1$, $\alpha_2 = R$, $R_1 = \infty$, $R_2 = R$ are set with coordinate axes (s, θ) measured along the generator of the cylinder and the circumferential direction, respectively.

Substitution of these results into the strain displacement equations yields

$$\epsilon_1 = \frac{\partial u}{\partial x}$$

$$\epsilon_2 = \frac{1}{R} \frac{\partial v}{\partial \theta} + \frac{w}{R}$$

$$\gamma_{12} = \frac{\partial v}{\partial x} + \frac{1}{R} \frac{\partial u}{\partial \theta}$$

$$\kappa_1 = -\frac{\partial^2 w}{\partial x^2}$$

(1.13-64)

$$\kappa_2 = -\frac{1}{R^2} \frac{\partial^2 w}{\partial \theta^2} + \frac{1}{R^2} \frac{\partial v}{\partial \theta}$$

$$\kappa_{12} = -\frac{2}{R} \frac{\partial^2 w}{\partial x \partial \theta} + \frac{1}{R} \frac{\partial v}{\partial x}$$

The equilibrium equations become

$$\frac{\partial N_x}{\partial x} + \frac{1}{R} \frac{\partial N_{x\theta}}{\partial \theta} + p_x = 0$$

$$\frac{1}{R} \frac{\partial N_\theta}{\partial \theta} + \frac{\partial N_{x\theta}}{\partial x} + \frac{Q_\theta}{R} + p_\theta = 0$$

$$\frac{\partial Q_x}{\partial x} + \frac{1}{R} \frac{\partial Q_\theta}{\partial \theta} - \frac{N_\theta}{R} + q = 0$$

(1.13-65)

$$\frac{1}{R} \frac{\partial M_\theta}{\partial \theta} + \frac{\partial M_{x\theta}}{\partial x} - Q_\theta = 0$$

$$\frac{\partial M_x}{\partial x} + \frac{1}{R} \frac{\partial M_{x\theta}}{\partial \theta} - Q_x = 0$$

The final system of three partial differential equations in the three displacement components are obtained by eliminating Q_x and Q_θ from equilibrium Eq. 1.13-65 and inserting the force-displacement relations obtained using Eq. 1.13-64. The resulting three equations contain certain terms which higher approximation theories have shown to be negligible. It is therefore permissible to simplify the equations by omitting such terms, as shown by Timoshenko (Ref. 1-26). Solutions to these Love-Timoshenko equations are also presented in Ref. 1-26 for particular problems of unsymmetrically loaded circular cylinders.

For the case of axisymmetrically loaded circular cylinders, Love's Eqs. 1.13-64 and -65 readily reduce to

$$\epsilon_1 = \frac{du}{dx}, \quad \epsilon_2 = \frac{w}{R}, \quad \kappa_1 = -\frac{d^2w}{dx^2} \quad (1.13-66)$$

$$\gamma_{12} = \kappa_2 = \kappa_{12} = 0$$

and

$$\begin{aligned} \frac{dN_x}{dx} + q_x &= 0 \\ \frac{dQ_x}{dx} - \frac{N_\theta}{R} + q &= 0 \\ \frac{dM_x}{dx} - Q_x &= 0 \end{aligned} \quad (1.13-67)$$

If only pressure is considered, $P_x = 0$ and $q = p$, and the above equations lead to a single fourth order equation in w . For a constant thickness shell the equation is (Ref. 1-26)

$$\frac{d^4 w}{dx^4} + 4\beta^4 w = \frac{P}{D} \quad (1.13-68)$$

where

$$\beta^4 = \frac{3(1 - \mu^2)}{R^2 t^2}, \quad D = \frac{Et^3}{12(1 - \mu^2)}$$

Eq. 1.13-68 is identical to that for a beam on an elastic foundation. Particular solutions are given in Refs. 1-26 and 1-43, and are summarized in Chapter 2.00.

Donnell simplified the strain displacement relations (Eq. 1.13-64) by ignoring the influence of the original shell curvature on the deformations due to bending and twisting moments. The change in hoop curvature and the change in twist thus become

$$\kappa_2 = \frac{1}{R^2} \frac{\partial^2 w}{\partial \theta^2}, \quad \kappa_{12} = -\frac{2}{R} \frac{\partial^2 w}{\partial \theta \partial x} \quad (1.13-69)$$

while the remainder of expressions (Eq. 1.13-64) are unchanged. By this approximation the relations between moments and change in curvature and twist become the same as for flat plates. A similar simplification was made in the previous section for shallow spherical shells.

Following Donnell's approximation, the terms $\frac{Q_\theta}{R}$ are also neglected in the second equilibrium equations so that the first two equations reduce in form to the corresponding equations of plane stress. A stress function F is defined for cylindrical coordinates as

$$N_x = \frac{\partial^2 F}{\partial s^2}, \quad N_s = \frac{\partial^2 F}{\partial x^2}; \quad N_{xs} = -\frac{\partial^2 F}{\partial x \partial s} \quad (1.13-70)$$

where

$$\frac{\partial}{\partial s} = \frac{1}{R} \frac{\partial}{\partial \theta}$$

and the compatibility expression is obtained as

$$\nabla^4 F = \frac{Et}{R} \frac{d^2 w}{dx^2} \quad (1.13-71)$$

Following a similar procedure to that described in the last section for shallow spherical caps, the equilibrium equations become

$$D \nabla^4 w + \frac{1}{R} \frac{\partial^2 F}{\partial x^2} - q = 0 \quad (1.13-72)$$

Elimination of the function F between the two equations above yields an eighth order partial differential equation in w of the form

$$\nabla^8 w + \frac{Et}{DR^2} \frac{\partial^4 w}{\partial x^4} = \frac{1}{D} \nabla^4 q \quad (1.13-73)$$

which is known as Donnell's linear theory (Ref. 1-44). A slightly more complex form of the above equation was obtained by Naghdi (Ref. 1-33)

when transverse shear distortion was considered. Donnell also proposed a simplified version of cylinder stability equations in the expanded form of the above equations. The details of this will be discussed in the section on shell stability.

E. Second-Order Approximation Theories for Shells of Revolution

The second order approximation theory of Flügge (Ref. 1-18) and Byrne (Ref. 1-19) retain the $\frac{z}{R}$ terms in comparison to unity in the stress resultant equations and in the strain-displacement relations. Flügge-Byrne type equations for a general shell are discussed by Kempner (Ref. 1-22) who obtains them as a special case of a unified thin-shell theory. Applications of this second approximation theory have generally been restricted to circular cylindrical shapes, for which case solutions are obtained in Refs. 1-19 and 1-45. In the latter reference, the Flügge-Byrne type equations are considered as a standard against which simplified first approximation theories are compared.

Second order approximation equations are derived by Vlasov (Ref. 1-16) directly from the general three-dimensional linear elasticity equations for a thick shell. The assumption $\epsilon_z = \gamma_{\phi z} = \gamma_{\phi \theta} = 0$ is made, and the remaining strains are represented by the first three terms of their series expansion. The assumption of zero normal strain as well as

zero transverse shear strains permits a rapid transition from the three-dimensional theory to the two-dimensional equations of shell theory, but it should not be interpreted in its strict sense as implying a state of plane strain. Rather, it is a convenient assumption equivalent to the basic Kirchhoff-Love hypothesis that normal lines remain normal and their extensions are negligible. An excellent discussion of this assumption is given by Novozhilov (Ref. 1-5).

1.13.5 Membrane Theory of Shells

The shell theories studied in the previous sections are generally referred to as "bending" theories of shells because this development includes the consideration of the flexural behavior of shells. If, in the study of equilibrium of a shell, all moment expressions are neglected, the resulting theory is the so-called "membrane" theory of shells.

A shell can be considered to act as a membrane if flexural strains are zero or negligible compared to direct axial strains. It is apparent that two types of shells comply with this definition of a membrane: (1) shells that lose stiffness sufficiently so that it is physically incapable of resisting bending, or (2) shells that are flexurally stiff but loaded and supported in a manner that avoids the introduction of bending strains. The state of stress in a membrane is referred to as a "momentless" state of stress. For an absolutely flexible shell, since it offers no

resistance to bending, only a momentless state of stress is possible. For shells with finite stiffness, such a state of stress is only one of the possible stress conditions and for a momentless state, several supplementary conditions relating to the shape of the shell, character of load applied, and support of its edges must be fulfilled.

Due to small thicknesses, shells badly adapt themselves to bending so that relatively small bending moments generate considerable stresses and deflections. Therefore, the pure bending stress condition is to be avoided and is technically disadvantageous to shells. The momentless state of stress condition is a desirable feature in the design of shell structures because it offers the advantage of uniform utilization of the strength capabilities of the shell material, in most cases using less material and, thus, resulting in less weight. The study of membrane theory is considerably simpler than the bending theory and, for this reason, historically preceded the latter theory. The first contributions to membrane theory were furnished by Lamé and Clapeyron early in the 19th century. These works considered symmetrical loading on shells of revolution. On the assumption that no moments could exist in the shell, the loading could only produce normal forces. On this basis, the calculation of the shell could be "statically

determined" (i. e., the analysis could be performed solely with the help of the force equilibrium equations without the need of the deformation relations).

The equilibrium equations for membrane theory are summarized in the following paragraph. These equations are based on the assumption of small deflections, and follow directly from the zero-ordered approximation to the linear theory of shells.

A. Equilibrium Equations

The equations of membrane theory can be obtained directly from the equations of general shell theory (Eq. 1.12-9). Since membrane theory, according to our classification of shells, represents a zero-ordered approximation, the strains are assumed to be uniform across the shell thickness and from Eq. 1-13-20 we find that

$$\begin{aligned}\epsilon_1 &= \epsilon_1^0 \\ \epsilon_2 &= \epsilon_2^0 \\ \gamma_{12} &= \gamma_{12}^0\end{aligned}\tag{1.13-74}$$

where it is noticed that curvature and rotation terms are neglected.

Accordingly, it is assumed that, although the shell may be resistant to bending, in view of the smallness of curvature and rotation, the moment terms in the equations of equilibrium for the shell element are unimportant. Therefore, from the consideration of Eq. 1.13-29,

$$M_1 = M_2 = M_{12} = 0 \quad (1.13-75)$$

which implies the neglect of transverse shear forces from Eq. 1.12-9b

$$Q_1 = Q_2 = 0 \quad (1.13-76)$$

and that in-plane shear forces are

$$N_{12} = N_{21} \quad (1.13-77)$$

Introducing the preceding values into Eq. 1.12-9a yields the equilibrium equations for a shell membrane

$$\begin{aligned} \frac{\partial \alpha_2 N_1}{\partial \xi_1} + \frac{\partial \alpha_1 N_{21}}{\partial \xi_2} + N_{12} \frac{\partial \alpha_1}{\partial \xi_2} - N_2 \frac{\partial \alpha_2}{\partial \xi_1} + \alpha_1 \alpha_2 p_1 &= 0 \\ \frac{\partial \alpha_1 N_2}{\partial \xi_2} + \frac{\partial \alpha_2 N_{12}}{\partial \xi_1} + N_{21} \frac{\partial \alpha_2}{\partial \xi_1} - N_1 \frac{\partial \alpha_1}{\partial \xi_2} + \alpha_1 \alpha_2 p_2 &= 0 \\ - N_1 \frac{\alpha_1 \alpha_2}{R_1} - N_2 \frac{\alpha_1 \alpha_2}{R_2} + \alpha_1 \alpha_2 q &= 0 \end{aligned} \quad (1.13-78)$$

The preceding equations, together with Eqs. 1-13-74 through 77 describe the momentless or membrane state of stress in shells.

In the system shown, the number of unknowns is equal to the number of equations, so that the problem in the membrane theory of shells is statically determinate. As pointed out by Novozhilov (Ref. 1-5), it should be noted that the problem is statically determinate in relation to the equilibrium of an infinitely small element of the shell, but not always in relation to the equilibrium of the shell as a whole. An

analogous situation occurs in the problem of the bending of a beam where likewise the number of unknowns in the equilibrium equations corresponds to the number of equations and where the determination of the reactions at the supports requires first the determination of the displacements.

With the forces and moments known, the displacements of the shell characterized by a membrane state of stress are given by

$$\begin{aligned} \epsilon_1 &= \frac{1}{\alpha_1} \frac{\partial u}{\partial \xi_1} + \frac{1}{\alpha_1 \alpha_2} \frac{\partial \alpha_1}{\partial \xi_2} v + \frac{w}{R_1} \\ \epsilon_2 &= \frac{1}{\alpha_2} \frac{\partial v}{\partial \xi_2} + \frac{1}{\alpha_1 \alpha_2} \frac{\partial \alpha_2}{\partial \xi_1} u + \frac{w}{R_2} \\ \gamma_{12} &= \frac{\alpha_2}{\alpha_1} \frac{\partial}{\partial \xi_1} \left(\frac{v}{\alpha_2} \right) + \frac{\alpha_1}{\alpha_2} \frac{\partial}{\partial \xi_2} \left(\frac{u}{R_1} \right) \end{aligned} \quad (1.13-79)$$

As shown by Novozhilov (Ref. 1-5), the solutions of the equations of membrane theory present pure bending displacements on an equal basis with displacement of the shell as a rigid body. Physically, this means that a freely flexible shell admits the appearance of bending displacements without offering any resistance.

Thus, in stating problems of membrane theory, the pure bending displacements must either be eliminated or, at least, bounded properly.

The indeterminacy of displacement magnitude and necessary bounds on displacements that characterize membrane state of stress effects boundary conditions as discussed in the following paragraph.

B. Boundary Conditions

Equilibrium Eq. 1.13-78, together with displacement Eq. 1.13-79, constitutes a fourth-order system of equations. Thus, in membrane theory, the differential equation for displacements have one-half the order of those in general bending theory of shell (Paragraph 1.13.1). Therefore, the number of edge conditions to be satisfied in membrane theory is one-half the order satisfied in general bending theory. In membrane theory, only two conditions may be specified on each edge of the shell.

The reduction of the order of the system of equations is a result of the assumption that moments and transverse shears are negligible in a membrane theory. Thus,

$$Q_1 = Q_2 = M_1 = M_{12} = M_{21} = M_2 = 0 \quad (1.13-80)$$

which hold at all points in the middle surface and, hence, on the boundary of the shell (the boundary conditions by general theory are given by Eq. 1.13-31).

Therefore, the edges of a shell in the membrane state of stress must be free from external edge loadings in the form of normal shearing

stresses and bending moments. As a result, membranes can only support tangential edge loadings and, consequently, only forces N_1 and N_{12} may act on an edge under consideration. Hence, boundary conditions must be formulated in terms of these quantities.

A special situation occurs if the boundary conditions are given in terms of displacements. For membrane theory, it is impossible to specify the edge displacement, w , and angle of rotation, β , since this would affect the corresponding general forces, Q_1 and M_1 (e. g., the conditions for membranes that $Q = 0$, $M = 0$ makes it impossible to specify $w = \beta = 0$ at the boundary). It follows that on the edge of a membrane only the tangential displacement components of the middle surface can be specified (i. e., u and v).

C. Conditions for the Existence of the Membrane State of Stress

It has been shown that one of the sources of contradiction in the membrane theory results from the fact that the solutions of this theory may not be subjected to general boundary conditions. Violation of these conditions is equivalent to disturbing the membrane state of stress. However, while these requirements are necessary, they are not sufficient, and additional requirements are necessary to ensure a membrane state of stress.

Another contradiction in membrane theory is the fact that its equations determine the forces in the shell without dependence on the compatibility relations of the middle surface. In addition, a membrane cannot be loaded by concentrated forces. The state of stress of a shell loaded by such forces will involve moments.

In summary, it should be emphasized that the existence of the membrane state of stress is related to the necessity of satisfying several conditions concerning the shape of the shell, the character of load applied, and the attachment of its edges.

D. Axisymmetric Load on Membrane Shaped as Shells of Revolution

In many practical problems, the external forces have the same symmetry as the shell itself. Forces are then independent of ξ_2 or θ , and all derivatives, with respect to θ , disappear from Eq. 1.13-78. There results

$$\frac{d}{d\phi} (rN_\phi) - R_1 N_\theta \cos \phi = -p_\phi rR_1 \quad (1.13-81a)$$

$$\frac{N_\phi}{R_1} + \frac{N_\theta}{R_2} = p_r \quad (1.13-81b)$$

When Eq. 1.13-81b is solved for N_θ and the result is substituted into Eq. 1.13-81a, a first-ordered differential equation for N_ϕ is obtained. Multiplication by $\sin \phi$ yields

$$\frac{d (rN_\phi)}{d\phi} \sin \phi + rN_\phi \cos \phi = R_1 R_2 p_r \cos \phi \sin \phi - R_1 R_2 p_\phi \sin^2 \phi \quad (1.13-82)$$

In combining we obtain, for one term on the left-hand side of equation (1.13-82).

$$\frac{d}{d\phi} (rN_{\phi} \sin \phi) = \frac{d}{d\phi} (R_2 N_{\phi} \sin^2 \phi)$$

hence

$$N_{\phi} = \frac{1}{R_1 \sin^2 \phi} \int R_1 R_2 (p_r \cos \phi - p_{\phi} \sin \phi) \sin \phi d\phi + C \quad (1.13-83)$$

The last equations may be considered as a condition of equilibrium for the part of the shell above a parallel circle, $\phi = \text{const}$. If F is a result of the total load, the equation of equilibrium is

$$2\pi r_0 N_{\phi} \sin \phi + F = 0 \quad (1.13-84)$$

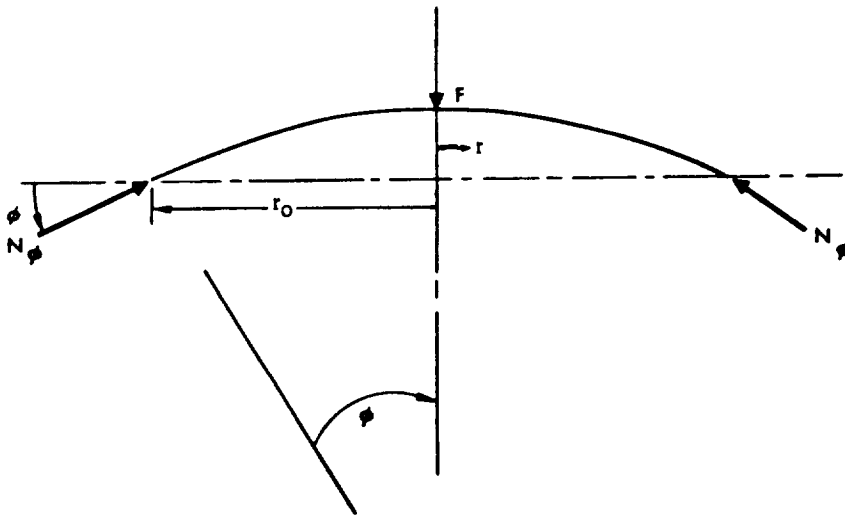


FIG. 1.13-3

Application of the membrane equation to a cylindrical shell under internal pressure (p) leads to the well known results

$$N_{\phi} = \frac{pR}{2}, \quad N_{\theta} = pR$$

For a conical shell under uniform internal pressure,

$$N_{\phi} = \frac{pR}{2 \sin \phi} , N_{\theta} = \frac{pR}{\sin \phi}$$

1.13.6 Summary

An introduction to linear theory of thin elastic shells was presented in this section. Basic relations necessary for deformation and stress analysis were provided and appropriate assumptions were indicated. Shell theories were categorized according to the assumptions, limitations, and restrictions for their usage described. Due to the quantity of material available on shells a complete treatment of the linear theory of shells was not possible. A more complete presentation is included in the literature (Novozhilov, Ref. 1-5; Goldenveiser, Ref. 1-46; Flügge, Ref. 1-47; Timoshenko, Ref. 1-26; Koiter, Ref. 1-48 and others).

1.20 NONLINEAR SHELL THEORY

1.21 INTRODUCTION

The small deflection field equations presented earlier were formulated from the classical linear theory of elasticity. It is known that these equations, which are based on Hooke's law and the omission of nonlinear terms both in the equations for strain components and the equilibrium equations, have a unique solution in every case. In other words, linear shell theory determines a unique position of equilibrium for every shell with prescribed load and constraints.

In reality, however, the solution of a physical shell problem is not always unique. A shell under identical conditions of loading and constraints may have several possible positions of equilibrium. The incorrect inference to which linear shell theory leads can be explained by the approximations introduced in the development of the shell equations. In this development rotations were neglected in the expressions for strains and equilibrium in order that the equations could be linearized. It is essential in the investigation of the multiple equilibrium states of a shell to include these rotation terms.

A theory of shells that is free of this hypothesis can be thought of as being "geometrically nonlinear" and requires formulation on the basis of the nonlinear elasticity theory. Additionally, the shell may be

"physically nonlinear" with respect to the stress-strain relations. This latter type of nonlinearity forms the basis of inelastic shell theory and will not be discussed here.

Theories based on nonlinear elasticity are required in analyzing the so-called "large" deformations of shells. "Large" or finite deflection shell theories form the basis for the investigation of the stability of shells. In the case of stability, the effects of deformation on equilibrium cannot be ignored. The stability of shells will be considered in the next section.

The subsequent development of nonlinear shell theory will be based on a general mathematical approach described by Novozhilov (Ref. 1-10) for problems of nonlinear elasticity. Starting with the general strain-displacement relations, approximate nonlinear strain-displacement relations and equilibrium equations are derived by the introduction of appropriate simplifying assumptions. The equilibrium equations will be obtained upon application of the principle of stationary potential energy. These concepts will be discussed in the following paragraphs.

1.22 GENERAL STRAIN-DISPLACEMENT RELATIONS

The strain-displacement relationships presented in Paragraph 1.12.2 are based on the classical (linear) theory of elasticity. In this formulation, several assumptions regarding the magnitude of strains and rotations were made. It was assumed that strains were small (i. e., $\epsilon \ll 1$) and that rotations were of the same order of magnitude as the strains (i. e., $\epsilon = O(\beta) \ll 1$). These assumptions permitted order of magnitude simplifications of the general strain-displacement relationships derived from nonlinear elasticity concepts.

In formulating a nonlinear shell theory, it is no longer permissible to restrict the rotations, and it becomes necessary to deal with the more complicated strain equations. The general strain-displacement relationships from nonlinear elasticity are given in terms of the curvilinear coordinate system ξ_1 , ξ_2 , and z by

$$\left. \begin{aligned} e_{11} &= \epsilon_1 + \frac{1}{2} \left[\epsilon_1^2 + \gamma_1^2 + \beta_1^2 \right] \\ e_{22} &= \epsilon_2 + \frac{1}{2} \left[\epsilon_2^2 + \gamma_2^2 + \beta_2^2 \right] \\ e_{12} &= \gamma_{12} + \epsilon_1 \gamma_2 + \epsilon_2 \gamma_1 + \beta_1 \beta_2 \end{aligned} \right\} (1.22-1a)$$

$$\left. \begin{aligned} e_{1z} &= \gamma_{1z} + \beta_1 \frac{\partial W}{\partial z} + \epsilon_1 \frac{\partial U}{\partial z} + \gamma_1 \frac{\partial V}{\partial z} \\ e_{2z} &= \gamma_{2z} + \beta_2 \frac{\partial W}{\partial z} + \epsilon_2 \frac{\partial V}{\partial z} + \gamma_2 \frac{\partial U}{\partial z} \end{aligned} \right\} (1.22-1b)$$

where the terms ϵ_1 , ϵ_2 , γ_{12} , γ_{1z} , and γ_{2z} are the linear strain expressions (Eq. 12.2-6) which in terms of displacements and their derivations, are given by:

$$\left. \begin{aligned}
 \epsilon_1 &= \frac{1}{1 + \frac{z}{R_1}} \left(\frac{1}{\alpha_1} \frac{\partial U}{\partial \xi_1} + \frac{V}{\alpha_1 \alpha_2} \frac{\partial \alpha_1}{\partial \xi_2} v + \frac{W}{R_1} \right) \\
 \epsilon_2 &= \frac{1}{1 + \frac{z}{R_2}} \left(\frac{1}{\alpha_2} \frac{\partial V}{\partial \xi_2} + \frac{U}{\alpha_1 \alpha_2} \frac{\partial \alpha_2}{\partial \xi_1} u + \frac{W}{R_2} \right) \\
 \gamma_{12} &= \frac{1}{1 + \frac{z}{R_1}} \left(\frac{1}{\alpha_1} \frac{\partial V}{\partial \xi_1} - \frac{U}{\alpha_1 \alpha_2} \frac{\partial \alpha_1}{\partial \xi_2} \right) + \frac{1}{1 + \frac{z}{R_2}} \left(\frac{1}{\alpha_2} \frac{\partial U}{\partial \xi_2} - \frac{V}{\alpha_1 \alpha_2} \frac{\partial \alpha_2}{\partial \xi_1} \right) \\
 \gamma_{1z} &= \frac{\partial u}{\partial z} + \frac{1}{1 + \frac{z}{R_1}} \left(\frac{1}{\alpha_1} \frac{\partial W}{\partial \xi_1} - \frac{U}{R_1} \right) \\
 \gamma_{2z} &= \frac{\partial v}{\partial z} + \frac{1}{1 + \frac{z}{R_2}} \left(\frac{1}{\alpha_2} \frac{\partial W}{\partial \xi_2} - \frac{V}{R_2} \right)
 \end{aligned} \right\} (1.22-2)$$

and the additional terms β_1 , β_2 , γ_1 , and γ_2 are given by:

$$\left. \begin{aligned}
 \gamma_1 &= \frac{1}{1 + \frac{z}{R_1}} \left(\frac{1}{\alpha_1} \frac{\partial V}{\partial \xi_1} - \frac{U}{\alpha_1 \alpha_2} \frac{\partial \alpha_1}{\partial \xi_2} u \right), \quad \beta_1 = \frac{1}{1 + \frac{z}{R_1}} \left(\frac{1}{\alpha_1} \frac{\partial W}{\partial \xi_1} - \frac{U}{R_1} \right) \\
 \gamma_2 &= \frac{1}{1 + \frac{z}{R_2}} \left(\frac{1}{\alpha_2} \frac{\partial U}{\partial \xi_2} - \frac{V}{\alpha_1 \alpha_2} \frac{\partial \alpha_2}{\partial \xi_1} v \right), \quad \beta_2 = \frac{1}{1 + \frac{z}{R_2}} \left(\frac{1}{\alpha_2} \frac{\partial W}{\partial \xi_2} - \frac{V}{R_2} \right)
 \end{aligned} \right\} (1.22-3)$$

It is noted that Eqs. 1.22-1a and b are a set of nonlinear differential equations considerably more complex than the strain-displacement expressions (Eqs. 12.2-6) of the linear theory.

Following a procedure similar to the one described in the linear shell theory section, the introduction of the Kirchhoff-Love assumptions permits considerable simplification of the above expressions. The "thinness" criterion permits the approximation that terms $\left(1 + \frac{z}{R_1}, 1 + \frac{z}{R_2}\right)$ can be replaced by unity; i. e.,

$$1 + \frac{z}{R_1} \approx 1 + \frac{z}{R_2} \approx 1.$$

The assumption that normals remain normal causes the transverse shear strains to vanish, i. e.,

$$\gamma_{1z} = 0$$

$$\gamma_{2z} = 0$$

(The normal strain ϵ_z vanishes from inextensibility of normals and, as a consequence, was not included in Eq. 1.22-1a.)

If the strains are assumed small ($\epsilon \ll 1$), order of magnitude considerations permit the neglecting of nonlinear terms in strain. The details of these simplifications are discussed by Novozhilov (Ref. 1-10) and Kempner (Ref. 1-22) and result in nonzero strain expressions of the form

$$\left. \begin{aligned} e_1 &= \epsilon_1 + \frac{\beta_1^2}{2} \\ e_2 &= \epsilon_2 + \frac{\beta_2^2}{2} \\ e_{12} &= \gamma_{12} + \beta_1 \beta_2 \end{aligned} \right\} \quad (1.22-4)$$

where ϵ_1 , ϵ_2 , γ_{12} , β_1 , and β_2 are the expressions obtained from Eqs. 1.22-2 and -3 with the $\frac{z}{R}$ term omitted.

From the assumption of planes remaining plane, the displacements may be expressed by

$$\left. \begin{aligned} U &= u_0 + z \beta_1 \\ V &= v_0 + z \beta_2 \\ W &= w_0 = w \end{aligned} \right\} \quad (1.22-5)$$

where u , v , and w are middle surface displacements and z is the coordinate transverse to the shells middle surface. By introducing these expressions into the strain-displacement relations (Eqs. 1.22-2 and Eqs. 1.22-4 and 5), there results the general form of the strains as

$$\left. \begin{aligned} e_1 &= e_1^0 + z \kappa_1 \\ e_2 &= e_2^0 + z \kappa_2 \\ e_{12} &= e_{12}^0 + z \kappa_{12} \end{aligned} \right\} \quad (1.22-6)$$

where e_1^0 , e_2^0 , and e_{12}^0 are the nonlinear middle surface extensional and in-plane shear strains given by Eq. 1.22-4 (superscripted with 0) and where

$$\left. \begin{aligned}
 \kappa_1 &= \frac{1}{\alpha_1} \frac{\partial \beta_1}{\partial \xi_1} + \frac{1}{\alpha_1 \alpha_2} \frac{\partial \alpha_1}{\partial \xi_2} \beta_2 \\
 \kappa_2 &= \frac{1}{\alpha_2} \frac{\partial \beta_2}{\partial \xi_2} + \frac{1}{\alpha_1 \alpha_2} \frac{\partial \alpha_2}{\partial \xi_1} \beta_1 \\
 \kappa_{12} &= \left[\frac{\alpha_2}{\alpha_1} \frac{\partial (\beta_2 / \alpha_2)}{\partial \xi_1} + \frac{\alpha_1}{\alpha_2} \frac{\partial (\beta_1 / \alpha_1)}{\partial \xi_2} \right]
 \end{aligned} \right\} \quad (1.22-7)$$

are the measures of bending distortion.

It should be noted that there are terms in z^2 contained in performing the outlined substitution; however, as discussed by Novozhilov (Ref. 1-10) for small strains, the correction introduced by these terms is insignificant. The κ_1 , κ_2 , and κ_{12} parameters characterize the change in curvature of the strained middle surface of the shell.

In the classical small deflection theory of shells it was shown that the strains (ϵ) were of the order of the magnitude of the rotations (β) or $\epsilon = O(\beta) \ll 1$. By relaxing the constraint on the middle surface rotations, the nonlinear strains of the middle surface are of the order of the rotations squared or $\epsilon = O(\beta^2) \ll 1$.

1.23 STRESS-STRAIN RELATIONS AND STRESS RESULTANTS

The isotropic stress-strain relations from Paragraph 1.12.5 are written as follows:

$$\left. \begin{aligned} \sigma_1 &= E/(1 - \mu^2) [e_1 + \mu e_2] \\ \sigma_2 &= E/(1 - \mu^2) [e_2 + \mu e_1] \\ \tau_{12} &= G_1 \gamma_{12} \end{aligned} \right\} \quad (1.23-8)$$

The stress-resultants may be obtained by appropriate integration of the above Hooke's law over the shell's thickness, i. e.,

$$\left\{ \begin{array}{l} N_1 \\ N_2 \\ N_{12} \end{array} \right\} = \int_t \left\{ \begin{array}{l} \sigma_1 \\ \sigma_2 \\ \tau_{12} \end{array} \right\} dz, \quad \left\{ \begin{array}{l} M_1 \\ M_2 \\ M_{12} \end{array} \right\} = \int_t \left\{ \begin{array}{l} \sigma_1 \\ \sigma_2 \\ \tau_{12} \end{array} \right\} z dz \quad (1.23-9)$$

where the integrals are taken over the shells thickness (t). If Eq. 1.23-8 and, subsequently, Eqs. 1.22-4 and -6 are inserted into Eq. 1.23-9, we may write the stress-resultant strain expressions as follows:

$$\left. \begin{aligned} N_1 &= B (e_1^0 + \mu e_2^0) + C (\kappa_1 + \mu \kappa_2) \\ N_2 &= B (e_2^0 + \mu e_1^0) + C (\kappa_2 + \mu \kappa_1) \\ N_{12} &= \bar{B} e_{12}^0 + \bar{C} \kappa_{12} = N_{21} \\ M_1 &= C (e_1^0 + \mu e_2^0) + D (\kappa_1 + \mu \kappa_2) \\ M_2 &= C (e_2^0 + \mu e_1^0) + D (\kappa_2 + \mu \kappa_1) \\ M_{12} &= \bar{C} e_{12}^0 + \bar{D} \kappa_{12} = M_{21} \end{aligned} \right\} \quad (1.23-10)$$

where

$$\left. \begin{aligned} B &= \int_t \frac{Edz}{1-\mu^2}, \quad C = \int_t \frac{Ezdz}{1-\mu^2}, \quad D = \int_t \frac{Ez^2dz}{1-\mu^2} \\ \bar{B} &= \int_t Gdz, \quad \bar{C} = \int_t Gzdz, \quad \bar{D} = \int_t Gz^2dz \end{aligned} \right\} \quad (1.23-11)$$

These expressions are presented for reference and will be utilized later in the development of the nonlinear equilibrium equation for shells. The stiffness parameters can be simplified by suitable choice of the reference surface within the shell wall.

The constitutive relations (Eq. 1.23-10) can be simplified considerably by proper selection of a reference surface within the shell wall. A convenient selection is one in which the stiffness parameters C, \bar{C} above vanish. Recall from Paragraph 1.13.1 for an isotropic monocoque shell this simplification was possible since the reference surface was selected at the middle surface.

1.24 PRINCIPLE OF POTENTIAL ENERGY

In the previous section, the linear shell force equilibrium equations were obtained from laws of statics by considering equilibrium of a differential shell element. In the formulation it was assumed that, since strains and rotations were negligibly small, the deformed and undeformed states of the shell element were identical. If the geometrical constraint on rotations is relaxed, the assumption made in the linear theory is no longer valid, and the effects of distortion of the deformed state must be considered in equilibrating forces. The equilibrium equations including the distortion effects can be obtained by considering equilibrium of the shell differential element in a similar manner as discussed in Paragraph 1.12.4. The equations that result are nonlinear. However, in this section, the use of energy principles for obtaining the nonlinear shell equilibrium equations will be illustrated.

The method is based on the fact that the governing equilibrium equations of a structural system can be obtained as a direct consequence of the minimization of a certain energy expression. In this context, the energy method that will be utilized is the principle of potential energy. In developing this method use shall be made of a branch of mathematics called calculus of variations; for this reason, these methods are sometimes referred to as variational methods.

The potential energy, \bar{V} , of a shell is given by the expression

$$\bar{V} = \bar{U} - \bar{W} \quad (1.24-12)$$

where \bar{U} is the potential energy of deformation or work done by the internal forces, and $(-\bar{W})$ is the potential energy of forces acting on the shell if the potential energy of these forces for the unstressed state is taken as zero. The potential energy of deformation, \bar{U} , is generally referred to as the strain energy. For a Hookean material, the strain energy expression for a shell is given by the expression

$$\bar{U} = \frac{1}{2} \iiint (\sigma_1 e_1 + \sigma_2 e_2 + \tau_{12} e_{12}) \alpha_1 \alpha_2 d\xi_1 d\xi_2 dz \quad (1.24-13)$$

where ξ_1 , ξ_2 , and z are shell curvilinear coordinates. This expression can be simplified by substituting Eq. 1.23-8 into the above, which yields the equation

$$\bar{U} = \frac{1}{2} \iiint \left[\frac{E}{1-\mu^2} (e_1^2 + e_2^2) + \frac{2\mu E}{1-\mu^2} e_1 e_2 + G e_{12}^2 \right] \alpha_1 \alpha_2 d\xi_1 d\xi_2 dz \quad (1.24-14)$$

It can be seen that, by substituting the strain-displacement relations (Eqs. 1.22-4, -6, -7) into the above, the strain energy expression described in terms of the middle surface displacement functions u_0 , v_0 , w_0 results. As a result, the potential energy can be described in terms of the displacement functions.

The principle of (stationary) potential energy (Wang, Ref. 1-9) states... "of all the displacements satisfying the given boundary

conditions, those which satisfy equilibrium conditions make the potential energy \bar{V} assume a stationary value." In addition, for stable equilibrium, the potential energy is a minimum. The operation of finding a stationary value or extremum point of the potential energy functional (i. e., function of displacement functions u, v, w) is analogous to operations performed in differential calculus. It may be recalled from the calculus (Ref. 1-49), that the derivative of a function vanishes at stationary values or extremum points. In addition, the point is a minimum point if the second derivative is positive. Using variational techniques, the operation analogous to the first derivative is called the first variation and the one analogous to the second derivative corresponds the second variation, resolving the problem to that of finding the displacement functions, $u, v,$ and $w,$ which make the potential energy stationary. The corresponding analog from calculus was to find points which made the function stationary. This, of course, should be understood to be an oversimplification of the problem and is only presented to give the engineer not familiar with variational methods some idea as to their nature. Those interested in more rigorous presentation should refer to many books on calculus of variations.

As stated above, the problem resolves itself to a matter of finding the displacement functions that make the potential energy function

stationary. In this connection, it will be assumed that the displacement functions can be represented in the form

$$\left. \begin{aligned} u(\xi_1, \xi_2) &= u^0(\xi_1, \xi_2) + \lambda \bar{u}(\xi_1, \xi_2) \\ v(\xi_1, \xi_2) &= v^0(\xi_1, \xi_2) + \lambda \bar{v}(\xi_1, \xi_2) \\ w(\xi_1, \xi_2) &= w^0(\xi_1, \xi_2) + \lambda \bar{w}(\xi_1, \xi_2) \end{aligned} \right\} \quad (1.24-15)$$

where u^0 , v^0 , and w^0 represent the displacements corresponding to the equilibrium configuration, and \bar{u} , \bar{v} , and \bar{w} are admissible variations of u , v , and w (called admissible displacements) that satisfy certain conditions of continuity and finiteness. The quantity λ represents an arbitrary small parameter that is independent of ξ_1 , ξ_2 . If the functions u , v , w are replaced in the potential energy expression (Eq. 1.24-14) by Eq. (1.24-15) the potential energy \bar{V} becomes a function of the parameter λ .

According to the principle of stationary potential energy, the potential energy becomes stationary at $\lambda = 0$. Thus, the requirement that the first variation, \bar{V}_1 , of the potential energy functional vanish at $\lambda = 0$ yields

$$\bar{V}_1 = \left. \frac{d\bar{V}(\lambda)}{d\lambda} \right|_{\lambda=0} = 0 \quad (1.24-16)$$

where $d()$ represents the usual differential operator. The use of the above operation to derive the equilibrium equation will be discussed in

the following section. A similar operation using the second variation of the potential energy will be used in obtaining the stability equations in Section 1.30.

The technique presented is quite similar to the principle of virtual work, in which the terms $\lambda \bar{u}$, $\lambda \bar{v}$, and $\lambda \bar{w}$ can be thought of as virtual displacements, where λ refers to a virtual change. In this case, the virtual work done is represented by $\delta(\bar{V})$. The principle of virtual work states that the displacements that actually occur in an elastic system under action of given forces are those that lead to zero variation of the total energy of the system for any virtual displacement from the position of equilibrium. The vanishing of the virtual work expressions requires that

$$\delta \bar{V} = \delta (\bar{U} - \bar{W}) = 0 \quad (1.24-17)$$

A more complete presentation of the principle of virtual work as applied to elastic systems is given by Wang (Ref. 1-9).

1.25 NONLINEAR EQUILIBRIUM EQUATIONS

The principle of stationary potential energy as a variational method was introduced in the previous section and will now be utilized to derive the differential equations of equilibrium of a shell. The nonlinear strain-displacement relations given by Eq. 1.22-4 will be utilized as a basis.

Following the format outlined in the previous section, substitution of the assumed displacement functions given by Eqs. 1.24-15 into Eqs. 1.22-4 yields expressions for the strains of the form

$$\begin{aligned} e_1 &= e_1^0 + \lambda \bar{e}_1 + \lambda^2 \bar{\bar{e}}_1 \\ e_2 &= e_2^0 + \lambda \bar{e}_2 + \lambda^2 \bar{\bar{e}}_2 \\ e_{12} &= e_{12}^0 + \lambda \bar{e}_{12} + \lambda^2 \bar{\bar{e}}_{12} \end{aligned} \quad (1.25-18)$$

where e_1^0 , e_2^0 , e_{12}^0 are given by Eq. 1.22-4 with appropriate superscript 0 and

$$\begin{aligned} \bar{e}_1 &= \bar{e}_1^0 + \frac{1}{2} \beta_1^0 \bar{\beta}_1 \\ \bar{e}_2 &= \bar{e}_2^0 + \frac{1}{2} \beta_2^0 \bar{\beta}_2 \\ \bar{e}_{12} &= \bar{e}_{12}^0 + \beta_2^0 \bar{\beta}_1 + \beta_1^0 \bar{\beta}_2 \end{aligned} \quad (1.25-19)$$

$$\begin{Bmatrix} \bar{\bar{e}}_1 \\ \bar{\bar{e}}_2 \\ \bar{\bar{e}}_{12} \end{Bmatrix} = \frac{1}{2} \begin{Bmatrix} (\bar{\beta}_1)^2 \\ (\bar{\beta}_2)^2 \\ \bar{\beta}_1 \bar{\beta}_2 \end{Bmatrix} \quad (1.25-20)$$

where ϵ and β are as defined previously provided these quantities are related to corresponding displacements described in Eq. 1.24-15.

Eq. 1.25-18 has an associated state of stress with components of the form

$$\begin{aligned}\sigma_1 &= \sigma_1^0 + \lambda \bar{\sigma}_1 + \lambda^2 \bar{\bar{\sigma}}_1 \\ \sigma_2 &= \sigma_2^0 + \lambda \bar{\sigma}_2 + \lambda^2 \bar{\bar{\sigma}}_2 \\ \tau_{12} &= \tau_{12}^0 + \lambda \bar{\tau}_{12} + \lambda^2 \bar{\bar{\tau}}_{12}\end{aligned}\tag{1.25-21}$$

where neglecting thermal terms the σ_1^0 , σ_2^0 , ---, $\bar{\tau}_{12}$ expressions are given by Eq. 1.23-8 with the appropriate superscript attached.

Inserting the right-hand side of Eqs. 1.25-18 and 1.25-21 into the strain energy expression (Eq. 1.24-13), dropping terms of higher order than λ^2 , and noting the well-known reciprocity relations, we arrive at the strain energy of the shell given by the form

$$\bar{U} = \bar{U}_0 + \lambda \bar{U}_1 + \lambda^2 \bar{U}_2\tag{1.25-22}$$

where

$$\bar{U}_0 = \frac{1}{2} \int_{\mathbf{v}} \left[\sigma_1^0 \epsilon_1^0 + \sigma_2^0 \epsilon_2^0 + \tau_{12}^0 \epsilon_{12}^0 \right] \alpha_1 \alpha_2 d\xi_1 d\xi_2 dz\tag{1.25-23}$$

$$\bar{U}_1 = \int_{\mathbf{v}} \left[\sigma_1^0 \bar{\epsilon}_1 + \sigma_2^0 \bar{\epsilon}_2 + \tau_{12}^0 \bar{\epsilon}_{12} \right] \alpha_1 \alpha_2 d\xi_1 d\xi_2 dz\tag{1.25-24}$$

$$\begin{aligned}\bar{U}_2 &= \frac{1}{2} \int_{\mathbf{v}} \left\{ \left[\bar{\sigma}_1 \bar{\epsilon}_1 + \bar{\sigma}_2 \bar{\epsilon}_2 + \bar{\tau}_{12} \bar{\epsilon}_{12} \right] \right. \\ &\quad \left. + 2 \left[\sigma_1^0 \bar{\bar{\epsilon}}_1 + \sigma_2^0 \bar{\bar{\epsilon}}_2 + \tau_{12}^0 \bar{\bar{\epsilon}}_{12} \right] \right\} \alpha_1 \alpha_2 d\xi_1 d\xi_2 dz\end{aligned}\tag{1.25-25}$$

An expression similar to Eq. 1.25-22 can be formed for the potential energy expression ($-\bar{W}$) due to applied external forces. For large deflections, it is appropriate to express (\bar{W}) as

$$-\bar{W} = - \int_{\xi_1^o}^{\hat{\xi}_1} \int_{\xi_2^o}^{\hat{\xi}_2} [f_1^o \bar{u} + f_2^o \bar{v} + f_z^o \bar{w}] \alpha_1 \alpha_2 d\xi_1 d\xi_2 \quad (1.25-26)$$

where the superscript, o, and roof, ($\hat{\quad}$), on the integration limits represent initial and final boundary coordinates, and the f's are a function of the applied forces p_1 , p_2 , and q .

The total potential energy expression, \bar{V} , obtained from Eqs. 1.25-22 and 1.25-26 can be described in terms of displacement function u^o , v^o , w^o and arbitrary variations \bar{u} , \bar{v} , \bar{w} by appropriate substitution of Eqs. 1.24-15 and 1.25-23 -25. The potential energy expressed similar to Eq. 1.25-22 is given by

$$\bar{V} = \bar{V}_0 + \lambda \bar{V}_1 + \lambda^2 \bar{V}_2 \quad (1.25-27)$$

Since \bar{V}_0 , \bar{V}_1 , \bar{V}_2 are independent of the arbitrary parameter λ according to the principle of potential energy the potential energy becomes stationary at $\lambda = 0$ when

$$\left. \frac{d\bar{V}}{d\lambda} \right|_{\lambda=0} = \bar{V}_1 = \bar{U}_1 - \bar{W}_1 = 0 \quad (1.25-28)$$

Thus, the first variation expression described by Eqs. 1.24-16 and its equivalent, Eq. 1.25-28, are used to establish the equilibrium equations. The insertion of Eqs. 1.23-8 and 1.25-19 into Eq. 1.25-24 and these into 1.25-28 and integrating by parts noting arbitrariness of admissible displacements \bar{u} , \bar{v} , \bar{w} leads to the large deflection equilibrium equations of the form

$$\begin{aligned} \frac{\partial \alpha_2 N_1^0}{\partial \xi_1} + \frac{\partial \alpha_1 N_{12}^0}{\partial \xi_2} + \frac{\partial \alpha_1}{\partial \xi_2} N_{12}^0 - \frac{\partial \alpha_2}{\partial \xi_1} N_2^0 + \frac{\alpha_1 \alpha_2}{R_1} Q_1^0 \\ - \frac{\alpha_1 \alpha_2}{R_1} (\beta_1 N_1^0 + \beta_2 N_{12}^0) + \alpha_1 \alpha_2 p_1 = 0 \end{aligned} \quad (1.25-29a)$$

$$\begin{aligned} \frac{\partial \alpha_2 N_{12}^0}{\partial \xi_1} + \frac{\partial \alpha_1 N_2^0}{\partial \xi_2} + \frac{\partial \alpha_2}{\partial \xi_1} N_{12}^0 - \frac{\partial \alpha_1}{\partial \xi_2} N_1^0 + \frac{\alpha_1 \alpha_2}{R_2} Q_2^0 \\ - \frac{\alpha_1 \alpha_2}{R_2} (\beta_1 N_{12}^0 + \beta_2 N_2^0) + \alpha_1 \alpha_2 p_2 = 0 \end{aligned} \quad (1.25-29b)$$

$$\begin{aligned} \frac{\partial \alpha_2 Q_1^0}{\partial \xi_1} + \frac{\partial \alpha_1 Q_2^0}{\partial \xi_2} - \alpha_1 \alpha_2 \left(\frac{N_1^0}{R_1} + \frac{N_2^0}{R_2} \right) - \frac{\partial}{\partial \xi_1} (\alpha_2 \beta_1 N_1^0 + \alpha_2 \beta_2 N_{12}^0) \\ - \frac{\partial}{\partial \xi_2} (\alpha_1 \beta_1 N_{12}^0 + \alpha_1 \beta_2 N_2^0) + \alpha_1 \alpha_2 q = 0 \end{aligned} \quad (1.25-29c)$$

$$\frac{\partial \alpha_2 M_1^0}{\partial \xi_1} + \frac{\partial \alpha_1 M_{12}^0}{\partial \xi_2} + \frac{\partial \alpha_1}{\partial \xi_2} M_{12}^0 - \frac{\partial \alpha_2}{\partial \xi_1} M_2^0 - \alpha_1 \alpha_2 Q_1^0 = 0 \quad (1.25-29d)$$

$$\frac{\partial \alpha_2 M_{12}^0}{\partial \xi_1} + \frac{\partial \alpha_1 M_2^0}{\partial \xi_2} + \frac{\partial \alpha_2}{\partial \xi_1} M_{12}^0 - \frac{\partial \alpha_1}{\partial \xi_2} M_1^0 - \alpha_1 \alpha_2 Q_2^0 = 0 \quad (1.25-29e)$$

where it is noted $N_{12}^0 = N_{21}^0$; $M_{12}^0 = M_{21}^0$

The details of the above operations can be found in Ref. 1-22. The above equations can be simplified when the effects of transverse shear distortion are neglected. Following a similar procedure as described in the Linear Shell Theory section a reduction in the number of equations may be realized. Solving for the last two equations for shear forces Q_1, Q_2 , in terms of the moments, and substituting the resulting expressions into the first three equations results in the following "large" deflection equilibrium equations:

$$\begin{aligned} \frac{\partial}{\partial \xi_1} (N_1^0 \alpha_2) + \frac{1}{\alpha_1} \frac{\partial}{\partial \xi_2} (N_{21}^0 \alpha_1^2) - N_2^0 \frac{\partial \alpha_2}{\partial \xi_1} + \frac{1}{R_1} \left[\frac{\partial}{\partial \xi_1} (M_1^0 \alpha_2) \right. \\ \left. + \frac{1}{\alpha_1} \frac{\partial}{\partial \xi_2} (M_{21}^0 \alpha_1^2) - M_2^0 \frac{\partial \alpha_2}{\partial \xi_1} - N_1^0 \beta_1^0 \alpha_1 \alpha_2 \right. \\ \left. - N_{12}^0 \beta_2^0 \alpha_1 \alpha_2 \right] + p_1^0 \alpha_1 \alpha_2 = 0 \end{aligned} \quad 1.25(30a)$$

$$\begin{aligned} \frac{\partial}{\partial \xi_2} (N_2^0 \alpha_1) + \frac{1}{\alpha_2} \frac{\partial}{\partial \xi_1} (\alpha_2^2 N_{12}^0) - N_1^0 \frac{\partial \alpha_1}{\partial \xi_2} + \frac{1}{R_2} \left[\frac{\partial}{\partial \xi_2} (M_2^0 \alpha_1) \right. \\ \left. + \frac{1}{\alpha_2} \frac{\partial}{\partial \xi_1} (M_{12}^0 \alpha_2^2) - M_1^0 \frac{\partial \alpha_1}{\partial \xi_2} - N_2^0 \beta_2^0 \alpha_1 \alpha_2 \right. \\ \left. - N_{21}^0 \beta_1^0 \alpha_1 \alpha_2 \right] + p_2^0 \alpha_1 \alpha_2 = 0 \end{aligned} \quad 1.25(30b)$$

$$\begin{aligned}
& -\alpha_1 \alpha_2 \left(\frac{N_1^{\circ}}{R_1} + \frac{N_2^{\circ}}{R_2} \right) + \frac{\partial}{\partial \xi_1} \left[\frac{1}{\alpha_1} \frac{\partial}{\partial \xi_1} (M_1^{\circ} \alpha_2) + \frac{1}{\alpha_1^2} \frac{\partial}{\partial \xi_2} (M_{21}^{\circ} \alpha_1^2) \right. \\
& \left. - \frac{M_2^{\circ}}{\alpha_1} \frac{\partial \alpha_2}{\partial \xi_1} - N_1^{\circ} \beta_1^{\circ} \alpha_2 + N_{12}^{\circ} \beta_2^{\circ} \alpha_2 \right] + \frac{\partial}{\partial \xi_2} \left[\frac{1}{\alpha_2} \frac{\partial}{\partial \xi_2} (M_2^{\circ} \alpha_1) \right. \\
& \left. + \frac{1}{\alpha_2^2} \frac{\partial}{\partial \xi_1} (M_{12}^{\circ} \alpha_2^2) - \frac{M_1^{\circ}}{\alpha_2} \frac{\partial \alpha_1}{\partial \xi_2} - N_2^{\circ} \beta_2^{\circ} \alpha_1 - N_{21}^{\circ} \beta_1^{\circ} \alpha_1 \right] + q^{\circ} \alpha_1 \alpha_2 = 0
\end{aligned}
\tag{1.25-30c}$$

In addition, the following natural boundary conditions result:

1. At $\xi = \xi_1^{\circ}$ and $\hat{\xi}_1$ where the superscript \circ and $(\hat{\ })$ stand for initial and final boundary curves for ξ_1 coordinate respectively.

Either of the following are prescribed:

$$u^{\circ} \text{ or } \alpha_2 \left(N_1^{\circ} + \frac{M_1^{\circ}}{R_1} \right)$$

$$v^{\circ} \text{ or } \alpha_2 \left(N_{12}^{\circ} + \frac{M_{12}^{\circ}}{R_2} \right)$$

$$w^{\circ} \text{ or } \left[\frac{1}{\alpha_1} \frac{\partial}{\partial \xi_1} (\alpha_2 M_1^{\circ}) + \frac{\partial}{\partial \xi_2} (M_{12}^{\circ}) - \frac{M_2^{\circ}}{\alpha_1 \alpha_2} \frac{\partial \alpha_2}{\partial \xi_1} \right.$$

$$\left. + \frac{1}{(\alpha_1)^2} \frac{\partial}{\partial \xi_2} (\alpha_1^2 M_{21}^{\circ}) - N_1^{\circ} \beta_1^{\circ} \alpha_2 - N_{12}^{\circ} \beta_2^{\circ} \alpha_2 \right]$$

$$\frac{1}{\alpha_1} \frac{\partial \omega^{\circ}}{\partial \xi_1} \text{ or } M_1^{\circ} \alpha_1$$

(1.25-31)

2. And at $\xi_2 = \xi_2^0$ and $\hat{\xi}_2$, initial and final boundary curves for the ξ_2 coordinate, the following are prescribed:

$$\begin{aligned}
 u^0 & \text{ or } \alpha_1 \left(N_{21}^0 + \frac{M_{21}^0}{R_1} \right) \\
 v^0 & \text{ or } \alpha_1 \left(N_2^0 + \frac{M_2^0}{R_2} \right) \\
 w^0 & \text{ or } \left[\frac{1}{\alpha_2} \frac{\partial}{\partial \xi_2} (\alpha_1 M_2^0) + \frac{\partial M_{21}^0}{\partial \xi_1} - \frac{M_1^0}{\alpha_2} \frac{\alpha \xi_1}{\partial \xi_2} + \frac{1}{(\alpha_1)^2} \frac{\partial}{\partial \xi_1} (M_{12}^0 \alpha_2^2) \right. \\
 & \quad \left. - \alpha_1 N_2^0 \beta_2^0 - \alpha_1 N_{21}^0 \beta_1^0 \right] \\
 \frac{1}{\alpha_2} \frac{\alpha \omega^0}{\alpha \xi_2} & \text{ or } -M_2^0
 \end{aligned} \tag{1.25-32}$$

It should be noted that if the linear strain-displacement equations Eqs. 1.22-2 were utilized instead of Eqs. 1.22-4 in the previous development the expressions resulting from the variational approach would be the simplified small deflection equilibrium equations identical to Eqs. 1.25-29. This fact could also be seen if ϵ^0 and β^0 are of same order of magnitude (linear elasticity assumption), the terms containing β^0 would vanish from the above and the classical equilibrium equations would result.

1.26 NONLINEAR EQUATIONS FOR CYLINDRICAL SHELLS

The nonlinear Eqs. 1.25-29 and 1.25-30 represent equilibrium conditions for shells of arbitrary shape. It will be useful for study of the principal characteristics of a nonlinear equation to consider a particular shell shape. A particularly simple set of equations for cylindrical shells was suggested by Donnell in 1934 (Ref. 1-50). Donnell simplified the strain-displacement relationships by ignoring the influence of the original shell curvature in the deformations due to bending and twisting moments. (Recall Eq. 1.13-69.) By this approximation, the relations between moments and changes in curvature and twist become the same as for flat plates. Although the simplifications imply certain limitations on their range of applicability, the equations have formed the basis of the nonlinear analyses that appear in the literature. Their relative simplicity also makes them ideally suited to illustrate the elements of a nonlinear theory.

The Donnell form of the nonlinear equilibrium equations for a cylindrical shell subjected to edge loading and to surface pressure $p = p(s, \theta)$ are given by

$$\frac{\partial N_x}{\partial x} + \frac{\partial N_{\theta x}}{\partial s} = 0$$

$$\frac{\partial N_{x\theta}}{\partial x} + \frac{\partial N_\theta}{\partial s} = 0$$

$$\left(\frac{\partial^2 M_x}{\partial x^2} + 2 \frac{\partial^2 M_{\theta x}}{\partial x \partial s} + \frac{\partial^2 M_\theta}{\partial s^2} \right) \frac{N_\theta}{R} - \frac{\partial(N_x \beta_\theta)}{\partial x} - \frac{\partial(N_{x\theta} \beta_x)}{\partial x} \quad (1.26-33)$$

$$- \frac{\partial(N_{\theta x} \beta_\theta)}{\partial s} - \frac{\partial(N_\theta \beta_x)}{\partial s} = -p$$

where s is circumferential coordinate given by

$$s = R \theta$$

$$\partial s = R \partial \theta$$

The elastic relations for the Donnell form of the equations are

$$N_x = \frac{Et}{1-\mu^2} (\epsilon_x + \mu \epsilon_\theta)$$

$$N_\theta = \frac{Et}{1-\mu^2} (\epsilon_\theta + \mu \epsilon_x)$$

$$N_{x\theta} = N_{\theta x} = \frac{Et}{2(1+\mu)} \gamma_{x\theta} \quad (1.26-34)$$

$$M_x = D(\kappa_x + \mu \kappa_\theta)$$

$$M_\theta = D(\kappa_\theta + \mu \kappa_x)$$

$$M_{x\theta} = M_{\theta x} = \frac{D(1-\mu)}{2} \kappa_{x\theta}$$

where the flexural rigidity of the shell is given by

$$D = Et^3 / [12 (1-\mu^2)]$$

The kinematical relations are

$$\epsilon_x = \frac{\partial u}{\partial x} + \frac{1}{2} \left(\frac{\partial w}{\partial x} \right)^2$$

$$\epsilon_\theta = \frac{\partial v}{\partial s} + \frac{w}{R} + \frac{1}{2} \left(\frac{\partial w}{\partial s} \right)^2$$

$$\gamma_{x\theta} = \frac{\partial u}{\partial s} + \frac{\partial v}{\partial x} + \frac{\partial w}{\partial x} \frac{\partial w}{\partial s}$$

$$\phi_x = \frac{\partial w}{\partial s}$$

$$\phi_\theta = \frac{\partial w}{\partial x}$$

$$\kappa_x = -\frac{\partial^2 w}{\partial x^2}$$

$$\kappa_\theta = -\frac{\partial^2 w}{\partial s^2}$$

$$\kappa_{x\theta} = -\frac{2\partial^2 w}{\partial x \partial s}$$

(1.26-35)

With these relations, the equilibrium equations may be expressed in the final form:

$$\frac{\partial N_x}{\partial x} + \frac{\partial N_{x\theta}}{\partial s} = 0$$

$$\frac{\partial N_{x\theta}}{\partial x} + \frac{\partial N_\theta}{\partial s} = 0$$

(1.26-36)

$$(D/R^2) \nabla^4 w + \frac{N_\theta}{R} + N_x \frac{\partial^2 w}{\partial x^2} + 2N_{x\theta} \frac{\partial^2 w}{\partial x \partial \theta} + N_\theta \frac{\partial^2 w}{\partial \theta^2} = p$$

where

$$\nabla^4 () = \frac{\partial^4 ()}{\partial x^4} + \frac{2 \partial^4 ()}{\partial x^2 \partial \theta^2} + \frac{\partial^4 ()}{\partial \theta^4}$$

Eqs. 1.26-36 may, of course, be explicitly expressed in terms of displacements u , v , and w , which in this case would represent three nonlinear differential equations in nondimensional displacement variables. Within the limitation of their accuracy they determine all linear and nonlinear equilibrium paths for the cylinder. The corresponding linear differential equations of equilibrium identical to those presented in Section 1.13.4-D are obtained from the above expressions by omission of all rotation terms in Eqs. 1.26-35 and 1.26-36.

The Donnell equations form the basis for a simplified version of cylinder stability equations which will be discussed in the next section. In addition, the Donnell equations in their homogeneous form have been widely used for problems of circular cylinders subjected to line, concentrated and arbitrary edge loads. A review of such solutions is presented in Ref. 1-51.

The system of equations that has been described is suitable for determining displacements and stresses corresponding to equilibrium configurations. To determine whether solutions of these equations represent stable or unstable states of equilibrium, it is necessary to study the second variations of the potential energy expression \bar{V} (Eq. 1.24-12). The discussion of stability and buckling of shells is presented in the next section.

1.27 SUMMARY

In this section, the equilibrium equations for shells based on the concepts of nonlinear elasticity were derived. The principle of potential energy was introduced and the use of variational techniques for obtaining the so-called "large deflection" equilibrium equations for shells was indicated. In addition, a simplified set of nonlinear equations frequently used in analyzing cylindrical shells was presented.

The concepts and equations presented in this section will be used in presenting the stability theory of shells described in the next section.

1.30 STABILITY THEORY OF SHELLS

1.31 INTRODUCTION

In the previous section, the governing nonlinear equations which determine the various equilibrium portions of a shell were derived. Possible equilibrium configurations which a shell can assume are stable, neutral, and unstable equilibrium. Therefore, in considering the problem of elastic equilibrium, it is necessary to consider the stability of the equilibrium configurations as well. It is essential to observe that, when there are several possible positions of equilibrium, that position which is given by the classical theory of elasticity is ordinarily unstable. The problem of shell buckling involves the determination of the particular values of the loading parameter at which various equilibrium positions are possible.

In a linear shell theory, displacements are proportional to loads. The essence of shell buckling, however, is a disproportionate increase in displacement resulting from a small increase in load. It becomes obvious that a nonlinear shell theory is required. Thus, shell buckling is fundamentally a subtopic of nonlinear shell theory.

The stability of shells can be determined from the equilibrium equations of nonlinear shell theory. Derivation of the nonlinear equations for

shells of arbitrary shape were presented in the previous section. Other forms may be found in many references, e. g. , Mushtari and Galimov (Ref. 1-52), and Sanders (Ref. 1-53).

An excellent survey of work in shell buckling was presented by Fung and Sechler (Ref. 1-54). A comprehensive description of research in progress may be found in the 1962 NASA collection of papers on shell stability (Ref. 1-55). Most attempts to obtain solutions to the equations for the buckling of shells have for the most part been restricted to only two shell shapes, the cylinder and the shallow spherical cap. The problem of the cylindrical shell will be utilized freely in subsequent discussion to illustrate the various methods used.

In principle, buckling loads for shells can be determined by suitably plotting all equilibrium paths given by the solutions to the nonlinear equilibrium equations, and observing the lowest load at which large lateral displacements result from small increases in applied load. Because of the obvious difficulty of such a procedure, it is usually preferred to determine only those particular points of the paths at which the equilibrium changes from a stable to a neutral state. To be more precise, the first appearance of a possible bifurcation in the solution corresponds to the critical load. That is, assume that some load on the shell is the critical load; then, according to this criteria, two possible infinitely close positions of

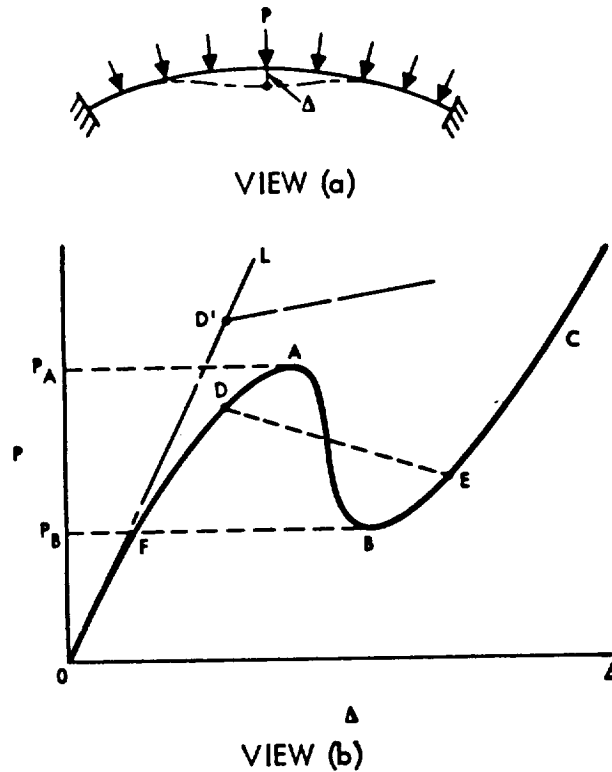
equilibrium exist. Two equivalent methods of the theory of elastic stability have been developed for determining the critical loads: the adjacent equilibrium theory and the minimum potential energy theorem (Ref. 1-9). The use of these methods for obtaining the shell stability equations will be illustrated in this section.

1.32 CONCEPT OF STABILITY

Before developing the shell stability equations, it may be worthwhile to briefly discuss the nature of the buckling process. It will be convenient to examine the load displacement characteristics of a representative shell model to introduce the concept of stability as related to shells. For purposes of illustration, consider the shallow spherical shell, shown in Fig. 1.32-1a, clamped at the outer edge and subjected to uniform external pressure. The displacement Δ at the apex of the shell will now be studied as a function of the applied load P . It will be assumed that representative but hypothetical load displacement curves for this model are given in Fig. 1.32-1b. The curves are introduced for discussion purposes and do not necessarily represent the actual physical solutions. Each position plotted in Fig. 1.32-b represents an equilibrium configuration. Points not on the line, of course, represent nonequilibrium configurations. The line itself is called an equilibrium path.

In linear shell theory, the load is proportional to the displacement, and the load displacement curve is a straight line, as shown by dashed line OL in Fig. 1.32-1b. Since yielding and large rotations are excluded, the line extends indefinitely in the direction indicated. Branching or bifurcation can occur from a linear elasticity path if rotation free equilibrium configurations

FIG. 1.32-1



exist for nonzero values of the load. A bifurcation point is illustrated by D' in Fig. 1.32-1b. The second path can slope upward, downward, or horizontal, depending on the shell configuration.

In general, the rotations of the elements of the shell effect the conditions of equilibrium. When this effect is taken into account, the conditions of equilibrium are given by a system of nonlinear equations. The resulting nonlinear load-displacement curve is illustrated by the solid line OABC in Fig. 1.32-1b.

It should be noted that the displacement Δ corresponding to a given load P is not unique unless $P > P_A$ or $P < P_B$. The behavior of the shell depends on whether P or Δ is the controlled variable. Under a controlled

displacement Δ (if this were possible), the equilibrium path is followed over its entire length, with the load P undergoing an appropriate decrease from A to B . However, if P is the controlled variable, a small increase in P above the value P_A causes the shell to jump from point A to point C without following the path. This large increase in displacement from a small increase in applied load is termed buckling. The load P_A is called the critical load.

For some shell configurations it is possible that there are two (or more) equilibrium paths between O and C . The configurations represented by points along $OABC$ are axisymmetric. Those along equilibrium path $ODEC$ are antisymmetric. Points at which an equilibrium path splits into two branches are called branch points or bifurcation points. They are denoted by small dots, as indicated. Buckling occurs at $P = P_D$. During buckling the shell can move along a nonequilibrium path from D to a point lying between B and C , viz., E .

A point in the equilibrium paths in Fig. 1.32-1b represents a condition of stable, neutral, or unstable equilibrium, depending upon whether the slope of the curve at the point is positive, zero, or negative. For example, points between O and A and between B and C on the line $OABC$ represent stable configurations whereas those between A and B represent unstable configurations.

1.33 ADJACENT EQUILIBRIUM METHOD

The adjacent equilibrium theory is based on the observation that at a critical load a second infinitesimally adjacent configuration exists for the same load. Therefore, the appearance of a possible bifurcation in the solution corresponds to the critical load. This criteria for determining critical loads will be used to obtain the differential equations representing stability of shells.

Denote u° , v° , w° , the prebuckled displacements corresponding to the initial equilibrium position which becomes unstable when the critical or buckling load is reached. The displacements corresponding to the new adjacent position occurring at buckling would then be represented by

$$\begin{aligned}u &= u^\circ + \lambda \bar{u} \\v &= v^\circ + \lambda \bar{v} \\w &= w^\circ + \lambda \bar{w}\end{aligned}\tag{1.33-1}$$

where \bar{u} , \bar{v} , \bar{w} represent arbitrary admissible displacement functions which satisfy appropriate laws of continuity, finiteness, and comply with the constraints. The parameter λ is an infinitesimally small quantity independent of shell coordinates. Thus, $\lambda \bar{u}$, $\lambda \bar{v}$, $\lambda \bar{w}$ are the incremental displacements to which positions on a shell shift from the initial configuration to the new adjacent position.

Now apply the nonlinear equations of equilibrium derived in the previous section (Eq. 1.25-29) to the second position of equilibrium of the shell. With the observation that u° , v° , w° are solutions to the nonlinear equilibrium equations, introduction of Eq. 1.33-1 into the equilibrium Eq. 1.25-29 with the omission of terms containing the factor λ to a degree higher than the second results in the following stability equations for the shell:

$$\begin{aligned}
& a_2 \frac{\partial \bar{N}_1}{\partial \xi_1} + \bar{N}_1 \frac{\partial a_2}{\partial \xi_1} + \frac{1}{a_1} \frac{\partial (\bar{N}_{21} a_1^2)}{\partial \xi_2} - \bar{N}_2 \frac{\partial a_2}{\partial \xi_1} \\
& + \frac{1}{R_1} \left[\frac{\partial (\bar{M}_1 a_2)}{\partial \xi_1} + \frac{1}{a_1} \frac{\partial}{\partial \xi_2} (\bar{M}_{21} a_1^2) - \bar{M}_2 \frac{\partial a_2}{\partial \xi_1} \right] \tag{1.33-2a}
\end{aligned}$$

$$+ \frac{a_1 a_2}{R_1} (-\beta_1^\circ \bar{N}_1 - \beta_2^\circ \bar{N}_{12} - \bar{\beta}_1 N_1^\circ - \bar{\beta}_2 N_{12}^\circ) + a_1 a_2 p_1 = 0$$

$$\begin{aligned}
& \frac{\partial}{\partial \xi_2} (\bar{N}_2 a_1) + \frac{1}{a_2} \frac{\partial (\bar{N}_{12} a_2^2)}{\partial \xi_1} - \bar{N}_1 \frac{\partial a_1}{\partial \xi_2} \\
& + \frac{1}{R_2} \left[\frac{\partial (\bar{M}_2 a_1)}{\partial \xi_2} + \frac{1}{a_2} \frac{\partial (\bar{M}_{12} a_2^2)}{\partial \xi_1} - \bar{M}_1 \frac{\partial a_1}{\partial \xi_2} \right] \tag{1.33-2b}
\end{aligned}$$

$$+ \frac{a_1 a_2}{R_2} (-\bar{N}_2 \beta_2^\circ - \bar{N}_{21} \beta_1^\circ - N_2^\circ \bar{\beta}_2 - N_{21}^\circ \bar{\beta}_1) + a_1 a_2 p_2 = 0$$

$$\begin{aligned}
& \alpha_1 \alpha_2 \left(\frac{\bar{N}_1}{R_1} + \frac{\bar{N}_2}{R_2} \right) + \frac{\partial}{\partial \xi_1} \left[\frac{1}{\alpha_1} \frac{\partial(\bar{M}_1 \alpha_2)}{\partial \xi_1} + \frac{1}{(\alpha_1)^2} \frac{\partial(\bar{M}_{21} \alpha_1^2)}{\partial \xi_2} \right. \\
& \left. - \frac{\bar{M}_2}{\alpha_1} \frac{\partial \alpha_2}{\partial \xi_1} + \alpha_2 (-\bar{N}_1 \beta_1^\circ - \bar{N}_{12} \beta_2^\circ - N_1^\circ \bar{\beta}_1 - N_{12}^\circ \bar{\beta}_2) \right] \\
& + \frac{\partial}{\partial \xi_2} \left[\frac{1}{\alpha_2} \frac{\partial}{\partial \xi_2} (\bar{M}_2 \alpha_1) - \frac{1}{(\alpha_2)^2} \frac{(\bar{M}_{12}^2 \alpha_2^2)}{\alpha \xi_1} - \frac{\bar{M}_1}{\alpha_2} \frac{\partial \alpha_1}{\partial \xi_2} \right. \\
& \left. - \alpha_1 (-\bar{N}_2 \beta_2^\circ - \bar{N}_{21} \beta_1^\circ + N_2^\circ \bar{\beta}_2 - N_{21}^\circ \bar{\beta}_1) \right] + \alpha_1 \alpha_2 q = 0
\end{aligned} \tag{1.33-2c}$$

where $(\bar{\quad})$ represents the contribution to the quantities (N and M) resulting from the incremental displacements \bar{u} , \bar{v} , \bar{w} . The \bar{N} and \bar{M} terms are obtained from Eq. 1.23-10.

For a cylindrical shell, utilizing the approximations of the Donnell theory discussed earlier (Section 1.26), the above stability equations for cylindrical shells, in terms of axial and circumferential coordinates x , and s are of the form

$$\begin{aligned}
\frac{\partial \bar{N}_x}{\partial x} + \frac{\partial \bar{N}_{x\theta}}{\partial s} &= 0 \\
\frac{\partial \bar{N}_{x\theta}}{\partial x} + \frac{\partial \bar{N}_\theta}{\partial s} &= 0
\end{aligned} \tag{1.33-3}$$

$$D \nabla^4 \bar{w} + \frac{\bar{N}_\theta}{R} + \left(N_x^\circ \frac{\partial^2 \bar{w}}{\partial x^2} + \frac{\partial^2 w^\circ}{\partial x^2} \bar{N}_x \right) \quad (1.33-3 \text{ cont})$$

$$+ 2 \left(N_{x\theta}^\circ \frac{\partial^2 \bar{w}}{\partial x \partial s} + \frac{\partial^2 w^\circ}{\partial x \partial s} \bar{N}_{x\theta} \right) + \left(N_\theta^\circ \frac{\partial^2 \bar{w}}{\partial s^2} + \frac{\partial^2 w^\circ}{\partial s^2} \bar{N}_\theta \right) = 0$$

where

$$N_x^\circ = \frac{Et}{1-\mu} \left[\frac{\partial u^\circ}{\partial x} + \frac{1}{2} \left(\frac{\partial w^\circ}{\partial x} \right)^2 + \mu \left(\frac{w^\circ}{R} \right) \right]$$

(1.33-4a)

$$N_\theta^\circ = \frac{Et}{1-\mu} \left[\frac{w^\circ}{R} + \mu \left(\frac{\partial u^\circ}{\partial x} \right) + \frac{1}{2} \left(\frac{\partial w^\circ}{\partial x} \right)^2 \right]$$

$$N_{x\theta}^\circ = \frac{Et}{2(1+\mu)} \left[\frac{\partial u^\circ}{\partial x} + \frac{\partial v^\circ}{\partial s} + 2 \frac{\partial w^\circ}{\partial x} \frac{\partial w^\circ}{\partial s} \right]$$

and the increment in nondimensional forces resulting from the incremental displacements are

$$\bar{N}_x = \frac{Et}{1-\mu} \left[\frac{\partial \bar{u}}{\partial x} + \frac{\partial w^\circ}{\partial x} \frac{\partial \bar{w}}{\partial x} + \mu \left(\frac{\partial \bar{v}}{\partial s} + \frac{\bar{w}}{R} + \frac{\partial w^\circ}{\partial s} \frac{\partial \bar{w}}{\partial s} \right) \right]$$

$$\bar{N}_\theta = \frac{Et}{1-\mu} \left[\frac{\partial \bar{v}}{\partial s} + \frac{\bar{w}}{R} + \frac{\partial w^\circ}{\partial s} \frac{\partial \bar{w}}{\partial s} + \mu \left(\frac{\partial \bar{u}}{\partial x} + \frac{\partial w^\circ}{\partial x} \frac{\partial \bar{w}}{\partial x} \right) \right]$$

(1.33-4b)

$$\bar{N}_{x\theta} = \frac{Et}{2(1+\mu)} \left[\frac{\partial \bar{u}}{\partial s} + \frac{\partial \bar{v}}{\partial x} + \frac{\partial w^\circ}{\partial x} \frac{\partial \bar{w}}{\partial s} + \frac{\partial w^\circ}{\partial s} \frac{\partial \bar{w}}{\partial x} \right]$$

When Eq. 1.33-4 is substituted into Eq. 1.33-3, the latter represents three linear differential equations in \bar{u} , \bar{v} and \bar{w} with variable coefficients corresponding to displacements u° , v° , w° which represent solutions for the initial positions of equilibrium. Since no restriction has been placed on u° , v° , and w° the stability equations permit the determination of critical loads whether the initial equilibrium paths are linear or nonlinear.

This procedure results in the replacement of nonlinear differential equations of equilibrium by linear differential equations of stability. However, in general, u° , v° , w° are solutions of the original nonlinear set; hence, Eq. 1.33-3 is of little use without additional simplifying restrictions. The most common simplification is to apply the equations of classical shell theory to the initial position of equilibrium such that u° , v° , w° are restricted to points along the linear elasticity path. This approximation assumes that angles of rotation which correspond to the initial position of equilibrium are of the same order as strains. Thus, the coefficients u° , v° , w° are given by the solution of the linear equilibrium equations instead of the nonlinear ones. This restriction of u° , v° , w° to points along the linear elasticity path is the distinguishing characteristic of linear stability theory. A further simplification is usually introduced in linear stability analysis. Since it is assumed that classical theory is applicable to the pre-buckled state, then for consistency, all terms explicitly containing prebuckled rotations can be omitted from Eq. 1.33-2.

If these terms are neglected, the stability equations (1.33-3) reduce to the form

$$\frac{\partial N_x}{\partial x} + \frac{\partial N_{x\theta}}{\partial s} = 0$$

$$\frac{\partial N_x}{\partial x} + \frac{\partial N_\theta}{\partial s} = 0 \quad (1.33-5)$$

$$D \nabla^4 \bar{w} + \frac{\bar{N}_\theta}{R} + N_x^\circ \frac{\partial^2 \bar{w}}{\partial x^2} + 2N_{x\theta}^\circ \frac{\partial^2 \bar{w}}{\partial x \partial s} + N_\theta^\circ \frac{\partial^2 \bar{w}}{\partial s^2} = 0$$

where

$$\bar{N}_x = \frac{Et}{1-\mu} \left[\frac{\partial \bar{u}}{\partial x} + \mu \left(\frac{\partial \bar{v}}{\partial s} + \frac{\bar{w}}{R} \right) \right]$$

$$\bar{N}_\theta = \frac{Et}{1-\mu} \left[\left(\frac{\partial \bar{v}}{\partial s} + \frac{\bar{w}}{R} \right) + \mu \frac{\partial \bar{u}}{\partial x} \right] \quad (1.33-6)$$

$$\bar{N}_{x\theta} = \frac{Et}{2(1+\mu)} \left[\frac{\partial \bar{u}}{\partial s} + \frac{\partial \bar{v}}{\partial x} \right]$$

Eq. 1.33-5 are referred to as the Donnell stability equations in coupled form. They may be written in terms of admissible displacement components \bar{u} , \bar{v} , \bar{w} by substitution of Eq. 1.33-1 into Eq. 1.33-5.

A more familiar uncoupled form is obtained by suitable differentiation and recombination (Ref. 1-44) to yield:

$$R\nabla^4 \bar{u} = -\mu \frac{\partial^3 \bar{w}}{\partial x^3} + \frac{\partial^3 \bar{w}}{\partial x \partial s^2}$$

$$R\nabla^4 \bar{v} = -(2 + \mu) \frac{\partial^3 \bar{w}}{\partial x^2 \partial s} - \frac{\partial^3 \bar{w}}{\partial s^3} \quad (1.33-7)$$

$$D\nabla^8 \bar{w} + \frac{Et}{R^2} \frac{\partial^4 \bar{w}}{\partial x^4} + \nabla^4 \left[N_x^\circ \frac{\partial^2 \bar{w}}{\partial x^2} + 2N_{x\theta}^\circ \frac{\partial^2 \bar{w}}{\partial x \partial s} + N_\theta^\circ \frac{\partial^2 \bar{w}}{\partial s^2} \right] = 0$$

Thus, for linear stability theory, the prebuckled displacements u° , v° , w° are obtained by solution of the linear shell equilibrium equations from the linear theory (Paragraph 1.13-4-D) with prescribed boundary conditions. These quantities are known functions of shell coordinates x and θ and of the magnitude of the applied load. By substituting these functions into Eq. 1.33-7, a set of linear homogeneous differential equations is arrived at for \bar{u} , \bar{v} , and \bar{w} .

The resulting system has a nontrivial solution only for certain definite values of the load parameter. These values represent the characteristic values of the system. To each such characteristic value, there corresponds a point of bifurcation of the solution of the equations.

The boundary conditions prescribed must be satisfied at both the initial and adjacent positions of equilibrium. As shown by Novozhilov (Ref. 1-10), for geometric boundaries, a set of homogeneous boundary conditions result for \bar{u} , \bar{v} , \bar{w} .

This adjacent equilibrium method is a basic technique for investigating elastic stability and reduces the problem of finding critical loads to that of determining the characteristics of a system of linear homogeneous differential equations with prescribed boundary conditions.

1.34 ENERGY METHOD

The adjacent equilibrium method has the advantage of yielding exact solutions. However, the mathematical complexity is such that it is more convenient in many instances to use a different criterion. For this purpose, the so-called potential energy method will be adopted for determination of buckling loads. The minimum potential energy theory of stability is based on the observation that the total potential energy of a loaded shell is a relative minimum for stable configurations along the equilibrium paths but is only stationary for unstable configurations. Recall from Section 1.24 that displacement functions which made the potential energy stationary corresponded to equilibrium positions. This characteristic was utilized in obtaining the nonlinear equilibrium equations; however, it was not possible to determine whether the potential energy was a minimum, thereby characterizing a stable configuration. The critical load on the shell can thus be defined as the lowest load at which the total potential energy ceases to be a relative minimum for configurations along the equilibrium path. The magnitude of the critical load may be determined by consideration of the second variation of the total potential energy expression. The equilibrium is stable only if the second variation of the total potential energy is positive definite.

The second variation expression using results of Section 1.24 is given by

$$\left. \frac{d^2 \bar{V}}{d\lambda^2} \right|_{\lambda=0} = \bar{V}_2 = \bar{U}_2 - \bar{W}_2 \quad (1.34-8)$$

$$\begin{aligned} \bar{V}_2 = \frac{1}{2} \int_{\xi_1^*}^{\hat{\xi}_1} \int_{\xi_2^*}^{\hat{\xi}_2} \int_{-t/2}^{t/2} & \left\{ \bar{\sigma}_1 \bar{e}_1 + \bar{\sigma}_2 \bar{e}_2 + \bar{\tau}_{12} \bar{e}_{12} \right. \\ & \left. + 2 \left[\sigma_1^{\circ} \bar{e}_1 + \sigma_2^{\circ} \bar{e}_2 + \tau_{12}^{\circ} \bar{e}_{12} \right] \right\} a_1 a_2 d\xi_1 d\xi_2 dz \quad (1.34-9) \end{aligned}$$

The strain and stress equations (1.25-18 and -21, respectively) can be substituted into the above to yield an expression in terms of the displacement functions u° , v° , and w° and admissible increments \bar{u} , \bar{v} , and \bar{w} . The resulting expression constitutes a second variation expression suitable for examination of the stability of any configuration along the equilibrium path. These equations are the energy counterpart of the differential equations of stability (Eq. 1.33-2) presented earlier. In fact, for a shell in a position of neutral equilibrium, the second variation expression vanishes; and the

appropriate integration by parts of Eq. 1.34-9, noting arbitrariness of the increments \bar{u} , \bar{v} , and \bar{w} , would result in the identical stability equations described by Eq. 1.33-2.

The energy counterpart of the Donnell stability equation for cylindrical shells can be obtained by substituting strain terms (Eq. 1.25-19) into the second variational energy expression. Neglecting prebuckling rotations β_1° and β_2° , in the expression (Eq. 1.34-9) results in the second variation of the potential energy of the form (integrating over the thickness):

$$\begin{aligned} \bar{V}_2 = & \frac{EtR^2}{(1-\mu^2)} \int_0^{2\pi} \int_0^{\frac{L}{a}} \left\{ \left[\bar{e}_x^2 + \bar{e}_\theta^2 + 2\mu \bar{e}_x \bar{e}_\theta + \frac{1-\mu}{2} \bar{e}_{x\theta}^2 \right] \right. \\ & + k \left[\left(\frac{\partial^2 \bar{w}}{\partial x^2} \right)^2 + \left(\frac{\partial^2 \bar{w}}{\partial \theta^2} \right)^2 + 2\mu \frac{\partial^2 \bar{w}}{\partial x^2} \frac{\partial^2 \bar{w}}{\partial \theta^2} + 2(1-\mu) \left(\frac{\partial^2 \bar{w}}{\partial x \partial \theta} \right)^2 \right] \\ & \left. + \frac{1-\mu}{Et} \left[N_x^\circ \left(\frac{\partial \bar{w}}{\partial x} \right)^2 + N_\theta^\circ \left(\frac{\partial \bar{w}}{\partial \theta} \right)^2 + 2N_{x\theta}^\circ \frac{\partial \bar{w}}{\partial x} \frac{\partial \bar{w}}{\partial \theta} \right] \right\} dx d\theta \end{aligned} \quad (1.34-10)$$

where

R = the middle surface radius,

$k = 1/12 (t/R)^2$,

$$N_x^{\circ} = \frac{Et}{1-\mu} (\epsilon_x^{\circ} + \mu \epsilon_{\theta}^{\circ}), \text{ etc;}$$

are recalled from Eq. 1.26-34.

According to the Trefftz condition (Refs. 1-24 and 1-55), the limit of positive-definiteness of the second variation expression is determined by the Euler equations for the integral, where the variations are taken with respect to \bar{u} , \bar{v} , and \bar{w} . Determination of the Euler equations for the integral in Eq. 1.34-10 again yields the Donnell stability equations (Eq. 1.33-3).

In summary, all linear and nonlinear equilibrium paths for shells can be determined from the nonlinear differential equations of equilibrium (Eq. 1.25-29) from the previous section. Complete determination of the equilibrium paths of course determines maximum and bifurcation points. Due to mathematical complexity, it is difficult to obtain complete solutions to the nonlinear equations. The differential equations of stability, (Eqs. 1.33-2a-c) or their energy counterpart (Eq. 1.34-10) permit determination of only those particular points along the path at which the equilibrium changes from stable to neutral. The linear stability equations determine such points along the linear elasticity path. To illustrate the significance of these various equations, two kinds of analyses for the axially compressed cylinder are examined in the following section. In one kind,

nonlinear equilibrium paths are determined by approximate solutions of the equilibrium equations. In the other kind, critical points on the nonlinear equilibrium path are determined by approximate solutions of the stability equations. These developments will proceed within the framework of the discussion on the discrepancy between theoretical results and experimental values.

1.35 "CLASSICAL" BUCKLING ANALYSIS

Previously, the shell stability equations were obtained from the nonlinear equilibrium equations by use of the adjacent equilibrium method. In general, the resulting equations are a set of linear homogeneous differential equations with variable coefficients. These coefficients represented solutions for the initial or prebuckled state with loading magnitudes implicit in the solution. The critical or buckling loads can be obtained from these equations by solution of the associated eigen or characteristic value problem. To illustrate the procedure involved, consider the so-called classical buckling problem. In particular, the (classical) buckling loads of axially loaded (perfect) cylindrical shells will be determined from the solution of the Donnell-type stability equations.

The stability equations from a nonlinear prebuckling form were given by Eq. 1.33-3. Let us consider now the problem of an axially compressed cylinder that is perfect before it is loaded. In this case, the prebuckled deformation is axisymmetric, therefore, from Eq. 1.33-1

$$\begin{aligned}u^0 &= u^0(x) \\v^0 &= 0 \\w^0 &= w^0(x)\end{aligned}\tag{1.35-11}$$

and Eq. 1.33-3 simplifies to

$$\frac{\partial \bar{N}_x}{\partial x} + \frac{\partial \bar{N}_{x\theta}}{\partial s} = 0$$

$$\frac{\partial \bar{N}_{x\theta}}{\partial x} + \frac{\partial \bar{N}_\theta}{\partial s} = 0 \quad (1.35-12)$$

$$D \nabla^4 \bar{w} + \frac{\bar{N}_\theta}{R} + \left(N_x^o \frac{\partial^2 \bar{w}}{\partial x^2} + \frac{\partial^2 w^o}{\partial x^2} \bar{N}_x \right) + N_\theta^o \frac{\partial^2 \bar{w}}{\partial s^2} = 0$$

with similar simplification of Eq. 1.33-5.

The prebuckled displacements are obtained by specializing the nonlinear equations of equilibrium for axial symmetry, as follows

$$\frac{\partial N_x^o}{\partial x} = 0$$

$$D \frac{\partial^4 w^o}{\partial x^4} + \frac{N_\theta^o}{R} + N_x^o \frac{\partial^2 w^o}{\partial x^2} = 0 \quad (1.35-13)$$

Because of the special circumstance that a uniform compressive load is applied only at the end of the cylinder, the nonlinear equations become linear constant coefficient equations since

$$N_x^o = \text{constant} = +P \text{ (applied compressive end load)} \quad (1.35-14a)$$

and

$$N_\theta^o = Et \frac{w^o}{R} - \mu P \quad (1.35-14b)$$

In the classical buckling problem, it is assumed that the cylinder ends are unrestrained until buckling occurs, then it becomes simply supported. Thus, for these special boundary conditions, the prebuckled configurations obtained from the solution of Eq. 1.35-13 becomes

$$w^0 = + \frac{\mu P}{Et} R \quad (1.35-15)$$

and

$$N_{\theta}^0 = 0$$

The solutions indicate a rotation-free equilibrium condition. For this special case, the solution to the nonlinear and linear equilibrium paths coincide. For this problem, stability is determined from the simplified equation obtained by substitution of Eqs. 1.35-14 and 15 into Eq. 1.35-12. The resulting equations can be combined to yield a simple eight order equation (Ref. 1-19) of the form

$$D \nabla^8 \bar{w} + P \nabla^4 \frac{\partial^2 \bar{w}}{\partial x^2} + \frac{Et}{R^2} \frac{\partial^4 \bar{w}}{\partial x^4} = 0 \quad (1.35-16)$$

Determination of the smallest P for the nontrivial solution of Eq. 1.35-16, in accordance with the adjacent equilibrium theory, yields the associated bifurcation points along the nonlinear and linear equilibrium path.

A solution of Eq. 1.35-16 that satisfies the boundary conditions of simple support at the end of the cylinder is

$$w = A \sin \frac{n\pi x}{L} \cos m \frac{s}{R} \quad (1.35-17)$$

Substitution of Eq. 1.35-17 into the stability equation (Eq. 1.35-16), yields the following stability criteria for the nontrivial solution, after appropriate minimization with respect to integers m and n

$$P = (N_x^0)_{cl} = \frac{Et^2}{\sqrt{3(1-\mu^2)} R} \quad (1.35-18)$$

This criteria is called the "classical buckling load" in the literature.

In the analyses discussed, the conditions of no edge restraint resulted in considerable simplification of the buckling problem for the assumption that the effect of boundary conditions had little effect on buckling, especially for long cylinders. If the cylinder shell has edge restraint throughout its loaded configuration, solution of Eq. 1.35-13 will not result in a constant deformation, w, but will be a function of x. Substitution of the prebuckled deformation into Eq. 1.35-12 results in a more complicated form, since the selection of the eigenvalue problem requires consideration of variable coefficients in the differential equations. The influences of these edge restraints on prebuckling deformations and, consequently, buckling loads will be discussed in the next section. A similar approach can be used in obtaining classical linear buckling loads for spherical and conical shells (Ref. 1-26).

1.36 DISCREPANCY BETWEEN THEORETICAL AND EXPERIMENTAL RESULTS

The solution of the linear stability equation Eq. (1.35-16) for a cylinder under axial compression yields

$$\sigma_{c1} \approx 0.606 \frac{Et}{R} \quad (1.36-19)$$

This value is called the "classical buckling stress." It represents the lowest bifurcation point on the linear elasticity path, as illustrated by Fig. 1.36-1. This theoretical value is compared with the experimental test data (Ref. 1-56) for axially compressed cylinders in Fig. 1.36-2. As can be seen, there is a serious disagreement between the results of classical and experiment stress for the buckling of isotropic cylindrical shells. Similar discrepancies can be observed for other shell shapes and loading conditions. Many investigators have attempted to explain this discrepancy.

One of the most significant of the early investigations was performed by Von Kármán and Tsien (Ref. 1-57) who first used nonlinear shell theory to investigate the large deflection behavior of an axially compressive cylinder. These investigators attempted to determine the nonlinear equilibrium path that branches off at the linear theory bifurcation point. In their analysis, they chose to determine the nonlinear branch by use of

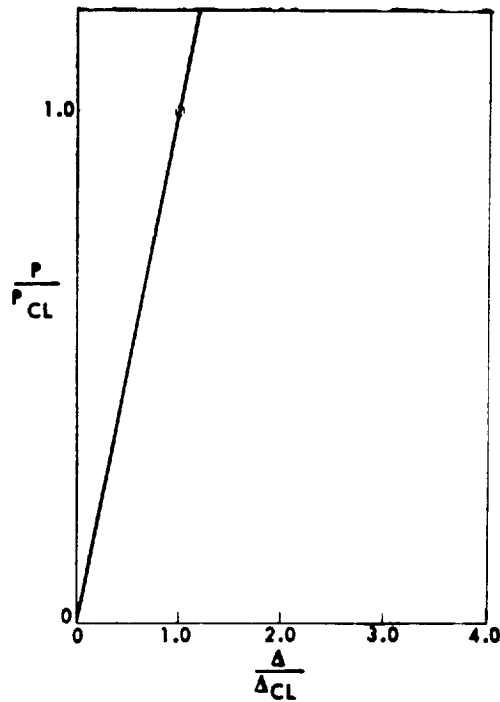


FIG. 1.36-1. Linear-Theory Bifurcation Point for the Axially Compressed Cylinder

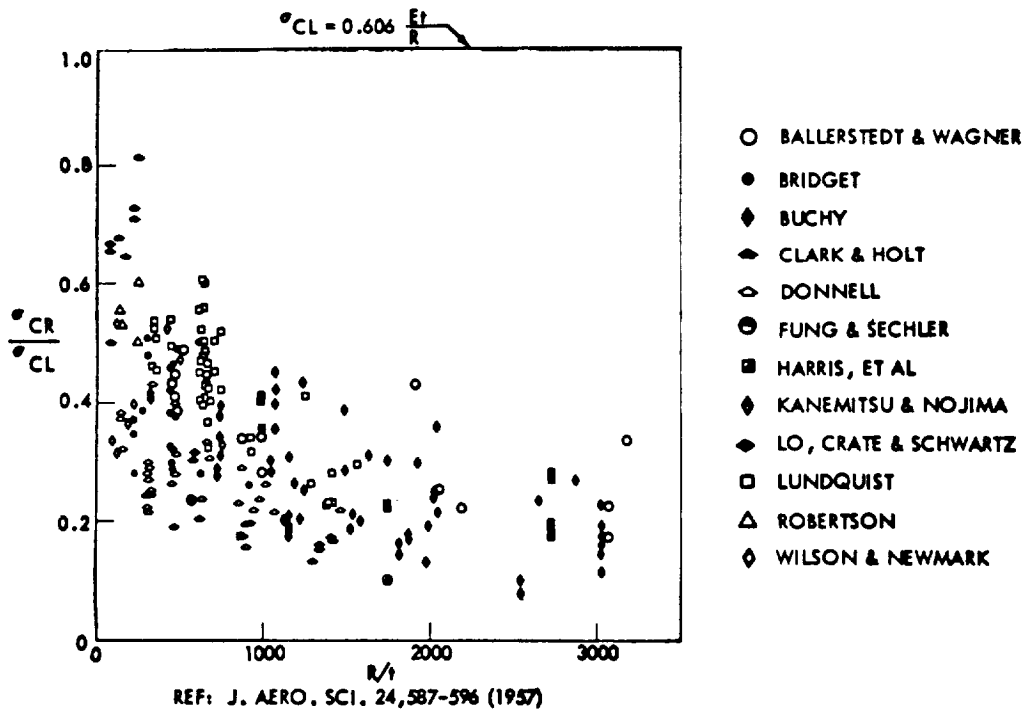


FIG. 1.36-2. Axially Compressed Cylinder Test Data

the potential energy expression and a Raleigh-Ritz approach rather than by solution of Eqs. 1.35-12 and -13. For a displacement function, w , these investigators assumed an expression

$$w = a_{00} + a_{11} \cos(m\pi x) \cos(n\pi\theta) + a_{20} \cos(2m\pi x) + a_{02} \cos(2n\pi\theta) \quad (1.36-20)$$

where m and n are wavelength parameters and the a_{ij} 's are constants. Substitution of Eq. 1.36-20 into the appropriate form of the potential energy expression (Ref. 1-57) yields a quartic polynomial in the a_{ij} 's. For equilibrium (see nonlinear theory section), the requirement that

$$\frac{\partial \bar{V}}{\partial a_{ij}} = 0 \quad (1.36-21)$$

must be satisfied. The results showed that existence of finite deflection equilibrium configurations at loads considerably less than the classical buckling load occurred. The results obtained by Von Kármán and Tsien are given by the curve in Fig. 1.36-3.

Several investigators have extended the Von Kármán-Tsien analysis in order to determine the effect of inclusion of more degrees of freedom in the assumed deflection function for the Raleigh-Ritz analysis. Curve A in Fig. 1.36-4 is the result of critical load obtained by Kempner (Ref. 1-58); curve B is the results obtained by Almroth (Ref. 1-59). It was hoped that a minimum postbuckling load could be established from such an approach. However, in recent studies performed by Hoff at

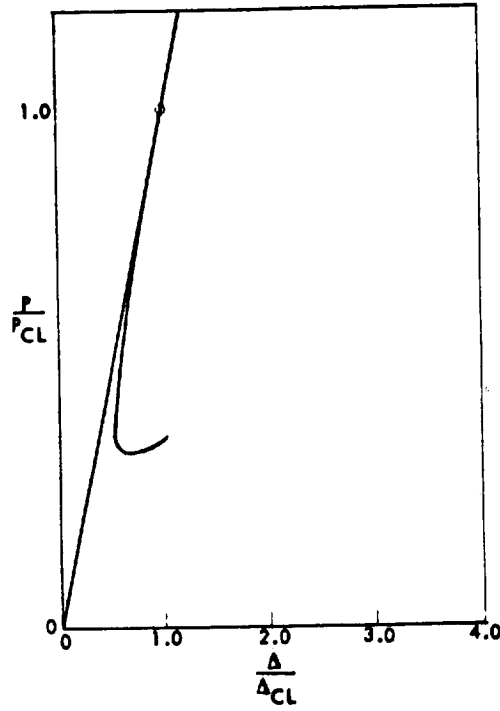


FIG. 1.36-3. Load-Displacement Curve for Perfect Cylinder

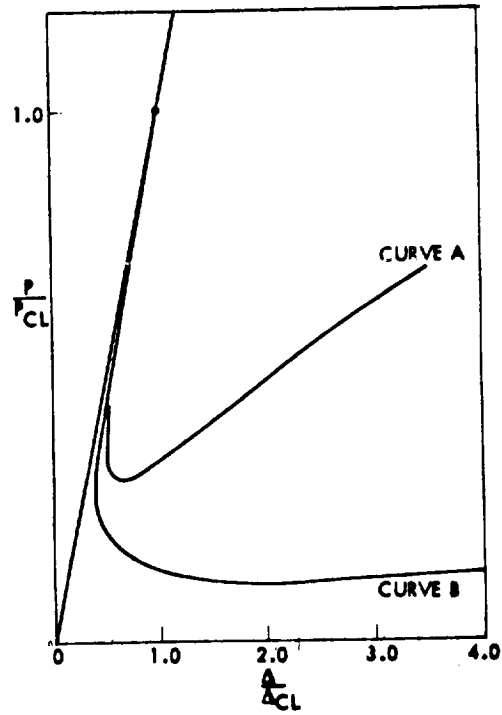


FIG. 1.36-4. Load Displacement Curves for Perfect Cylinder

Stanford University (Ref. 1-60), postbuckling equilibrium configurations approaching a zero loading condition were obtained using a refinement of this approach.

Although these analyses determined the nonlinear equilibrium path, it did not change the bifurcation point load. Tests show that the cylinder jumps from the unbuckled configuration to one of the nonlinear branches without passing through the linear theory bifurcation point. There has been much speculation concerning the cause of this cylinder jump and the resulting discrepancy between observed and calculated loads. Weak stability has been one of the first explanations suggested as to a possible cause of the jump. (Ref. 1-57.) Von Kármán and Tsien showed that the stability of an axially compressed cylinder is weak, and suggested that accidental vibrations of the test machine or disturbances in the laboratory caused the cylinder to jump over a potential barrier to a lower load. This suggestion was a reasonable one, however, various test programs conducted since the work of Von Kármán and Tsien have strongly indicated that accidental disturbances are not the major reason for the reduction in critical loads in laboratory tests (Ref. 1-59). This is not meant to imply that the loss of stability due to external disturbances is not an important design consideration, but simply that it is not believed to be an important factor in ordinary laboratory buckling tests.

Von Kármán and Tsien also suggested that imperfections which were inevitable in manufacture, such as initial shape irregularities in the test cylinder, might cause a roundoff of the sharp peak between the linear and nonlinear branches of the load-displacement curve, and, thus, result in a lower maximum point.

To perform an initial imperfection analysis for cylindrical shells, it is necessary to modify the nonlinear equations of equilibrium for slightly noncylindrical shells. The nonlinear equations of the imperfect cylinder (Eq. 1.33-3) become (Ref. 1-61)

$$\begin{aligned}\frac{\partial N_x}{\partial x} + \frac{\partial N_{x\theta}}{\partial \theta} &= 0 \\ \frac{\partial N_{x\theta}}{\partial x} + \frac{\partial N_\theta}{\partial \theta} &= 0\end{aligned}\quad (1.36-22)$$

$$D\nabla^4 w + \frac{N_\theta}{R} + N_x \frac{\partial^2 (w^* + w)}{\partial x^2} + 2N_{x\theta} \frac{\partial^2 (w^* + w)}{\partial x \partial \theta} + N_\theta \frac{\partial^2 (w^* + w)}{\partial \theta^2} = 0$$

where w^* is the initial imperfection from the cylindrical form; w^* would also cause a modification in the form of the strain displacement relations.

The initial imperfection, w^* , in these equations is an arbitrary function of x and θ . Solution of the equations for a particular w^* determines the corresponding nonlinear equilibrium path and critical load. A systematic study of various initial shapes will firmly establish the role

of initial imperfections in buckling analysis. A general evaluation of various values of w^* has not been performed to date due to the mathematical difficulties involved. However, two specialized initial imperfection analyses of particular significance have been reported in literature.

In 1950, Donnell and Wan (Ref. 1-62) presented analysis with consideration of an initiator imperfection of the form

$$w^* = \frac{K-1}{2} w \quad (1.36-23)$$

where K is an imperfection constant. This form does not represent a particular initial shape but probably does represent one of the most influential imperfections for each equilibrium configuration. Instead of attempting to solve Eqs. 1.36-22, Donnell and Wan used the corresponding potential energy expression and the Raleigh-Ritz procedure for their analysis. Donnell and Wan selected a displacement function of the general form of Eq. 1.36-20 and, following a similar procedure as Von Kármán and Tsien, were able to determine a nonlinear equilibrium path for a given imperfection parameter, K . The results of their analysis is shown in Fig. 1.36-5. The critical load for cylindrical shells is characterized by a maximum point on a nonlinear path. Although the Donnell and Wan results substantially contribute to an understanding of the role of imperfections, the analysis has two limitations: (1) relatively few degrees of freedom were considered in the Raleigh-Ritz analysis and,

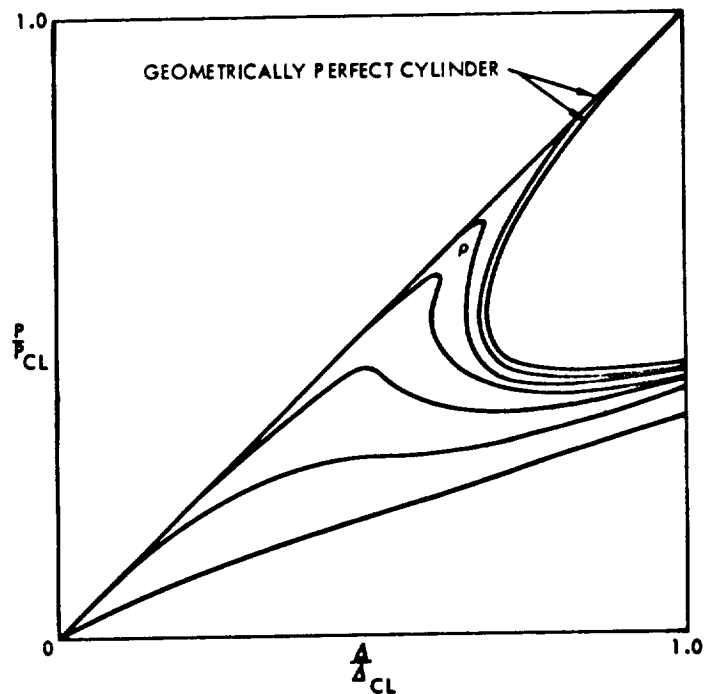


FIG. 1.36-5. Load-Displacement Curves for Imperfect Cylinders

as previously noted, (2) the imperfection does not represent a particular initial shape.

An imperfection analysis which does represent a particular initial shape was reported by Koiter in Ref. 1-63. The solution of the nonlinear equations can be significantly simplified by considering initial imperfections to be axisymmetric. As shown in Section 1.35, such a specialization of the set of nonlinear partial differential equations yields a set of nonlinear ordinary differential equations. For the particular case of an axially loaded cylinder the fact that $N_x^0 = P$, (a constant), for any prebuckled displacement $w_0 = w_0(x)$ yields a set of linear ordinary

differential equations with constant coefficients. Eq. 1.36-22, with appropriate modification to include initial imperfection, can be solved explicitly for arbitrary axisymmetric imperfections. Koiter investigated the form

$$w^* = -\mu t \cos 2\rho x \quad (1.36-24)$$

where μ is amplitude of imperfection as a fraction of shell thickness, and ρ is a wave length parameter. A Galerkin (Ref. 1-63) procedure was used to solve the variable coefficient equations. The results of the Koiter analysis are shown in Fig. 1.36-6 for the case where ρ was selected to coincide with the axisymmetric buckled mode of a perfect cylindrical shell. It can be seen that an initial imperfection amplitude equal to the shell thickness is sufficient to reduce the buckling load to only 20 percent of the corresponding value for the perfect cylinder.

In careful tests performed at Lockheed (Ref. 1-61 and at the California Institute of Technology (Ref. 1-73), unusually high buckling loads (85 to 90 percent of classical) have been obtained when initial imperfections were carefully minimized. Brush and Almroth (Ref. 1-59) were able to repeat buckling loads in their tests for a given cylinder, but the results were quite different for different cylinders. The results of these tests and the analytical results described have given a strong indication that initial imperfections have a serious effect of buckling loads.

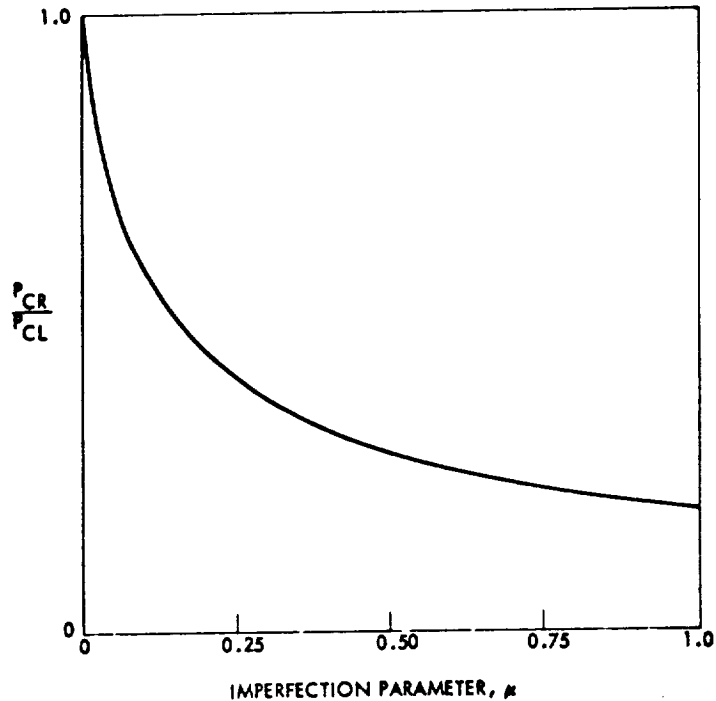


FIG. 1.36-6. Critical Loads for Imperfect Cylinders

A possible cause of the discrepancies observed between theory and the influence of edge effects was suggested by Stein (Ref. 1-64) and Fischer (Ref. 1-65) who investigated the influence of prebuckled deformations. In the classical analysis described in Section 1.35 the influence of edge restraint on prebuckling deformation was neglected. However, in reality, the diameter of the restrained cylinder tends to increase under axial compression loading due to Poisson's ratio effects. This increase is prevented at the ends of the cylinder by its boundary restraints. Hence, the generators of the cylinders are distorted prior to buckling and axial forces in the cylinder at the ends are eccentric relative to portions of the shell wall near midlength. When this eccentricity is

considered, the theoretical prebuckling equilibrium becomes nonlinear. Stein and Fischer sought a bifurcation point along this nonlinear path.

The analysis proceeds similarly to that described in this section except that the prebuckled deformations obtained from the solution of Eq. 1.36-22 is now a function of the x coordinate for restrained boundaries. In the classical theory, w^0 was constant. In this case, the resulting stability equations have variable coefficients and it becomes more complicated to determine the bifurcation points. Both Stein and Fischer considered simply supported shells and solved the equations numerically. The approaches were quite similar except for differences in the in-plane boundary condition. Stein assumed zero tangent restraint ($N_{x0} = 0$) at the boundary, while Fischer assumed the perhaps more likely restraint that the tangential displacement vanishes ($v = 0$). The results obtained were substantially different as shown by the results given in Fig. 1.36-7. These results appear to indicate that different in-plane boundary conditions can lead to a wide variation in results. Almroth (Ref. 1-66) recently presented solutions for other boundary restraint conditions.

In an earlier investigation based on linear stability theory, Ohira (Ref. 1-67) used boundary conditions similar to Stein and found a bifurcation point at a relatively low load along the linear elasticity path. His results are also shown in Fig. 1.36-7. Hoff also reported lower buckling

loads based on linear stability theory in Ref. 1-68. All these results show that the edge effect can be a significant factor in reducing the theoretical buckling loads.

The results discussed to this point have related to the buckling of cylindrical shells under axial compression. Similar discrepancies have been observed for other loading conditions and shell shapes. For example, Fig. 1.36-8 shows a comparison of experimental and theoretical values (e. g., Ref. 1-72), for the case of a spherical cap under uniform normal pressure. This problem has been treated extensively in the literature. Here again there is a significant discrepancy between theoretical

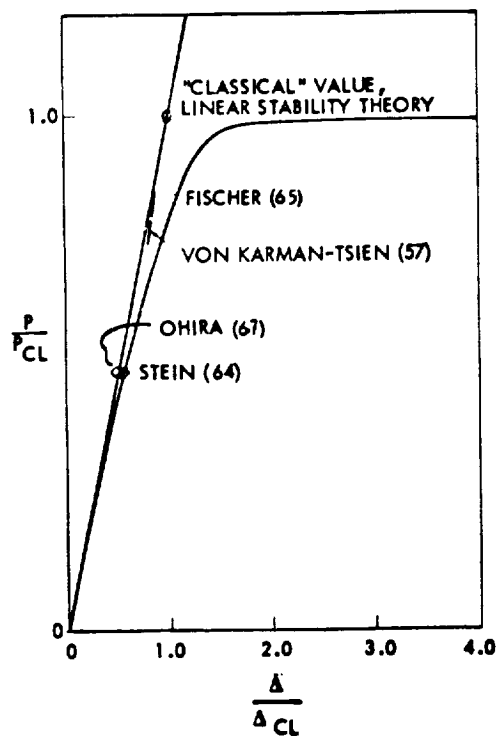


FIG. 1.36-7. Axially Compressed Cylinder Bifurcation Points

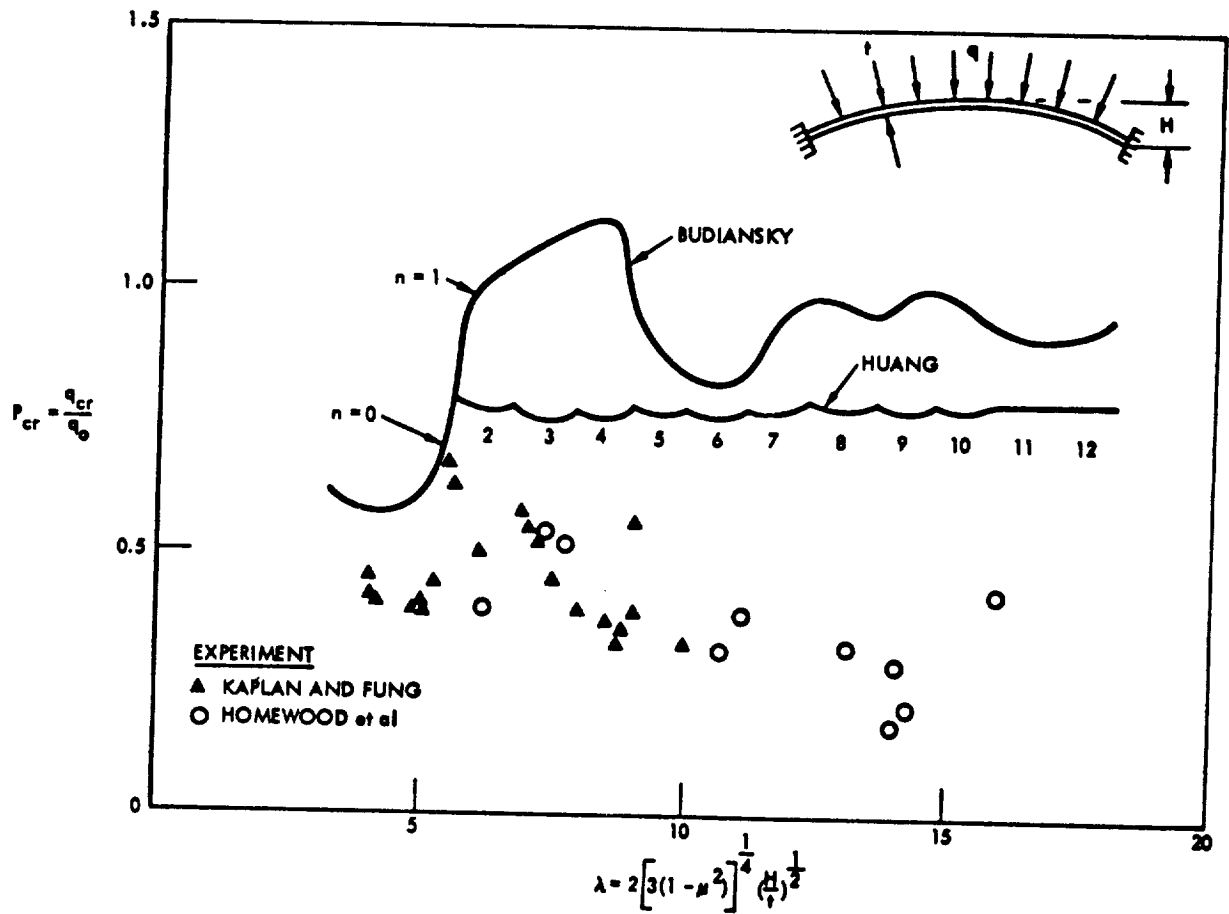


FIG. 1.36-8. Consolidated Buckling Pressures of Clamped, Shallow, Spherical Shells and Experimental Results

values and test data. The theoretical results shown for axisymmetric buckling were obtained by Budiansky (Ref. 1-69); and results shown for an unsymmetric buckling load were obtained by Huang (Ref. 1-70).

Additional information pertinent to the design and stability analysis of shells may be found in the excellent texts of Gerard (1-71), Timoshenko (1-74), Bleich (1-75) and Cox (1-76).

SHELL ANALYSIS MANUAL

By E. H. Baker, A. P. Cappelli, L. Kovalevsky,
F. L. Rish, and R. M. Verette

Distribution of this report is provided in the interest of information exchange. Responsibility for the contents resides in the author or organization that prepared it.

Prepared under Contract No. NAS 9-4387 by
NORTH AMERICAN AVIATION, INC.
Downey, Calif.

for Manned Spacecraft Center

NATIONAL AERONAUTICS AND SPACE ADMINISTRATION

For sale by the Clearinghouse for Federal Scientific and Technical Information
Springfield, Virginia 22151 - CFSTI price \$3.00

155 A.

1.37 SUMMARY AND CONCLUSIONS

The static nonlinear stability theory of thin shells has been discussed in relation to its use in shell buckling analysis. The stability equation of shells were derived based on the nonlinear equilibrium equation. Certain well-known approximate solutions of the nonlinear equations for axially compressed cylinders were discussed. The severe discrepancy between theoretical and experimental results was noted.

From the foregoing discussions, it is not difficult to see why there has been little agreement between theoretical and experimental results for critical loads of shell structures since apparently infinitesimal deviations in boundary conditions and in the shape of the shell yield drastic reduction in critical loads. For the researcher, these results indicate that he must always be aware of the problem to which his investigations actually apply and of the implication of the assumptions he makes. Nonlinear theory can be used to consider the influence of both initial imperfections and edge effects in shell buckling analysis. It is believed that accurate formulation of a problem in terms of this theory and exact solution of the equations would result in a close agreement between theoretical and experimental results. At present, for actual practice, however, this procedure is prohibitively difficult. Nonlinear theory serves to broaden our knowledge of shell buckling analysis and to clarify the meaning and limitations of

linear stability theory, but at present it is not a design tool for direct determination of the buckling load.

The designer must be exceedingly careful in applying results of analysis and experimentation in order that the shell structures for which the results were obtained apply to the structures for which he is designing.

REFERENCES

- 1-1 Aron, H. J. reine angew. Math., Vol. 78 (1874) p. 136.
- 1-2 Love, A. E. H. Phil. Trans. Royal Soc., Vol. 17A (1888) pp. 491-546.
- 1-3 Love, A. E. H. A Treatise on the Mathematical Theory of Elasticity, 4th Edition, New York: Dover Publications (1944).
- 1-4 Naghdj, P. M. "A Survey of Recent Progress in the Theory of Elastic Shells," Applied Mechanics Review, Vol. 9, No. 9 (Sept. 1956) pp. 365-368.
- 1-5 Novozhilov, V. V. The Theory of Thin Shells. Groningen, The Netherlands: P. Noordhoff Ltd., (1959).
- 1-6 Striuk, Dirk, J. Differential Geometry. Reading, Massachusetts: Addison-Wesley Publishing Co., Inc. (1957).
- 1-7 Kreszig, E. Differential Geometry. University of Toronto Press (1959).
- 1-8 Eisenhart, L. P. An Introduction to Differential Geometry. Princeton University Press (1947).
- 1-9 Wang, Chi-Teh. Applied Elasticity. New York: McGraw-Hill Book Co., Inc. (1953).
- 1-10 Novozhilov, V. V. Foundations of the Nonlinear Theory of Elasticity. Rochester, New York: Graylock Press (1953).

- 1-11 Reissner, E. "A New Derivation of the Equations for the Deformation of Elastic Shells," American Mathematical Society (Dec. 1940).
- 1-12 Sokolnikoff, I.S. *Mathematical Theory of Elasticity*. New York: McGraw-Hill Book Co., Inc. (1956) p. 59.
- 1-13 Naghdi, P.M. "On the Theory of Thin Elastic Shells," Quar. Jour. of App. Math., Vol. 14 (1956) pp. 369-380.
- 1-14 Sanders, J.L. An Improved First-Approximation Theory for Thin Shells. NASA TR R 24 (1959).
- 1-15 Hildebrand, Reissner, and Thomas. Notes on the Foundations of the Theory of Small Displacements of Orthotropic Shells. NACA TN 1833 (March 1949).
- 1-16 Vlasov, V. Z. General Theory of Shells and Its Applications in Engineering. NASA Technical Translations, NASA TTF-99 (1949).
- 1-17 Budiansky, B. and J.L. Sanders, Jr. "On the Best First Order Linear Shell Theory," Progress in Applied Mechanics. New York: Macmillan Co. (1963).
- 1-18 Flügge, W., "Statik und Dynamik der Schalen," Berlin, Germany: Springer-Verlag (1957).
- 1-19 Byrne, Ralph, Jr., "Theory of Small Deformations of a Thin Elastic Shell," *Seminar Reports in Mathematics, Univ. of Calif., at Los Angeles*, published in Math, N. S. Vol. 2, No. 1 (1944), pp. 103-152.

- 1-20 Biezene, C.B. and R. Grammel. Technische Dynamik. Berlin: Julius Springer (1939) pp. 466-469.
- 1-21 Lure, A.I. "The General Theory of Thin Elastic Shell," Publ. Mat. Mech. Akademiya Nauk. S.S.R., IV, 2 (1940).
- 1-22 Kempner, J. Unified Thin-Shells Theory, Symposium on the Mechanics of Plates and Shells for Industry Research Associates, Polv. Inst. of Brooklyn, PIBAL No. 566 (Mar. 9-11, 1960).
- 1-23 Bassett, A. B. VI "On the Extension and Flexure of Cylindrical and Spherical Thin Elastic Shells," Phil. Trans. Ray. Soc. (London) Ser. A, Vol. 181, No. 6 (1890) pp. 433-480.
- 1-24 Trefftz, E. Ableitung der Schalenbiegungs-gleichungen mit dem Castizhano schem Prinzip, Z. f. a. M. M., Bd 15 (1935).
- 1-25 Reissner, E. "The Effect of Transverse Shear Deformation on the Bending of Elastic Plates," Jour. Appl. Mech., Vol. 12, No. 2 (June 1945).
- 1-26 Timoshenko, S.P. and S. Woinowsky-Krieger. Theory of Plates and Shells. New York: McGraw-Hill Book Co., Inc. (1959).
- 1-27 Reissner, H. Spannungen in Kurzschaalen, Müller-Breslau, Festschr. (1912).
- 1-28 Meissner, E. "Das Elastizitätsgesetz für dünne Schalen von Ringflächen, Kugel- and Kegelform," Phys. Zeitschr, Bd. 14 (1913).

- 1-29 Meissner, E. "Über Elastizität und Festigkeit dünner Schalen," Viertelschr. d. natur. Ges., Bd 60, Zurich (1915).
- 1-30 Reissner, E. On the Theory of Thin Elastic Shells. H. Reissner Anniversary Volume (1949), pp. 231-247.
- 1-31 Clark, R.A. "On the Theory of Thin Elastic Toroidal Shells," Journal of Mathematics and Physics, Vol. 29 (1950) pp. 146-178.
- 1-32 Naghdi, P.M., and C.N. De Silva. "Deformation of Elastic Ellipsoidal Shells of Revolution," Proc. 2nd U.S. National Congress of Applied Mechanics (1954), pp. 333-343.
- 1-33 Naghdi, P.M. On the Theory of Thin Elastic Shells. Office of Naval Research Proj. NR-064-400, Contract No. 1224 (01), Technical Report 1, University of Michigan (Jan 1958).
- 1-34 Hildebrand, F. "On Asymptotic Integration in Shell Theory," Proc. Symp. Applied Mathematics, Vol. 3 (1950), pp. 53-66.
- 1-35 Geckeler, J. Über die Festigkeit Achsensymmetrischer Schalen, Forsch, Arb. a. d., Geb. Ing. West (1926).
- 1-36 Esslinger, M. Statische Berechnung von Kesselbenden. Berlin: Springer-Verlag (1952).
- 1-37 Structures Manual, "Section 6, Thin Shells." Aerojet General (1960).
- 1-38 Bleich, H.H. and M.G. Salvadori. "Bending Moments on Shell Boundaries," Proc. ASCE, Journal Structures Division (Dec 1950), pp. 396-398.
- 1-39 Blumenthal, G. "Über die Asymptotische Integration," etc., Zeitschrift für Mathematik and Physik, Vol. 62 (1914), p. 343.

- 1-40 Hetenyi, M. "Spherical Shells Subjected to Axial Symmetrical Bending," Intern. Assoc. of Bridge and Struct. Engr., Pub., Vol. 5, Zurich (1938), pp. 173-185.
- 1-41 Coates, W.M. "State of Stress in Full Heads of Pressure Vessels," ASME Trans. Vol. 52, No. 22 (1930), pp. 117-131.
- 1-42 Reissner, E. "Stresses and Small Displacements of Shallow Spherical Shells," Journal of Math. Physics, 25 (1946).
- 1-43 Hetenyi, M. Beams on Elastic Foundation. University of Michigan Press (1946).
- 1-44 Donnell, L.H. Stability of Thin Walled Tubes Under Torsion. NACA, TR No. 479 (1933).
- 1-45 Kempner, J. "Remarks on Donnell's Equations," Journal of Applied Mechanics, Vol. 22, No. 1 (March 1955).
- 1-46 Goldenveizer. Theory of Elastic Thin Shells, New York: Pergamon Press (1961).
- 1-47 Flügge, Wilhelm. Stresses in Shells, Berlin, Germany: Springer-Verlag (1962).
- 1-48 Koiter, W. T. "The Theory of Thin Elastic Shells," Proceedings of the Symposium on, I. U. T. A. M. Delft 24-28 Aug. (1959). Amsterdam: North Holland Pub. Co. (1960).
- 1-49 Courant, R. and D. Hilbert. Methods of Mathematical Physics, Vol. 1. New York: Interscience Publishers (1953).

- 1-50 Donnell, L.H. "A New Theory for the Buckling of Thin Cylindrical Shells Under Axial Compression and Bending," *ASME Trans.*, Vol. 56 (Nov. 1934), pp. 795-806.
- 1-51 Pohle, F.V. "Solutions for Simplified Circular Cylindrical Shell Equations," *Symposium on the Mechanics of Plates and Shells for Industry Research Associates, Polytechnic Institute of Brooklyn* (March 1960).
- 1-52 Mushtau, Kh.M. and K.Z. Galinov. Non-Linear Theory of Thin Elastic Shells, Russian translational series (NASA TT-F62), Wash. 25, D.C.: U.S. Department of Commerce (1957).
- 1-53 Sanders, Lyell J., Jr. Nonlinear Theories for Thin Shells. Contract NONR 1866(02), Office of Naval Research, Tech. Report No. 10, Cambridge, Massachusetts: Harvard Press (Feb. 1961).
- 1-54 Fung, Y.C., and E.E. Sechler. "Instability of Thin Elastic Shells," Structural Mechanics, New York: Pergamon Press (1960), pp. 115-168.
- 1-55 Collected Papers on Instability of Shell Structures, Langley Research Center, NASA TND-1510 (December 1962).
- 1-56 Harris, L.A., H.S. Suer, W.T. Skene, and R.J. Benjamin. "The Stability of Thin-Walled Unstiffened Circular Cylinders Under Axial Compression Including the Effects of Internal Pressure," J. Aero. Sci., Vol. 24 (Aug. 1957), pp. 587-596.

- 1-57 Von Kármán, Th and H.S. Tsien. "The Buckling of Thin Cylindrical Shells Under Axial Compression," J. Aero. Sci., Vol. 8 (June 1941), pp. 303-312.
- 1-58 Kempner, J. "Postbuckling Behavior of Axially Compressed Circular Cylindrical Shells," J. Aero. Sci. 21 (1954), pp. 329-342.
- 1-59 Almroth, B., A. Holmes, and D. Brush. "An Experimental Study of the Buckling of Cylinders Under Axial Compression," presented at SESA Spring Meeting, Salt Lake City, May 6-8, 1964.
- 1-60 Hoff, N. J., W. A. Madsen, and J. Mayers. "Postbuckling Equilibrium of Axially Compressed Circular Cylindrical Shells," AIAA Journ., Vol. 4, No. 1 (January 1966).
- 1-61 Brush, D. O. Lecture Notes on Static and Dynamic Stability of Structure Short Course, UCLA, June 22-July 3, 1965.
- 1-62 Donnell, L. H. and C. C. Wan. "Effects of Imperfections on Buckling of Thin Cylinders and Columns Under Axial Compression," J. Appl. Mech., Vol. 13 (March 1950), pp. 73-83.
- 1-63 Koiter, W. T. The Effect of Axisymmetric Imperfections on the Buckling of Cylindrical Shells Under Axial Compression. Lockheed Missiles and Space Company Report 6-90-63-86 (Aug. 1963).
- 1-64 Stein, M. Notes on the Influence of Prebuckling Deformations and Stresses on the Buckling of Perfect Cylinders. Lecture on the Static and Dynamic Stability of Structures, UCLA (Sept. 23-Oct. 4, 1963).

- 1-65 Fischer, G. "Über den Einfluss der Gelenkigen Lagerung auf die Stabilität dünnwandiger Kreiszyinderschalen unter Axiallast und Innendruck." Z. Flugwissenschaften, Jahrg. 11, Heft 3 (March 1963) pp. 111-119.
- 1-66 Almroth, B.O. "Influence of Edge Conditions on the Stability of Axially Compressed Cylindrical Shells," AIAAJ. Vol. 4, No. 1 (Jan. 1966).
- 1-67 Ohira, H. "Local Buckling Theory of Axially Compressed Cylinders," Proc. Eleventh Japan Natl. Cong. for Appl. Mech., Tokyo (1961).
- 1-68 Hoff, N.J. and Tsai-Chen Soong. Buckling of Circular Cylindrical Shells in Axial Compression N65-14484, Stanford University, Dept. of Aeronautics and Astronautics, SUDAER No. 204 (1964).
- 1-69 Budiansky, B. "Buckling of Clamped Shallow Spherical Shells," Proc. of IUTAM Symposium on the Theory of Thin Elastic Shells. Amsterdam: North-Holland Publishing Co. (1960), pp. 64-85.
- 1-70 Huang, N.C. "Unsymmetrical Buckling of Shallow Spherical Shells," AIAA J., Vol. 1 (1963), pp. 945-946.
- 1-71 Gerard, G. Introduction to Structural Stability Theory. New York: McGraw-Hill Book Co., Inc. (1962).
- 1-72 Parameter, R.R. "The Buckling of Clamped Shallow Spherical Shells Under Uniform Pressure," U.S. Air Force Office of Scientific Research Dept. 5362 (Nov. 1963).

- 1-73 Parameter, R. R. "The Buckling of Clamped Shallow Spherical Shells Under Uniform Pressure." Ph. D Thesis, California Institute of Technology, Pasadena, California (1964).
- 1-74 Timoshenko, S. P. and J. M. Gere. Theory of Elastic Stability, McGraw-Hill Book Co., New York (1961).
- 1-75 Bleich, F. Buckling Strength of Metal Structures, McGraw-Hill Book Co., New York (1952).
- 1-76 Cox, H. L. The Buckling of Plates and Shells, The Macmillan Co., New York (1963).

2.00 PROCEDURES FOR STATIC ANALYSIS OF SHELL STRUCTURES

2.10 INTRODUCTION

GENERAL

In this chapter some of the results of Chapter 1.00 will be applied to solve shell problems. Chapter 1.00 defined the structural shell and several shell theories, with their limitations and ramifications. It was pointed out that the thickness-to-radius-of-curvature ratio, material behavior, type of construction (e. g. , honeycomb sandwich or ring-stiffened shells), types of loadings, and other factors all play a role in establishing which theory is applicable. Furthermore, shallow versus nonshallow shells required different approaches even though they fell into the same thin shell theory.

In this chapter, nonshallow shells will be analyzed. The resulting differential equations for nonshallow shells have solutions which will be tabulated for the solution of simple and complex rotationally symmetric geometries subjected to arbitrary rotationally symmetric loads. There are certain restraining conditions, called edge restraints, that the solution must satisfy. The edge restraints are reduced to unit loads and, by making the solution of the differential equations satisfy these unit edge restraints, the influence coefficients for the geometry are obtained. These influence

coefficients, etc., are then used to solve problems that involve determining stresses, strains, and displacements in simple and complex geometries.

In the following sections, surface loads, inertia loads, and thermally induced loads are included in the equilibrium equations and will be part of the so-called "membrane solution." The membrane solutions are called "primary solutions" and solutions for the unit edge restraints are called "secondary solutions."

GEOMETRICAL CONSIDERATIONS OF SHELL SEGMENTS

In this portion of the manual, a shell or the combination of shells shown in Fig. 2.10-1, having the characteristics of (a) nonshallow thin shell of revolution, (b) rotationally symmetrically loaded, and (c) rotationally symmetrical distribution of materials, are treated. In addition, the described procedure is limited to the so-called "thin" shell category described in Chapter 1.00.

A thin shell is defined as a shell that conforms to the Navier hypothesis and the Bernoulli-Euler theory of bending. A basic assumption in this theory is that a normal plane section before bending remains a normal plane section after bending, and without extension. Also, in this theory, anticlastic bending is neglected. A characteristic of a nonshallow shell is that the bending moment exists only in the neighborhood of the edge of the shell or in the area where a concentrated load is applied.

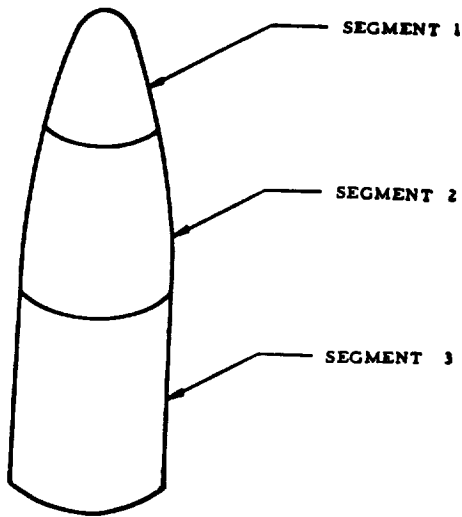


FIG. 2.10-1. Combined Shell

Novozhilov (Ref. 2-1)

recommends the criterion that a thin shell be defined as a shell where the relation t/R (where t is the thickness, and R is the radius of average curvature) can be neglected in comparison to unity. If this relationship

does not exist, the so-called "thick" shell theory may have to be used. The division into thin and thick shells is still artificial and arbitrary unless those values which are negligible in comparison to unity are defined. For example, if it is assumed that the usual error of 5 percent is permissible, then the range of thin monocoque shells will generally be dictated by the relation $t/R < 1/20$. The great majority of monocoque shells commonly used in practice are in the $1/1000 < t/R < 1/50$ range which means that they belong to the thin shell family. However, as was noted above, the division into thin and thick shells is arbitrary and depends on degree of accuracy that is required for the solution of the problem. If an error of 20 to 30 percent is permissible, the theory of thin shells can be used with caution even where $t/R \leq 1/3$.

Furthermore, only thin shells with small deflections in the elastic range will be discussed in this section (i. e., the deflection of the shell must

be small in comparison to the wall thickness). Loads and material restrictions are such that the laws of the linear theory of elasticity are applicable.

After the analysis is conducted, the result should be qualified to ensure that the deflection is small in comparison with the wall thickness.

MEMBRANE SOLUTION

The membrane theory for shells assumes that the basic resistance of the shell to load is by inplane tension, compression, and shear. Bending and twisting are neglected.

A membrane is a two-dimensional equivalent of the cable that resists loading through tensile stresses. This is illustrated in Fig. 2.10-2.

The shape of the cable or membrane as defined below is a function of the loading; with a change or redistribution of the loading, its shape immediately will change to allow response to the loading with tension stresses only.

BENDING FORCES AND THEIR INTERACTION WITH MEMBRANE FORCES

Consider a membrane made from catenaries as shown in Fig. 2.10-2 which found its equilibrium position under the illustrated loading condition. If this deflected membrane could be made rigid by some technique and the loading reversed, as shown in Fig. 2.10-3, then the loading will be resisted by internal compressive stresses.

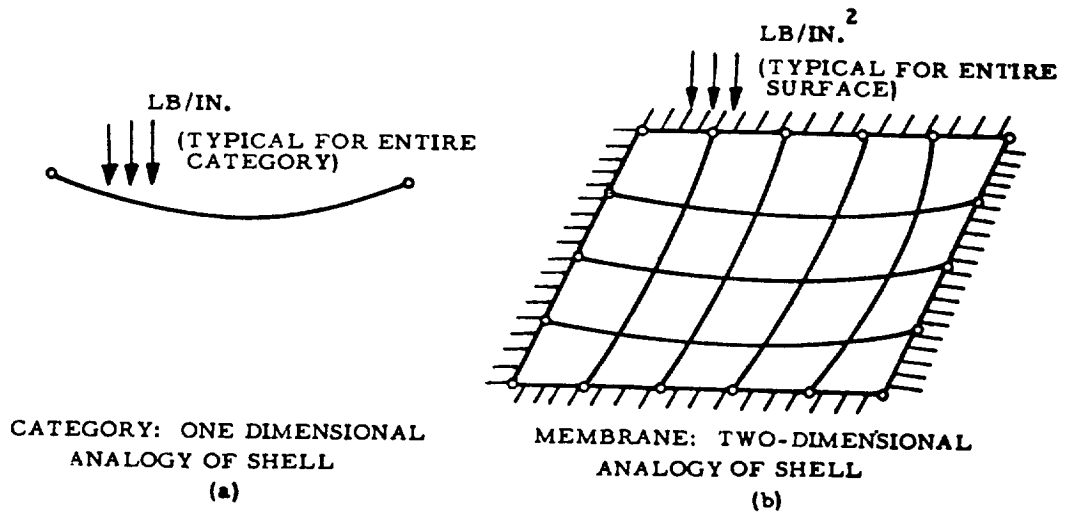


FIG. 2.10-2. Analogs of Shell

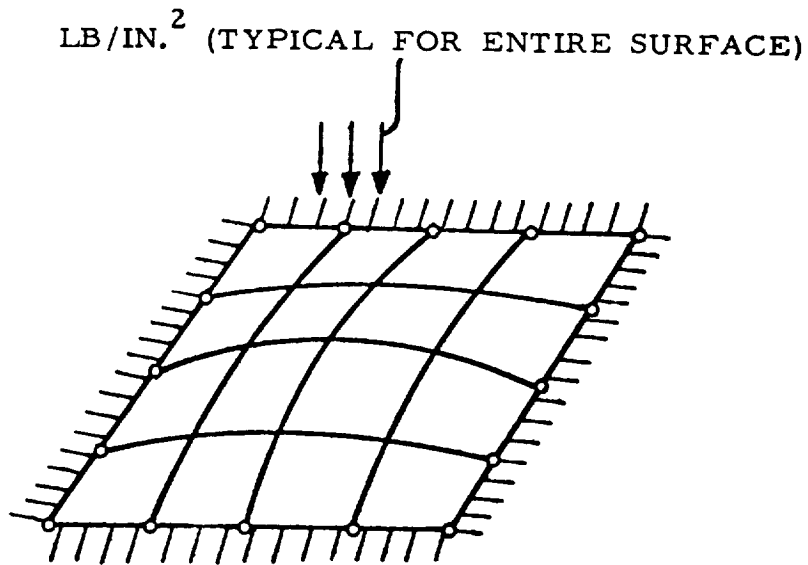


FIG. 2.10-3. Shell

The thin shell must be capable of resisting both tension and compression. In reality, the similarity between the thin shell and membrane is not complete, because of so-called boundary disturbances. For nonshallow shells, the effects of edge moments and shears are usually localized in the region immediately adjacent to the boundary. (In shallow shells the edge effects and concentrated loads are felt throughout the entire shell.) Consequently, the shell, unlike the membrane, will also be able to resist some moments, but this resistance is not the prime function of the ideal shell.

For better understanding of the shell bending action, the following analogies can be given: A plate supported along the edges and loaded perpendicularly to the plate surfaces, is actually a two-dimensional equivalent of a beam supported at the ends and loaded perpendicularly to the beam axis. In this case the plate, like the beam, resists loads by two-dimensional bending and shear. Beams resist loads by one-dimensional moment and shear. The plate is a two-dimensional surface. A shell is also a surface, but is three-dimensional. Bending is resisted by the shell in a similar manner to the plate, except that for the plate, bending is the main characteristic resistance and for a shell it is only secondary.

UNIT EDGE LOADING METHOD OF SOLUTION

The unit-loading method, generally regarded in practice as an economical and effective way of solving this type of problem, is treated briefly in this section. Unit-loads, which will be defined in detail in subsequent sections, are unit moment, unit shear, and unit in-plane edge loads from which the so-called influence coefficients are determined. These influence coefficients are used to build up solutions of shell segments (see Fig. 2.10-1), to get the solution of a complicated shell. This method has the advantage of being applicable to most practical problems because it enables the stress analyst to solve complex geometries in terms of combinations of known solutions for simple geometries. This is done by substituting the complex geometry by cones, spheres, cylinders, tori, etc., for which solutions are generally known, and then piecing the solutions together. These solutions, when pieced together, must satisfy continuity conditions as well as the equilibrium condition at the junction of the shell segments. The unit loads are used in the equilibrium condition.

2.20 GENERAL APPROACH OF UNIT-LOADING METHOD

In this section, membrane and bending theories will be discussed for application in the unit loading method; then, the interaction process between the shell geometries will be presented. This permits any complicated shell structure to be broken down into simpler shell elements; the unit-loading method will then be applied to obtain the solution for the complicated shell.

2.21 INTRODUCTION

2.21.1 Nature of Statically Indeterminate Structures

Generally, a shell is a statically indeterminate structure. The internal forces of the shell are determined from six equations of equilibrium, which are derived from the three force and three moment equilibrium conditions.

There are ten unknowns that make the problem internally statically indeterminate because determination of the unknowns does not depend on the supports. The situation is similar to a truss which, as used in practice, is a highly statically indeterminate system. If reactions to the applied loading can be found with the help of known equations of statical equilibrium, the system is externally determinate; however, a truss is a statically indeterminate system internally because instead of the assumed simplification (which introduces hinges at the joints), all joints are welded or riveted together. This introduces the moment into the members. However, this additional influence is known to be negligible. To find the statically indeterminate values, deformations must be considered.

The main objective of the following sections is to bypass the elaborate calculations by replacing the classical methods of elasticity theory with the simplified but accurate procedure called the unit loading method. This is accomplished by enforcing the conditions of equilibrium, compatibility in

displacement, and rotations at the junctions. The following paragraphs will review the membrane and bending theories.

2.22 MEMBRANE AND BENDING THEORIES

After discussion of the membrane and bending theories, it will be shown how both theories can be combined to achieve a simpler and more accurate method to determine stresses and deformations.

2.22.1 Membrane Theory

The elaborate calculation of statically indeterminate values may be bypassed with the help of an approximation method that can lead to useful results for most cases in practice. This method is called the membrane theory. Its justification and success are closely connected with the interplay of forces in curved surface structures, as explained in the introduction.

Of ten unknown stresses acting on the differential element of a shell (two bending moments, two torsional moments, two normal shears, two in-plane shears, and two in-plane loads), only four are of any significance. Consequently, a simplified theory was formed which assumes that normal shears, bending moments, and twisting moments are negligibly small compared to other terms; hence, they are set equal to zero.

The membrane theory is based on the assumption that only two in-plane shears and two in-plane loads are significant. This theory neglects all rest of the above-mentioned loads. The membrane theory is applicable only if boundary conditions are compatible with conditions of equilibrium, as shown in Fig. 2.22-1. It is noted in Fig. 2.22-2 that the concentrated loads

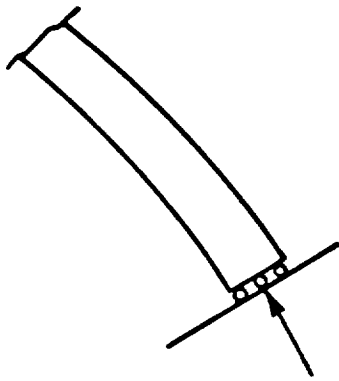


FIG. 2.22-1. Boundary Conditions Compatible With the Membrane Theory

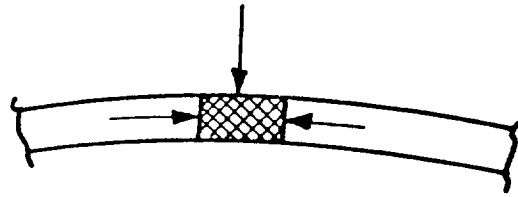


FIG. 2.22-2. Disequilibrium Due to Concentrated Load

normal to the middle surface are not compatible with the membrane theory because of local out-of-plane forces.

2.22.2 Bending Theory

The bending theory, in which all stresses, including vertical shear, bending, and twisting are considered, is more general and exact than the membrane theory. Unfortunately, as shown in previous discussion in the introductory chapters, this method is much more elaborate. However, in certain instances, this theory can be simplified when applied to rotationally symmetric geometries subjected to rotationally symmetric loads.

2.22.3 Comparison of Membrane and Bending Theories for Nonshallow Shells

The bending theory is more general than the membrane theory because it permits use of all possible boundary conditions. To compare the two theories, assume a nonshallow spherical shell with some axisymmetrical loading and built in along the edges. When the results are compared, the following conclusions can be made:

1. The stresses and deformations are almost identical for all locations of the shells with the exception of a narrow strip on the shell surface which is adjacent to the boundary. This narrow strip is generally no wider than \sqrt{Rt} , where R is the radius and t is the thickness of the spherical shell.
2. Except for the strip along the boundary, all bending moments, twisting moments, and vertical shears are negligible; this causes the entire solution to be practically identical to the membrane solution.
3. Disturbances along the supporting edge are very significant; however, the local bending and shear decrease rapidly along the meridian, and may become negligible outside of the narrow strip, as described in item 1.

2.22.4 Combined Bending and Membrane Theory

Since the bending and membrane theories give practically the same results except for a strip adjacent to the boundary, the simple membrane theory can be used; then, at the edges, the influences (moments and shears) can be applied to bring the displaced edge of the shell into the position prescribed by boundary conditions. The bending theory is used for this operation leading to final formulas. Consequently, once the solutions are obtained, they can be used later without any special derivation. The results obtained from application of both theories can be superimposed, which will lead to the final results being almost identical to those obtained by using the exact bending theory.

2.22.5 Unit-Loading Method Applied to the Combined Theory

The solution of a shell of revolution under axisymmetrical loading can be conducted in a simplified way, known as the unit-loading method;

1. Assume that the shell under consideration is a free membrane. Obtain a solution for this membrane. Find the overall stresses and distortions of the edge. This is the primary solution. The primary solutions for frequently used loadings and geometries can be collected and tabulated. The category of primary solutions includes a list of such solutions obtained by other methods when the membrane theory failed to provide the answer.

2. Apply the following edge loadings:

- a. Moment in pound inches per inch along the edge
- b. Horizontal shear in pounds per inch along the edge
- c. Vertical shear in pounds per inch along the edge.

These loadings should be of such magnitude as to be able to return the distorted edge of membrane into a position prescribed by the nature of supports (edge condition). The third edge loading in the majority of cases is not necessary. The amount of applied corrective loadings depend on the magnitude of edge deformations due to the primary solution. The exact magnitude will be determined by the interaction procedure to be explained later. However, to start the interaction process, formulas will be necessary for deformations due to the following:

- a. Unit-edge moment: $M = 1$ pound inches per inch
- b. Unit-edge horizontal shear: $Q = 1$ pound per inch
- c. Unit-edge vertical shear: $V = 1$ pound per inch

These solutions will be referred to as unit edge influences, or as secondary solutions.

3. Having the primary and unit edge solutions, these can be entered into the interaction process. This will

determine the correct amount of corrective loadings M , Q , and V ; all stresses and distortions due to these loadings can then be determined.

4. Superposition of stresses and distortions obtained by primary solution and corrective loadings lead to the final solution.

The solution obtained is almost equivalent to that solution obtained by the application of the exact bending theory.

2.23 INTERACTION BETWEEN SHELLS OF VARIOUS GEOMETRIES

Usually, structures are represented by a system of simple members that mechanically interact with each other. A shell can be regarded as one of these possible members. For example, missiles, boosters, and space vehicles contain bulkhead and cylinder combinations; both shells are built into each other; and consequently, a stress-strain discontinuity relationship exists for each of these shell elements. Analytical methods are required to determine stresses and deflections including the effects of interaction.

2.23.1 Breakdown for Complicated Shell Geometry

Complicated shell configurations usually can be broken down into simple elements. Very often the combination of shells and rings must be dealt with. Usual shapes include spherical, elliptical, conical, conoidal, toroidal, or compound (irregular) shapes of bulkhead. Fig. 2.23-1, for example, illustrates a compound bulkhead which consists of the spherical transition and conical shell. By analysis of such a shell, the analyst must choose between two methods: he can consider such a system as an irregular one and use some approximation, or he can calculate it as a compound shell, using the method of interaction, depending on the accuracy required.

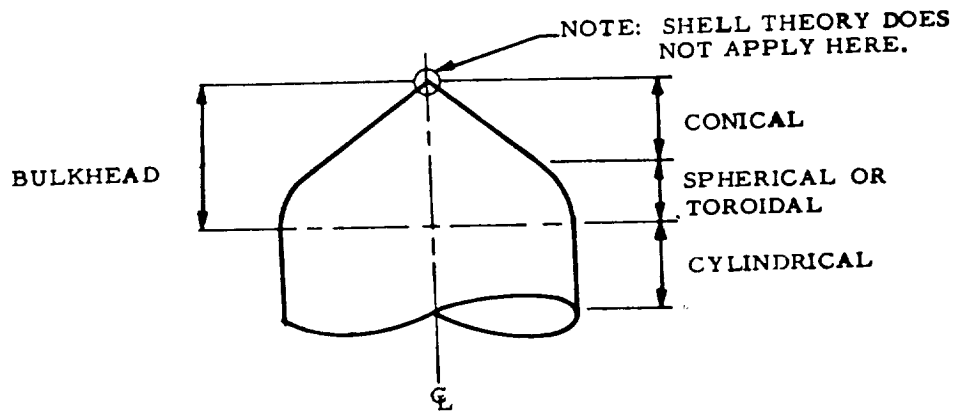


FIG. 2.23-1. Compound Bulkhead

In this section, the interaction method, which is applicable not only to the monocoque shells but also to sandwich and orthotropic shells, is presented. The interacting elements are often from different materials. The loading can vary considerably too. The most frequently used loadings are internal or external pressure, axial tension or compression load, thermally induced loads, and the thrust loads.

2.23.2 Interaction Between Two Shell Elements

After this brief introduction, the method of interaction can now be described. For simplicity, the interaction between two structural elements will be described first. Second to be described is the more general case

of interaction of several elements, as is usually the case if the combined bulkhead is under consideration. For the purpose of presentation, a system consisting of a bulkhead and cylinder, pressurized internally, is selected. The bulkhead can be considered as a unit-element of some defined shape and will not be subdivided into separate portions in the great majority of cases. For example, assume the pressurized container to be theoretically separated into two main parts: the cylindrical shell and dome, as shown in Fig. 2.23-2. Stresses and deformations introduced by internal pressure

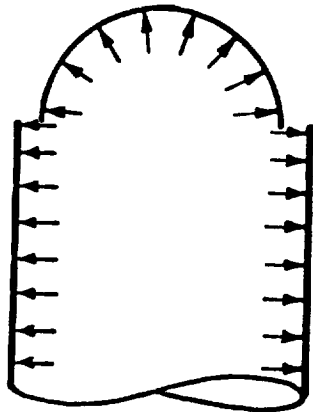


FIG. 2.23-2. Cylindrical Shell and Dome

(or another external loading) can be determined for each part separately.

Assume that the membrane analysis (primary solution) supplied the radial displacements $\Delta r = \delta_c$ and rotation β_c for the cylinder along the discontinuity line and $\Delta r = \delta_d$ and β_d for the dome. Since the structure is separated into two elements,

$$\delta_c \neq \delta_d$$

$$\beta_c \neq \beta_d$$

Consequently, there exists the discontinuity:

(a) in displacement $\delta_c - \delta_d$

(b) in slope $\beta_c - \beta_d$

To close this gap, unknown forces Q and M will be introduced around the junction to hold the two pieces together.

Displacements and rotation of the cylinder due to unit values of Q and M are defined as follows:

$$Q_c^\delta, Q_c^\beta \quad \text{and} \quad M_c^\delta, M_c^\beta$$

The corresponding values for the dome for the same unit loadings will be:

$$Q_d^\delta, Q_d^\beta \quad \text{and} \quad M_d^\delta, M_d^\beta$$

These unit-deformations and unit-loadings at the junctions are presented in Fig. 2.23-3.

To close the gap, the following equations can be written:

$$\begin{cases} (Q_c^\delta + Q_d^\delta) Q + (M_c^\delta + M_d^\delta) M = \delta_c - \delta_d \\ (Q_c^\beta + Q_d^\beta) Q + (M_c^\beta + M_d^\beta) M = \beta_c - \beta_d \end{cases} \quad (2.23-1)$$

Assume that all coefficients δ and β are known. For any shell geometry and any loading of practical values, these coefficients will be given in the further presentation of this chapter as an algebraic formula. Thus, the following can be indicated:

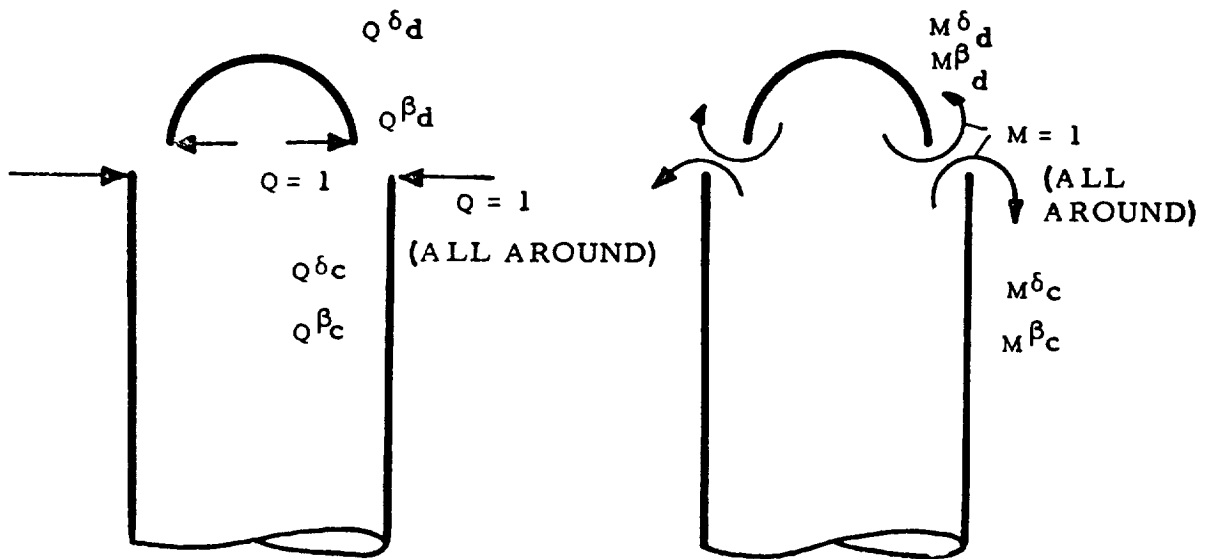


FIG. 2.23-3. Unit Deformations and Unit Loadings

$$\begin{aligned}
 Q\delta_c + Q\delta_d &= \delta_Q & ; & & Q\beta_c + Q\beta_d &= \beta_Q \\
 M\delta_c + M\delta_d &= \delta_M & ; & & M\beta_c + M\beta_d &= \beta_M \\
 \delta_c - \delta_d &= \delta & ; & & \beta_c - \beta_d &= \beta
 \end{aligned}
 \tag{2.23-2}$$

As illustrated, 12 coefficients are known in general. In the special case of interaction of a cylindrical shell and a dome (not toroidal) with the same tangent on intersection, the number of coefficients are reduced to ten because

$$\beta_c = 0 \quad \text{and} \quad \beta_d = 0$$

Finally, Eq. 2.23-1 is reduced to a system of two equations with the two unknowns, Q and M:

$$\delta_Q Q + \delta_M M = \delta$$

$$\beta_Q Q + \beta_M M = \beta$$

Define the determinants of the above system as follows:

$$D = \begin{vmatrix} \delta_Q & \delta_M \\ \beta_Q & \beta_M \end{vmatrix}, \quad D_1 = \begin{vmatrix} \delta & \delta_M \\ \beta & \beta_M \end{vmatrix}, \quad D_2 = \begin{vmatrix} \delta_Q & \delta \\ \beta_Q & \beta \end{vmatrix}$$

The statically indeterminate values of Q and M are determined:

$$Q = \frac{D_1}{D}, \quad M = \frac{D_2}{D}$$

It is noted that one cut through the shell lead to two algebraic equations with two unknowns.

The following sign convention is adopted:

1. Horizontal deflection δ is positive outward.
2. Shears are positive if they cause deflection outward.
3. Moments are positive if they cause tension on the inside fibers of the shell.
4. Rotations are positive if they correspond to a positive moment.

In general, this sign convention is arbitrary. Any rule of signs may be adopted if it does not conflict with the logic and is used consistently.

It is noted that in addition to M and Q, there is an axial force distributed around the junction between the cylinder and dome (reaction of bulkhead), but the effect of this force on the displacement, due to M and Q, is negligible.

2.23.3 Interaction Between Three or More Shell Elements

In practice, most cases are similar to the above described two-member interaction. However, at times it may be convenient to consider interaction of more than two members. This can be performed in two ways:

1. Interact first the two members; then, when this combination is solved, interact it with the third member, etc.
2. Simultaneously interact all members at the same time.

The first method is self-explanatory. The second method requires further explanation: If the shape of the bulkhead is such that its meridian cannot be approximated with one definite analytical curve, such a bulkhead is called a compound bulkhead and can be approximated with many curves. Such a bulkhead was illustrated in Fig. 2.23-1.

In such a case, two or more imaginary cuts through the shell will be required to separate the compound bulkhead into component shells of a basic shape. This is shown in Fig. 2.23-4, which has two imaginary cuts and the compound shell consists of three elementary shells: circular, toroidal, and cylindrical. Fig. 2.23-4 illustrates also the loading and

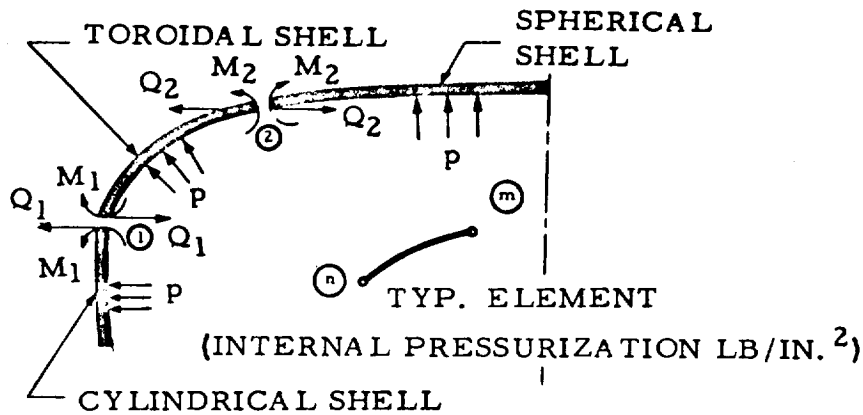


FIG. 2.23-4. Discontinuity Loads

discontinuity influences that belong to each cut. The discontinuity influences will restore the continuity of the compound shell.

The symbols used for the two successive cuts m and n are also shown in Fig. 2.23-4.

$M_{nn}^{\beta} \cdot Q_{nn}^{\beta}$ = rotation at point n due to a unit moment M or unit horizontal shear Q acting at point n

$M_{nn}^{\delta} \cdot Q_{nn}^{\delta}$ = horizontal displacement due to the same loading in application points as above.

$M_{nm}^{\beta} \cdot Q_{nm}^{\beta}$ = rotation at point n due to a unit moment or unit horizontal shear acting at point m, respectively

$M_{nm}^{\delta} \cdot Q_{nm}^{\delta}$ = horizontal displacement due to the same loading in application points as above.

Indicating $n = 1$ and $m = 2$, the above nomenclature can be considered as a proper indication to cover the toroidal portion ① , ② as shown in Fig. 2.23-4.

Additional nomenclature needed to cover the spherical shell is shown in Fig. 2.23-4.

M^{β}_s , Q^{β}_s = rotations at point ② on the spherical shell due to a unit moment or unit shear at the same point.

M^{δ}_s , Q^{δ}_s = horizontal displacements due to the same conditions as above.

Similarly, displacements and rotations of point ① on the cylindrical shell will be defined. Subscript c (cylinder) will be used instead of s (sphere).

Due to the primary loading (internal pressure), the rotations and displacements will be indicated with β and $\Delta r = \Delta$. As before, the subscripts c and s refer to the cylinder and sphere. The subscripts 1t and 2t will be used to denote the toroidal shell at the edge ① and ②

Now the equations for the total rotation and displacement can be formed.

Spherical Shell:

$$\delta_s = M^{\delta}_s M_2 + Q^{\delta}_s Q_2 + \Delta_s p$$

$$\beta_s = M^{\beta}_s M_2 + Q^{\beta}_s Q_2 + \beta_s p$$

Toroidal Shell:

$$\delta_{2t} = M \delta_{22} M_2 + Q \delta_{22} Q_2 + M \delta_{21} M_1 + Q \delta_{21} Q_1 + \Delta_{2t} P$$

$$\beta_{2t} = M \beta_{22} M_2 + Q \beta_{22} Q_2 + M \beta_{21} M_1 + Q \beta_{21} Q_1 + \beta_{2t} P$$

$$\delta_{1t} = M \delta_{12} M_2 + Q \delta_{12} Q_2 + M \delta_{11} M_1 + Q \delta_{11} Q_1 + \Delta_{1t} P$$

$$\beta_{1t} = M \beta_{12} M_2 + Q \beta_{12} Q_2 + M \beta_{11} M_1 + Q \beta_{11} Q_1 + \beta_{1t} P$$

Cylindrical Shell:

$$\delta_c = M \delta_c M_1 + Q \delta_c Q_1 + \Delta_c P$$

$$\beta_c = M \beta_c M_1 + Q \beta_c Q_1 + \beta_c P$$

The following compatibility equations must be satisfied:

$$\delta_s = \delta_{2t} \quad \beta_s = \beta_{2t}$$

$$\delta_c = \delta_{1t} \quad \beta_c = \beta_{1t}$$

Following consideration of the above relations and some mathematical rearrangements, a system of four linear equations with four unknowns will finally be obtained.

$$M \delta_{21} M_1 + (M \delta_{22} - M \delta_s) M_2 + Q \delta_{21} Q_1 + (Q \delta_{22} - Q \delta_s) Q_2 + (\Delta_{2t} - \Delta_s) P = 0$$

$$(M \delta_{11} - M \delta_c) M_1 + M \delta_{12} M_2 + (Q \delta_{11} - Q \delta_c) Q_1 + Q \delta_{12} Q_2 + (\Delta_{1t} - \Delta_c) P = 0 \quad (2.23-3)$$

$$M \beta_{21} M_1 + (M \beta_{22} - M \beta_s) M_2 + Q \beta_{21} Q_1 + (Q \beta_{22} - Q \beta_s) Q_2 + (\beta_{2t} - \beta_s) P = 0$$

$$(M \beta_{11} - M \beta_c) M_1 + M \beta_{12} M_2 + (Q \beta_{11} - Q \beta_c) Q_1 + Q \beta_{12} Q_2 + (\beta_{1t} - \beta_c) P = 0$$

It is noted that two imaginary cuts lead to four equations with four unknowns:

$$M_1, M_2, Q_1 \text{ and } Q_2$$

Previously, when considering only one imaginary cut, only two equations with two unknowns were obtained. Consequently, if n imaginary cuts are introduced simultaneously, $2n$ linear equations with $2n$ unknowns can be obtained.

Depending on adopted sign-convention, some of the introduced coefficients may be negative and, as such, would have been introduced in the preceding equations.

2.23.4 Summary

This section has presented breakdowns of a shell structure into a set of simple elements and one way to perform the interaction process. This includes the use of two or more elements at a junction.)

It can be concluded that the problem of interaction is reduced to the problem of finding rotation β and displacements $\Delta r = \delta$ of interacting structural elements due to the primary loadings and the secondary loadings $M = Q = 1$ (around the junction). The rotations and displacements then will be introduced into a set of linear equations, as shown in Eq. 2.23-3. Statically indeterminate values M and Q will be found.

2.24 CONCLUSION

This section presented the background for understanding and applying the unit loadings method. The following section will be limited to monocoque shells of revolution loaded with the axisymmetrical loadings. Numerous solutions will be presented to make the design procedure of the complicated shell as simple as possible. The following two sections are associated with determination of deformations and stresses due to primary loadings (membrane solutions) and secondary loadings (unit-loadings). Only homogeneous materials and monocoque shells will be considered in these sections. Later, the necessary modifications of derived formulas for nonhomogeneous material and nonmonocoque shells will be presented.

2.30 MONOCOQUE SHELLS

2.31 INTRODUCTION

The shells considered in this section are homogeneous isotropic monocoque shells of revolution. Thin shells are considered and all loadings are axisymmetrical. The membrane and bending theories have been previously discussed in Section 2.22. An extensive literature search was made to collect and present as many existing solutions as possible within the scope of this manual. These solutions will be designated as primary solutions or unit edge loading solutions. The geometry of every shell being considered will be described, and limitations will be indicated.

2.32 PRIMARY SOLUTIONS

This section contains general information regarding the membrane solutions.

The internal forces and displacements must be calculated, to solve shell problems.

2.32.1 Determination of Membrane Internal Forces

The forces acting on the sides of shell element are denoted with symbols as indicated in Fig. 2.32-1.

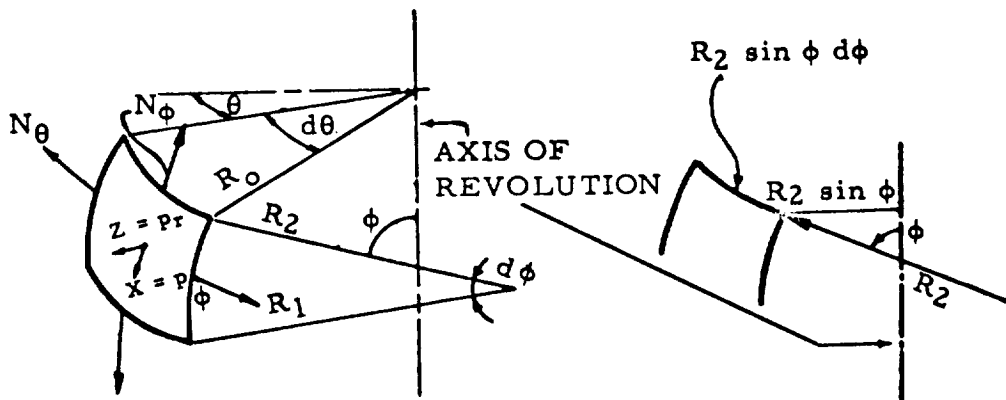


FIG. 2.32-1. Shell Element Forces

θ = angle in horizontal plane, which controls the location of any point of the shell

ϕ = angle in vertical plane (measured from axis of rotation)

R_1 = radius of curvature of meridian at any point

R_2 = radial distance between point on the shell and the axis of rotation

$Z = p_r$ }
 and } = the radial and meridional components of existing loading,
 $X = p_\phi$ } which act on the differential element (because of assumed
 axisymmetrical loading, the component in circumferential
 direction is zero)

N_ϕ }
 and } = loads on meridional and circumferential side of differential
 N_θ } element

In general, the shells of revolution will be loaded with some kind of external/internal pressure in combination with some vertical loading at the vertex or around the hole at the vertex. A solution of the following shape can be given for such shells as mentioned above (axial symmetry), loaded with any external (internal) pressure:

$$\frac{N_\phi}{R_1} + \frac{N_\theta}{R_2} = P_r \dots \dots \dots \quad (2.32-1)$$

where

$$N_\phi = \frac{1}{R_2 \sin^2 \phi} \left[\int R_1 R_2 (p_r \cos \phi - p_\phi \sin \phi) \sin \phi d\phi + C \right]$$

where the constant C represents the effect of loads which may be applied above the circle $\phi = \phi_0$ in accordance with Fig. 2.32-2. The angle ϕ_0 defines the opening in the shell of the revolution. The resultant of these

forces will be $2\pi C$. If the shell were closed, such loading would degenerate to the concentrated load P in the vertex of the shell.

$$2\pi C = -P$$

P = Vertical load in pounds

N_ϕ, N_θ = unit resultants in pounds per inch

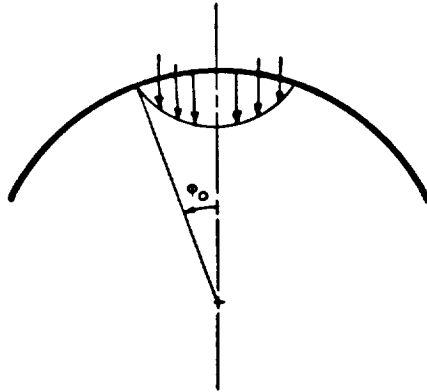


FIG. 2.32-2. Partial Loading Above Circle $\phi = \phi_0$

If no other loads are present except P , the meridional and circumferential forces will be given as

$$N_\phi = -\frac{P}{2\pi R_2 \sin^2 \phi} \quad \text{and} \quad N_\theta = +\frac{P}{2\pi R_1 \sin^2 \phi}$$

These loads may always be treated as additive loads due to the loaded opening at the vertex of the shell. If the shell is closed, other influences will be present besides membrane influences in the range of application of the load. The feasibility of this will be discussed later.

2.32.2 Determination of Membrane Displacements

It was shown that determination of stress components in axisymmetrically loaded shell of revolution is a statically determinate case, and the membrane forces N_θ and N_ϕ are easily obtained. However, the displacements must be determined for the interaction process of two or more shells.

In the symmetrical deformation of a shell, a small displacement of a point can be resolved into two components:

u - in the direction of the tangent to the meridian

w - in the direction of the normal to the middle surface

The strain components ϵ_ϕ and ϵ_θ can be expressed in terms of the forces N_ϕ and N_θ :

$$\left. \begin{aligned} \epsilon_\phi &= \frac{1}{Et} (N_\phi - \mu N_\theta) \\ \epsilon_\theta &= \frac{1}{Et} (N_\theta - \mu N_\phi) \end{aligned} \right\} \quad (2.32-2)$$

where

E = Young's modulus

t = thickness of the shell

μ = Poisson's ratio

The next step is to make use of the following differential equation:

$$\frac{du}{d\phi} - u \cot\phi = \frac{1}{Et} \left[N_\phi (R_1 + \mu R_2) - N_\theta (R_2 + \mu R_1) \right] = f(\phi)$$

where

ϕ is the angle which locates any point on shell-middle surface along the meridian in respect to the axis of revolution.

Then the general solution for u is

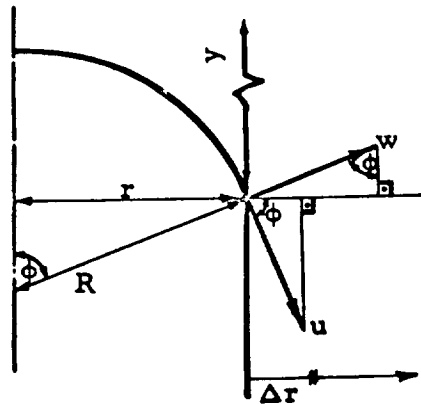
$$u = \sin \phi \left[\int \frac{f(\phi)}{\sin \phi} d\phi + C \right]$$

where C is the constant of integration to be determined from the condition at the support. The displacement w will be found from the equation

$$w = u \cot \phi - R_2 \epsilon_\theta$$

substituting the value ϵ_θ from the Eq. 2.32-2.

Having u and w , the corresponding displacement can be found in the horizontal and vertical direction using simple trigonometric relations in connection with Fig. 2.32-3.



$$\Delta r = w \sin \phi + u \cos \phi$$

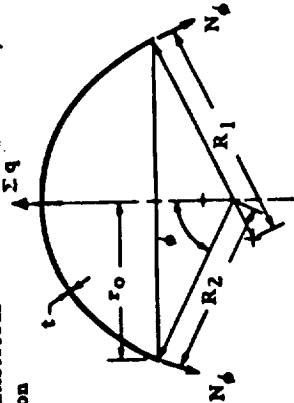
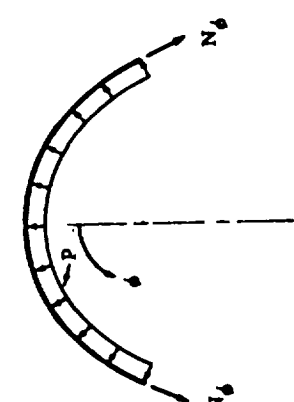
$$y = -w \cos \phi + u \sin \phi$$

FIG. 2.32-3. Geometric Relations Between Displacements

2. 32. 3 Any Shape of Meridian

Table 2. 32-1 presents a summary of equations of the linear membrane theory in more convenient form for a general case of shell of revolution loaded axisymmetrically with uniform pressure. Special cases will be presented after the above general introduction.

TABLE 2.32-1. AXISYMMETRICALLY LOADED SHELL OF REVOLUTION SUMMARY OF EQUATIONS FOR LINEAR MEMBRANE THEORY

| | |
|--|---|
| <p>General Complete Shell of Revolution, General Axisymmetrical Load Distribution</p>  <p>Σq is the resultant of the applied load above the parallel circle defined by θ</p> <p>$q_\theta = q_\theta(\theta)$ $q_z = q_z(\theta)$ $q_0 = 0$</p> | <p>General Complete Shell of Revolution, Uniform Pressure</p>  <p>$q_z = p$ $q_\theta = q_0 = 0$</p> |
| <p>N_θ</p> <p>N_ϕ</p> | <p>$2\epsilon r_0 N_\theta \sin \theta - \Sigma q = 0$</p> <p>This system shall be solved in order to obtain N_θ and N_ϕ</p> <p>$\left\{ \begin{aligned} N_\theta + \frac{N_\phi}{R_1 + R_2} - q_z &= 0 \end{aligned} \right.$</p> <p>$\frac{R_2 P}{2}$</p> <p>$\frac{R_2 P}{2} \left[2 - \frac{R_2}{R_1} \right]$</p> |
| <p>Δr</p> <p>γ</p> <p>ρ</p> | <p>$\epsilon_2 r_0$</p> <p>$\epsilon_2 r_0 \cot \theta - \int \frac{\tilde{i}(\theta)}{\sin \theta} d\theta + C$</p> <p>$\frac{1}{R_1} \left[\frac{\tilde{i}(\theta)}{\tan \theta} - \frac{d}{d\theta} (\epsilon_2 R_2) \right]$</p> <p>where:</p> <p>$\epsilon_1 = \frac{1}{Et} (N_\theta - \mu N_\phi)$</p> <p>$\epsilon_2 = \frac{1}{Et} (N_\phi - \mu N_\theta)$</p> <p>$\tilde{i}(\theta) = R_1 \epsilon_1 - R_2 \epsilon_2$</p> <p>and C is an integration constant</p> <p>$\epsilon_2 r_0 = \frac{r_0}{Et} (N_\phi - \mu N_\theta) = \frac{R_2^2 \sin \theta P}{2Et} \left[2 - \mu - \frac{R_2}{R_1} \right]$</p> <p>$w \cot \theta = \int \frac{R_1 (N_\theta - \mu N_\phi) - R_2 (N_\phi - \mu N_\theta)}{Et \sin \theta} d\theta + C$</p> <p>$\frac{p R_2}{2Et \tan \theta} \left[\left(\frac{R_2}{R_1} - 1 \right) \left(-2 \frac{R_2}{R_1} + 3 \right) \right] - \frac{P}{2Et} \left(\frac{R_2}{R_1} \right)^3 \frac{dR_1}{d\theta}$</p> |

2. 32. 4 Spherical Shells

This subsection presents the solutions for nonshallow spherical shells exposed to axisymmetrical loading. Both closed and open spherical shells will be considered.

Listed below are the loading cases under consideration, which are divided into the circumferential, meridional, and normal components X, Y, Z. Additional designations are indicated on the figures that correspond to each loading case. The spherical shells, which satisfy the relation

$$\cot \theta = \frac{\cos \theta}{\sin \theta} \approx \frac{1}{\theta}$$

are not in the scope of this section and fall into the category of shallow shells.

In order that a membrane state of stress exist, the boundaries of the shell must be free to rotate and deflect normal to the shell middle surface.

Abrupt discontinuities in shell thickness must not be present.

The following loading cases are considered:

1. Dead Weight (Fig 2. 32-4)

$$X = q \sin \theta, \quad Y = 0,$$

$$Z = q \cos \theta$$

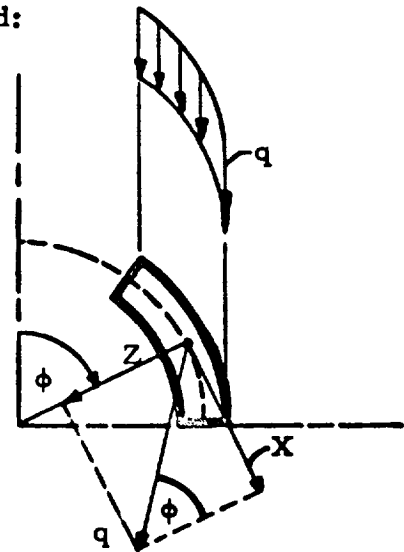


FIG. 2. 32-4. Loading of Spherical Shell With Dead Weight

2. Uniformly Distributed Loading over the Base (Fig. 2.32-5)

$$X = p \cos \phi \sin \phi$$

$$Y = 0$$

$$Z = p \cos^2 \phi$$

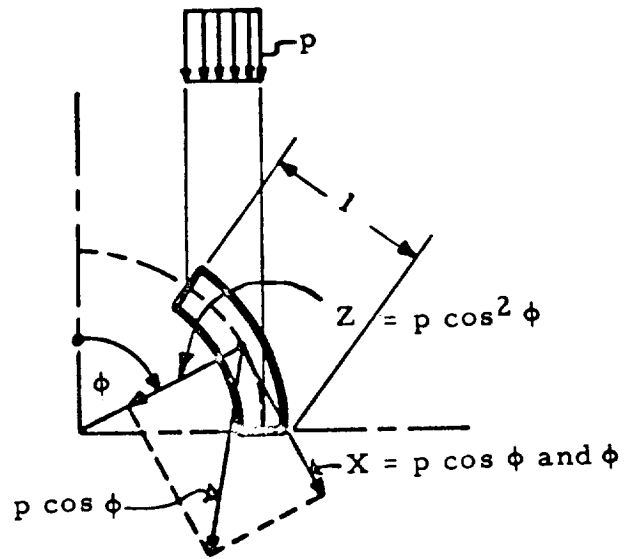


FIG. 2.32-5. Loading of Spherical Shell With Equally Distributed Loading Over Base Area

3. Hydrostatic Pressure Loading (Fig. 2.32-6).

ρ = specific weight

$$X = Y = 0$$

$$Z = \rho [f + R (1 - \cos \phi)]$$

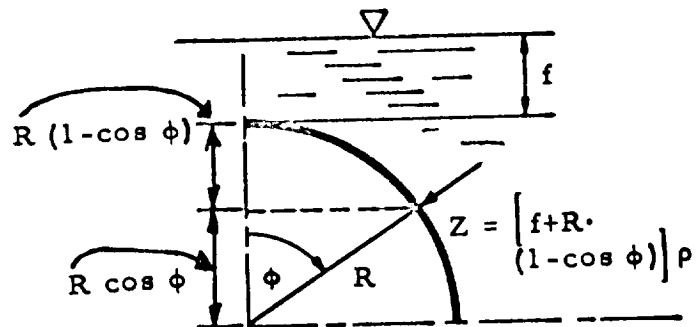


FIG. 2.32-6. Hydrostatic Pressure Loading of Spherical Shell

For reversed spherical shell, f is the distance from the surface of liquid to the apex of the reversed shell, and, $Z = [f - R (1 - \cos \phi)] \rho$

4. Uniform Loading in z-direction (pressurization; Fig. 2.32-7)

$$X = Y = 0$$

$$Z = p$$

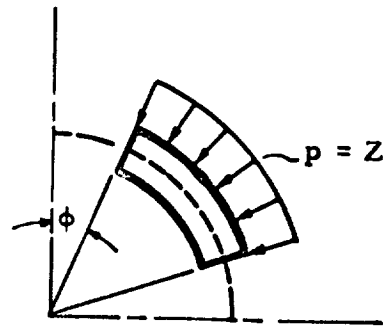


FIG. 2.32-7. Loading of Spherical Shell With Normal Pressure

5. Lantern - Loading p - Load per unit of length of the upper shell edge (Fig. 2.32-8).

$$X = Y = Z = 0$$

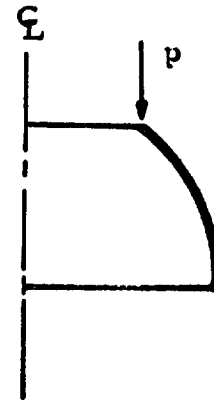


FIG. 2.32-8. Lantern Loading

The corresponding formulas and deformations are listed in tabular form for each loading case indicated for the closed and open spherical shell (Tables 2.32-2 and 2.32-3).

TABLE 2.32-2. STRESS AND DEFORMATION IN SPHERICAL SHELL MEMBRANE SOLUTION (REF. 2-2)

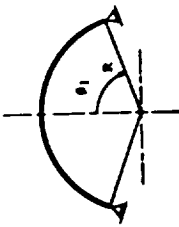
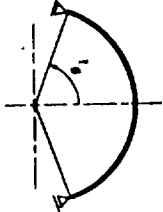
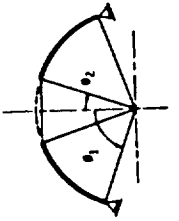
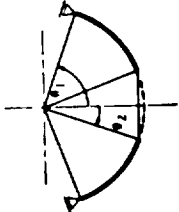
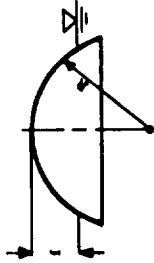
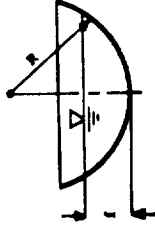
| |  |  |  |  |
|------------------------------------|---|--|--|---|
| 1. DEADWEIGHT LOADING | | | | |
| M_θ | $-\frac{Rq}{1 + \cos\theta}$ | $\frac{Rq}{1 + \cos\theta}$ | $-\frac{Rq}{\sin\theta} (\cos\theta_2 - \cos\theta)$ | $\frac{Rq}{\sin^2\theta} (\cos\theta_2 - \cos\theta)$ |
| N_θ | $-Rq \left(\cos\theta - \frac{1}{1 + \cos\theta} \right)$ | $Rq \left(\cos\theta - \frac{1}{1 + \cos\theta} \right)$ | $Rq \left(\cos\theta - \frac{1}{\sin\theta} (\cos\theta_2 - \cos\theta) \right)$ | $Rq \left[\cos\theta - \frac{1}{\sin\theta} (\cos\theta_2 - \cos\theta) \right]$ |
| Δr | $\frac{R^2 q}{Et} \sin\theta \left[-\cos\theta + \frac{1 + \mu}{2} (1 - \cos\theta) \right]$ | $-\frac{R^2 q}{Et} \sin\theta \left[-\cos\theta + \frac{1 + \mu}{2} (1 - \cos\theta) \right]$ | $\frac{R^2 q}{Et} \sin\theta \left[-\cos\theta + \frac{1 + \mu}{2} (\cos\theta_2 - \cos\theta) \right]$ | $-\frac{R^2 q}{Et} \sin\theta \left[-\cos\theta + \frac{1 + \mu}{2} (\cos\theta_2 - \cos\theta) \right]$ |
| ρ | $-\frac{Rq}{Et} (2 + \mu) \sin\theta$ | $-\frac{Rq}{Et} (2 + \mu) \sin\theta$ | $-\frac{Rq}{Et} (2 + \mu) \sin\theta$ | $-\frac{Rq}{Et} (2 + \mu) \sin\theta$ |
| 2. UNIFORM LOAD ON PROJECTED AREAS | | | | |
| M_θ | $-\frac{PR}{2}$ | $\frac{PR}{2}$ | $-\frac{PR}{2} \left(1 - \frac{\sin^2\theta_2}{\sin^2\theta} \right)$ | $\frac{PR}{2} \left(1 - \frac{\sin^2\theta_2}{\sin^2\theta} \right)$ |
| N_θ | $-\frac{PR}{2} \cos 2\theta$ | $\frac{PR}{2} \cos 2\theta$ | $-\frac{PR}{2} \left(2 \cos^2\theta - 1 + \frac{\sin^2\theta_2}{\sin^2\theta} \right)$ | $\frac{PR}{2} \left(2 \cos^2\theta - 1 + \frac{\sin^2\theta_2}{\sin^2\theta} \right)$ |
| Δr | $\frac{R^2 P}{Et} \sin\theta \left[-\cos^2\theta + \frac{1 + \mu}{2} \right]$ | $-\frac{R^2 P}{Et} \sin\theta \left[-\cos^2\theta + \frac{1 + \mu}{2} \right]$ | $-\frac{R^2 P}{Et} \sin\theta \left[-\cos^2\theta + \frac{1 + \mu}{2} \right]$ | $-\frac{R^2 P}{Et} \sin\theta \left[-\cos^2\theta + \frac{1 + \mu}{2} \right]$ |
| ρ | $-\frac{RP}{Et} (3 + \mu) \sin\theta \cos\theta$ | $\frac{RP}{Et} (3 + \mu) \sin\theta \cos\theta$ | $-\frac{RP}{Et} (3 + \mu) \sin\theta \cos\theta$ | $-\frac{RP}{Et} (3 + \mu) \sin\theta \cos\theta$ |

TABLE 2.32-2 (CONT)

| 3. HYDROSTATIC PRESSURE LOADING | | | |
|---|--|--|--|
| M_0 | $\frac{\rho R^2}{6} \left(1 + 3 \frac{f}{R} - \frac{2 \cos^2 \phi}{1 + \cos \phi} \right)$ | $\frac{\rho R^2}{6} \left(1 + 3 \frac{f}{R} + \frac{2 \cos^2 \phi}{1 + \cos \phi} \right)$ | $-\frac{\rho R^2}{6} \left[3 \left(1 + \frac{f}{R} \right) \left(1 - \frac{\sin^2 \phi_2}{\sin^2 \phi} \right) - \frac{\cos^3 \phi_2 - \cos^3 \phi}{\sin^2 \phi} \right]$ |
| M_0 | $-\frac{\rho R^2}{6} \left(1 + 3 \frac{f}{R} - \frac{4 \cos^2 \phi - 6}{1 + \cos \phi} \right)$ | $\frac{\rho R^2}{6} \left(1 + 3 \frac{f}{R} + \frac{4 \cos^2 \phi - 6}{1 + \cos \phi} \right)$ | $-\frac{\rho R^2}{6} \left[3 \left(1 + \frac{f}{R} \right) \left(1 + \frac{\sin^2 \phi_2}{\sin^2 \phi} \right) + \frac{2(2 \cos^3 \phi + \cos^3 \phi_2) - 6 \cos \phi}{\sin^2 \phi} \right]$ |
| d_r | $-\frac{\rho R^3}{6 E t} \sin \phi \left[3 \left(1 + \frac{f}{R} \right) (1 - \mu) - 6 \cos \phi - \frac{2(1 + \mu)}{\sin^2 \phi} (\cos^3 \phi - 1) \right]$ | $\frac{\rho R^3}{6 E t} \sin \phi \left[3 \left(1 + \frac{f}{R} \right) (1 - \mu) - \left[1 - \mu + (1 + \mu) \frac{\sin^2 \phi_2}{\sin^2 \phi} \right] - 6 \cos \phi + 2(1 + \mu) \frac{\cos^3 \phi_2 - \cos^3 \phi}{\sin^2 \phi} \right]$ | $\frac{\rho R^3}{6 E t} \sin \phi \left[3 \left(1 + \frac{f}{R} \right) - \left[1 - \mu + (1 + \mu) \frac{\sin^2 \phi_2}{\sin^2 \phi} \right] - 6 \cos \phi + 2(1 + \mu) \frac{\cos^3 \phi_2 - \cos^3 \phi}{\sin^2 \phi} \right]$ |
| ρ | $\frac{\rho R^2}{E t} \sin \phi$ | $\frac{\rho R^2}{E t} \sin \phi$ | $\frac{\rho R^2}{E t} \sin \phi$ |
| 4. UNIFORM LOADING IN NORMAL DIRECTION (PRESSURIZATION) | | | |
| M_0 | $-\frac{R^2 P}{2}$ | $\frac{R^2 P}{2}$ | $\frac{R^2 P}{2} \left(1 - \frac{\sin^2 \phi_2}{\sin^2 \phi} \right)$ |
| M_0 | $-\frac{R^2 P}{2}$ | $\frac{R^2 P}{2}$ | $\frac{R^2 P}{2} \left(1 + \frac{\sin^2 \phi_2}{\sin^2 \phi} \right)$ |
| d_r | $-\frac{R^2 P}{2 E t} (1 - \mu) \sin \phi$ | $\frac{R^2 P}{2 E t} (1 - \mu) \sin \phi$ | $\frac{R^2 P}{E t} \sin \phi \left[1 - \frac{1 + \mu}{2} \left(1 - \frac{\sin^2 \phi_2}{\sin^2 \phi} \right) \right]$ |
| ρ | 0 | 0 | 0 |
| 5. LANTERN LOADING | | | |
| M_0 | No case | No case | $\frac{P \sin \phi_2}{\sin^2 \phi}$ |
| M_0 | No case | No case | $-\frac{P \sin \phi_2}{\sin^2 \phi}$ |
| d_r | No case | No case | $-\frac{P R (1 + \mu)}{E t} \frac{\sin \phi_2}{\sin \phi}$ |
| ρ | 0 | 0 | 0 |

TABLE 2.32-3. HYDROSTATIC-PRESSURE LOADING OVER PORTION OF SPHERICAL SHELL (Ref. 2-3)

| Shell | Loading | N_θ | N_ϕ | T |
|--|--|---|--|---|
|  | <p>a</p> $Z = p(R-R \cos \phi - l)$ | <p>Points above the liquid level:</p> 0 | <p>Points below the liquid level:</p> $- \rho \frac{R^2}{6} \left[\frac{l}{R} \left[\frac{1}{\sin^2 \theta} \left(3 - \frac{l}{R} \right) - 3 \right] + 1 - \frac{2 \cos^2 \theta}{1 + \cos \theta} \right] - N_\theta$ | 0 |
| | | <p>Points above the liquid level:</p> $\rho \frac{l^2}{6} \left(3 - \frac{l}{R} \right) \frac{1}{\sin^2 \theta}$ | <p>Points below the liquid level:</p> $\rho \frac{R^2}{6} \left[3 \frac{l}{R} - 1 + \frac{2 \cos^2 \theta}{1 + \cos \theta} \right]$ | $- \rho \frac{l^2}{6} \left(3 - \frac{l}{R} \right) \frac{1}{\sin^2 \theta}$ |
|  <p>$\phi = 180^\circ - \theta$</p> | <p>b</p> $Z = -p(R - R \cos \theta - l)$ | <p>Points above the liquid level:</p> 0 | <p>Points below the liquid level:</p> $- \rho \frac{l^2}{6} \left(3 - \frac{l}{R} \right) \frac{1}{\sin^2 \theta}$ | 0 |
| | | <p>Points above the liquid level:</p> $\rho \frac{l^2}{6} \left(3 - \frac{l}{R} \right) \frac{1}{\sin^2 \theta}$ | <p>Points below the liquid level:</p> $\rho \frac{R^2}{6} \left[\frac{l}{R} - 1 + \cos \theta \right] - N_\theta$ | $- \rho \frac{l^2}{6} \left(3 - \frac{l}{R} \right) \frac{1}{\sin^2 \theta}$ |

2.32.5 Conical Shells

This section presents the solutions for nonshallow conical shells exposed to axisymmetrical loading. The closed and open conical shell is considered.

The loading cases under consideration are categorized in the circumferential, meridional and normal components X , Y , Z .

Additional designations are indicated on the figures that correspond to each loading case. In order to be in the category of nonshallow shell, angle α_0 must be larger than 45 degrees.

In order for a membrane state of stress to exist at the boundaries of the shell it must be free to rotate and deflect normal to the middle shell surface. Abrupt discontinuities in shell thickness must not be present. All presented formulas are based on small deflection membrane theory.

The following loading cases are considered:

(a) Dead Weight (Fig. 2.32-9)

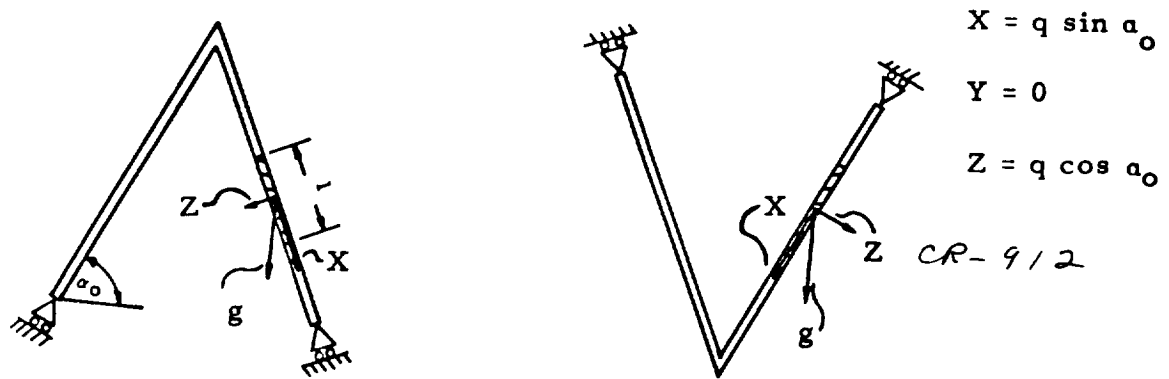


FIG. 2.32-9. Loading Dead Weight

(b) Uniformly Distributed Loading over the Base (Fig. 2.32-10)

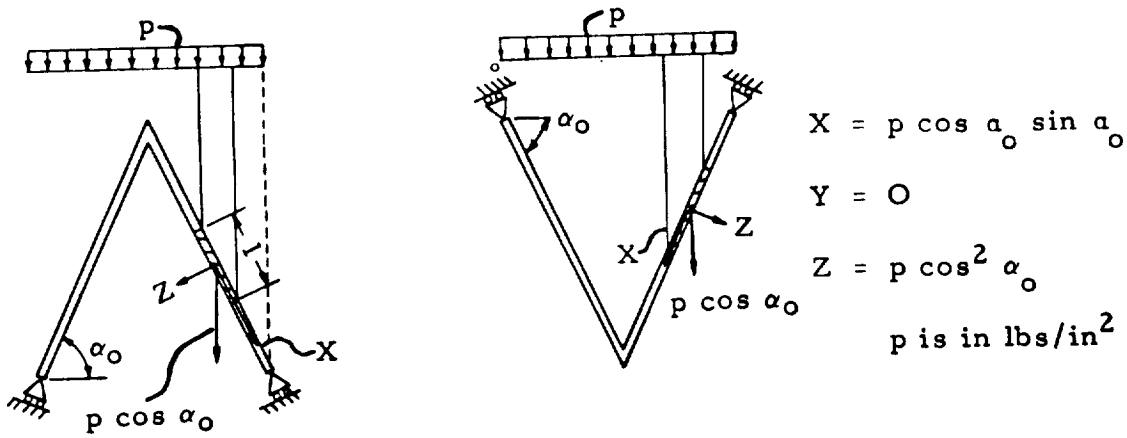


FIG. 2.32-10. Loading Uniformly Distributed Over the Base

(c) Hydrostatic Pressure Loading (Fig. 2.32-11)

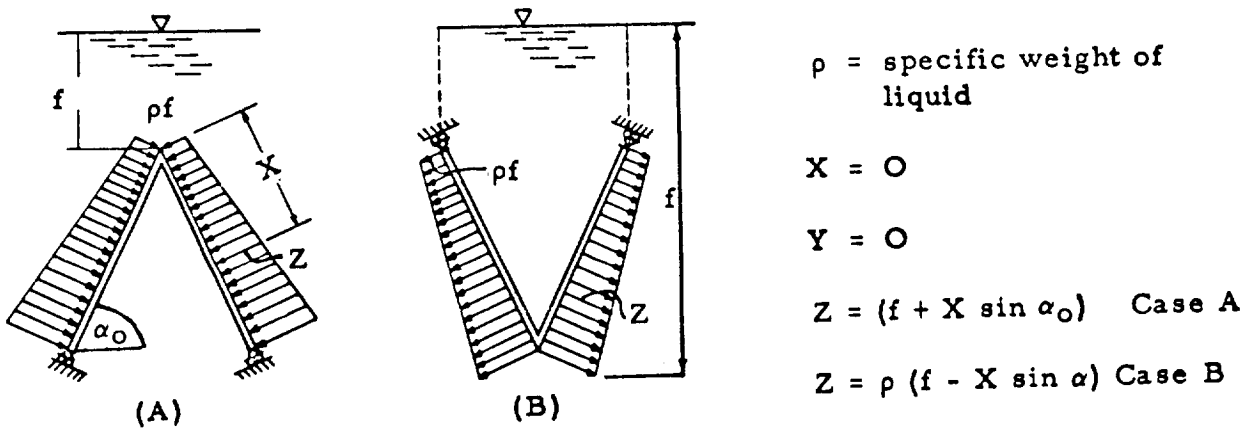


FIG. 2.32-11. Hydrostatic Pressure Loading

(d) Uniform Normal Pressure p (psi) (Fig. 2.32-12)

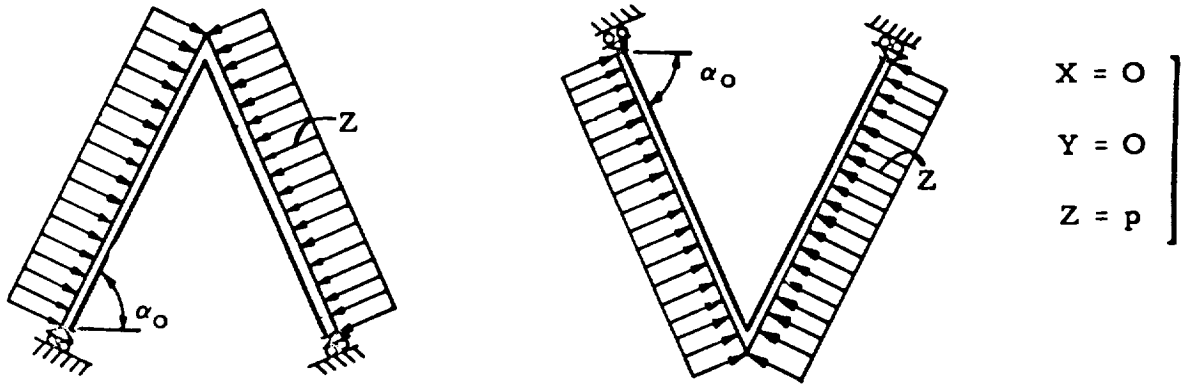


FIG. 2.32-12. Loading With Normal Pressure

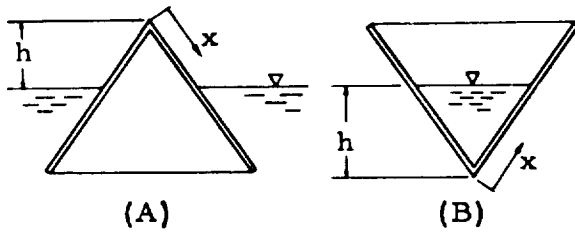
(e) Equally Distributed Loading Along the Opening Edge (Lantern Load)

(See Fig. 2.32-13)



FIG. 2.32-13. Equally Distributed Loading Along the Opening Edge

(f) Hydrostatic Pressure Over Portion of Shell (Fig. 2.32-14)



ρ = specific weight liquid

$X = 0$

$Y = 0$

$Z = \rho (x \sin \alpha_0 - h)$ for (A)

$Z = p_z = \rho (h - x \sin \alpha_0)$

for (B)

FIG. 2.32-14. Hydrostatic Pressure Over Portion of Shell

The corresponding formulas and deformations are assembled in tabular form (Table 2.32-4) for each loading case as indicated for "closed" and "open" conical shell.

TABLE 2.32-4. MEMBRANE SOLUTIONS FOR CONICAL SHELL (REF. 2-2)
(SHEET 1 OF 4)

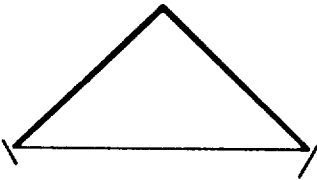
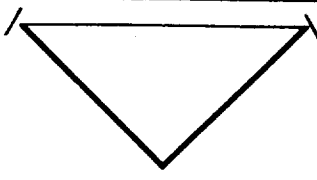
| |  |  |
|---|---|---|
| | Closed Conical Shell (Supported) | Closed Conical Shell (Hinged) |
| (a) DEADWEIGHT | | |
| N_θ | $-\frac{q x \cos^2 \alpha_0}{\sin \alpha_0}$ | $q \frac{\cos^2 \alpha_0}{\sin \alpha_0}$ |
| N_x | $-\frac{1}{x} \left(\frac{q x^2}{2 \sin \alpha_0} \right)$ | $\frac{q}{2 \sin \alpha_0} x$ |
| Δr | $-\frac{x^2}{2t} q \cot \alpha_0 \left(\cos^2 \alpha_0 - \frac{\mu}{2} \right)$ | $\frac{q x^2}{2t} \cot \alpha_0 \left(\cos^2 \alpha_0 - \frac{\mu}{2} \right)$ |
| ρ | $\frac{q x \cos \alpha_0}{Et \sin^2 \alpha_0} \left[(2 + \mu) \cos^2 \alpha_0 - \frac{1}{2} - \mu \right]$ | $\frac{q x \cos \alpha_0}{Et \sin^2 \alpha_0} \left[(2 + \mu) \cos^2 \alpha_0 - \frac{1}{2} + \mu \right]$ |
| (b) UNIFORMLY DISTRIBUTED LOADING OVER THE BASE | | |
| N_θ | $-p \frac{\cos^3 \alpha_0}{\sin \alpha_0} x$ | $p x \frac{\cos^3 \alpha_0}{\sin \alpha_0}$ |
| N_x | $-p \frac{x}{2} \cot \alpha_0$ | $p \frac{x}{2} \cot \alpha_0$ |
| Δr | $-p \frac{x^2}{2t} \cos \alpha_0 \cot \alpha_0 \left(\cos^2 \alpha_0 - \frac{\mu}{2} \right)$ | $p \frac{x^2}{2t} \cos \alpha_0 \cot \alpha_0 \left(\cos^2 \alpha_0 - \frac{\mu}{2} \right)$ |
| ρ | $\frac{p x}{2t} \cot^2 \alpha_0 \left[(2 + \mu) \cos^2 \alpha_0 - \mu - \frac{1}{2} \right]$ | $\frac{p x}{2t} \cot^2 \alpha_0 \left[(2 + \mu) \cos^2 \alpha_0 - \mu - \frac{1}{2} \right]$ |
| (c) HYDROSTATIC PRESSURE LOADING | | |
| N_θ | $-p x \cos \alpha_0 \left(\frac{f}{\sin \alpha_0} + x \right)$ | $-p x \cos \alpha_0 \left(x - \frac{f}{\sin \alpha_0} \right)$ |
| N_x | $-p x \cos \alpha_0 \left(\frac{f}{2 \sin \alpha_0} + \frac{x}{3} \right)$ | $-p x \cos \alpha_0 \left(\frac{x}{3} - \frac{f}{2 \sin \alpha_0} \right)$ |
| Δr | $\frac{p x^2}{2t} \cos^2 \alpha_0 \left[\frac{f}{\sin \alpha_0} \left(\frac{\mu}{2} - 1 \right) + x \left(\frac{\mu}{2} - 1 \right) \right]$ | $\frac{p x^2}{2t} \cos^2 \alpha_0 \left[x \left(\frac{\mu}{2} - 1 \right) - \frac{f}{\sin \alpha_0} \left(\frac{\mu}{2} - 1 \right) \right]$ |
| ρ | $\frac{p x \cos^2 \alpha_0}{Et \sin \alpha_0} \left(\frac{1}{2} \frac{f}{\sin \alpha_0} + \frac{2}{3} x \right)$ | $\frac{p x \cos^2 \alpha_0}{Et \sin \alpha_0} \left(-\frac{2}{3} x + \frac{1}{2} \frac{f}{\sin \alpha_0} \right)$ |

TABLE 2.32-4 (SHEET 2 OF 4)

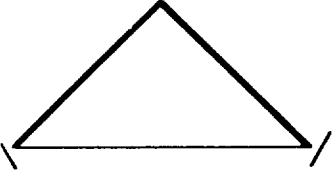
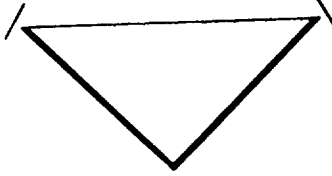
| | | |
|--|---|---|
| |  <p>Closed Conical Shell (Supported)</p> |  <p>Closed Conical Shell (Hinged)</p> |
| (d) UNIFORM NORMAL PRESSURE | | |
| N_θ | $-p x \cot \alpha_0$ | $-p x \cot \alpha_0$ |
| N_x | $-p \frac{x}{2} \cot \alpha_0$ | $-p \frac{x}{2} \cot \alpha_0$ |
| Δr | $-p \frac{x^2}{E t} \cos \alpha_0 \cot \alpha_0 \left(1 - \frac{\mu}{2}\right)$ | $-p \frac{x^2}{E t} \cos \alpha_0 \cot \alpha_0 \left(1 - \frac{\mu}{2}\right)$ |
| ρ | $\frac{3}{2} \frac{p x}{E t} \cot^2 \alpha_0$ | $-\frac{3}{2} \frac{p x}{E t} \cot^2 \alpha_0$ |
| (f) HYDROSTATIC PRESSURE OVER PORTION OF THE SHELL | | |
| N_θ | <p>0 for points above ∇ For points below ∇</p> $-p x (x \cos \theta - h \cot \theta)$ | <p>Points above the ∇: 0 For points below ∇:</p> $p x (h \cot \theta - x \cos \theta)$ |
| N_x | <p>0 for points above ∇ For points below ∇</p> $-\frac{p}{6x} \frac{\cos \theta}{\sin^3 \theta} h^3 + x^2 (2x \cos \theta - 3h \cot \theta)$ | <p>Points above ∇: $\frac{p h^3}{6x} \frac{\cos \theta}{\sin^3 \theta}$ For points below ∇:</p> $\frac{p x}{2} (3h \cot \theta - 2x \cos \theta)$ |

TABLE 2.32-4 (SHEET 3 OF 4)

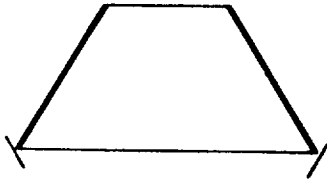
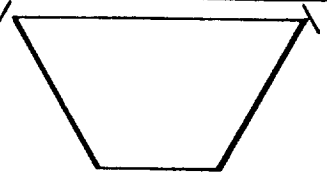
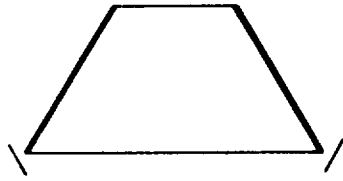
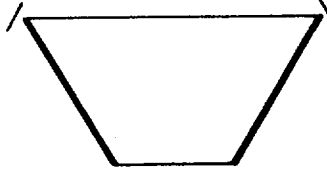
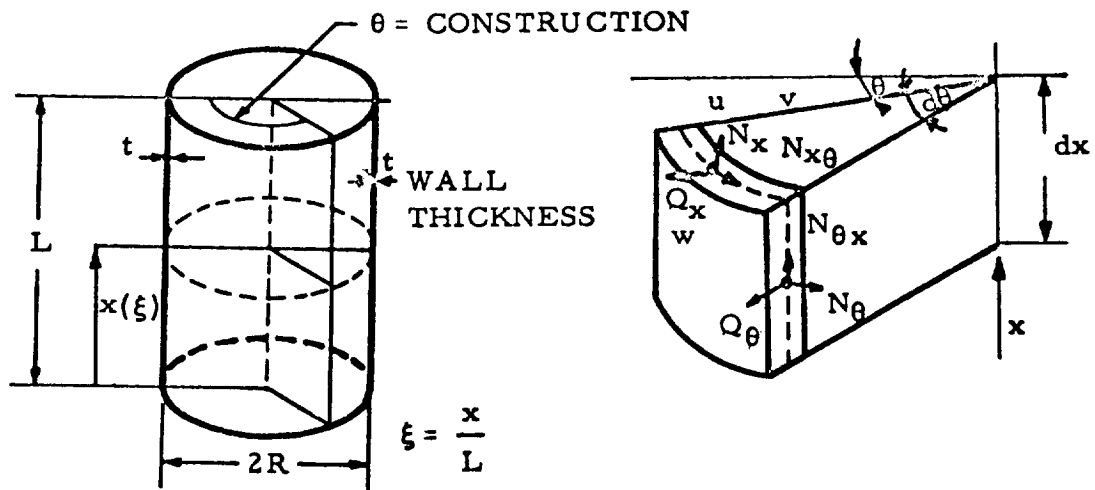
| |  |  |
|---|---|---|
| | Open Conical Shell (Supported) | Open Conical Shell (hanged) |
| (a) DEADWEIGHT | | |
| N_θ | $-q \frac{\cos^2 \theta_0}{\sin \theta_0} x$ | $\frac{\cos^2 \theta_0}{\sin \theta_0} q x$ |
| N_x | $-\frac{q x}{2 \sin \theta_0} \left[1 - \left(\frac{x_1}{x} \right)^2 \right]$ | $\frac{q x}{2 \sin \theta_0} \left[1 - \left(\frac{x_1}{x} \right)^2 \right]$ |
| Δr | $-\frac{q x^2}{2 E t} \cot \theta_0 \left\{ 2 \cos^2 \theta_0 - \mu \left[1 - \left(\frac{x_1}{x} \right)^2 \right] \right\}$ | $\frac{q x^2 \cot \theta_0}{2 E t} \left\{ 2 \cos^2 \theta_0 - \mu \left[1 - \left(\frac{x_1}{x} \right)^2 \right] \right\}$ |
| ρ | $\frac{q x \cos \theta_0}{2 E t \sin^2 \theta_0} \left[2(2 + \mu) \cos^2 \theta_0 - 1 + \left(\frac{x_1}{x} \right)^2 - 2\mu \right]$ | $\frac{q x \cos \theta_0}{2 E t \sin^2 \theta_0} \left[2(2 + \mu) \cos^2 \theta_0 - 1 + \left(\frac{x_1}{x} \right)^2 - 2\mu \right]$ |
| (b) UNIFORMLY DISTRIBUTED LOADING OVER THE BASE | | |
| N_θ | $-\frac{p x \cos^3 \theta_0}{\sin \theta_0}$ | $\frac{p x \cos^3 \theta_0}{\sin \theta_0}$ |
| N_x | $-\frac{1}{2} p x \left[1 - \left(\frac{x_1}{x} \right)^2 \right] \cot \theta_0$ | $\frac{1}{2} p x \left[1 - \left(\frac{x_1}{x} \right)^2 \right] \cot \theta_0$ |
| Δr | $-\frac{p x^2 \cos^2 \theta_0}{2 E t \sin \theta_0} \left\{ 2 \cos^2 \theta_0 - \mu \left[1 - \left(\frac{x_1}{x} \right)^2 \right] \right\}$ | $\frac{p x^2 \cos^2 \theta_0}{2 E t \sin \theta_0} \left\{ 2 \cos^2 \theta_0 - \mu \left[1 - \left(\frac{x_1}{x} \right)^2 \right] \right\}$ |
| ρ | $\frac{p x}{2 E t} \cot^2 \theta_0 \left[2(2 + \mu) \cos^2 \theta_0 - 2\mu + \left(\frac{x_1}{x} \right)^2 - 1 \right]$ | $\frac{p x}{2 E t} \cot^2 \theta_0 \left[2(2 + \mu) \cos^2 \theta_0 - 2\mu + \left(\frac{x_1}{x} \right)^2 - 1 \right]$ |
| (c) HYDROSTATIC PRESSURE LOADING | | |
| N_θ | $-p x \cos \theta_0 \left(\frac{f}{\sin \theta_0} + x \right)$ | $-p x \cos \theta_0 \left(x - \frac{f}{\sin \theta_0} \right)$ |
| N_x | $-p x \cos \theta_0 \left\{ \frac{f}{2 \sin \theta_0} \left[1 - \left(\frac{x_1}{x} \right)^2 \right] + \frac{x}{3} \left[1 - \left(\frac{x_1}{x} \right)^3 \right] \right\}$ | $-p x \cos \theta_0 \left\{ \frac{x}{3} \left[1 - \left(\frac{x_1}{x} \right)^3 \right] - \frac{f}{2 \sin \theta_0} \left[1 - \left(\frac{x_1}{x} \right)^2 \right] \right\}$ |
| Δr | $\frac{p x^2}{E t} \cos^2 \theta_0 \left\{ \mu \left[\frac{f}{2 \sin \theta_0} \left[1 - \left(\frac{x_1}{x} \right)^2 \right] + \frac{x}{3} \left[1 - \left(\frac{x_1}{x} \right)^3 \right] \right] - \frac{f}{\sin \theta_0} x \right\}$ | $\frac{p x^2}{E t} \cos^2 \theta_0 \left\{ \mu \left[\frac{x}{3} \left[1 - \left(\frac{x_1}{x} \right)^3 \right] - \frac{f}{2 \sin \theta_0} \left[1 - \left(\frac{x_1}{x} \right)^2 \right] \right] + \frac{f}{\sin \theta_0} x \right\}$ |
| ρ | $\frac{p x \cos^2 \theta_0}{E t \sin \theta_0} \left[\frac{f}{2 \sin \theta_0} \left[3 + \left(\frac{x_1}{x} \right)^2 \right] + \frac{x}{3} \left[8 + \left(\frac{x_1}{x} \right)^3 \right] \right]$ | $\frac{p x \cos^2 \theta_0}{E t \sin \theta_0} \left[\frac{f}{2 \sin \theta_0} \left[3 + \left(\frac{x_1}{x} \right)^2 \right] - \frac{x}{3} \left[8 + \left(\frac{x_1}{x} \right)^3 \right] \right]$ |

TABLE 2.32-4 (SHEET 4 OF 4)

| | | |
|---|---|---|
| |  <p>Open Conical Shell (Supported)</p> |  <p>Open Conical Shell (hanged)</p> |
| (d) UNIFORM NORMAL PRESSURE | | |
| N_θ | $-px \cot \alpha_0$ | $-px \cot \alpha_0$ |
| N_x | $-\frac{p}{2} x \cot \alpha_0 \left[1 - \left(\frac{x_1}{x} \right)^2 \right]$ | $-\frac{p}{2} x \cot \alpha_0 \left[1 - \left(\frac{x_1}{x} \right)^2 \right]$ |
| Δr | $\frac{p}{Et} x^2 \cos \alpha_0 \cot \alpha_0 \left\{ 1 - \frac{\mu}{2} \left[1 - \left(\frac{x_1}{x} \right)^2 \right] \right\}$ | $-\frac{px^2}{Et} \cos \alpha_0 \cot \alpha_0 \left\{ 1 - \frac{\mu}{2} \left[1 - \left(\frac{x_1}{x} \right)^2 \right] \right\}$ |
| β | $\frac{px}{2Et} \cot^2 \alpha_0 \left[3 + \left(\frac{x_1}{x} \right)^2 \right]$ | $-\frac{px}{2Et} \cot^2 \alpha_0 \left[3 + \left(\frac{x_1}{x} \right)^2 \right]$ |
| (e) EQUALLY DISTRIBUTED LOADING ALONG THE OPENING EDGE (LANTERN LOAD) | | |
| N_θ | 0 | 0 |
| N_x | $-\frac{p_{kl}}{\sin \alpha_0} \frac{x_1}{x}$ | $\frac{p_{kl}}{\sin \alpha_0} \frac{x_1}{x}$ |
| Δr | $\frac{\mu p_{kl} x_1 \cot \alpha_0}{Et}$ | $-\mu \frac{p_{kl} x_1}{Et} \cot \alpha_0$ |
| β | $-\frac{p_{kl}}{Et} \frac{x_1}{x} \frac{\cot \alpha_0}{\sin \alpha_0}$ | $-\frac{p_{kl}}{Et} \frac{x_1}{x} \frac{\cot \alpha_0}{\sin \alpha_0}$ |

2. 32. 6 Cylindrical Shells

The primary solution for cylindrical shells with different axisymmetrical loading conditions will be presented in this section. All solutions are based on the membrane theory. In order that a membrane state of stress may exist, the boundaries of the shell must be free to rotate and to deflect normal to the shell middle surface. Abrupt discontinuity in shell thickness must not be present. The following designations, in connection with Fig. 2. 32-15, will be adopted.



a. Main Designations

b. Differential Element

FIG. 2. 32-15. Cylindrical Shell

$$\xi = \frac{x}{L} \quad \text{where } 0 \leq \xi \leq 1$$

$$B = \frac{Et}{1 - \mu^2}$$

$$k = \frac{\sqrt[4]{3(1 - \mu^2)}}{\sqrt{Rt}}$$

The following loadings will be considered:

1. Linear loading, as a result of the superposition of equally distributed and triangular loading (Fig. 2.32-16)

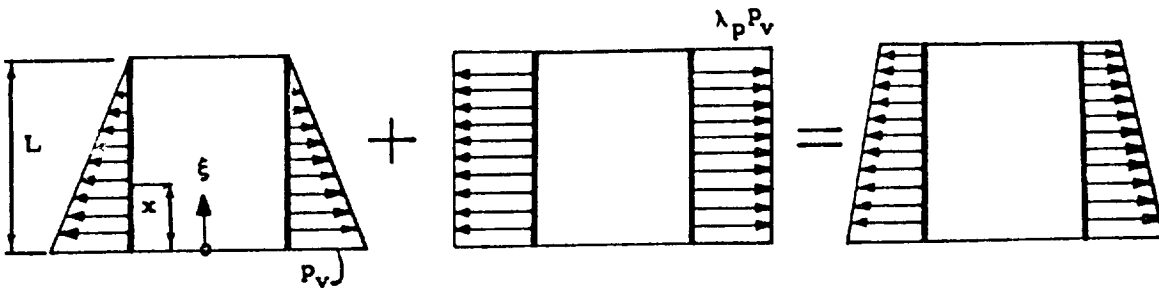


FIG. 2.32-16. Linear Loadings

$$Y = X = 0; \quad Z = p_v (1 + \lambda_p - \xi)$$

2. Trigonometrical loading as a result of superposition

(Fig. 2.32-17)

$$Y = X = 0 \quad Z = p(\xi) = -p_0 (\sin \alpha \xi + \lambda_p \cos \beta \xi)$$

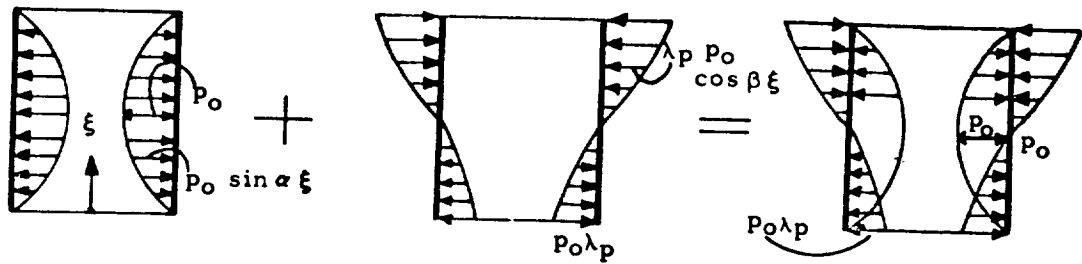


FIG. 2.32-17. Trigonometrical Loadings

3. Exponential loading (Fig. 2.32-18)

$$Z = p(\xi) = -p_0 \exp(-\alpha\xi)$$

also special case:

$$Z = p(\xi) = -\sum_i p_i \exp(-\alpha_i \xi)$$

$$= p \sum_i \lambda_{pi} \exp(-\alpha_i \xi)$$

$$X = Y = 0$$

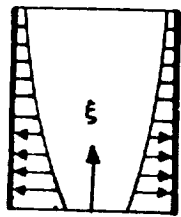
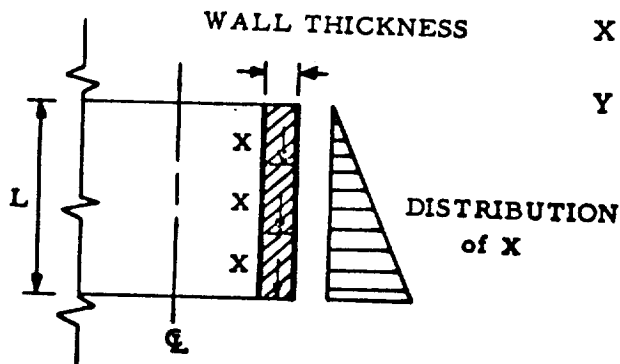


FIG. 2.32-18.
Exponential
Loading Case

λ_i obtainable as in previous cases.

4. Linear loading as per Fig. 2.32-19. (Dead Weight Loading)

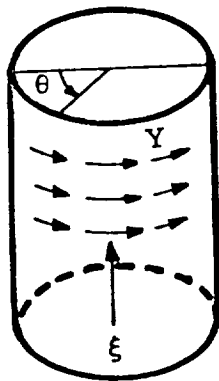


$$X = p_x(\xi) = p_{x0}(1 - \xi)$$

$$Y = Z = 0$$

FIG. 2.32-19. Dead Weight Loading.

5. The constant function Y in circumferential direction (Fig. 2.32-20).

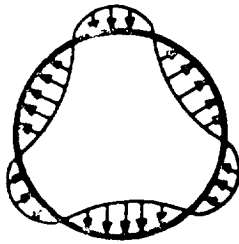


$$Y = p_y$$

$$X = Z = 0$$

FIG. 2.32-20. Circumferential Loading

6. Periodical loading (Fig. 2.32-21). As before, the one dimensionless factor λ_{pi} can be entered. The following periodical loading will be considered here:



$$Z = - p_0 \sum_i \lambda_{pi} \cos \alpha_i \theta$$

$$X = Y = 0$$

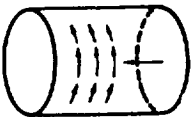
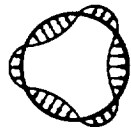
FIG. 2.32-21. Periodic Loading

Membrane solutions for the above listed loading are presented in Table 2.32-5.

TABLE 2.32-5. MEMBRANE SOLUTIONS FOR CYLINDRICAL SHELLS (REF. 2-2)

| Item | Loading | Stresses | | | Deformations | | |
|------|--|--|---|---------------|--|------|--|
| | | N_θ | N_x | $N_{x\theta}$ | u | v | w |
| (1) | Linear Loading $p_v \lambda p$ | $p_v R (1 + \lambda_p - \xi)$ | Zero | Zero | $\frac{1}{Et} \left[-\mu p_v R L \xi \right. \\ \left. (1 + \lambda_p - \frac{1}{2} \xi) \right]$ | Zero | $\frac{1}{Et} \left[p_v R^2 \right. \\ \left. (1 + \lambda_p - \xi) \right]$ |
| (2) | Trigonometrical Loading | $p_o R (\sin \alpha \xi + \lambda_p \cos \beta \xi)$ | Zero | Zero | $\frac{\mu}{Et} p_o R L \left(\frac{\cos \alpha \xi}{\alpha} \right. \\ \left. - \lambda_p \frac{\sin \beta \xi}{\beta} \right)$ | Zero | $\frac{1}{Et} p_o R^2 (\sin \alpha \xi \\ + \lambda_p \cos \beta \xi)$ |
| (3) | Exponential Loading | $p R \sum_1^{\lambda} p_i \exp(-\alpha_i \xi)$ | Zero | Zero | $\frac{1}{Et} \mu p R L \sum_1^{\lambda} \frac{p_i}{\alpha_i} \exp \\ (-\alpha_i \xi)$ | Zero | $\frac{1}{Et} p R^2 \sum_1^{\lambda} p_i \exp \\ (-\alpha_i \xi)$ |
| (4) | Linear Loading Applied to Segments | Zero | $p_{x0} L \left(\frac{1}{2} - \xi + \frac{\xi^2}{2} \right)$ | Zero | $\frac{1}{Et} \left[p_{x0} L^2 \xi \left(\frac{1}{2} \right. \right. \\ \left. \left. - \frac{\xi}{2} + \frac{\xi^2}{6} \right) \right]$ | Zero | $\frac{1}{Et} \mu p_{x0} \sigma L \left(-\frac{1}{2} \right. \\ \left. + \xi - \frac{\xi^2}{2} \right)$ |

TABLE 2.32-5 (CONT)

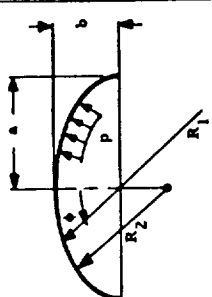
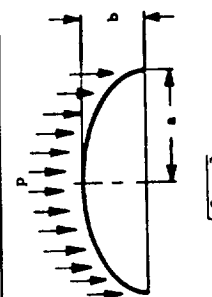
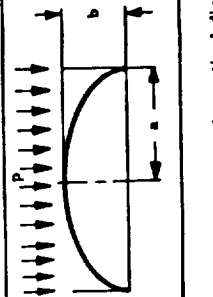
| ITEM | SHELL AND LOADING | STRESSES | | | DEFORMATIONS | | |
|------|--|---|---|--|--|--|---|
| | | N_θ | N_x | $N_{x\theta}$ | u | v | w |
| 5 | <p>CIRCUMFERENTIAL LOADING</p>  | ZERO | ZERO | $P_y L (1 - \xi)$ | ZERO | $\frac{1}{E t} \left[2(1 + \mu) P_y L^2 \left(\xi - \frac{\xi^2}{2} \right) \right]$ | ZERO |
| 6 | <p>PERIODICAL LOADING</p>  | $P_0 R \sum \lambda p_i \cos \alpha_i \theta$ | $\frac{P_0 L^2}{2R} \sum \lambda p_i \sigma_i^2 \cos \alpha_i \theta$ $\sigma_i \theta (-\xi^2 + 2\xi - 1)$ | $P_0 L \sum \lambda p_i \sigma_i \sin \alpha_i \theta$ $\sigma_i \theta (\xi - 1)$ | $\frac{P_0 R^2}{E t} \left[\frac{L^3}{2R^3} \sum \lambda p_i \sigma_i^2 \cos \alpha_i \theta \left(\frac{\xi^3}{3} + \xi^2 - \xi \right) - \frac{1}{R} \xi \sum \lambda p_i \sigma_i \sin \alpha_i \theta \right]$ | $\frac{P_0 R^2}{E t} \left[\frac{L^4}{24R^4} \sum \lambda p_i \sigma_i^3 \sin \alpha_i \theta (-\xi + 4\xi^3 - 6\xi^2) + \frac{L^2}{2R^2} \sum \lambda p_i \sigma_i \sin \alpha_i \theta (2 + \mu) \right]$ $\xi^2 - 4(1 - \mu)\xi$ | $\frac{P_0 R^2}{E t} \left[\frac{\lambda}{1} p_i \cos \alpha_i \theta + \frac{L^4}{24R^4} \sum \lambda p_i \sigma_i^3 \cos \alpha_i \theta + \frac{L^2}{2R^2} \sum \lambda p_i \sigma_i^2 \cos \alpha_i \theta \right]$ $\theta (\xi^4 - 4\xi^3 + 6\xi^2) + \frac{L^2}{2R^2} \sum \lambda p_i \sigma_i^2 \cos \alpha_i \theta$ $\left[-2\xi^2 + 2(2 + \mu) \xi + \mu \right]$ |

2. 32. 7 Elliptical Shell

This subsection presents the solutions for elliptical shells exposed to axisymmetrical loadings. Only closed elliptical shells are considered. The loadings under consideration are presented in Table 2. 32-6. The boundaries of the elliptical shell must be free to rotate and deflect normal to the shell middle surface. Abrupt discontinuities in shell **thickness** must not be present.

The formulas for stresses and deformations are presented in Table 2. 32-6 and are obtained with membrane theory (small deflections) (Table 2. 32-6 and graphs on Figs. 2. 32-22, 23, and 24).

TABLE 2.32-6. ELLIPTICAL MEMBRANE SHELL

| LOADING CASE | LOADING | FORCES | | DISPLACEMENTS* |
|--------------|---|---|---|--|
| | | N_ϕ | N_θ | |
| 1 |  <p>Uniform pressure $Z = P$ $X = Y = 0$</p> | $\frac{R_2 P}{2}$ | $\frac{R_2 P}{2} \left(2 - \frac{R_2}{R_1} \right)$ | $\frac{p R_2 \sin \phi}{2 E t} \left[2 - \mu - \frac{R_2}{R_1} \right]$ |
| 2 |  <p>$\sqrt{\frac{2-Z}{a-b}} = 1$</p> | $-\frac{P}{2} \frac{\sqrt{a^2 \tan^2 \phi + b^2}}{a^2 \sin \phi \tan \phi} \left[2 - \frac{a^2 b^2 \sqrt{1 + \tan^2 \phi}}{b^2 + a^2 \tan^2 \phi} + \frac{b^2}{a} \ln \frac{(1 + \epsilon) \sqrt{b^2 + a^2 \tan^2 \phi}}{b (\epsilon + \sqrt{1 + \tan^2 \phi})} \right]$ | $P \left[\frac{(b^2 + a^2 \tan^2 \phi)^{3/2}}{2 \tan^2 \phi \sqrt{1 + \tan^2 \phi}} \times \left(\frac{1}{a^2} \ln \frac{(1 + \epsilon) \sqrt{b^2 + a^2 \tan^2 \phi}}{b (\epsilon + \sqrt{1 + \tan^2 \phi})} + \frac{1}{b^2} \frac{\sqrt{1 + \tan^2 \phi}}{b^2 + a^2 \tan^2 \phi} \right) - \frac{a^2}{\sqrt{b^2 + a^2 \tan^2 \phi}} \right]$ | See Ref. 2-4 |
| 3 |  | $-\frac{P}{2} \frac{a^2 \sqrt{1 + \tan^2 \phi}}{\sqrt{b^2 + a^2 \tan^2 \phi}}$ | $-\frac{P}{2} \frac{a^2}{b} \frac{b^2 - a^2 \tan^2 \phi}{\sqrt{b^2 + a^2 \tan^2 \phi} \sqrt{1 + \tan^2 \phi}}$ | See Ref. 2-4 |

The stresses are plotted in non-dimensional form according to following equation:

$$\frac{N_\phi}{ap} = \frac{a}{2b} \left[1 - \left(\frac{Z}{a} \right)^2 \left[1 - \left(\frac{b}{a} \right)^2 \right] \right]^{1/2}$$

$$\frac{N_\theta}{ap} = \frac{N_\phi}{ap} \left[2 - \frac{1}{1 - \left(\frac{Z}{a} \right)^2 \left[1 - \left(\frac{b}{a} \right)^2 \right]} \right]$$

*In this case γ represents vertical displacement if Δr is horizontal $\eta = \frac{a}{b} K = \eta^2 - 1$

FIG. 2.32-22 MEMBRANE FORCE PARAMETERS FOR ELLIPSOIDAL SHELLS UNDER UNIFORM PRESSURE (CASE 1)

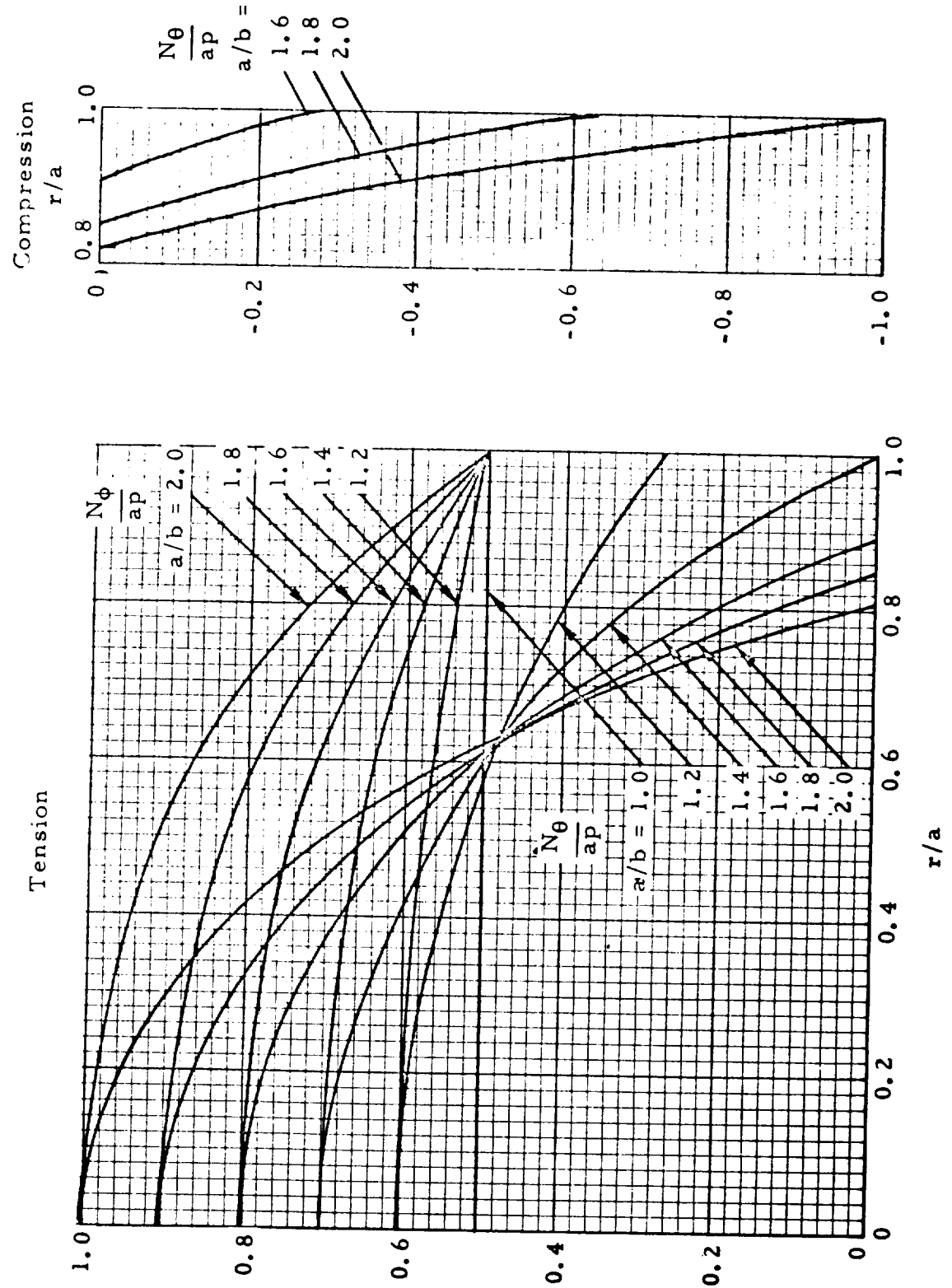


FIG. 2.32-23 DISPLACEMENT AND ROTATION PARAMETERS FOR ELLIPSOIDAL SHELLS UNDER UNIFORM PRESSURE

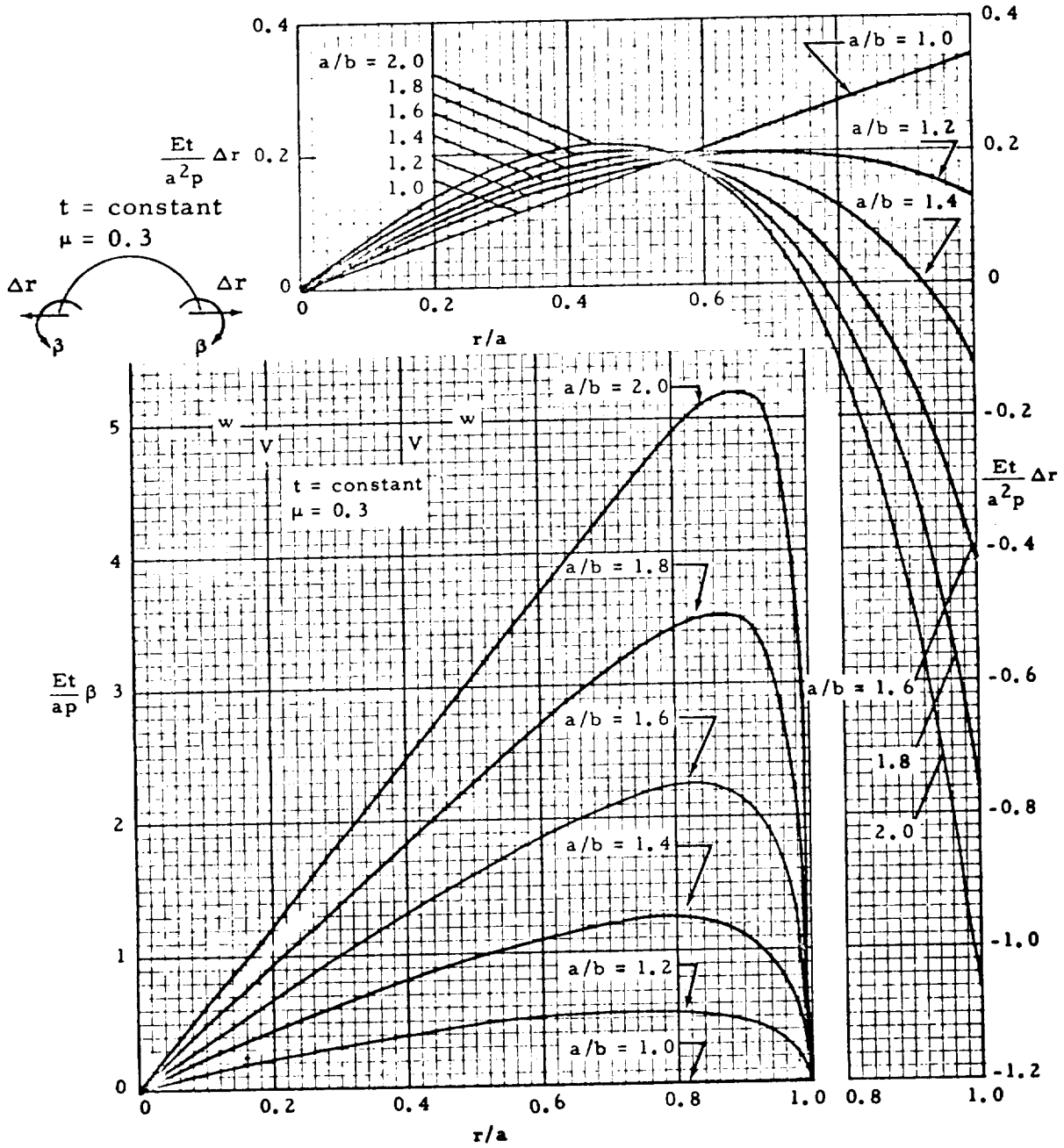
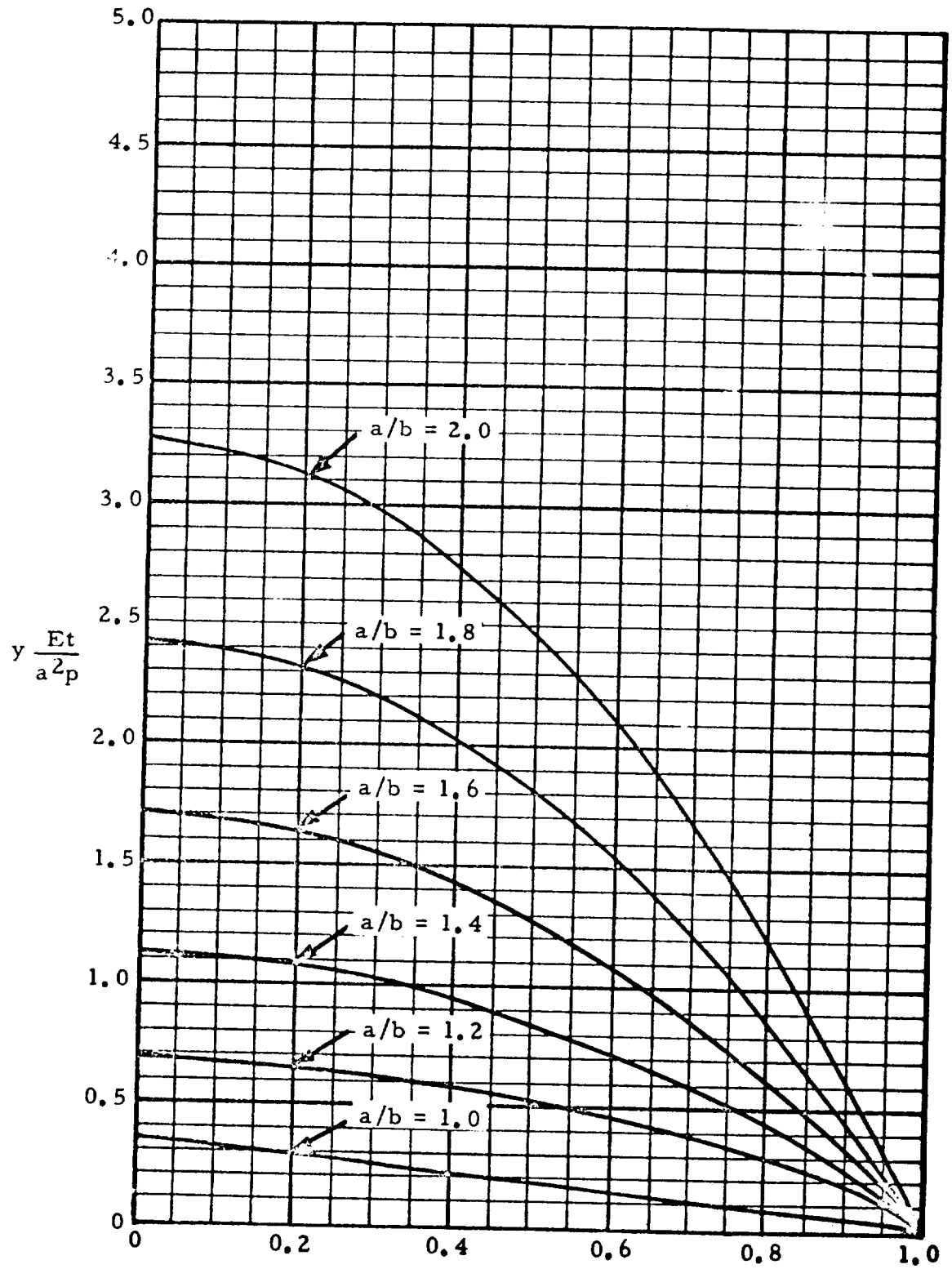


FIG. 2.32-24. DISPLACEMENT PARAMETER FOR ELLIPSOIDAL SHELLS UNDER UNIFORM PRESSURE



2. 32. 8 Cassini Shells

These shells are useful as boiler bulkheads. The discrepancy of the hoop forces of the boiler and the boiler drum may be avoided by choosing one family of Cassinian curves as a meridian shape. Its equation is

$$(r^2 + n^2 z^2)^2 + 2a^2 (r^2 - n^2 z^2) = 3a^4$$

where n is a number > 1 , r and z are variables along r and z lines, and $a = \max z$ as per Fig. 2. 32-25.

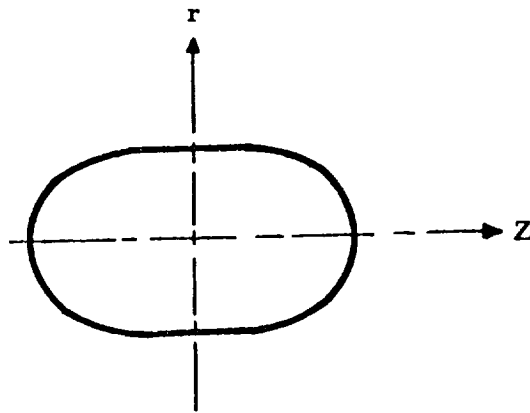


FIG. 2. 32-25. Cassini's Curve

The formulas presented are based on the membrane small deflection theory. Consequently, the boundaries of the shell must be free to rotate and deflect normal to the middle shell surface. Abrupt discontinuities in shell thickness must not be present. The only loading that will be considered is pressurization.

The second loading case is plotted (Fig. 2. 32-26) in nondimensional form according to the following equations:

$$\frac{N_{\phi}}{ap} = \frac{2}{5(4K+3)} \left[5(16K^4 + 24K^3 - 7K^2 + 8K + 3) \right]^{1/2}$$
$$\frac{N_{\phi}}{ap} = \frac{4 \left[64K^5 + 144K^4 + 44K^3 - 85K^2 - 36K + 23 \right]}{(4K+3)^2 \left[5(16K^4 + 24K^3 - 7K^2 + 8K + 3) \right]^{1/2}}$$

where K is given in Table 2. 32-7.

Additional graphs for Δr , y , and β are given in Fig. 2. 32-27 and 2. 32-28.

TABLE 2.32-7. CASSINI SHELLS—MEMBRANE SOLUTIONS

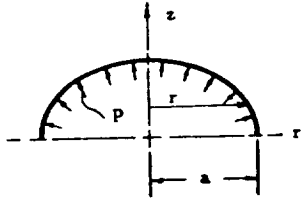
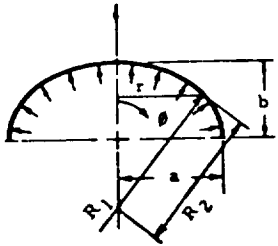
| | | Case ① | Case ② |
|-------------------|------------|---|--|
| Loading and Shape | | $n > 1$  | Special Case: $n = 2$ $b = 0.743a$  |
| | | | |
| Forces | N_θ | $pa \left[\frac{r^2(a^2 + n^2 z^2) + n^4 z^2(a^2 - r^2)}{a^2 + r^2 + n^2 z^2} \right]^{1/2}$ | $\frac{R_2 p}{2}$ |
| | N_ϕ | $N_\phi \left[2 - \frac{3n^2 a^4}{(a^2 + r^2 + n^2 z^2)} \frac{(a^2 - r^2 + n^2 z^2)}{\left[r^2(a^2 + n^2 z^2) + n^4 z^2(a^2 - r^2) \right]} \right]$ | $\frac{R_2 p}{2} \left[2 - \frac{R_2}{R_1} \right]$ |
| Displacements | Δr | | $\frac{p R_2^2 \sin \theta}{2Et} \left[2 - \mu - \frac{R_2}{R_1} \right]$ |
| | y | For determination of Δr , y , and β , see Section 2.32.2 | $\Delta r \cot \phi - \int \frac{R_1 (N_\phi - \mu N_\theta) - R_2 (N_\theta - \mu N_\phi)}{Et \sin \phi} d\phi + C$ |
| | β | | $\frac{p R_2}{2Et \tan \phi} \left[\left(\frac{R_2}{R_1} - 1 \right) \left(\frac{R_2}{R_1} + 3 \right) - R_2^2 \sin^4 \theta Z \right]$ |
| Remarks | | | $Z = \frac{2160}{a^2 K(3+4K)^4}$ $K = \left[1 - 0.94 \left(\frac{r}{a} \right)^2 \right]^{1/2}$ |

FIG. 2.32-26 MEMBRANE FORCE PARAMETERS FOR CASSINI SHELLS UNDER UNIFORM PRESSURE (CASE ②)

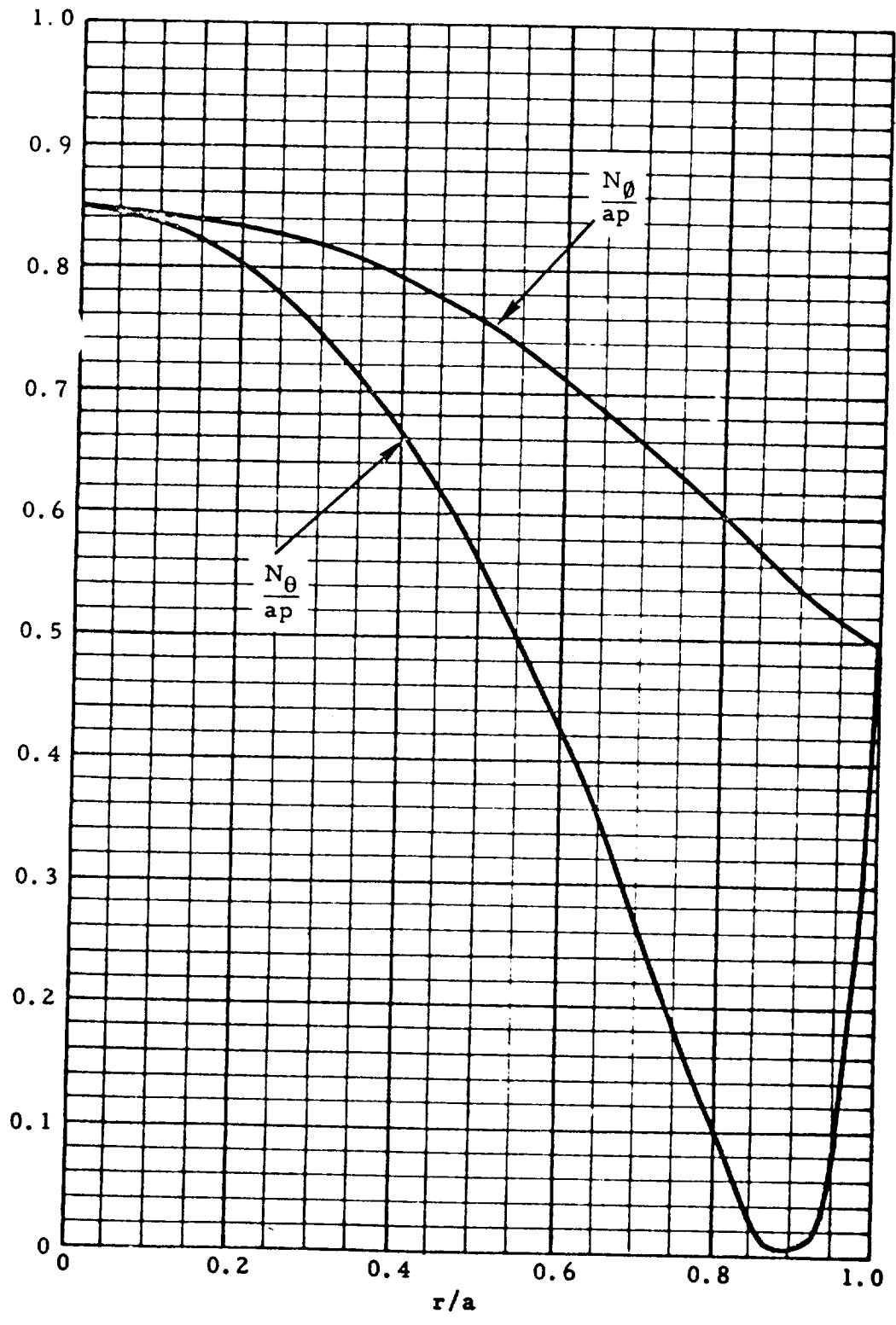


FIG. 2.32-27 DISPLACEMENT AND ROTATION PARAMETERS FOR CASSINI DOMES UNDER UNIFORM PRESSURE (CASE 1)

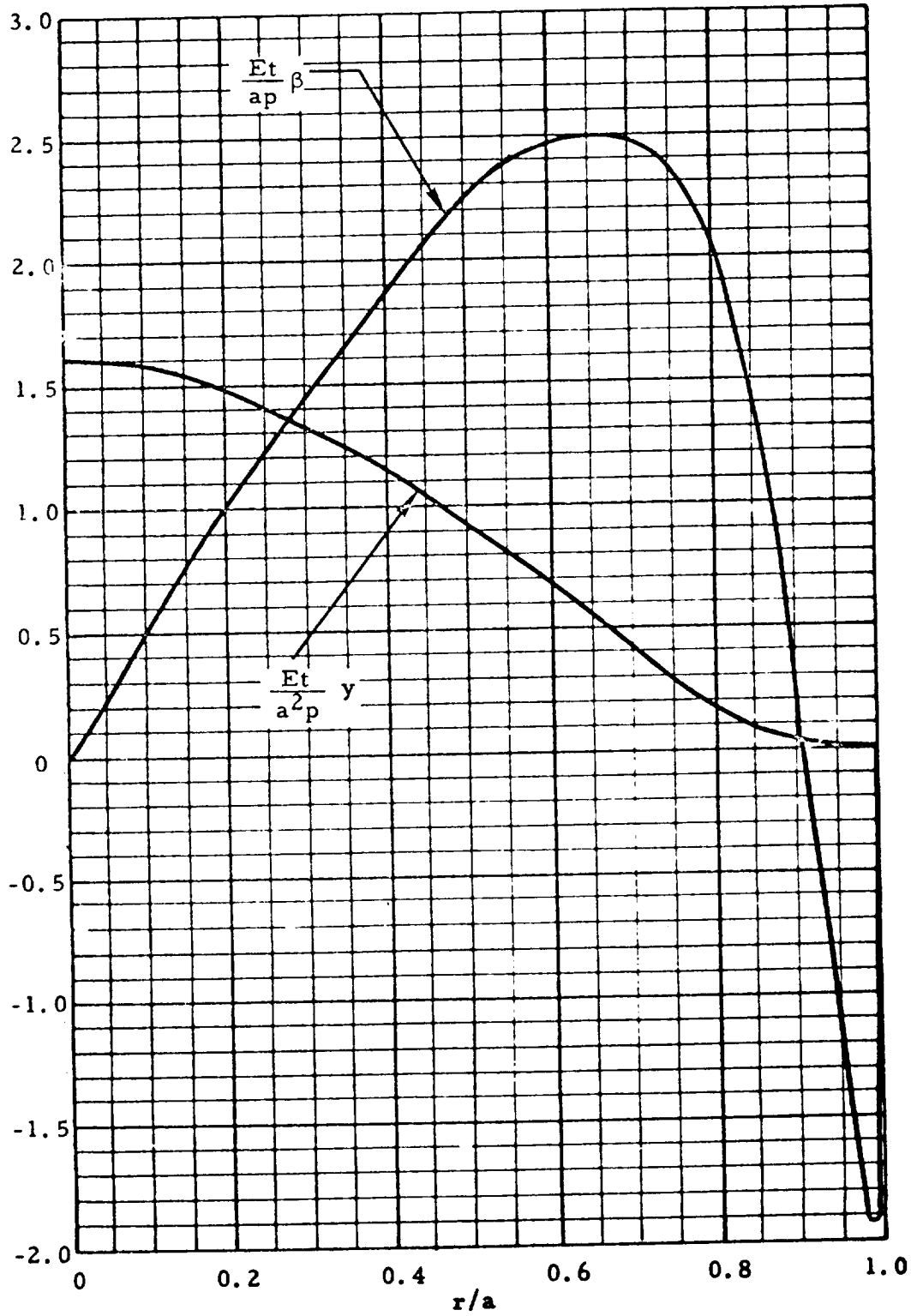
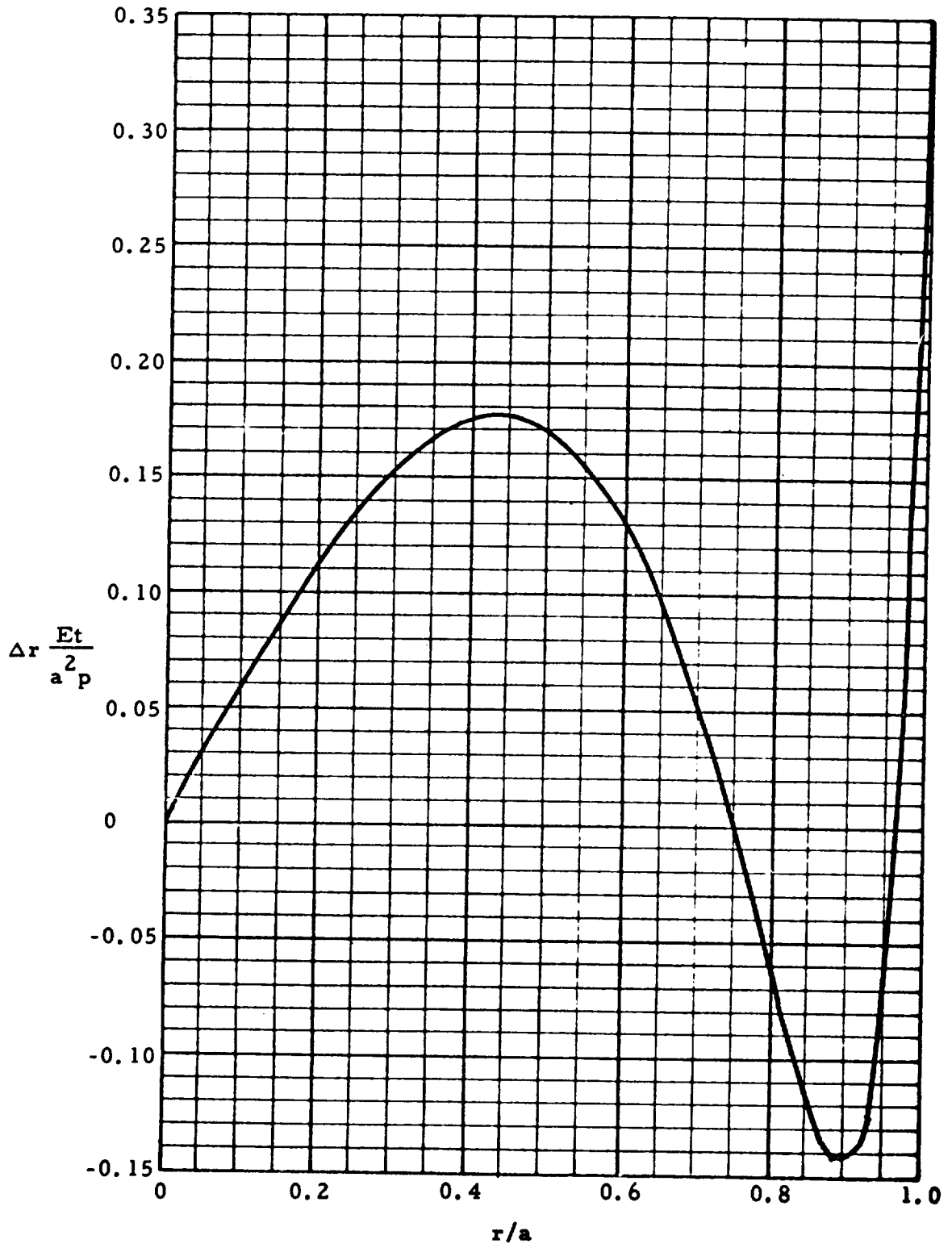


FIG. 2.32-28 DISPLACEMENT PARAMETER FOR CASSINIAN DOMES UNDER UNIFORM PRESSURE (CASE 1)



2.32.9 Toroidal Shells

This section presents some known solutions for closed and open toroidal shells. The loading and systems under consideration are indicated in the Tables 2.32-8 and 2.32-9. The solutions are based on membrane-small deflection theory; consequently, the boundaries must be free to rotate and deflect normal to the shell middle surface. Abrupt discontinuities in shell thickness must not be present. The walls of the shells are assumed to be of uniform thickness.

TABLE 2.32-8. TOROIDAL SHELL PRIMARY SOLUTIONS

| Loading Case | Loading and Shell | Forces | | Horizontal Displacement Δr | Displacements | | Rotation β |
|--------------|-------------------|---|---|--|--|---|-------------------|
| | | N_θ | N_ϕ | | Vertical Displacement y | | |
| ① | | $\frac{pR}{Z} \left[\frac{b}{R \sin \theta} + 1 \right]$ | $\frac{pR}{Z}$ | $\frac{pR^2}{2Et} \left[\frac{b}{R} (1 - 2\mu) + (1 - \mu) \sin \theta \right] + (1 - \mu) \sin \theta$ | (See footnote. *) | (See footnote. *) | (See footnote. *) |
| ② | | $\frac{pR}{Z} \left[\frac{b}{R \sin \theta} + 1 \right]$ | $\frac{pR}{Z} \left[1 - \frac{b^2}{R^2 \sin^2 \theta} \right]$ | $\frac{pR^2}{2Et} \left[\frac{b}{R} (1 - 2\mu) + (1 - \mu) \sin \theta + \frac{b^2(1 + \mu)}{R^2 \sin \theta} - \frac{b^3}{R^3 \sin^2 \theta} \right]$ | $\frac{pR^2}{2Et} \left[(1 - \mu) \cos \theta + \frac{b}{R} \left(1 - \frac{2b^2}{3R^2} \right) \cot \theta + \frac{b^2}{R^2} \left(\frac{3}{2} + 2\mu \right) \frac{\cot \theta}{\sin \theta} - \frac{b^2}{R^2} \left(1 + \frac{b}{3R} \right) \frac{\cot \theta}{\sin^2 \theta} - \frac{b^2}{2R^2} (1 + 2\mu) \frac{1}{\sin^2 \theta} \right]$ | $\frac{pR \cot \theta}{2Et \sin \theta} \left[\frac{b}{R} \left(\frac{2b}{R \sin \theta} - 1 \right) \left(\frac{b}{R \sin \theta} + 1 \right) \right]$ | |
| ③ | | $\frac{pR}{Z} \left[\frac{b}{R \sin \theta} - 1 \right]$ | $\frac{pR}{Z} \left[\frac{b^2}{R^2 \sin^2 \theta} - 1 \right]$ | $\frac{pR^2}{2Et} \left[-\frac{b}{R} (1 - 2\mu) + (1 - \mu) \sin \theta - \frac{b^2(1 + \mu)}{R^2 \sin \theta} + \frac{b^3}{R^3 \sin^2 \theta} \right]$ | $\frac{pR^2}{2Et} \left[(1 - \mu) \cos \theta + \frac{b}{R} \left(1 + \frac{2b^2}{3R^2} \right) \cot \theta + \frac{b^2}{R^2} \left(\frac{3}{2} + 2\mu \right) \frac{\cot \theta}{\sin \theta} - \frac{b^2}{R^2} \left(1 - \frac{b}{3R} \right) \frac{\cot \theta}{\sin^2 \theta} - \frac{b^2}{2R^2} (1 + 2\mu) \frac{1}{\sin^2 \theta} \right]$ | $-\frac{pR \cot \theta}{2Et \sin \theta} \left[\frac{b}{R} \left(\frac{2b}{R \sin \theta} + 1 \right) \left(\frac{b}{R \sin \theta} - 1 \right) \right]$ | |

*The equations for the displacement y , and rotation β , as derived from the Linear Membrane Theory, are discontinuous and incompatible at $\theta = 0^\circ$ and π . **For approximate useful range: $35^\circ \leq \theta \leq 75^\circ$

TABLE 2.32-9. TOROIDAL SHELL (Ref. 2-4)

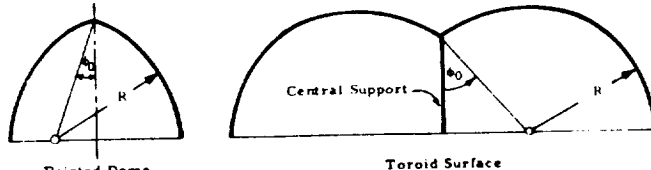
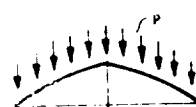
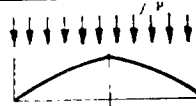
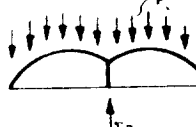

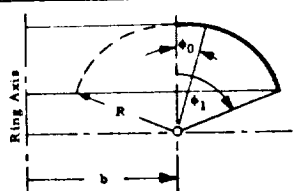
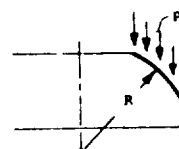
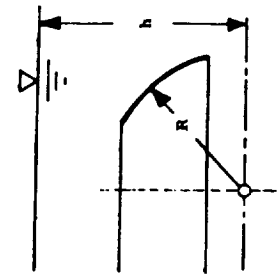
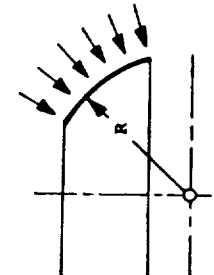
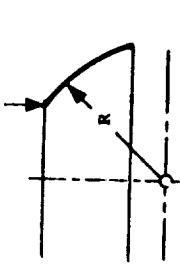
| (a) Ring axis bisects the cross-section  | | | | |
|---|---|--|---|---|
| No. | Shell | Loading Condition | N_ϕ | N_θ |
| ① |  | $P_x = p \sin \phi$ $P_z = p \cos \phi$ | $-pR \frac{\cos \phi_0 - \cos \phi - (\phi - \phi_0) \sin \phi_0}{(\sin \phi - \sin \phi_0) \sin \phi}$ | $-p \frac{R}{\sin^2 \phi} \left[(\phi - \phi_0) \sin \phi_0 - (\cos \phi_0 - \cos \phi) + (\sin \phi - \sin \phi_0) \sin \phi \cos \phi \right]$ |
| ② |  | $P_x = p \sin \phi \cos \phi$ $P_z = p \cos^2 \phi$ | $-p \frac{R}{2} \left(1 - \frac{\sin \phi_0}{\sin \phi} \right)$ | $-p \frac{R}{2} \left(\cos 2\phi + 2 \sin \phi \sin \phi_0 - \frac{\sin^2 \phi_0}{\sin^2 \phi} \right)$ |
| ③ |  | $P_x = p \sin \phi$ $P_z = p \cos \phi$ $\Sigma p = 2p\pi \left(R \phi_0 \sin \phi_0 - 2 \sin^2 \frac{\phi_0}{2} \right)$ | $-pR \frac{1 - \cos \phi + \phi \sin \phi_0}{\sin \phi (\sin \phi + \sin \phi_0)}$ | $-pR \left[\cos \phi - \frac{1 - \cos \phi}{\sin^2 \phi} + \sin \phi \left(\cot \phi - \frac{\phi}{\sin^2 \phi} \right) \right]$ |
| ④ |  | $P_x = p \sin \phi \cos \phi$ $P_z = p \cos^2 \phi$ $\Sigma p = p\pi R^2 \sin^2 \phi_0$ | $-p \frac{R}{2} \frac{\sin \phi + 2 \sin \phi_0}{\sin \phi + \sin \phi_0}$ | $p \frac{R}{2} (\cos 2\phi - 2 \sin \phi \sin \phi_0)$ |
| (b) Ring axis does not bisect the cross-section  | | | | |
| No. | Shell | Loading Condition | N_ϕ | N_θ |
| ⑤ |  | $P_x = p \sin \phi$ $P_z = p \cos \phi$ | $-p \frac{bR(\phi - \phi_0) + R^2(\cos \phi_0 - \cos \phi)}{(b + R \sin \phi) \sin \phi}$ <p style="text-align: center;">For $\phi_0 = -\phi_1$ (symmetrical cross-section)</p> $-p \frac{bR\phi + R^2(1 - \cos \phi)}{(b + R \sin \phi) \sin \phi}$ | $-\frac{p}{\sin \phi} \left[(b + R \sin \phi) \cos \phi - b(\phi - \phi_0) - R(\cos \phi_0 - \cos \phi) \right]$ $-\frac{p}{\sin \phi} \left[(b + R \sin \phi) \cos \phi - b\phi - R(1 - \cos \phi) \right]$ |

TABLE 2.32-9. (CONT)

| No. | Shell | Loading Condition | N_ϕ | N_θ |
|-----|---|---|--|--|
| ⑨ |  | $P_x = P(h - R \cos \phi)$ | $-\frac{\rho R}{(b + R \sin \phi) \sin \phi} \left[-bh (\sin \phi_0 - \sin \phi) + \frac{Rh}{2} (\cos^2 \phi_0 - \cos^2 \phi) + \frac{bR}{2} (\sin \phi_0 \cos \phi_0 - \sin \phi \cos \phi - \phi + \phi_0) - \frac{R^2}{3} (\cos^3 \phi_0 - \cos^3 \phi) \right]$ <p style="text-align: center;">For $\phi_0 = -\phi$, (symmetrical cross-section)</p> | $-\frac{P}{\sin^2 \phi} \left[(h - R \cos \phi) (b - R \sin \phi) \times \sin \phi + bh (\sin \phi_0 - \sin \phi) - \frac{Rh}{2} (\cos^2 \phi_0 - \cos^2 \phi) - \frac{bR}{2} \times (\sin \phi_0 \cos \phi_0 - \sin \phi \cos \phi - \phi + \phi_0) + \frac{R^2}{3} (\cos^3 \phi_0 - \cos^3 \phi) \right]$ |
| ⑩ |  | $P_x = P$ | $-\frac{\rho R}{(b + R \sin \phi) \sin \phi} \left[bh \sin \phi + \frac{Rh}{2} \sin^2 \phi - \frac{bR}{2} (\sin \phi \cos \phi + \phi) - \frac{R^2}{3} (1 - \cos^3 \phi) \right]$ <p style="text-align: center;">For $\phi_0 = -\phi$, (symmetrical cross-section)</p> | $-\frac{P}{2 \sin^2 \phi} \left[2b \sin \phi_0 + R (\sin^2 \phi_0 + \sin^2 \phi) \right]$ |
| ⑪ |  | <p style="text-align: center;">Edge load P_L</p> | $-\frac{P_L}{R} \frac{b + R \sin \phi_0}{(b + R \sin \phi) \sin \phi}$ | $-\frac{P_L}{R} \frac{b + R \sin \phi_0}{\sin^2 \phi}$ |

2. 32. 10 Other Geometries of Shells

Some solutions for shells of other geometries—modified elliptical, pointed, parabolical, and cycloidal shells—are presented herein. The shells considered will be loaded with internal and external pressure, or with evenly distributed loading over the shell-surface on shell base. For parabolical shells, the hydrostatic pressure is also considered. All loadings are axisymmetrical.

The formulas for the internal forces are obtained with linear membrane theory; consequently, the boundaries must be free to rotate and deflect normal to the shell middle surface. The thickness of the shell is assumed to be constant. Abrupt discontinuities in shell thickness must not be present. Table 2. 32-10 presents the stresses in different shells. For determining displacements, the procedure described in paragraph 2. 32. 2 shall be used.

TABLE 2.32-10. OTHER SHELLS OF REVOLUTION WITH CURVED MERIDIAN (Ref. 2-4)

| Case | Shell Geometry | Loading | Shell Normal | |
|------|--|--|--|--|
| | | | N_ϕ | N_θ |
| | <p> r_0 Radius of curvature at vertex X, Z Surface load components N_ϕ, N_θ Unit normal forces </p> | | | |
| ① | | $X = p \sin \phi$ $Z = p \cos \phi$ | $-p \frac{r_0}{3} \frac{1 - \cos^3 \phi}{\sin^2 \phi \cos^2 \phi}$ | $-p \frac{r_0}{3} \frac{2 - 3 \cos^2 \phi + \cos^3 \phi}{\sin^2 \phi}$ |
| ② | | $X = p \sin \phi \cos \phi$ $Z = p \cos^2 \phi$ | $-p \frac{r_0}{2} \frac{1}{\cos \phi}$ | $-p \frac{r_0}{2} \cos \phi$ |
| ③ | | $Z = p \left(h + \frac{r_0}{2} \tan^2 \phi \right)$ | $-p \frac{r_0}{2} \left(h + \frac{r_0}{4} \tan^2 \phi \right) \frac{1}{\cos \phi}$ | $-p \frac{r_0}{2} \left[h (2 \tan^2 \phi + 1) + r_0 \tan^2 \phi \left(\tan^2 \phi + \frac{3}{4} \right) \right] \cos \phi$ |
| ④ | | $Z = p$ | $-p \frac{r_0}{2} \frac{1}{\cos \phi}$ | $-p \frac{r_0}{2} \frac{1 + \sin^2 \phi}{\cos \phi}$ |
| ⑤ | | $X = p \sin \phi$ $Z = p \cos \phi$ | $-p \frac{r_0}{2} \frac{\phi \sin \phi + \cos \phi - \frac{1}{3} \cos^3 \phi - \frac{2}{3}}{(2\phi + \sin 2\phi) \sin \phi}$ | $-p \frac{r_0}{2} \left[\frac{1 - \cos \phi}{3 \sin^2 \phi} \cos \phi - \frac{\phi}{2} \tan \phi - \frac{1}{2} \sin^2 \phi \right]$ |
| ⑥ | | $X = p \sin \phi \cos \phi$ $Z = p \cos^2 \phi$ | $-p \frac{r_0}{8} \frac{2\phi + \sin 2\phi}{\sin \phi}$ | $-p \frac{r_0}{16} \frac{2\phi + \sin 2\phi}{\sin \phi} \times \left(4 \cos^2 \phi - \frac{2\phi}{\sin 2\phi} - 1 \right)$ |

TABLE 2.32-10. (CONT)

| Case | Geometry | Loading | Stresses | | Remarks |
|------|--|----------------|---|--|--|
| | | | N_ϕ | N_θ | |
| ⑦ | <p>Modified Elliptical Shell Equation of meridian</p> $y = - \int \frac{x^3 dx}{\sqrt{(1-x^2)(x^2-a_1)(x^2-a_2)}}$ | Pressurization | $\frac{1}{2} \frac{p R m^2}{2 x^2}$ <p>For the bottom-edge:</p> $N_\phi \left(2 - \frac{x}{n} \right)$ | $N_\theta \left(2 - \frac{x}{n} \right)$ | $a_1 = \frac{1}{2} \left(\sqrt{\frac{4x_0^2}{1-x_0^2}} - 1 \right)$ $a_2 = -\frac{1}{2} \left(\sqrt{\frac{4x_0^2}{1-x_0^2}} + 1 \right)$ $m = (1-x^2)(x^2-a_1)(x^2-a_2)$ $n = 1 + \frac{6}{m}$ |
| ⑧ | | Pressurization | $\frac{p R m}{2}$ | $p m \left(1 - \frac{m}{2} \right)$ <p>where $m = 1 - \frac{\sin \phi_0}{\sin \phi}$</p> | <p>Solution is not valid at Apex.</p> <p>Reference 2-5.</p> |

2. 32. 11 Irregular Shell

Regardless of the shape of the meridian and kind of loading, determination of membrane forces appears to be relatively simple because it is a statically determinate problem. Table 2. 32-1 may be used for this purpose.

Determination of the displacements is a complicated and possibly time-consuming problem. A simplified method for obtaining the approximate solution is presented by M. G. Salvadori (Ref. 2-6).

Consider a shell of revolution generated by the rotation of a meridian curve $y(x)$ around the y -axis, as is shown on Fig. 2. 32-29. The following conditions shall be satisfied:

1. The shell is vertical at the edge ($y = 0$).
2. The meridian curve is symmetrical about the equator.
3. The shell thickness is practically constant near the edge.

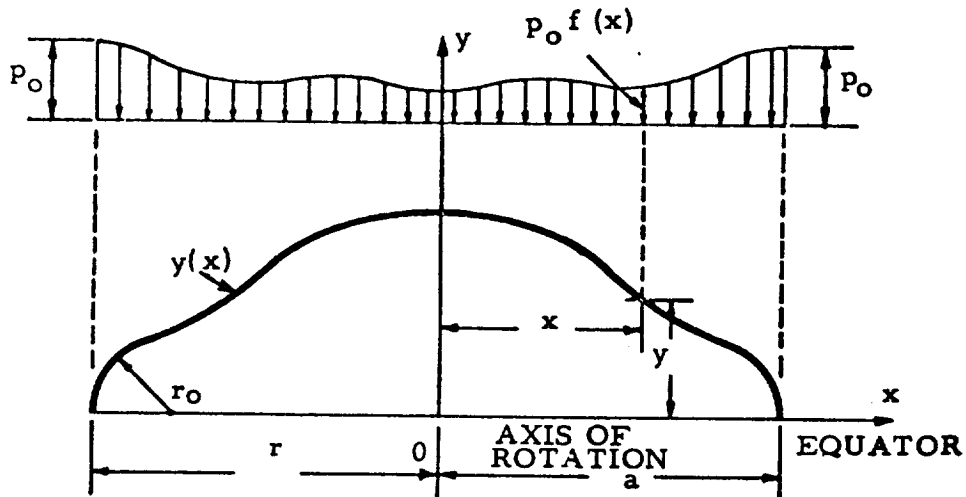


FIG. 2. 32-29. Shell of Revolution Under Vertical Load

The shell is loaded by a distributed load, p , per unit of horizontal projection, whose intensity varies with the law:

$$p(x) = p_0 f(x)$$

Salvadori (Ref. 2-6) proved that, under conditions 1, 2, and 3 and assuming the membrane conditions, the following is correct:

- (a) The edge of the shell does not rotate.
- (b) The radial displacement of the edge of the shell is independent of the meridian shape.
- (c) The displacement (positive outward) is given by

$$\Delta r = \frac{p_0 r^2}{E t_s} \left(\frac{r}{r_0} \right) S_p$$

where

r = equator radius = a

r_0 = radius of curvature of meridian at equator

t_s = shell thickness at equator

E = modulus of elasticity

$S_p = \frac{2}{r^2} \int_0^r f(x)x \cdot dx$ is the static moment of the load about the axis of rotation in nondimensional form.

Poisson ratio, μ , is assumed to be zero. For the load distribution not representable by a simple formula, S_p may be evaluated numerically by means of the approximate summation formula:

$$S_p = \frac{2}{P_o r} \sum_{i=1}^n p(x_i) x_i \Delta x$$

as shown in Fig. 2.32-30.

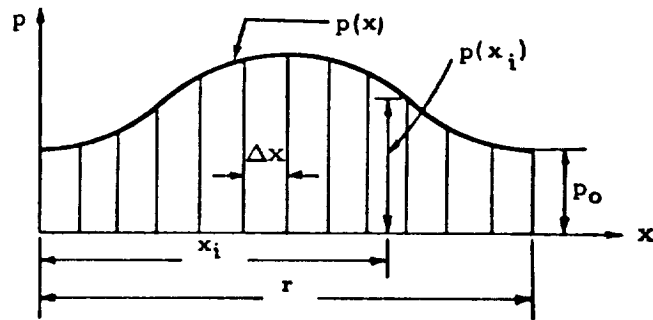


FIG. 2.32-30. Numerical Evaluation of S_p

The value of the radius of curvature r_o in connection with Fig. 2.32-31 is

$$r_o = R \text{ for spherical shells}$$

$$r_o = R^* \text{ for conoidal shells}$$

$$r_o = \frac{b^2}{a} \text{ for elliptical shell of rise } b$$

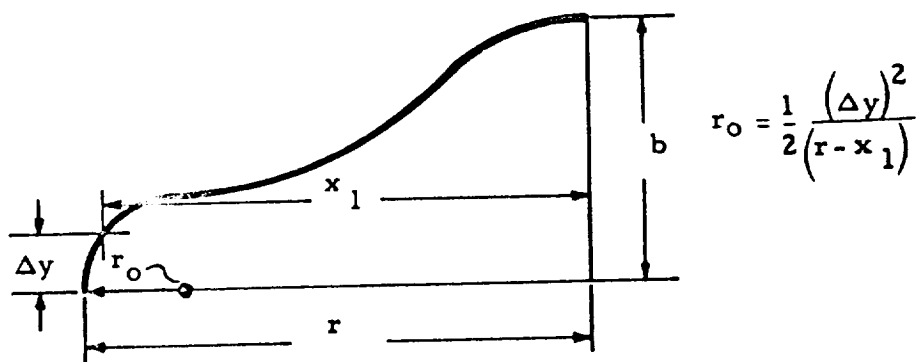
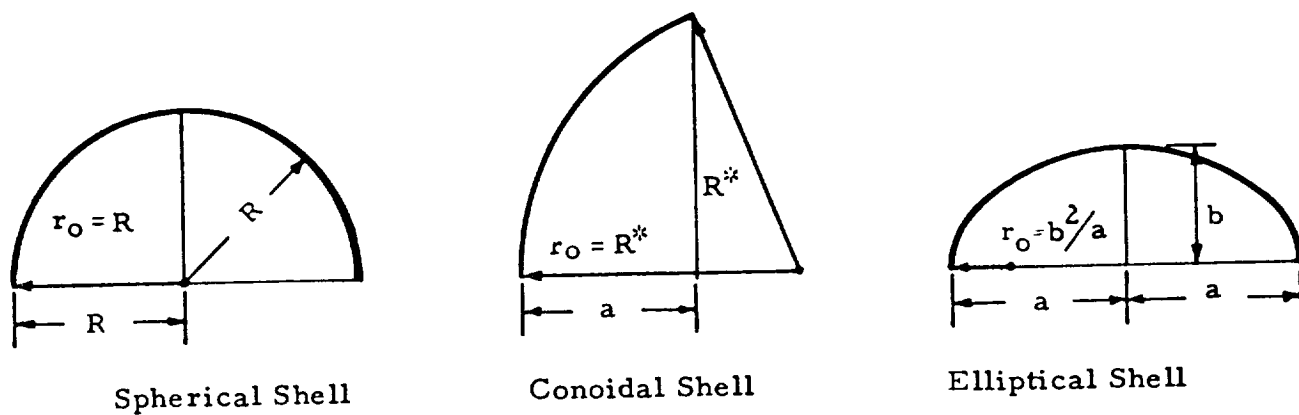
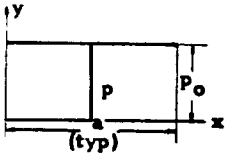
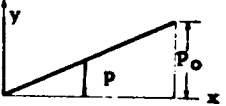
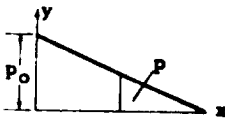
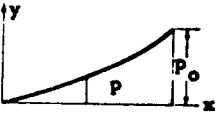
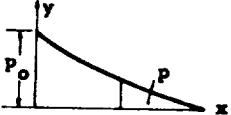
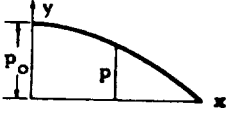
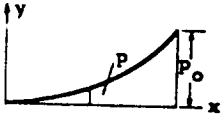
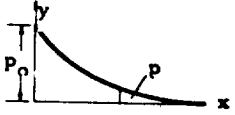



FIG. 2.32-31. Radius of Curvature r_o for Various Types of Shells

Finally, for common loading distributions, $p(x)$, Table 2.32-11 gives correspondent S_p factors. This approximate method is very handy if time is a pressing element.

A similar "short cut" for determining deformations due to unit-edge loadings is given by Salvadori (Ref. 2-6) and will be presented later.

TABLE 2.32-11. S_p FACTORS

| Distribution of Loading | Equation of Loading Intensity | S_p Factor |
|---|---|----------------|
|  | $p = P_0$ | 1 |
|  | $p = P_0 \frac{x}{a}$ | $\frac{2}{3}$ |
|  | $p = P_0 \left(1 - \frac{x}{a}\right)$ | $\frac{1}{3}$ |
|  | $p = P_0 \left(\frac{x}{a}\right)^2$ | $\frac{1}{2}$ |
|  | $p = P_0 \left(1 - \frac{x}{a}\right)^2$ | $\frac{1}{6}$ |
|  | $p = P_0 \left[1 - \left(\frac{x}{a}\right)^2\right]$ | $\frac{1}{2}$ |
|  | $p = P_0 \left(\frac{x}{a}\right)^3$ | $\frac{2}{5}$ |
|  | $p = P_0 \left(1 - \frac{x}{a}\right)^3$ | $\frac{1}{10}$ |
|  | $p = P_0 \left[1 - \left(\frac{x}{a}\right)^3\right]$ | $\frac{3}{5}$ |

2. 32. 12 Conclusion

The collection of membrane solutions presented above for special cases of geometry and loading represent the majority of the problems that any analyst may face in actual practice. The exact and approximate approaches are given. This concludes the presentation of primary solutions.

To perform the interaction of different shell elements, there must also be secondary solutions known. This task will be performed in the following section.

2. 33 SECONDARY SOLUTIONS

2. 33.1 Introduction and General Discussion

Unit loadings (defined in Section 2. 22. 5) are the loadings acting on upper or lower edge of shell:

$$M = 1 \text{ lb-in/in}$$

$$Q = 1 \text{ lb/in}$$

Unit influences are deformations and forces in a shell of revolution due to unit loadings. Influences of this nature are of local character and do not progress very far into the shell from the disturbed edge.

Various differently shaped shells are covered in this section. Of special interest is a shell that represents a bulkhead, which is characterized with $\phi_{\max} = 90^\circ$; such bulkheads are very common in air space vehicles and pressure vessels. The bulkhead shells are tangent to the cylindrical body of the vehicle.

When the values of deformations due to the unit loadings are available, the deformations can be entered together with the primary deformations into set of equations 2. 23-1 or 3, and discontinuity stresses can be determined.

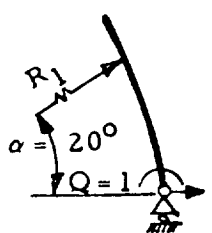





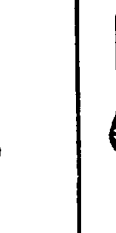

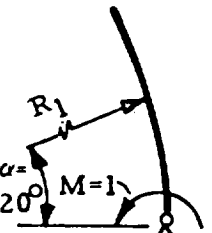






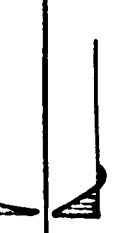
The bending theory is used to obtain the influence coefficients due to unit loadings. The fundamentals of this procedure were explained in the

introductory sections. Some conclusions will be discussed and the final formulas for different geometries of shells will be presented.

It has been mentioned that deflections and internal loads due to unit loadings are of local importance. It can be concluded that all disturbances due to edge-unit loadings will disappear completely for $\alpha \geq 20^\circ$ and will become negligible for $\alpha \geq 10^\circ$, as shown on Table 2.33-1 for a spherical shell.

Table 2.33-1 illustrates a very important conclusion: due to the unit-edge loadings, practically all parts of the shell, satisfying the condition $\alpha \geq 20^\circ$, will remain unstressed and undisturbed. These parts will

TABLE 2.33-1. UNIT EDGE LOADING SOLUTIONS

| | N_θ | N_ϕ | M_θ | M_ϕ | Q | Δr | θ |
|---|---|---|---|---|--|---|---|
|  |  |  |  |  |  |  |  |
|  |  |  |  |  |  |  |  |

not be needed for satisfying equilibrium. They do not effect the stresses and deformations in disturbed zone $0 < \alpha < 20^\circ$ in any way. We can delete all material above $\alpha = 20^\circ$ because this material does not contribute to the stresses or strains, which are computed for the zone defined with $0 < \alpha < 20^\circ$. Nothing will be changed in the regime of stresses or deformations in zone $0 < \alpha < 20^\circ$ if we replace the removed material with any shape of shell, as shown in Fig. 2.33-1, which illustrates imaginary operations. Consequently, cases A, B, and C in Fig. 2.33-1 are statically equivalent. This discussion leads to the following conclusions:

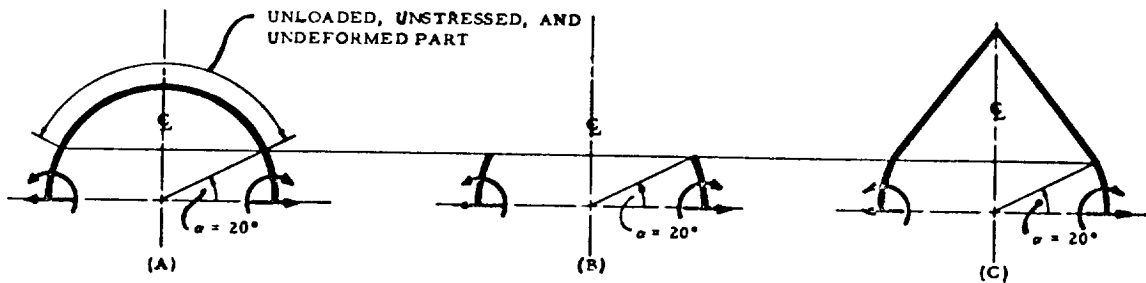


FIG. 2.33-1. Statically Analogous Shells

1. The spherical shell of revolution, loaded with the unit loadings ($M = Q = 1$), acts as a lower segment would act under the same loading (segment defined with $\alpha = 20^\circ$). Consequently, it is indifferent what shape the rest of the shell has (Fig. 2.33-2).
2. If any shell at the lower portion (which is adjusted to the loaded edge) can be approximated with the spherical shell to a satisfactory degree, the solution obtained for the spherical shell

which is loaded with $V = Q = 1$ all around the edges (Fig. 2.33-3) can be used for the actual shell.

3. When extreme accuracy is required, $\alpha = 10^\circ$ may be used in place of $\alpha = 20^\circ$.

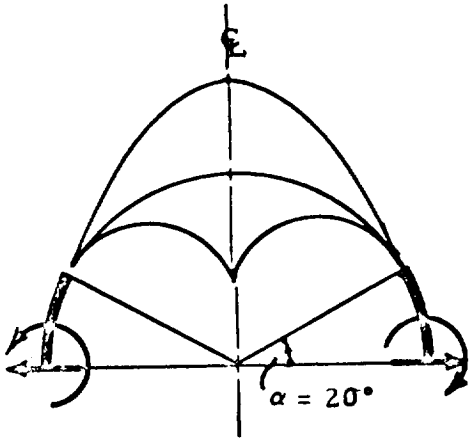


FIG. 2.33-2. Different Variants for Unstressed Portion

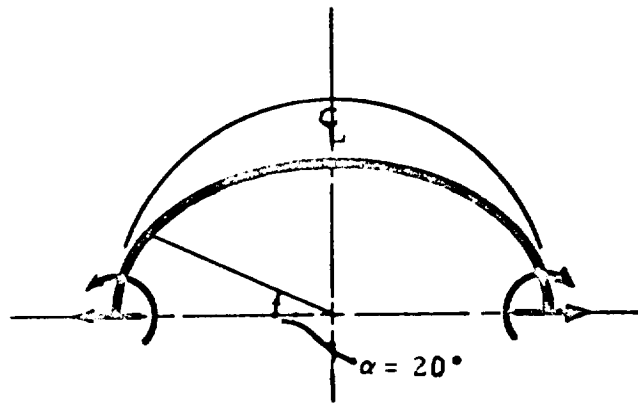


FIG. 2.33-3. Approximation With the Sphere

Another approximation, known as a Geckeler's assumption, may be useful, i. e.:

If the thickness of the shell t is small in comparison with equatorial radius $r_1 = a$ and limited by relation $a/t > 50$, the bending stresses at the edge may be determined by cylindrical shell theory. Meissner even recommends $a/t > 30$. This means that the bulkhead-shell can be approximated with a cylinder for finding unit-influences.

The bending theory was described and explained in the introductory sections of this manual. The small element of shell of revolution (loaded

with unit loadings) in equilibrium is shown in Fig. 2. 33-4. The nomenclature is the same as before, except that

M_ϕ = moment for meridional direction

M_θ = moment for circumferential direction

Q = shear for meridional direction

Shear in circumferential direction for the shell of revolution loaded with the axisymmetrical loading is 0.

Fig. 2. 33-5 shows the meridional deformations of the element from Fig. 2. 33-4. Due to deformation, point A was displaced to the position A'.

Δr = horizontal displacement

β = angle of rotation of element

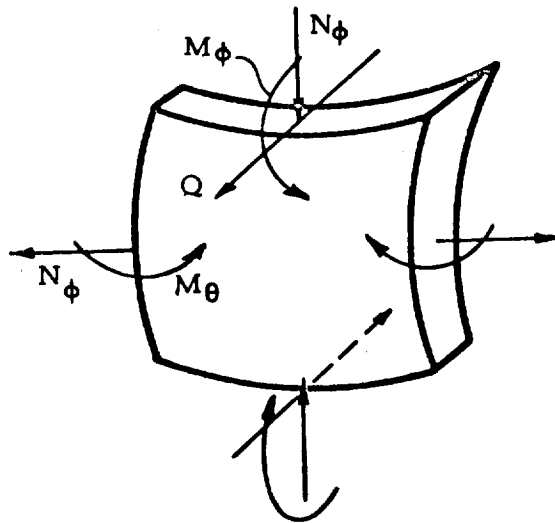


FIG. 2. 33-4. Designations in Connection With Differential Element of Stressed Shell

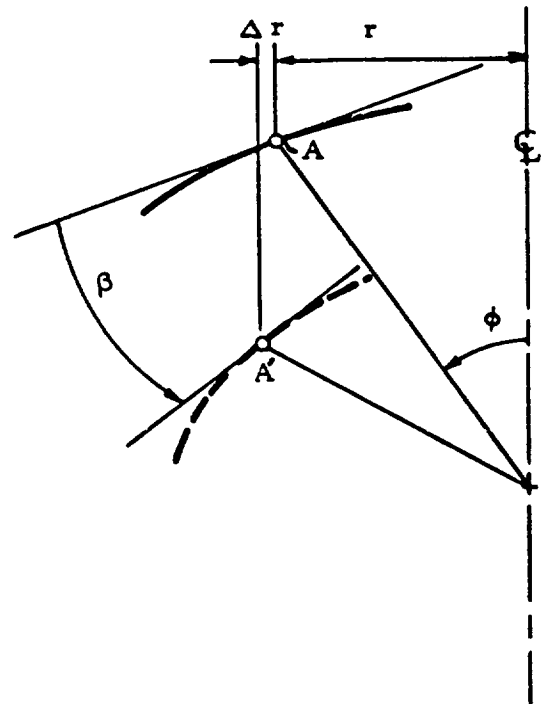


FIG. 2. 33-5. Meridional Deformations of Differential Element

The circumferential deformations are not independent. They are related to the meridional deformations and, consequently, will not be considered.

After this discussion, many existing solutions can be presented due to the unit loading action. This will be done in the following presentation.

2. 33. 2 Spherical Shells (Open, Closed)

This section presents the solutions for non-shallow spherical shell, which does not satisfy the relation

$$\cot\phi \approx \frac{1}{\phi} \quad (\text{Ref. 2-2})$$

which is characteristic for the category of shallow spherical shells. Physically, it means that for shallow shells, the disturbances due to unit edge loadings will not die before reaching the apex. Consequently, from diametrically opposite edge loadings, disturbances will be superimposed in some area around the apex.

The boundaries of shells must be free to rotate and deflect vertically and horizontally due to the action of unit loadings. Abrupt discontinuities in the shell thickness must not be present. Thickness of the shell must be uniform in the range in which the stresses are present.

The formulas are listed for closed and open spherical shells. Open spherical shells are shells that have an axisymmetrical circular opening at the apex. The spherical segment must have such meridional length that the disturbances due to the unit-edge loading will die or become insignificant before the opposite edge ($\phi_{\min} \approx 20^\circ$) will be reached. Unit-edge loadings may act at the lower or upper edge of the open shell. For derivation of the formulas presented, linear bending theory was used.

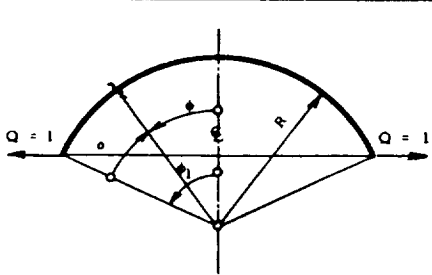
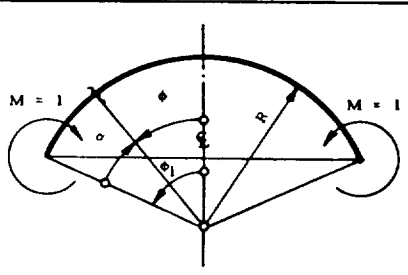
The following designations will be used:

$$k = \sqrt[4]{\left(\frac{R}{t}\right)^2 3(1-\mu^2)}; \alpha = \phi_1 - \phi$$

Table 2.33-2 presents the formulas for closed spherical shells. The table can be used for open shells, however, if the segment is such that the influences due to the unit loadings will die before reaching the edge of the opening.

Usually, the central opening is in an unstressed area of the shell. Therefore, for the analysis all formulas as presented below may be used, for open shells too provided that $\alpha_0 \geq 20^\circ$. Otherwise, the analyst shall be dealing with a ring instead of a shell.

TABLE 2.33-2. SPHERICAL SHELL (REF. 2-9)¹

| |  |  |
|--------------------------------------|--|--|
| Q_ϕ | $-\sqrt{2} \sin \phi_1 \cdot e^{-k\alpha} \cos(k\alpha + \frac{\pi}{4})$ | $+\frac{2k}{R} e^{-k\alpha} \sin k\alpha$ |
| N_ϕ | $-Q_\phi \cot \phi$ | $-Q_\phi \cot \phi$ |
| N_θ | $2k \sin \phi_1 \cdot e^{-k\alpha} \cos k\alpha$ | $+2\sqrt{2} \frac{k^2}{R} e^{-k\alpha} \cos(k\alpha + \frac{\pi}{4})$ |
| M_ϕ | $\frac{R}{k} \sin \phi_1 e^{-k\alpha} \sin k\alpha$ | $\sqrt{2} e^{-k\alpha} \sin(k\alpha + \frac{\pi}{4})$ |
| M_θ | $-\frac{R}{k^2 \sqrt{2}} \sin \phi_1 (\cot \phi) \cdot e^{-k\alpha} \sin(k\alpha + \frac{\pi}{4})$ $+ \mu M_\phi$ | $\frac{1}{k} \cot \phi \cdot e^{-k\alpha} \cos k\alpha + \mu M_\phi$ |
| DEFORMATIONS | | |
| $Et\beta$ | $-2\sqrt{2} k^2 \sin \phi_1 \cdot e^{-k\alpha} \sin(k\alpha + \frac{\pi}{4})$ | $-\frac{4k^3}{R} e^{-k\alpha} \cos k\alpha$ |
| $Et(\Delta r)$ | $R \sin \phi_1 \cdot e^{-k\alpha} \left[2k \sin \phi \cos k\alpha \right.$ $\left. - \sqrt{2} \mu \cos \phi \cos(k\alpha + \frac{\pi}{4}) \right]$ | $+ R \sin \phi (N_\theta - \mu N_\phi) + 2k e^{-k\alpha} \left[\sqrt{2} \cdot k \right.$ $\left. \sin \phi \cdot \cos(k\alpha + \frac{\pi}{4}) + \mu \cos \phi \sin k\alpha \right]$ |
| FOR $\alpha = 0$ AND $\phi = \phi_1$ | | |
| $Et\beta$ | $-2k^2 \sin \phi_1$ | $-\frac{4k^3}{R}$ |
| $Et(\Delta r)$ | $R \sin \phi_1 (2k \sin \phi_1 - \mu \cos \phi_1)$ | $+ 2k^2 \sin \phi_1$ |
| FOR $\phi_1 = 90^\circ$ | | |
| $Et\beta$ | $-2k^2$ | $-\frac{4k^3}{R}$ |
| $Et(\Delta r)$ | $2Rk$ | $+ 2k^2$ |

¹For k factors, see paragraph 2.33.2

A. Open Spherical Shell, Unit Loading at Upper Edge

Fig. 2.33-6 represents the case in which $M = P = 1$ loading acts on the upper edge of an open shell. These cases can be reduced easily to the previous case, as shown in Fig. 2.33-7, and the same formulas can be used, except that $\phi_1 > 90^\circ$. The actual shell (Fig. 2.33-6) will be imagined turned at 180 degrees (Fig. 2.33-7), and the shell can be calculated in the usual way.

An additional set of formulas for spherical closed and open shells is presented in Tables 2.33-3, -4 and -5. These formulas are expressed with functions F_1 and $F_1(\alpha)$. These functions are tabulated in the Section 2.42.6. In the case of the spherical shell, instead of parameter ξ in the above-mentioned tables, α shall be used.

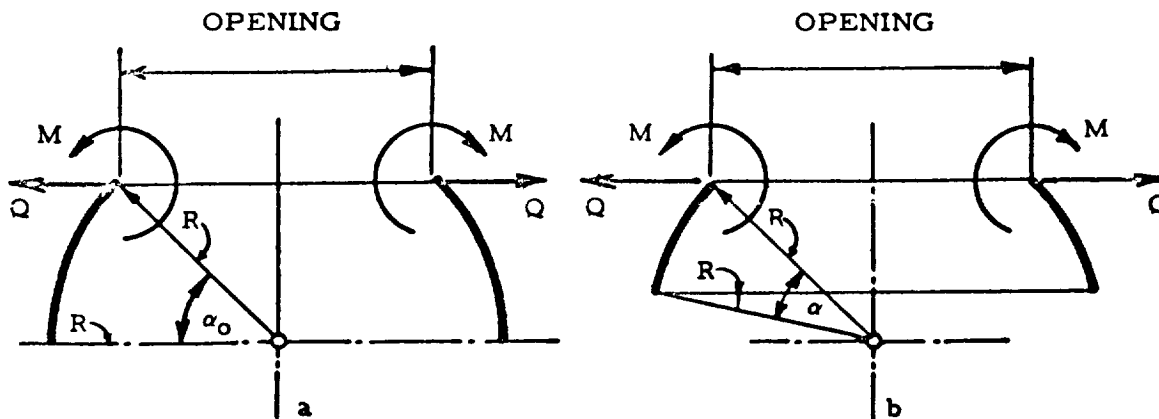


FIG. 2.33-6. Unit Loadings at Upper Edge

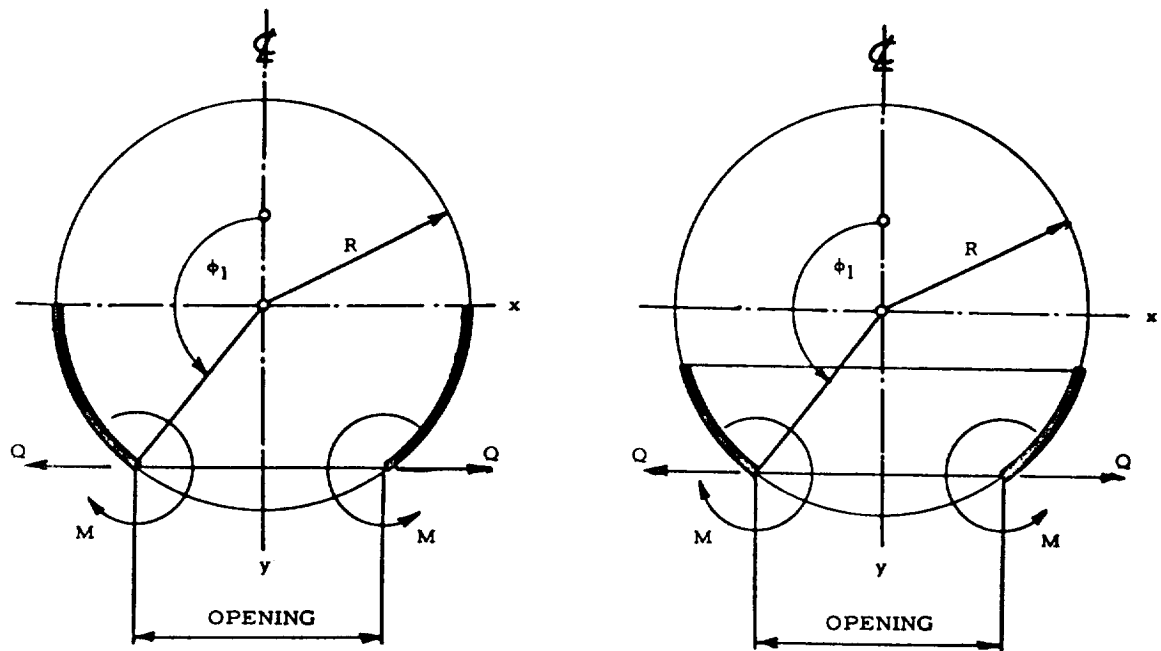


FIG. 2.33-7. Spherical Shell, $\phi_1 < 90^\circ$

TABLE 2.33-3. OPEN (OR CLOSED) SPHERICAL SHELL EXPOSED TO UNIT DISTORTIONS AT LOWER EDGE¹

Reference 2.2

| | Displacement ΔV_{1k} | Displacement Δr_{1k} |
|---|--|--|
| | | |
| Boundary Conditions | Boundary Conditions | Boundary Conditions |
| $\alpha = 0$ ($\theta = \theta_1$): $\Delta r = 0$, $\beta = 0$ $\alpha = \theta_0$ ($\theta = \theta_2$): $\Delta r = 0$, $\beta = 0$ | $\alpha = 0$ ($\theta = \theta_1$): $\beta = 0$, $\Delta V = \Delta V_{1k}$ $\alpha = \theta_0$ ($\theta = \theta_2$): $\beta = 0$, $\Delta V = 0$ | $\alpha = 0$ ($\theta = \theta_1$): $\Delta r = 2r_0$, $\beta = 0$ $\alpha = \theta_0$ ($\theta = \theta_2$): $\Delta r = 0$, $\beta = 0$ |
| Internal Forces and Deformations | | |
| N_k | $\frac{\Delta V_{1k} \cos \theta}{2k} \left[\frac{r_2}{r_1} F_7(\theta) + \frac{r_3}{r_1} F_8(\theta) - F_9(\theta) \right]$ | $\frac{\Delta V_{1k} \cos \theta}{2k} \left[\frac{r_2}{r_1} F_7(\theta) + \frac{r_3}{r_1} F_8(\theta) - F_9(\theta) \right]$ |
| M_k | $-\frac{\Delta V_{1k}}{2k} \left[-\frac{r_2}{r_1} F_5(\theta) + 2 \frac{r_3}{r_1} F_6(\theta) - F_{10}(\theta) \right]$ | $-\frac{\Delta V_{1k}}{2k} \left[-\frac{r_2}{r_1} F_5(\theta) + 2 \frac{r_3}{r_1} F_6(\theta) - F_{10}(\theta) \right]$ |
| Q_k | $\frac{\Delta V_{1k}}{2k} \left[\frac{r_2}{r_1} F_1(\theta) + \frac{r_3}{r_1} F_2(\theta) - F_3(\theta) \right]$ | $\frac{\Delta V_{1k}}{2k} \left[\frac{r_2}{r_1} F_1(\theta) + \frac{r_3}{r_1} F_2(\theta) - F_3(\theta) \right]$ |
| M_θ | $-\frac{\Delta V_{1k}}{2k} \left[-\frac{r_2}{r_1} F_{10}(\theta) + 2 \frac{r_3}{r_1} F_{11}(\theta) - F_9(\theta) \right]$ | $-\frac{\Delta V_{1k}}{2k} \left[-\frac{r_2}{r_1} F_{10}(\theta) + 2 \frac{r_3}{r_1} F_{11}(\theta) - F_9(\theta) \right]$ |
| M_ϕ | $\frac{\Delta V_{1k}}{2k} \left[\frac{r_2}{r_1} \left[\frac{\cos \theta}{k} F_8(\theta) - F_{10}(\theta) \right] + \frac{r_3}{r_1} \left[\frac{\cos \theta}{k} F_{10}(\theta) - 2 F_9(\theta) \right] \right.$ $\left. - \left[\frac{\cos \theta}{k} F_7(\theta) + F_9(\theta) \right] \right]$ | $\frac{\Delta V_{1k}}{2k} \left[\frac{r_2}{r_1} \left[\frac{\cos \theta}{k} F_8(\theta) - F_{10}(\theta) \right] + \frac{r_3}{r_1} \left[\frac{\cos \theta}{k} F_{10}(\theta) - 2 F_9(\theta) \right] \right.$ $\left. - \left[\frac{\cos \theta}{k} F_7(\theta) + F_9(\theta) \right] \right]$ |
| Δr | $-\frac{\Delta V_{1k}}{2k} \sin \theta \left[-\frac{r_2}{r_1} F_9(\theta) + 2 \frac{r_3}{r_1} F_{10}(\theta) - F_{10}(\theta) \right]$ | $-\frac{\Delta V_{1k}}{2k} \sin \theta \left[-\frac{r_2}{r_1} F_9(\theta) + 2 \frac{r_3}{r_1} F_{10}(\theta) - F_{10}(\theta) \right]$ |
| β | $-\frac{\Delta V_{1k}}{2k} \left[-\frac{r_2}{r_1} F_6(\theta) + \frac{r_3}{r_1} F_{10}(\theta) - F_9(\theta) \right]$ | $-\frac{\Delta V_{1k}}{2k} \left[-\frac{r_2}{r_1} F_6(\theta) + \frac{r_3}{r_1} F_{10}(\theta) - F_9(\theta) \right]$ |
| Internal Forces and Deformations | | |
| N_k | $\frac{\Delta V_{1k} \cos \theta}{2k} \left[\frac{r_2}{r_1} F_7(\theta) + \frac{r_3}{r_1} F_8(\theta) - F_9(\theta) \right]$ | $\frac{\Delta V_{1k} \cos \theta}{2k} \left[\frac{r_2}{r_1} F_7(\theta) + \frac{r_3}{r_1} F_8(\theta) - F_9(\theta) \right]$ |
| M_k | $-\frac{\Delta V_{1k}}{2k} \left[-\frac{r_2}{r_1} F_5(\theta) + 2 \frac{r_3}{r_1} F_6(\theta) - F_{10}(\theta) \right]$ | $-\frac{\Delta V_{1k}}{2k} \left[-\frac{r_2}{r_1} F_5(\theta) + 2 \frac{r_3}{r_1} F_6(\theta) - F_{10}(\theta) \right]$ |
| Q_k | $\frac{\Delta V_{1k}}{2k} \left[\frac{r_2}{r_1} F_1(\theta) + \frac{r_3}{r_1} F_2(\theta) - F_3(\theta) \right]$ | $\frac{\Delta V_{1k}}{2k} \left[\frac{r_2}{r_1} F_1(\theta) + \frac{r_3}{r_1} F_2(\theta) - F_3(\theta) \right]$ |
| M_θ | $-\frac{\Delta V_{1k}}{2k} \left[-\frac{r_2}{r_1} F_{10}(\theta) + 2 \frac{r_3}{r_1} F_{11}(\theta) - F_9(\theta) \right]$ | $-\frac{\Delta V_{1k}}{2k} \left[-\frac{r_2}{r_1} F_{10}(\theta) + 2 \frac{r_3}{r_1} F_{11}(\theta) - F_9(\theta) \right]$ |
| M_ϕ | $\frac{\Delta V_{1k}}{2k} \left[\frac{r_2}{r_1} \left[\frac{\cos \theta}{k} F_8(\theta) - F_{10}(\theta) \right] + \frac{r_3}{r_1} \left[\frac{\cos \theta}{k} F_{10}(\theta) - 2 F_9(\theta) \right] \right.$ $\left. - \left[\frac{\cos \theta}{k} F_7(\theta) + F_9(\theta) \right] \right]$ | $\frac{\Delta V_{1k}}{2k} \left[\frac{r_2}{r_1} \left[\frac{\cos \theta}{k} F_8(\theta) - F_{10}(\theta) \right] + \frac{r_3}{r_1} \left[\frac{\cos \theta}{k} F_{10}(\theta) - 2 F_9(\theta) \right] \right.$ $\left. - \left[\frac{\cos \theta}{k} F_7(\theta) + F_9(\theta) \right] \right]$ |
| Δr | $-\frac{\Delta V_{1k}}{2k} \sin \theta \left[-\frac{r_2}{r_1} F_9(\theta) + 2 \frac{r_3}{r_1} F_{10}(\theta) - F_{10}(\theta) \right]$ | $-\frac{\Delta V_{1k}}{2k} \sin \theta \left[-\frac{r_2}{r_1} F_9(\theta) + 2 \frac{r_3}{r_1} F_{10}(\theta) - F_{10}(\theta) \right]$ |
| β | $-\frac{\Delta V_{1k}}{2k} \left[-\frac{r_2}{r_1} F_6(\theta) + \frac{r_3}{r_1} F_{10}(\theta) - F_9(\theta) \right]$ | $-\frac{\Delta V_{1k}}{2k} \left[-\frac{r_2}{r_1} F_6(\theta) + \frac{r_3}{r_1} F_{10}(\theta) - F_9(\theta) \right]$ |

¹For F factors, see paragraph 2.42.6
For k factors, see paragraph 2.33.2

TABLE 2.33-4. OPEN SPHERICAL SHELL—UNIT EDGE LOADINGS AT UPPER BOUNDARY¹

| Boundary Conditions | |
|---------------------------------------|---|
| $\alpha = 0 \ (\phi = \phi_1)$ | $M_\phi = 0$ |
| | $Q_\phi = 0$ |
| $\alpha = \alpha_0 \ (\phi = \phi_2)$ | $M_\phi = 0$ |
| | $H_{ki} = -Q_{ki} \sin \phi_2 - N_{ki} \cos \phi_2$ |
| Internal Forces and Deformations | |
| N_ϕ | $H_{ki} \cot \phi \sin \phi_2 \left[\frac{F_9}{F_1} F_{10}(\alpha) - 2 \frac{F_8}{F_1} F_8(\alpha) \right]$ |
| N_θ | $H_{ki} 2k \sin \phi_2 \left[-\frac{F_9}{F_1} F_7(\alpha) + \frac{F_8}{F_1} F_{10}(\alpha) \right]$ |
| Q_ϕ | $H_{ki} \sin \phi_2 \left[\frac{F_9}{F_1} F_{10}(\alpha) - \frac{2F_8}{F_1} F_8(\alpha) \right]$ |
| M_ϕ | $H_{ki} \frac{R}{k} \sin \phi_2 \left[\frac{F_9}{F_1} F_8(\alpha) - \frac{F_8}{F_1} F_9(\alpha) \right]$ |
| M_θ | $H_{ki} \frac{R}{2k} \sin \phi_2 \left\{ \frac{F_9}{F_1} \left[-\frac{\cot \phi}{k} F_9(\alpha) + \mu 2F_8(\alpha) \right] - \frac{2F_8}{F_1} \left[\frac{\cot \phi}{k} F_7(\alpha) + \mu F_9(\alpha) \right] \right\}$ |
| Δr | $-H_{ki} \sin \phi_2 \frac{Rk}{Et} 2 \sin \phi \left[\frac{F_9}{F_1} F_7(\alpha) - \frac{F_8}{F_1} F_{10}(\alpha) \right]$ |
| β | $H_{ki} \sin \phi_2 \frac{2k^2}{Et} \left[\frac{F_9}{F_1} F_9(\alpha) + \frac{2F_8}{F_1} F_7(\alpha) \right]$ |

¹For F factors, see paragraph 2.42.6

¹For k factors, see paragraph 2.42.6

TABLE 2.33-4 (CONT)¹

| Boundary Conditions | |
|---------------------------------------|--|
| $\alpha = 0 (\phi = \phi_1) :$ | $M_\phi = 0$ $Q_\phi = 0$ |
| $\alpha = \alpha_0 (\phi = \phi_2) :$ | $M_\phi = M_{ki}$ $Q_\phi = 0$ |
| Internal Forces and Deformations | |
| N_ϕ | $M_{ki} \frac{2k}{R} \cot \phi \left[\frac{F_8}{F_1} F_{10}(\alpha) - \frac{F_{10}}{F_1} F_8(\alpha) \right]$ |
| N_θ | $M_{ki} \frac{2k^2}{R} \left[-2 \frac{F_8}{F_1} F_7(\alpha) + \frac{F_{10}}{F_1} F_{10}(\alpha) \right]$ |
| Q_ϕ | $-M_{ki} \frac{2k}{R} \left[-\frac{F_8}{F_1} F_{10}(\alpha) + \frac{F_{10}}{F_1} F_8(\alpha) \right]$ |
| M_ϕ | $M_{ki} \left[2 \frac{F_8}{F_1} F_8(\alpha) - \frac{F_{10}}{F_1} F_9(\alpha) \right]$ |
| M_θ | $-M_{ki} \left\{ \frac{F_8}{F_1} \left[\frac{\cot \phi}{k} F_9(\alpha) - \mu 2F_8(\alpha) \right] + \frac{F_{10}}{F_1} \left[\frac{\cot \phi}{k} F_7(\alpha) + \mu F_7(\alpha) \right] \right\}$ |
| Δr | $M_{ki} \frac{2k^2}{Et} \sin \phi \left[-2 \frac{F_8}{F_1} F_7(\alpha) + \frac{F_{10}}{F_1} F_{10}(\alpha) \right]$ |
| β | $M_{ki} \frac{4k^3}{EtR} \left[\frac{F_8}{F_1} F_9(\alpha) + \frac{F_{10}}{F_1} F_7(\alpha) \right]$ |

¹For F factors, see paragraph 2.42.6

For k factors, see paragraph 2.33.2

TABLE 2.33-5. OPEN SPHERICAL SHELL—UNIT EDGE LOADINGS
AT LOWER BOUNDARY¹

| BOUNDARY CONDITIONS | | |
|----------------------------------|---|---|
| | $\begin{aligned} \sigma = 0 \text{ (} \phi = \phi_1 \text{): } & M_{\phi} = 0 \\ & H_{1k} = Q_{1k} \sin \phi_1 + M_{1k} \cos \phi_1 \\ \sigma = \sigma_0 \text{ (} \phi = \phi_2 \text{): } & M_{\phi} = 0 \\ & Q_{\phi} = 0 \end{aligned}$ | $\begin{aligned} \sigma = 0 & \quad M_{\phi} = -M_{1k} \\ Q_{\phi} & = 0 \\ \sigma = \sigma_0 & \quad M_{\phi} = 0 \\ Q_{\phi} & = 0 \end{aligned}$ |
| INTERNAL FORCES AND DEFORMATIONS | | |
| N_{ϕ} | $H_{1k} \sin \phi \cos \phi \left[F_7(\sigma) - \frac{F_4}{F_1} F_{10}(\sigma) + \frac{F_2}{F_1} F_8(\sigma) \right]$ | $M_{1k} \cos \phi \frac{2k}{R} \left[\frac{F_6}{F_1} F_{15}(\sigma) + \frac{F_5}{F_1} F_{16}(\sigma) - \frac{F_3}{F_1} F_8(\sigma) \right]$ |
| N_{θ} | $-H_{1k} k \sin \phi_1 \left[-F_9(\sigma) - 2 \frac{F_4}{F_1} F_7(\sigma) + \frac{F_2}{F_1} F_{10}(\sigma) \right]$ | $-M_{1k} \frac{2k^2}{R} \left[\frac{F_6}{F_1} F_{14}(\sigma) + \frac{F_5}{F_1} F_{13}(\sigma) - \frac{F_3}{F_1} F_{10}(\sigma) \right]$ |
| Q_{ϕ} | $H_{1k} \sin \phi_1 \left[F_7(\sigma) - \frac{F_4}{F_1} F_{10}(\sigma) + \frac{F_2}{F_1} F_8(\sigma) \right]$ | $M_{1k} \frac{2k}{R} \left[\frac{F_6}{F_1} F_{15}(\sigma) + \frac{F_5}{F_1} F_{16}(\sigma) - \frac{F_3}{F_1} F_8(\sigma) \right]$ |
| M_{ϕ} | $-H_{1k} \frac{R}{2k} \sin \phi_1 \left[-F_{10}(\sigma) + 2 \frac{F_4}{F_1} F_8(\sigma) - \frac{F_2}{F_1} F_9(\sigma) \right]$ | $M_{1k} \left[\frac{F_6}{F_1} \left[\frac{\cos \phi}{k} F_{16}(\sigma) - \nu F_{13}(\sigma) \right] - \frac{F_5}{F_1} \left[\frac{\cos \phi}{k} F_{15}(\sigma) - \nu F_{14}(\sigma) \right] - \frac{F_3}{F_1} \frac{\cos \phi}{k} F_7(\sigma) + \nu F_9(\sigma) \right]$ |
| M_{θ} | $H_{1k} \frac{R}{2k} \sin \phi_1 \left[-\left[\frac{\cos \phi}{k} F_8(\sigma) + \nu F_{10}(\sigma) \right] + \frac{F_4}{F_1} \left[\frac{\cos \phi}{k} F_9(\sigma) - 2 \nu F_8(\sigma) \right] + \frac{F_2}{F_1} \left[\frac{\cos \phi}{k} F_7(\sigma) + \nu F_9(\sigma) \right] \right]$ | $-M_{1k} \left[\frac{F_6}{F_1} F_{13}(\sigma) - \frac{F_5}{F_1} F_{14}(\sigma) + \frac{F_3}{F_1} F_9(\sigma) \right]$ |
| Δr | $-H_{1k} \frac{Rk}{Et} \sin \phi \sin \phi_1 \left[-F_9(\sigma) - 2 \frac{F_4}{F_1} F_7(\sigma) + \frac{F_2}{F_1} F_{10}(\sigma) \right]$ | $-M_{1k} \frac{2k^2}{Et} \sin \phi \left[\frac{F_6}{F_1} F_{14}(\sigma) + \frac{F_5}{F_1} F_{13}(\sigma) - \frac{F_3}{F_1} F_{10}(\sigma) \right]$ |
| ρ | $-H_{1k} \frac{2k^2}{Et} \sin \phi_1 \left[-F_8(\sigma) - \frac{F_4}{F_1} F_9(\sigma) + \frac{F_2}{F_1} F_7(\sigma) \right]$ | $-M_{1k} \frac{4k^3}{EIR} \left[\frac{F_6}{F_1} F_{16}(\sigma) - \frac{F_5}{F_1} F_{15}(\sigma) - \frac{F_3}{F_1} F_7(\sigma) \right]$ |

¹For F factors, see paragraph 2.42.6
For k factors, see paragraph 2.33.2

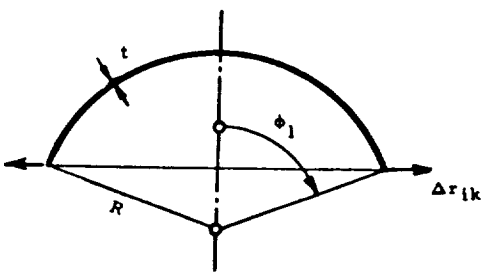
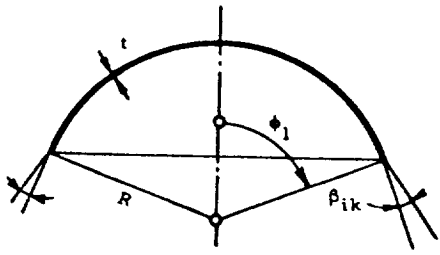
B. Unit of Distortions

In connection with some problems, it may be of interest to know the stresses and displacements in the circular shell (closed or open), if unit displacements at the edges are acting instead of M and Q :

$$\text{At lower edge } i \quad \left\{ \begin{array}{l} \Delta r_{ik} = \text{unit displacement in } r \text{ direction} \\ \Delta V_{ik} = \text{unit displacement in vertical direction} \\ \beta_{ik} = \text{unit rotation} \end{array} \right.$$
$$\text{At upper edge } k \quad \left\{ \begin{array}{l} \Delta r_{ki} = \text{unit displacement in } r \text{ direction} \\ \Delta V_{ki} = \text{unit displacement in vertical direction} \\ \beta_{ki} = \text{unit rotation} \end{array} \right.$$

Tables 2.33-6 and 7 contain the answer to this problem.

TABLE 2.33-6. CLOSED SPHERICAL SHELL SOLUTIONS DUE TO UNIT EDGE LOADING/DEFORMATIONS¹ (REF. 2-2)

| | | | |
|---|--|--|--|
|  | |  | |
| Boundary Conditions | | | |
| $\sigma = 0 \quad (\phi = \phi_1) \quad \Delta r = \Delta r_{ik} \quad \beta = 0$ | | $\sigma = 0 \quad (\phi = \phi_1) \quad \Delta r = 0 \quad \beta = \beta_{ik}$ | |
| Internal Forces and Deformations | | | |
| N_ϕ | $\Delta r_{ik} \frac{Et \cot \phi}{Rk \sin \phi_1} F_{17}(\alpha)$ | $\beta_{ik} \frac{Et}{2k^2} \cot \phi F_{19}(\alpha)$ | |
| N_θ | $\Delta r_{ik} \frac{Et}{R \sin \phi} F_{19}(\alpha)$ | $\beta_{ik} \frac{Et}{k} F_{18}(\alpha)$ | |
| Q_ϕ | $\Delta r_{ik} \frac{Et}{Rk \sin \phi_1} F_{17}(\alpha)$ | $\beta_{ik} \frac{Et}{2k^2} F_{19}(\alpha)$ | |
| M_ϕ | $\Delta r_{ik} \frac{Et}{2k^2 \sin \phi_1} F_{20}(\alpha)$ | $-\beta_{ik} \frac{REt}{2k^3} F_{17}(\alpha)$ | |
| M_θ | $\Delta r_{ik} \frac{Et}{2k^2 \sin \phi_1} \left[\frac{\cot \phi}{k} F_{18}(\alpha) - \mu F_{20}(\alpha) \right]$ | $-\beta_{ik} \frac{REt}{4k^3} \left[\frac{\cot \phi}{k} F_{20}(\alpha) + 2\mu F_{17}(\alpha) \right]$ | |
| Δr | $\Delta r_{ik} \frac{\sin \phi}{\sin \phi_1} F_{19}(\alpha)$ | $\beta_{ik} \frac{R \sin \phi}{k} F_{18}(\alpha)$ | |
| β | $-\Delta r_{ik} \frac{2k}{R \sin \phi_1} F_{18}(\alpha)$ | $\beta_{ik} F_{20}(\alpha)$ | |

¹For F factors, see paragraph 2.42.6
For k factors, see paragraph 2.33.2

TABLE 2.33-6 (CONT)¹

| | | |
|--|---|---|
| | | |
| Boundary Conditions | | |
| $\alpha = 0 \quad (\phi = \phi_1) \quad M = -M_{ik} \quad Q = 0$ | $\alpha = 0 \quad (\phi = \phi_1) \quad M_\phi = 0$ $H_{ik} = Q_{ik} \sin \phi_1 + N_{ik} \cos \phi_1$ | |
| Internal Forces and Deformations | | |
| N_ϕ | $M_{ik} \frac{2k \cot \phi}{R} F_{1d}(\alpha)$ | $H_{ik} \sin \phi_1 \cot \phi F_{20}(\alpha)$ |
| N_θ | $-M_{ik} \frac{2k^2}{R} F_{20}(\alpha)$ | $H_{ik} 2k \sin \phi_1 F_{17}(\alpha)$ |
| Q_ϕ | $M_{ik} \frac{2k}{R} F_{18}(\alpha)$ | $H_{ik} \sin \phi_1 F_{20}(\alpha)$ |
| M_ϕ | $-M_{ik} F_{19}(\alpha)$ | $H_{ik} \frac{R \sin \phi_1}{k} F_{18}(\alpha)$ |
| M_θ | $-M_{ik} \left[\frac{\cot \phi}{k} F_{17}(\alpha) + \mu F_{19}(\alpha) \right]$ | $H_{ik} \frac{R \sin \phi_1}{2k} \left[\frac{\cot \phi}{k} F_{19}(\alpha) + 2\mu F_{18} \right]$ |
| Δr | $-M_{ik} \frac{2k^2 \sin \phi}{Et} F_{20}(\alpha)$ | $H_{ik} \frac{2Rk}{Et} \sin \phi_1 \sin \phi F_{17}(\alpha)$ |
| δ | $M_{ik} \frac{4k^3}{EtR} F_{17}(\alpha)$ | $-H_{ik} \frac{2k^2}{Et} \sin \phi_1 F_{19}(\alpha)$ |

¹For F factors, see paragraph 2.42.6
 For k factors, see paragraph 2.33.2

TABLE 2.33-7. OPEN SPHERICAL SHELL—UNIT EDGE DEFORMATIONS AT UPPER BOUNDARY

| Boundary Condition | | |
|---|---|--|
| $\alpha = 0 (\phi = \phi_1): \Delta r = 0$ $\beta = 0$ $\alpha = \alpha_0 (\phi = \phi_2): \Delta r = \Delta r_{kl}$ $\beta = 0$ | $\alpha = 0 (\phi = \phi_1): \Delta r = 0$ $\beta = 0$ $\alpha = \alpha_0 (\phi = \phi_2): \beta = 0$ $\Delta v = \Delta V_{kl}$ | $\alpha = 0 (\phi = \phi_1): \Delta r = 0$ $\beta = 0$ $\alpha = \alpha_0 (\phi = \phi_2): \Delta r = 0$ $\beta = \beta_{kl}$ |
| Internal Forces and Deformations | | |
| N_ϕ | N_ϕ | N_ϕ |
| N_θ | N_θ | N_θ |
| Q_ϕ | Q_ϕ | Q_ϕ |
| M_ϕ | M_ϕ | M_ϕ |
| M_θ | M_θ | M_θ |
| Δr | Δr | Δr |
| β | β | β |

¹For F factors, see paragraph 2.42.6
 For k factors, see paragraph 2.33.3(b)

2.33.3 Conical Shells

This section presents the solutions for non-shallow open or closed conical shells, in which α_0 is not small. There is no exact information about limiting angle α_0 . It is recommended that consideration be limited to the range of $\alpha_0 \geq 45^\circ$. If $\alpha_0 = 90^\circ$, the cone degenerates into a cylinder.

Another limitation must be applied to the height of the cone. As in the case of the sphere, the disturbances due to unit-edge loadings will die at a short distance from the disturbed edge (for practical purposes, approximately at \sqrt{Rt}). Consequently, a "high" cone is characterized by an undisturbed edge (or apex) due to unit loading influences on the respective opposite edge.

The boundaries must be free to rotate and deflect vertically and horizontally due to the action of the unit-edge loadings. The abrupt discontinuities in the shell thickness must not be present. The thickness of shell must be uniform in the range in which the stresses are present.

The formulas are assembled for closed and open conical shells. Open conical shells are characterized by removal of the upper part above some circumference in the plane parallel to the base.

Linear bending theory was used to derive the following formulas. If the height of the segment is less than \sqrt{Rt} , the analyst is practically dealing with a circular ring instead of the shell. The following constants are important:

$$k = \frac{l}{\sqrt{Rt} \sin\phi} \sqrt[4]{3(1-\mu^2)}$$

$$D = \frac{Et^3}{12(1-\mu^2)}$$

Additional designations are indicated on Fig. 2.33-8.

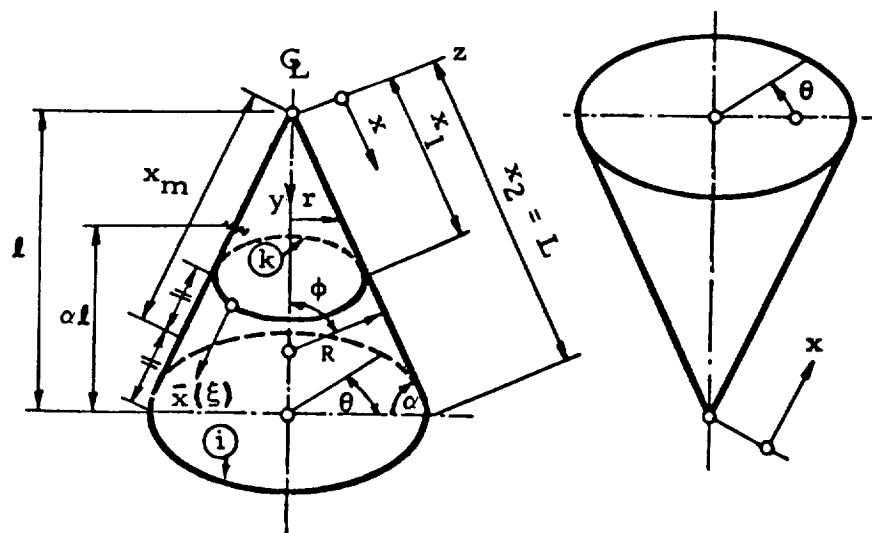


FIG. 2.33-8. Cone Nomenclature

R is variable and perpendicular to the meridian. Angle ϕ is constant. Table 2.33-8 presents the formulas for a closed conical shell.

TABLE 2.33-8. CONICAL SHELL—UNIT EDGE LOADING SOLUTIONS¹

| | HORIZONTAL UNIT LOAD | UNIT MOMENT LOADING |
|------------------|--|---|
| | | |
| N_ϕ | $-\sqrt{2} \cos \phi \cdot e^{-k\alpha} \cos(k\alpha + \frac{\pi}{4})$ | $-\frac{2k \cos \phi}{l} e^{-k\alpha} \sin k\alpha$ |
| N_θ | $-\frac{2R^2 k \sin^2 \phi}{l} e^{-k\alpha} \cos k\alpha$ | $\frac{2\sqrt{2} R k^2 \sin^2 \phi}{l^2} e^{-k\alpha} \cos(k\alpha + \frac{\pi}{4})$ |
| M_ϕ | $\frac{l}{k} e^{-k\alpha} \sin k\alpha$ | $-\sqrt{2} e^{-k\alpha} \sin(k\alpha + \pi/4)$ |
| M_θ | $\frac{l^2}{\sqrt{2} R k^2} \frac{\cot \phi}{\sin \phi} e^{-k\alpha} \sin(k\alpha + \frac{\pi}{4}) + \mu M_\phi$ | $-\frac{l \cot \phi}{R k \sin \alpha} e^{-k\alpha} \cos k\alpha + \mu M_\phi$ |
| Q | $-\sqrt{2} \sin \phi \cdot e^{-k\alpha} \cos(k\alpha + \frac{\pi}{4})$ | $-\frac{2k \sin \phi}{l} e^{-k\alpha} \sin k\alpha$ |
| DEFORMATIONS | | |
| Δr | $\frac{l^3 e^{-k\alpha}}{2D k^3 \sin \phi} \left[\cos k\alpha - \mu \frac{l}{\sqrt{2} R k} \right. \\ \left. - \frac{\cos \phi}{\sin \phi} \cdot \cos(k\alpha + \frac{\pi}{4}) \right]$ | $\frac{-l^2 e^{-k\alpha}}{2D k^2 \sin \phi} \left[\sqrt{2} \cos(k\alpha + \frac{\pi}{4}) + \mu \frac{l}{R} \right. \\ \left. \frac{\cos \phi \sin k\alpha}{k \sin^2 \phi} \right]$ |
| β | $-\frac{l^2 e^{-k\alpha} \sin(k\alpha + \pi/4)}{\sqrt{2} D k^2 \sin \phi}$ | $\frac{l e^{-k\alpha} \cos k\alpha}{D k \sin \phi}$ |
| FOR $\alpha = 0$ | | |
| Δr | $\frac{l^3}{2D k^3 \sin \phi} \left[1 - \frac{\mu l \cot \phi}{2R k \sin \phi} \right]$ | $-\frac{l^2}{2D k^2 \sin \phi}$ |
| β | $-\frac{l^2}{2D k^2 \sin \phi}$ | $\frac{l}{D k \sin \phi}$ |

¹For k factors, see paragraph 2.33.3

(a) Open Conical Shell—Unit Loading at Lower Edge

Since unit influences are not progressing very far from the edge into the cone, the formulas presented in Table 2. 33-8 can be used for the cone with opening at vertex (Fig. 2. 33-9).

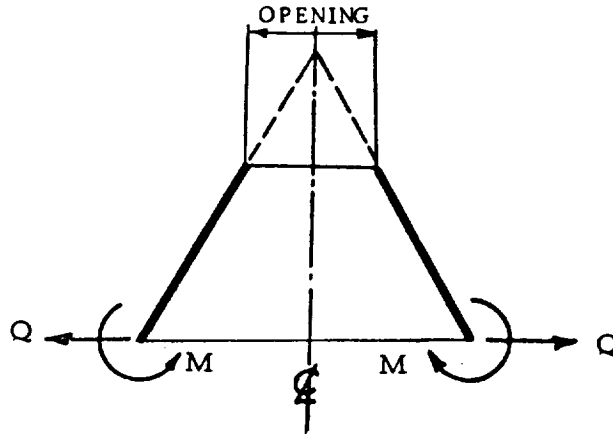


FIG. 2. 33-9. Open Conical Shell Loading at Lower Edge

(b) Open Conical Shell—Unit Loading at Upper Edge

If it is imagined that the shell, loaded as per Fig. 2. 33-10A, is replaced with shell as per Fig 2. 33-10B, the result is a conical shell

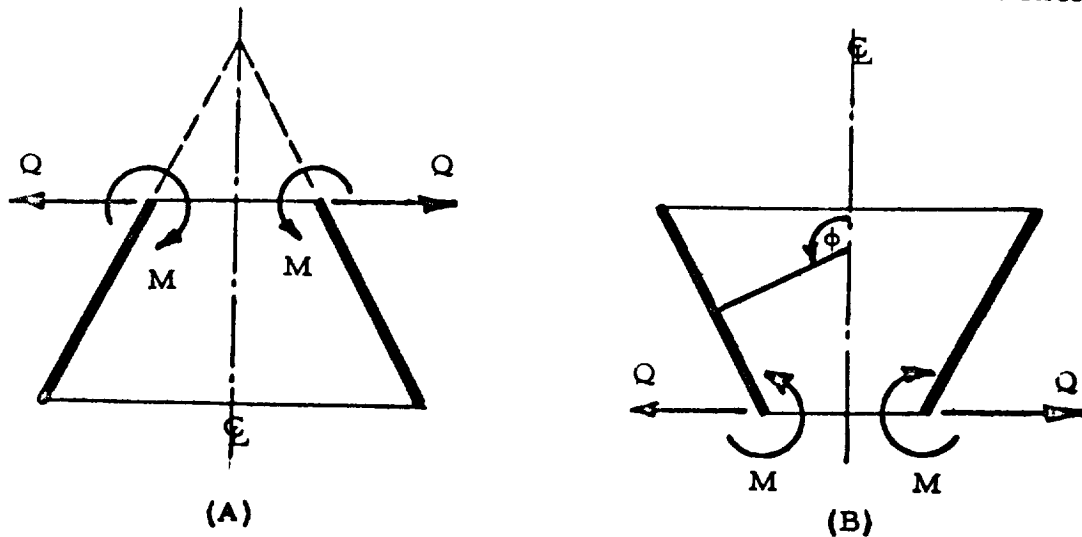


FIG. 2. 33-10. Open Conical Shell Loading at Upper Edge

loaded with unit loading at the lower edge. The same formulas are used, for determining edge influence but it is noted that $\phi > 90^\circ$.

An additional set of formulas for open conical shells (that can be also used for closed cone) is presented in Table 2.33-9. These formulas are expressed with the functions F_i and $F_i(\xi)$, which are tabulated in Paragraph 2.42.6. The following constant is used for k :

$$k = \frac{\sqrt[4]{3(1 - \mu^2)}}{\sqrt{t x_m \cot \alpha_o}}$$

TABLE 2.33-9. OPEN CONICAL SHELL - UNIT EDGE
LOADING SOLUTIONS¹ (REF. 2-2)

| | | |
|------------|---|--|
| | | |
| N_x | $M_{ki} 2k \cot \alpha_0 \left[\frac{F_6}{F_1} F_{15}(\xi) + \frac{F_5}{F_1} F_{16}(\xi) - \frac{F_3}{F_1} F_8(\xi) \right]$ | $M_{ik} 2k \cot \alpha_0 \left[\frac{F_8}{F_2} F_{10}(\xi) - \frac{F_{10}}{F_1} F_8(\xi) \right]$ |
| N_θ | $M_{ki} 2k^2 x_m \cot \alpha_0 \left[\frac{F_6}{F_1} F_{14}(\xi) + \frac{F_5}{F_1} F_{13}(\xi) - \frac{F_3}{F_1} F_{10}(\xi) \right]$ | $M_{ik} 2k^2 x_m \cot \alpha_0 \left[\frac{2F_8}{F_1} F_7(\xi) - \frac{F_{10}}{F_1} F_{10}(\xi) \right]$ |
| M_x | $M_{ki} \left[\frac{F_6}{F_1} F_{13}(\xi) - \frac{F_5}{F_1} F_{14}(\xi) + \frac{F_3}{F_1} F_9(\xi) \right]$ | $-M_{ik} \left[\frac{2F_8}{F_1} F_8(\xi) - \frac{F_{10}}{F_1} F_9(\xi) \right]$ |
| Q_x | $M_{ki} 2k \left[\frac{F_6}{F_1} F_{15}(\xi) + \frac{F_5}{F_1} F_{16}(\xi) - \frac{F_3}{F_1} F_8(\xi) \right]$ | $M_{ik} 2k \left[\frac{F_8}{F_1} F_{10}(\xi) - \frac{F_{10}}{F_1} F_8(\xi) \right]$ |
| Δr | $M_{ki} \frac{\sin \alpha_0}{2Dk^2} \left[\frac{F_6}{F_1} F_{14}(\xi) + \frac{F_5}{F_1} F_{13}(\xi) - \frac{F_3}{F_1} F_{10}(\xi) \right]$ | $M_{ik} \frac{\sin \alpha_0}{2Dk^2} \left[\frac{2F_8}{F_1} F_7(\xi) - \frac{F_{10}}{F_1} F_{10}(\xi) \right]$ |
| β | $-\frac{M_{ki}}{Dk} \left[\frac{F_6}{F_1} F_{16}(\xi) - \frac{F_5}{F_1} F_{15}(\xi) - \frac{F_3}{F_1} F_7(\xi) \right]$ | $M_{ik} \frac{1}{Dk} \left[\frac{F_8}{F_1} F_9(\xi) + \frac{F_{10}}{F_1} F_7(\xi) \right]$ |

¹For F factors, see paragraph 2.42.6

For k factors, see paragraph 2.33.3(b)

TABLE 2.33-9. (CONT)¹

| | |
|--|--|
| | |
| N_x $- H_{ki} \cos \alpha_0 \left[F_7 (\xi) - \frac{F_4}{F_1} F_{10} (\xi) + \frac{F_2}{F_1} F_8 (\xi) \right]$ | $H_{ki} \cos \alpha_0 \left[- \frac{F_9}{F_1} F_{10} (\xi) + \frac{2F_8}{F_1} F_8 (\xi) \right]$ |
| N_θ $H_{ki} x_m k \cos \alpha_0 \left[F_9 (\xi) + \frac{2F_4}{F_1} F_7 (\xi) - \frac{F_2}{F_1} F_{10} (\xi) \right]$ | $2H_{ik} x_m \cos \alpha_0 \left[- \frac{F_9}{F_1} F_7 (\xi) + \frac{F_8}{F_1} F_{10} (\xi) \right]$ |
| M_x $H_{ki} \frac{\sin \alpha_0}{2} \left[F_{10} (\xi) - \frac{2F_4}{F_1} F_8 (\xi) + \frac{F_2}{F_1} F_9 (\xi) \right]$ | $H_{ik} \frac{\sin \alpha_0}{k} \left[\frac{F_9}{F_1} F_8 (\xi) - \frac{F_8}{F_1} F_9 (\xi) \right]$ |
| Q_x $- H_{ki} \sin \alpha_0 \left[F_7 (\xi) - \frac{F_4}{F_1} F_{10} (\xi) + \frac{F_2}{F_1} F_8 (\xi) \right]$ | $H_{ik} \sin \alpha_0 \left[- \frac{F_9}{F_1} F_{10} (\xi) + \frac{2F_8}{F_1} F_8 (\xi) \right]$ |
| Δr $H_{ki} \frac{\sin^2 \alpha_0}{4Dk^3} \left[F_9 (\xi) + \frac{2F_4}{F_1} F_7 (\xi) - \frac{F_2}{F_1} F_{10} (\xi) \right]$ | $H_{ik} \frac{\sin^2 \alpha_0}{2Dk^3} \left[- \frac{F_9}{F_1} F_7 (\xi) + \frac{F_8}{F_1} F_{10} (\xi) \right]$ |
| β $H_{ki} \frac{\sin \alpha_0}{2Dk^2} \left[- F_8 (\xi) + \frac{F_4}{F_1} F_9 (\xi) + \frac{F_2}{F_1} F_7 (\xi) \right]$ | $- H_{ik} \frac{\sin \alpha_0}{2Dk^2} \left[+ \frac{F_9}{F_1} F_9 (\xi) + \frac{2F_8}{F_1} F_7 (\xi) \right]$ |

¹For F factors, see paragraph 2.42.6
For k factors, see paragraph 2.33.3(b)

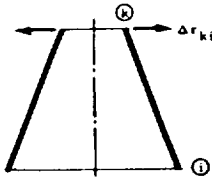
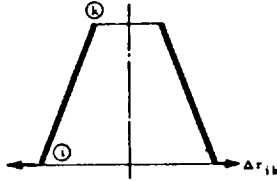
In connection with some problems, it may be of interest to know the stresses and displacements in the conical shell (closed or open), if unit displacements at the edges are acting instead of M and Q:

$$\text{At lower boundary } i \quad \begin{cases} \Delta r_{ik} = \text{unit displacement in horizontal direction} \\ \beta_{ik} = \text{unit rotation} \end{cases}$$

$$\text{At upper boundary } k \quad \begin{cases} \Delta r_{ki} = \text{unit displacement in horizontal direction} \\ \beta_{ki} = \text{unit rotation} \end{cases}$$

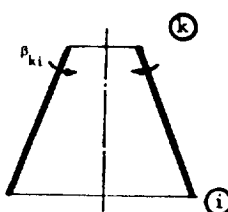
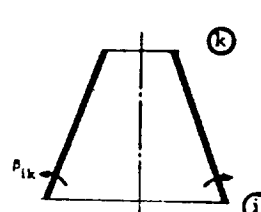
Table 2.33-10 supplies the answer to this problem.

TABLE 2.33-10. OPEN CONICAL SHELL—UNIT EDGE
LOADING SOLUTIONS¹ (REF. 2-2)

| | |
|--|--|
|  |  |
| $N_x = \frac{4Dk^3 \cot \alpha_0 \Delta r_{ki}}{\sin \alpha_0} \left[-\frac{F_3}{F_1} \right.$ $F_7(\xi) - \frac{F_5}{F_1} F_{15}(\xi)$ $\left. + \frac{F_6}{F_1} F_{16}(\xi) \right]$ | $\frac{4Dk^3 \cot \alpha_0 \Delta r_{ik}}{\sin \alpha_0} \left[\frac{F_{10}}{F_1} F_7(\xi) \right.$ $\left. + \frac{F_8}{F_1} F_9(\xi) \right]$ |
| $N_\theta = \frac{Et \Delta r_{ki}}{r_m \cos \alpha_0} \left[\frac{F_3}{F_1} F_9(\xi) \right.$ $\left. - \frac{F_5}{F_1} F_{14}(\xi) + \frac{F_6}{F_1} F_{13}(\xi) \right]$ | $\frac{Et \Delta r_{ik}}{r_m \cos \alpha_0} \left[-\frac{F_{10}}{F_1} F_9(\xi) \right.$ $\left. + \frac{2F_8}{F_1} F_8(\xi) \right]$ |
| $M_x = \frac{2Dk^2 \Delta r_{ki}}{\sin \alpha_0} \left[\frac{F_3}{F_1} F_{10}(\xi) \right.$ $\left. - \frac{F_5}{F_1} F_{13}(\xi) - \frac{F_6}{F_1} F_{14}(\xi) \right]$ $M_\theta = \mu M_x$ | $\frac{2Dk^2 \Delta r_{ik}}{\sin \alpha_0} \left[-\frac{F_{10}}{F_1} F_{10}(\xi) \right.$ $\left. + \frac{2F_8}{F_1} F_7(\xi) \right]$ |
| $Q_x = \frac{4Dk^3 \Delta r_{ki}}{\sin \alpha_0} \left[-\frac{F_3}{F_1} F_7(\xi) \right.$ $\left. - \frac{F_5}{F_1} F_{15}(\xi) + \frac{F_6}{F_1} F_{16}(\xi) \right]$ | $\frac{4Dk^3 \Delta r_{ik}}{\sin \alpha_0} \left[\frac{F_{10}}{F_1} F_9(\xi) \right.$ $\left. + \frac{F_8}{F_1} F_9(\xi) \right]$ |
| $\Delta r = \Delta r_{ki} \left[\frac{F_3}{F_1} F_9(\xi) - \frac{F_5}{F_1} F_{14}(\xi) \right.$ $\left. + \frac{F_6}{F_1} F_{13}(\xi) \right]$ | $\Delta r_{ik} \left[-\frac{F_{10}}{F_1} F_9(\xi) \right.$ $\left. + \frac{2F_8}{F_1} F_8(\xi) \right]$ |
| $p = -\frac{2k}{\sin \alpha_0} \Delta r_{ki} \left[\frac{F_3}{F_1} F_8(\xi) \right.$ $\left. - \frac{F_5}{F_1} F_{16}(\xi) - \frac{F_6}{F_1} F_{15}(\xi) \right]$ | $\frac{2k \Delta r_{ik}}{\sin \alpha_0} \left[\frac{F_{10}}{F_1} F_8(\xi) \right.$ $\left. - \frac{F_8}{F_1} F_{16}(\xi) - \frac{F_8}{F_1} F_{15}(\xi) \right]$ |

¹For F factors, see paragraph 2.42.6
For k factors, see paragraph 2.33.3(b)

TABLE 2.33-10. (CONT)¹

| |  |  |
|------------|---|--|
| N_x | $2Dk^2 \cot \alpha_o \beta_{kl} \left[\frac{F_2}{F_1} F_7 (\xi) + \frac{F_4}{F_1} F_9 (\xi) - F_8 (\xi) \right]$ | $2Dk^2 \cot \alpha_o \beta_{ik} \left[\frac{2F_8}{F_1} F_7 (\xi) + \frac{F_9}{F_1} F_9 (\xi) \right]$ |
| N_θ | $2Dk^3 x_m \cot \alpha_o \beta_{kl} \left[-\frac{F_2}{F_1} F_9 (\xi) + \frac{2F_4}{F_1} F_8 (\xi) - F_{10} (\xi) \right]$ | $4Dk^3 x_m \cot \alpha_o \beta_{ik} \left[-\frac{F_8}{F_1} F_9 (\xi) + \frac{F_9}{F_1} F_8 (\xi) \right]$ |
| M_x | $Dk \beta_{kl} \left[-\frac{F_2}{F_1} F_{10} (\xi) + \frac{2F_4}{F_1} F_7 (\xi) + F_9 (\xi) \right]$ | $2Dk \beta_{ik} \left[-\frac{F_8}{F_1} F_{10} (\xi) + \frac{F_9}{F_1} F_7 (\xi) \right]$ |
| Q_x | $2Dk^2 \beta_{kl} \left[\frac{F_2}{F_1} F_7 (\xi) + \frac{F_4}{F_1} F_9 (\xi) - F_8 (\xi) \right]$ | $2Dk^2 \beta_{ik} \left[\frac{2F_8}{F_1} F_7 (\xi) + \frac{F_9}{F_1} F_9 (\xi) \right]$ |
| Δr | $\frac{\sin \alpha_o}{2k} \beta_{kl} \left[-\frac{F_2}{F_1} F_9 (\xi) + \frac{2F_4}{F_1} F_8 (\xi) - F_{10} (\xi) \right]$ | $\frac{\sin \alpha_o}{k} \beta_{ik} \left[-\frac{F_8}{F_1} F_9 (\xi) + \frac{F_9}{F_1} F_8 (\xi) \right]$ |
| ρ | $\beta_{kl} \left[\frac{F_2}{F_1} F_8 (\xi) - \frac{F_4}{F_1} F_{10} (\xi) + F_7 (\xi) \right]$ | $\beta_{ik} \left[\frac{2F_8}{F_1} F_8 (\xi) - \frac{F_9}{F_1} F_{10} (\xi) \right]$ |

¹For F factors, see paragraph 2.42.6
For k factors, see paragraph 2.33.3(b)

2.33.4 Cylindrical Shell

This section presents the solutions for long and short cylinders, loaded along the boundary with the unit-edge loadings (moment, shear, forced horizontal displacement, forced rotation at the boundary). All disturbances in the cylindrical wall caused by edge loading will become, for practical purposes, negligible at distance $x = \sqrt{Rt}$. If the height of the cylinder is less than x , then the analyst is dealing with a circular ring instead of a shell. Further, to be on the safe side, the following precautions should be observed:

- a. If $\beta L \leq 5$, the more exact theory is used, and such cylinders are designated as short cylinders.
- b. If $\beta L \geq 5$, the simplified formulas is used, and this is a special case of the more general case a.

The factor β is defined as follows:

$$\beta^4 = 3(1 - \mu^2) / R^2 t^2$$

and shall be distinguished from the similar designation β_i (with subscript) which is an angle of rotation due to the unit edge loadings.

The primary solutions (membrane theory) will not be affected by the length of the cylinder. (See paragraph 2.32.6.) The boundaries must be free to rotate and deflect because of the action of the unit edge loadings. The shell thickness must be uniform in the range where the stresses are present.

(a). Long Cylinders

The following constants will be noted:

$$k = \frac{L}{\sqrt{Rt}} \sqrt[4]{3(1 - \mu^2)}$$

$$D = \frac{Et^3}{12(1 - \mu^2)}$$

The formulas for the disturbances caused by the unit-edge loadings are presented in Table 2.33-11.

TABLE 2.33-11. LONG CYLINDRICAL SHELLS—UNIT EDGE LOADING SOLUTIONS (Ref. 2-7)¹

| | Q = 1 | M = 1 |
|--------------------------------|--|--|
| | | |
| N_x | 0 | 0 |
| N_θ | $-\frac{2Rk}{L} e^{-k\bar{\beta}} \cos k\bar{\beta}$ | $\frac{2\sqrt{2} \cdot Rk^2}{L^2} e^{-k\bar{\beta}} \cos(k\bar{\beta} + \pi/4)$ |
| M_x | $\frac{L}{k} e^{-k\bar{\beta}} \sin k\bar{\beta}$ | $-\sqrt{2} \cdot e^{-k\bar{\beta}} \sin(k\bar{\beta} + \pi/4)$ |
| M_θ | μM_x | μM_x |
| Q | $\sqrt{2} \cdot e^{-k\bar{\beta}} \cos(k\bar{\beta} + \frac{\pi}{4})$ | $\frac{2k}{L} e^{-k\bar{\beta}} \sin k\bar{\beta}$ |
| β | $\frac{L^2}{\sqrt{2} \cdot k^2 D} e^{-k\bar{\beta}} \sin(k\bar{\beta} + \pi/4)$ | $-\frac{L}{Dk} e^{-k\bar{\beta}} \cos k\bar{\beta}$ |
| Δr | $-\frac{R}{Et} (N_\theta - \mu N_x) = \frac{L^3}{2Dk^3} e^{-k\bar{\beta}} \cos k\bar{\beta}$ | $-\frac{R}{Et} (N_\theta - \mu N_x) = -\frac{L^3}{\sqrt{2} Dk^2} e^{-k\bar{\beta}} \cos(k\bar{\beta} + \pi/4)$ |
| FOR THE CASE $\bar{\beta} = 0$ | | |
| β | $L^2/2k^2 D$ | $-L/Dk$ |
| Δr | $L^3/2k^3 D$ | $-L^2/2Dk^2$ |

¹For k factors, see paragraph 2.33.4

(b) Short Cylinders with Uniform Wall Thickness Without Abrupt
Discontinuity

The following constants are used for tables 2.33-12 and 2.33-13:

$$\beta^4 = 3(1 - \mu^2)/R^2 t^2$$

$$\rho = \sinh^2 \beta L - \sin^2 \beta L$$

$$K_1 = (\sinh \beta L \cosh \beta L - \sin \beta L \cos \beta L)/\rho$$

$$K_2 = (\sin \beta L \cosh \beta L - \cos \beta L \sinh \beta L)/\rho$$

$$K_3 = (\sinh^2 \beta L + \sin^2 \beta L)/\rho$$

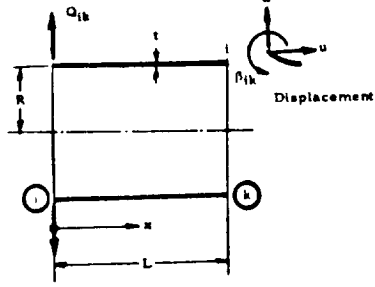
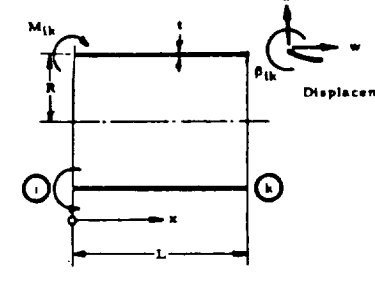
$$K_4 = 2 \sinh \beta L \sin \beta L/\rho$$

$$K_5 = 2(\sin \beta L \cos \beta L + \sinh \beta L \cosh \beta L)/\rho$$

$$K_6 = 2(\sin \beta L \cosh \beta L + \cos \beta L \sinh \beta L)/\rho$$

The formulas for unit-edge loading disturbances are presented in Tables 2.33-12 and 2.33-13. To use these formulas the relation $\beta L \leq 5$ must be satisfied. Distinguish the coefficient β (no subscript) from the adopted notation for rotation angle β (with subscript).

TABLE 2.33-12. SHORT CYLINDRICAL SHELLS—UNIT EDGE LOADING SOLUTIONS¹

| |  |  | Remarks |
|--|--|---|-------------------------------------|
| w_x β_x | $\frac{Q_{ik}}{4\beta^3 D} \left[(\sinh 2\beta L - \sin 2\beta L) \cosh \beta x \cos \beta x - 2 \sinh^2 \beta L \cdot \sinh \beta x \cos \beta x - 2 \sin^2 \beta L \cosh \beta x \sin \beta x \right]$ $\frac{Q_{ik}}{2\beta^2 D} \left[\sinh \beta x \sin \beta x - K_3 \cosh \beta x \cos \beta x - K_1 (\cosh \beta x \cdot \sin \beta x - \sinh \beta x \cos \beta x) \right]$ | $\frac{M_{ik}}{2\beta^2 D} \left[K_3 \cosh \beta x \cos \beta x + \sinh \beta x \sin \beta x - \frac{K_5}{2} (\cosh \beta x \sin \beta x + \sinh \beta x \cos \beta x) \right]$ $\frac{M_{ik}}{2\beta^2 D} \left(\frac{K_5}{2} \rho \cosh \beta x - \sinh^2 \beta L \sinh \beta x \cos \beta x + \sin^2 \beta L \cosh \beta x \sin \beta x \right)$ | |
| w_{ik} β_{ik} w_{ki} β_{ki} | $- Q_{ik} K_1 / 2\beta^3 D$ $+ Q_{ik} K_3 / 2\beta^2 D$ $- Q_{ik} K_2 / 2\beta^3 D$ $- Q_{ik} K_4 / 2\beta^2 D$ | $M_{ik} K_3 / 2\beta^2 D$ $- M_{ik} K_5 / 2\beta D$ $- M_{ik} K_4 / 2\beta^2 D$ $- M_{ik} K_6 / 2\beta D$ | |
| N_x N_θ M_x M_θ Q_x | 0 $\Sigma t w / R$ $\frac{Q_{ik}}{\rho \beta} (\sin^2 \beta L \sinh \beta x \cos \beta x - \sinh^2 \beta L \cosh \beta x \cdot \sin \beta x + \rho K_1 \sinh \beta x \sin \beta x)$ μM_x $Q_{ik} \left[(\cosh \beta x \cos \beta x + K_3 \sinh \beta x \sin \beta x - K_1 (\sinh \beta x \cdot \cos \beta x + \cosh \beta x \sin \beta x)) \right]$ | 0 $+ \Sigma t w / R$ $M_{ik} \left[\cosh \beta x \cos \beta x - K_3 (\sinh \beta x \sin \beta x) + \frac{K_5}{2} (\cosh \beta x \cdot \sin \beta x - \sinh \beta x \cos \beta x) \right]$ μM_x $\beta \frac{M_{ik}}{\rho} (K_5 \rho \sinh \beta x \sin \beta x - 2 \sinh^2 \beta L \cosh \beta x \sin \beta x - 2 \sin^2 \beta L \sinh \beta x \cos \beta x)$ | |
| Edge Influence Coefficients | | | |
| w_{ik} w_{ki} β_{ik} β_{ki} | $- K_1 / 2\beta^3 D$ $- K_2 / 2\beta^3 D$ $K_3 / 2\beta^2 D$ $- K_4 / 2\beta^2 D$ | $K_3 / 2\beta^2 D$ $- K_4 / 2\beta^2 D$ $- K_5 / 2\beta D$ $- K_6 / 2\beta D$ | Due to Unit Loadings $M = Q = 1$ |

¹For k factors, see paragraph 2.33.4(b)

TABLE 2.33-13. K-COEFFICIENTS (SHEET 1 OF 4)

| βL | K_1 | K_2 | K_3 | K_4 | K_5 | K_6 |
|-----------|---------|---------|----------|----------|-----------|-----------|
| 0.100 | 20.0000 | 10.0000 | 300.0010 | 299.9993 | 6000.0726 | 5999.9726 |
| 0.102 | 19.6078 | 9.8038 | 288.3502 | 288.3484 | 5653.9797 | 5653.8777 |
| 0.104 | 19.2307 | 9.6153 | 277.3661 | 277.3643 | 5334.0202 | 5333.9163 |
| 0.106 | 18.8680 | 9.4340 | 267.0011 | 266.9992 | 5037.8137 | 5037.7076 |
| 0.108 | 18.5185 | 9.2592 | 257.2024 | 257.2004 | 4763.0654 | 4762.9574 |
| 0.110 | 18.1818 | 9.0909 | 247.9354 | 247.9334 | 4507.9753 | 4507.8654 |
| 0.112 | 17.8572 | 8.9286 | 239.1601 | 239.1580 | 4270.7759 | 4270.6639 |
| 0.114 | 17.5438 | 8.7718 | 230.8407 | 230.8385 | 4049.8977 | 4049.7837 |
| 0.116 | 17.2414 | 8.6206 | 222.9497 | 222.9474 | 3844.0227 | 3843.9067 |
| 0.118 | 16.9492 | 8.4745 | 215.4565 | 215.4542 | 3651.8686 | 3651.7506 |
| 0.120 | 16.6667 | 8.3333 | 208.3347 | 208.3323 | 3472.3100 | 3472.1900 |
| 0.122 | 16.3934 | 8.1967 | 201.5600 | 201.5576 | 3304.3290 | 3304.2070 |
| 0.124 | 16.1291 | 8.0645 | 195.1109 | 195.1083 | 3147.0173 | 3146.8933 |
| 0.126 | 15.8730 | 7.9364 | 188.9657 | 188.9631 | 2999.5240 | 2999.3979 |
| 0.128 | 15.6250 | 7.8124 | 183.1071 | 183.1044 | 2861.1180 | 2860.9900 |
| 0.130 | 15.3847 | 7.6923 | 177.5168 | 177.5140 | 2731.0977 | 2730.9677 |
| 0.135 | 14.8148 | 7.4074 | 164.6109 | 164.6079 | 2438.7537 | 2438.6187 |
| 0.140 | 14.2858 | 7.1428 | 153.0632 | 153.0600 | 2186.6934 | 2186.5533 |
| 0.145 | 13.7932 | 6.8965 | 142.6899 | 142.6864 | 1968.2148 | 1968.0698 |
| 0.150 | 13.3334 | 6.6666 | 133.3360 | 133.3323 | 1777.8949 | 1777.7449 |
| 0.155 | 12.9033 | 6.4515 | 124.8725 | 124.8685 | 1611.3412 | 1611.1862 |
| 0.160 | 12.5001 | 6.2499 | 117.1905 | 117.1862 | 1464.9675 | 1464.8076 |
| 0.165 | 12.1213 | 6.0605 | 110.1957 | 110.1912 | 1335.7945 | 1335.6295 |
| 0.170 | 11.7648 | 5.8823 | 103.8095 | 103.8047 | 1221.3795 | 1221.2095 |
| 0.175 | 11.4287 | 5.7142 | 97.9624 | 97.9573 | 1119.6639 | 1119.4889 |
| 0.180 | 11.1112 | 5.5555 | 92.5962 | 92.5908 | 1028.9436 | 1028.7636 |
| 0.185 | 10.8109 | 5.4053 | 87.6591 | 87.6534 | 947.7650 | 947.5800 |
| 0.190 | 10.5265 | 5.2631 | 83.1066 | 83.1005 | 874.9079 | 874.7179 |
| 0.195 | 10.2566 | 5.1281 | 78.8997 | 78.8933 | 809.3321 | 809.1371 |
| 0.20 | 10.0002 | 4.9999 | 75.0043 | 74.9976 | 750.1503 | 749.9503 |
| 0.21 | 9.5240 | 4.7618 | 68.0319 | 68.0246 | 648.0355 | 647.8255 |
| 0.22 | 9.0911 | 4.5453 | 61.9887 | 61.9806 | 563.6514 | 563.4314 |
| 0.23 | 8.6959 | 4.3477 | 56.7164 | 56.7076 | 493.3093 | 493.0794 |
| 0.24 | 8.3336 | 4.1665 | 52.0895 | 52.0799 | 434.2073 | 433.9673 |
| 0.25 | 8.0003 | 3.9998 | 48.0066 | 47.9962 | 384.1866 | 383.9366 |

TABLE 2.33-13. (CONT) (SHEET 2 OF 4)

| βL | K_1 | K_2 | K_3 | K_4 | K_5 | K_6 |
|-----------|--------|--------|---------|---------|----------|----------|
| 0.26 | 7.6927 | 3.8459 | 44.3859 | 44.3747 | 341.5695 | 341.3095 |
| 0.27 | 7.4078 | 3.7034 | 41.1601 | 41.1479 | 305.0342 | 304.7642 |
| 0.28 | 7.1433 | 3.5711 | 38.2737 | 38.2607 | 273.5341 | 273.2541 |
| 0.29 | 6.8970 | 3.4479 | 35.6809 | 35.6668 | 246.2304 | 245.9405 |
| 0.30 | 6.6672 | 3.3330 | 33.3430 | 33.3280 | 222.4478 | 222.1478 |
| 0.31 | 6.4522 | 3.2254 | 31.2278 | 31.2118 | 201.6362 | 201.3262 |
| 0.32 | 6.2507 | 3.1245 | 29.3079 | 29.2908 | 183.3460 | 183.0260 |
| 0.33 | 6.0613 | 3.0298 | 27.5599 | 27.5418 | 167.2068 | 166.8768 |
| 0.34 | 5.8831 | 2.9406 | 25.9640 | 25.9447 | 152.9116 | 152.5716 |
| 0.35 | 5.7151 | 2.8566 | 24.5030 | 24.4826 | 140.2046 | 139.8547 |
| 0.36 | 5.5565 | 2.7771 | 23.1621 | 23.1405 | 128.8710 | 128.5111 |
| 0.37 | 5.4064 | 2.7020 | 21.9285 | 21.9057 | 118.7305 | 118.3605 |
| 0.38 | 5.2642 | 2.6308 | 20.7911 | 20.7670 | 109.6302 | 109.2503 |
| 0.39 | 5.1294 | 2.5633 | 19.7401 | 19.7148 | 101.4402 | 101.0503 |
| 0.40 | 5.0013 | 2.4991 | 18.7671 | 18.7404 | 94.0496 | 93.6496 |
| 0.41 | 4.8794 | 2.4381 | 17.8644 | 17.8364 | 87.3630 | 86.9531 |
| 0.42 | 4.7634 | 2.3799 | 17.0256 | 16.9962 | 81.2989 | 80.8790 |
| 0.43 | 4.6527 | 2.3245 | 16.2447 | 16.2138 | 75.7865 | 75.3566 |
| 0.44 | 4.5471 | 2.2715 | 15.5164 | 15.4842 | 70.7646 | 70.3247 |
| 0.45 | 4.4462 | 2.2209 | 14.8363 | 14.8026 | 66.1798 | 65.7299 |
| 0.46 | 4.3497 | 2.1725 | 14.2001 | 14.1649 | 61.9856 | 61.5258 |
| 0.47 | 4.2573 | 2.1262 | 13.6042 | 13.5674 | 58.1415 | 57.6716 |
| 0.48 | 4.1688 | 2.0818 | 13.0452 | 13.0069 | 54.6117 | 54.1318 |
| 0.49 | 4.0839 | 2.0392 | 12.5202 | 12.4802 | 51.3647 | 50.8749 |
| 0.50 | 4.0024 | 1.9982 | 12.0264 | 11.9848 | 48.3729 | 47.8731 |
| 0.51 | 3.9241 | 1.9589 | 11.5613 | 11.5180 | 45.6104 | 45.1006 |
| 0.52 | 3.8488 | 1.9211 | 11.1230 | 11.0780 | 43.0583 | 42.5385 |
| 0.53 | 3.7764 | 1.8847 | 10.7094 | 10.6627 | 40.6957 | 40.1659 |
| 0.54 | 3.7067 | 1.8496 | 10.3187 | 10.2701 | 38.5055 | 37.9657 |
| 0.55 | 3.6395 | 1.8158 | 9.9491 | 9.8987 | 36.4721 | 35.9224 |
| 0.56 | 3.5748 | 1.7832 | 9.5993 | 9.5470 | 34.5819 | 34.0222 |
| 0.57 | 3.5123 | 1.7518 | 9.2678 | 9.2137 | 32.8226 | 32.2529 |
| 0.58 | 3.4520 | 1.7214 | 8.9533 | 8.8973 | 31.1830 | 30.6033 |
| 0.59 | 3.3938 | 1.6920 | 8.6548 | 8.5968 | 29.6531 | 29.0635 |
| 0.60 | 3.3375 | 1.6636 | 8.3712 | 8.3112 | 28.2241 | 27.6245 |

TABLE 2.33-13. (CONT) (SHEET 3 OF 4)

| βL | K_1 | K_2 | K_3 | K_4 | K_5 | K_6 |
|-----------|--------|--------|--------|--------|---------|---------|
| 0.61 | 3.2830 | 1.6361 | 8.1015 | 8.0395 | 26.8876 | 26.2781 |
| 0.62 | 3.2304 | 1.6095 | 7.8448 | 7.7808 | 25.6365 | 25.0170 |
| 0.63 | 3.1794 | 1.5838 | 7.6003 | 7.5342 | 24.4641 | 23.8346 |
| 0.64 | 3.1300 | 1.5588 | 7.3673 | 7.2991 | 23.3642 | 22.7248 |
| 0.65 | 3.0822 | 1.5346 | 7.1450 | 7.0747 | 22.3314 | 21.6820 |
| 0.66 | 3.0358 | 1.5111 | 6.9328 | 6.8603 | 21.3606 | 20.7013 |
| 0.67 | 2.9908 | 1.4883 | 6.7302 | 6.6555 | 20.4475 | 19.7782 |
| 0.68 | 2.9472 | 1.4661 | 6.5365 | 6.4595 | 19.5876 | 18.9084 |
| 0.69 | 2.9048 | 1.4446 | 6.3512 | 6.2720 | 18.7773 | 18.0882 |
| 0.70 | 2.8637 | 1.4237 | 6.1739 | 6.0924 | 18.0131 | 17.3140 |
| 0.72 | 2.7849 | 1.3836 | 5.8415 | 5.7552 | 16.6102 | 15.8913 |
| 0.74 | 2.7105 | 1.3456 | 5.5359 | 5.4449 | 15.3565 | 14.6178 |
| 0.76 | 2.6400 | 1.3096 | 5.2545 | 5.1585 | 14.2328 | 13.4742 |
| 0.78 | 2.5732 | 1.2753 | 4.9948 | 4.8936 | 13.2229 | 12.4445 |
| 0.80 | 2.5098 | 1.2427 | 4.7546 | 4.6482 | 12.3128 | 11.5147 |
| 0.82 | 2.4495 | 1.2117 | 4.5321 | 4.4204 | 11.4908 | 10.6729 |
| 0.84 | 2.3923 | 1.1821 | 4.3256 | 4.2084 | 10.7466 | 9.9089 |
| 0.86 | 2.3377 | 1.1538 | 4.1337 | 4.0109 | 10.0718 | 9.2139 |
| 0.88 | 2.2857 | 1.1267 | 3.9550 | 3.8265 | 9.4573 | 8.5802 |
| 0.90 | 2.2361 | 1.1008 | 3.7884 | 3.6541 | 8.8979 | 8.0012 |
| 0.92 | 2.1887 | 1.0759 | 3.6329 | 3.4926 | 8.3874 | 7.4710 |
| 0.94 | 2.1435 | 1.0521 | 3.4875 | 3.3411 | 7.9206 | 6.9846 |
| 0.96 | 2.1001 | 1.0292 | 3.3515 | 3.1988 | 7.4930 | 6.5375 |
| 0.98 | 2.0587 | 1.0071 | 3.2239 | 3.0649 | 7.1008 | 6.1258 |
| 1.00 | 2.0190 | 0.9859 | 3.1043 | 2.9388 | 6.7405 | 5.7460 |
| 1.05 | 1.9267 | 0.9361 | 2.8360 | 2.6538 | 5.9598 | 4.9169 |
| 1.10 | 1.8434 | 0.8904 | 2.6052 | 2.4056 | 5.3209 | 4.2298 |
| 1.15 | 1.7678 | 0.8482 | 2.4058 | 2.1881 | 4.7941 | 3.6551 |
| 1.20 | 1.6991 | 0.8091 | 2.2322 | 1.9957 | 4.3561 | 3.1697 |
| 1.25 | 1.6365 | 0.7727 | 2.0813 | 1.8253 | 3.9916 | 2.7582 |
| 1.30 | 1.5795 | 0.7386 | 1.9492 | 1.6732 | 3.6859 | 2.4061 |
| 1.35 | 1.5273 | 0.7066 | 1.8333 | 1.5366 | 3.4286 | 2.1029 |
| 1.40 | 1.4795 | 0.6764 | 1.7314 | 1.4135 | 3.2113 | 1.8402 |
| 1.45 | 1.4357 | 0.6477 | 1.6416 | 1.3019 | 3.0271 | 1.6115 |

TABLE 2.33-13. (CONT) (SHEET 4 OF 4)

| βL | K_1 | K_2 | K_3 | K_4 | K_5 | K_6 |
|-----------|--------|--------|--------|--------|--------|---------|
| 1.50 | 1.3955 | 0.6205 | 1.5623 | 1.2004 | 2.8707 | 1.4113 |
| 1.55 | 1.3586 | 0.5945 | 1.4923 | 1.1076 | 2.7376 | 1.2352 |
| 1.60 | 1.3247 | 0.5697 | 1.4303 | 1.0226 | 2.6243 | 1.0797 |
| 1.65 | 1.2936 | 0.5458 | 1.3755 | 0.9444 | 2.5276 | 0.9418 |
| 1.70 | 1.2651 | 0.5229 | 1.3269 | 0.8722 | 2.4452 | 0.8192 |
| 1.75 | 1.2389 | 0.5007 | 1.2840 | 0.8054 | 2.3748 | 0.7097 |
| 1.80 | 1.2149 | 0.4793 | 1.2461 | 0.7435 | 2.3149 | 0.6118 |
| 1.85 | 1.1929 | 0.4586 | 1.2126 | 0.6859 | 2.2638 | 0.5240 |
| 1.90 | 1.1727 | 0.4385 | 1.1831 | 0.6321 | 2.2204 | 0.4451 |
| 1.95 | 1.1543 | 0.4189 | 1.1570 | 0.5819 | 2.1835 | 0.3740 |
| 2.00 | 1.1376 | 0.3999 | 1.1341 | 0.5350 | 2.1524 | 0.3101 |
| 2.05 | 1.1223 | 0.3814 | 1.1141 | 0.4911 | 2.1261 | 0.2525 |
| 2.10 | 1.1084 | 0.3634 | 1.0966 | 0.4500 | 2.1039 | 0.2005 |
| 2.15 | 1.0959 | 0.3459 | 1.0813 | 0.4114 | 2.0854 | 0.1536 |
| 2.20 | 1.0845 | 0.3288 | 1.0680 | 0.3751 | 2.0699 | 0.1114 |
| 2.25 | 1.0742 | 0.3121 | 1.0566 | 0.3411 | 2.0571 | 0.0734 |
| 2.30 | 1.0650 | 0.2958 | 1.0467 | 0.3091 | 2.0465 | 0.0392 |
| 2.35 | 1.0567 | 0.2800 | 1.0382 | 0.2791 | 2.0379 | 0.0086 |
| 2.40 | 1.0493 | 0.2646 | 1.0310 | 0.2510 | 2.0309 | -0.0188 |
| 2.45 | 1.0427 | 0.2496 | 1.0249 | 0.2246 | 2.0252 | -0.0433 |
| 2.50 | 1.0368 | 0.2350 | 1.0198 | 0.1998 | 2.0207 | -0.0649 |
| 2.55 | 1.0316 | 0.2208 | 1.0155 | 0.1766 | 2.0172 | -0.0841 |
| 2.60 | 1.0270 | 0.2071 | 1.0119 | 0.1549 | 2.0144 | -0.1009 |
| 2.65 | 1.0230 | 0.1938 | 1.0090 | 0.1347 | 2.0123 | -0.1155 |
| 2.70 | 1.0195 | 0.1809 | 1.0067 | 0.1158 | 2.0108 | -0.1281 |
| 2.75 | 1.0165 | 0.1685 | 1.0048 | 0.0982 | 2.0096 | -0.1389 |
| 2.80 | 1.0138 | 0.1565 | 1.0033 | 0.0819 | 2.0088 | -0.1479 |
| 2.85 | 1.0115 | 0.1449 | 1.0022 | 0.0668 | 2.0082 | -0.1553 |
| 2.90 | 1.0096 | 0.1338 | 1.0014 | 0.0528 | 2.0079 | -0.1613 |

CR-912

(c) Special Formulas

Hampe (Ref. 2-2) gives exact solutions for cylinders, based on linear bending theory. Tables 2.33-14 and 2.33-15 presents the influences caused by the unit-edge loadings: $M_{ik} = 1$, $Q_{ik} = 1$, forced rotation of the edge $\beta_{ik} = 1$ and forced displacement of the edge $\Delta r_{ik} = 1$. All formulas are valid for long and short cylinders.

If the length of cylinder is such that $L \geq 3.1 \sqrt{Rt}$, the formulas can be simplified. The simplification is also considered in Tables 2.33-16 and 2.33-17. The functions, F_i and $F_i(\xi)$, are from Paragraph 2.42.6.

TABLE 2.33-14. CYLINDRICAL SHELLS—EXACT FORMULAS FOR UNIT-EDGE LOADING SOLUTIONS (REF. 2-2)¹

| | | |
|--------------|--|---|
| | | |
| N_{θ} | $M_{ik} 2k^2 R \left[-\frac{F_2}{F_1} F_7(\xi) + \frac{F_3}{F_1} F_{10}(\xi) - F_8(\xi) \right]$ | $Q_{ik} 2kR \left[\frac{F_4}{F_1} F_7(\xi) - \frac{F_5}{F_1} F_{15}(\xi) - \frac{F_6}{F_1} F_{16}(\xi) \right]$ |
| M_x | $M_{ik} \left[\frac{F_2}{F_1} F_8(\xi) - \frac{F_3}{F_1} F_9(\xi) - F_7(\xi) \right]$ | $\frac{Q_{ik}}{k} \left[-\frac{F_4}{F_1} F_8(\xi) - \frac{F_5}{F_1} F_{16}(\xi) + \frac{F_6}{F_1} F_{15}(\xi) \right]$ |
| Q_x | $-k M_{ik} \left[\frac{F_2}{F_1} F_{10}(\xi) - \frac{2F_3}{F_1} F_8(\xi) + F_8(\xi) \right]$ | $Q_{ik} \left[\frac{F_4}{F_1} F_{10}(\xi) + \frac{F_5}{F_1} F_{13}(\xi) - \frac{F_6}{F_1} F_{14}(\xi) \right]$ |
| Δr | $\frac{M_{ik}}{2Dk} \left[\frac{F_2}{F_1} F_7(\xi) + \frac{F_3}{F_1} F_{10}(\xi) - F_8(\xi) \right]$ | $\frac{Q_{ik}}{2Dk} \left[\frac{F_4}{F_1} F_7(\xi) - \frac{F_5}{F_1} F_{15}(\xi) - \frac{F_6}{F_1} F_{16}(\xi) \right]$ |
| β | $\frac{M_{ik}}{2Dk} \left[\frac{F_2}{F_1} F_9(\xi) + \frac{2F_3}{F_1} F_7(\xi) - F_{10}(\xi) \right]$ | $-\frac{Q_{ik}}{2Dk^2} \left[\frac{F_4}{F_1} F_9(\xi) + \frac{F_5}{F_1} F_{14}(\xi) + \frac{F_6}{F_1} F_{13}(\xi) \right]$ |

¹For F factors, see paragraph 2.42.6

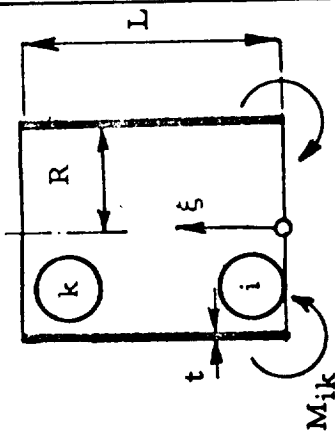
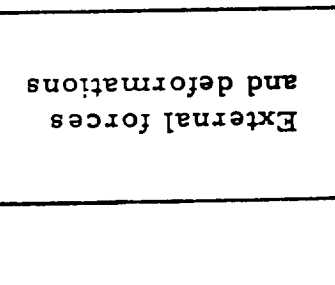
For k factors, see paragraph 2.33.4

TABLE 2.33-15. CYLINDRICAL SHELLS—EXACT FORMULAS FOR UNIT-EDGE DEFORMATIONS¹ (REF. 2-2)

| | | |
|--------------|--|---|
| | | |
| N_{θ} | $\Delta r_{ik} \frac{Et}{R} \left[F_7(\xi) + \frac{F_3}{F_1} F_9(\xi) - \frac{F_2}{F_1} F_8(\xi) \right]$ | $\frac{\beta_{ik} Et}{k} \left[\frac{F_6}{F_1} F_{15}(\xi) - \frac{F_5}{F_1} F_{16}(\xi) - \frac{F_4}{F_1} F_8(\xi) \right]$ |
| M_x | $\Delta r_{ik} 2Dk^2 \left[-F_8(\xi) + \frac{F_3}{F_1} F_{10}(\xi) - \frac{F_2}{F_1} F_7(\xi) \right]$ | $\beta_{ik} 2Dk \left[\frac{F_6}{F_1} F_{16}(\xi) + \frac{F_5}{F_1} F_{15}(\xi) - \frac{F_4}{F_1} F_7(\xi) \right]$ |
| Q_x | $\Delta r_{ik} 2Dk^3 \left[-F_{10}(\xi) + 2 \frac{F_3}{F_1} F_7(\xi) + \frac{F_2}{F_1} F_9(\xi) \right]$ | $-\beta_{ik} 2Dk^2 \left[\frac{F_6}{F_1} F_{13}(\xi) + \frac{F_5}{F_1} F_{14}(\xi) + \frac{F_4}{F_1} F_9(\xi) \right]$ |
| Δr | $\Delta r_{ik} k \left[F_7(\xi) + \frac{F_3}{F_1} F_9(\xi) - \frac{F_2}{F_1} F_8(\xi) \right]$ | $\frac{\beta_{ik}}{k} \left[\frac{F_6}{F_1} F_{15}(\xi) - \frac{F_5}{F_1} F_{16}(\xi) - \frac{F_4}{F_1} F_8(\xi) \right]$ |
| β | $\Delta r_{ik} k \left[-F_9(\xi) + 2 \frac{F_3}{F_1} F_8(\xi) - \frac{F_2}{F_1} F_{10}(\xi) \right]$ | $\beta_{ik} \left[\frac{F_6}{F_1} F_{14}(\xi) - \frac{F_5}{F_1} F_{13}(\xi) - \frac{F_4}{F_1} F_{10}(\xi) \right]$ |

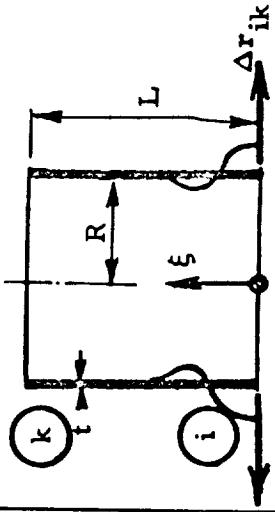
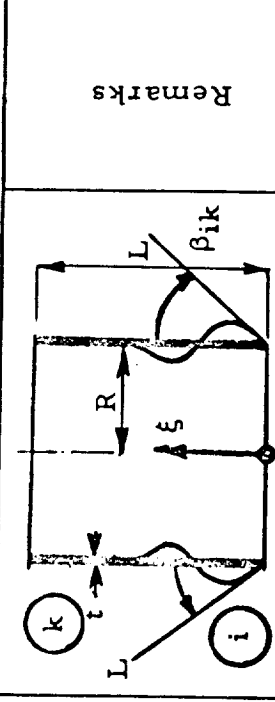
¹For F factors, see paragraph 2.42.6
For k factors, see paragraph 2.33.4

TABLE 2.33-16. LONG CYLINDRICAL SHELLS—APPROXIMATE SOLUTIONS
FOR UNIT-EDGE LOADING (REF 2-2)¹

| External forces and deformations |  |  | Remarks |
|----------------------------------|--|---|--|
| N_{θ} | $-M_{ik} 2k^2 R F_{20} (\xi)$ | $Q_{ik} 2k R F_{17} (\xi)$ | Must be satisfied: $kL > 4$ or $L \geq 3.1 \sqrt{Rt}$ |
| M_x | $-M_{ik} F_{19} (\xi)$ | $Q_{ik} \frac{F_{18}}{k} (\xi)$ | |
| Q_x | $-M_{ik} 2k F_{18} (\xi)$ | $-Q_{ik} F_{20} (\xi)$ | |
| Δr | $\frac{M_{ik}}{2Dk^2} F_{20} (\xi)$ | $\frac{Q_{ik}}{2Dk^3} F_{17} (\xi)$ | |
| β | $\frac{M_{ik}}{Dk} F_{17} (\xi)$ | $-\frac{Q_{ik}}{2Dk^2} F_{19} (\xi)$ | |
| Used approximation | $\frac{F_3}{F_1} \approx \frac{F_2}{F_1} \approx 1$ | $\frac{F_4}{F_1} \approx \frac{F_6}{F_1} \approx 1$ | $\frac{F_5}{F_1} \approx 0$ |

¹For F factors, see paragraph 2.42.6
For k factors, see paragraph 2.33.4

TABLE 2.33-17. CYLINDRICAL SHELLS—APPROXIMATE SOLUTIONS FOR UNIT-EDGE DEFORMATIONS (REF. 2-2)¹

| Internal Forces and Deformations |  |  | Remarks |
|----------------------------------|--|---|---|
| N_{θ} | $\Delta r_{ik} \frac{Et}{R} F_{19} (\xi)$ | $\frac{\beta_{ik}}{k} \frac{Et}{R} F_{18} (\xi)$ | |
| M_x | $-\Delta r_{ik} 2Dk^2 F_{20} (\xi)$ | $-\beta_{ik} 2Dk F_{17} (\xi)$ | |
| Q_x | $-\Delta r_{ik} 4Dk^3 F_{17} (\xi)$ | $-\beta_{ik} 2Dk^2 F_{19} (\xi)$ | |
| Δr | $\Delta r_{ik} F_{19} (\xi)$ | $\frac{\beta_{ik}}{k} F_{18} (\xi)$ | |
| β | $-\Delta r_{ik} 2k F_{18} (\xi)$ | $\beta_{ik} F_{20} (\xi)$ | |
| Used Approximation | $\frac{F_3}{F_1} \approx \frac{F_2}{F_1} \approx 1$ | $\frac{F_6}{F_1} = \frac{F_4}{F_1} \approx 1$ $\frac{F_5}{F_1} \approx 0$ | Must be satisfied: $KL \geq 4$ or $L \geq 3.1 \sqrt{Rt}$ |

¹For F factors, see paragraph 2.42.6
For k factors, see paragraph 2.33.4

2.33.5 Salvadori's Approximate Method for Irregular Shell

Consider a shell of revolution of any meridional shape loaded with axisymmetrical loading with restricting assumptions as stated in Paragraph 2.32.11.

A. Displacements

The following simplified formulas for displacements are given by Salvadori in Ref. 2-6 (see Table 2.33-18).

TABLE 2.33-18. IRREGULAR SHELLS—UNIT EDGE LOADING SOLUTIONS

| | | |
|---|--------------------------------|--------------------------------|
| | | |
| Δr | $\frac{Q_0}{2 \beta_s^3 D_s}$ | $-\frac{M_0}{2 \beta_s^2 D_s}$ |
| β | $-\frac{Q_0}{2 \beta_s^2 D_s}$ | $\frac{M_0}{\beta_s D_s}$ |
| <p>Where: $\beta_s = \sqrt[4]{3/\sqrt{at}}$, $D_s = Et_s^3/12$ Poisson's ratio assumed to be zero.</p> | | |

Ratio t_s/a is assumed to be small enough for displacements, rotations, and stresses in the shell to be approximated by the same quantities in a cylinder of constant thickness, t_s , tangent to the shell at the equator. This approximation is satisfactory for shells whose ratio, t_s/a , is less than 1/50 and whose thickness near the edge does not change abruptly.

B. Interaction

Considering displacements of the primary and secondary solutions, the interaction leads to the following formulas for discontinuity forces:

$$M_0 = m_0 p_0 a t_s \left(\frac{a}{r_0}\right) S_p$$

$$Q_0 = q_0 p_0 a \sqrt{\frac{t_s}{a}} \left(\frac{a}{r_0}\right) S_p$$

where

$$m_0 = \frac{1}{4\sqrt{3}} \frac{(1 - \chi^2)}{(1 + \chi^2)^2 + 2\chi^{3/2}(1 + \chi)}$$

$$q_0 = \frac{1}{2\sqrt[4]{3}} \frac{(1 + \chi^{5/2})}{(1 + \chi^2)^2 + 2\chi^{3/2}(1 + \chi)}$$

$$\chi = t_s/t_c$$

where

t_c is thickness of cylinder

S_p = factor, dependent on loading, see Table 2.32-11.

C. The Maximum Values

The maximum value of M may be larger than M_0 ; consequently, it has to be determined. It was shown by Salvadori that a maximum value of M appears at a distance \bar{x}_s , in the bulkhead, defined as follows:

$$\tan \beta_s \bar{x}_s = \frac{q_0}{q_0 - 2 \sqrt[4]{3} \cdot m_0}$$

This distance is measured along the meridian, starting from the discontinuity section. In a cylinder, the correspondent distance is \bar{x}_c , defined as follows:

$$\tan \beta_c \bar{x}_c = \frac{q_0}{q_0 + 2 \sqrt[4]{3} \sqrt{m_0}}$$

Then, for both bulkhead and cylinder, special values M_s (bulkhead) and M_c (cylinder) have to be determined. The larger value, M_0 or M , as defined above represents the actual maximum moment.

This work will be performed using Fig. 2.33-11 and the formulas that are given on this graph for M and Q . To obtain M_s or M_c , use the formula in Fig. 2.33-11, entering m_s or m_c or m , as shown in the formula.

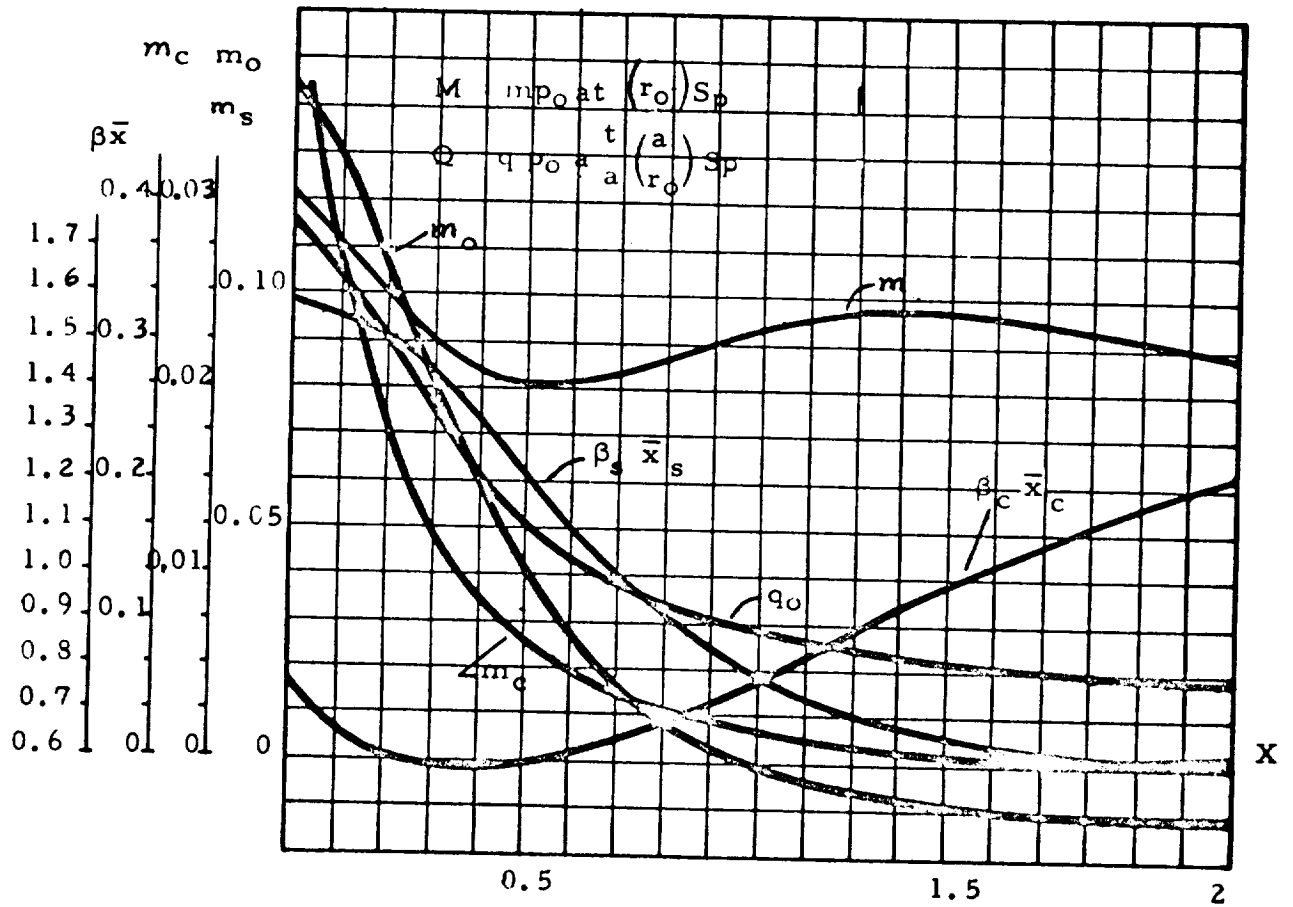


FIG. 2.33-11. Graphical Form of Data

The simplicity of the results obtained allow the checking of shell design for boundary moments (the most dangerous condition in most practical cases) without any difficulty and in a routine manner.

2.33.6 Conclusion

The influences due to the unit edge loadings were covered in this section. The disturbing influences at the boundary were as follows:

Unit-edge loadings: moments and shears.

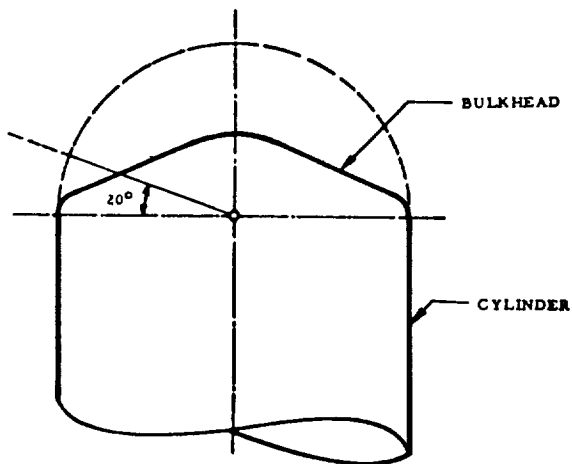
Unit-edge deformations: horizontal displacement and rotation.

The correspondent disturbances along the meridian were membrane stresses, internal moments, shear, and rotation and deflections. A combination of these influences with the influences due to primary loadings lead to the resulting stresses and deformations, if the interaction process is used as was described in Paragraph 2.23.2.

2. 34 SUMMARY

The unit-load method was presented in detail. The interaction process between shells was discussed at the beginning, and then the primary and secondary solutions were systematically presented for use in an interaction process. It was shown that a large family of axisymmetrically loaded shells of revolution can be solved using this method.

Sometimes, there are bulkheads that cannot be easily approximated at boundary zone with the spherical or cylindrical shell to obtain unit influences. Fig. 2. 34-1 is an example of such shells. It is clear that within the range of 20 degrees, the shell at junction with the cylinder cannot be approximated with the sphere. In such case, however, two



spherical shells or toroidal and spherical shell will be needed for the approximation, as shown in Fig. 2. 34-2. The determination of discontinuity stresses will be performed with the more complicated process as was shown with the system of Eq. 2. 23-3.

FIG. 2. 34-1. Bulkhead, Which Cannot be Approximated With a Sphere Alone

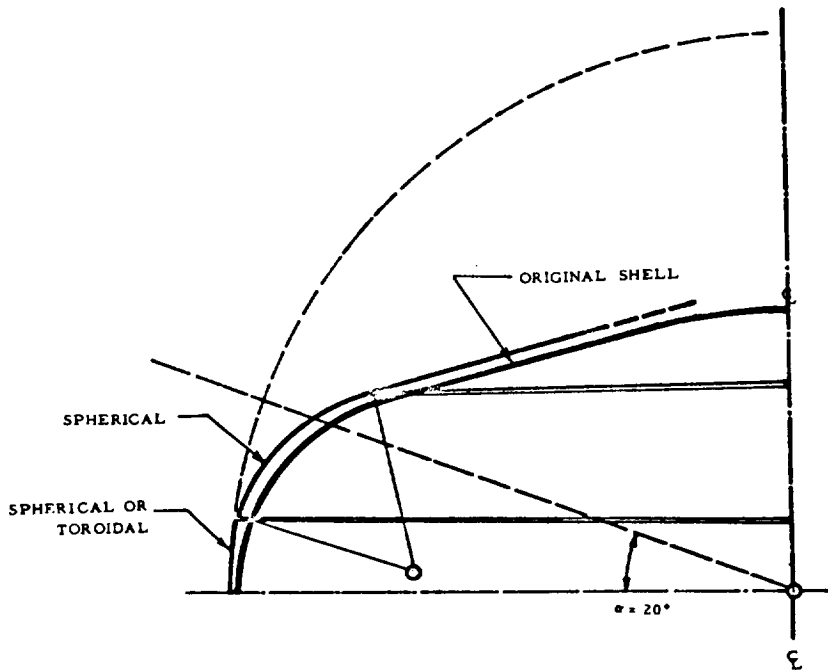


FIG. 2.34-2. Combined Bulkhead

Up to this point, solutions were discussed and presented for the isotropic material and homogeneous section of constant thickness t .

This presentation covers the most common shell configurations; however, the presentation would not be complete, unless a brief treatment of circular plates and rings is included, because the more complicated configurations known as the "multishells" always have these elements as interacting parts. Also, sometimes it is simpler to use already collected formulas than to go into the interaction process for the most used simple shells with different restrictions on the boundaries. That is the subject of Section 2.40.

2.40 SPECIAL SOLUTIONS

2.41 INTRODUCTION

The "unit-loads" method for obtaining the solutions for combined shells has been discussed. Problems can be solved in the same manner, for various idealized boundary conditions (such as simply supported or fixed) which can approximate some practical conditions. Consequently, the following definitions can be made:

The "fixed" (or "built-in") boundary does not permit any displacements or rotation along the boundary.

The "pinned" boundary permits rotation of support but not displacement. A special case of "pinned" boundary, (the so-called "simply supported" edge condition) permits the movement in one prescribed direction.

All of the aforementioned supporting conditions may be considered during the interaction process to obtain the solution. In order to save time, Hampe's method (Ref. 2-2) is presented. This method, with simple formulas, covers all possible cases of circular cylinders and spheres with various supporting conditions along the boundaries. Similarly, the abrupt discontinuity in the wall thickness may be covered by this method.

In addition, the formulas will be presented for circular plates (with and without a circular hole at the center) under different loading conditions. The same treatment will be given to circular rings. Circular plates and rings usually are the common interacting elements in the multishells; consequently, they can not be omitted in a shell manual.

2.42 HAMPE METHOD

Hampe (Ref. 2-2) derived a set of general formulas for the stresses and deformations of cylindrical shells with various boundary conditions and loadings. The results of his derivations (based on classical linear bending theory) are presented in tabular form in this section. The following constants are used:

F and $F(\xi)$: These functions of geometry are presented in Paragraph 2.42.6

S : These factors are dependent on the type of boundary and loading. (Tables 2.42-1 through 2.42-8.)

w factors for particular solution of differential equations are as follows:

w_p = the ordinates of the deflection line

w'_p = inclination of deflection line

w''_p = the second derivative of the deflection line

w'''_p = the third derivative of the deflection line

These factors, for different loadings, are tabulated in Table 2.42-8.

The scope of this manual does not permit a breakdown of the derivations or a more rigorous explanation of the method. For further information refer to Hampe (Ref. 2-2). The general formulas are given in the following text for the factors that presented in the tables.

The stresses and deformations of the cylinder with any fixity at the boundary can be described by the formulas given below.

2.42.1 Stresses

A. General

The circumferential load is

$$N_{\theta} = \frac{Et}{R} \left[w_p(\xi) + S_1 F_7(\xi) + S_2 F_{15}(\xi) + S_3 F_{16}(\xi) + S_4 F_8(\xi) \right]$$

The location (ξ_N) of the max N_{θ} is obtained from the relation: $(N_{\theta})' = 0$

$$S_1 F_9(\xi_N) - S_2 F_{14}(\xi_N) - S_3 F_{13}(\xi_N) + S_4 F_{10}(\xi_N) - \frac{w_p'(\xi_N)}{k} = 0$$

The moment is

$$M_x = D \left\{ w_p''(\xi) + 2k^2 \left[-S_1 F_8(\xi) + S_2 F_{16}(\xi) - S_3 F_{15}(\xi) + S_4 F_7(\xi) \right] \right\}$$

The location (ξ_M) of the max, M_x , is obtainable from the relation, $M_x' = 0$:

$$S_1 F_{10}(\xi_M) - S_2 F_{13}(\xi_M) + S_3 F_{14}(\xi_M) + S_4 F_9(\xi_M) - \frac{w_p'''(\xi_M)}{2k^3} = 0$$

The shear is

$$Q_x = -D \left\{ w_p''''(\xi) + 2k^3 \left[-S_1 F_{10}(\xi) + S_2 F_{13}(\xi) - S_3 F_{14}(\xi) - S_4 F_9(\xi) \right] \right\}$$

B. Special Case: $kL \geq 4$ (Long Cylinders)

With the same notation as before, the circumferential force is

$$N_\theta = \frac{Et}{R} \left[w_p(\xi) + S_1 F_{17}(\xi) + S_2 F_{18}(\xi) \right]$$

The location (ξ_N) of max N is determinable with relation to

$$S_1 F_{19}(\xi_N) - S_2 F_{20}(\xi_N) - \frac{w_p'(\xi_N)}{k} = 0$$

The moment is

$$M_x = D \left\{ w_p''(\xi) + 2k^2 \left[S_1 F_{18}(\xi) - S_2 F_{17}(\xi) \right] \right\}$$

The location (ξ_M) of max M is determined by the relation

$$S_1 F_{20}(\xi_M) + S_2 F_{19}(\xi_M) + \frac{w_p'''(\xi_M)}{2k^3} = 0$$

The shear is

$$Q_x = -D \left\{ w_p''''(\xi) + 2k^3 \left[S_1 F_{20}(\xi_M) + S_2 F_{19}(\xi_M) \right] \right\}$$

2.42.2 Distortions

A. General

The deflection line is

$$w = w_p(\xi) + S_1 F_7(\xi) + S_2 F_{15}(\xi) + S_3 F_{16}(\xi) + S_4 F_8(\xi)$$

Inclination of the tangent of the deflection line is

$$w' = w'_p(\xi) + k \left[-S_1 F_9(\xi) + S_2 F_{14}(\xi) + S_3 F_{13}(\xi) + S_4 F_{10}(\xi) \right]$$

B. Special Case $kL \geq 4$ (Long Cylinders)

The deflection line is

$$w = w_p(\xi) + S_1 F_{17}(\xi) + S_2 F_{18}(\xi)$$

Inclination of the deflection line is

$$w' = w'_p(\xi) + k \left[S_1 F_{19}(\xi) + S_2 F_{20}(\xi) \right]$$

2.42.3 Coefficients and Tables

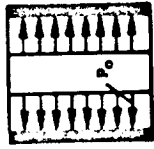
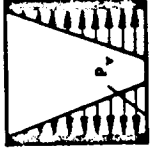
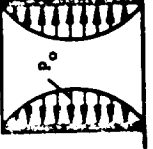
The w_p to w_p coefficients for the different loadings and geometries are presented in Table 2.42-1. S_i coefficients are presented similarly in Tables 2.42-2 to 9.

These tables are prepared for different kinds of distributed loadings. For hinged edges of the shell (rotation but not displacement permitted, moment = 0), the S_i coefficients are presented in Tables 2.42-4 and 5.

Table 2.42-6 presents the coefficients S_i for cylinders with both boundaries fixed. The coefficients S_i are presented in Table 2.42-7 for one boundary fixed and another hinged.

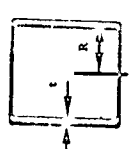
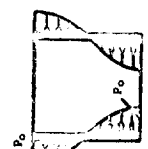
When the cylindrical shells are loaded with nonuniform loadings, bending will be involved, and the membrane theory will not be adequate to solve the shell problem even if the edges are free to rotate and deflect; therefore, these cases are tabulated in Tables 2.42-8 and 9. These cases are assembled for the free boundary conditions, however S_i factors are determined with linear bending theory in most of the cases. Dash over S_i factors (Table 2.42-9) indicates that the length of the cylinder is such that the supporting condition of one boundary does not effect the stresses and deformations on another boundary.

TABLE 2.42-1. $w_p, w'_p, w''_p, w'''_p, w''''_p$ - FUNCTIONS (Ref. 2-2)

| Load Condition | $w_p(\xi)$ | $w'_p(\xi)$ | $w''_p(\xi)$ | $w'''_p(\xi)$ |
|---|--|--|--|--|
|  | $+\frac{P_0 R^2}{EI}$ | 0 | 0 | 0 |
|  | $+\frac{P_0 R^2}{EI} (1 - \xi)$ | $-\frac{P_0 R^2}{EI L}$ | 0 | 0 |
|  | $+\frac{P_0 R^2}{EI} \frac{4(kL)^4}{\alpha^4 + 4(kL)^4} \sin \alpha \xi$ | $+\frac{P_0 R^2}{EI} \left(\frac{\alpha}{L}\right) \frac{4(kL)^4}{\alpha^4 + 4(kL)^4} \cos \alpha \xi$ | $-\frac{P_0 R^2}{EI} \left(\frac{\alpha}{L}\right)^2 \frac{4(kL)^4}{\alpha^4 + 4(kL)^4} \sin \alpha \xi$ | $-\frac{P_0 R^2}{EI} \left(\frac{\alpha}{L}\right)^3 \frac{4(kL)^4}{\alpha^4 + 4(kL)^4} \cos \alpha \xi$ |
| | $\alpha < kL$ | $+\frac{P_0 R^2}{EI} \cos \alpha \xi$ | $+\frac{P_0 R^2}{EI} \left(\frac{\alpha}{L}\right)^2 \sin \alpha \xi$ | $-\frac{P_0 R^2}{EI} \left(\frac{\alpha}{L}\right)^3 \cos \alpha \xi$ |

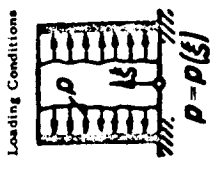
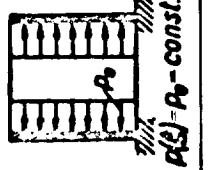
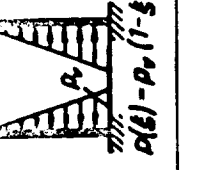
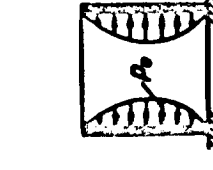
For k factors, see paragraph 2.42.6

TABLE 2.42-1 (CONT.)¹

| Load Condition | $w_p(\xi)$ | $w_p'(\xi)$ | $w_p''(\xi)$ | $w_p'''(\xi)$ |
|--|---|--|---|---|
|  | $+ \frac{P_0 R^2}{Et} \frac{4(kL)^4}{\alpha^4 + 4(kL)^4} \cos \alpha \xi$ | $- \frac{P_0 R^2}{Et} \frac{\alpha}{L} \frac{4(kL)^4}{\alpha^4 + 4(kL)^4} \sin \alpha \xi$ | $- \frac{P_0 R^2}{Et} \left(\frac{\alpha}{L} \right)^2 \frac{4(kL)^4}{\alpha^4 + 4(kL)^4} \cos \alpha \xi$ | $+ \frac{P_0 R^2}{Et} \left(\frac{\alpha}{L} \right)^3 \frac{4(kL)^4}{\alpha^4 + 4(kL)^4} \sin \alpha \xi$ |
| | $+ \frac{P_0 R^2}{Et} \cos \alpha \xi$ | $- \frac{P_0 R^2}{Et} \frac{\alpha}{L} \sin \alpha \xi$ | $- \frac{P_0 R^2}{Et} \left(\frac{\alpha}{L} \right)^2 \cos \alpha \xi$ | $+ \frac{P_0 R^2}{Et} \left(\frac{\alpha}{L} \right)^3 \sin \alpha \xi$ |
|  <p>$P(\xi) = P_0 \cos \alpha \xi$</p> | $+ \frac{P_0 R^2}{Et} \frac{4(kL)^4}{\alpha^4 + 4(kL)^4} \exp(-\alpha \xi)$ | $- \frac{P_0 R^2}{Et} \frac{\alpha}{L} \frac{4(kL)^4}{\alpha^4 + 4(kL)^4} \exp(-\alpha \xi)$ | $+ \frac{P_0 R^2}{Et} \left(\frac{\alpha}{L} \right)^2 \frac{4(kL)^4}{\alpha^4 + 4(kL)^4} \exp(-\alpha \xi)$ | $- \frac{P_0 R^2}{Et} \left(\frac{\alpha}{L} \right)^3 \frac{4(kL)^4}{\alpha^4 + 4(kL)^4} \exp(-\alpha \xi)$ |
| | $+ \frac{P_0 R^2}{Et} \exp(-\alpha \xi)$ | $- \frac{P_0 R^2}{Et} \frac{\alpha}{L} \exp(-\alpha \xi)$ | $+ \frac{P_0 R^2}{Et} \left(\frac{\alpha}{L} \right)^2 \exp(-\alpha \xi)$ | $- \frac{P_0 R^2}{Et} \left(\frac{\alpha}{L} \right)^3 \exp(-\alpha \xi)$ |

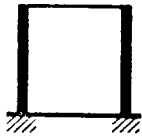
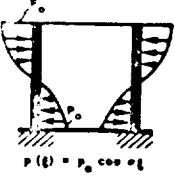
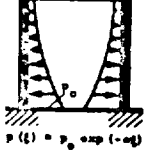
¹For k factors, see paragraph 2.42.6

TABLE 2.42-2. COEFFICIENTS S_i , $kL < 4.0$ (Ref. 2-2)

| Loading Conditions | s_1 | s_2 | s_3 | s_4 |
|--|-----------------------|---|---|---|
|  $P = P(\xi)$ | $-\frac{P_0 R^2}{Et}$ | $-\frac{P_0 R^2}{Et} \frac{F_3}{F_1 + 2}$ | $+\frac{P_0 R^2}{Et} \frac{F_3}{F_1 + 2}$ | $+\frac{P_0 R^2}{Et} \frac{F_2}{F_1 + 2}$ |
|  $P(\xi) = P_0 = \text{const.}$ | $-\frac{P_0 R^2}{Et}$ | $-\frac{P_0 R^2}{Et} \left(\frac{F_3}{F_1 + 2} - \frac{1}{kL} \frac{F_6 + 1}{F_1 + 2} \right)$ | $+\frac{P_0 R^2}{Et} \left(\frac{F_3}{F_1 + 2} - \frac{1}{kL} \frac{F_5 - 1}{F_1 + 2} \right)$ | $+\frac{P_0 R^2}{Et} \left(\frac{F_2}{F_1 + 2} - \frac{1}{kL} \frac{F_4}{F_1 + 2} \right)$ |
|  $P(\xi) = P_0 (1 - \xi)$ | 0 | $-\frac{P_0 R^2}{Et} \frac{4(kL)^4}{\sigma^4 + 4(kL)^4} \left[\frac{\sigma}{kL} \frac{F_6 + 1}{F_1 + 2} - \frac{\sigma^2}{2(kL)^2} \left(\frac{F_9}{F_1 + 2} \sin \sigma + \frac{F_7}{F_1 + 2} \cos \sigma \right) + \frac{\sigma}{kL} \frac{F_7}{F_1 + 2} \cos \sigma \right]$ | $+\frac{P_0 R^2}{Et} \frac{4(kL)^4}{\sigma^4 + 4(kL)^4} \left[\frac{\sigma}{kL} \frac{F_5 - 1}{F_1 + 2} - \frac{\sigma^2}{2(kL)^2} \left(\frac{F_9}{F_1 + 2} \sin \sigma + \frac{F_7}{F_1 + 2} \cos \sigma \right) + \frac{\sigma}{kL} \frac{F_7}{F_1 + 2} \cos \sigma \right]$ | $+\frac{P_0 R^2}{Et} \frac{4(kL)^4}{\sigma^4 + 4(kL)^4} \left[\frac{\sigma}{kL} \frac{F_4}{F_1 + 2} - \frac{\sigma^2}{2(kL)^2} \left(\frac{2F_7}{F_1 + 2} \sin \sigma - \frac{\sigma}{kL} \frac{F_{10}}{F_1 + 2} \cos \sigma \right) \right]$ |
|  $P(\xi) = P_0 \sin \alpha \xi$ | 0 | $-\frac{P_0 R^2}{Et} \left[\frac{\sigma}{kL} \frac{F_6 + 1}{F_1 + 2} - \frac{\sigma^2}{2(kL)^2} \left(\frac{F_9}{F_1 + 2} \sin \sigma + \frac{F_7}{F_1 + 2} \cos \sigma \right) \right]$ | $+\frac{P_0 R^2}{Et} \left[\frac{\sigma}{kL} \frac{F_5 - 1}{F_1 + 2} - \frac{\sigma^2}{2(kL)^2} \left(\frac{F_9}{F_1 + 2} \sin \sigma + \frac{F_7}{F_1 + 2} \cos \sigma \right) \right]$ | $+\frac{P_0 R^2}{Et} \left[\frac{\sigma}{kL} \frac{F_4}{F_1 + 2} - \frac{\sigma^2}{2(kL)^2} \left(\frac{2F_7}{F_1 + 2} \sin \sigma - \frac{\sigma}{kL} \frac{F_{10}}{F_1 + 2} \cos \sigma \right) \right]$ |

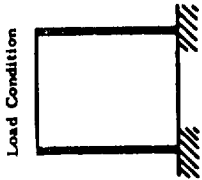
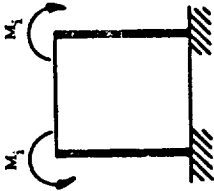
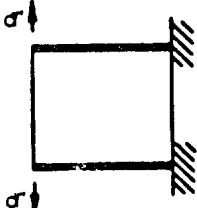
¹For F factors and F factors, see paragraph 2.42.6

TABLE 2.42-2. (CONT)

| <p>Load Condition</p>  | S_1 | | S_2 | | S_3 | | S_4 | |
|--|--|--|--|---|---------------|---|---|--|
|  <p>$p(x) = p_0 \cos \alpha x$</p> | $-\frac{p_0 R^2}{Et} \frac{4(kL)^4}{\alpha^4 + 4(kL)^4}$ | $-\frac{p_0 R^2}{Et} \frac{4(kL)^4}{\alpha^4 + 4(kL)^4} \left[\frac{F_3}{F_1 + 2} \right.$ $-\frac{\alpha^2}{2(kL)^2} \left(\frac{F_9}{F_1 + 2} \cos \alpha \right.$ $\left. \left. - \frac{\alpha}{kL} \frac{F_7}{F_1 + 2} \sin \alpha \right) \right]$ | $+\frac{p_0 R^2}{Et} \frac{4(kL)^4}{\alpha^4 + 4(kL)^4} \left[\frac{F_3}{F_1 + 2} \right.$ $-\frac{\alpha^2}{2(kL)^2} \left(\frac{F_9}{F_1 + 2} \cos \alpha \right.$ $\left. \left. - \frac{\alpha}{kL} \frac{F_7}{F_1 + 2} \sin \alpha \right) \right]$ | $+\frac{p_0 R^2}{Et} \frac{4(kL)^4}{\alpha^4 + 4(kL)^4} \left[\frac{F_2}{F_1 + 2} \right.$ $+\frac{\alpha^2}{2(kL)^2} \left(\frac{2F_7}{F_1 + 2} \cos \alpha \right.$ $\left. \left. + \frac{\alpha}{kL} \frac{F_{10}}{F_1 + 2} \sin \alpha \right) \right]$ | $\alpha < kL$ | $-\frac{p_0 R^2}{Et} \left[\frac{F_3}{F_1 + 2} - \frac{\alpha^2}{2(kL)^2} \right.$ $\left. \left(\frac{F_9}{F_1 + 2} \cos \alpha \right. \right.$ $\left. \left. - \frac{\alpha}{kL} \frac{F_7}{F_1 + 2} \sin \alpha \right) \right]$ | $+\frac{p_0 R^2}{Et} \left[\frac{F_3}{F_1 + 2} - \frac{\alpha^2}{2(kL)^2} \right.$ $\left. \left(\frac{F_9}{F_1 + 2} \cos \alpha \right. \right.$ $\left. \left. - \frac{\alpha}{kL} \frac{F_7}{F_1 + 2} \sin \alpha \right) \right]$ | $+\frac{p_0 R^2}{Et} \left[\frac{F_2}{F_1 + 2} \right.$ $+\frac{\alpha^2}{2(kL)^2} \left(\frac{2F_7}{F_1 + 2} \cos \alpha \right.$ $\left. \left. + \frac{\alpha}{kL} \frac{F_{10}}{F_1 + 2} \sin \alpha \right) \right]$ |
|  <p>$p(x) = p_0 \exp(-\alpha x)$</p> | $-\frac{p_0 R^2}{Et} \frac{4(kL)^4}{\alpha^4 + 4(kL)^4}$ | $-\frac{p_0 R^2}{Et} \frac{4(kL)^4}{\alpha^4 + 4(kL)^4} \left[\frac{F_3}{F_1 + 2} \right.$ $-\frac{\alpha}{kL} \frac{F_6 + 1}{F_1 + 2} + \left(\frac{F_9}{F_1 + 2} \right.$ $\left. \left. - \frac{\alpha}{kL} \frac{F_7}{F_1 + 2} \right) \frac{\alpha^2}{2(kL)^2} \exp(-\alpha) \right]$ | $+\frac{p_0 R^2}{Et} \frac{4(kL)^4}{\alpha^4 + 4(kL)^4} \left[\frac{F_3}{F_1 + 2} \right.$ $-\frac{\alpha}{kL} \frac{F_5 - 1}{F_1 + 2} + \left(\frac{F_9}{F_1 + 2} \right.$ $\left. \left. - \frac{\alpha}{kL} \frac{F_7}{F_1 + 2} \right) \frac{\alpha^2}{2(kL)^2} \exp(-\alpha) \right]$ | $+\frac{p_0 R^2}{Et} \frac{4(kL)^4}{\alpha^4 + 4(kL)^4} \left[\frac{F_2}{F_1 + 2} + \frac{\alpha}{kL} \frac{F_4}{F_1 + 2} \right.$ $\left. \left. - \left(\frac{2F_7}{F_1 + 2} + \frac{\alpha}{kL} \frac{F_{10}}{F_1 + 2} \right) \right.$ $\left. \left. - \frac{\alpha^2}{2(kL)^2} \exp(-\alpha) \right) \right]$ | $\alpha < kL$ | $-\frac{p_0 R^2}{Et} \left[\frac{F_3}{F_1 + 2} - \frac{\alpha}{kL} \frac{F_6 + 1}{F_1 + 2} \right.$ $+ \left(\frac{F_9}{F_1 + 2} - \frac{\alpha}{kL} \frac{F_7}{F_1 + 2} \right)$ $\left. \frac{\alpha^2}{2(kL)^2} \exp(-\alpha) \right]$ | $+\frac{p_0 R^2}{Et} \left[\frac{F_3}{F_1 + 2} - \frac{\alpha}{kL} \frac{F_5 - 1}{F_1 + 2} \right.$ $+ \left(\frac{F_9}{F_1 + 2} - \frac{\alpha}{kL} \frac{F_7}{F_1 + 2} \right)$ $\left. \frac{\alpha^2}{2(kL)^2} \exp(-\alpha) \right]$ | $+\frac{p_0 R^2}{Et} \left[\frac{F_2}{F_1 + 2} - \frac{\alpha}{kL} \frac{F_4}{F_1 + 2} \right.$ $\left. - \left(\frac{2F_7}{F_1 + 2} + \frac{\alpha}{kL} \frac{F_{10}}{F_1 + 2} \right) \right.$ $\left. - \frac{\alpha^2}{2(kL)^2} \exp(-\alpha) \right]$ |

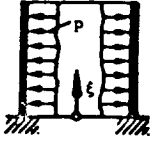
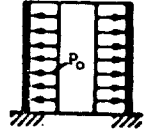
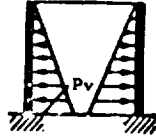
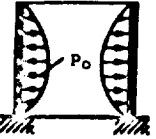
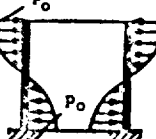
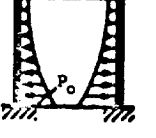
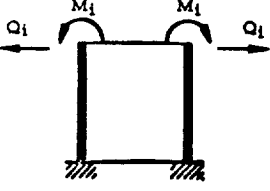
¹For F factors, see paragraph 2.42.6

TABLE 2.42-2. (CONT)

| | | | | |
|---|----------------------|--|--|---|
| <p>Load Condition</p>  | <p>S₁</p> | <p>S₂</p> | <p>S₃</p> | <p>S₄</p> |
|  | <p>0</p> | $+\frac{M_1 R^2}{Et} - 2k^2 \frac{F_9}{F_1 + 2}$ | $-\frac{M_1 R^2}{Et} + 2k^2 \frac{F_9}{F_1 + 2}$ | $+\frac{M_1 R^2}{Et} - 2k^2 \frac{2F_7}{F_1 + 2}$ |
|  | <p>0</p> | $-\frac{Q_1 R^2}{Et} - 2k \frac{F_7}{F_1 + 2}$ | $+\frac{Q_1 R^2}{Et} + 2k \frac{F_7}{F_1 + 2}$ | $+\frac{Q_1 R^2}{Et} - 2k \frac{F_{10}}{F_1 + 2}$ |

¹For k factors, see paragraph 2.42.6

TABLE 2.42-3. S_1 AND S_2 COEFFICIENTS, $kL \geq 4.0$ (Ref. 2-2)¹

| Load Condition  $p = p(\xi)$ | S_1 | | S_2 |
|---|-----------------------|--|---|
|  $p(\xi) = p_0 = \text{const}$ | $-\frac{P_0 R^2}{Et}$ | | $-\frac{P_0 R^2}{Et}$ |
|  $p(\xi) = p_v (1 - \xi)$ | $-\frac{P_v R^2}{Et}$ | | $-\frac{P_v R^2}{Et} \left(1 - \frac{1}{kL}\right)$ |
|  $p(\xi) = p_0 \sin \alpha \xi$ | | 0 | $-\frac{P_0 R^2}{Et} \frac{\alpha}{kL} \frac{4(kL)^4}{\alpha^4 + 4(kL)^4}$ |
| | $\alpha < kL$ | 0 | $-\frac{P_0 R^2}{Et} \frac{\alpha}{kL}$ |
|  $p(\xi) = p_0 \cos \alpha \xi$ | | $-\frac{P_0 R^2}{Et} \frac{4(kL)^4}{\alpha^4 + 4(kL)^4}$ | $-\frac{P_0 R^2}{Et} \frac{4(kL)^4}{\alpha^4 + 4(kL)^4}$ |
| | $\alpha < kL$ | $-\frac{P_0 R^2}{Et}$ | $\frac{P_0 R^2}{Et}$ |
|  $p(\xi) = p_0 \exp(-\alpha \xi)$ | | $-\frac{P_0 R^2}{Et} \frac{4(kL)^4}{\alpha^4 + 4(kL)^4}$ | $-\frac{P_0 R^2}{Et} \frac{4(kL)^4}{\alpha^4 + 4(kL)^4} \left(1 - \frac{\alpha}{kL}\right)$ |
| | $\alpha < kL$ | $-\frac{P_0 R^2}{Et}$ | $-\frac{P_0 R^2}{Et} \left(1 - \frac{\alpha}{kL}\right)$ |
|  | 0 | | 0 |

¹For k factors, see paragraph 2.42.6

TABLE 2.42-4. S_i - VALUES, $kL < 4.0$ (REF. 2-2)

| Load Condition | S_1 | S_2 | S_3 | S_4 |
|----------------|---|--|--|---|
| | | | | |
| | $-\frac{P_0 R^2}{Et}$ | $+\frac{P_0 R^2 F_5}{Et F_4}$ | $+\frac{P_0 R^2 F_6}{Et F_4}$ | 0 |
| | $-\frac{P_v R^2}{Et}$ | $+\frac{P_v R^2 F_5}{Et F_4}$ | $+\frac{P_v R^2 F_6}{Et F_4}$ | 0 |
| | 0 | $+\frac{P_0 R^2}{Et} \frac{4(kL)^4}{a^4 + 4(kL)^4} \frac{a^2}{2(kL)^2} \left(\frac{F_{14} \sin \theta}{F_4} - \frac{a}{kL} \frac{F_{15} \cos \theta}{F_4} \right)$ | $+\frac{P_0 R^2}{Et} \frac{4(kL)^4}{a^4 + 4(kL)^4} \frac{a^2}{2(kL)^2} \left(\frac{F_{13} \sin \theta}{F_4} - \frac{a}{kL} \frac{F_{16} \cos \theta}{F_4} \right)$ | 0 |
| | 0 | $+\frac{P_0 R^2}{Et} \frac{a^2}{2(kL)^2} \left(\frac{F_{14} \sin \theta}{F_4} - \frac{a}{kL} \frac{F_{15} \cos \theta}{F_4} \right)$ | $+\frac{P_0 R^2}{Et} \frac{a^2}{2(kL)^2} \left(\frac{F_{13} \sin \theta}{F_4} - \frac{a}{kL} \frac{F_{16} \cos \theta}{F_4} \right)$ | 0 |
| | $-\frac{P_0 R^2}{Et} \frac{4(kL)^4}{a^4 + 4(kL)^4}$ | $+\frac{P_0 R^2}{Et} \frac{4(kL)^4}{a^4 + 4(kL)^4} \left[\frac{F_5}{F_4} - \frac{a^2}{2(kL)^2} \frac{F_6 + 1}{F_4} + \frac{a^2}{2(kL)^2} \left(\frac{F_{14} \cos \theta}{F_4} + \frac{a}{kL} \frac{F_{15} \sin \theta}{F_4} \right) \right]$ | $+\frac{P_0 R^2}{Et} \frac{4(kL)^4}{a^4 + 4(kL)^4} \left[\frac{F_6}{F_4} - \frac{a^2}{2(kL)^2} \frac{F_5 - 1}{F_4} + \frac{a^2}{2(kL)^2} \left(\frac{F_{13} \cos \theta}{F_4} + \frac{a}{kL} \frac{F_{16} \sin \theta}{F_4} \right) \right]$ | $+\frac{P_0 R^2}{Et} \frac{a^2}{2(kL)^2} \frac{4(kL)^4}{a^4 + 4(kL)^4}$ |
| | $-\frac{P_0 R^2}{Et}$ | $+\frac{P_0 R^2}{Et} \left[\frac{F_5}{F_4} - \frac{a^2}{2(kL)^2} \frac{F_6 + 1}{F_4} + \frac{a^2}{2(kL)^2} \left(\frac{F_{14} \cos \theta}{F_4} + \frac{a}{kL} \frac{F_{15} \sin \theta}{F_4} \right) \right]$ | $+\frac{P_0 R^2}{Et} \left[\frac{F_6}{F_4} - \frac{a^2}{2(kL)^2} \frac{F_5 - 1}{F_4} + \frac{a^2}{2(kL)^2} \left(\frac{F_{13} \cos \theta}{F_4} + \frac{a}{kL} \frac{F_{16} \sin \theta}{F_4} \right) \right]$ | $+\frac{P_0 R^2}{Et} \frac{a^2}{2(kL)^2}$ |

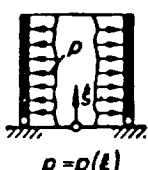
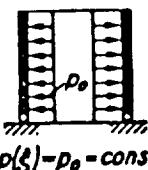

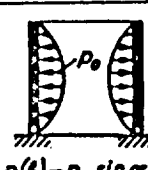
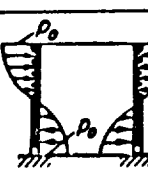
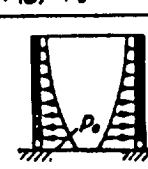
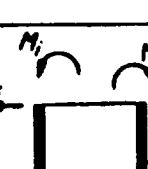
¹For F factors, see paragraph 2.42.6
For k factors, see paragraph 2.42.6

TABLE 2.42-4. (CONT)

| Load Condition | S1 | S2 | S3 | S4 |
|--|------------------------|---|---|---|
| | | $+ \frac{P_0 R^2}{EI} \frac{4 (kL)^4}{\sigma^4 + 4 (kL)^4} \left[\frac{F_5}{F_4} \right]$ $+ \frac{\sigma^2}{2 (kL)^2} \frac{F_6 + 1}{F_4} \cdot \frac{\sigma^2}{2 (kL)^2}$ $\left(\frac{F_{14}}{F_4} + \frac{\sigma}{kL} \frac{F_{15}}{F_4} \right) \exp(-\sigma)$ | $+ \frac{P_0 R^2}{EI} \frac{4 (kL)^4}{\sigma^4 + 4 (kL)^4} \left[\frac{F_6}{F_4} \right]$ $- \frac{\sigma^2}{2 (kL)^2} \frac{F_5 - 1}{F_4} \cdot \frac{\sigma^2}{2 (kL)^2}$ $\left(\frac{F_{13}}{F_4} + \frac{\sigma}{kL} \frac{F_{16}}{F_4} \right) \exp(-\sigma)$ | $- \frac{P_0 R^2}{EI} \frac{\sigma^2}{2 (kL)^2} \frac{4 (kL)^4}{\sigma^4 + 4 (kL)^4}$ |
| <p>$p(x) = P_0 \exp(-\sigma x)$</p> | $- \frac{P_0 R^2}{EI}$ | $+ \frac{P_0 R^2}{EI} \left[\frac{F_5}{F_4} + \frac{\sigma^2}{2 (kL)^2} \frac{F_6 + 1}{F_4} \right]$ $- \frac{\sigma^2}{2 (kL)^2} \left(\frac{F_{14}}{F_4} \right)$ $+ \frac{\sigma}{kL} \frac{F_{15}}{F_4} \exp(-\sigma)$ | $+ \frac{P_0 R^2}{EI} \left[\frac{F_6}{F_4} + \frac{\sigma^2}{2 (kL)^2} \frac{F_5 - 1}{F_4} \right]$ $- \frac{\sigma^2}{2 (kL)^2} \left(\frac{F_{13}}{F_4} \right)$ $+ \frac{\sigma}{kL} \frac{F_{16}}{F_4} \exp(-\sigma)$ | $- \frac{P_0 R^2}{EI} \frac{\sigma^2}{2 (kL)^2}$ |
| | • | $+ \frac{M_1 R^2}{EI} \frac{2 k^2}{2 k} \frac{F_{14}}{F_4}$ | $+ \frac{M_2 R^2}{EI} \frac{2 k^2}{2 k} \frac{F_{13}}{F_4}$ | 0 |
| | • | $+ \frac{Q_1 R^2}{EI} \frac{2 k}{2 k} \frac{F_{15}}{F_4}$ | $+ \frac{Q_2 R^2}{EI} \frac{2 k}{2 k} \frac{F_{16}}{F_4}$ | 0 |

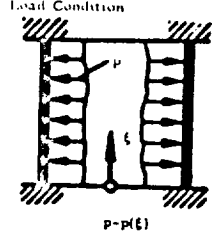
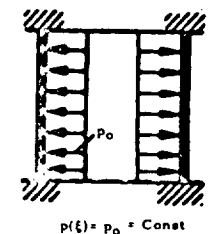
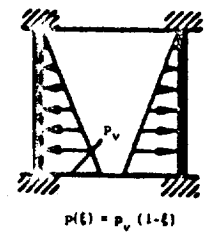
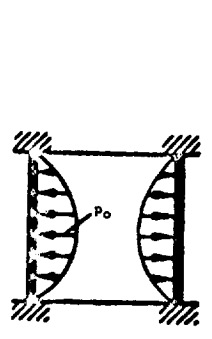
For F and k factors, see paragraph 2.42.6

TABLE 2.42-5. S_1 AND S_2 COEFFICIENTS, $KL > 4.0$ (REF. 2-2)¹

| Load Condition | S_1 | S_2 |
|--|-----------------------|---|
|  $p = p(\xi)$ | S_1 | S_2 |
|  $p(\xi) = p_0 = \text{const}$ | $-\frac{p_0 R^2}{Et}$ | 0 |
|  $p(\xi) = p_v(1-\xi)$ | $-\frac{p_v R^2}{Et}$ | 0 |
|  $p(\xi) = p_0 \sin \alpha \xi$ | 0 | 0 |
|  $p(\xi) = p_0 \cos \alpha \xi$ | | $-\frac{p_0 R^2}{Et} \frac{4(kL)^4}{\alpha^4 + 4(kL)^4} \frac{\alpha^2}{2(kL)^2}$ |
| | $\alpha < kL$ | $-\frac{p_0 R^2}{Et}$ |
|  $p(\xi) = p_0 \exp(\alpha \xi)$ | | $+\frac{p_0 R^2}{Et} \frac{4(kL)^4}{\alpha^4 + 4(kL)^4} \frac{\alpha^2}{2(kL)^2}$ |
| | $\alpha < kL$ | $-\frac{p_0 R^2}{Et}$ |
|  | 0 | 0 |

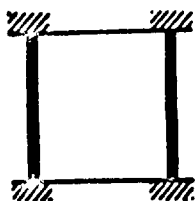
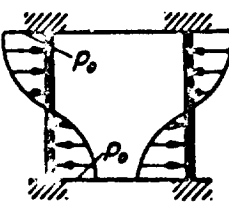
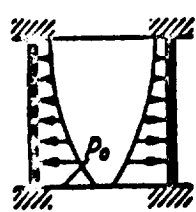
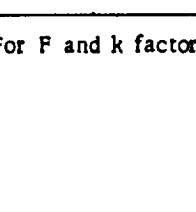

¹For k factors, see paragraph 2.42.6

TABLE 2.42-6. S_i -COEFFICIENTS (REF. 2-2)¹

| Load Condition | S_1 | S_2 | S_3 | S_4 |
|--|-----------------------|---|---|---|
|  $p = p(\xi)$ | | | | |
|  $p(\xi) = p_0 = \text{Const}$ | $-\frac{p_0 R^2}{Et}$ | $-\frac{p_0 R^2}{Et} \left(\frac{F_3}{F_1} - \frac{F_{10}}{F_1} \right)$ | $+\frac{p_0 R^2}{Et} \left(\frac{F_3}{F_1} - \frac{F_{10}}{F_1} \right)$ | $+\frac{p_0 R^2}{Et} \left(\frac{F_2}{F_1} - \frac{2F_8}{F_1} \right)$ |
|  $p(\xi) = p_v (1-\xi)$ | $-\frac{p_v R^2}{Et}$ | $-\frac{p_v R^2}{Et} \left[\frac{F_3}{F_1} - \frac{1}{kL} \left(\frac{F_6}{F_1} + \frac{F_8}{F_1} \right) \right]$ | $+\frac{p_v R^2}{Et} \left[\frac{F_3}{F_1} - \frac{1}{kL} \left(\frac{F_5}{F_1} + \frac{F_8}{F_1} \right) \right]$ | $+\frac{p_v R^2}{Et} \left[\frac{F_2}{F_1} - \frac{1}{kL} \left(\frac{F_4}{F_1} + \frac{F_9}{F_1} \right) \right]$ |
|  $p(\xi) = p_0 \sin \xi$ | 0 | $+\frac{p_0 R^2}{Et} \frac{4(kL)^4}{a^4 + 4(kL)^4} \left[\frac{F_{10}}{F_1} \sin a - \frac{a}{kL} \left(\frac{F_6}{F_1} + \frac{F_8}{F_1} \cos a \right) \right]$ | $-\frac{p_0 R^2}{Et} \frac{4(kL)^4}{a^4 + 4(kL)^4} \left[\frac{F_{10}}{F_1} \sin a - \frac{a}{kL} \left(\frac{F_5}{F_1} + \frac{F_8}{F_1} \cos a \right) \right]$ | $-\frac{p_0 R^2}{Et} \frac{4(kL)^4}{a^4 + 4(kL)^4} \left[\frac{2F_8}{F_1} \sin a - \frac{a}{kL} \left(\frac{F_4}{F_1} + \frac{F_9}{F_1} \cos a \right) \right]$ |
| | $a < kL$ | 0 | $-\frac{p_0 R^2}{Et} \left[\frac{F_{10}}{F_1} \sin a - \frac{a}{kL} \left(\frac{F_6}{F_1} + \frac{F_8}{F_1} \cos a \right) \right]$ | $-\frac{p_0 R^2}{Et} \left[\frac{F_{10}}{F_1} \sin a - \frac{a}{kL} \left(\frac{F_5}{F_1} + \frac{F_8}{F_1} \cos a \right) \right]$ |

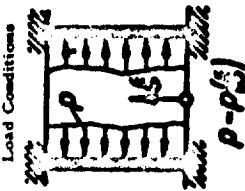
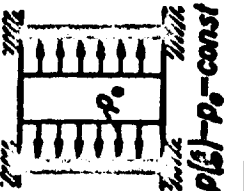
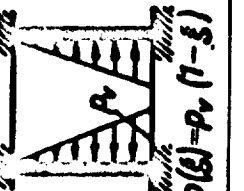
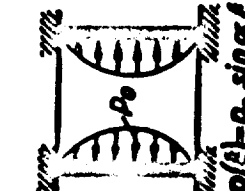
¹For F and k factors, see paragraph 2.42.6

TABLE 2.42-6. (CONT)

| Load Condition | S_1 | | S_2 | | S_3 | | S_4 | |
|---|----------|--|--|--|--|--|--|--|
|  | | | | | | | | |
|  $p(\xi) = P_0 \cos \alpha \xi$ | $a < kL$ | $-\frac{P_0 R^2}{Et} \frac{4(kL)^4}{\alpha^4 + 4(kL)^4}$ | $-\frac{P_0 R^2}{Et} \frac{4(kL)^4}{\alpha^4 + 4(kL)^4}$ | $\left(\frac{F_3}{F_1} - \frac{F_{10}}{F_1} \cos \alpha \right.$ $\left. - \frac{\alpha}{kL} \frac{F_8}{F_1} \sin \alpha \right)$ | $+\frac{P_0 R^2}{Et} \frac{4(kL)^4}{\alpha^4 + 4(kL)^4}$ | $\left(\frac{F_3}{F_1} - \frac{F_{10}}{F_1} \cos \alpha \right.$ $\left. - \frac{\alpha}{kL} \frac{F_8}{F_1} \sin \alpha \right)$ | $+\frac{P_0 R^2}{Et} \frac{4(kL)^4}{\alpha^4 + 4(kL)^4}$ | $\left(\frac{F_2}{F_1} - \frac{2F_8}{F_1} \cos \alpha \right.$ $\left. - \frac{\alpha}{kL} \frac{F_9}{F_1} \sin \alpha \right)$ |
|  $p(\xi) = P_0 \cos \alpha \xi$ | $a < kL$ | $-\frac{P_0 R^2}{Et}$ | $-\frac{P_0 R^2}{Et} \left(\frac{F_3}{F_1} - \frac{F_{10}}{F_1} \cos \alpha \right.$ $\left. - \frac{\alpha}{kL} \frac{F_8}{F_1} \sin \alpha \right)$ | $+\frac{P_0 R^2}{Et} \left(\frac{F_3}{F_1} - \frac{F_{10}}{F_1} \cos \alpha \right.$ $\left. - \frac{\alpha}{kL} \frac{F_8}{F_1} \sin \alpha \right)$ | $+\frac{P_0 R^2}{Et} \left(\frac{F_2}{F_1} - \frac{2F_8}{F_1} \cos \alpha \right.$ $\left. - \frac{\alpha}{kL} \frac{F_9}{F_1} \sin \alpha \right)$ | | | |
|  $p(\xi) = P_0 \exp(-\alpha \xi)$ | $a < kL$ | $-\frac{P_0 R^2}{Et} \frac{4(kL)^4}{\alpha^4 + 4(kL)^4}$ | $-\frac{P_0 R^2}{Et} \frac{4(kL)^4}{\alpha^4 + 4(kL)^4}$ | $\left[\frac{F_3}{F_1} - \frac{F_{10}}{F_1} \exp(-\alpha) \right.$ $\left. - \frac{\alpha}{kL} \left(\frac{F_6}{F_1} + \frac{F_8}{F_1} \exp(-\alpha) \right) \right]$ | $+\frac{P_0 R^2}{Et} \frac{4(kL)^4}{\alpha^4 + 4(kL)^4}$ | $\left[\frac{F_3}{F_1} - \frac{F_{10}}{F_1} \exp(-\alpha) \right.$ $\left. - \frac{\alpha}{kL} \left(\frac{F_3}{F_1} + \frac{F_8}{F_1} \exp(-\alpha) \right) \right]$ | $+\frac{P_0 R^2}{Et} \frac{4(kL)^4}{\alpha^4 + 4(kL)^4}$ | $\left[\frac{F_2}{F_1} - \frac{2F_8}{F_1} \exp(-\alpha) \right.$ $\left. - \frac{\alpha}{kL} \left(\frac{F_4}{F_1} + \frac{F_9}{F_1} \exp(-\alpha) \right) \right]$ |
|  $p(\xi) = P_0 \exp(-\alpha \xi)$ | $a < kL$ | $-\frac{P_0 R^2}{Et}$ | $-\frac{P_0 R^2}{Et} \left[\frac{F_3}{F_1} - \frac{F_{10}}{F_1} \exp(-\alpha) \right.$ $\left. - \frac{\alpha}{kL} \left(\frac{F_6}{F_1} + \frac{F_8}{F_1} \exp(-\alpha) \right) \right]$ | $+\frac{P_0 R^2}{Et} \left[\frac{F_3}{F_1} - \frac{F_{10}}{F_1} \exp(-\alpha) \right.$ $\left. - \frac{\alpha}{kL} \left(\frac{F_3}{F_1} + \frac{F_8}{F_1} \exp(-\alpha) \right) \right]$ | $+\frac{P_0 R^2}{Et} \left[\frac{F_2}{F_1} - \frac{2F_8}{F_1} \exp(-\alpha) \right.$ $\left. - \frac{\alpha}{kL} \left(\frac{F_4}{F_1} + \frac{F_9}{F_1} \exp(-\alpha) \right) \right]$ | | | |

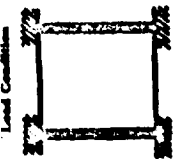
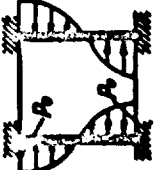
¹For F and k factors, see paragraph 2.42.6

TABLE 2.42-7. S_1 -COEFFICIENTS, $kL \geq 4.0$ (REF. 2-2)¹

| Load Conditions | S_1 | S_2 | S_3 | S_4 |
|---|------------------------------|--|---|-------|
|  $P - P_0$ | $-\frac{P_0 R^2}{E\epsilon}$ | $\frac{P_0 R^2}{E\epsilon} \left(\frac{F_5 - 1}{F_4} + \frac{F_{13}}{F_4} \right)$ | $\frac{P_0 R^2}{E\epsilon} \left(\frac{F_6 + 1}{F_4} - \frac{F_{14}}{F_4} \right)$ | 0 |
|  $P(\xi) - P_0 - \text{const}$ | $-\frac{P_0 R^2}{E\epsilon}$ | $\frac{P_0 R^2}{E\epsilon} \left(\frac{F_5 - 1}{F_4} + \frac{1}{kL} \frac{F_{16}}{F_4} \right)$ | $\frac{P_0 R^2}{E\epsilon} \left(\frac{F_6 + 1}{F_4} - \frac{1}{kL} \frac{F_{15}}{F_4} \right)$ | 0 |
|  $P(\xi) - P_0 (\eta - \xi)$ | 0 | $\frac{P_0 R^2}{E\epsilon} \frac{4(kL)^4}{\epsilon^4 + 4(kL)^4} \left(\frac{F_{13} \sin \epsilon}{F_4} - \frac{F_{16}}{kL} \frac{\cos \epsilon}{F_4} \right)$ | $-\frac{P_0 R^2}{E\epsilon} \frac{4(kL)^4}{\epsilon^4 + 4(kL)^4} \left(\frac{F_{14} \sin \epsilon}{F_4} - \frac{F_{15}}{kL} \frac{\cos \epsilon}{F_4} \right)$ | 0 |
|  $P(\xi) - P_0 \sin \epsilon \xi$ | 0 | $-\frac{P_0 R^2}{E\epsilon} \left(\frac{F_{13} \sin \epsilon}{F_4} - \frac{F_{16}}{kL} \frac{\cos \epsilon}{F_4} \right)$ | $-\frac{P_0 R^2}{E\epsilon} \left(\frac{F_{14} \sin \epsilon}{F_4} - \frac{F_{15}}{kL} \frac{\cos \epsilon}{F_4} \right)$ | 0 |


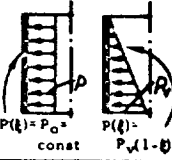
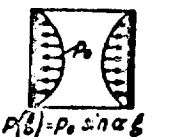
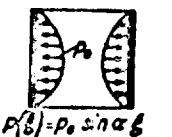
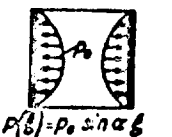


¹For F and k factors, see paragraph 2.42.6

TABLE 2. 42-7 (CONT)

| Load Condition | θ_1 | θ_2 | θ_3 | θ_4 |
|---|--|--|---|--|
|  $P(t) = P_0 \cos \omega t$ | $-\frac{P_0 R^2}{EI} \frac{4(NL)^4}{\omega^4 + 4(NL)^2}$ | $\frac{P_0 R^2}{EI} \frac{4(NL)^4}{\omega^4 + 4(NL)^2} \left[\frac{F_5 - 1}{F_4} + \frac{F_{13}}{F_4} \cos \omega t + \frac{\omega}{kL} \left(\frac{F_{16} \sin \omega t}{F_4} - \frac{\omega}{2kL} \frac{F_6 \cos \omega t}{F_4} \right) \right]$ | $\frac{P_0 R^2}{EI} \frac{4(NL)^4}{\omega^4 + 4(NL)^2} \left[\frac{F_6 + 1}{F_4} - \frac{F_{13}}{kL} \frac{\sin \omega t}{F_4} - \frac{\omega}{2kL} \left(\frac{F_{15}}{F_4} \cos \omega t + \frac{F_5}{F_4} \right) \right]$ | $\frac{P_0 R^2}{EI} \frac{\omega^2}{2(NL)^2} \frac{4(NL)^4}{\omega^4 + 4(NL)^2} \cos \omega t$ |
| | $-\frac{P_0 R^2}{EI}$ | $\frac{P_0 R^2}{EI} \left[\frac{F_5 - 1}{F_4} + \frac{F_{13}}{F_4} \cos \omega t + \frac{\omega}{kL} \left(\frac{F_{16} \sin \omega t}{F_4} - \frac{\omega}{2kL} \frac{F_6 \cos \omega t}{F_4} \right) \right]$ | $\frac{P_0 R^2}{EI} \left[\frac{F_6 + 1}{F_4} - \frac{F_{13}}{kL} \frac{\sin \omega t}{F_4} - \frac{\omega}{2kL} \left(\frac{F_{15}}{F_4} \cos \omega t + \frac{F_5}{F_4} \right) \right]$ | $\frac{P_0 R^2}{EI} \frac{\omega^2}{2(NL)^2} \cos \omega t$ |
|  $P(t) = P_0 \cos \omega t$ | $-\frac{P_0 R^2}{EI} \frac{4(NL)^4}{\omega^4 + 4(NL)^2}$ | $\frac{P_0 R^2}{EI} \frac{4(NL)^4}{\omega^4 + 4(NL)^2} \left[\frac{F_5 - 1}{F_4} + \frac{F_{13}}{F_4} \exp(-\omega t) + \frac{\omega}{kL} \left(\frac{F_{16} \exp(-\omega t)}{F_4} + \frac{\omega}{2kL} \frac{F_6}{F_4} \right) \right]$ | $\frac{P_0 R^2}{EI} \frac{4(NL)^4}{\omega^4 + 4(NL)^2} \left[\frac{F_6 + 1}{F_4} - \frac{F_{13}}{kL} \exp(-\omega t) - \frac{\omega}{2kL} \left(\frac{F_{15}}{F_4} \exp(-\omega t) + \frac{F_5}{F_4} \right) \right]$ | $-\frac{P_0 R^2}{EI} \frac{\omega^2}{2(NL)^2} \frac{4(NL)^4}{\omega^4 + 4(NL)^2}$ |
| | $-\frac{P_0 R^2}{EI}$ | $\frac{P_0 R^2}{EI} \left[\frac{F_5 - 1}{F_4} + \frac{F_{13}}{F_4} \exp(-\omega t) + \frac{\omega}{kL} \left(\frac{F_{16} \exp(-\omega t)}{F_4} + \frac{\omega}{2kL} \frac{F_6}{F_4} \right) \right]$ | $\frac{P_0 R^2}{EI} \left[\frac{F_6 + 1}{F_4} - \frac{F_{13}}{kL} \exp(-\omega t) - \frac{\omega}{2kL} \left(\frac{F_{15}}{F_4} \exp(-\omega t) + \frac{F_5}{F_4} \right) \right]$ | $-\frac{P_0 R^2}{EI} \frac{\omega^2}{2(NL)^2}$ |



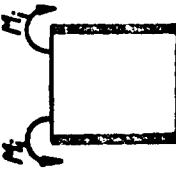

For F and k factors, see paragraph 2. 42. 6

TABLE 2.42-8. S_i —COEFFICIENTS, $kL < 4.0$ (Ref. 2-2)

| Load Condition | S_1 | S_2 | S_3 | S_4 |
|--|---|---|---|---|
|  <p>$p = p(s)$</p> | | | | |
|  <p>$P(s) = P_0 = \text{const}$</p>  <p>$P(s) = P_0 \sin \alpha s$</p> | | | | |
|  <p>$P(s) = P_0 \sin \alpha s$</p> | $\frac{P_0 R^2}{Et} \frac{\alpha^2}{2 (kL)^2} \frac{4 (kL)^4}{\alpha^4 + 4 (kL)^4}$ $\left(\frac{\alpha}{kL} \frac{F_2}{F_1} - \frac{2F_8}{F_1} \sin \alpha \right)$ $+ \frac{\alpha}{kL} \frac{F_9}{F_1} \cos \alpha$ | $\frac{P_0 R^2}{Et} \frac{\alpha^2}{2 (kL)^2} \frac{4 (kL)^4}{\alpha^4 + 4 (kL)^4}$ $\left(\frac{\alpha}{kL} \frac{F_3}{F_1} - \frac{F_{10}}{F_1} \sin \alpha \right)$ $+ \frac{\alpha}{kL} \frac{F_8}{F_1} \cos \alpha$ | $\frac{P_0 R^2}{Et} \frac{\alpha^2}{2 (kL)^2} \frac{4 (kL)^4}{\alpha^4 + 4 (kL)^4}$ $\left(\frac{\alpha}{kL} \frac{F_6}{F_1} - \frac{F_{10}}{F_1} \sin \alpha \right)$ $+ \frac{\alpha}{kL} \frac{F_8}{F_1} \cos \alpha$ | |
|  <p>$P(s) = P_0 \sin \alpha s$</p> | $\frac{P_0 R^2}{Et} \frac{\alpha^2}{2 (kL)^2} \left(\frac{\alpha}{kL} \frac{F_4}{F_1} \right)$ $- \frac{2F_8}{F_1} \sin \alpha + \frac{\alpha}{kL} \frac{F_9}{F_1} \cos \alpha$ | $\frac{P_0 R^2}{Et} \frac{\alpha^2}{2 (kL)^2} \left(\frac{\alpha}{kL} \frac{F_5}{F_1} \right)$ $- \frac{F_{10}}{F_1} \sin \alpha + \frac{\alpha}{kL} \frac{F_8}{F_1} \cos \alpha$ | $\frac{P_0 R^2}{Et} \frac{\alpha^2}{2 (kL)^2} \left(\frac{\alpha}{kL} \frac{F_6}{F_1} \right)$ $- \frac{F_{10}}{F_1} \sin \alpha + \frac{\alpha}{kL} \frac{F_8}{F_1} \cos \alpha$ | |
|  <p>$P(s) = P_0 \cos \alpha s$</p> | $\frac{P_0 R^2}{Et} \frac{\alpha^2}{2 (kL)^2} \frac{4 (kL)^4}{\alpha^4 + 4 (kL)^4}$ $\left(\frac{F_2}{F_1} - \frac{2F_8}{F_1} \cos \alpha \right)$ $+ \frac{\alpha}{kL} \frac{F_9}{F_1} \sin \alpha$ | $\frac{P_0 R^2}{Et} \frac{\alpha^2}{2 (kL)^2} \frac{4 (kL)^4}{\alpha^4 + 4 (kL)^4}$ $\left(\frac{F_3}{F_1} - \frac{F_{10}}{F_1} \cos \alpha \right)$ $+ \frac{\alpha}{kL} \frac{F_8}{F_1} \sin \alpha$ | $\frac{P_0 R^2}{Et} \frac{\alpha^2}{2 (kL)^2} \frac{4 (kL)^4}{\alpha^4 + 4 (kL)^4}$ $\left(\frac{F_6}{F_1} - \frac{F_{10}}{F_1} \cos \alpha \right)$ $+ \frac{\alpha}{kL} \frac{F_8}{F_1} \sin \alpha$ | $\frac{P_0 R^2}{Et} \frac{\alpha^2}{2 (kL)^2} \frac{4 (kL)^4}{\alpha^4 + 4 (kL)^4}$ |
|  <p>$P(s) = P_0 \cos \alpha s$</p> | $\frac{P_0 R^2}{Et} \frac{\alpha^2}{2 (kL)^2} \left(\frac{F_4}{F_1} \right)$ $- \frac{2F_8}{F_1} \cos \alpha + \frac{\alpha}{kL} \frac{F_9}{F_1} \sin \alpha$ | $\frac{P_0 R^2}{Et} \frac{\alpha^2}{2 (kL)^2} \left(\frac{F_5}{F_1} \right)$ $- \frac{F_{10}}{F_1} \cos \alpha + \frac{\alpha}{kL} \frac{F_8}{F_1} \sin \alpha$ | $\frac{P_0 R^2}{Et} \frac{\alpha^2}{2 (kL)^2} \left(\frac{F_6}{F_1} \right)$ $- \frac{F_{10}}{F_1} \cos \alpha + \frac{\alpha}{kL} \frac{F_8}{F_1} \sin \alpha$ | $\frac{P_0 R^2}{Et} \frac{\alpha^2}{2 (kL)^2}$ |

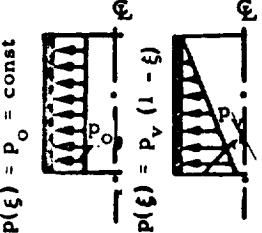
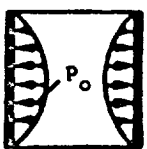
¹For F and k factors, see paragraph 2.42.6

TABLE 2.42-8. (CONT)¹

| Load Condition | S_1 | S_2 | S_3 | S_4 |
|--|--|--|--|---|
|  | $-\frac{P_0 R^2 \sigma^2}{E t} \frac{4 (kL)^4}{2 (kL)^2 \sigma^4 + 4 (kL)^4}$ $\left[\frac{F_2}{F_1} - \frac{\sigma}{kL} \frac{F_4}{F_1} - \left(\frac{2F_8}{F_1} \right) \right]$ $+ \left(\frac{F_9}{kL} \frac{F_1}{F_1} \right) \exp(-\sigma)$ | $+\frac{P_0 R^2 \sigma^2}{E t} \frac{4 (kL)^4}{2 (kL)^2 \sigma^4 + 4 (kL)^4}$ $\left[\frac{F_3}{F_1} - \frac{\sigma}{kL} \frac{F_5}{F_1} \right]$ $- \left(\frac{F_{10}}{F_1} + \frac{\sigma}{kL} \frac{F_6}{F_1} \right) \exp(-\sigma)$ | $+\frac{P_0 R^2 \sigma^2}{E t} \frac{4 (kL)^4}{2 (kL)^2 \sigma^4 + 4 (kL)^4}$ $\left[\frac{F_3}{F_1} - \frac{\sigma}{kL} \frac{F_6}{F_1} \right]$ $- \left(\frac{F_{10}}{F_1} + \frac{\sigma}{kL} \frac{F_6}{F_1} \right) \exp(-\sigma)$ | $-\frac{P_0 R^2 \sigma^2}{E t} \frac{4 (kL)^4}{2 (kL)^2 \sigma^4 + 4 (kL)^4}$ |
|  $p(x) = p_0 \exp(-x/b)$ | $-\frac{P_0 R^2 \sigma^2}{E t} \frac{4 (kL)^4}{2 (kL)^2 \sigma^4 + 4 (kL)^4} \left[\frac{F_2}{F_1} - \frac{\sigma}{kL} \frac{F_4}{F_1} - \left(\frac{2F_8}{F_1} \right) \right]$ $+ \left(\frac{F_9}{kL} \frac{F_1}{F_1} \right) \exp(-\sigma)$ | $+\frac{P_0 R^2 \sigma^2}{E t} \frac{4 (kL)^4}{2 (kL)^2 \sigma^4 + 4 (kL)^4} \left[\frac{F_3}{F_1} - \frac{\sigma}{kL} \frac{F_5}{F_1} \right]$ $- \left(\frac{F_{10}}{F_1} + \frac{\sigma}{kL} \frac{F_6}{F_1} \right) \exp(-\sigma)$ | $+\frac{P_0 R^2 \sigma^2}{E t} \frac{4 (kL)^4}{2 (kL)^2 \sigma^4 + 4 (kL)^4} \left[\frac{F_3}{F_1} - \frac{\sigma}{kL} \frac{F_6}{F_1} \right]$ $- \left(\frac{F_{10}}{F_1} + \frac{\sigma}{kL} \frac{F_6}{F_1} \right) \exp(-\sigma)$ | $-\frac{P_0 R^2 \sigma^2}{E t} \frac{4 (kL)^4}{2 (kL)^2 \sigma^4 + 4 (kL)^4}$ |
|  | $-\frac{M_1 R^2}{E t} \frac{2 k^2}{2 k} \frac{2 F_8}{F_1}$ | $+\frac{M_1 R^2}{E t} \frac{2 k^2}{2 k} \frac{2 F_{10}}{F_1}$ | $+\frac{M_1 R^2}{E t} \frac{2 k^2}{2 k} \frac{2 F_{10}}{F_1}$ | 0 |
|  | $-\frac{Q_L R^2}{E t} \frac{F_9}{2 k} \frac{F_1}{F_1}$ | $+\frac{Q_L R^2}{E t} \frac{F_8}{2 k} \frac{F_1}{F_1}$ | $+\frac{Q_L R^2}{E t} \frac{2 k} {2 k} \frac{F_8}{F_1}$ | 0 |

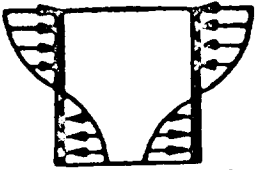
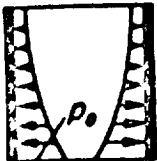
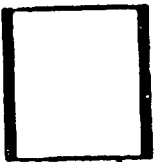
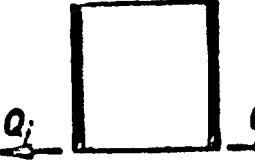
¹For F and k factors, see paragraph 2.42.6

TABLE 2.42-9. S_1 AND S_2 COEFFICIENTS $kL > 4.0$ (Ref. 2-2)¹

| Load Condition | S_1 | S_2 |
|---|---|-------|
|  <p>$p(\xi) = p_0 = \text{const}$</p> <p>$p(\xi) = p_v(1 - \xi)$</p> <p>Symmetrical About Centerline</p> | 0 | 0 |
|  <p>$p(\xi) = p_0 \sin \alpha \xi$</p> | $+ \frac{p_0 R^2}{Et} \frac{4 (kL)^4}{\alpha^4 + 4 (kL)^4} \frac{\alpha^3}{2 (kL)^3}$ | 0 |
| | $\alpha < kL$ $+ \frac{p_0 R^2}{Et} \frac{\alpha^3}{2 (kL)^3}$ | 0 |

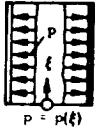
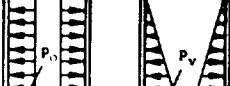

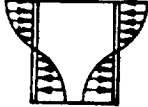
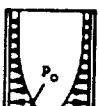
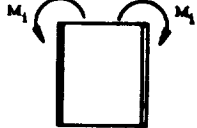
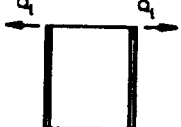
¹For k factors, see paragraph 2.42.6

TABLE 2.42-9 (CONT)¹

| Load Condition | S ₁ | | S ₂ |
|--|----------------|--|---|
|  <p>$p(\xi) = p_0 \cos \alpha \xi$</p> | | $+ \frac{p_0 R^2}{Et} \frac{4 (kL)^4}{\alpha^4 + 4 (kL)^4} \frac{\alpha^2}{2 (kL)^2}$ | $- \frac{p_0 R^2}{Et} \frac{4 (kL)^4}{\alpha^4 + 4 (kL)^4} \frac{\alpha^2}{2 (kL)^2}$ |
| | $\alpha < kL$ | $+ \frac{p_0 R^2}{Et} \frac{\alpha^2}{2 (kL)^2}$ | $- \frac{p_0 R^2}{Et} \frac{\alpha^2}{2 (kL)^2}$ |
|  <p>$p(\xi) = p_0 \exp(-\alpha \xi)$</p> | | $- \frac{p_0 R^2}{Et} \frac{4 (kL)^4}{\alpha^4 + 4 (kL)^4} \frac{\alpha^2}{2 (kL)^2} \left(1 - \frac{\alpha}{kL}\right)$ | $+ \frac{p_0 R^2}{Et} \frac{4 (kL)^4}{\alpha^4 + 4 (kL)^4} \frac{\alpha^2}{2 (kL)^2}$ |
| | $\alpha < kL$ | $- \frac{p_0 R^2}{Et} \frac{\alpha^2}{2 (kL)^2} \left(1 - \frac{\alpha}{kL}\right)$ | $+ \frac{p_0 R^2}{Et} \frac{\alpha^2}{2 (kL)^2}$ |
|  <p>M_i</p> | | $- \frac{M_i R^2}{Et} 2 k^2$ | $+ \frac{M_i R^2}{Et} 2 k^2$ |
|  <p>q_i</p> | | $+ \frac{Q_i R^2}{Et} 2 k$ | <p>0</p> |

¹For k factors, see paragraph 2.42.6

TABLE 2.42-9 (CONT)¹

| LOAD CONDITION  $P = P(\xi)$ | \bar{S}_1 | \bar{S}_2 |
|--|--|--|
|  $P(\xi) = P_0 = \text{const}$ $P(\xi) = P_v(1-\xi)$ | 0 | 0 |
|  $P(\xi) = P_0 \sin \alpha \xi$ | $\sigma < kL$ $+ \frac{P_0 R^2}{Et} \frac{\sigma^2}{2(kL)^2} \frac{4(kL)^4}{\sigma^4 + 4(kL)^4}$ $\left(\sin \sigma - \frac{\sigma}{kL} \cos \sigma \right)$ | $- \frac{P_0 R^2}{Et} \frac{\sigma^2}{2(kL)^2}$ $\frac{4(kL)^4}{\sigma^4 + 4(kL)^4} \sin \sigma$ |
|  $P(\xi) = P_0 \cos \alpha \xi$ | $\sigma < kL$ $+ \frac{P_0 R^2}{Et} \frac{\sigma^2}{2(kL)^2}$ $\left(\cos \sigma + \frac{\sigma}{kL} \sin \sigma \right)$ | $- \frac{P_0 R^2}{Et} \frac{\sigma^2}{2(kL)^2}$ $\frac{4(kL)^4}{\sigma^4 + 4(kL)^4} \cos \sigma$ |
|  $P(\xi) = P_0 \exp(-\alpha \xi)$ | $\sigma < kL$ $- \frac{P_0 R^2}{Et} \frac{\sigma^2}{2(kL)^2} \frac{4(kL)^4}{\sigma^4 + 4(kL)^4}$ $\left(1 + \frac{\sigma}{kL} \right) \exp(-\sigma)$ | $+ \frac{P_0 R^2}{Et} \frac{\sigma^2}{2(kL)^2}$ $\frac{4(kL)^4}{\sigma^4 + 4(kL)^4} \exp(-\sigma)$ |
|  | $+ 2k^2 \frac{M_1 R^2}{Et}$ | $- 2k^2 \frac{M_1 R^2}{Et}$ |
|  | $+ 2k \frac{Q_1 R^2}{Et}$ | 0 |

¹For k factors, see paragraph 2.42.6

2.42.4 Analysis of Cylinders with Rotationally Symmetric Discontinuities
in Geometry or Loading.

Rotationally symmetric discontinuities are of special importance, especially if they are located not far from the edges of the cylinder. As before, the tables are prepared for many possible discontinuity types (Ref. 2-2).

Assume that (i) represents the place where discontinuities will occur. Fig. 2.42-1 shows the designations and the system of coordinates which will be used.

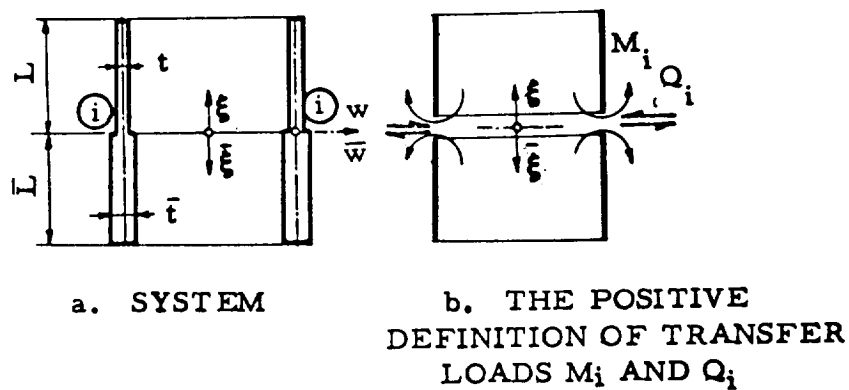


FIG. 2.42-1. Cylinders with Discontinuities

The imaginary cut at (i) is introduced, and an attempt is made to determine discontinuity loads M_i and Q_i . This is a usual problem of interaction and it will be solved as such; the following formulas will be obtained:

$$M_i = \frac{2Dk}{\phi} \left(k\phi_{M_2} \Delta w_p + \phi_{M_1} \Delta w'_p \right)$$

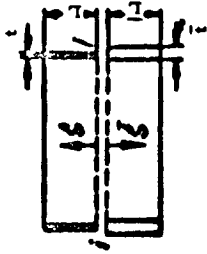
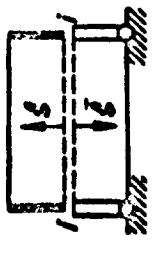
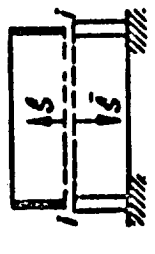
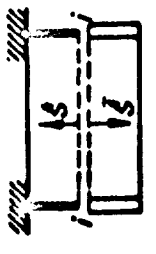
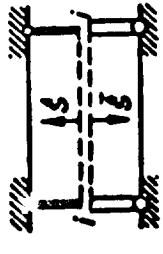
$$Q_i = \frac{2Dk^2}{\phi} \left(k\phi_{Q_2} \Delta w_p + \phi_{M_2} \Delta w'_p \right)$$

where

$$\phi = \phi_{M_2}^2 - \phi_{M_1} \phi_{Q_2}$$

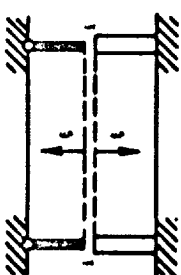
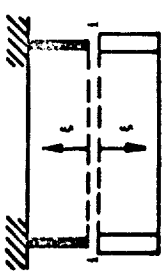
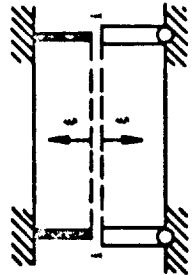
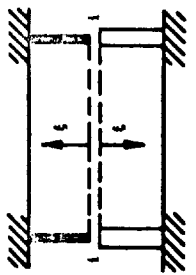
The values $\phi_{M, Q}$ are given in the Table 2.42-10. Some special cases of discontinuity loads M_1 and Q_1 are presented in the Table 2.42-11.

TABLE 2.42-10. ϕ FUNCTIONS (Ref. 2-2)¹

| Shell Geometry | ϕ_{M_1} | ϕ_{M_2} | ϕ_{a_2} |
|---|--|--|---|
|  | $\frac{F_4}{F_1} + \left(\frac{t}{T}\right)^{3/2} \frac{\bar{F}_4}{F_1}$ | $\frac{F_2}{F_1} - \left(\frac{t}{T}\right)^2 \frac{\bar{F}_2}{F_1}$ | $2 \left[\frac{F_3}{F_1} + \left(\frac{t}{T}\right)^{5/2} \frac{\bar{F}_3}{F_1} \right]$ |
|  | $\frac{F_4}{F_1} + \left(\frac{t}{T}\right)^{3/2} \frac{\bar{F}_2}{F_4}$ | $\frac{F_2}{F_1} - \left(\frac{t}{T}\right)^2 \frac{\bar{F}_3}{F_4}$ | $2 \left[\frac{F_3}{F_1} + \left(\frac{t}{T}\right)^{5/2} \frac{\bar{F}_{1+1}}{F_4} \right]$ |
|  | $\frac{F_4}{F_1} + \left(\frac{t}{T}\right)^{3/2} \frac{\bar{F}_4}{F_1 + 2}$ | $\frac{F_2}{F_1} - \left(\frac{t}{T}\right)^2 \frac{\bar{F}_2}{F_1 + 2}$ | $2 \left[\frac{F_3}{F_1} + \left(\frac{t}{T}\right)^{5/2} \frac{\bar{F}_3}{F_1 + 2} \right]$ |
|  | $\frac{F_2}{F_4} + \left(\frac{t}{T}\right)^{3/2} \frac{\bar{F}_4}{F_1}$ | $\frac{F_3}{F_4} - \left(\frac{t}{T}\right)^2 \frac{\bar{F}_1}{F_1}$ | $2 \left[\frac{F_{1+1}}{F_4} + \left(\frac{t}{T}\right)^{5/2} \frac{\bar{F}_3}{F_1} \right]$ |
|  | $\frac{F_2}{F_4} + \left(\frac{t}{T}\right)^{3/2} \frac{\bar{F}_2}{F_4}$ | $\frac{F_3}{F_4} - \left(\frac{t}{T}\right)^2 \frac{\bar{F}_3}{F_4}$ | $2 \left[\frac{F_{1+1}}{F_4} + \left(\frac{t}{T}\right)^{5/2} \frac{\bar{F}_{1+1}}{F_4} \right]$ |


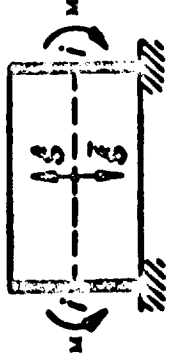
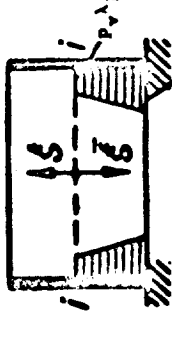
¹For F factors, see paragraph 2.42.6

TABLE 2.42-10 (CONT)

| Shell Geometry | ϕ_{M_1} | $\phi_{Q_1} = \phi_{M_2}$ | ϕ_{Q_2} |
|---|--|--|---|
|  | $\frac{F_2}{F_4} + \left(\frac{t}{T}\right)^{3/2} \frac{F_4}{F_1+2}$ | $\frac{F_3}{F_4} - \left(\frac{t}{T}\right)^2 \frac{F_2}{F_1+2}$ | $2 \left[\frac{F_1+1}{F_4} + \left(\frac{t}{T}\right)^{5/2} \frac{F_3}{F_1+2} \right]$ |
|  | $\frac{F_4}{F_1+2} + \left(\frac{t}{T}\right)^{3/2} \frac{F_4}{F_1}$ | $\frac{F_2}{F_1+2} - \left(\frac{t}{T}\right)^2 \frac{F_3}{F_4}$ | $2 \left[\frac{F_3}{F_1+2} + \left(\frac{t}{T}\right)^{5/2} \frac{F_3}{F_1} \right]$ |
|  | $\frac{F_4}{F_1+2} + \left(\frac{t}{T}\right)^{3/2} \frac{F_2}{F_4}$ | $\frac{F_2}{F_1+2} - \left(\frac{t}{T}\right)^2 \frac{F_3}{F_4}$ | $2 \left[\frac{F_3}{F_1+2} + \left(\frac{t}{T}\right)^{5/2} \frac{F_3}{F_1+2} \right]$ |
|  | $\frac{F_4}{F_1+2} + \left(\frac{t}{T}\right)^{3/2} \frac{F_4}{F_1+2}$ | $\frac{F_2}{F_1+2} - \left(\frac{t}{T}\right)^2 \frac{F_2}{F_1+2}$ | $2 \left[\frac{F_3}{F_1+2} + \left(\frac{t}{T}\right)^{5/2} \frac{F_1+1}{F_4+2} \right]$ |

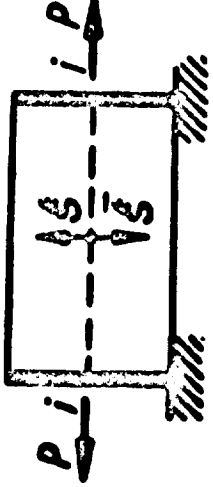
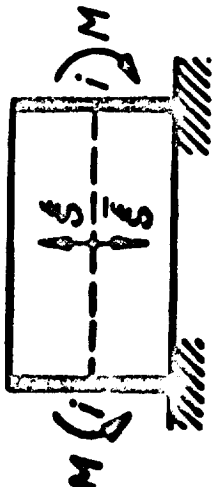

For F factors, see paragraph 2.42.6

TABLE 2.42-11 DETERMINATION OF M_i and Q_i (REF. 2-2)¹

| Load Condition | M_i | Q_i |
|---|--|--|
|  | $+\frac{P}{k\phi} \left(\phi_{M2} \frac{\bar{F}_4}{\bar{F}_1+2} + \phi_{M1} \frac{\bar{F}_2}{\bar{F}_1+2} \right)$ | $+\frac{P}{\phi} \left(\phi_{Q2} \frac{\bar{F}_4}{\bar{F}_1+2} + \phi_{M2} \frac{\bar{F}_2}{\bar{F}_1+2} \right)$ |
|  | $+\frac{M}{\phi} \left(\phi_{M2} \frac{\bar{F}_2}{\bar{F}_1+2} + \phi_{M1} \frac{2\bar{F}_3}{\bar{F}_1+2} \right)$ | $+\frac{Mk}{\phi} \left(\phi_{Q2} \frac{\bar{F}_2}{\bar{F}_1+2} + \phi_{M1} \frac{2\bar{F}_3}{\bar{F}_1+2} \right)$ |
|  | $+\frac{P_v}{\phi 2k2} \left\{ \phi_{M2} \left[\lambda_p - \frac{2\bar{F}_7}{\bar{F}_1+2} (\lambda_p+1) + \frac{1}{kL} \frac{\bar{F}_{10}}{\bar{F}_1+2} \right] \right. \\ \left. + \phi_{M1} \left[\frac{\bar{F}_9}{\bar{F}_1+2} (\lambda_p+2) - \frac{1}{kL} \left(1 - \frac{2\bar{F}_7}{\bar{F}_1+2} \right) \right] \right\}$ | $+\frac{P_v}{\phi 2k2} \left\{ \phi_{Q2} \left[\lambda_p - \frac{2\bar{F}_7}{\bar{F}_1+2} (\lambda_p+1) + \frac{1}{kL} \frac{\bar{F}_{10}}{\bar{F}_1+2} \right] \right. \\ \left. + \phi_{M2} \left[\frac{\bar{F}_9}{\bar{F}_1+2} (\lambda_p+2) - \frac{1}{kL} \left(1 - \frac{2\bar{F}_7}{\bar{F}_1+2} \right) \right] \right\}$ |

¹For F and k factors, see paragraph 2.42.6
 For λ_p coefficient, see paragraph 2.32.6(a)

TABLE 2.42-11 (CONT)¹

| Load Condition | M_i | Q_i |
|---|---|---|
|  | $+\frac{P}{\phi k} \left(\phi_{M2} \frac{\bar{F}_2}{\bar{F}_4} + \phi_{M1} \frac{\bar{F}_3}{\bar{F}_4} \right)$ | $+\frac{P}{\phi} \left(\phi_{Q2} \frac{\bar{F}_2}{\bar{F}_4} + \phi_{M2} \frac{\bar{F}_3}{\bar{F}_4} \right)$ |
|  | $+\frac{M}{\phi} \left(\phi_{M2} \frac{\bar{F}_3}{\bar{F}_4} + \phi_{M1} \frac{\bar{F}_1 + 1}{\bar{F}_4} \right)$ | $+\frac{M\bar{k}}{\phi} \left(\phi_{Q2} \frac{\bar{F}_3}{\bar{F}_4} + \phi_{M2} \frac{\bar{F}_1 + 1}{\bar{F}_4} \right)$ |
|  | $+\frac{P_v}{\phi 2k^2} \left\{ \phi_{M2} \left[\lambda_p + \frac{\bar{F}_1}{\bar{F}_4} (\lambda_p + 1) \right] + \phi_{M1} \left[\frac{2\bar{F}_8}{\bar{F}_4} (\lambda_p + 1) - \frac{1}{kL} \right] \right\}$ | $+\frac{P_v}{\phi 2k} \left\{ \phi_{Q2} \left[\lambda_p + \frac{\bar{F}_9}{\bar{F}_4} (\lambda_p + 1) \right] + \phi_{M2} \left[\frac{2\bar{F}_8}{\bar{F}_4} (\lambda_p + 1) - \frac{1}{kL} \right] \right\}$ |

¹For F and k factors, see paragraph 2.42.6
 For λ_p coefficient, see paragraph 2.32.6(a)

2.42.5 Spherical Shell, Any Fixity at the Lower Boundary

General formulas for open or closed spherical shells are presented herein in the same manner as for the cylindrical shell. The boundary conditions along the lower edge can be assumed to be "fixed" or "pinned." The formulas are dependent upon certain factors, S_i , that are the functions of integration constants, C , that appeared by derivation of formulas (bending theory). For the "fixed" lower boundary

$$S_1 = -\frac{Et}{2Rk} \left(\frac{\Delta r_m}{\sin \phi_1} \frac{2F_3}{F_1+2} + \beta_m \frac{R}{k} \frac{F_2}{F_1+2} \right)$$

$$S_2 = -\frac{Et}{1Rk} \left(\frac{\Delta r_m}{\sin \phi_1} 2 \frac{F_5-1}{F_1+2} + \beta_m \frac{R}{k} \frac{F_4}{F_1+2} \right)$$

$$S_3 = \frac{Et}{2Rk} \left(\frac{\Delta r_m}{\sin \phi_1} 2 \frac{F_6+1}{F_1+2} + \beta_m \frac{R}{k} \frac{F_4}{F_1+2} \right)$$

$$S_4 = \frac{Et}{2Rk} \beta_m \frac{R}{k}$$

where k and F are factors as shown in Paragraph 2.42.6.

For the special case of "closed" spherical shells, the only constants needed are:

$$S_1 = -\frac{Et}{2k} \left(\beta_m + \frac{\Delta r_m}{\sin \phi_1} \frac{2k}{R} \right)$$

$$S_2 = -\frac{Et}{2k^2} \beta_m$$

In the preceding formulas Δr_m is the radial movement of the membrane and β_m is the angle or rotation of the membrane.

For the "pinned" lower boundary

$$S_1 = -\frac{\Delta r_m Et F_1}{2 \sin \phi_1 R k F_4}$$

$$S_2 = \frac{\Delta r_m Et}{2 \sin \phi_1 R k}$$

$$S_3 = \frac{\Delta r_m Et}{2 \sin \phi_1 R k}$$

$$S_4 = \frac{\Delta r_m Et}{2 \sin \phi_1 R k} \frac{F_2}{F_4}$$

For the special case of the "closed" spherical shell, the only constants needed are

$$S_1 = -\frac{\Delta r_m Et}{2 \sin \phi_1 R k}$$

$$S_2 = \frac{\Delta r_m Et}{2 \sin \phi_1 R k}$$

With these indications the general formulas can be given.

A. General Case of Open Spherical Shell, Any Boundary at Lower Edge

Longitudinal Load:

$$N_{\phi} = N_{\phi\text{membr}} + \cot \phi \left[S_1 F_7(a) + S_2 F_{15}(a) + S_3 F_{16}(a) + S_4 F_8(a) \right]$$

Circumferential Load:

$$N_{\theta} = N_{\theta\text{membr}} - k \left[-S_1 F_9(a) + S_2 F_{14}(a) + S_3 F_{13}(a) + S_4 F_{10}(a) \right]$$

Shear:

$$Q_{\phi} = S_1 F_7(a) + S_2 F_{15}(a) + S_3 F_{16}(a) + S_4 F_8(a)$$

Moment M_{ϕ} :

$$M_{\phi} = -\frac{R}{2k} \left[-S_1 F_{10}(a) + S_2 F_{13}(a) - S_3 F_{14}(a) - S_4 F_9(a) \right]$$

Moment M_{θ} :

$$M_{\theta} = \mu \frac{R}{2k} \left[-S_1 F_{10}(a) + S_2 F_{13}(a) - S_3 F_{14}(a) - S_4 F_9(a) \right]$$

Deformations:

Horizontal Movements:

$$\Delta r = \frac{Rk}{Et} \sin \phi \left[-S_1 F_9(a) + S_2 F_{14}(a) + S_3 F_{13}(a) + S_4 F_{10}(a) \right]$$

Rotation of Meridian:

$$\beta = -\frac{2k^2}{Et} \left[-S_1 F_8(a) + S_2 F_{16}(a) - S_3 F_{15}(a) + S_4 F_7(a) \right]$$

B. General Case of Closed Spherical Shell, Any Boundaries at Lower Edge

Longitudinal Load:

$$N_\phi = N_{\phi\text{memb}} + \cot \phi \left[S_1 F_{17}(a) + S_2 F_{18}(a) \right]$$

Circumferential Load:

$$N_\theta = N_{\theta\text{memb}} + k \left[S_1 F_{19}(a) - S_2 F_{20}(a) \right]$$

Shear:

$$Q_\phi = S_1 F_{17}(a) + S_2 F_{18}(a)$$

Moment M_ϕ :

$$M_\phi = \frac{-R}{2k} \left[S_1 F_{20}(\alpha) + S_2 F_{19}(\alpha) \right]$$

Moment M_θ :

$$M_\theta = -\frac{R}{2k} \left[-S_1 \left(\frac{\cot \phi}{k} F_{18}(\alpha) - \mu F_{20}(\alpha) \right) + S_2 \left(\frac{\cot \phi}{k} F_{17}(\alpha) + \mu F_{19}(\alpha) \right) \right]$$

Deformations:

Horizontal Displacement:

$$\Delta r = \frac{Rk}{Et} \sin \phi \left[S_1 F_{19}(\alpha) - S_2 F_{20}(\alpha) \right]$$

Rotation of the Tangent of the Meridian:

$$\beta = -\frac{2k^2}{Et} \left[S_1 F_{18}(\alpha) - S_2 F_{17}(\alpha) \right]$$

2.42.6 Definition of F-Factors

The general solution of the homogeneous differential equation,

$$w'''' + 4k^4 w = 0$$

can be represented with the following combination of trigonometrical and hyperbolic functions:

$$\begin{array}{ll} \cosh kL\xi \cos kL\xi & \sinh kL\xi \cos kL\xi \\ \cosh kL\xi \sin kL\xi & \sinh kL\xi \sin kL\xi \end{array}$$

where kL is a dimensionless parameter and ξ is a dimensionless ordinate. Figs. 2.42-2 through 2.42-4 present the F -factors that simplify the analysis. As a special parameter for determining the F -factors, η is considered as follows

$$F = F(\eta) \quad \text{i. e., } F_1 = \sinh^2 \eta + \sin^2 \eta$$

For a cylindrical shell

$$\eta = kL \quad \text{or} \quad \eta = kL\xi \quad \text{and} \quad k = \frac{\sqrt[4]{3(1-\mu^2)}}{\sqrt{Rt}}$$

For a conical shell

$$\eta = kL \quad \text{or} \quad \eta = kL\xi \quad \text{and} \quad k = \frac{\sqrt[4]{3(1-\mu^2)}}{\sqrt{tx_m \cot \alpha_0}}$$

For a spherical shell

$$\eta = k \text{ for } F_i; \quad \eta = k\alpha \text{ for } F_i(\alpha); \quad \text{and} \quad k = \sqrt[4]{3(1-\mu^2) \left(\frac{R}{t}\right)^2}$$

Definition of the F-factors is given in Table 2.42-12. If the required accuracy is high, it is suggested that the F values be calculated as presented in Table 2.42-12. If the required values are estimated and extreme accuracy is not required, the graphs in Figs. 2.42-2 through 2.42-4 should be used. These graphs also present the values F_i .

TABLE 2.42-12. $F_i(\xi)$ AND F_i FACTORS, (Ref. 2-2)

| i | $F_i(\xi)$ | F_i |
|----|---|---------------------------------------|
| 1 | $\sinh^2 kL\xi - \sin^2 kL\xi$ | $\sinh^2 kL - \sin^2 kL$ |
| 2 | $\sinh^2 kL\xi + \sin^2 kL\xi$ | $\sinh^2 kL + \sin^2 kL$ |
| 3 | $\sinh kL\xi \cosh kL\xi + \sin kL\xi \cos kL\xi$ | $\sinh kL \cosh kL + \sin kL \cos kL$ |
| 4 | $\sinh kL\xi \cosh kL\xi - \sin kL\xi \cos kL\xi$ | $\sinh kL \cosh kL - \sin kL \cos kL$ |
| 5 | $\sin^2 kL\xi$ | $\sin^2 kL$ |
| 6 | $\sinh^2 kL\xi$ | $\sinh^2 kL$ |
| 7 | $\cosh kL\xi \cos kL\xi$ | $\cosh kL \cos kL$ |
| 8 | $\sinh kL\xi \sin kL\xi$ | $\sinh kL \sin kL$ |
| 9 | $\cosh kL\xi \sin kL\xi - \sinh kL\xi \cos kL\xi$ | $\cosh kL \sin kL - \sinh kL \cos kL$ |
| 10 | $\cosh kL\xi \sin kL\xi + \sinh kL\xi \cos kL\xi$ | $\cosh kL \sin kL + \sinh kL \cos kL$ |
| 11 | $\sin kL\xi \cos kL\xi$ | $\sin kL \cos kL$ |
| 12 | $\sinh kL\xi \cosh kL\xi$ | $\sinh kL \cosh kL$ |
| 13 | $\cosh kL\xi \cos kL\xi - \sinh kL\xi \sin kL\xi$ | $\cosh kL \cos kL - \sinh kL \sin kL$ |
| 14 | $\cosh kL\xi \cos kL\xi + \sinh kL\xi \sin kL\xi$ | $\cosh kL \cos kL + \sinh kL \sin kL$ |
| 15 | $\cosh kL\xi \sin kL\xi$ | $\cosh kL \sin kL$ |
| 16 | $\sinh kL\xi \cos kL\xi$ | $\sinh kL \cos kL$ |
| 17 | $\exp(-kL\xi \cos kL\xi)$ | $\exp(-kL \cos kL)$ |
| 18 | $\exp(-kL\xi \sin kL\xi)$ | $\exp(-kL \sin kL)$ |
| 19 | $\exp[-kL\xi (\cos kL\xi + \sin kL\xi)]$ | $\exp[-kL (\cos kL + \sin kL)]$ |
| 20 | $\exp[-kL\xi (\cos kL\xi - \sin kL\xi)]$ | $\exp[-kL (\cos kL - \sin kL)]$ |

FIG. 2.42-2. F_i FACTORS ($i = 1, 2, 3, 4, 6, 12$)
(SHEET 1 OF 3)

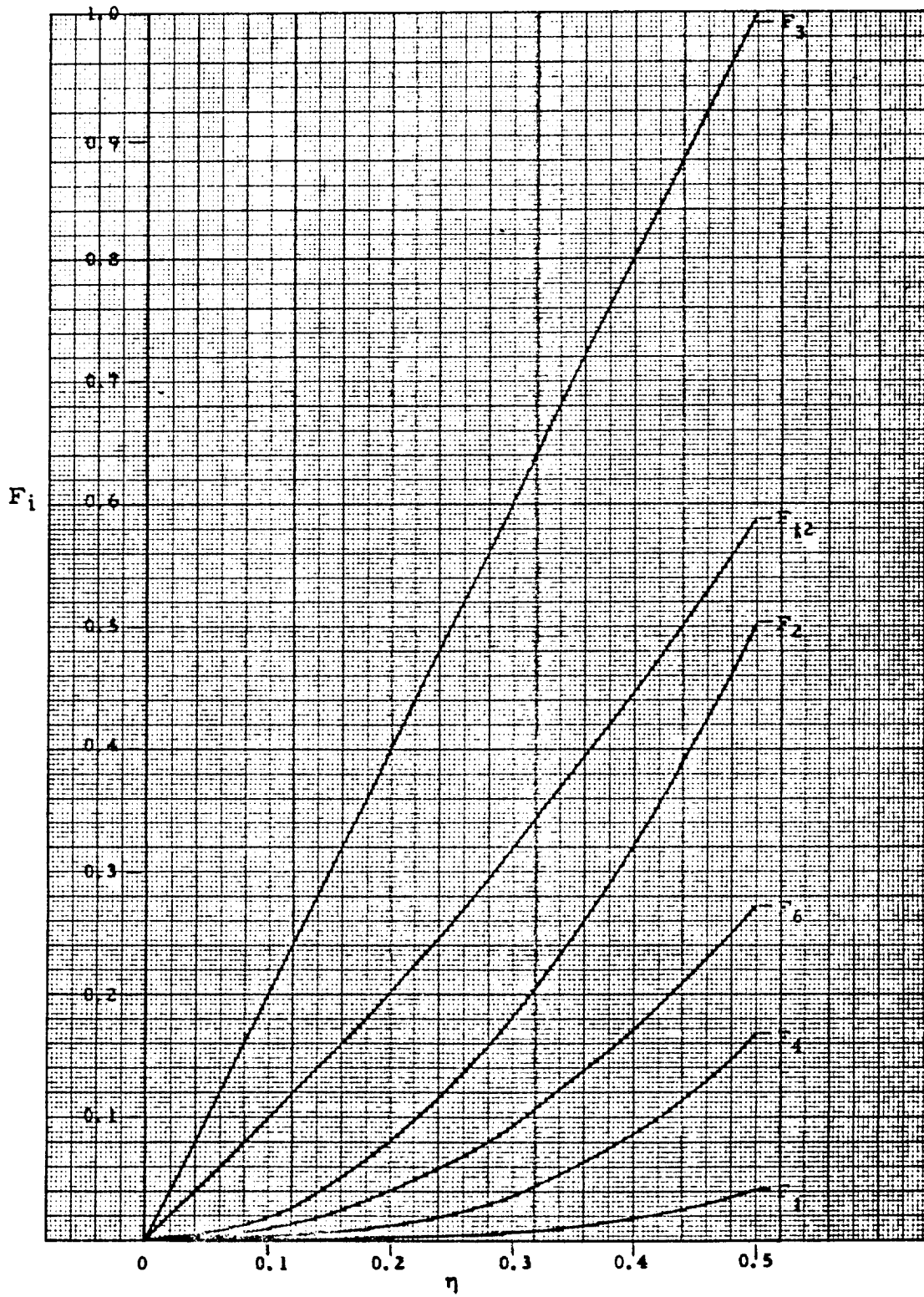


FIG. 2.42-2. (SHEET 2 OF 3)

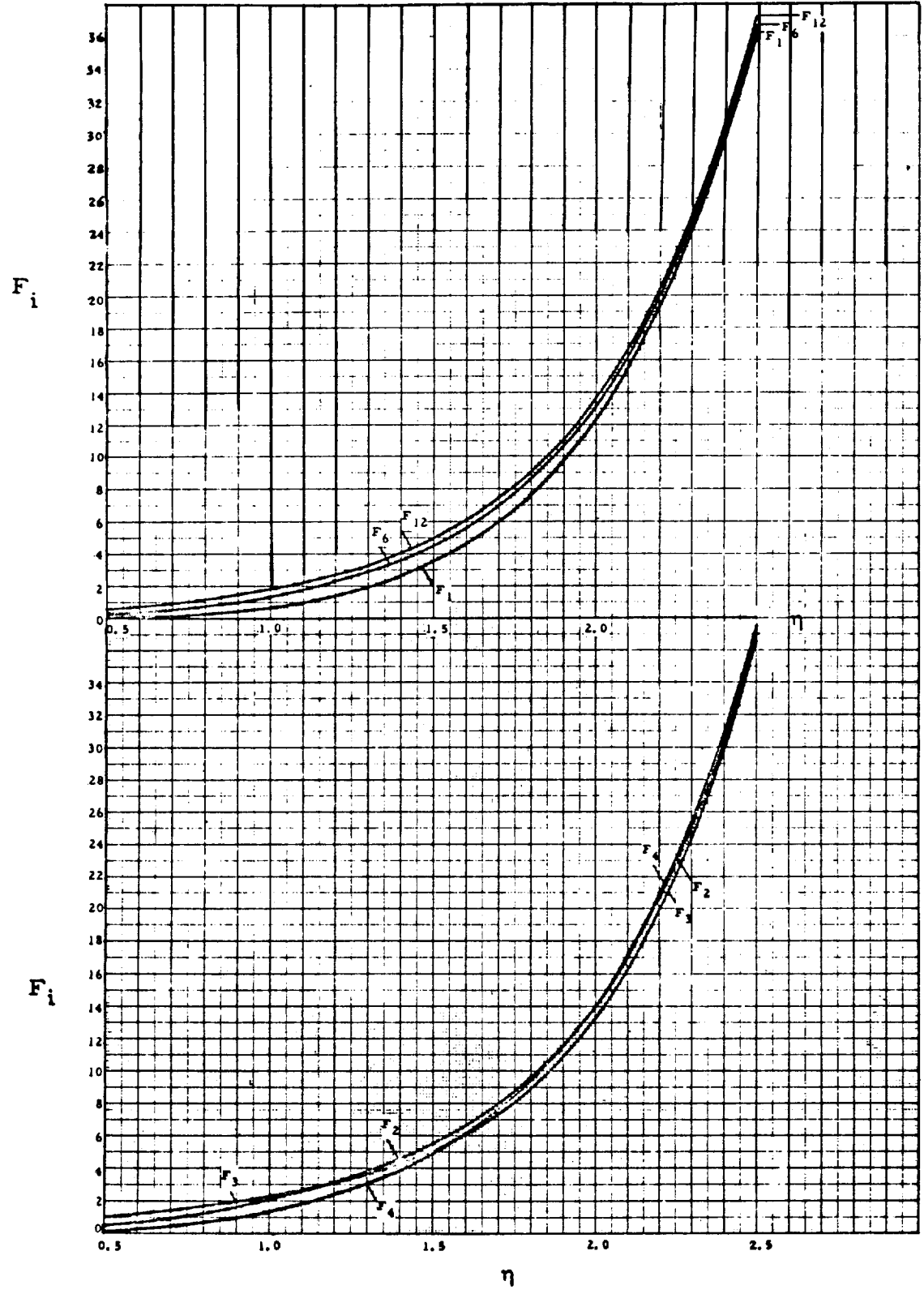


FIG. 2.42-2. (SHEET 3 OF 3)

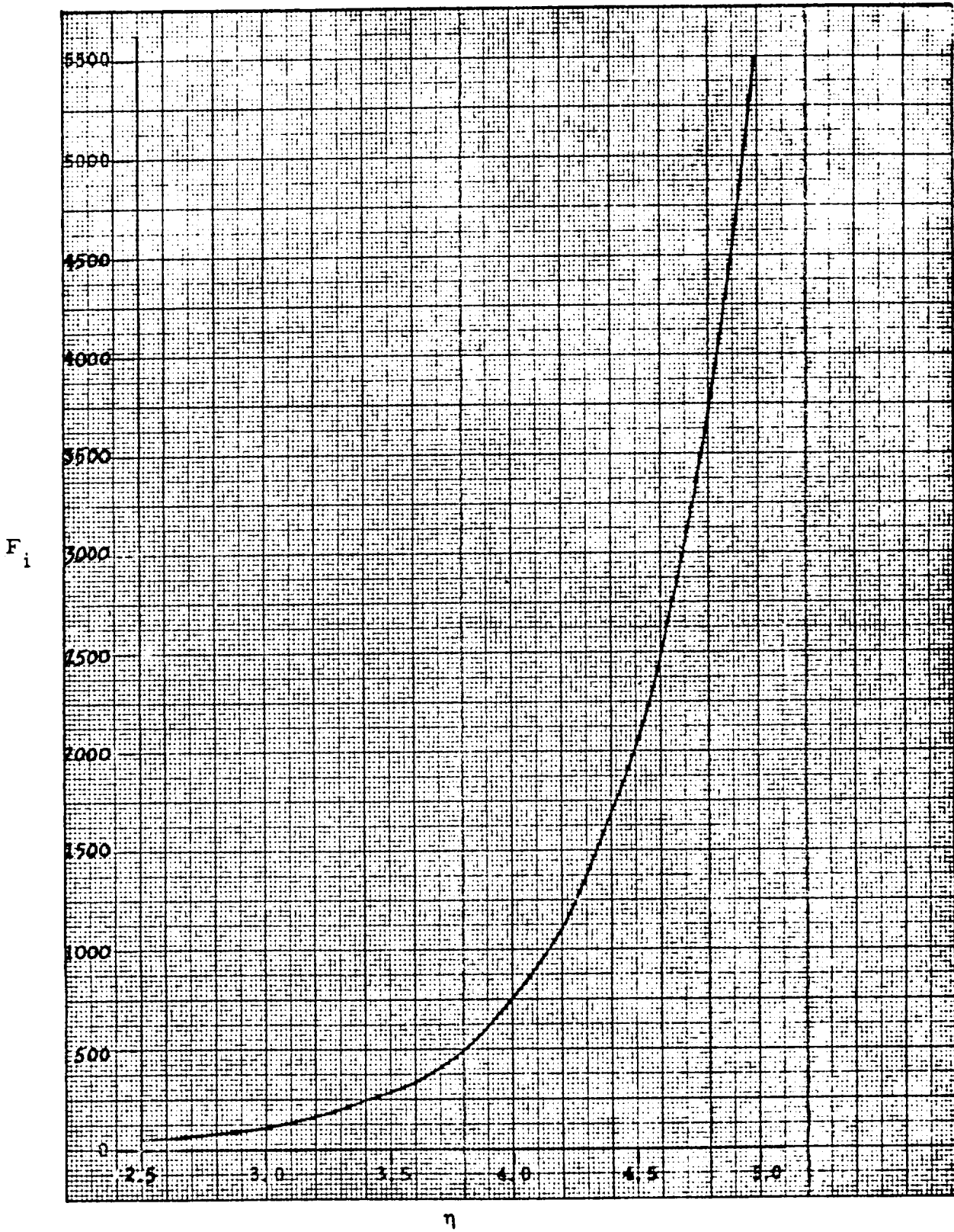


FIG. 2.42-3. F_i FACTORS ($i = 7, 8, 9, 10, 13, 14, 15, 16$)
(SHEET 1 OF 3)

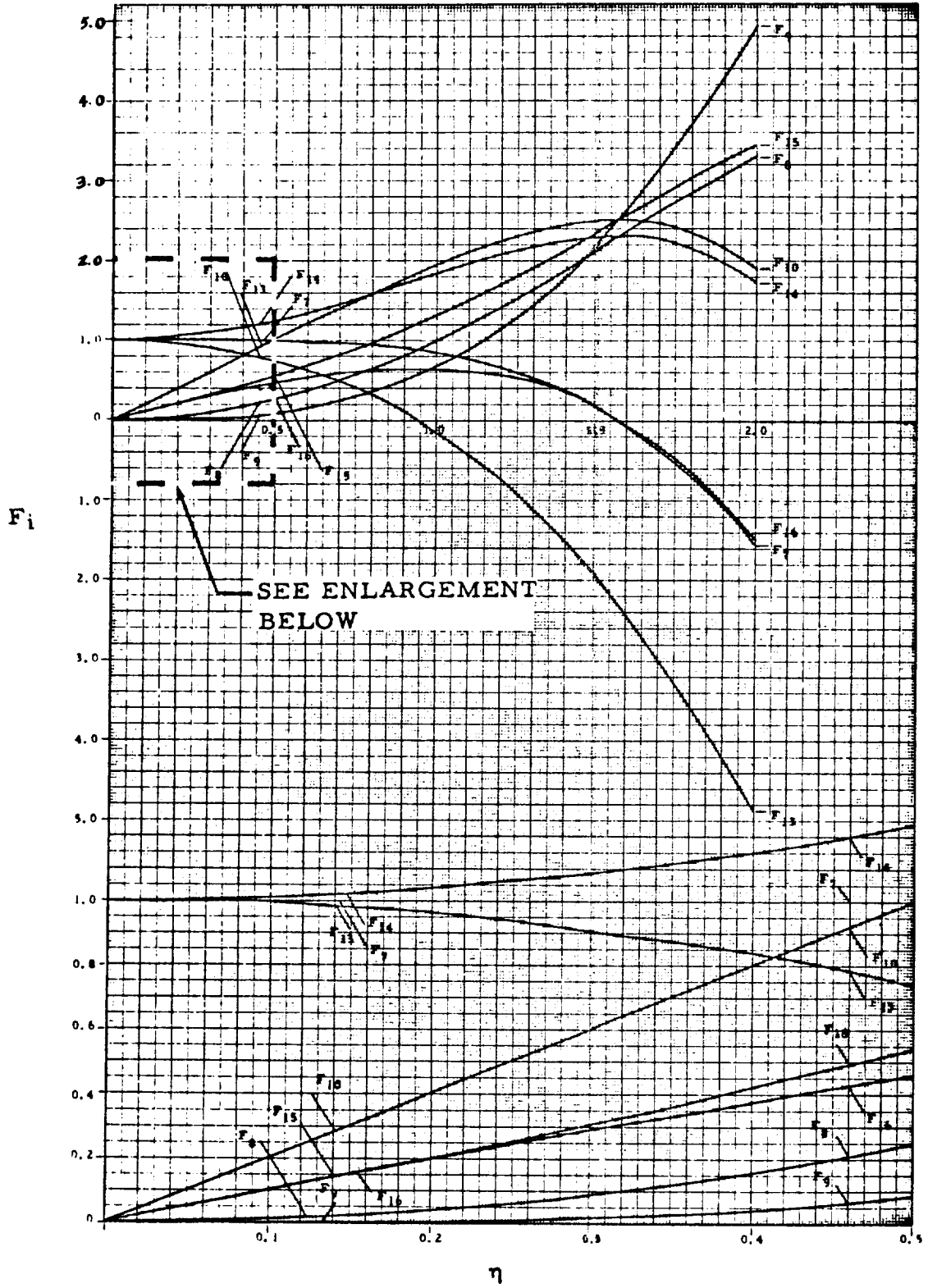
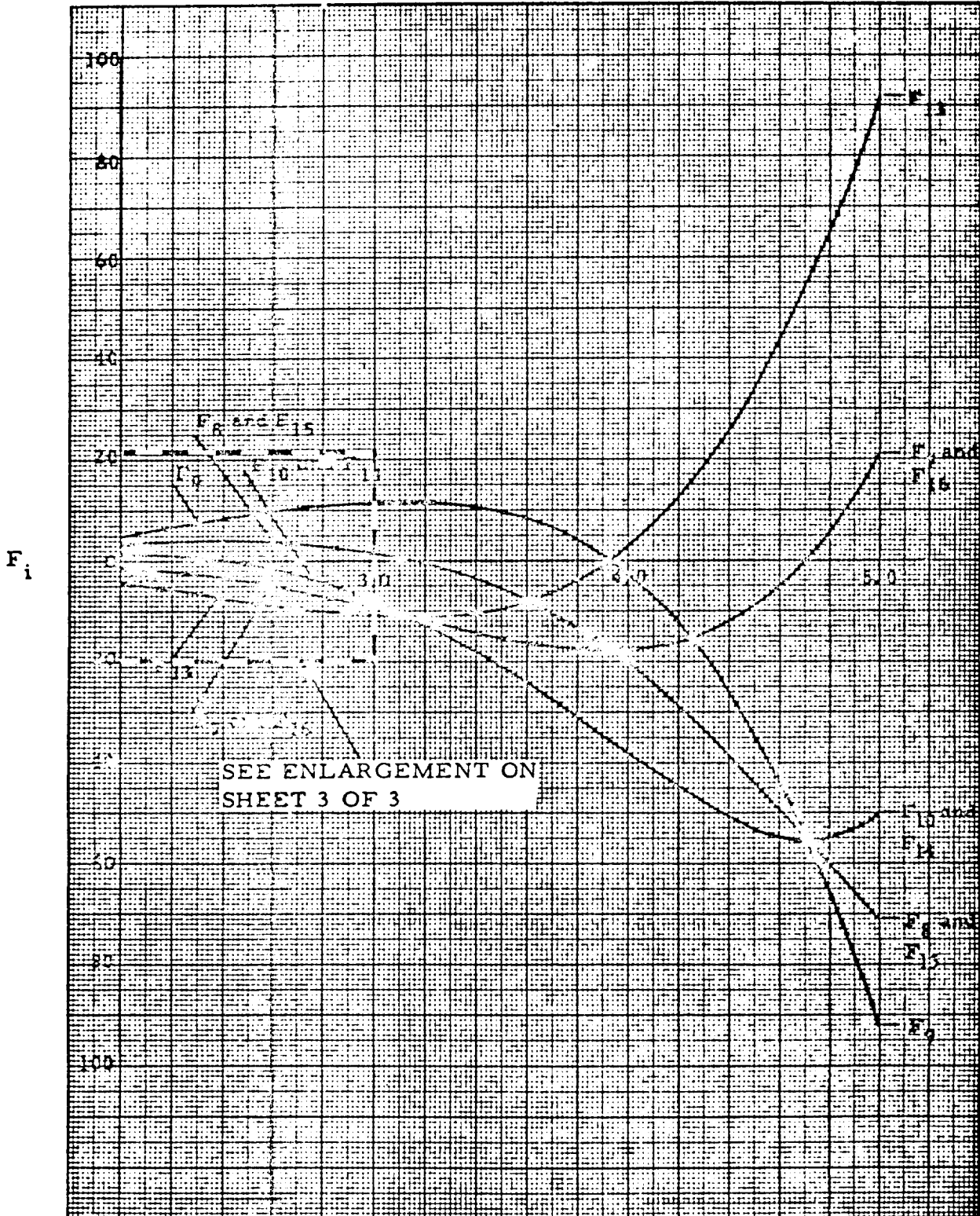


FIG. 2.42-3. (SHEET 2 OF 3)



η

FIG. 2.42-3. (SHEET 3 OF 3)

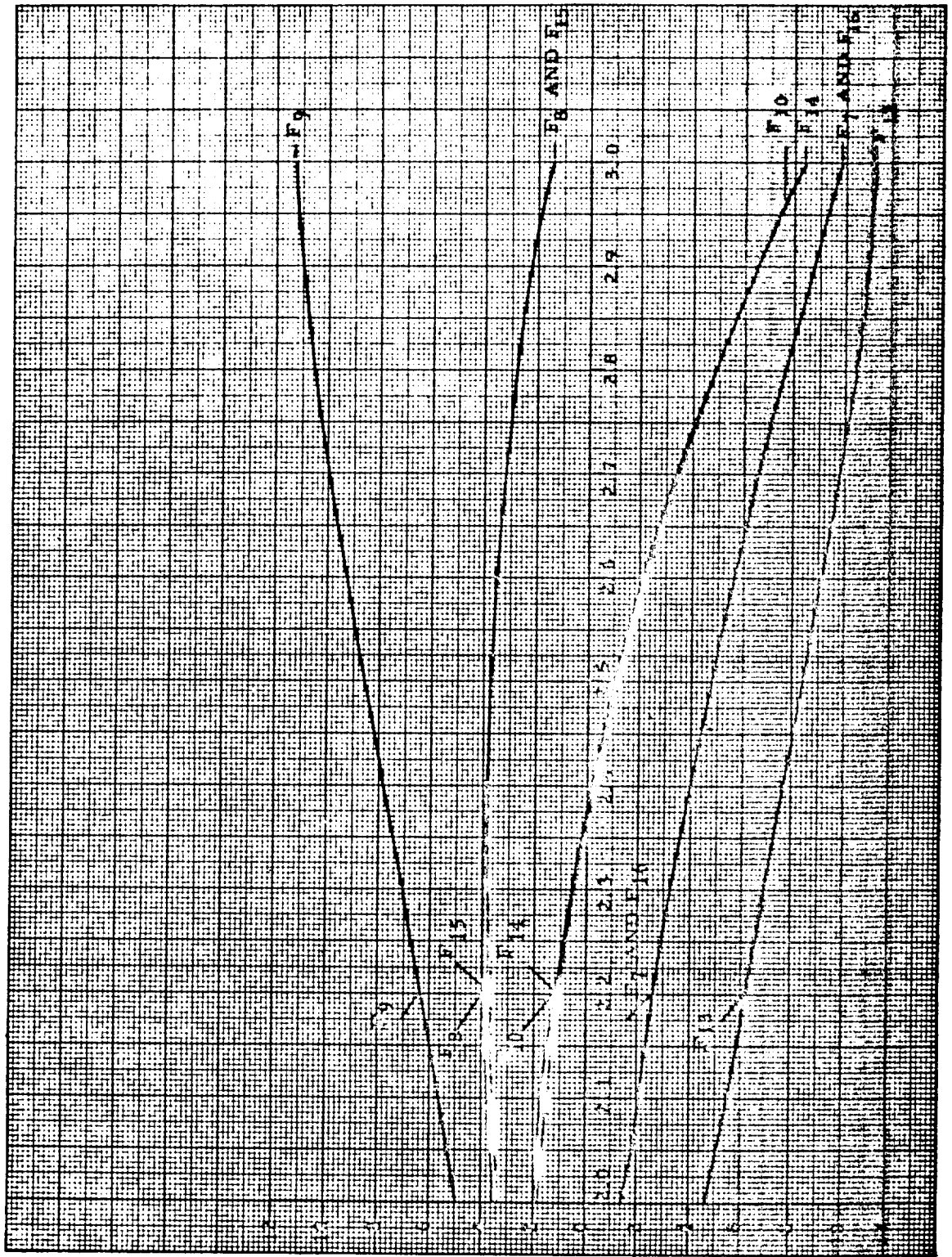


FIG. 2.42-4. F_i FACTORS ($i = 5, 11, 17, 18, 19, 20$)
 (SHEET 1 OF 2)

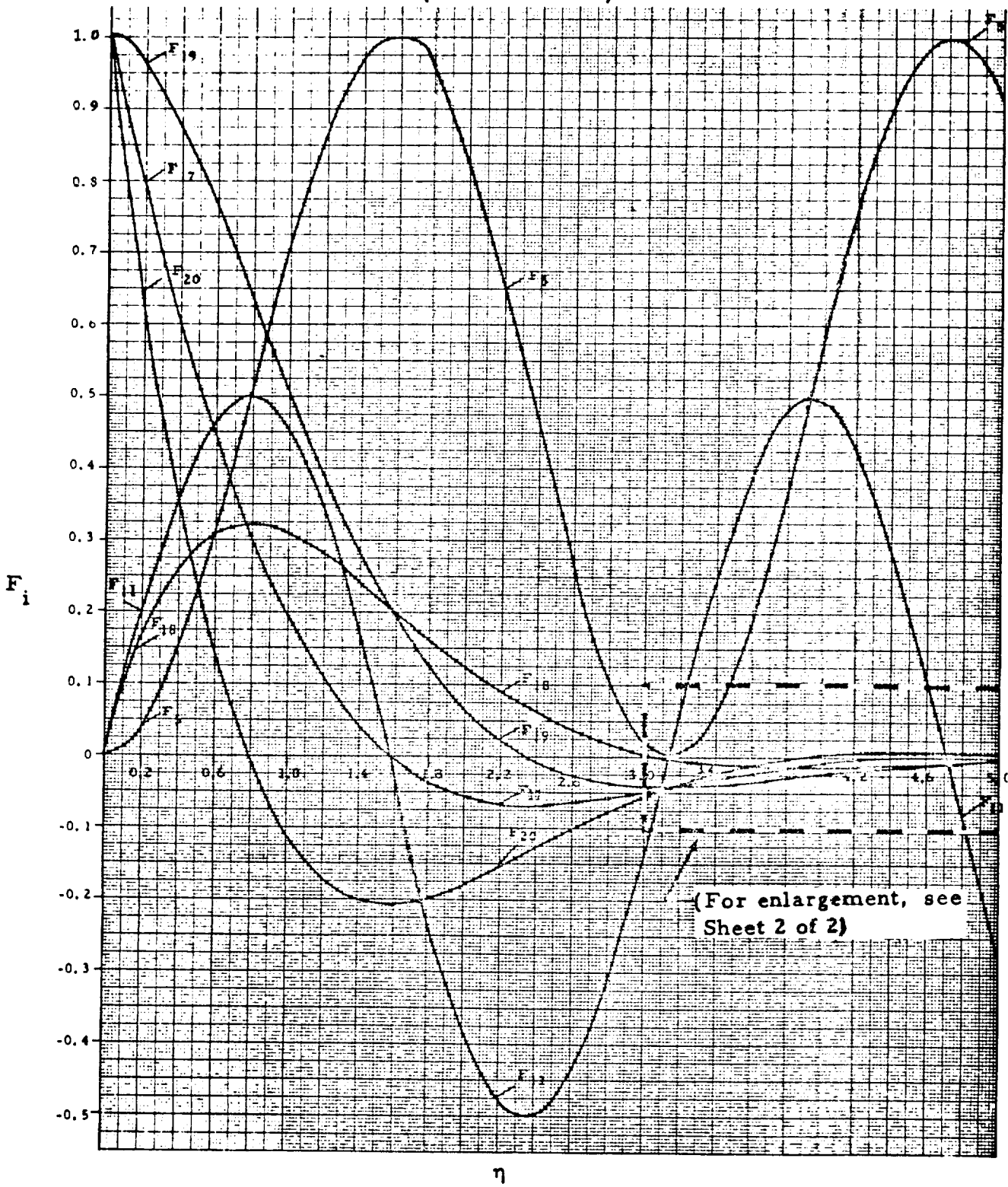
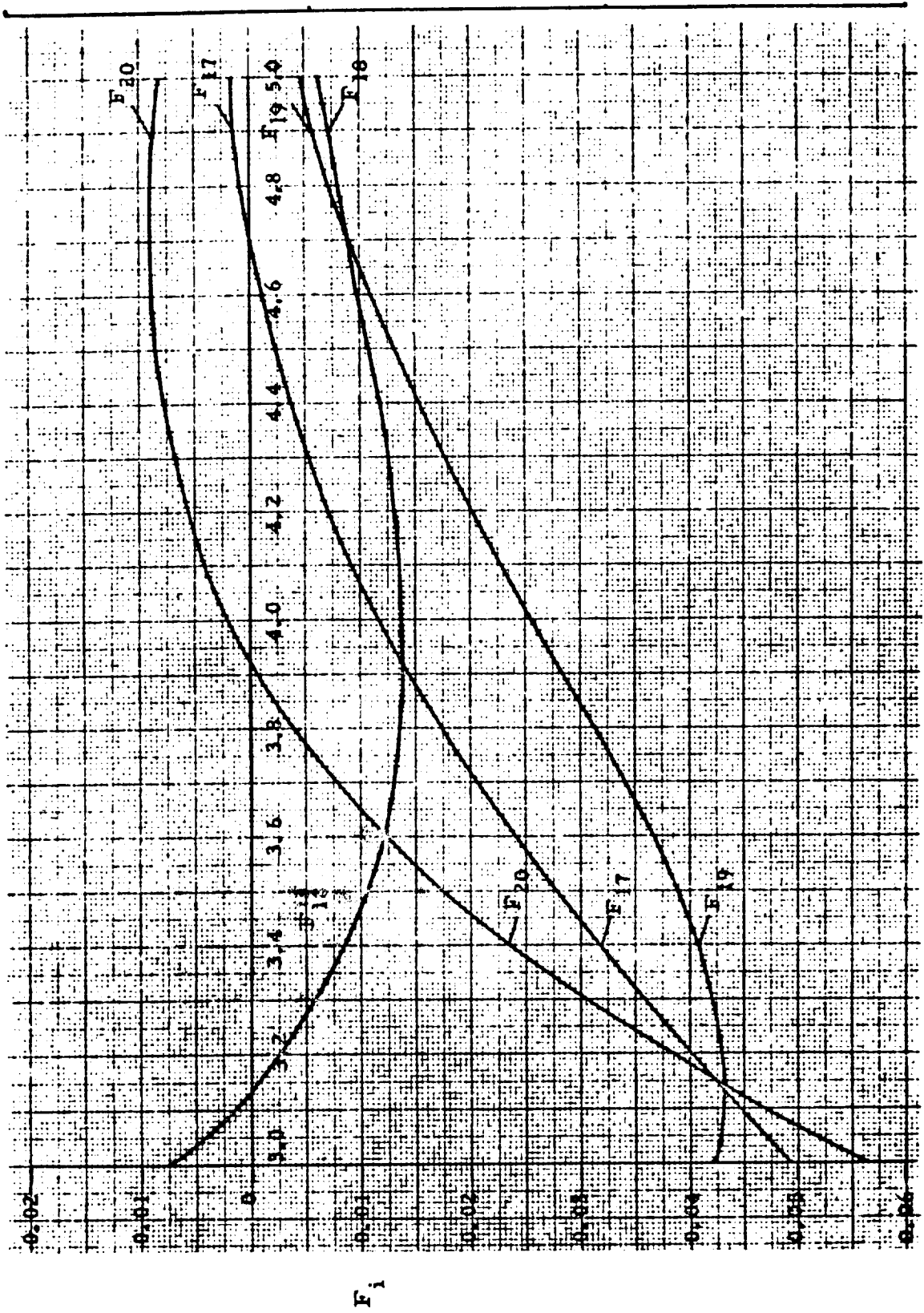


FIG. 2.42-4. (SHEET 2 OF 2)



2.43 APPROXIMATE METHOD FOR DETERMINATION OF LOCATION AND MAXIMUM STRESSES IN CYLINDERS (REF. 2-2)

The approximate method is useful for preliminary design.

ξ_N and ξ_M are nondimensional values that represent the location of maximum circumferential stress and maximum moment due to any linear loading, characterized with p_v and λ_p . (See Paragraph 2.32.6.) N_{max} is the maximum circumferential force, and M_{max} is the maximum moment along the meridian. Q_F and M_F are the reactionary forces at the boundary (discontinuity forces). The graphs are plotted for different geometries of cylinders represented with parameter kL where $k = \frac{\sqrt[4]{3(1-\mu^2)}}{\sqrt{Rt}}$. There are two similar sets of graphs: one for the fixed lower boundary and the other for pinned. Consequently,

Graphs on Fig. 2.43-1 and Fig. 2.43-2 lead to determination of ξ_N and N_{max} .

Graphs on Fig. 2.43-3 or Fig. 2.43-4 lead to determination of ξ_M .

Graphs on Fig. 2.43-5 or Fig. 2.43-6 lead to determination of M_{max} .

Graphs on Fig. 2.43-7 or Fig. 2.43-8 lead to determination of Q_F .

Graphs on Fig. 2.43-9 lead to determination of M_F .

These graphs were plotted by Hampe and are based on his method which was described before (Section 2.42).

FIG. 2.43-1. DETERMINATION OF LOCATION AND VALUE OF MAXIMUM CIRCUMFERENTIAL LOAD IN CYLINDERS LOADED LINEARLY, WITH FIXED BOUNDARY

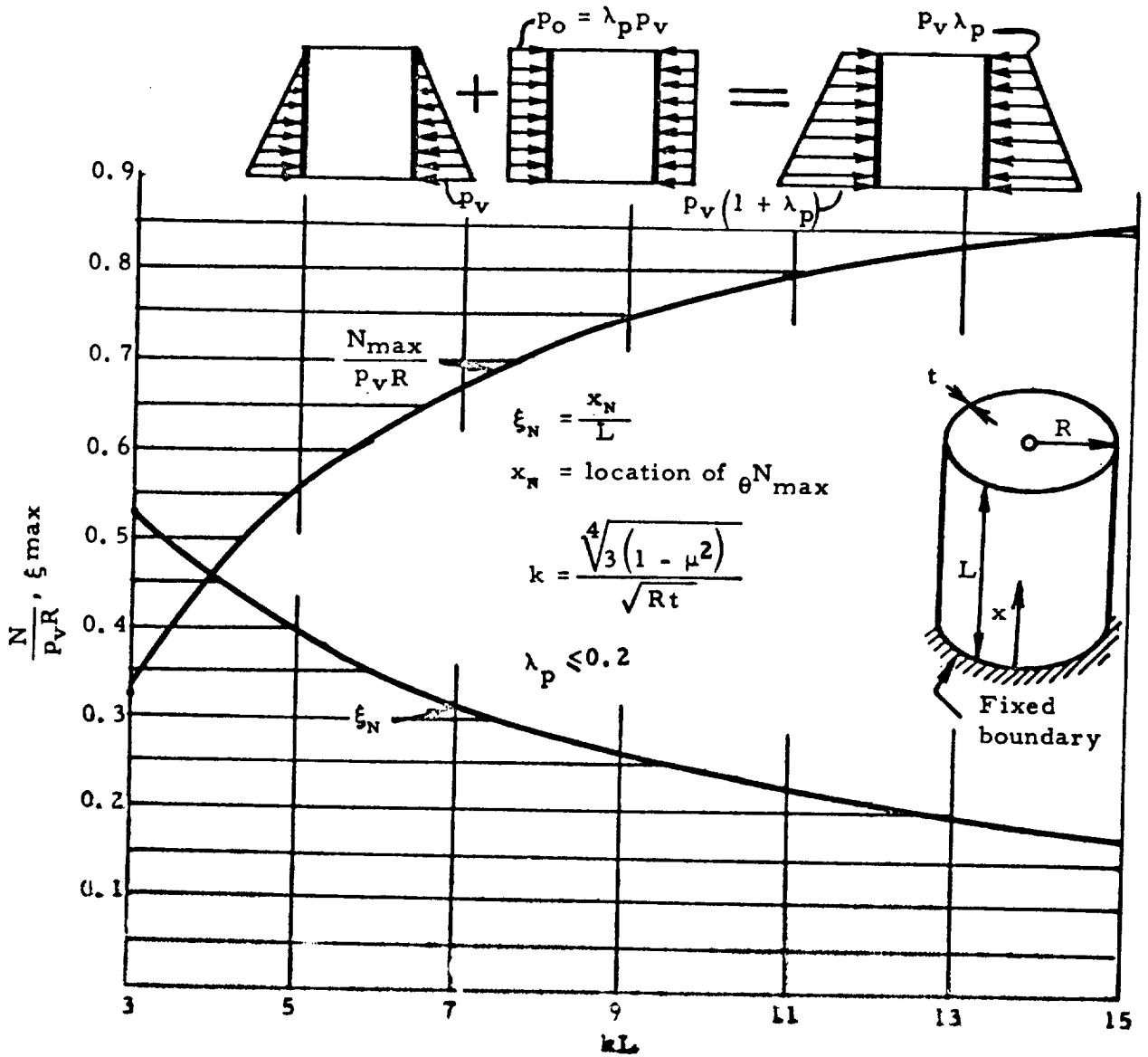


FIG. 2.43-2. DETERMINATION OF LOCATION AND VALUE OF MAXIMUM CIRCUMFERENTIAL LOAD IN CYLINDERS LOADED LINEARLY, SIMPLY SUPPORTED AT LOWER BOUNDARY

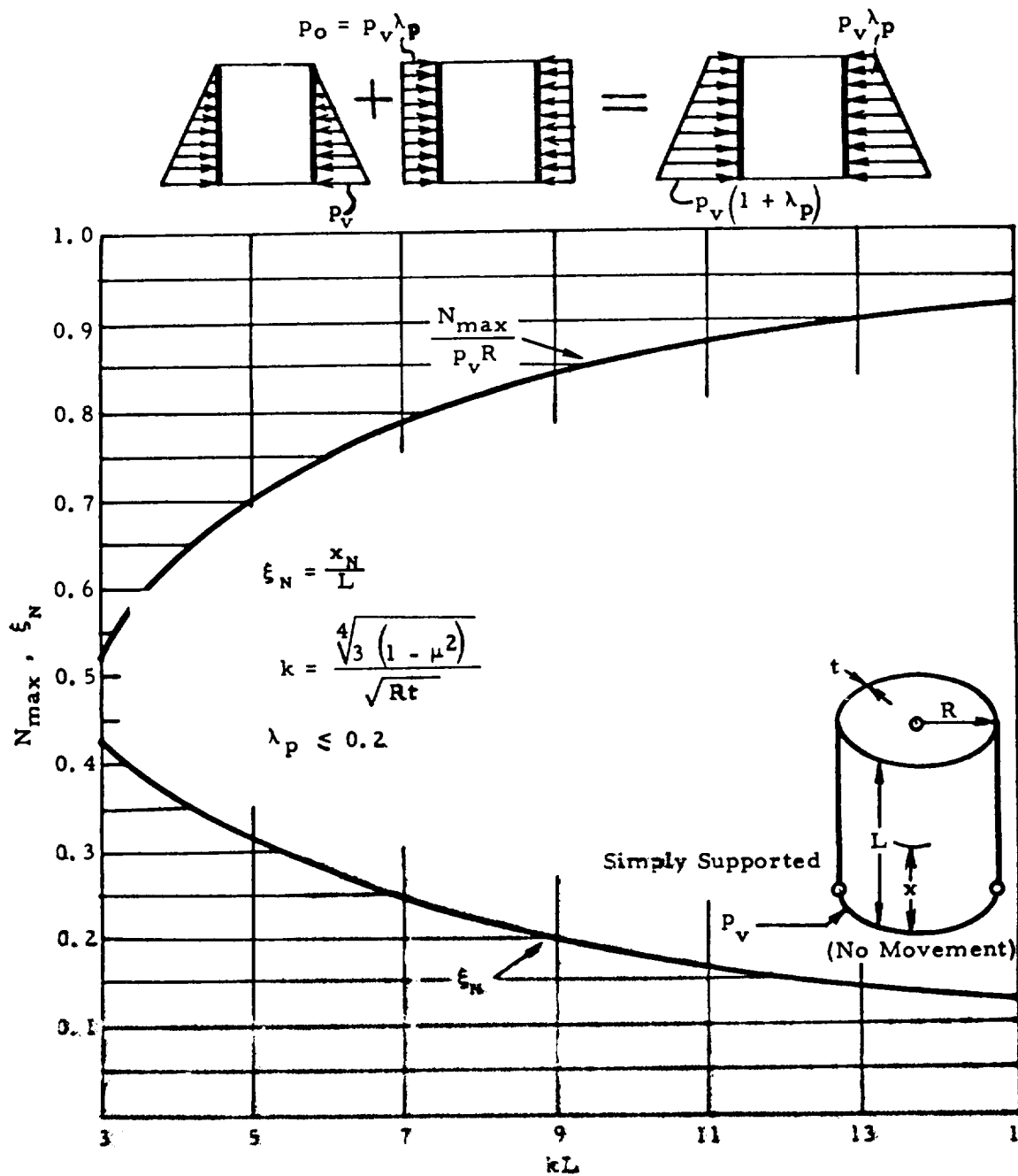


FIG. 2.43-3. DETERMINATION OF LOCATION FOR MAXIMUM MOMENT FOR CYLINDER LOADED LINEARLY WITH FIXED LOWER BOUNDARY

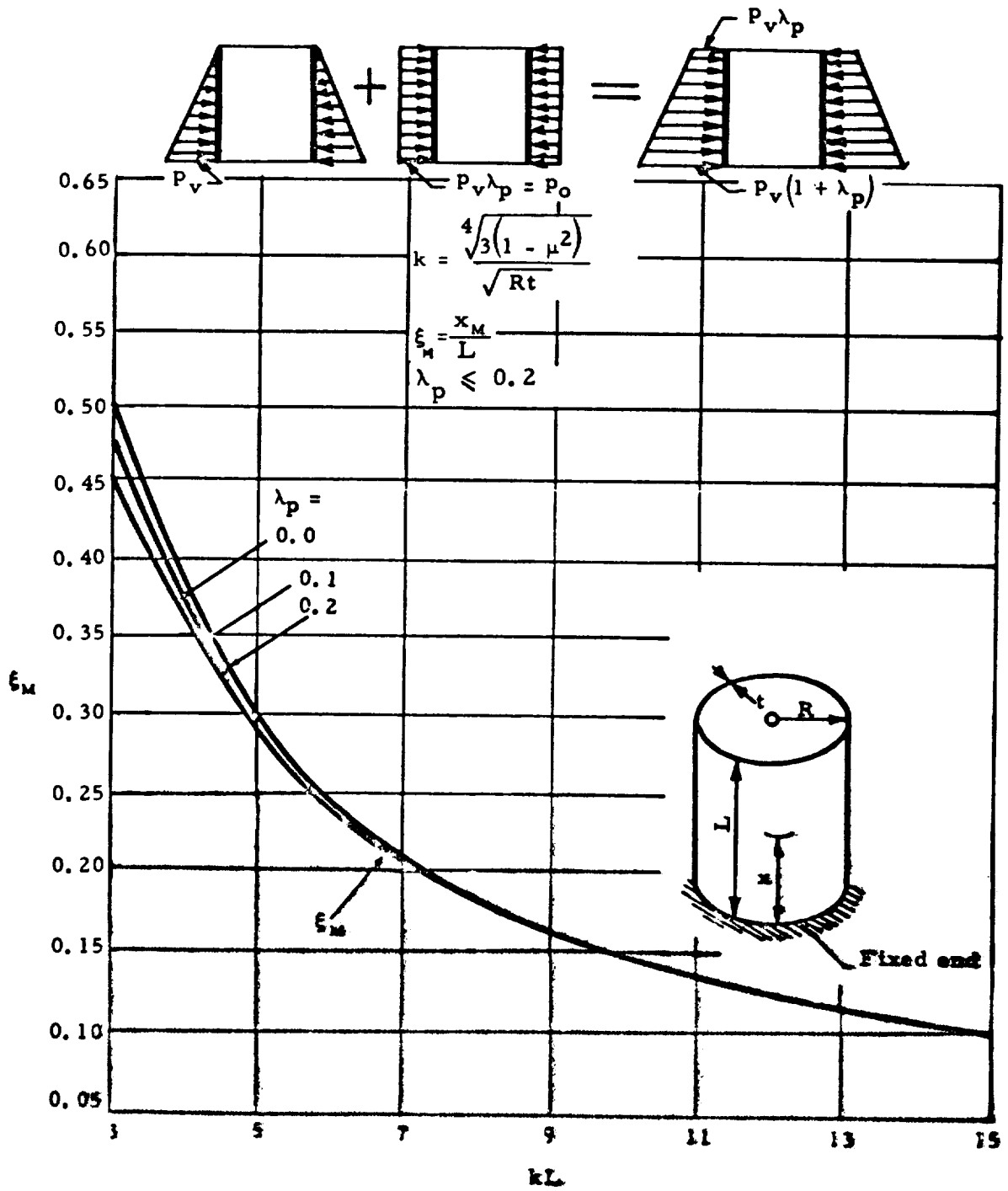


FIG. 2.43-4. DETERMINATION OF LOCATION FOR MAXIMUM MOMENT FOR CYLINDERS LOADED LINEARLY WITH SIMPLY SUPPORTED LOWER BOUNDARY

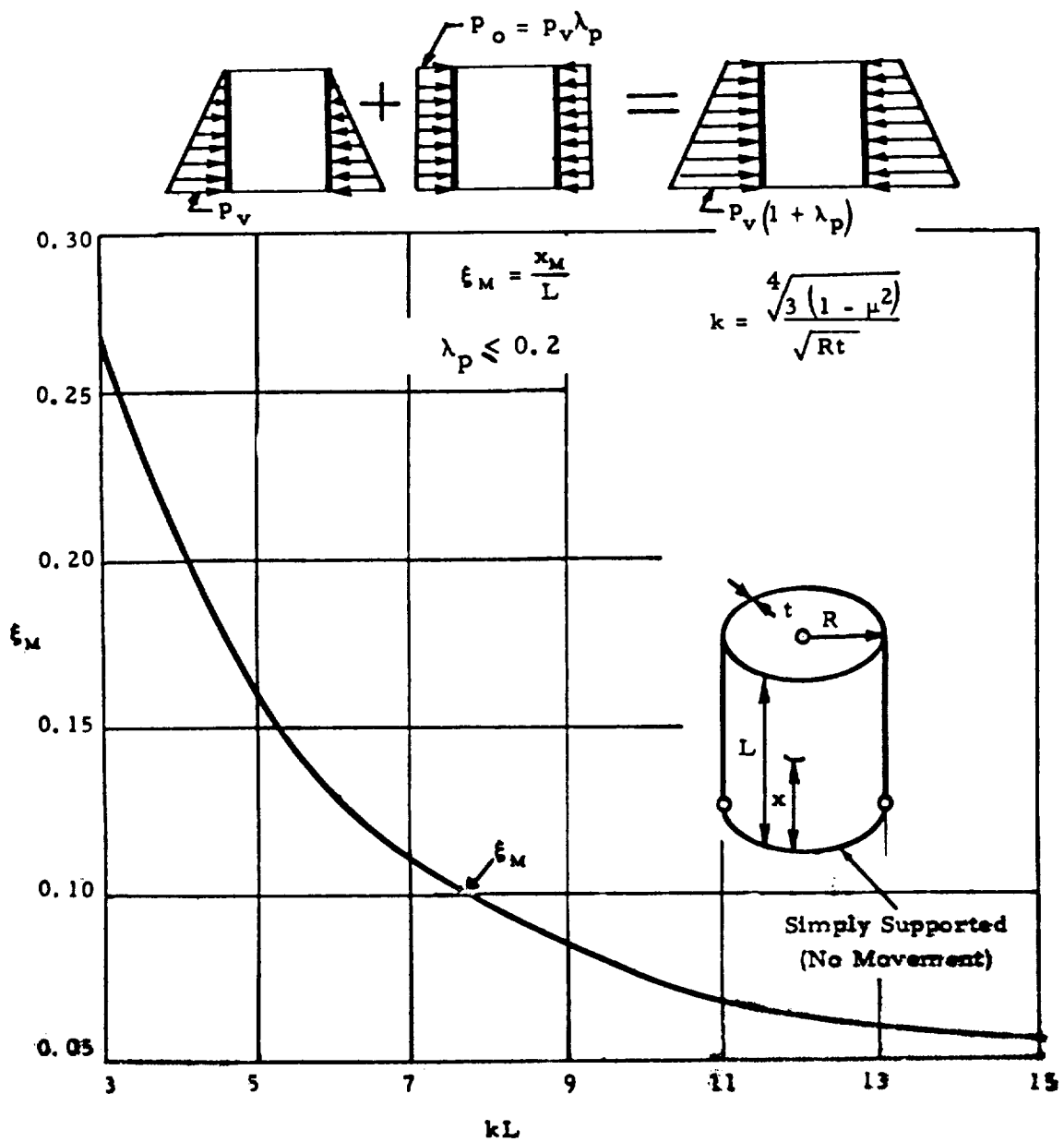


FIG. 2.43-5. DETERMINATION OF MAXIMUM MOMENT FOR LINEARLY LOADED CYLINDERS, FIXED AT LOWER BOUNDARY

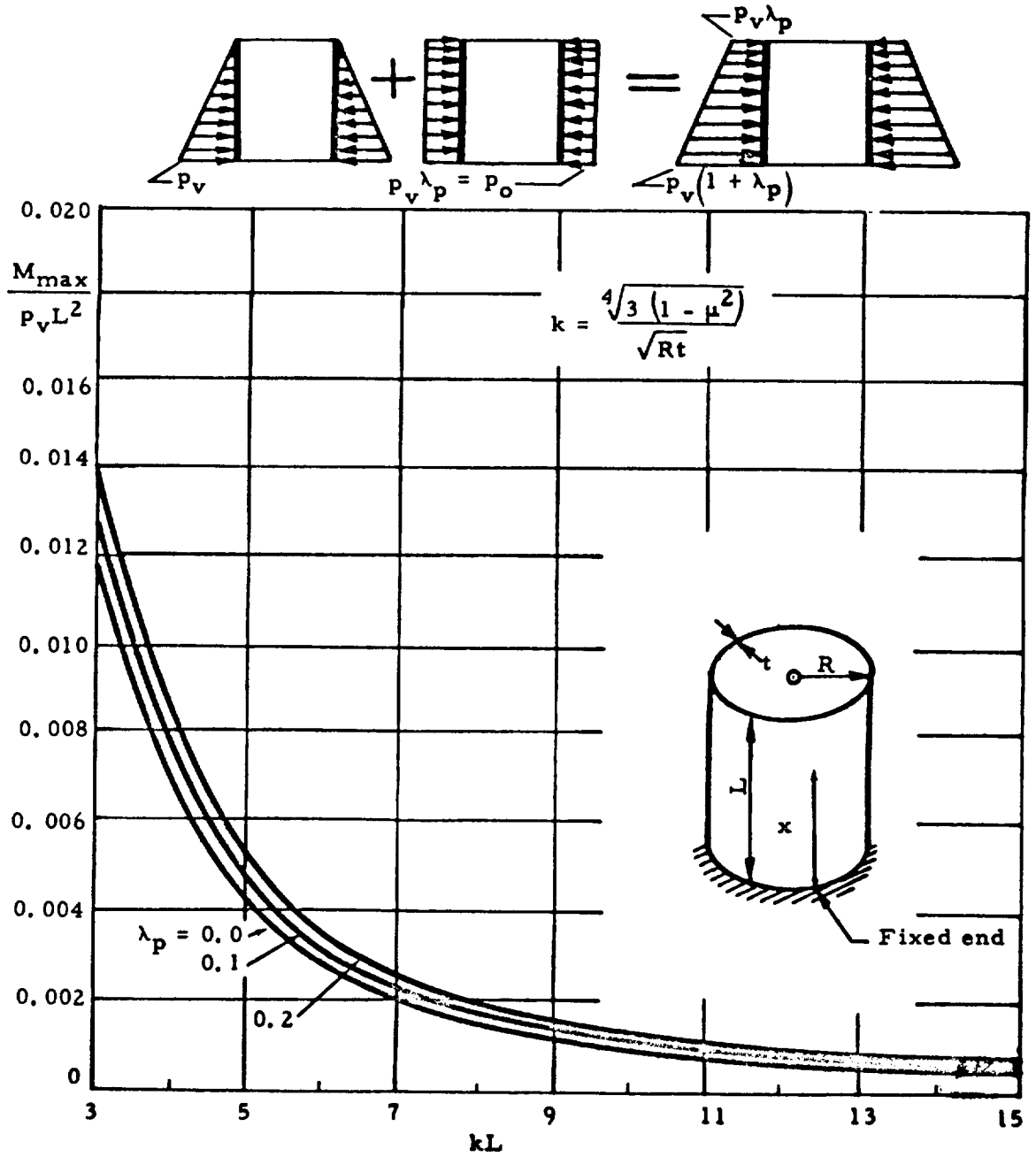


FIG. 2.43-6. DETERMINATION OF MAXIMUM MOMENT FOR LINEARLY LOADED CYLINDERS, SIMPLY SUPPORTED AT LOWER BOUNDARY

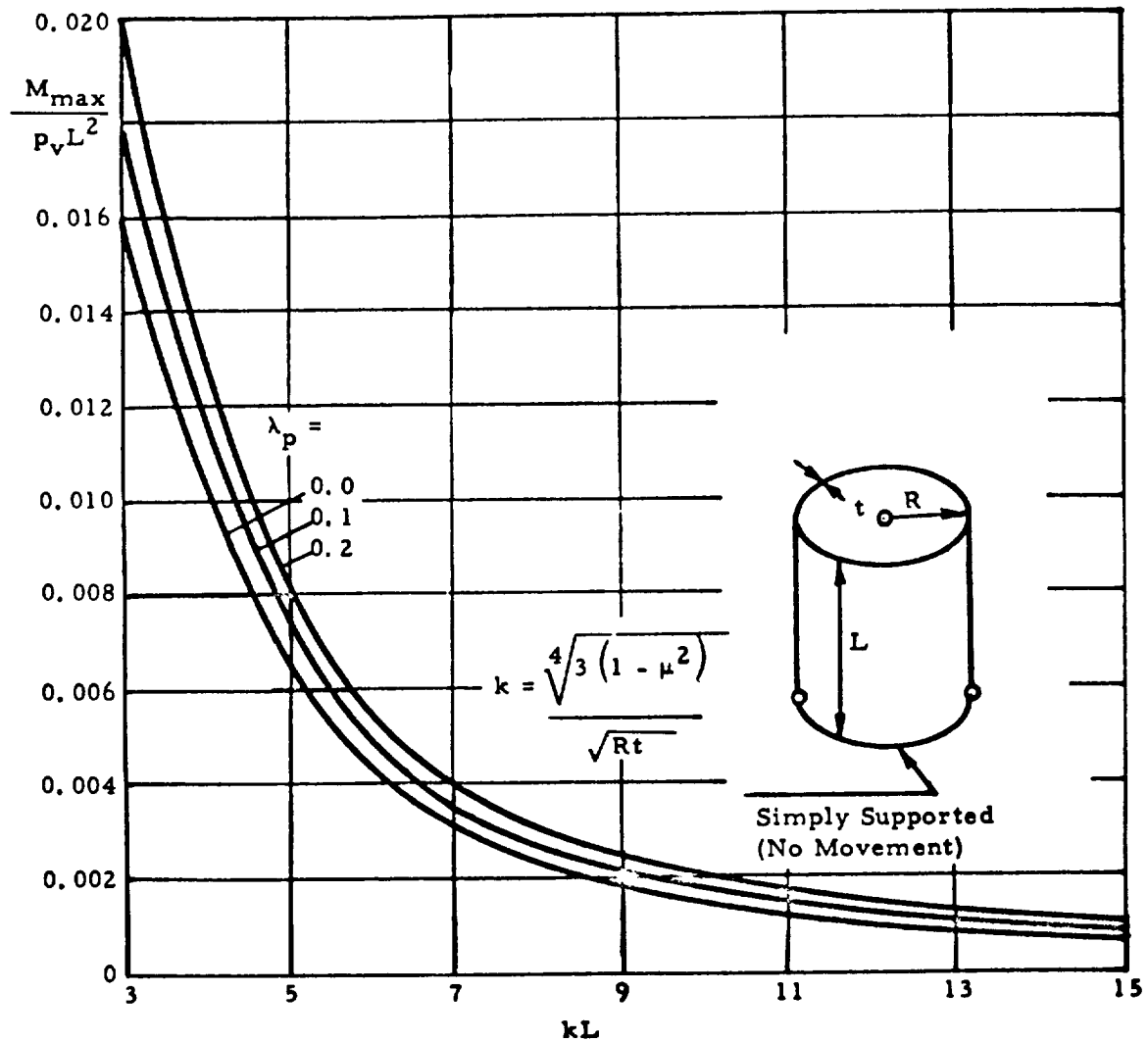
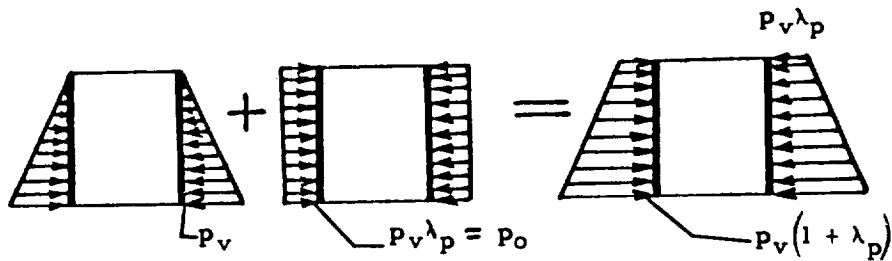


FIG. 2.43-7. DETERMINATION OF SHEAR AT LOWER FIXED BOUNDARY OF CYLINDERS LOADED WITH LINEARLY DISTRIBUTED PRESSURE

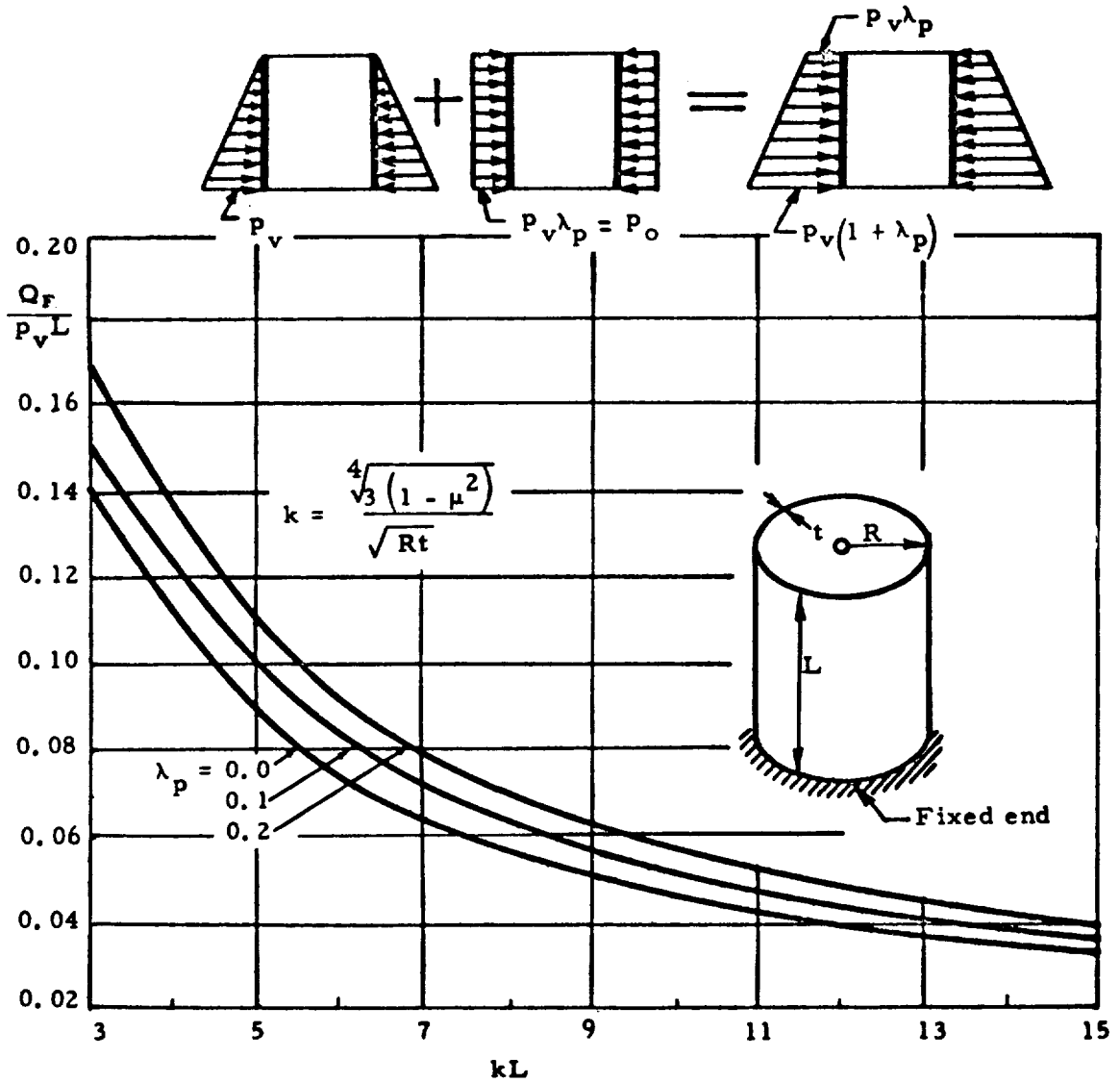


FIG. 2.43-8. DETERMINATION OF SHEAR AT LOWER SIMPLY SUPPORTED BOUNDARY OF CYLINDERS LOADED WITH LINEARLY DISTRIBUTED PRESSURE

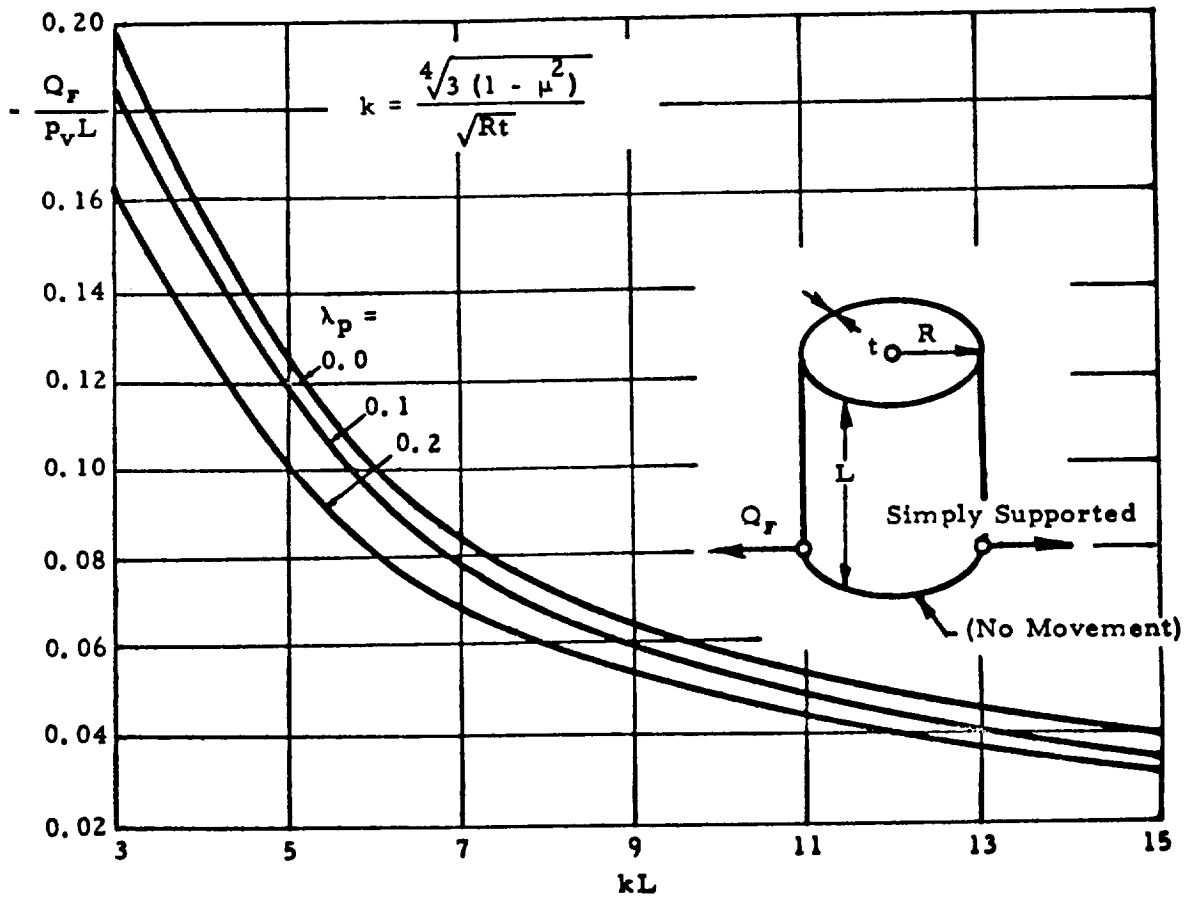
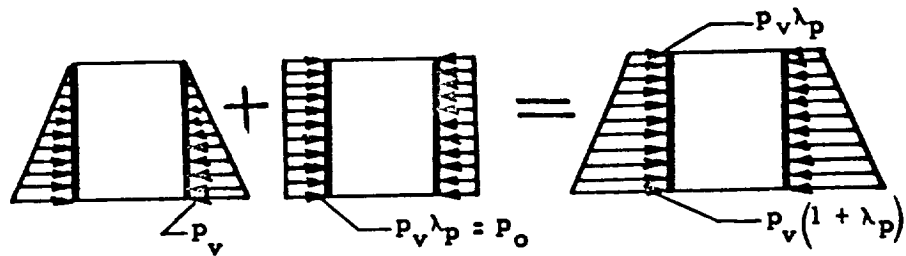
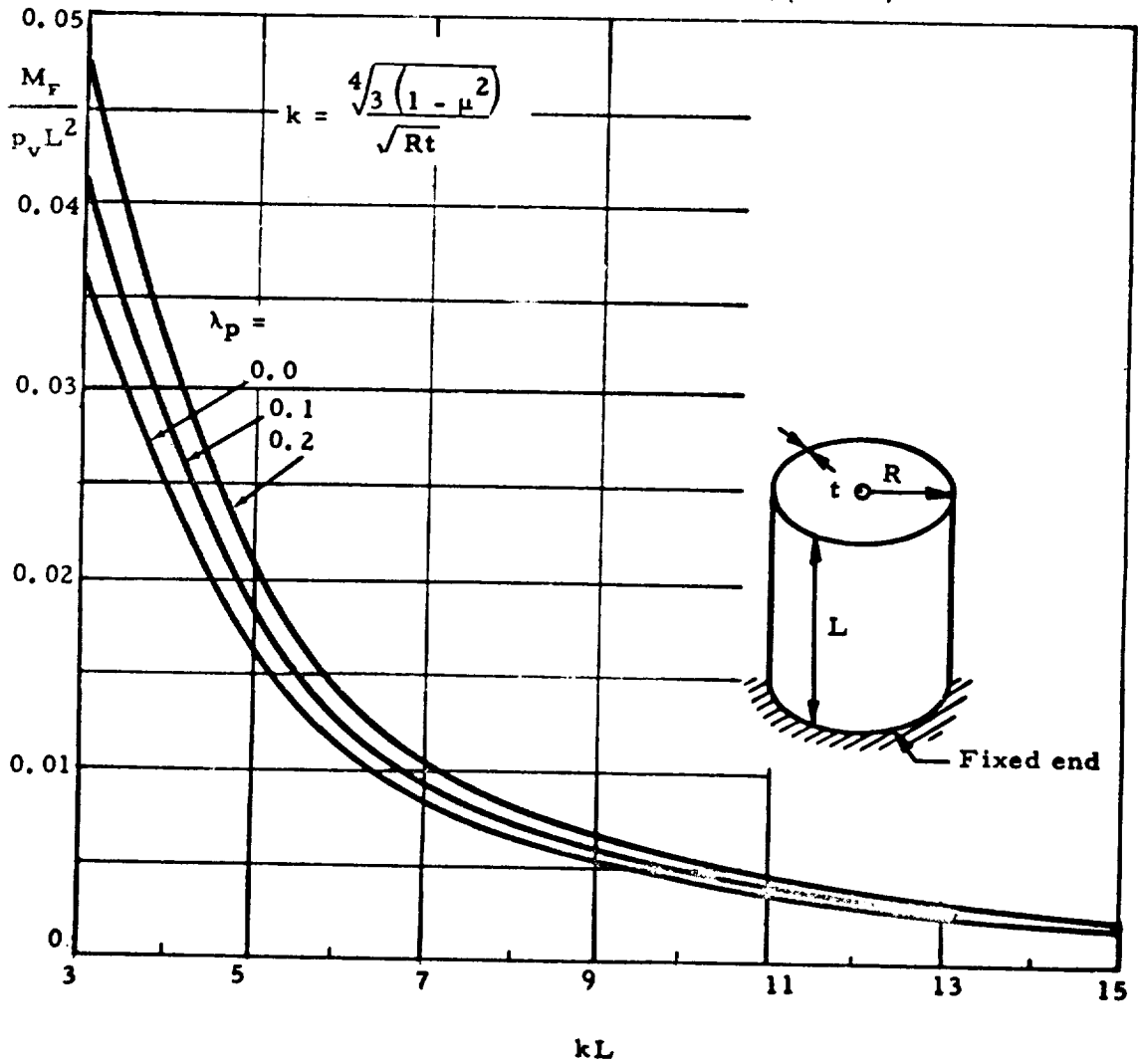
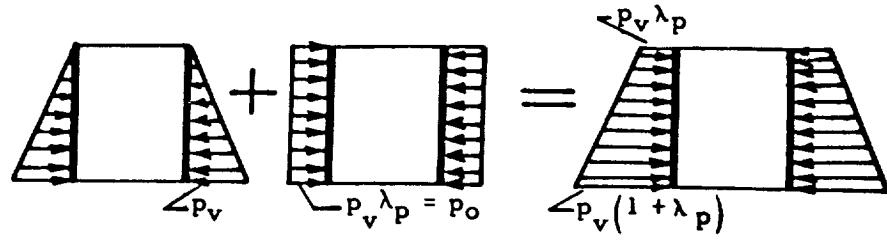


FIG. 2.43-9. DETERMINATION OF THE FIXTY MOMENT AT THE BOTTOM OF THE FIXED CYLINDERS FOR LINEAR LOADING



2.44 CIRCULAR PLATES

A collection of solutions for circular plates with different axisymmetrical loading conditions is presented in this section. The circular plates with and without a central circular hole are considered. These solutions can be used individually or in the process of interaction with more complicated structures. The following nomenclature will be used:

w = deflection

β = rotation

E = Young's modulus

μ = Poisson's ratio

t = thickness of plate

$$D = \frac{Et^3}{12(1 - \mu^2)}$$

M_r = radial moment

M_t = tangential moment

Q_r = radial shear

Other designations are indicated in tables presented in this section.

The formulas presented were derived by using the linear bending theory. The "primary" solution is presented first; then "secondary" solutions are presented in the same way as for the shells. Finally, special cases (fixed boundary conditions) will be given.

2.44.1 Primary Solutions

Primary solutions are assembled in Tables 2.44-1 and 2.

TABLE 2.44-1. SIMPLY SUPPORTED CIRCULAR PLATES (REF. 2-8)

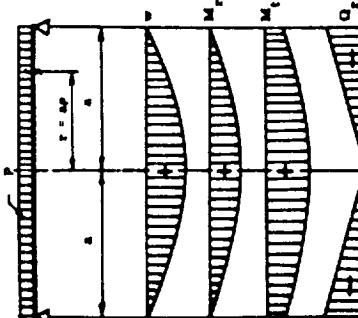
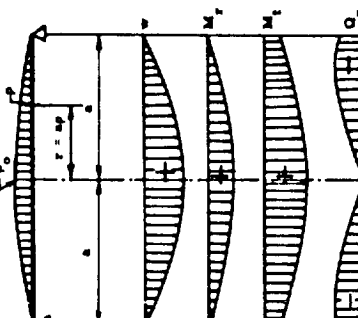
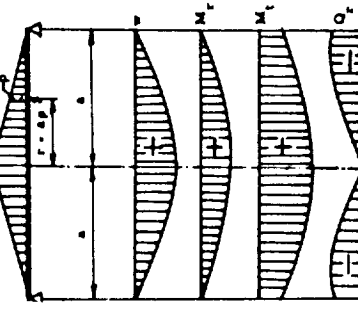
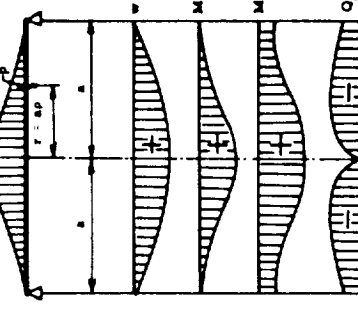
| | LOADING CONSTANT | PARABOLIC DISTRIBUTION | CONICAL DISTRIBUTION | REVERSE PARABOLIC |
|-------|--|---|---|--|
| | $P = \text{const.}; p = p_0 \frac{r^2}{a^2}$ $A = \frac{P}{2\pi a}; Q_r = \frac{Pr}{2\pi a}$  | $P = P_0(1-r^2); P = P_0 a^2 \frac{r^2}{a^2}$ $A = \frac{P}{2\pi a}; Q_r = \frac{Pr(2-r^2)}{2\pi a}$  | $P = P_0(1-r); P = P_0 a \frac{r^2}{a^2}$ $A = \frac{P}{2\pi a}; Q_r = \frac{Pr(1-2r)}{2\pi a}$  | $P = P_0(1-r)^2; P = P_0 a^2 \frac{r^2}{a^2}$ $A = \frac{P}{2\pi a}; Q_r = \frac{Pr(6-8r+3r^2)}{2\pi a}$  |
| w | $\frac{P_0 a^2}{64D\pi} \left(\frac{5+\nu}{1+\nu} - \rho^2 \right)$ | $\frac{P_0 a^2}{240D\pi} \left(\frac{39+15\nu}{1+\nu} - \frac{2}{1+\nu} \rho^2 + 9\rho^4 - \rho^6 \right)$ | $\frac{P_0 a^2}{480D\pi} \left[\frac{3(183+43\nu)}{1+\nu} - \frac{10(71+29\nu)}{1+\nu} \rho^2 + 225\rho^4 - 64\rho^6 \right]$ | $\frac{P_0 a^2}{240D\pi} \left[\frac{5(89+41\nu)}{1+\nu} - \frac{2}{1+\nu} \rho^2 + 225\rho^4 - 128\rho^6 + 25\rho^8 \right]$ |
| P | $\frac{P_0 a \rho}{16D\pi} (3+\nu - \rho^2)$ | $\frac{P_0 a \rho}{48D\pi} \left(\frac{13+5\nu}{1+\nu} - 6\rho^2 + \rho^4 \right)$ | $\frac{P_0 a \rho}{240D\pi} \left(\frac{71+29\nu}{1+\nu} - 45\rho^2 + 16\rho^4 \right)$ | $\frac{P_0 a \rho}{240D\pi} \left(\frac{89+41\nu}{1+\nu} - 90\rho^2 + 64\rho^4 - 15\rho^6 \right)$ |
| M_r | $\frac{P}{16\pi} (3+\nu)(1-\rho^2)$ | $\frac{P}{48\pi} \left[13+5\nu - 6(3+\nu)\rho^2 + (5+\nu)\rho^4 \right]$ | $\frac{P}{240\pi} \left[71+29\nu - 45\rho^2(3+\nu) + 16\rho^4(4+\nu) \right]$ | $\frac{P}{240\pi} \left[89+41\nu - 90\rho^2(3+\nu) + 64\rho^4(4+\nu) - 15\rho^6(5+\nu) \right]$ |
| M_t | $\frac{P}{16\pi} \left[3+\nu - (1+3\nu)\rho^2 \right]$ | | | $\frac{P}{240\pi} \left[89+41\nu - 90\rho^2(1+3\nu) + 64\rho^4(1+3\nu) - 15\rho^6(1+3\nu) \right]$ |

TABLE 2.44-1. (CONT)

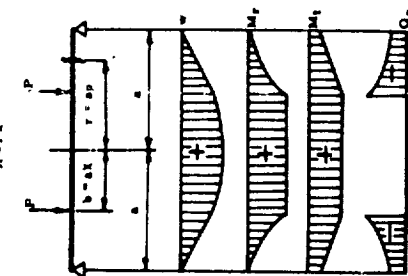
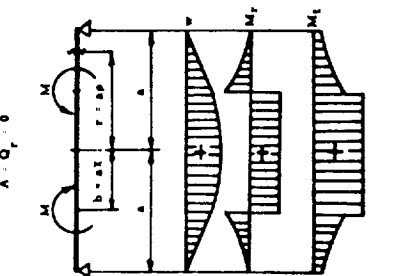
| CIRCUMFERENTIAL LOADING (LINEAR) | | CIRCUMFERENTIAL LOADING (MOMENT) | |
|--|--|--|--|
| <p>$A = PK$</p>  <p>$P \frac{ba}{\pi}$</p> <p>For $0 \leq \rho \leq \lambda$, $Q_r = 0$</p> <p>For $\lambda \leq \rho \leq 1$, $Q_r = -\frac{PK}{\rho}$</p> | | <p>$A = Q_r = 0$</p>  <p>$M \frac{ba \cdot \ln}{\pi}$</p> <p>For $0 \leq \rho \leq \lambda$</p> <p>For $\lambda \leq \rho \leq 1$</p> | |
| w | $\frac{Pc^2}{2D} \frac{\lambda}{1+\nu} \left[(1+\nu)(1+x^2) + 2(1+\nu) \right. \\ \left. - x^2 \ln x - (1-\nu)(1-x^2) - x \right. \\ \left. (1+\nu) \ln x \right] \rho^2$ | $\frac{M\lambda^2}{2D} \frac{x}{1+\nu} \left[(3+\nu - (1-\nu)x^2) \right. \\ \left. - (1-\nu^2) + 2(1+\nu)(x^2 + \rho^2) \ln \rho \right]$ | $\frac{M\lambda^2}{2D} \frac{x^2}{1+\nu} \left[(1-\nu)(1-\rho^2) \right. \\ \left. - 2(1+\nu) \ln \rho \right]$ |
| ρ | $\frac{Pc^2}{2D} \frac{x}{1+\nu} \rho \left[(1-\nu)(1-x^2) \right. \\ \left. - 2(1+\nu) \ln x \right]$ | $\frac{Pc^2}{2D} \frac{x}{1+\nu} \rho \left[2 - (1-\nu)x^2 - (1+\nu) \frac{x^2}{\rho^2} \right. \\ \left. - 2(1+\nu) \ln \rho \right]$ | $\frac{M\lambda^2}{2D(1+\nu)} \left[(1-\nu)\rho + \frac{1+\nu}{\rho} \right]$ |
| M_r | $\frac{P\lambda}{4} \left[(1-\nu)(1-x^2) - 2(1+\nu) \ln x \right]$ | $\frac{P\lambda}{4} \left[(1-\nu)x^2 \left(\frac{\rho^2}{x^2} - 1 \right) - 2(1+\nu) \right. \\ \left. \cdot \ln \rho \right]$ | $\frac{M}{2} \left[\rho + \nu + (1-\nu)x^2 \right]$ |
| M_c | $\frac{P\lambda}{4} \left[(1-\nu)(1-x^2) - 2(1+\nu) \ln x \right]$ | $\frac{P\lambda}{4} \left[(1-\nu) \left[2 - x^2 \left(\frac{\rho^2}{x^2} + 1 \right) \right] - 2(1+\nu) \right. \\ \left. \cdot \ln \rho \right]$ | $\frac{M}{2} \left[\rho + \nu + (1-\nu)x^2 \right]$ |
| Q_r | 0 | 0 | 0 |

TABLE 2.44-1. (CONT)

| PARTIALLY EQUAL LOADING | | CONCENTRATED LOADING | |
|--|--|--|---|
| $p = \text{constant}; P = pb^2 = pa^2 + \mu X^2; A = \frac{P}{2a}$ | | $A = \frac{P}{2a}$; For $p \neq X$, $Q_r = -2ap$ For $p = 0$, $Q_r = 0$ | |
| | | | |
| For $0 \leq p \leq X$ $Q_r = -\frac{Pp}{2aX^2}$ | | For $X \leq p \leq L$ $Q_r = -\frac{P}{2aX}$ | |
| w | $\frac{Pb^2}{64D} \frac{1}{1+\mu} \left[4(3+\mu)X^2 - 7(3+\mu)X^2 + 4(1+\mu)X^2 \right. \\ \left. - \ln X - 2 \left[4 - (1-\mu)X^2 - 4(1+\mu) \ln X \right] \right. \\ \left. - p^2 + (1+\mu) \frac{p^4}{X^2} \right]$ | $\frac{Pa^2}{32D} \frac{1}{1+\mu} \left[2(3+\mu) - (1-\mu)X^2 \right] (1-p^2) \\ + 2(1+\mu)X^2 \ln p + 4(1+\mu)p^2 \ln p$ | $\frac{Pa^2}{16D} \left[\frac{3+\mu}{1+\mu} (1-p^2) + 2p^2 \ln p \right]$ |
| p | $\frac{Pa}{16D} \frac{1}{1+\mu} \left[4 - (1-\mu)X^2 - 4(1+\mu) \ln X \right. \\ \left. - \frac{1+\mu}{X^2} p^2 \right]$ | $\frac{Pa}{16D} \frac{1}{1+\mu} \left[4 - (1-\mu)X^2 \right] p - (1+\mu) \frac{p^2}{2}$ | $\frac{Pa}{4D} p \left(\frac{1}{1+\mu} - \ln p \right)$ |
| M_r | $\frac{P}{16\pi} \left[4 - (1-\mu)X^2 - 4(1+\mu) \ln X \right. \\ \left. - 3 + \mu \right]$ | $\frac{P}{16\pi} \left[(1-\mu)X^2 \left(\frac{1}{2} - 1 \right) - 4(1+\mu) \ln p \right]$ | For $p \geq X$, $-\frac{P}{4\pi} (1+\mu) \ln p$ For $p = 0$, $\frac{P}{4\pi} \left[1 - (1+\mu) \ln X \right]$ |
| M_t | $\frac{P}{16\pi} \left[4 - (1+\mu)X^2 - 4(1+\mu) \ln X \right. \\ \left. - \frac{1+3\mu}{2} p^2 \right]$ | $\frac{P}{16\pi} \left[(1-\mu) \left[4 - X^2 \left(\frac{1}{2} + 1 \right) \right] - 4(1+\mu) \ln p \right]$ | For $p \geq X$, $\frac{P}{4\pi} \left[1 - \mu - (1+\mu) \ln p \right]$ For $p = 0$, $\frac{P}{4\pi} \left[1 - (1+\mu) \ln X \right]$ |

TABLE 2.44-2. SIMPLY SUPPORTED CIRCULAR PLATES WITH CENTRAL HOLE, (REF. 2-8)

| | Equally Distributed Loading (lb/in. ²) | Concentrated Edge Loading (lb/in.) |
|--------|--|--|
| | $Q_r = \frac{P_0}{2} \left(\rho - \frac{r^2}{\rho^2} \right); A = \frac{P_0}{2} (1 - \rho^2); X < 1;$ $A = \frac{P_0}{2} (X^2 - 1); X > 1; h_2 = X^2 \left[3 + \rho + 4(1 + \rho) \frac{X^2}{1 + X^2} \ln X \right]$ | $Q_r = -Pr/\rho; A = Pr \text{ for } X < 1; A = -Pr \text{ for } X > 1$ $h_2 = 1 + \rho - \frac{X^2}{1 + X^2} \ln X$ |
| v | $\frac{P_0^3}{640} \left[\frac{2}{1 + \rho} \left[(3 + \rho)(1 - 2X^2) + h_2 \right] (1 - \rho^2) - (1 - \rho^4) - \frac{4h_2 \ln \rho}{1 - \rho} - 8X^2 \rho^2 \ln \rho \right]$ | $\frac{Pr^3 X}{80D} \left[\frac{3 + \rho - 2h_2}{1 + \rho} (1 - \rho^2) + 4 \frac{h_2}{1 - \rho} \ln \rho + 2\rho^2 \ln \rho \right]$ |
| ρ | $\frac{P_0^3}{160} \left[\frac{1}{1 + \rho} \left[(3 + \rho - 4X^2 + h_2)\rho - \rho^3 + \frac{h_2}{1 - \rho} \rho + 4X^2 \rho \ln \rho \right] \right]$ | $\frac{Pr^2 X}{2D} \left[\frac{1 - h_2}{1 + \rho} \rho - \frac{h_2}{1 - \rho} - \frac{1}{\rho} - \rho \ln \rho \right]$ |
| M_r | $\frac{P_0^2}{16} \left[(3 + \rho)(1 - \rho^2) + h_2 \left(-\frac{1}{\rho^2} \right) + 4(1 + \rho) X^2 \ln \rho \right]$ | $\frac{PrX}{2} \left[h_2 \left(\frac{1}{\rho^2} - 1 \right) - (1 + \rho) \ln \rho \right]$ |
| M_t | $\frac{P_0^2}{16} \left[2(1 - \rho)(1 - 2X^2) + (1 + 3\rho)(1 - \rho^2) + h_2 \left(1 + \frac{1}{\rho^2} \right) + 4(1 + \rho) X^2 \ln \rho \right]$ | $\frac{PrX}{2} \left[1 - \rho - h_2 \left(\frac{1}{\rho^2} + 1 \right) - (1 + \rho) \ln \rho \right]$ |

2.44.2 Secondary Solutions

The only unit edge loading of importance is a unit moment loading along the edges (Fig. 2.44-1). Table 2.44-3 presents solutions for this loading for different cases of circular plate with and without the circular opening at the center.

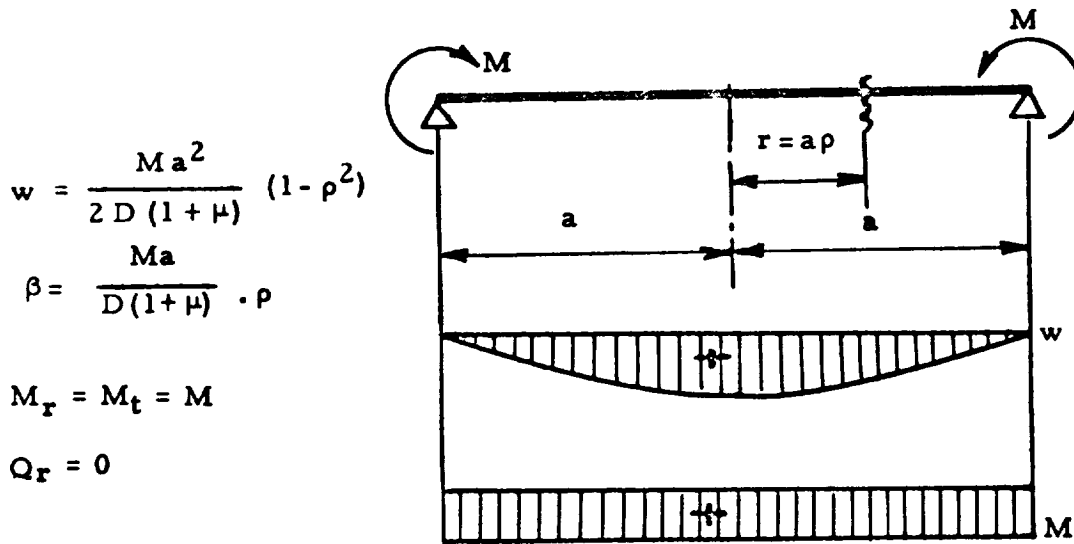


FIG. 2.44-1. Formulas of Influences for a Simply Supported Circular Plate Loaded With Equally Distributed End-Moment

TABLE 2.44-3. SIMPLY SUPPORTED CIRCULAR PLATES WITH
CENTRAL HOLE (REF. 2-8)

| | EQUALLY DISTRIBUTED EDGE MOMENT ($\rho = \chi$) | EQUALLY DISTRIBUTED EDGE MOMENT ($\rho = 1$) |
|--------|--|---|
| | <p>M is in lb-in./in.; $Q_r = 0$; $A = 0$; $k_0 = \chi^2 / (1 - \chi^2)$ $b = a\chi$; $r = ap$</p> | <p>M is in lb-in./in.; $Q_r = 0 = A$; $k_0 = 1 / (1 - \chi^2)$ $b = a\chi$; $r = ap$</p> |
| V | $\frac{M_0^2}{2D} \frac{b_0}{1+\mu} (1-\rho^2 - 2 \frac{1+\mu}{1-\mu} \cdot \ln \rho)$ | $\frac{M_0^2}{2D} \frac{b_0}{1+\mu} (1-\rho^2 - 2 \frac{1+\mu}{1-\mu} \chi^2 \cdot \ln \rho)$ |
| ρ | $\frac{M_0}{D} \frac{b_0}{1+\mu} (\rho + \frac{1+\mu}{1-\mu} \cdot \frac{1}{\rho})$ | $\frac{M_0}{D} \frac{b_0}{1+\mu} (\rho + \frac{1+\mu}{1-\mu} \chi^2 \cdot \frac{1}{\rho})$ |
| M_r | $M_0 \chi (1 - \frac{1}{\rho^2})$ | $M_0 \chi^2 b_0 (\frac{1}{\rho^2} - \frac{1}{\rho})$ |
| M_t | $M_0 \chi (1 + \frac{1}{\rho^2})$ | $M_0 \chi^2 b_0 (\frac{1}{\rho^2} + \frac{1}{\rho})$ |

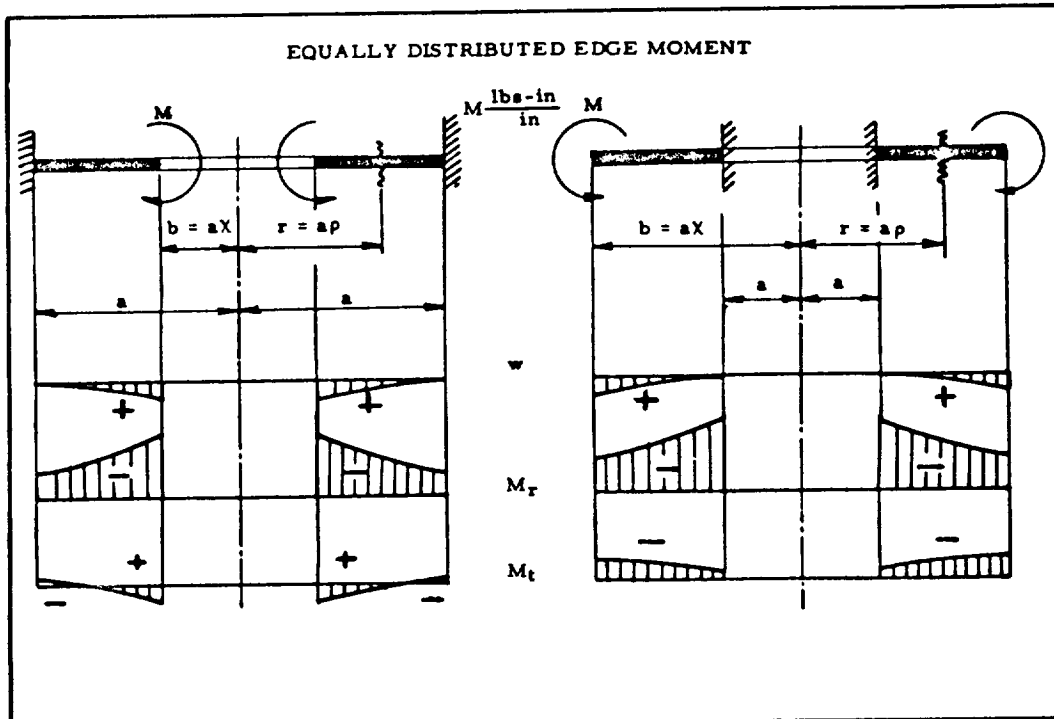
2.44.3 Special Cases

Special cases and solutions for circular plates that occur commonly in practice are presented in this section. The geometry, boundary conditions, and loadings for special circular plates (with and without a central hole) are shown in Tables 2.44-4 and 2.44-5. The information for these tables was obtained from Ref. 2-2. and 2-8.

TABLE 2.44-4. CIRCULAR PLATE WITH CENTRAL HOLE (REF. 2-8)

| EQUALLY DISTRIBUTED LOADING OVER THE SURFACE AREA | | EQUALLY DISTRIBUTED LOADING OVER THE EDGE-CIRCUMFERENCE | |
|--|--|--|--|
| $k_1 = x^2 \cdot \frac{(1-\nu)x^2 + (1+\nu)(1+x^2 \ln x)}{1-\nu + (1+\nu)x^2}$ | | $k_3 = x^2 \frac{1 + (1+\nu) \ln x}{1-\nu + (1+\nu)x^2}$ | |
| | | | |
| w | $\frac{Pa^6}{64D} [-1 + 2(1-k_1 - 2x^2)(1-\nu^2) + \nu^4 - 4k_1 \ln \rho - 8x^2 \rho^2 \ln \rho]$ | $\frac{Pa^3}{8D} [(1-2k_3)(1-\nu^2) + 4k_3 \ln \rho + 2\rho^2 \ln \rho]$ | |
| ρ | $\frac{Pa^3}{16D} [(1-k_1)\rho - \rho^3 + k_1 \cdot \frac{1}{\rho} + 4x^2 \rho \cdot \ln \rho]$ | $\frac{Pa^2 x}{2D} [k_3(\rho - \frac{1}{\rho}) - \rho \ln \rho]$ | |
| M_r | $\frac{Pa^2}{16} [(1+\nu)(1-k_1) + 4x^2 - (3+\nu)\rho^2 - (1-\nu)k_1 \cdot \frac{1}{\rho^2} + 4x^2(1+\nu) \ln \rho]$ | $\frac{Pa^2 x}{2} [-1 + (1+\nu)k_3 + (1-\nu)k_3 \cdot \frac{1}{\rho^2} - (1+\nu) \ln \rho]$ | |
| M_t | $\frac{Pa^2}{16} [(1+\nu)(1-k_1) + 4\nu x^2 - (1+3\nu)\rho^2 + (1-\nu) \cdot \frac{2}{\rho^2} + 4(1+\nu)x^2 \ln \rho]$ | $\frac{Pa^2 x}{2} [-\nu + (1+\nu)k_3 - (1-\nu) \cdot \frac{k_3}{\rho^2} - (1+\nu) \ln \rho]$ | |
| Q_r | $-\frac{Pa}{2} (\rho - x^2 \frac{1}{\rho})$ | $-Px \frac{1}{\rho}$ | |

TABLE 2.44-4. (CONT)



$$k_5 = \frac{\chi^2}{1 - \mu + (1 + \mu)\chi^2}$$

$$w = \frac{Ma^2}{2D} k_5 (-1 + \rho^2 - 2 \cdot \ln \rho)$$

$$\rho = \frac{Ma}{D} \cdot k_5 \left(\frac{1}{\rho} - \rho \right)$$

$$M_r = -Mk_5 \left[1 + \mu + (1 - \mu) \frac{1}{\rho^2} \right]$$

$$M_t = -Mk_5 \left[1 + \mu - (1 - \mu) \frac{1}{\rho^2} \right]$$

$$Q_r = 0$$


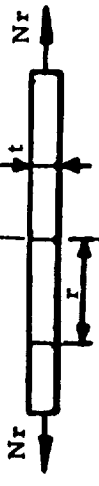
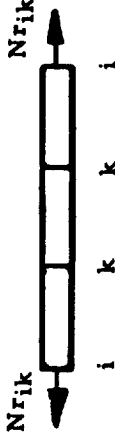
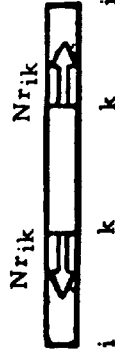
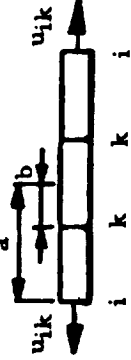
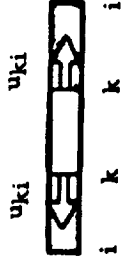
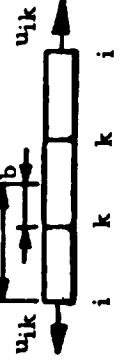
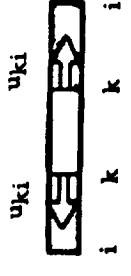
TABLE 2.44-5. CIRCULAR PLATES WITH CLAMPED EDGES (Ref. 2-8)

| | LOADING CONSTANT | PARABOLIC DISTRIBUTION | CONICAL DISTRIBUTION | REVERSE PARABOLIC |
|---------|--|--|---|---|
| | | | | |
| w | $\frac{P_0 a^2}{64 D^*} (1 - r^2)^2$ | $\frac{P_0 a^2}{288 D^*} (7 - 15r^2 + 9r^4 - r^6)$ | $\frac{P_0 a^2}{480 D^*} (11.9 - 5.96r^2 + 2.55r^4 - 64r^5)$ | $\frac{P_0 a^2}{240 D^*} (83 - 20.5r^2 + 2.25r^4 - 1.28r^5 + 2.5r^6)$ |
| β | $\frac{P_0 a^2}{16 D^*} r(1 - r^2)$ | $\frac{P_0 a^2}{48 D^*} (5 - 6r^2 + r^4)$ | $\frac{P_0 a^2}{240 D^*} (29 - 45r^2 + 16r^3)$ | $\frac{P_0 a^2}{240 D^*} (41 - 90r^2 + 64r^3 - 15r^4)$ |
| M_l | $\frac{P}{16 r} [1 + \nu - (3 + \nu)r^2]$ | $\frac{P}{48 r} [5(1 + \nu) - 6(3 + \nu)r^2 + r^4(5 + \nu)]$ | $\frac{P}{240 r} [29(1 + \nu) - 45(3 + \nu)r^2 + 16(4 + \nu)r^3]$ | $\frac{P}{240 r} [41(1 + \nu) - 90(3 + \nu)r^2 + 64(4 + \nu)r^3 - 15(5 + \nu)r^4]$ |
| M_r | $\frac{P}{16 r} [1 + \nu - (1 + 3\nu)r^2]$ | $\frac{P}{48 r} [5(1 + \nu) - 6(1 + 3\nu)r^2 + (1 + 5\nu)r^4]$ | $\frac{P}{240 r} [29(1 + \nu) - 45(1 + 3\nu)r^2 + 16(1 + 4\nu)r^3]$ | $\frac{P}{240 r} [41(1 + \nu) - 90(1 + 3\nu)r^2 + 64(1 + 4\nu)r^3 - 15(1 + 5\nu)r^4]$ |
| Q_r | $-\frac{P}{24 r} r$ | $-\frac{P}{24 r} r(2 - r^2)$ | $-\frac{P}{24 r} r(3 - 2r)$ | $-\frac{P}{24 r} r(6 - 8r + 3r^2)$ |

TABLE 2.44-5. (CONT)

| | Partially Equally Distributed Loading | Concentrated Loading | Circumferential Loading (Linear) | |
|-------|---|---|---|--|
| w | $\frac{P_0^2}{64D^2} \left[4 - 3x^2 + 4x^2 \ln x \right]$ $- 2 \left[(x^2 - 4 \ln x) \rho^2 + \frac{1}{x^2} \rho^4 \right]$ | $\frac{P_0^2}{160D^2} (1 - \rho + 2\rho^2 \ln \rho)$ | $\frac{P_0^2 X^3}{80D^2} \left[(1 + x^2)(1 - \rho^2) + 2 \left(x^2 + \rho^2 \right) \ln \rho \right]$ | $-\frac{M_0^2}{4D} \left[2x^2 \ln x + \rho^2 (1 - x^2) \right]$ |
| P | $\frac{P_0}{160D} \rho \left(x^2 - 4 \ln x - \frac{1}{x^2} \rho^2 \right)$ | $-\frac{P_0}{4D} \rho \ln \rho$ | $\frac{P_0^2 X \rho}{4D} \left[x^2 \left(1 - \frac{1}{\rho^2} \right) - 2 \ln \rho \right]$ | $\frac{M_0 X^2}{2D} \left(\frac{1}{\rho} - \rho \right)$ |
| M_1 | $\frac{P}{160D} \left[(1 + \mu) (x^2 - 4 \ln x) - \frac{2x^2}{x^2} \rho^2 \right]$ | $-\frac{P}{4\mu} (1 + \mu) \ln x$ | $-\frac{P_0^2 X}{4} \left[2 - (1 + \mu) \frac{x^2}{\rho^2} - (1 + \mu) (x^2 - 2 \ln \rho) \right]$ | $-\frac{M_0^2}{2} \left[(1 + \mu) \frac{1}{\rho^2} \right]$ |
| M_2 | $\frac{P}{160D} \left[(1 + \mu) (x^2 - 4 \ln x) + (1 + \mu) (x^2 - 4 \ln \rho) \right]$ | $-\frac{P}{4\mu} \left[\mu + (1 + \mu) \ln \rho \right]$ | $-\frac{P_0^2 X}{4} \left[2\mu + (1 + \mu) \frac{x^2}{\rho^2} - (1 + \mu) (x^2 - 2 \ln \rho) \right]$ | $-\frac{M_0^2}{2} \left[(1 + \mu) (1 - x^2) \right]$ |
| Q_1 | $-\frac{P}{24x^2} \rho$ | $-\frac{P}{24x} \frac{1}{\rho}$ | 0 | 0 |

TABLE 2.44-6. CIRCULAR PLATES, STRESSES IN PLATES DUE TO EDGE ELONGATION

| | | | |
|--|---|--|---|
| <p>Elongation</p>  | <p>Stress</p>  | <p>Stress</p>  | <p>Stress</p>  |
| <p>Elongation</p>  | <p>Elongation</p>  | <p>Stress</p>  | <p>Stress</p>  |
| $\frac{uEt}{a(1-\mu)}$ | | $u_{ik} \frac{Et(\lambda^2 - 1)}{2a}$ | |
| $u_{ik} \frac{Et(1-\lambda^{-2})}{a[1-\mu + \lambda^{-2}(1+\mu)]}$ | | $u_{ki} \frac{Et(\lambda^2 - 1)}{b[1-\mu + \lambda^2(1+\mu)]}$ | |
| <p>NOTE $\lambda = \frac{a}{b}$</p> | | | |

2.45 CIRCULAR RINGS

Circular rings are important structural elements which often interact with shells. The theory of shells would not be complete without information about circular rings. In this section, such information are summarized and presented for symmetrical loading in respect to the center of the ring.

Nomenclature employed is as follows:

A = area of the cross section

I_1, I_2 = moment of inertia for the centroidal axis in the plane or normal to the plane of the ring

J = torsional rigidity factor of the section.

Table 2.45-1 presents the solutions for different loads on rings.

This information was obtained from Ref. 2-5.

TABLE 2.45-1. SYMMETRICALLY LOADED CIRCULAR RINGS (Ref. 2-5)

| Item | Loading Condition | n > 1 | | n = 1 | | n = 0 | |
|------|---|--|---|--|--|--|---------------|
| | | Stresses | Displacements | Stresses | Displacements | Stresses | Displacements |
| 1 | <p>RADIAL LOADING</p> <p>$P = P_n \cos n\theta$, where n is an integer: n = 1, 2, 3, ...</p> | $N = \frac{P_n a^2}{n^2 - 1} \cos n\theta$ $M = \frac{P_n a^2}{n^2 - 1} \cos n\theta$ | $v = \frac{P_n a^2}{n(n^2 - 1)} \left[\frac{a^2}{(n^2 - 1)EI_2} + \frac{1}{EA} \right] \cos n\theta$ $w = \frac{P_n a^4}{(n^2 - 1)^2 EI_2} \cos n\theta$ | <p>PROBLEM DOES NOT EXIST BECAUSE THE LOADING IS NOT IN SELF-EQUILIBRIUM</p> | $N = P_n$ $M = 0$ | $v = 0$ $w = \frac{P_n a^2}{EA}$ | |
| 2 | <p>TANGENTIAL LOADING</p> <p>$P = P_n \sin n\theta$</p> | $N = \frac{n P_n a^2}{n^2 - 1} \cos n\theta$ $M = \frac{P_n a^2}{n(n^2 - 1)} \cos n\theta$ | $v = \frac{P_n a^2}{n^2 - 1} \left[\frac{a^2}{(n^2 - 1)EI_2} + \frac{1}{EA} \right] \sin n\theta$ $w = \frac{P_n a^4}{n(n^2 - 1)^2 EI_2} \cos n\theta$ | <p>PROBLEM DOES NOT EXIST BECAUSE THE LOADING IS NOT IN SELF-EQUILIBRIUM</p> | <p>PROBLEM DOES NOT EXIST BECAUSE THE LOADING IS NOT IN SELF-EQUILIBRIUM</p> | <p>PROBLEM DOES NOT EXIST BECAUSE THE LOADING IS NOT IN SELF-EQUILIBRIUM</p> | |
| 3 | <p>LOADING NORMAL TO THE PLANE OF THE RING</p> <p>$P = P_n \cos n\theta$</p> | $M_1 = \frac{P_n a^2}{n^2 - 1} \cos n\theta$ $M_T = \frac{P_n a^2}{n(n^2 - 1)} \sin n\theta$ | $u = \frac{P_n a^4}{(n^2 - 1)^2} \left[\frac{1}{EI_1} + \frac{\cos n\theta}{n^2 GJ} \right]$ $\beta = \frac{P_n a^3}{(n^2 - 1)^2} \left[\frac{1}{EI_1} + \frac{1}{GJ} \right] \cos n\theta$ | <p>PROBLEM DOES NOT EXIST BECAUSE THE LOADING IS NOT IN SELF-EQUILIBRIUM</p> | <p>PROBLEM DOES NOT EXIST BECAUSE THE LOADING IS NOT IN SELF-EQUILIBRIUM</p> | <p>PROBLEM DOES NOT EXIST BECAUSE THE LOADING IS NOT IN SELF-EQUILIBRIUM</p> | |
| 4 | <p>EXTERNAL MOMENTS, ABOUT THE RING AXIS</p> <p>$m = m_n \cos n\theta$</p> | $M_1 = \frac{m_n a^2}{n^2 - 1} \cos n\theta$ $M_T = \frac{m_n a^2}{n^2 - 1} \cos n\theta$ | $u = \frac{m_n a^3}{(n^2 - 1)^2} \left[\frac{1}{EI_1} + \frac{1}{GJ} \right] \cos n\theta$ $\beta = \frac{m_n a^2}{(n^2 - 1)^2} \left[\frac{1}{EI_1} + \frac{2}{GJ} \right] \cos n\theta$ | <p>PROBLEM DOES NOT EXIST BECAUSE THE LOADING IS NOT IN SELF-EQUILIBRIUM</p> | $M_1 = m_n$ $M_T = 0$ | $u = \text{may assume any desired value}$ $\beta = \frac{m_n a^2}{EI_1}$ | |

2.46 CONCLUSION

In this section, supplemental information on the unit-edge loading method was presented and special attention was given to the cylinders and spheres. To make the collection of formulas more complete and general, the necessary information for circular plates and rings was provided. With all the information on numerous shell plates and ring elements, two or more shells can be combined and analyzed. The following section is devoted to this subject.

2.50 MULTISHELL STRUCTURES (Ref. 2-2)

2.51 INTRODUCTION

Up to this point, only single-shell systems were considered. In the introductory sections of this chapter, instruction was given for the treatment of "combined shells," i. e., shells that are a combination of two or three shell segments.

This section presents a simple approach for dealing with the multishell systems, similar to that shown in Fig. 2.52-1(a). Such systems usually are a combination of spherical, cylindrical, and conical shells, and circular plates and circular rings located axisymmetrically.

The multishell system is analogous to the statically indeterminate frame system and can be handled similarly. The shell elements, however, shall be high enough in order that one boundary is not to be influenced by disturbances at another boundary.

Several known methods are useful for this purpose. In this chapter, two methods, (1) the force-method and (2) the displacement-method, are presented.

Basically, the philosophy is similar for each of the methods. It is clear that, if the deformation is known, the forces at each section can be determined and, vice versa, if the forces are known, the

displacement can be determined. Consequently, there is no basic difference between the ways in which the loads (moments) or deformations as statically indeterminate values are chosen, but in some cases one or the other way may be preferred.

2.52 FORCE METHOD

2.52.1 Introduction

This method is an analog to the method employed in statics for solving rigid frames, which is called the "force method" and which introduces the cuts in the system under consideration and then, in order to restore the integrity of the structure, applies the statically indeterminate force.

2.52.2 Analysis

The system will be separated into the elementary shell, plate, or ring elements as shown in Fig. 2.52-1(b).

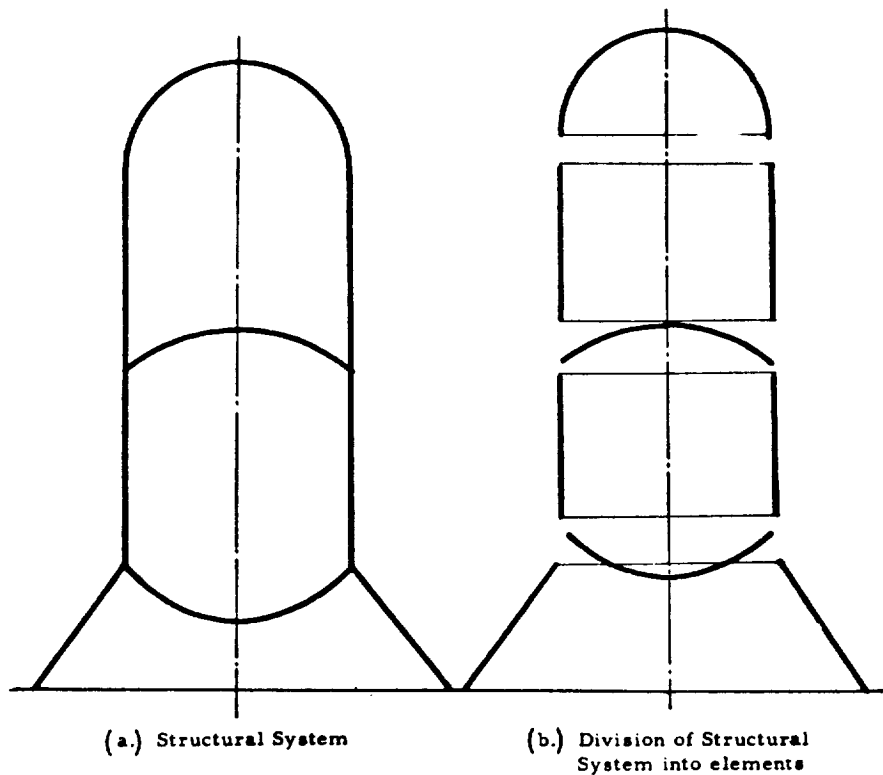


FIG. 2.52-1. Multishell

Each element (Fig. 2.52-1(b)) is statically determinate, and is loaded with the primary loading (pressurization) and with the secondary loadings (unit-loadings) in order to restore the integrity of the system, as it was explained in the introductory section of this chapter.

Fig. 2.52-2 shows the necessary statically indeterminate loadings that are applied at each point of separation in order to restore the integrity of the system.

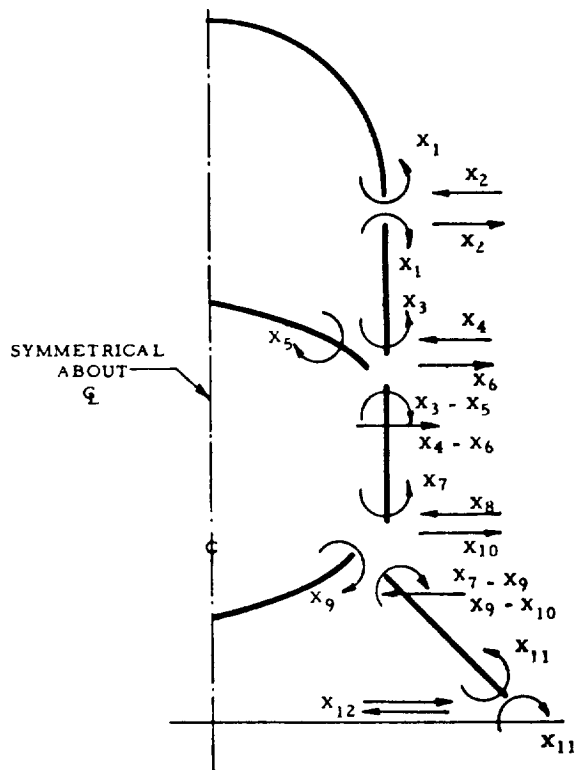


FIG. 2.52-2. Statically Indeterminate Forces Acting on the Free-Body Diagram-System With Statically Determinate Elements

The following sign convention is adapted here:

Call the values on the right-side positive, as noted:

A. Shell-Element

(1) Upper Edge of a Shell Element:

Moment in the clockwise direction.

Horizontal load directed outside.

Vertical load directed up.

(2) Lower Edge of a Shell-Element:

Moments in counterclockwise direction of rotation.

Horizontal load directed in inside direction.

Vertical load downward.

B. For Circular Plates.

(1) Inside Edge of Circular Plate With Hole:

As upper edge under A(1)

(2) Outside Edge of a Circular Plate With or Without Holes:

As lower edge under A(2)

As shown in the introductory portions of this chapter (Paragraphs 2.23.2 and 2.23.3), a system of linear equations can be written for determining the statically unknown values X_i .

Two cases which usually are considered when the system is built up from the statically determinate elements (Fig. 2.52-2) will be distinguished. The next paragraph discusses these cases.

2.52.3 System Combined From Statically Determinate Elements

A. Case 1

The length of each element is such that unit influences due to unit loading will overlap. In other words, stresses due to unit loading will depend in every joint on both edge unit influence. For such a case, the matrix for determination of X_i has the shape shown in Fig. 2.52-3.

| i | X ₁ | X ₂ | X ₃ | X ₄ | X ₅ | X ₆ | X ₇ | X ₈ | X ₉ | X ₁₀ | X ₁₁ | X ₁₂ | δ _{io} |
|----|----------------|----------------|----------------|----------------|----------------|----------------|----------------|----------------|----------------|-----------------|-----------------|-----------------|-------------------|
| 1 | == | — | — | — | | | | | | | | | δ ₁₀ |
| 2 | — | == | — | — | | | | | | | | | δ ₂₀ |
| 3 | — | — | == | — | — | — | — | — | | | | | δ ₃₀ |
| 4 | — | — | — | == | — | — | — | — | | | | | δ ₄₀ |
| 5 | | | — | — | == | — | — | — | | | | | δ ₅₀ |
| 6 | | | — | — | — | == | — | — | | | | | δ ₆₀ |
| 7 | | | — | — | — | — | == | — | — | — | — | — | δ ₇₀ |
| 8 | | | — | — | — | — | — | == | — | — | — | — | δ ₈₀ |
| 9 | | | | | | | — | — | == | — | — | — | δ ₉₀ |
| 10 | | | | | | | — | — | — | == | — | — | δ _{10,0} |
| 11 | | | | | | | — | — | — | — | == | — | δ _{11,0} |
| 12 | | | | | | | — | — | — | — | — | == | δ _{12,0} |

FIG. 2.52-3. The Matrix of Unknowns if the Boundary Disturbances at Opposite Boundaries are Influencing Each Other. (Force Method, With the Statically Determinate Elements)

B. Case 2

The length of the element is such that the disturbances caused by the unit loadings will die at short distance from the edge and will not overlap with the disturbances due to the unit loading on opposite edge of statically determinate shell element.

In this case the matrix will have the shape shown in Fig. 2.52-4.

| i | X ₁ | X ₂ | X ₃ | X ₄ | X ₅ | X ₆ | X ₇ | X ₈ | X ₉ | X ₁₀ | X ₁₁ | X ₁₂ | δ _{io} |
|----|----------------|----------------|----------------|----------------|----------------|----------------|----------------|----------------|----------------|-----------------|-----------------|-----------------|-------------------|
| 1 | == | — | | | | | | | | | | | δ ₁₀ |
| 2 | — | == | | | | | | | | | | | δ ₂₀ |
| 3 | | | == | — | — | — | | | | | | | δ ₃₀ |
| 4 | | | — | == | — | — | | | | | | | δ ₄₀ |
| 5 | | | — | — | == | — | | | | | | | δ ₅₀ |
| 6 | | | — | — | — | == | | | | | | | δ ₆₀ |
| 7 | | | | | | | == | — | — | — | | | δ ₇₀ |
| 8 | | | | | | | — | == | — | — | | | δ ₈₀ |
| 9 | | | | | | | — | — | == | — | | | δ ₉₀ |
| 10 | | | | | | | — | — | — | == | | | δ _{10,0} |
| 11 | | | | | | | | | | | == | — | δ _{11,0} |
| 12 | | | | | | | | | | | — | == | δ _{12,0} |

FIG. 2.52-4. The Matrix of Unknowns if the Boundary Disturbances at Opposite Boundaries are not Influencing Each Other. (Loads Method With Statically Determinate Elements)

It can be seen that case 2 can be split into four independent systems of linear equations. The solution will be much faster and simpler than under case 1.

2.52.4 Structural System Combined From Statically Indeterminate Elements

In reality, the separation of the multishell into simpler components does not necessarily need to be made as shown in Fig. 2.52-1(b). The separation can be performed as shown in Fig. 2.52-5,

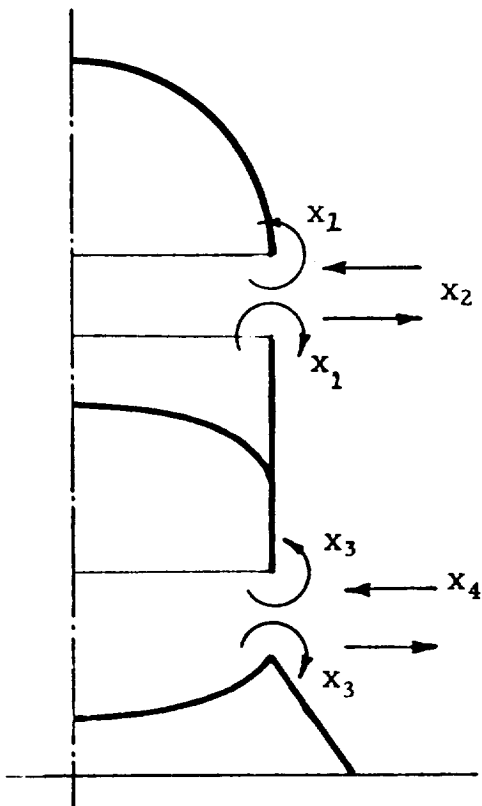


FIG. 2.52-5. Free-Body Diagram. The System is Divided Into the Statically Indeterminate Elements

but then the elements are of a "statically indeterminate" type. It does not change the philosophy, but the analysis will be much faster if formulas are available for the statically indeterminate elements subjected to the primary and secondary loadings, because fewer elements will be present. These influences can also be obtained by calculation if the collection of

formulas does not cover the particular case. As before, two cases are considered.

A. Case 1

The length of the element is such that the unit influences due to the unit loads on opposite edges will be overlapped. In other words, stresses due to the unit-loadings will depend, in every point of the shell, on both opposite edge unit-loadings. For this case the correspondent matrix is shown in Fig. 2.52-6.

| i | X ₁ | X ₂ | X ₃ | X ₄ | δ _{io} |
|---|----------------|----------------|----------------|----------------|-----------------|
| 1 | == | | — | — | δ ₁₀ |
| 2 | — | == | — | — | δ ₁₂ |
| 3 | — | — | == | — | δ ₁₃ |
| 4 | — | — | — | == | δ ₁₄ |

FIG. 2.52-6. The Matrix of Unknowns if the Boundary Disturbances at Opposite Boundaries are Influencing Each Other (Loads Method With the Statically Indeterminate Elements)

B. Case 2

The lengths of the elements are such that the unit influences due to the unit loading does not depend on unit loading of the opposite edge.

For such a case, the corresponding matrix is shown in Fig. 2.52-7.

| i | X ₁ | X ₂ | X ₃ | X ₄ | δ _{io} |
|---|----------------|----------------|----------------|----------------|-----------------|
| 1 | == | — | | | δ ₁₀ |
| 2 | — | == | | | δ ₂₀ |
| 3 | | | == | — | δ ₃₀ |
| 4 | | | — | == | δ ₄₀ |

FIG. 2.52-7. The Matrix of Unknowns if the Boundary Disturbances at Opposite Boundaries are not Influencing Each Other (Loads Method With Statically Indeterminate Elements)

In case 2, the system of four linear equations will be split into two independent systems of only two linear equations to make the solution simpler. Also, use of the externally statically indeterminate elements greatly reduces the number of the statically unknowns, thus making the solution much simpler.

The method of handling these systems was extensively explained, in detail in Section 2.23 of this chapter.

2.52.5 Conclusion

In this section, analysis of a "multishell system" by the set of linear algebraic equations was shown. This method was explained in general, since a detailed description was presented in the Introduction of this chapter.

To simplify the application of the method described, tables are presented in Subsection 2.54, containing the formulas for the edge-deformations due to different loadings of primary and secondary nature. The formulas in this section are shorter and simpler than the general formulas given in Section 2.30 because they cover the special cases of loads and displacements at the edge only. Use of these formulas simplifies the procedure.

2.53 DEFLECTION METHOD

2.53.1 Introduction

The deflection method is applicable to the solutions of statically indeterminate structures. To make simple comparisons between the previous method and this method, the same multishell system will be used. In general, if the deformations in any section of the shell are known, the loads at this section are also known.

2.53.2 Analysis

Designate the edge rotations with β_i and the end horizontal movements with $\Delta r = \delta_{Hi}$. Unknown deformations at any junction of statically determinate shell elements are shown in Fig. 2.53-1. Note that δ_{vi} (vertical movements) are negligible at junctions (3) and (4). Also note that there is 100-percent fixity at support in junction (1); consequently, all deformations are zero's.

The following deformations are unknown:

Rotations: $\beta_2, \beta_3, \beta_4$

Horizontal displacements: $\delta_{2H}, \delta_{3H}, \delta_{4H}$

Vertical displacements: δ_{2v}

Determination of the unknowns delineated is analogous to the known "slope deflection" method applicable to the rigid frames.

THE VALUES $\beta_1 = \delta_{H1} = \delta_{v1} = 0$.

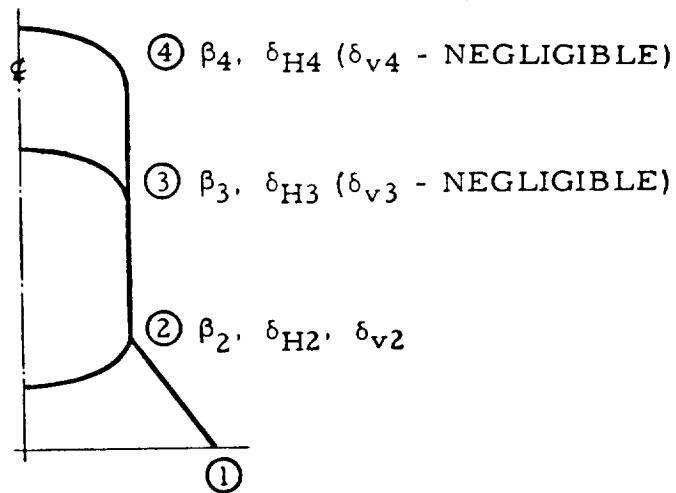


FIG. 2.53-1. Multishell With Statically Indeterminate Deformations

First, a 100-percent fixity against rotation and movement of each element is assumed. This can be determined by the "fixed-end-moments" and "fixed-end-loads," which are designated by M_x° and N_x° . In reality, these loads do not exist, and correspondingly, deformations β_i and δ_i will not be zero, but will be of such an amount to make M_x° and N_x° zero. For example, junction (2) will be rotated by some angle β_2 , resulting in the following moments at this junction:

$$M_{21}(\beta_2), M_{22}(\beta_2), M_{23}(\beta_2)$$

Similarly, junction 2 will be moved horizontally by the amount δ_{2H} , resulting in the moments

$$M_{21}(\delta_{2H}), M_{23}(\delta_{2H})$$

(moment $M_{22}(\delta_{2H})$ was neglected here, assuming the curvature of shell 2-2 to be small).

Also, junction (2) will be moved vertically to the amount δ_{2V} , resulting in the moment $M_{21}(\delta_{2V})$.

The adjusted junction(3) will be rotated in a similar manner, and will influence the joint (2) by delivering $M_{23}(\beta_3)$ to it. The joint (3) also moved horizontally by amount δ_{3H} , and again influenced joint (2) by delivering $M_{23}(\delta_{3H})$ to it. However, because of equilibrium which must be $\Sigma M_{2i} = 0$, this can be expressed algebraically as

$$M_2^o = M_{23}^o + M_{22}^o + M_{21}^o$$

then

$$\begin{aligned} M_2^o + M_{21}(\beta_2) + M_{22}(\beta_2) + M_{23}(\beta_2) \\ + M_{23}(\beta_3) + M_{21}(\delta_{2H}) + M_{23}(\delta_{2H}) \\ + M_{23}(\delta_{3H}) + M_{21}(\delta_{2V}) = 0 \end{aligned}$$

Similar equations can be derived for any junction (i), leading to the system of linear algebraic equations. Again, as in the previously described methods, two possibilities exist:

1. End-deformations of each shell element mutually influence each other (as was assumed in the example previously presented).
2. End-deformations of each shell element are independent of each other, and the stresses in the element always will be the function of only one end-deformation.

A corresponding matrix is given in Fig. 2.53-2 for case 1, and in Fig. 2.53-3 for case 2. Again, it can be noted that in case 2, the system will be reduced to three simple independent systems, thus making the solution faster.

| | β_4 | δ_{4H} | β_3 | δ_{3H} | β_2 | δ_{2H} | δ_{2V} | δ_{io} |
|---|-----------|---------------|-----------|---------------|-----------|---------------|---------------|---------------|
| 1 | == | --- | --- | --- | | | | δ_{10} |
| 2 | --- | == | --- | --- | | | | δ_{20} |
| 3 | --- | --- | == | --- | --- | --- | --- | δ_{30} |
| 4 | --- | --- | --- | == | --- | --- | --- | δ_{40} |
| 5 | --- | --- | --- | --- | == | --- | --- | δ_{50} |
| 6 | | | --- | --- | --- | == | --- | δ_{60} |
| 7 | | | --- | --- | --- | --- | == | δ_{70} |

FIG. 2.53-2. The Matrix of Unknowns if the Boundaries of Elements Influence Each Other. (Deflections Method)

| | β_4 | δ_{4H} | β_3 | δ_{3H} | β_2 | δ_{2H} | δ_{2V} | δ_{io} |
|---|-----------|---------------|-----------|---------------|-----------|---------------|---------------|---------------|
| 1 | == | --- | | | | | | δ_{10} |
| 2 | --- | == | | | | | | δ_{20} |
| 3 | | | == | | | | | δ_{30} |
| 4 | | | | == | | | | δ_{40} |
| 5 | | | | | == | --- | --- | δ_{50} |
| 6 | | | | | --- | == | --- | δ_{60} |
| 7 | | | | | --- | --- | == | δ_{70} |

FIG. 2.53-3. The Matrix of Unknowns if the Boundaries of Elements are far Enough and Consequently do not Influence Each Other (Deflections Method)

Similarly, as before, the use of statically indeterminate elements will reduce the number of equations and, consequently, simplify the solution. The tables are given in Section 2.54.

2.53.3 Conclusion

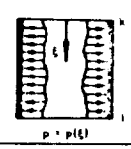
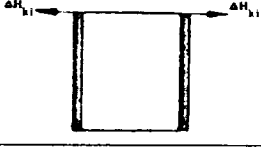
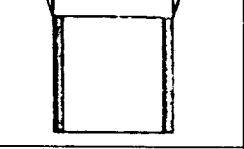
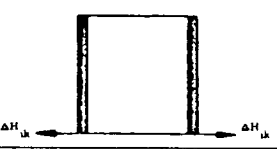
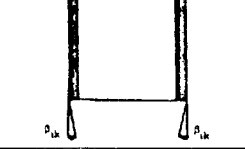
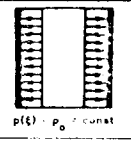
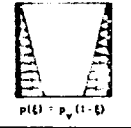
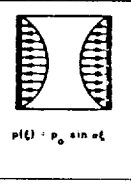
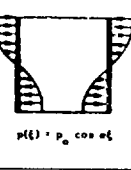
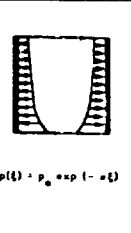
In this section, the outline of the special procedure for determining stresses and deformations in axisymmetrical multishell structures was presented. It was shown that the suggested procedure is analogous to the "slope-deflection" procedure usually applicable to the rigid frames. As soon as the statically indeterminate values are found, the stresses and deformations in any point of the structure can be determined in the usual manner.

A set of formulas was assembled by Hampe (Ref. 2-2) for faster determination of influences at the edges. These formulas are presented in the tables included in Section 2.54.

2.54 TABLES FOR MULTISHELL ANALYSIS

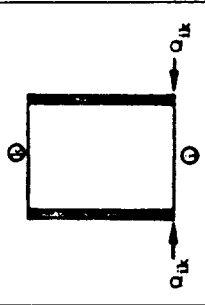
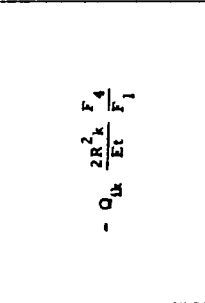
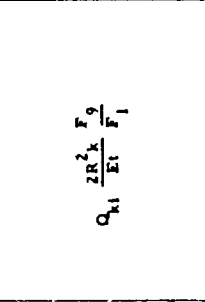
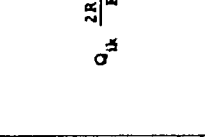
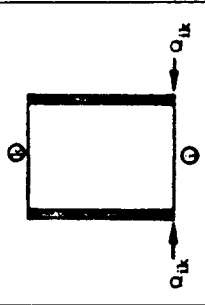
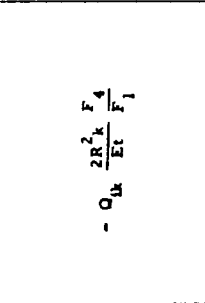
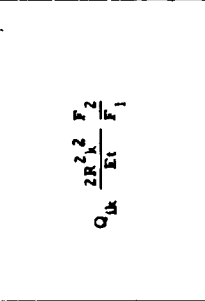
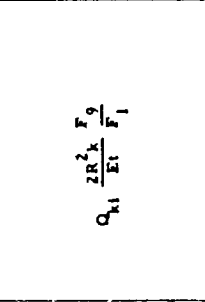
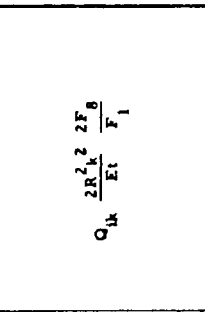
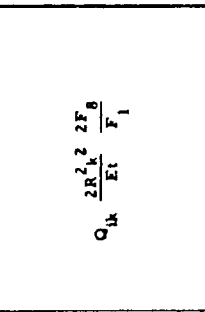
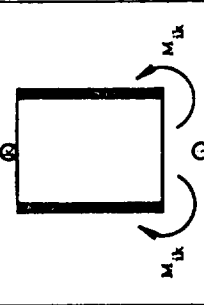
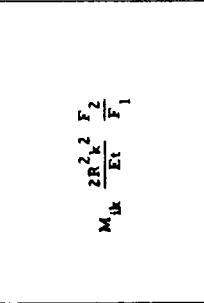
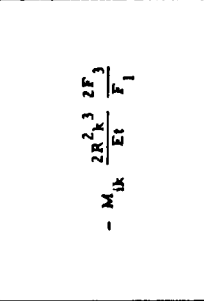
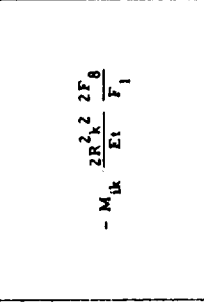
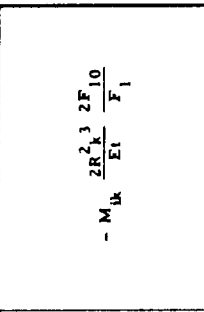
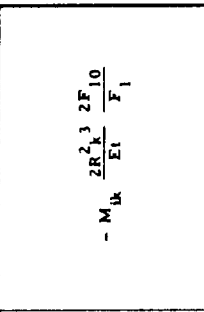
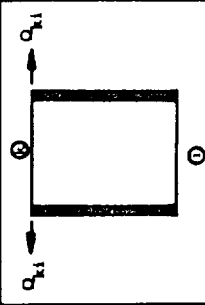
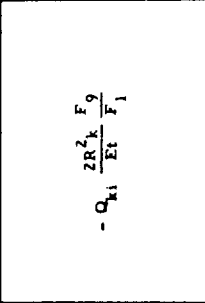
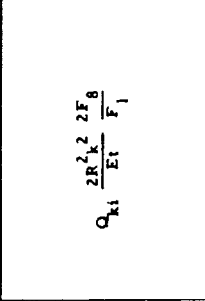
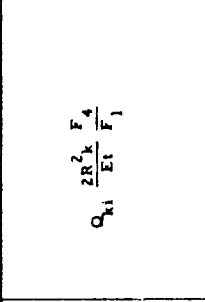
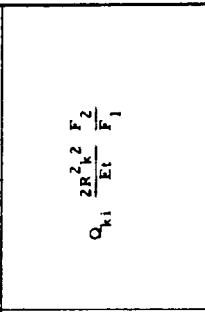
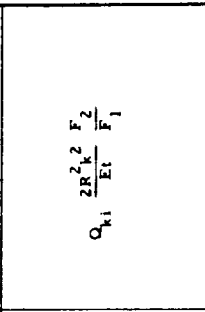
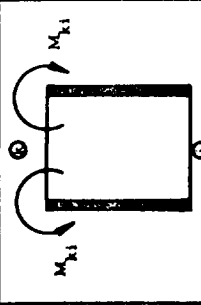
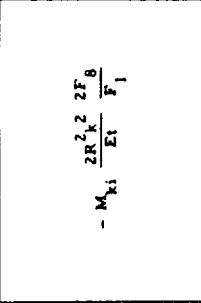
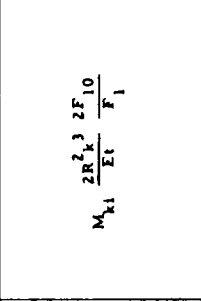
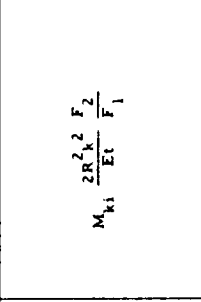
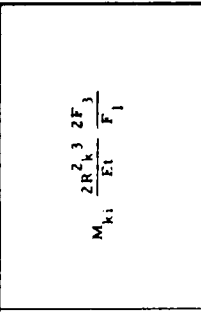
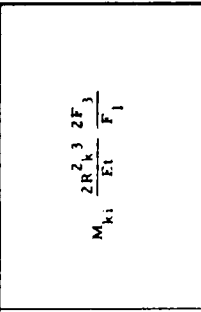
Tables 2.54-1 through -12 contain the formulas for the edge-deformations due to different loadings of primary and secondary nature. The formulas are shorter and simpler than those given in Section 2.30 because they cover the special cases of loads only at the boundary. Use of these formulas shortens the calculation. These tables present formulas for cylinders, cones, and spheres with different boundary conditions.

TABLE 2.54-1. CYLINDRICAL SHELL WITH FREE EDGES. EDGE DISTORTIONS DUE TO PRIMARY LOADINGS (Ref. 2-2)¹

| Shell Geometry | Boundary distortions | | | |
|---|---|---|---|---|
|  |  |  |  |  |
| Loading Condition | ΔH_{k1} | P_{k1} | ΔH_{1k} | P_{1k} |
|  | $\frac{p_0 R^2}{Et}$ | 0 | $\frac{p_0 R^2}{Et}$ | 0 |
|  | 0 | $-\frac{p_0 R^2}{EtL}$ | $\frac{p_0 R^2}{Et}$ | $-\frac{p_0 R^2}{EtL}$ |
|  | $\frac{p_0 R^2}{Et} \frac{4(DL)^4}{\alpha^4 + 4(DL)^4} \left[\sin \alpha \right. \\ \left. - \frac{2(DL)^2}{\alpha^2} \left(\frac{\alpha F_9}{F_1} - \frac{F_2}{F_1} \right) \sin \alpha \right. \\ \left. + \frac{\alpha}{KL} F_4 \cos \alpha \right]$ | $\frac{p_0 R^2}{Et} \frac{4(DL)^4}{\alpha^4 + 4(DL)^4} k \left[\frac{\alpha}{KL} \cos \alpha \right. \\ \left. + \frac{\alpha^2}{2(DL)^2} \left(\frac{2F_3}{F_1} \right) \sin \alpha \right. \\ \left. - \frac{\alpha}{KL} \frac{2F_8}{F_1} - \frac{\alpha}{KL} \frac{F_2}{F_1} \cos \alpha \right]$ | $\frac{p_0 R^2}{Et} \frac{\alpha^2}{2(DL)^2} \frac{4(DL)^4}{\alpha^4 + 4(DL)^4} \\ \left(\frac{\alpha F_4}{F_1} - \frac{2F_8}{F_1} \right) \sin \alpha \\ + \frac{\alpha}{KL} F_9 \cos \alpha$ | $\frac{p_0 R^2}{Et} \frac{4(DL)^4}{\alpha^4 + 4(DL)^4} k \left[\frac{\alpha}{KL} \right. \\ \left. - \frac{\alpha^2}{2(DL)^2} \left(\frac{\alpha F_2}{F_1} - \frac{2F_{10}}{F_1} \right) \sin \alpha \right. \\ \left. + \frac{\alpha}{KL} \frac{2F_8}{F_1} \cos \alpha \right]$ |
|  | $\frac{p_0 R^2}{Et} \frac{4(DL)^4}{\alpha^4 + 4(DL)^4} \left[\cos \alpha \right. \\ \left. - \frac{\alpha^2}{2(DL)^2} \left(\frac{2F_8}{F_1} - \frac{F_2}{F_1} \right) \cos \alpha \right. \\ \left. - \frac{\alpha}{KL} F_4 \sin \alpha \right]$ | $-\frac{p_0 R^2}{Et} \frac{4(DL)^4}{\alpha^4 + 4(DL)^4} k \left[\frac{\alpha}{KL} \sin \alpha \right. \\ \left. + \frac{\alpha^2}{2(DL)^2} \left(\frac{2F_{10}}{F_1} - \frac{2F_3}{F_1} \right) \cos \alpha \right. \\ \left. - \frac{\alpha}{KL} \frac{F_2}{F_1} \sin \alpha \right]$ | $\frac{p_0 R^2}{Et} \frac{4(DL)^4}{\alpha^4 + 4(DL)^4} \left[1 + \frac{\alpha^2}{2(DL)^2} \left(\frac{F_2}{F_1} - \frac{2F_8}{F_1} \right) \cos \alpha \right. \\ \left. - \frac{\alpha}{KL} F_9 \sin \alpha \right]$ | $-\frac{p_0 R^2}{Et} \frac{4(DL)^4}{\alpha^4 + 4(DL)^4} k \left[\frac{\alpha}{KL} \right. \\ \left. - \frac{\alpha^2}{2(DL)^2} \left(\frac{2F_3}{F_1} - \frac{2F_{10}}{F_1} \right) \cos \alpha - \frac{2F_8}{KL F_1} \sin \alpha \right]$ |
|  | $\frac{p_0 R^2}{Et} \frac{4(DL)^4}{\alpha^4 + 4(DL)^4} \left[\exp(-\alpha) \right. \\ \left. + \frac{\alpha^2}{2(DL)^2} \left(\frac{2F_8}{F_1} - \frac{\alpha F_9}{KL F_1} \right) \right. \\ \left. - \frac{\alpha^2}{2(DL)^2} \left(\frac{F_2}{F_1} \right) \right. \\ \left. + \frac{\alpha}{KL} \frac{F_4}{F_1} \exp(-\alpha) \right]$ | $-\frac{p_0 R^2}{Et} \frac{4(DL)^4}{\alpha^4 + 4(DL)^4} k \left[\frac{\alpha}{KL} \right. \\ \left. \exp(-\alpha) - \frac{\alpha^2}{2(DL)^2} \left(\frac{2F_{10}}{F_1} \right) \right. \\ \left. - \frac{\alpha}{KL} \frac{2F_8}{F_1} - \frac{\alpha^2}{2(DL)^2} \right. \\ \left. \left(\frac{2F_3}{F_1} + \frac{\alpha F_2}{KL F_1} \right) \exp(-\alpha) \right]$ | $\frac{p_0 R^2}{Et} \frac{4(DL)^4}{\alpha^4 + 4(DL)^4} \left[1 - \frac{\alpha^2}{2(DL)^2} \left(\frac{F_2}{F_1} - \frac{\alpha F_4}{KL F_1} \right) \right. \\ \left. + \frac{\alpha^2}{2(DL)^2} \left(\frac{2F_8}{F_1} + \frac{\alpha F_9}{KL F_1} \right) \exp(-\alpha) \right]$ | $-\frac{p_0 R^2}{Et} \frac{4(DL)^4}{\alpha^4 + 4(DL)^4} k \left[\frac{\alpha}{KL} - \frac{\alpha^2}{2(DL)^2} \left(\frac{2F_3}{F_1} - \frac{F_2}{KL F_1} \right) \right. \\ \left. + \frac{\alpha^2}{2(DL)^2} \right. \\ \left. \left(\frac{2F_{10}}{F_1} + \frac{\alpha F_2}{KL F_1} \right) \exp(-\alpha) \right]$ |

¹For F factors, see paragraph 2.42.6
For k factors, see paragraph 2.42.6

TABLE 2.54-2. CONICAL SHELL, FREE EDGES. EDGE DISTORTIONS DUE TO PRIMARY LOADINGS¹

| Loading Condition | Edge Distortions |  |  |  |  |
|---|---|--|---|---|---|
|  |  |  |  |  |  |
|  |  |  |  |  |  |
|  |  |  |  |  |  |
|  |  |  |  |  |  |

¹For F factors, see paragraph 2.42.6
For k factors, see paragraph 2.42.6

TABLE 2.54-3. CONICAL SHELL WITH FREE EDGES. EDGE DISTORTIONS DUE TO PRIMARY LOADINGS

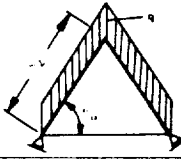
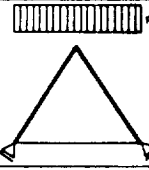
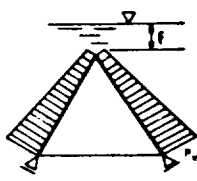
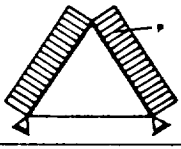
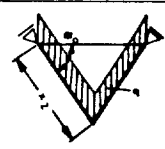
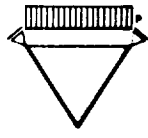
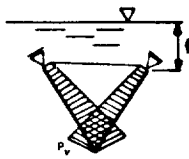
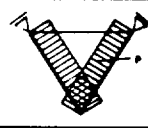
| Edge Distortions | | | |
|---|---|--|---------|
| Loading Condition | Fig. 2 | Fig. 3 | Fig. 4 |
|  | $-\frac{q r_0^2}{E t} \cot \alpha_0 \left(\cos^2 \alpha_0 - \frac{\nu}{2} \right)$ | $\frac{q r_0^2}{E t} \frac{\cos \alpha_0}{\sin^2 \alpha_0} \left[\cos^2 \alpha_0 (2 + \nu) - \frac{1}{2} - \nu \right]$ | |
|  | $-\frac{p r_0^2}{E t} \cos \alpha_0 \cot \alpha_0 \left(\cos^2 \alpha_0 - \frac{\nu}{2} \right)$ | $\frac{p r_0^2}{E t} \cos^2 \alpha_0 \left[\cos^2 \alpha_0 (2 + \nu) - \frac{1}{2} - \nu \right]$ | |
|  | $\frac{P r_0^2}{E t} \cos^2 \alpha_0 \left[\frac{f}{\sin \alpha_0} \left(\frac{1}{2} - \nu \right) + \nu \left(\frac{\nu}{2} - 1 \right) \right]$ | $\frac{P r_0^2}{E t} \frac{\cos^2 \alpha_0}{\sin \alpha_0} \left(\frac{1}{2} \frac{f}{\sin \alpha_0} + \frac{\nu}{2} \nu \right)$ | |
|  | $-\frac{p r_0^2}{E t} \cos \alpha_0 \cot \alpha_0 \left(1 - \frac{\nu}{2} \right)$ | $-\frac{p r_0^2}{E t} \frac{1}{2} \cos^2 \alpha_0$ | |
| Edge Distortion | Fig. 5 | Fig. 6 | Fig. 7 |
| Loading Condition | Fig. 8 | Fig. 9 | Fig. 10 |
|  | $\frac{q r_0^2}{E t} \cos \alpha_0 \left(\cos^2 \alpha_0 - \frac{\nu}{2} \right)$ | $\frac{q r_0^2}{E t} \frac{\cos \alpha_0}{\sin^2 \alpha_0} \left[\cos^2 \alpha_0 (2 + \nu) - \frac{1}{2} - \nu \right]$ | |
|  | $\frac{p r_0^2}{E t} \cos \alpha_0 \cot \alpha_0 \left(\cos^2 \alpha_0 - \frac{\nu}{2} \right)$ | $\frac{p r_0^2}{E t} \cot^2 \alpha_0 \left[\cos^2 \alpha_0 (2 + \nu) - \frac{1}{2} - \nu \right]$ | |
|  | $-\frac{P r_0^2}{E t} \cos^2 \alpha_0 \cdot \left[\frac{f}{\sin \alpha_0} \left(\frac{\nu}{2} - 1 \right) + \nu \left(\frac{\nu}{2} - 1 \right) \right]$ | $\frac{P r_0^2}{E t} \frac{\cos^2 \alpha_0}{\sin \alpha_0} \left(\frac{1}{2} \frac{f}{\sin \alpha_0} - \frac{\nu}{2} \nu \right)$ | |
|  | $-\frac{p r_0^2}{E t} \cos \alpha_0 \cot \alpha_0 \left(1 - \frac{\nu}{2} \right)$ | $-\frac{p r_0^2}{E t} \frac{1}{2} \cos^2 \alpha_0$ | |

TABLE 2.54-4. CONICAL SEGMENT WITH FREE EDGES, EDGE DISTORTIONS DUE TO PRIMARY LOADINGS

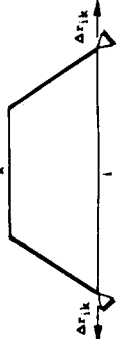
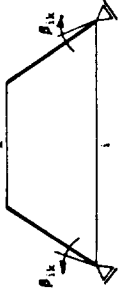
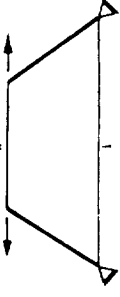
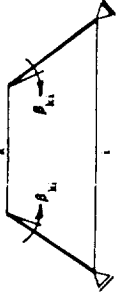
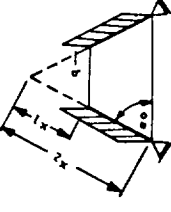
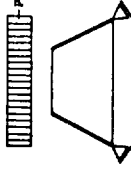
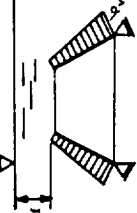
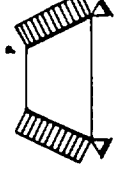
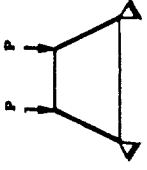
| Edge Distortion Loading Condition |  |  |  |  |
|---|---|---|--|---|
|  | $-\frac{q x_2^2 \cos \epsilon_0}{Et} \left[2 \cos^2 \epsilon_0 - \mu \left(1 - \frac{x_1^2}{x_2^2} \right) \right]$ | $\frac{q x_2 \cos \epsilon_0}{Et} \frac{\cos \epsilon_0}{2 \sin^2 \epsilon_0} \left[2 \cos^2 \epsilon_0 (2 + \mu) - 1 - 2\mu + \left(\frac{x_1}{x_2} \right)^2 \right]$ | $-\frac{q x_1^2 \cos^3 \epsilon_0}{Et} \frac{\cos^3 \epsilon_0}{2 \sin \epsilon_0}$ | $\frac{q x_1 \cos^2 \epsilon_0}{Et} \frac{\cos^2 \epsilon_0}{\sin^2 \epsilon_0} \left[\cos^2 \epsilon_0 (2 + \mu) - \mu \right]$ |
|  | $-\frac{P x_2^2 \cos^2 \epsilon_0}{Et} \frac{\cos^2 \epsilon_0}{2 \sin \epsilon_0} \left[2 \cos^2 \epsilon_0 - \mu \left(1 - \frac{x_1^2}{x_2^2} \right) \right]$ | $\frac{P x_2 \cos^2 \epsilon_0}{Et} \frac{\cos^2 \epsilon_0}{2} \left[2 \cos^2 \epsilon_0 (2 + \mu) - 1 - 2\mu + \left(\frac{x_1}{x_2} \right)^2 \right]$ | $-\frac{P x_1^2 \cos^4 \epsilon_0}{Et} \frac{\cos^4 \epsilon_0}{\sin \epsilon_0}$ | $\frac{P x_1 \cot^2 \epsilon_0}{Et} \frac{\cot^2 \epsilon_0}{\sin^2 \epsilon_0} \left[\cos^2 \epsilon_0 (2 + \mu) - \mu \right]$ |
|  | $\frac{P x_2^2 \cos^2 \epsilon_0}{Et} \frac{\cos^2 \epsilon_0}{3} \left[\frac{l}{2 \sin \epsilon_0} \left(1 - \frac{x_1^2}{x_2^2} \right) + \frac{x_2}{3} \left(1 - \frac{x_1^2}{x_2^2} \right) - \frac{l}{\sin \epsilon_0} - x_2 \right]$ | $\frac{P x_2^2 \cos^2 \epsilon_0}{Et} \frac{\cos^2 \epsilon_0}{\sin \epsilon_0} \left[\frac{l}{2 \sin \epsilon_0} \left(3 + \frac{x_1^2}{x_2^2} \right) + \frac{x_2}{3} \left(8 + \frac{x_1^2}{x_2^2} \right) \right]$ | $-\frac{P x_1^2 \cos^2 \epsilon_0}{Et} \frac{\cos^2 \epsilon_0}{\sin \epsilon_0} \left(\frac{l}{\sin \epsilon_0} + x_1 \right)$ | $\frac{P x_1 \cot^2 \epsilon_0}{Et} \frac{\cot^2 \epsilon_0}{\sin \epsilon_0} \left(\frac{2l}{\sin \epsilon_0} + 3 x_1 \right)$ |
|  | $-\frac{P x_2^2 \cos \epsilon_0 \cot \epsilon_0}{Et} \left[1 - \frac{x_1^2}{x_2^2} \left(1 - \frac{x_1^2}{x_2^2} \right) \right]$ | $\frac{P x_2 \cos^2 \epsilon_0}{Et} \frac{\cos^2 \epsilon_0}{2} \left[3 + \left(\frac{x_1}{x_2} \right)^2 \right]$ | $-\frac{P x_1^2 \cos \epsilon_0 \cot \epsilon_0}{Et}$ | $-\frac{P x_1 \cot^2 \epsilon_0}{Et}$ |
|  | $\frac{P x_1 \cot \epsilon_0}{Et}$ | $\frac{P \cot \epsilon_0 x_1}{Et} \frac{\cot \epsilon_0}{\sin \epsilon_0} \frac{x_1}{x_2}$ | $\frac{P x_1 \mu \cot \epsilon_0}{Et}$ | $\frac{P \cot \epsilon_0}{Et} \frac{\cot \epsilon_0}{\sin \epsilon_0}$ |

TABLE 2.54-4. (CONT)

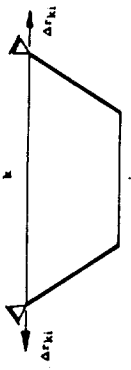
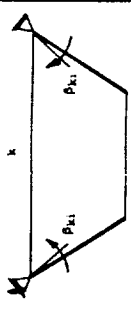
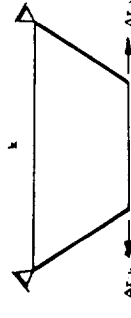

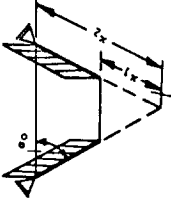
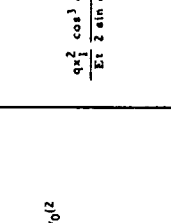
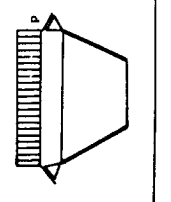
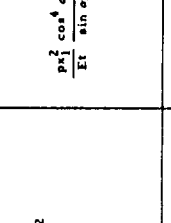
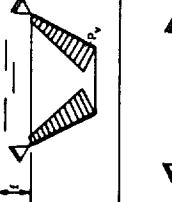
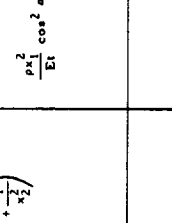
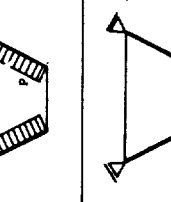
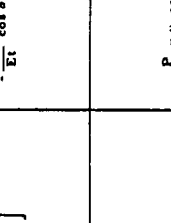
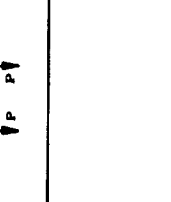
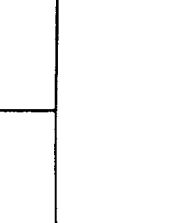
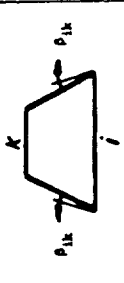
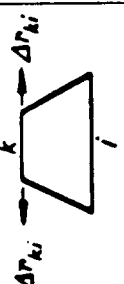
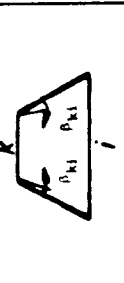
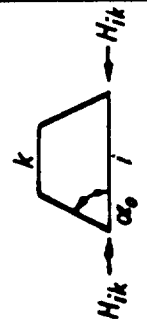
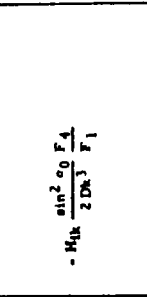
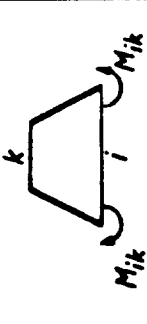
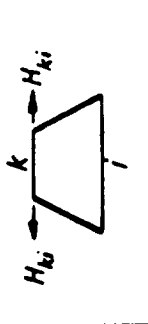
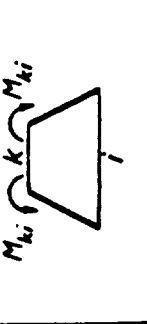
| Edge Distortion | Loading Condition |  |  |  |  |
|---|---|---|--|--|--|
|  |  | $\frac{qx_2^2 \cot \epsilon_0}{Et} \frac{2}{2} \left[2 \cos^2 \epsilon_0 - \mu \left(1 - \frac{x_1^2}{x_2^2} \right) \right]$ | $\frac{qx_2^2 \cot \epsilon_0}{Et} \frac{2 \cos^2 \epsilon_0}{2} \left[2 \cos^2 \epsilon_0 (2 + \mu) - 1 - 2\mu + \left(\frac{x_1}{x_2} \right)^2 \right]$ | $\frac{qx_2^2 \cot^3 \epsilon_0}{Et} \frac{2 \sin \epsilon_0}{2 \sin \epsilon_0}$ | $\frac{qx_1 \cos \epsilon_0}{Et \sin^2 \epsilon_0} \left[\cos^2 \epsilon_0 (2 + \mu) - \mu \right]$ |
|  |  | $\frac{px_2^2 \cos^2 \epsilon_0}{Et} \frac{2 \cos^2 \epsilon_0}{2 \sin \epsilon_0} \left[2 \cos^2 \epsilon_0 - \mu \left(1 - \frac{x_1^2}{x_2^2} \right) \right]$ | $\frac{px_2^2 \cos^2 \epsilon_0}{Et} \frac{2 \cos^2 \epsilon_0}{2} \left[2 \cos^2 \epsilon_0 (2 + \mu) - 1 - 2\mu + \left(\frac{x_1}{x_2} \right)^2 \right]$ | $\frac{px_2^2 \cos^4 \epsilon_0}{Et \sin \epsilon_0}$ | $\frac{px_1 \cot^2 \epsilon_0}{Et} \left[\cos^2 \epsilon_0 (2 + \mu) - \mu \right]$ |
|  |  | $\frac{px_2^2 \cos^2 \epsilon_0}{Et} \left\{ \left[\frac{x_2}{3} \left(1 - \frac{x_1}{x_2} \right) \right] - \frac{l}{2 \sin \epsilon_0} \left(1 - \frac{x_1^2}{x_2^2} \right) + \frac{l}{\sin \epsilon_0} x_2 \right\}$ | $\frac{px_2 \cos^2 \epsilon_0}{Et \sin \epsilon_0} \left[\frac{l}{3} \left(\frac{x_1}{x_2} \right)^2 - \frac{x_2}{3} \left(\frac{x_1}{x_2} \right) \right]$ | $\frac{px_1^2 \cos^2 \epsilon_0}{Et} \cos^2 \epsilon_0 \left(\frac{l}{\sin \epsilon_0} - x_1 \right)$ | $\frac{px_1 \cos^2 \epsilon_0}{Et \sin \epsilon_0} \left(\frac{2}{\sin \epsilon_0} - 3x_1 \right)$ |
|  |  | $-\frac{px_2^2 \cos \epsilon_0 \cot \epsilon_0}{Et} \left[1 - \frac{x_1}{2} \left(1 - \frac{x_1}{x_2} \right) \right]$ | $-\frac{px_2^2 \cos^2 \epsilon_0}{Et} \frac{2 \cos^2 \epsilon_0}{2} \left[3 + \left(\frac{x_1}{x_2} \right)^2 \right]$ | $-\frac{px_1^2}{Et} \cos \epsilon_0 \cot \epsilon_0$ | $-\frac{px_1}{Et} 2 \cot^2 \epsilon_0$ |
|  |  | $-\frac{P}{Et} x_1 \mu \cot \epsilon_0$ | $-\frac{P \cot \epsilon_0 x_1}{Et \sin \epsilon_0 x_2}$ | $-\frac{P}{Et} x_1 \mu \cot \epsilon_0$ | $-\frac{P \cot \epsilon_0}{Et \sin \epsilon_0}$ |

TABLE 2.54-5. CONICAL SEGMENT WITH FREE EDGES. EDGE DISTORTIONS DUE TO SECONDARY LOADINGS (Ref. 2-2)¹

| Loading Condition | Edge Distortion |  |  |  |
|---|---|--|---|---|
|  |  | $+\frac{\sin^2 \alpha_0 F_4}{2 DK^3 F_1}$ | $+\frac{\sin^2 \alpha_0 F_9}{2 DK^3 F_1}$ | $+\frac{\sin \alpha_0 F_8}{2 DK^2 F_1}$ |
|  | $+\frac{\sin \alpha_0 F_2}{2 DK F_1}$ | $+\frac{\sin \alpha_0 F_2}{2 DK^2 F_1}$ | $-\frac{\sin \alpha_0 F_8}{2 DK^2 F_1}$ | $-\frac{1}{2 DK} \frac{2F_{10}}{F_1}$ |
|  | $-\frac{\sin^2 \alpha_0 F_4}{2 DK^3 F_1}$ | $+\frac{\sin \alpha_0 F_8}{2 DK^2 F_1}$ | $+\frac{\sin^2 \alpha_0 F_9}{2 DK^3 F_1}$ | $+\frac{\sin \alpha_0 F_2}{2 DK^2 F_1}$ |
|  | $-\frac{\sin \alpha_0 F_2}{2 DK F_1}$ | $+\frac{\sin \alpha_0 F_2}{2 DK^2 F_1}$ | $+\frac{\sin \alpha_0 F_8}{2 DK^2 F_1}$ | $+\frac{1}{2 DK} \frac{2F_{10}}{F_1}$ |

¹For F factors, see paragraph 2.42.6
For k factors, see paragraph 2.42.6

TABLE 2.54-6. SPHERICAL SHELL WITH FREE EDGES. EDGE DISTORTIONS DUE TO PRIMARY LOADING (Ref. 2-2)



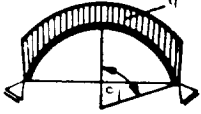
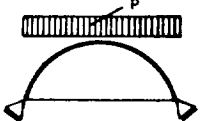
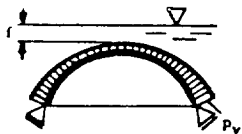
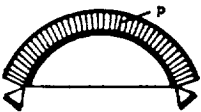
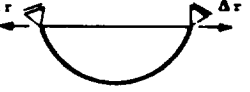

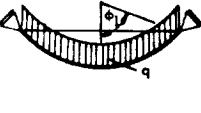
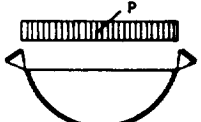
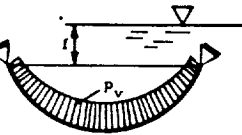
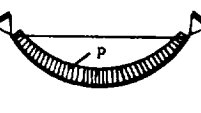
| Edge Distortions / Loading Condition |  |  |
|---|---|---|
|  | $\frac{R^2 q}{Et} \sin \phi_1 \left[-\cos \phi_1 + \frac{1 + \mu}{\sin^2 \phi_1} (-\cos \phi_1 + 1) \right]$ | $-\frac{Rq}{Et} (2 + \mu) \sin \phi_1$ |
|  | $\frac{R^2 p}{Et} \sin \phi_1 \left(-\cos^2 \phi_1 + \frac{1 + \mu}{2} \right)$ | $\frac{Rp}{Et} (3 + \mu) \sin \phi_1 \cos \phi_1$ |
|  | $-\frac{pR^3}{6Et} \sin \phi_1 \left[3 \left(1 + \frac{f}{R} \right) (1 - \mu) - 6 \cos \phi_1 - 2 \frac{1 + \mu}{\sin^2 \phi_1} (\cos^3 \phi_1 - 1) \right]$ | $\frac{pR^2}{Et} \sin \phi_1$ |
|  | $-\frac{R^2 p}{2Et} (1 - \mu) \sin \phi_1$ | 0 |
| Edge Distortions / Loading Condition |  |  |
|  | $-\frac{R^2 q}{Et} \sin \phi_1 \left[-\cos \phi_1 + \frac{1 + \mu}{\sin^2 \phi_1} (-\cos \phi_1 + 1) \right]$ | $-\frac{Rq}{Et} (2 + \mu) \sin \phi_1$ |
|  | $-\frac{R^2 p}{Et} \sin \phi_1 \left(-\cos^2 \phi_1 + \frac{1 + \mu}{2} \right)$ | $-\frac{Rp}{Et} (3 + \mu) \sin \phi_1 \cos \phi_1$ |
|  | $+\frac{pR^3}{6Et} \sin \phi_1 \left[3 \left(1 + \frac{f}{R} \right) (1 - \mu) - 6 \cos \phi_1 - 2 \frac{1 + \mu}{\sin^2 \phi_1} (\cos^3 \phi_1 - 1) \right]$ | $-\frac{pR^2}{Et} \sin \phi_1$ |
|  | $\frac{R^2 p}{Et} (1 - \mu) \sin \phi_1$ | 0 |

TABLE 2.54-7. SPHERICAL SEGMENT WITH FREE EDGES, EDGE DISTORTIONS DUE TO PRIMARY LOADINGS (Ref. 2-2)


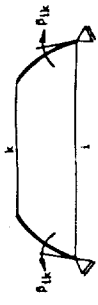

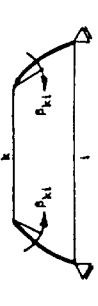
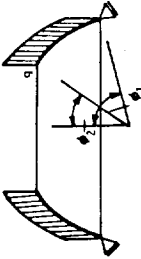
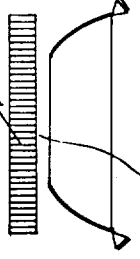
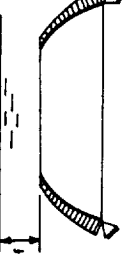


| Edge Distortions Loading Condition |  |  |  |  |
|---|--|--|---|---|
|  | $\frac{Rq}{Et} \sin \phi_1 \left[-\cos \phi_1 + \frac{1+\mu}{\sin^2 \phi_1} (-\cos \phi_1 + \cos \phi_2) \right]$ | $-\frac{Rq}{Et} (2+\mu) \sin \phi_1$ | $-\frac{R^2 q}{Et} \sin \phi_2 \cos \phi_2$ | $-\frac{Rq}{Et} (2+\mu) \sin \phi_2$ |
|  | $\frac{R^2 P}{Et} \sin \phi_1 \left[-\cos^2 \phi_1 + \frac{1+\mu}{\left(1 - \frac{\sin^2 \phi_2}{\sin^2 \phi_1}\right)} \right]$ | $-\frac{RP}{Et} (3+\mu) \sin \phi_1 \cos \phi_1$ | $-\frac{R^2 P}{Et} \sin \phi_2 \cos^2 \phi_2$ | $-\frac{RP}{Et} (3+\mu) \sin \phi_2 \cos \phi_2$ |
|  | $\frac{PR^3}{6Et} \sin \phi_1 \left[3 \left(1 + \frac{1}{R}\right) \left(1 - \mu + (1+\mu) \frac{\sin^2 \phi_2}{\sin^2 \phi_1}\right) - 6 \cos \phi_1 + 2(1+\mu) \frac{\cos^3 \phi_2 - \cos^3 \phi_1}{\sin^2 \phi_1} \right]$ | $+\frac{PR^2}{Et} \sin \phi_1$ | $-\frac{PR^3}{Et} \sin \phi_2 \left(1 + \frac{1}{R} - \cos \phi_2\right)$ | $+\frac{PR^2}{Et} \sin \phi_2$ |
|  | $-\frac{R^2 P}{Et} \sin \phi_1 \left[1 - \frac{1+\mu}{2} \left(1 - \frac{\sin^2 \phi_2}{\sin^2 \phi_1}\right) \right]$ | 0 | $-\frac{R^2 P}{Et} \sin \phi_2$ | 0 |
|  | $\frac{PR}{Et} (1+\mu) \frac{\sin \phi_2}{\sin \phi_1}$ | 0 | $\frac{PR}{Et} (1+\mu)$ | 0 |

TABLE 2.54-7. (CONT)


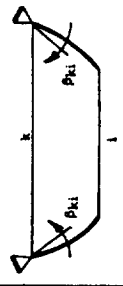
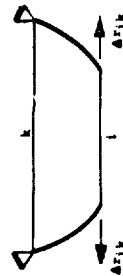
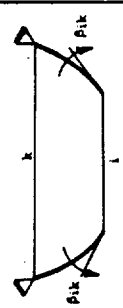
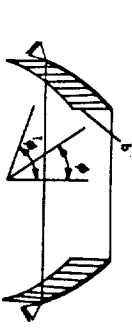
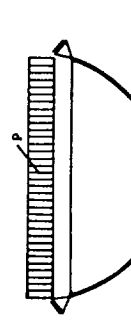

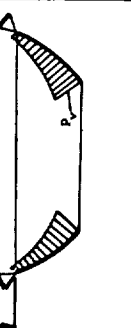
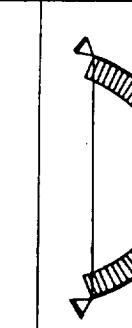
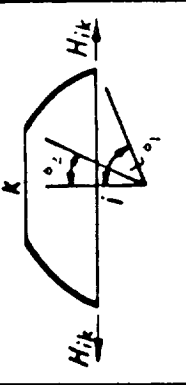
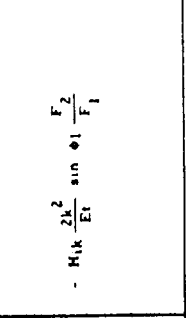
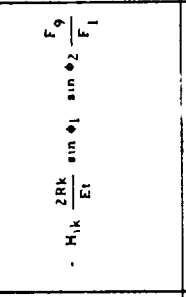
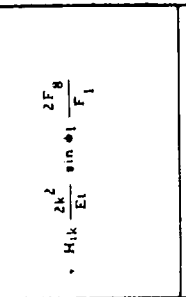
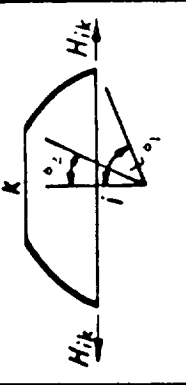
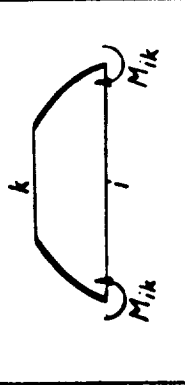
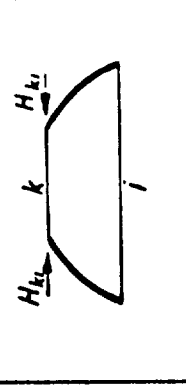
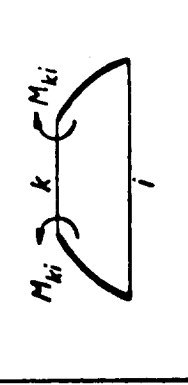
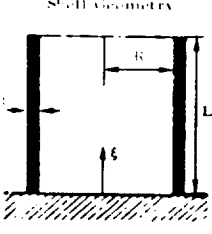
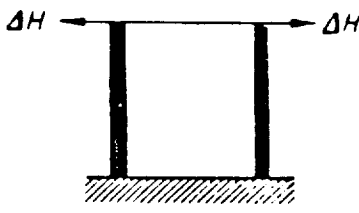
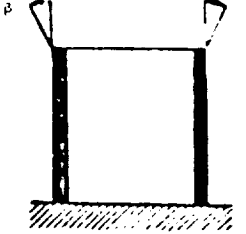
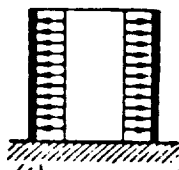
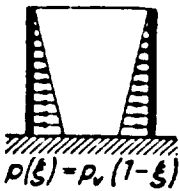
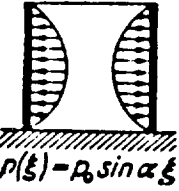
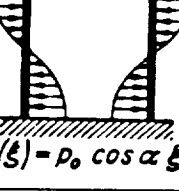
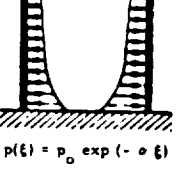
| | | | |
|--|--|---|---|
| <p>Edge Distortion</p>  |  |  |  |
| <p>Loading Condition</p>  | $-\frac{R^2 q}{Et} \sin \phi_1 \left[-\cos \phi_1 + \frac{1+\mu}{2} \frac{1}{\sin \phi_1} \right]$ $(-\cos \phi_1 + \cos \phi_2)$ | $-\frac{Rq}{Et} (2+\mu) \sin \phi_1$ | $-\frac{Rq}{Et} (2+\mu) \sin \phi_2$ |
|  | $-\frac{R^2 P}{Et} \sin \phi_1 \left[-\cos^2 \phi_1 + \frac{1+\mu}{2} \left(1 - \frac{\sin^2 \phi_2}{\sin^2 \phi_1} \right) \right]$ | $-\frac{Rp}{Et} (3+\mu) \sin \phi_1 \cos \phi_1$ | $-\frac{Rp}{Et} (3+\mu) \sin \phi_2 \cos \phi_2$ |
|  | $\frac{PR^3}{6Et} \sin \phi_2 \left\{ 3 \left(1 + \frac{l}{R} \right) \left[1 - \mu + (1+\mu) \frac{\sin^2 \phi_2}{\sin^2 \phi_1} \right] - 6 \cos \phi_2 + 2(1+\mu) \frac{\cos^3 \phi_2 - \cos^3 \phi_1}{\sin^2 \phi_1} \right\}$ | $-\frac{PR^2}{Et} \sin \phi_1$ | $+\frac{PR^3}{Et} \sin \phi_2 \left(1 + \frac{l}{R} - \cos \phi_2 \right)$ |
|  | $\frac{R^2 P}{Et} \sin \phi_1 \left[1 - \frac{1+\mu}{2} \left(1 - \frac{\sin^2 \phi_2}{\sin^2 \phi_1} \right) \right]$ | 0 | 0 |
|  | $-\frac{PR}{Et} (1+\mu) \frac{\sin \phi_2}{\sin \phi_1}$ | 0 | 0 |

TABLE 2.54-8. SPHERICAL SEQUENT, FREE EDGES-EDGE DISTORTIONS DUE TO SECONDARY LOADINGS (Ref. 2-2)¹

| Edge-Distortions Loading Condition |  |  |  |  |
|---|---|--|---|---|
|  | $+ M_{ik} \frac{2Rk}{Et} \sin^2 \phi_1 \frac{F_4}{F_1}$ | $- M_{ik} \frac{2k^2}{Et} \sin \phi_1 \frac{F_2}{F_1}$ | $- M_{ik} \frac{2Rk}{Et} \sin \phi_1 \sin \phi_2 \frac{F_9}{F_1}$ | $+ M_{ik} \frac{2k^2}{Et} \sin \phi_1 \frac{2F_8}{F_1}$ |
|  | $- M_{ik} \frac{2k^2}{Et} \sin \phi_1 \frac{F_2}{F_1}$ | $+ M_{ik} \frac{2k^3}{EtR} \frac{2F_3}{F_1}$ | $- M_{ik} \frac{2k^2}{Et} \sin \phi_2 \frac{2F_8}{F_1}$ | $+ M_{ik} \frac{2k^3}{EtR} \frac{2F_{10}}{F_1}$ |
|  | $+ M_{ki} \frac{2Rk}{Et} \sin \phi_1 \sin \phi_2 \frac{F_9}{F_1}$ | $- M_{ki} \frac{2k^2}{Et} \sin \phi_2 \frac{2F_8}{F_1}$ | | $- M_{ki} \frac{2k^2}{Et} \sin \phi_2 \frac{F_2}{F_1}$ |
|  | $- M_{ki} \frac{2k^2}{Et} \sin \phi_1 \frac{2F_8}{F_1}$ | $- M_{ki} \frac{2k^3}{EtR} \frac{2F_{10}}{F_1}$ | | $+ M_{ki} \frac{2k^3}{EtR} \frac{2F_3}{F_1}$ |

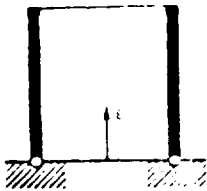
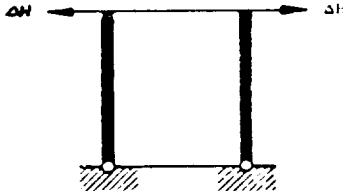
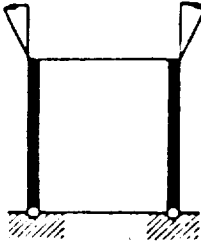
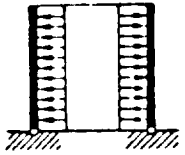
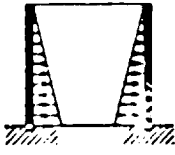
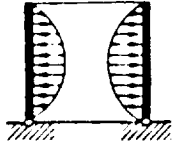
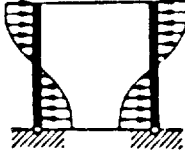
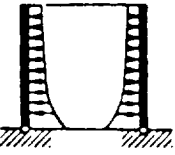
¹For F and k factors, see paragraph 2.42.6

TABLE 2.54-9. CYLINDRICAL SHELL WITH ONE EDGE FREE, OTHER EDGE FIXED. EDGE DISTORTIONS DUE TO PRIMARY LOADING (Ref. 2-2)¹

|  <p>Shell geometry</p> |  <p>ΔH = Deflection</p> |  <p>β = Rotation of Edge</p> |
|--|--|--|
|  <p>$p(\xi) = p_0 = \text{const}$</p> | $p_0 \frac{R^2}{Et} \left(1 - \frac{2F_7}{F_1 + 2} \right)$ | $p_0 \frac{R^2 k}{Et} \frac{2F_9}{F_1 + 2}$ |
|  <p>$p(\xi) = p_0(1 - \xi)$</p> | $p_0 \frac{R^2}{Et} \left(\frac{1}{kL} \frac{F_{10}}{F_1 + 2} - \frac{2F_7}{F_1 + 2} \right)$ | $-\frac{R^2 p_0}{EtL} \left(1 - kL \frac{2F_9}{F_1 + 2} - \frac{2F_7}{F_1 + 2} \right)$ |
|  <p>$p(\xi) = p_0 \sin \alpha \xi$</p> | $\frac{p_0 R^2}{Et} \frac{4(kL)^4}{\alpha^4 + 4(kL)^4} \left[\sin \alpha - \frac{\alpha}{kL} \frac{F_{10}}{F_1 + 2} + \frac{\alpha^2}{2(kL)^2} \left(\frac{F_2}{F_1 + 2} \sin \alpha - \frac{\alpha}{kL} \frac{F_4}{F_1 + 2} \cos \alpha \right) \right]$ | $\frac{p_0 R^2 k}{Et} \frac{4(kL)^4}{\alpha^4 + 4(kL)^4} \left[\frac{\alpha}{kL} \cos \alpha - \frac{\alpha}{kL} \frac{2F_7}{F_1 + 2} + \frac{\alpha^2}{2(kL)^2} \left(\frac{2F_3}{F_1 + 2} \sin \alpha - \frac{\alpha}{kL} \frac{F_2}{F_1 + 2} \cos \alpha \right) \right]$ |
|  <p>$p(\xi) = p_0 \cos \alpha \xi$</p> | $\frac{p_0 R^2}{Et} \frac{4(kL)^4}{\alpha^4 + 4(kL)^4} \left[\cos \alpha - \frac{2F_7}{F_1 + 2} + \frac{\alpha^2}{2(kL)^2} \left(\frac{F_2}{F_1 + 2} \cos \alpha + \frac{\alpha}{kL} \frac{F_4}{F_1 + 2} \sin \alpha \right) \right]$ | $-\frac{p_0 R^2 k}{Et} \frac{4(kL)^4}{\alpha^4 + 4(kL)^4} \left[\frac{\alpha}{kL} \sin \alpha - \frac{2F_9}{F_1 + 2} - \frac{\alpha^2}{2(kL)^2} \left(\frac{2F_3}{F_1 + 2} \cos \alpha + \frac{\alpha}{kL} \frac{F_2}{F_1 + 2} \sin \alpha \right) \right]$ |
|  <p>$p(\xi) = p_0 \exp(-\alpha \xi)$</p> | $p_0 \frac{R^2}{Et} \frac{4(kL)}{\alpha^4 + 4(kL)^4} \left[\exp(-\alpha) - \frac{2F_7}{F_1 + 2} + \frac{\alpha}{kL} \frac{F_{10}}{F_1 + 2} + \frac{\alpha^2}{2(kL)^2} \left(\frac{F_2}{F_1 + 2} + \frac{\alpha}{kL} \frac{F_4}{F_1 + 2} \exp(-\alpha) \right) \right]$ | $-\frac{p_0 R^2 k}{Et} \frac{4(kL)^4}{\alpha^4 + 4(kL)^4} \left[\frac{\alpha}{kL} \exp(-\alpha) - \frac{2F_9}{F_1 + 2} - \frac{\alpha}{kL} \frac{2F_7}{F_1 + 2} + \frac{\alpha^2}{2(kL)^2} \left(\frac{2F_3}{F_1 + 2} + \frac{\alpha}{kL} \frac{F_2}{F_1 + 2} \right) \exp(-\alpha) \right]$ |



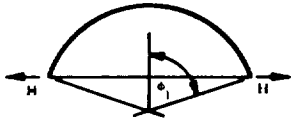

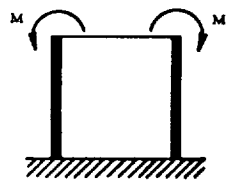
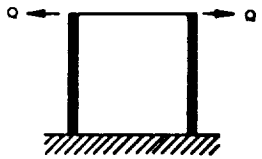
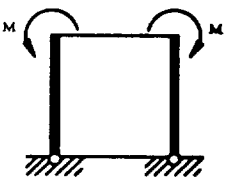
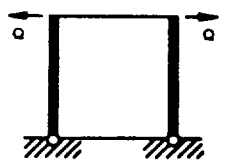
¹For F and k factors, see paragraph 2.42.6

TABLE 2.54-10. CYLINDRICAL SHELL WITH ONE BOUNDARY SIMPLY SUPPORTED OTHER FREE. EDGE INFLUENCE DUE TO PRIMARY LOADING (Ref. 2-2)¹

|  |  |  |
|--|--|---|
| Loading Condition | ΔH - deflection | β - rotation |
|  <p>$p(\xi) = p_0 \text{ const}$</p> | $\frac{p_0 R^2}{Et} \left(1 + \frac{F_9}{F_4} \right)$ | $-\frac{p_0 R^2}{Et} k \left(\frac{1}{kL} - \frac{2F_8}{F_9} \right)$ |
|  <p>$p(\xi) = p_0(1-\xi)$</p> | $\frac{p_0 R^2}{Et} \frac{F_9}{F_4}$ | $\frac{p_0 R^2}{Et} k \frac{2F_8}{F_4}$ |
|  <p>$p(\xi) = p_0 \sin \xi$</p> | $\frac{p_0 R^2}{Et} \frac{4(kL)^4}{\sigma^4 + 4(kL)^4} \left[\sin \sigma + \frac{\sigma^2}{2(kL)^2} \left(-\sin \sigma \frac{F_3}{F_4} - \frac{\sigma}{kL} \cos \sigma \frac{F_2}{F_4} \right) \right]$ | $\frac{p_0 R^2}{Et} k \frac{4(kL)^4}{\sigma^4 + 4(kL)^4} \left[\cos \sigma + \frac{\sigma^2}{2(kL)^2} \left(-\sin \sigma \frac{2(F_1 + 1)}{F_4} - \frac{\sigma}{kL} \cos \sigma \frac{F_3}{F_4} \right) \right]$ |
|  <p>$p(\xi) = p_0 \cos \xi$</p> | $\frac{p_0 R^2}{Et} \frac{4(kL)^4}{\sigma^4 + 4(kL)^4} \left[\cos \sigma + \frac{F_9}{F_4} + \frac{\sigma^2}{2(kL)^2} \frac{F_{10}}{F_4} + \frac{\sigma^2}{2(kL)^2} \left(\cos \sigma \frac{F_3}{F_4} + \frac{\sigma}{kL} \sin \sigma \frac{F_2}{F_4} \right) \right]$ | $-\frac{p_0 R^2}{Et} k \frac{4(kL)^4}{\sigma^4 + 4(kL)^4} \left[\frac{\sigma}{kL} \sin \sigma - \frac{2F_8}{F_4} + \frac{\sigma^2}{2(kL)^2} \frac{2F_7}{F_4} - \frac{\sigma^2}{2(kL)^2} \left(\cos \sigma \frac{2(F_1 + 1)}{F_4} + \frac{\sigma}{kL} \sin \sigma \frac{F_3}{F_4} \right) \right]$ |
|  <p>$p(\xi) = p_0 \exp(-\alpha \xi)$</p> | $\frac{p_0 R^2}{Et} \frac{4(kL)^4}{\sigma^4 + 4(kL)^4} \left[\exp(-\sigma) + \frac{F_9}{F_4} + \frac{\sigma^2}{2(kL)^2} \times \frac{F_{10}}{F_4} - \frac{\sigma^2}{2(kL)^2} \left(\frac{F_3}{F_4} + \frac{\sigma}{kL} \frac{F_2}{F_4} \right) \exp(-\sigma) \right]$ | $-\frac{p_0 R^2}{Et} k \frac{4(kL)^4}{\sigma^4 + 4(kL)^4} \left[\frac{\sigma}{kL} \exp(-\sigma) - \frac{2F_8}{F_4} - \frac{\sigma^2}{2(kL)^2} \frac{2F_7}{F_4} + \frac{\sigma^2}{2(kL)^2} \left(\frac{2(F_1 + 1)}{F_4} + \frac{\sigma}{kL} \frac{F_3}{F_4} \right) \exp(-\sigma) \right]$ |

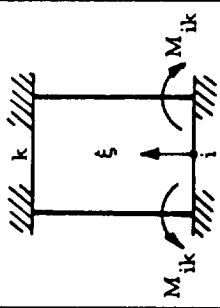
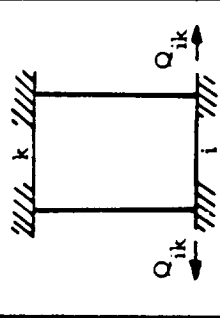
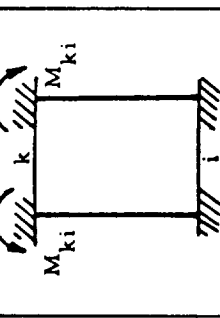
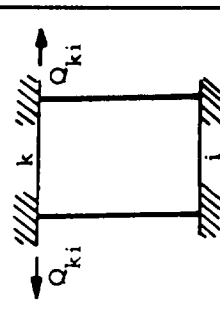
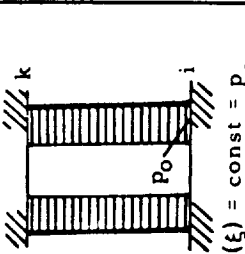
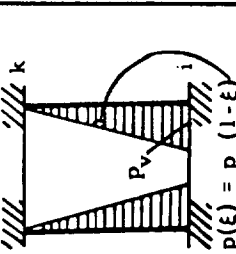
¹For F and k factors, see paragraph 2.42.6

TABLE 2.54-11. DISTORTIONS DUE TO SECONDARY LOADINGS (Ref. 2-2)

| | | |
|---|--|---|
| <p>Edge Distortions</p> <p>Shell Geometry and Loading Condition</p> |  |  |
|  | $+ H \frac{2Rk}{Et} \sin^2 \phi_1$ | $- H \frac{2k^2}{Et} \sin \phi_1$ |
|  | $- M \frac{2k^2}{Et} \sin \phi_1$ | $+ M \frac{4k^3}{EtR}$ |
| <p>Shell Loading Condition</p> | <p>$\Delta H =$ deflection</p> | <p>$\beta =$ rotation</p> |
|  | $M \frac{R^2 k^2}{Et} \frac{2F_2}{F_1 + 2}$ | $M \frac{R^2 k^3}{Et} \frac{4F_3}{F_1 + 2}$ |
|  | $Q \frac{R^2 k}{Et} \frac{2F_4}{F_1 + 2}$ | $Q \frac{R^2 k^2}{Et} \frac{2F_2}{F_1 + 2}$ |
|  | $M \frac{R^2 k^2}{Et} \frac{2F_3}{F_4}$ | $M_2 \frac{R^2 k^3}{Et} \frac{4(F_1 + 1)}{F_4}$ |
|  | $Q \frac{R^2 k}{Et} \frac{2F_2}{F_4}$ | $Q_1 \frac{R^2 k^2}{Et} \frac{2F_3}{F_4}$ |

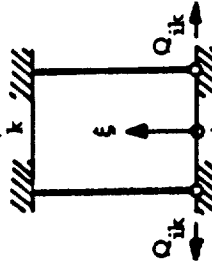
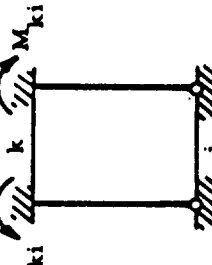
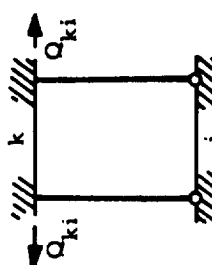
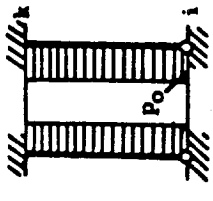
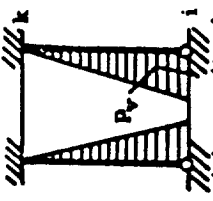
¹For F and k factors, see paragraph 2.42.6

TABLE 2.54-12. CYLINDRICAL SHELL WITH VARIOUS EDGE CONDITIONS -
 EDGE REACTIONS DUE TO PRIMARY AND
 SECONDARY LOADINGS (Ref. 2-2)¹

| Edge Reactions |  |  |  |  |
|--|--|--|---|---|
| Loading Condition  $p(\xi) = \text{const} = p_0$ | $-\frac{p_0}{2k} \left(\frac{F_2}{F_1} - \frac{2F_8}{F_1} \right)$ | $\frac{p_0}{k} \left(\frac{F_3}{F_1} - \frac{F_{10}}{F_1} \right)$ | $+\frac{p_0}{2k} \left(\frac{F_2}{F_1} - \frac{2F_8}{F_1} \right)$ | $-\frac{p_0}{k} \left(\frac{F_3}{F_1} - \frac{F_{10}}{F_1} \right)$ |
|  $p(\xi) = p_v(1-\xi)$ | $-\frac{p_v}{2k} \left[\frac{F_2}{F_1} - \frac{1}{kL} \left(\frac{F_4}{F_1} + \frac{F_9}{F_1} \right) \right]$ | $-\frac{p_v}{2k} \left[\frac{2F_3}{F_1} - \frac{1}{kL} \left(\frac{F_2}{F_1} + \frac{2F_8}{F_1} \right) \right]$ | $-\frac{p_v}{2k} \left[\frac{2F_8}{F_1} - \frac{1}{kL} \left(\frac{F_4}{F_1} + \frac{F_9}{F_1} \right) \right]$ | $+\frac{p_v}{2k} \left[\frac{2F_{10}}{F_1} - \frac{1}{kL} \left(\frac{F_2}{F_1} + \frac{2F_8}{F_1} \right) \right]$ |

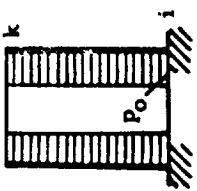
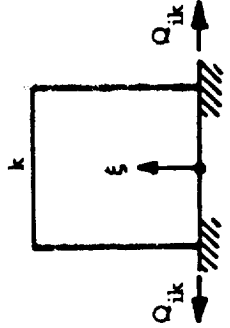
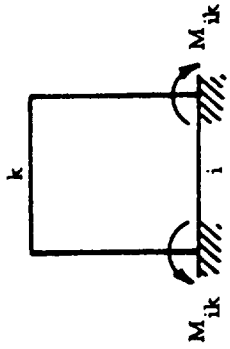
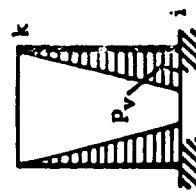
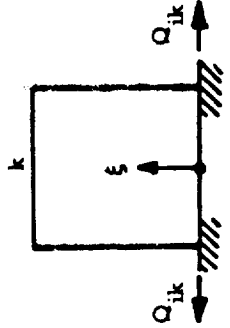
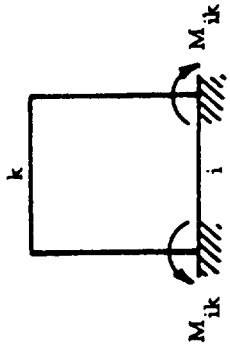
¹For F factors, see paragraph 2.42.6
 For k factors, see paragraph 2.42.6

TABLE 2.54-12 (CONT)¹

| Edge Reactions Loading Condition |  |  |  |
|---|--|---|---|
|  <p>$p(\xi) = \text{const} = p_0$</p> | $p_0 \left(\frac{2F_7}{F_4} - \frac{F_1 + 2}{F_4} \right) + \frac{2F_7}{F_4} - \frac{F_1 + 2}{F_4}$ | $+ \frac{p_0}{2k} \left(\frac{F_3}{F_4} - \frac{F_4}{F_4} \right)$ | $- \frac{p_0}{2k} \left(\frac{2(F_1 + 1)}{F_4} - \frac{2F_7}{F_4} \right)$ |
|  <p>$p(\xi) = p_v (1 - \xi)$</p> | $- \frac{p_v}{2k} \left(\frac{F_1 + 2}{F_4} - \frac{1}{kL} \frac{F_{10}}{F_4} \right)$ | $- \frac{p_v}{2k^2} \left(\frac{F_{10}}{F_4} - \frac{1}{kL} \frac{F_2}{F_4} \right)$ | $+ \frac{p_v}{2k} \left(\frac{2F_7}{F_4} - \frac{1}{kL} \frac{F_3}{F_4} \right)$ |

¹For F and k factors, see paragraph 2.42.6

TABLE 2.54-12. (CONT)¹

| Loading Condition | Edge Reactions | |
|---|--|---|
|  <p>$P(\xi) = \text{const} = P_0$</p> |  |  $-\frac{P_0}{2k} \frac{F_2}{F_1 + 2}$ |
|  <p>$P(\xi) = P_v (1 - \xi)$</p> |  |  $-\frac{P_v}{2k} \left(\frac{F_2}{F_1 + 2} - \frac{1}{kL} \frac{F_4}{F_1 + 2} \right)$ |

¹For F_1 and k factors, see paragraph 2.42.6

2.55 SUMMARY

In this section, the two basic methods used to solve multi-shells were described, and tables were presented for simple and fast operation. If the matrixes are large, computer programs can be used to solve the systems of linear algebraic equations. In most cases, however, the systems can be solved manually by using a slide rule if certain methods, such as "iteration," are applied.

Preceding sections have presented methods of analyzing multi-shells characterized with the axisymmetrical geometry and loading. By using the extended interaction process (as shown in this section) many cases can be analyzed with discontinuity in loading (Fig. 2.55-1); or with discontinuity in wall thickness (Fig. 2.55-2); different combinations of shells with other shells, with rings (foundations), or with plates (Fig. 2.55-3).

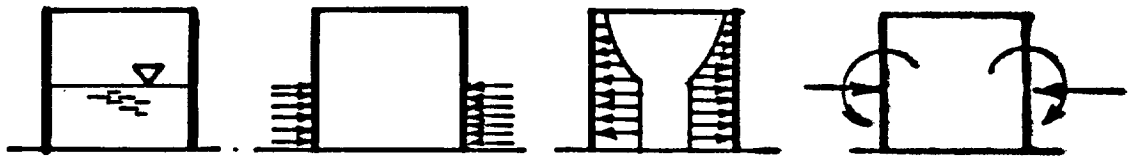


FIG. 2.55-1. Discontinuities Due to the Loading

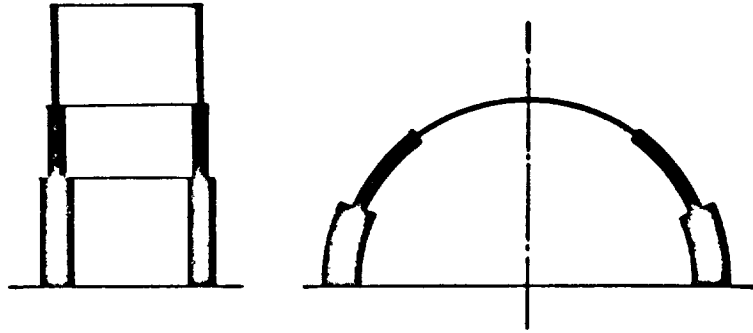


FIG. 2.55-2. Discontinuities in the Wall Thickness

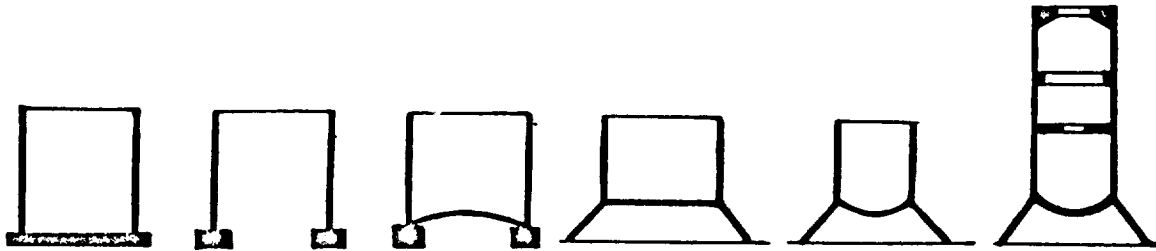


FIG. 2.55-3. Common Interactions of Shell
(Slab, Ring) Elements

However, to this point, the limitation exists regarding the condition that the material must be isotropic. In the logical process of generalization of the method, the next step is to consider the possible anisotropy. The shells may be reinforced with the circumferential or longitudinal stiffeners or may be represented by some kind of sandwich. Such cases will be discussed in the following section.

2.60 COMPOSITE SHELLS

2.61 INTRODUCTION

Up to this point, only homogeneous, isotropic monocoque shells have been considered.

It is known that certain rearrangements of the material in the section increase the rigidity and, consequently, less material is needed, and this effects the efficiency of design. Consequently, in order to obtain a more efficient and economical structure, the material in the section should be arranged to make the section most resistant to certain stresses that are predominant in this section.

Chapter 4.00 deals with the minimum weight design. This approach will only be mentioned here. The minimum weight design should not be confused with the known economical design of structural members, which is commonly used for heavy constructions. The latter method leads to the proper selection of different materials from which the corresponding section will be made to obtain minimum cost. In some cases, the minimum cost design actually corresponds to the minimum weight design, but not necessarily. In aerospace structures, weight is usually a governing factor, even if the "minimum weight" structure costs more.

If the section is stressed axially, excluding the stability considerations (Chapter 3.00), the distribution of material does not affect the stresses if the material is arranged symmetrically with respect to the center of gravity of the cross-section of the member.

If the structural member is under a bending load, consideration should be given to the material in the two flanges, which will be stressed approximately axially (one flange stressed in tension, the other in compression) and will absorb most of the moment. This arrangement is shown in Fig. 2.61-1. A small amount of material is

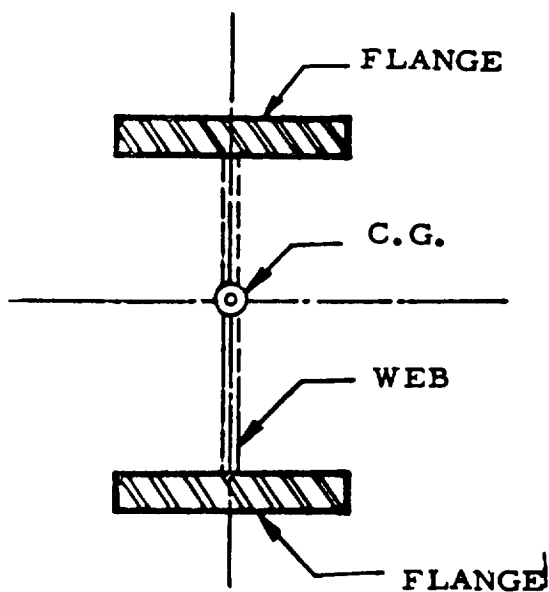


FIG. 2.61-1.
Concept of I-Beams

used for the "web" which contributes very little to the resistance to the moments; however, it absorbs most of the shear. The simplifying scheme of structural action of these elements is as follows: The moments are absorbed entirely by the flanges; the shear is absorbed entirely by the web. The weight savings in comparison with the monocoque section is very significant.

Based on the principle explained, the stiffened structures were developed. The philosophy previously described is applied mostly in stiffened and sandwich constructions.

2.62 STIFFENED SHELLS

2.62.1 General

Stiffened shells are commonly used in the aerospace and civil engineering fields. The shell functions more efficiently if the meridional, circumferential, or a combination of both systems of stiffeners is used. The meridional stiffeners usually have all the characteristics of beams and are designed to take the compressional and bending influences more effectively than the monocoque section. The circumferential stiffeners provide most of the lateral support for the meridional stiffeners. However, circumferential stiffeners are capable of withstanding the moments, shears, and axial stresses.

Basically, two approaches are possible. If the stiffeners cover considerable cross-sectional area and are arranged at a wide spacing, the whole construction can actually be interpreted as a three-dimensional frame. The plates between the stiffeners distribute and transfer loading to the frame, which will be analyzed accordingly as a space frame. This problem is beyond the scope of this manual.

If the stiffeners are located closer together, it appears more logical to replace the stiffened section with an equivalent monocoque section with the corresponding ideal modulus of elasticity. Then the shell can be analyzed as a monocoque shell. More details on this

approach will be given later. The geometry included is for cylindrical, spherical, and conical shells.

2.62.2 Cylindrical Shell

This shell may have longitudinal stiffening, circumferential stiffening, or both. Stiffening may be placed on the internal side or the external side of the surface, or it may be located on both sides. If cut-outs are needed, they will usually be located between the stiffeners.

2.62.3 Spherical Shell

This shell, if stiffened, will usually be stiffened in both meridional and circumferential directions. The problem may be slightly more complicated in the meridional direction because, obviously, the section that corresponds to this direction will decrease in size toward the apex. This leads to the nonuniform ideal thickness.

2.62.4 Conical Shell

This configuration is structurally between cases 1 and 2.

2.62.5 Approach for Analysis

The approach of the analysis is similar for all shells. If only circumferential stiffening exists, the structure can be cut into simple elements consisting of cylindrical, conical, or spherical elements and rings as shown in Fig. 2.62-1 and, considering the primary loading,

the interaction will be performed as shown in Section 2.50. If only longitudinal stiffeners are present, interaction of cylindrical panels with longitudinal beams (stiffeners) will be performed, as shown in Fig. 2.62-2.

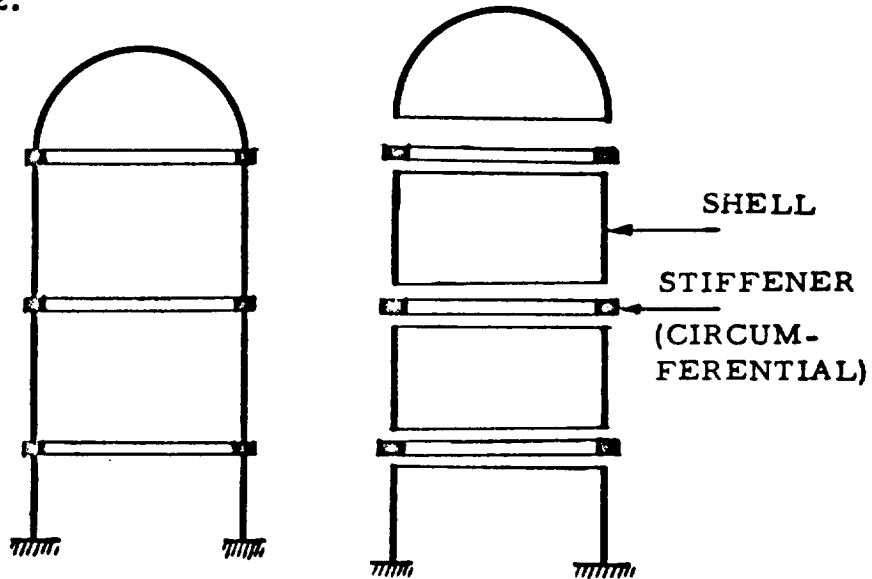


FIG. 2.62-1. Circumferentially Stiffened Shell

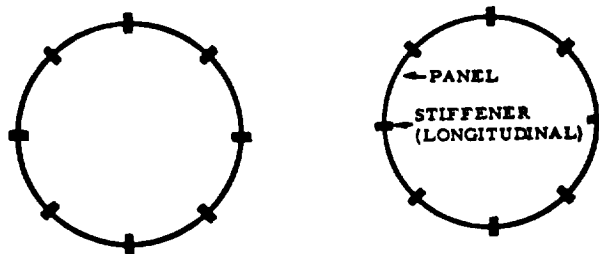


FIG. 2.62-2. Longitudinally Stiffened Shell

If both circumferential and longitudinal stiffeners are present, the panel will be supported on all four sides. The ratio of circumferential to longitudinal distances between the stiffeners is very important. These panels loaded with pressure (external or internal) will transmit the reactions to the circumferential and the longitudinal stiffeners. It is significant to note the analogy of the rectangular plate loadings equally distributed over the plate surface and perpendicular to the middle surface. Plates with the ratio of side equal to one are most effective; they transmit one half of the load in one direction and the other half in another direction. If, however, the ratio of sides is equal or greater than two, for all practical purposes, the whole loading can be considered to be carried by one shorter direction. The reader is referred to the Markus (Ref. 2-10) method for analysis of such plates. Curved panels react similarly but, due to increased curvature, these panels deviate more from the plates. The curved span under pressurization usually deflects less than the noncurved span; consequently, more loading will be carried by the curved direction. The system of beams (stiffeners) will be analyzed as a three-dimensional frame. Such analysis belongs to the theory of frames; consequently, no further discussion on this subject will be provided here.

There are no fixed formulas in existence for the case previously discussed or for stiffened shells in general. As was previously mentioned, if the stiffeners are positioned close together, the structure can be analyzed as a shell (not as a spaceframe). Then the stiffened section, for the purpose of analysis, should be replaced with the equivalent monocoque section, which is characterized with the equivalent modulus of elasticity. This replacement has to be done for both, meridional and circumferential direction. Both sections will possess ideal monocoque properties, the same thickness, but different ideal moduli of elasticity. This leads to the idea of orthotropic material. The concept of orthotropy will be studied in detail in a later section, and a proper analysis procedure will be suggested.

2.62.6 Method of Transformed Section

This approximate method covers all variations of stiffened (and sandwich) construction, regardless of the kind of elements that make up the section. This method shows how the combined section can be substituted with an equivalent monocoque section of the same stiffness. This idealized section should be determined for the circumferential and meridional directions of the shell. Then the analyst deals with an orthotropic, monocoque shell. The analysis of orthotropic shells is similar to the analysis of monocoque shells discussed previously, if

certain corrections are entered into the previous formulas. The analysis for the shells where the shear distortions cannot be neglected is more complicated, as will be explained in detail in the following sections.

Assume a composite section (stiffened, sandwich, or composite) which consists of different layers of material, as shown in the Fig. 2.62-3. Each layer, (i), is characterized by a modulus of

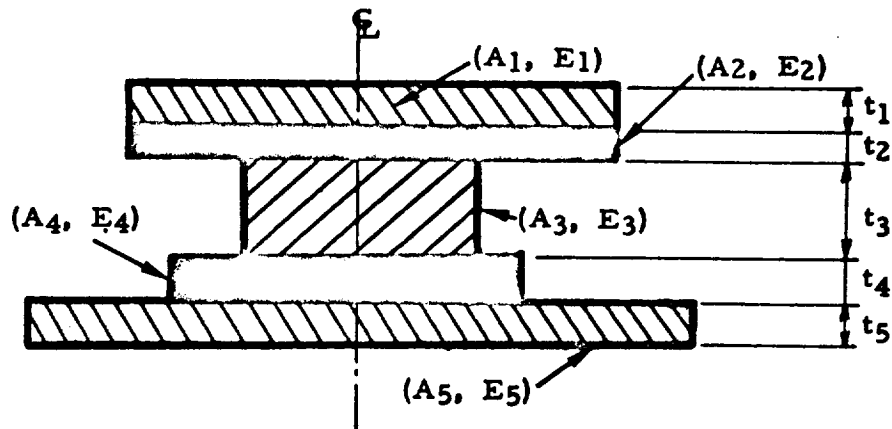


FIG. 2.62-3. Original Composite Section

elasticity, E_i , and a cross-sectional area, A_i . First select one convenient modulus of elasticity, E^* , as a basis for the equivalent monocoque section which will be established. Accordingly, all layers will be modified and reduced to one equivalent material which is characterized with E^* . In this manner, the ideal transformed section (Fig. 2.62-4) is determined. It should be noted that, for the convenience of design,

the thickness, t_i , of individual layers was not changed, but areas A_i become A_i^* . The same modulus of elasticity, E^* , now corresponds to every A_i^* , thus making the entire section homogeneous.

The necessary computations are presented in Table 2.62-1.

Designations are given on the sketch included in the table.

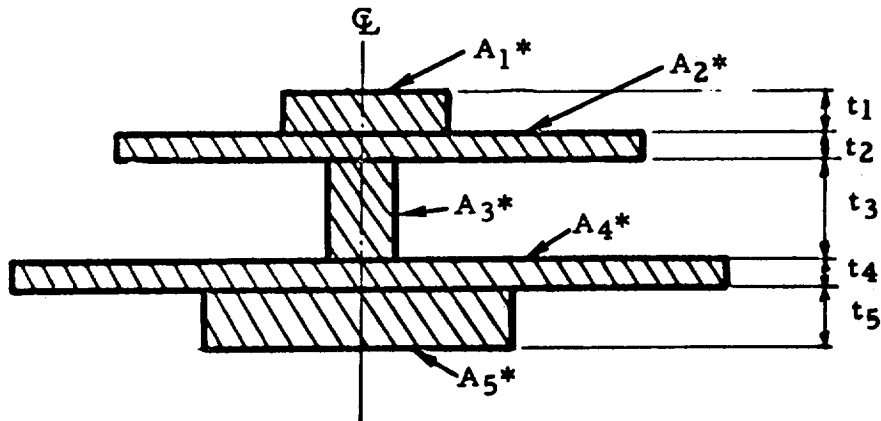


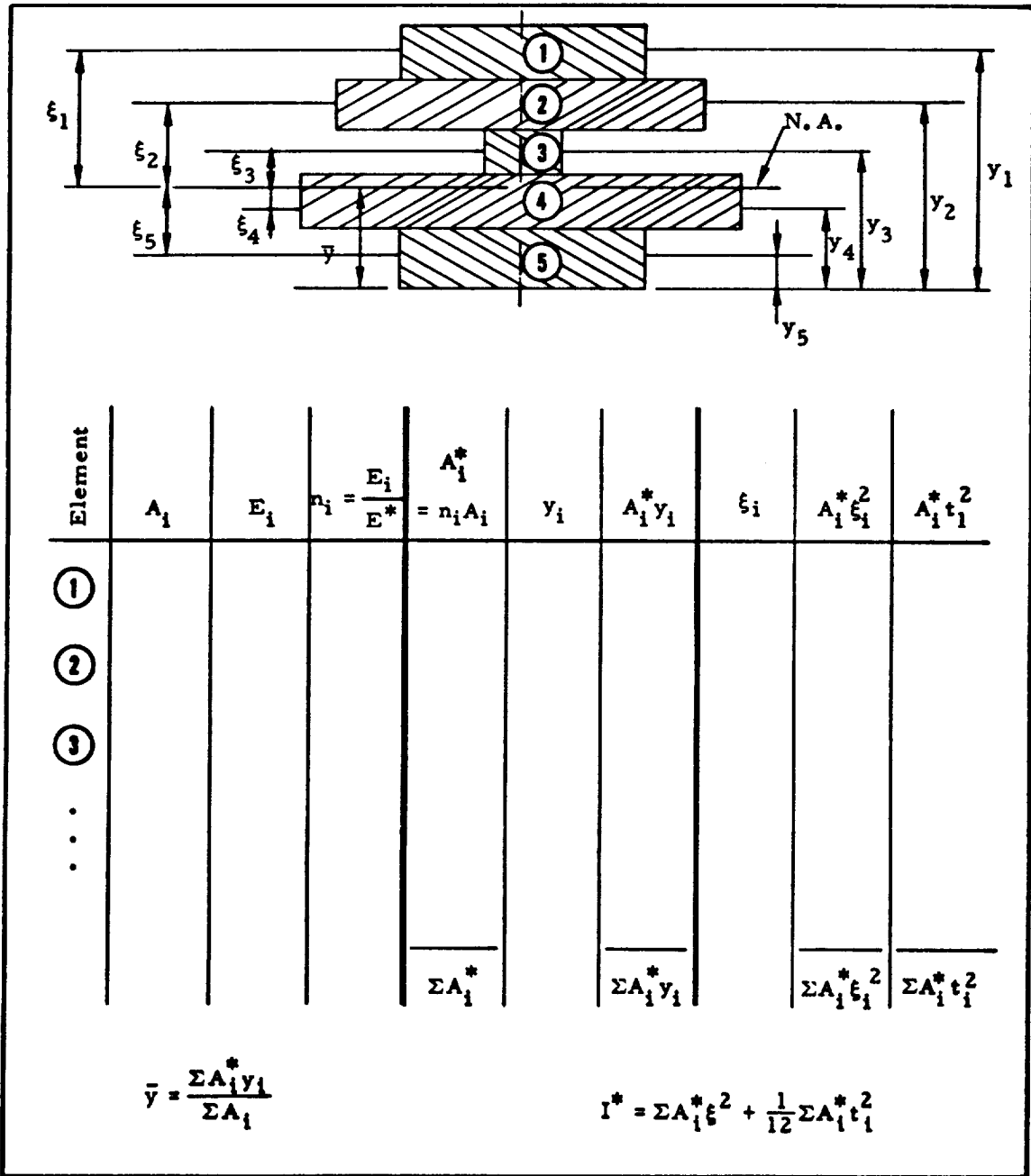
FIG. 2.62-4. Transformed Section

The computations lead to the determination of the moment of inertia of equivalent section. The ideal monocoque rectangular section can be determined as having the same bending resistance as the original section. For example, if the section is symmetrical about the neutral axis, the thickness, t , can be found for the new monocoque rectangular section of the same resistance as follows:

$$I = \frac{bt^3}{12} = I^*; \quad t = 2.29 \sqrt[3]{\frac{I^*}{b}}$$

where b is the selected width of the new section.

TABLE 2.62-1. TRANSFORMED SECTION METHOD



2.63 SANDWICH SHELLS

2.63.1 Introduction

The basic philosophy which the analyst applies to a sandwich structure is precisely the same as would apply to any structural element. This procedure consists of determining a set of design allowables against which the set of applied loads is compared.

In the analysis, external loads are applied to a configuration and a set of internal loads is computed. These loads apply to the internal substructural elements such as columns, plates, shells, tension elements, etc. The precise computation of internal loads will not be considered herein except to mention that additional complication might be introduced by the use of sandwich because of the additional lag in the distribution of load between facings caused by the relatively low shear modulus of the core.

2.63.2 Modes of Failure of Sandwich Elements

Generally, two types of allowable data exists. The first type is determined by simple material tests and is associated with material more than with geometry; the second type is dependent on the geometry of the element. If, in a sandwich construction, the materials of construction are considered to be the core, the facings, and the bonding media, the basic material properties would be associated with the

properties of these three independent elements. Table 2.63-1 presents a list of some of the important structural material properties of these three materials.

TABLE 2.63-1. BASIC PROPERTIES OF SANDWICH MATERIALS

| FACINGS |
|--|
| Compressive yield strength Tensile yield strength Tensile ultimate strength Shear yield strength Shear ultimate strength Modulus of elasticity Poisson's ratio |
| CORE |
| Shear strength Shear modulus Flatwise compressive strength Flatwise compressive modulus Flatwise tensile strength Flatwise tensile modulus Bending rigidity (if present) |
| BOND MEDIA |
| Shear strength Shear modulus Tensile strength Peel strength |

In general, there are properties which are unaffected by the configuration of the sandwich element as a whole, but are present regardless of the configuration. If the yield strength of the skins is exceeded, yielding will take place regardless of whether the sandwich is in the configuration of a flat plate, a column, or a cylinder. Similarly, the core shear strength is independent of geometry, etc.

The second class of allowable data is those which are dependent on configuration as well as the basic properties of the facings, core, and bond media. This class of failure modes may be further subdivided into modes of failure that include the entire configuration, and those that are localized to a portion of the structure but still limit the overall load-carrying capacity.

The most important local modes of failure are dimpling, wrinkling, and crimping. These modes of failure are dependent on the local geometry and on the basic properties of the materials of the sandwich. The general modes of failure generally are associated with the buckling

strength of sandwich structural elements. Excessive deflections or flexibility of the element might govern for specific designs, but these factors are generally specific for a particular application. This factor will be discussed in Chapter 3.00.

Another local mode of failure which may occur is associated with failure at local details such as edge members and close-outs or at points of introduction of concentrated loads. Unfortunately, exact analysis of all these many types of "foreign" elements that must be introduced into the sandwich by the design requirements is seldom possible. As a consequence, the analyst must either determine the allowables experimentally or must make simplifying conservative analytical approximations.

The comparison between the allowable and the applied loads is a basic function of the analyst. The importance of this comparison cannot be overemphasized. In order to be able to apply sandwich construction on a logical basis, it is imperative that the modes of failure be identified and analyzed. Then the applied stresses (or loads) can be compared with the allowable stresses (or loads) and a margin (or factor) of safety can be computed.

2.63.3 Structural Function of Sandwich

Basically, many of the structural reasons for the use of sandwich construction are related to attempts at achieving a high bending rigidity-

to-weight ratio. From a structural standpoint, the minimum weight arrangement of material in a bending or compression element would be two membranes separated by nothing, this nothing being capable of transferring shear between the membranes and allowing the membranes to bend about a common neutral axis. Although this Utopia has not been reached, attempts have been made to come as close as possible. In a beam, the I-beam is a good example in which the engineer attempts to place as much material as far away as possible from the neutral axis. The weight of the web member is reduced further in a tension field beam in which the web may buckle (Ref. 2-14).

In a surface application, the structure analogous to the I-beam is the sandwich. In the case of the sandwich, we replace the Utopian nothing with a core and bond media. It should be pointed out that the minimum weight tension element is composed of the highest strength-to-weight material available and is independent of the cross-section shape. As a consequence, sandwich is inefficient as a tension element because the core and bond may not add materially to the tensile strength. In a sandwich, then, the facing sheets perform much as membranes (although the bending rigidity of the facings about their own neutral axis may become an important factor for some sandwich designs), and the core acts principally to transmit shear through the facings, thereby, allowing the facings to act about a common neutral axis.

In practice, the achievement of a high bending rigidity is used structurally in problems in which stability may govern (Chapter 3.00) or in which stress or deflection limitation may govern. A high bending rigidity can, of course, be achieved without recourse to sandwich construction. However, some very simple calculations of the bending rigidity of a sandwich as contrasted to, for instance, a flat sheet readily indicate the important weight advantage of the sandwich-type construction. Conventionally stiffened structures are more competitive than unstiffened sheet with respect to a weight/strength comparison with sandwich.

In addition to the structural reasons for the use of sandwich, there may be a number of other reasons for which sandwich construction might be used, in spite of the fact that it may weigh more or cost more than some other configuration. It may be advantageous from a temperature control standpoint to utilize sandwich. It is obviously advantageous, in some cases, to use sandwich construction to achieve some particular architectural effect. It may be also advantageous in some designs to be able to design into the structure large areas or volumes which are uninterrupted by support members. Additionally, there is the advantage of being able to design with fewer parts.

2.63.4 Types of Sandwich Cores

As far as the analyst is concerned, the core is a basic material of the sandwich and is treated as a material. It has a shear strength, a shear modulus, a flatwise tensile and compressive strength and modulus, and it may have some bending strength.

Cores may be classified either by their properties or by their geometrical configuration. Analytically, cores are generally categorized by their properties in the xz and yz planes. Cores in which the properties on these two planes are equal are termed isotropic cores, whereas those with different properties in the two planes are termed orthotropic cores. Cores may be orthotropic with respect to bending and/or shear rigidity and strength parameters. The foam-type cores generally are isotropic, at least in the xz and yz planes. (The properties in the third plane, xy plane, may be different.) The honeycomb-type cellular cores are generally nearly isotropic with respect to shear (about 3-to-1 ratio maximum) although there are some configurations in which efforts are made to increase properties in one of the two planes. The corrugated cores are highly orthotropic, having orthotropic properties both with respect to strength, bending rigidity, and shear rigidity.

Practically speaking, there are three types of cores which are commercially available. There are the solid cores, the cellular cores,

and the corrugated cores. Solid cores are typified by the balsa wood or plywood cores in which the core can be used by itself as a structural member. Such cores generally have bending and shear rigidities and strengths in three planes. Consequently, the properties of the resulting sandwich may be greater with the same facing sheets than one in which one of the cellular cores is used.

Actually, there are two types of cellular cores. The first type consists of materials like cellular cellulose acetate in which a mass of bubbles has been solidified. These cores, of course, were widely used in the inception of the very low density core materials. The more recently developed cellular core is the honeycomb-type core. In this material, the core has a regular geometrical pattern which, in the case of at least one common product, has the appearance of the cross-section of a beehive. Actually, any geometrical pattern of closed cells with the axis of the cell perpendicular to the surface could be considered of this type. There are a multitude of such cores, each with somewhat different properties. It is pointed out that when the core has bending rigidity in either plane, it accepts bending loads and stresses and must be checked to determine allowable bending stresses. This is especially true when different facing and core materials are used.

The corrugated cores are orthotropic, both with respect to bending and to shear properties. Both the bending and the shear properties of the corrugated core are many times greater in the plane parallel to the axis of the corrugations than in the plane perpendicular to the corrugations. As a consequence, different analyses are generally required for the corrugated core sandwiches than for the cellular core sandwich.

The most important thing to remember about cores in design of sandwich is that, analytically, they have basic properties similar to those of the facing sheets. Some of these properties are included in the basic analytical parameters of the entire sandwich and govern the behavior of the resulting sandwich in stability, stress, and deflection applications.

2.63.5 Design Requirements for Inspection and Structural Test

One of the easily overlooked, but important aspects of a sandwich design is a requirement for inspection of the completed production parts and for structural test to verify design and analysis assumptions. Unfortunately, all is not known about the local modes of failure and detail analysis of local inserts, edge members, closeouts, etc. As has been indicated, the best the analyst can do is work with experimental data which give some of the basic allowables. In the case of wrinkling, for instance, neither theory nor test has yet yielded a reliable method of analysis. As a consequence, for structures in which

the design margins are low, the analyst should request a structural test. Although the structural test may not be of any significance for the overall stability or deflection analysis, it may uncover difficulties in local detail.

The acceptance of a structural part is somewhat difficult in a sandwich structure. Only recently have electronic and x-ray techniques become reasonably reliable. The analyst should play a contributing role in a decision as to the type of acceptance test because he is versed in the areas which are critical from the analysis standpoint.

2.63.6 Analysis of Sandwich Shells

The similarity between the sandwich and stiffened shells was mentioned previously. The analysis of most instability (general and local) is presented in Chapter 3.00 of this manual. Here the general design of sandwich shells under pure static conditions will be presented. Two fundamental cases will be recognized:

1. Shear deformations can be neglected. In many cases, shear deformations may be neglected if deformations appear to be extensive, and the core cannot take the shear. In such a case the core must be substituted with another core which is heavier, stronger, and correspondingly will be sufficient to resist extensive shear stresses. In this case, however, the

deformation of such a core will be usually small and not entered into the analysis.

2. Shear deformations are extensive; however, shear can be taken by the core. The shear deformations must be considered in the analysis. The primary analytical difference between the behavior of a sandwich element and a homogeneous isotropic element is the necessity of accounting for the shear deformation. No new basic theories are required for the analysis of sandwich structural elements, only the application of established theory. Once the shear deformation is properly included in the analysis, the analysis is complete.

2.63.7 Conclusion

Section 2.63 basically was taken without change from Ref. 2-11. In this section, the physical concepts of sandwich were reviewed and difficulties that are connected with the exact analysis of sandwich shells were listed. Although, any analysis still is only an approximation. Assuming the reader's familiarity with the basic sandwich concepts, the following sections will continue to put forth the theory for the approximate sandwich analysis. The first most logical approximation would be to replace actual sandwich with orthotropic material. The concepts of orthotropy actually may cover not only large family of

sandwiches but also other materials, such as stiffened shells (if stiffeners are very closely spaced), corrugated shells, etc.

To give a systematical description of orthotropic analysis, attention will again be directed to the mathematical structure of the analytical formulas for the monocoque shells presented previously in this manual. This will make clear what kind of modifications can be made, in order to apply the same formulas (that were derived for monocoque material) to the orthotropic shells.

2.64 ORTHOTROPIC SHELLS

2.64.1 Introduction

A material is orthotropic if the characteristics of the materials are not the same in two mutually orthogonal directions (two dimensional space). Such material has different values for E , G , and μ for each direction. The Poisson ratio μ also may be different in the case of bending and axial stresses. In the majority of cases this difference is negligible but in order to distinguish one from another μ' will be designated for the Poisson ratio which corresponds to the bending, and μ for axial stresses. The behavior of the shell under loading is a function of certain constants that depend on the previously mentioned material constants and geometry. The special case of orthotropy is isotropy (the material characteristics in both directions of two dimensional space are the same). In order to see the dependence of stresses and deformations in shells from previously mentioned constants, a short review of isotropic concepts of shells is provided. These constants are designated with strain and bending rigidities.

2.64.2 Extensional and Bending Rigidities in Shells Theory (Ref. 2-15)

In the past only isotropic monocoque shells were considered, and numerous formulas were presented. For isotropic shells the following definitions hold.

Strain rigidity

$$B = \frac{Et}{1 - \mu^2}$$

Bending rigidity

$$D = \frac{Et^3}{12(1 - \mu^2)}$$

B and D have appeared in many previous formulas.

The following characteristic stress-formulas apply for rotationally symmetric thin shells.

$$N_\phi = B(\epsilon_\phi + \mu\epsilon_\theta)$$

$$N_\theta = B(\epsilon_\theta + \mu\epsilon_\phi)$$

The bending loads are

$$M_\phi = -D \left(\frac{1}{R_\phi} \frac{d\beta}{d\phi} + \mu \frac{\beta}{R_\theta} \cot \phi \right)$$

$$M_\theta = D \left(\frac{\beta}{R_\theta} \cos \phi + \mu \frac{1}{R_\phi} \frac{d\beta}{d\phi} \right)$$

The final stresses can be obtained as follows:

$$\left. \begin{aligned} \sigma_\phi &= \frac{E}{1 - \mu^2} \left(\frac{N_\phi}{B} + \frac{M_\phi}{D} z \right) \\ \sigma_\theta &= \frac{E}{1 - \mu^2} \left(\frac{N_\theta}{B} - \frac{M_\theta}{D} z \right) \end{aligned} \right\} \quad (2.64-1)$$

For monocoque section of rectangular shape

$$\left. \begin{aligned} \sigma_{\phi} &= \frac{N_{\phi}}{t} + \frac{M_{\phi}}{\frac{t^3}{12}} z \\ \sigma_{\theta} &= \frac{N_{\theta}}{t} - \frac{M_{\theta}}{\frac{t^3}{12}} z \end{aligned} \right\} \quad (2.64-2)$$

The physical meaning of D and B is obvious if Eqs. (2.64-1) and (2.64-2) are compared.

The componental stresses due to membrane forces are

$$1 \sigma_{\phi} = \frac{EN_{\phi}}{(1-\mu^2)B} = \frac{E}{1-\mu^2} \cdot N_{\phi} \frac{1-\mu^2}{Et} = \frac{N_{\phi}}{1 \cdot t} = \frac{N_{\phi}}{A}$$

$$1 \sigma_{\theta} = \frac{EN_{\theta}}{(1-\mu^2)B} = \frac{E}{1-\mu^2} \cdot N_{\theta} \frac{1-\mu^2}{Et} = \frac{N_{\theta}}{1 \cdot t} = \frac{N_{\theta}}{A}$$

where

$$A = 1 \times t$$

It is convenient to chose the width of the section strip that is equal to unity.

The componental stresses due to bending:

$$2 \sigma_{\phi} = \frac{M_{\phi} z}{D} \cdot \frac{E}{1-\mu^2} = M_{\phi} z \frac{E}{(1-\mu^2)} \frac{12(1-\mu^2)}{Et^3} = \frac{12 M_{\phi} z}{1 \times t^3} = \frac{M_{\phi} z}{I}$$

$$2 \sigma_{\theta} = \frac{M_{\theta} z}{D} \cdot \frac{E}{1-\mu^2} = M_{\theta} z \frac{E}{(1-\mu^2)} \frac{12(1-\mu^2)}{Et^3} = \frac{12 M_{\theta} z}{1 \times t^3} = \frac{M_{\theta} z}{I}$$

where

$$I = \frac{1 \times t^3}{12}$$

Evidently, if stiffened or sandwich shell is being dealt with, a modified B and D shall be used in the equations, then all previously derived equations for monocoque shells may be used for stiffened and sandwich shells. If the values from the "transformed section" are used, then

$$B = \frac{A^* E^*}{1 - \mu^2} \quad ; \quad D = \frac{I^* E^*}{1 - \mu^2}$$

In the preceding formulas $\mu' \approx \mu$ is assumed.

2.64.3 Orthotropic Characteristics

Now the orthotropy is defined if, for two mutual orthogonal main directions, 1 and 2, the following constants are known or determined:

D_1, B_1, μ_1, μ_1' and shear rigidity D_{Q_1}

D_2, B_2, μ_2, μ_2' and shear rigidity D_{Q_2}

In order to use the previously given formulas (for the isotropic case) for the analysis of the orthotropic structures, the formulas must be modified. For this purpose, a systematical modification of the primary and secondary solutions will be provided in the following section in order to make possible the use of the unit edge loading method for the orthotropic case. In the analysis of monocoque shells, the shear distortions usually are neglected. With sandwich, in most cases, such neglect is justified. The previously collected formulas for the isotropic case do not include the shear distortion. Consequently,

orthotropic analyses which neglect the shear distortions will be examined first. Later, additional study will be presented, which considers the distortions due to the shear.

2.64.4 Orthotropic Analysis, If Shear Distortions are Neglected

A. Primary Solutions

It was previously stated that in most cases, the primary solutions are membrane-solutions. For the purpose of interaction, the following set of values is needed (considering axisymmetrically loaded shells of revolution).

N_{θ} - membrane load in circumferential direction

N_{ϕ} - membrane load in meridional direction

u - displacement in the direction of tangent to the meridian

w - displacement in the direction of the normal-to-the-middle surface.

Actually, having u and w , any componential displacements can be obtained from the pure geometric relations if only the axisymmetrical cases are considered. Consequently, for this purpose, it will be adequate to investigate u and w .

To determine N_{θ} and N_{ϕ} all formulas that were presented for the isotropic case can be used, because the membrane is a statically determinate system and does not depend on the material properties.

When N_θ and N_ϕ are obtained, u and w can be obtained in the following manner. (See Ref. 2-15.)

First determine the strains components ϵ_ϕ and ϵ_θ . For the isotropic case, the correspondent formulas are

$$\epsilon_\phi = \frac{1}{Et} (N_\phi - \mu N_\theta)$$

$$\epsilon_\theta = \frac{1}{Et} (N_\theta - \mu N_\phi)$$

For the orthotropic case the same formulas may be written

$$\epsilon_\phi = \frac{1}{B_\phi (1 - \mu_\phi \mu_\theta)} (N_\phi - \mu_\theta N_\theta)$$

$$\epsilon_\theta = \frac{1}{B_\theta (1 - \mu_\theta \mu_\phi)} (N_\theta - \mu_\phi N_\phi)$$

$$\text{Note: } D = B \frac{t^2}{12}$$

Displacement can now be obtained from the following differential equation:

$$\frac{du}{d\phi} - u \cot \phi = R_1 \epsilon_\phi - R_2 \epsilon_\theta \quad (\text{call}) = f(\phi)$$

The solution of the above equation is

$$u = \sin \phi \left(\int \frac{f(\phi)}{\sin \phi} d\phi + C \right)$$

where C is the constant of integration to be determined from the condition at the support. Then, the displacement w is obtained from the following equation:

$$\epsilon_{\theta} = \frac{u}{R_2} \cot \phi - \frac{w}{R_2}$$

Consequently, for every symmetrically loaded shell of revolution the stresses and deformations are determined for the orthotropic case.

B. Secondary Solutions (Ref. 2-15)

To obtain the secondary solutions, the formulas that were derived for the isotropic case can be used and then, using the substitution of proper constants, they can be transformed into formulas for the orthotropic case. Generally, due to any edge disturbance (unit loading) the formulas give direct solutions for

$$N_{\phi}, N_{\theta}, M_{\phi}, M_{\theta}, Q, \beta, \Delta r$$

in the form of

$$\text{Solution} = (\text{Edge disturbance}) \times (\text{Function of Significant Constant}) \\ \times (\text{Function of Geometry})$$

The most important geometries of the orthotropic shells are spherical, conical and cylindrical. Any other geometry in the majority of the cases can be approximated with these three types, as was shown in Section 2.34.

The significant constants which appear in Section 2.33 are

$$k, \bar{\beta}, \lambda, B \text{ and } D$$

These constants, in order to transform the "isotropic" formulas into "orthotropic," should be modified, as will be shown in the following discussion, except for those modifications that are self evident.

Spherical Shell (See Fig. 2.64-1). The discussion here makes reference to the analysis for the isotropic case. To make the transformation into the orthotropic case factor

$$k^4 = 3(1 - \mu^2) \left(\frac{R}{t}\right)^2$$

will be replaced with the similar factor where the orthotropy

$$k^4 = 3(1 - \mu_1 \mu_2) \left(\frac{R}{t}\right)^2$$

is considered. Then, to make the discussion shorter, for both unit

edge loadings, M and H, the com-

bined formulas obtained are

$$N_\theta = -\cot(\phi_1 - \alpha) C_1 e^{-k\alpha} \cdot \sin(k\alpha + C_2)$$

$$N_\phi = k\sqrt{2} C_1 e^{-k\alpha} \sin(k\alpha + C_2 - \frac{\pi}{4})$$

$$Q_\phi = -N_\phi / \cot \phi$$

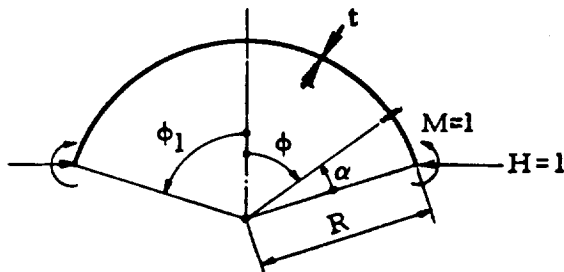


FIG. 2.64-1. Spherical Shell
Loaded With Unit Edge
Loadings

where C_1 and C_2 are the constants. These constants are different for unit moment and unit shear loadings:

$$M_{\theta} = \frac{R}{k \sqrt{2}} C_1 e^{-k\alpha} \sin\left(k\alpha + C_2 + \frac{\pi}{4}\right)$$

$$M_{\theta} = \mu_{\theta} M_{\theta}$$

Displacements are given by the following formulas:

$$\Delta r = - \frac{R}{Et} \sin(\theta_1 - \alpha) k \sqrt{2} C_1 e^{-k\alpha} \sin\left(k\alpha + C_2 - \frac{\pi}{4}\right)$$

$$= - \frac{12R}{D_{\theta} (1 - \mu_1' \mu_2') t^2} \sin(\theta_1 - \alpha) k \sqrt{2} C_1 e^{-k\alpha}$$

$$\cdot \sin\left(k\alpha + C_2 - \frac{\pi}{4}\right)$$

$$\beta = - \frac{2k^2}{Et} C_1 e^{-k\alpha} \cos(k\alpha + C_2)$$

$$= - \frac{24k^2}{t^2 D_{\theta} (1 - \mu_1' \mu_2')} C_1 e^{-k\alpha} \cos(k\alpha + C_2)$$

(a) Special Case, $M = 1$ all around. Then,

$$C_1 = 2kM/R \quad ; \quad C_2 = 0$$

The correspondent deformations at the edge are

$$\beta = - \frac{4 k^3 M}{E R t} = \frac{48 k^3 M}{t^2 R D_{\theta} (1 - \mu'_1 \mu'_2)}$$

$$\Delta r = \frac{2 k^2 \sin \theta_1}{E t} M = \frac{24 k^2 \sin \theta_1}{t^2 D_{\theta} (1 - \mu'_1 \mu'_2)} M$$

To obtain N_{θ} , N_{θ} , Q_{θ} , M_{θ} , M_{θ} enter C_1 and C_2 into general formulas that were presented before.

(b) Special Case $H = 1$ all around the edge. Then,

$$C_1 = - \frac{2 H \sin \theta_1}{\sqrt{2}} ; \quad C_2 = - \frac{\pi}{4}$$

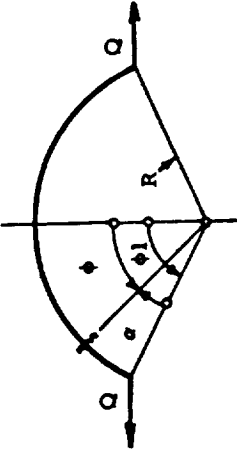
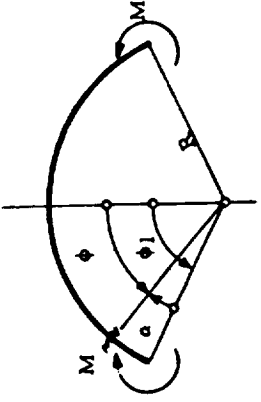
The correspondent deformations at the edge are

$$\beta = \frac{2 k^2 \sin \theta_1}{E t} H = \frac{24 k^2 \sin \theta_1}{t^2 D_{\theta} (1 - \mu'_1 \mu'_2)} H$$

$$\Delta r = - \frac{2 R k \sin^2 \theta_1}{E t} H = \frac{-24 R k \sin^2 \theta_1}{t^2 D_{\theta} (1 - \mu'_1 \mu'_2)} H$$

To obtain N_{θ} , N_{θ} , Q_{θ} , M_{θ} , M_{θ} enter C_1 and C_2 in the preceding general formulas. Table 2.64-1 presents a modification of Table 2.33-2 in above-described manner. Similar modifications may be obtained for the formulas presented in Tables 2.33-3 through 2.33-7.

TABLE 2.64-1. ORTHOTROPIC SPHERE-UNIT EDGE LOADING SOLUTIONS¹

| |  |  |
|---|--|--|
| Q_ϕ | $-\sqrt{2} \sin\phi_1 \cdot e^{-k\alpha} \cos(k\alpha + \frac{\pi}{4})$ | $+\frac{2k}{R} e^{-k\alpha} \sin k\alpha$ |
| N_ϕ | $-Q_\phi \cot\phi$ | $-Q_\phi \cot\phi$ |
| N_θ | $2k \sin\phi_1 \cdot e^{-k\alpha} \cos k\alpha$ | $+2\sqrt{2} \frac{k}{R} e^{-k\alpha} \cos(k\alpha + \frac{\pi}{4})$ |
| M_ϕ | $\frac{R}{k} \sin\phi_1 e^{-k\alpha} \sin k\alpha$ | $\sqrt{2} e^{-k\alpha} \sin(k\alpha + \frac{\pi}{4})$ |
| M_θ | $-\frac{R}{k} \frac{\sin\phi_1 \cot\phi}{2\sqrt{2}} \cdot e^{-k\alpha} \sin(k\alpha + \frac{\pi}{4}) + \mu'_\phi M_\phi$ | $\frac{1}{k} \cot\phi \cdot e^{-k\alpha} \cos k\alpha + \mu'_\phi M_\phi$ |
| β | $-\frac{2\sqrt{2}k \sin\phi_1}{D_\phi(1 - \mu'_\phi \mu'_\theta)} e^{-k\alpha} \sin(k\alpha + \frac{\pi}{4})$ | $-\frac{4k}{RD_\phi} \frac{e^{-k\alpha}}{(1 - \mu'_\phi \mu'_\theta)} \cos k\alpha$ |
| Δr | $\frac{R \sin\phi_1 \cdot e^{-k\alpha}}{D_\phi(1 - \mu'_\phi \mu'_\theta)} \left[2k \sin\phi \cos k\alpha - \sqrt{2} \mu_\theta \cos\phi \cos(k\alpha + \frac{\pi}{4}) \right]$ | $+\frac{2ke^{-k\alpha}}{D_\phi(1 - \mu'_\phi \mu'_\theta)} \left[\sqrt{2} \cdot k \sin\phi \cos(k\alpha + \frac{\pi}{4}) + \mu'_\phi \cos\phi \sin k\alpha \right]$ |
| $k = \sqrt[4]{\frac{R}{t}} \sqrt[3]{(1 - \mu'_\phi \mu'_\theta)}$ | | |

¹See Table 2.33-2.

Conical Shell. In the same manner the formulas previously given for the isotropic case of conical geometry may be modified to be useful for the orthotropic case. The following constants shall replace those previously given. (See Paragraph 2. 32. 5.)

$$D = \frac{Et^3}{12(1 - \mu^2)} \Rightarrow D_x = \frac{E_x t^3}{12(1 - \mu'_x \mu'_\theta)}$$

$$k = \frac{\sqrt[4]{3(1 - \mu^2)}}{\sqrt{t x_m \cot \alpha_o}} \Rightarrow \frac{\sqrt[4]{3(1 - \mu'_x \mu'_\theta)}}{\sqrt{t x_m \cot \alpha_o}}$$

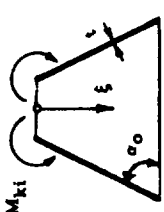
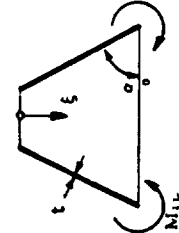
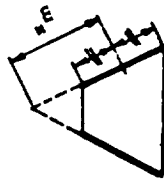
Then the previously given formulas can be used.

It shall be noted, that since the formulas presented before, came from different sources, in Table 2. 33-8, instead of k as shown above, includes k as follows:

$$k = \frac{l}{\sqrt{R t \sin \theta}} \sqrt[4]{3(1 - \mu^2)}$$

The modification in this case is the same (μ^2 is replaced with $\mu'_x \mu'_\theta$). In this way, all formulas given in Tables 2. 33-8 through 2. 33-10 can be modified to be useful for the orthotropic case. Tables 2. 64-2 and 2. 64-3 are such modifications of Table 2. 33-9.

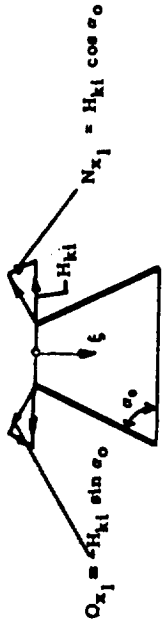
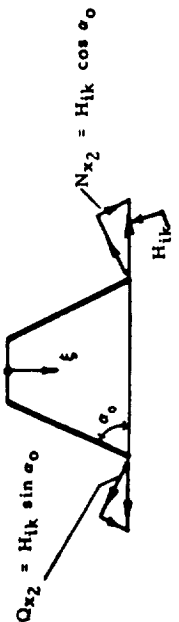
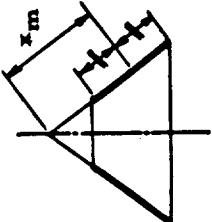
TABLE 2.64-2. ORTHOTROPIC CONE-UNIT MOMENT EDGE LOADING SOLUTIONS ¹

| | | |
|--------------------|--|---|
| |  |  |
| N_x | $M_{ki} 2k \cot \alpha_0 \left[\frac{F_6}{F_1} F_{15}(\xi) + \frac{F_5}{F_1} F_{16}(\xi) - \frac{F_3}{F_1} F_8(\xi) \right]$ | $M_{ik} 2k \cot \alpha_0 \left[\frac{F_8}{F_2} F_{10}(\xi) - \frac{F_{10}}{F_1} F_8(\xi) \right]$ |
| \tilde{N}_θ | $M_{ki} 2k^2 x_m \cot \alpha_0 \left[\frac{F_6}{F_1} F_{14}(\xi) + \frac{F_5}{F_1} F_{13}(\xi) - \frac{F_3}{F_1} F_{10}(\xi) \right]$ | $M_{ik} 2k^2 x_m \cot \alpha_0 \left[\frac{2F_8}{F_1} F_7(\xi) - \frac{F_{10}}{F_1} F_{10}(\xi) \right]$ |
| M_x | $M_{ki} \left[\frac{F_6}{F_1} F_{13}(\xi) - \frac{F_5}{F_1} F_{14}(\xi) + \frac{F_3}{F_1} F_4(\xi) \right]$ | $-M_{ik} \left[\frac{2F_8}{F_1} F_8(\xi) - \frac{F_{10}}{F_1} F_9(\xi) \right]$ |
| Q_x | $M_{ki} 2k \left[\frac{F_6}{F_1} F_{15}(\xi) + \frac{F_5}{F_1} F_{16}(\xi) - \frac{F_3}{F_1} F_8(\xi) \right]$ | $M_{ik} 2k \left[\frac{F_8}{F_1} F_{10}(\xi) - \frac{F_{10}}{F_1} F_8(\xi) \right]$ |
| $\Delta r'$ | $M_{ki} \frac{\sin \alpha_0}{2D_x k^2} \left[\frac{F_6}{F_1} F_{14}(\xi) + \frac{F_5}{F_1} F_{13}(\xi) - \frac{F_3}{F_1} F_{10}(\xi) \right]$ | $M_{ik} \frac{\sin \alpha_0}{2D_x k^2} \left[\frac{2F_8}{F_1} F_7(\xi) - \frac{F_{10}}{F_1} F_{10}(\xi) \right]$ |
| β | $-\frac{M_{ki}}{D_x} \left[\frac{F_6}{F_1} F_{16}(\xi) - \frac{F_5}{F_1} F_{15}(\xi) - \frac{F_3}{F_1} F_7(\xi) \right]$ | $M_{ik} \frac{1}{D_x^2} \left[\frac{F_3}{F_1} F_4(\xi) + \frac{F_{10}}{F_1} F_7(\xi) \right]$ |
| |  | $D_x = \frac{E_x t^3}{12(1 - \nu_x^2)}$ |

¹See Table 2.33-9

For F factors, see paragraph 2.42.6

TABLE 2.64-3. ORTHOTROPIC CONE-UNIT SHEAR EDGE LOADING SOLUTIONS ¹

| |  $Q_{x_1} = H_{kl} \sin \alpha_0$ $N_{x_1} = H_{kl} \cos \alpha_0$ |  $Q_{x_2} = H_{ik} \sin \alpha_0$ $N_{x_2} = H_{ik} \cos \alpha_0$ |
|------------|---|---|
| N_x | $-H_{kl} \cos \alpha_0 \left[F_7(\xi) - \frac{F_4}{F_1} F_{10}(\xi) + \frac{F_2}{F_1} F_8(\xi) \right]$ | $H_{ik} \cos \alpha_0 \left[\frac{F_9}{F_1} F_{10}(\xi) + \frac{2F_8}{F_1} F_8(\xi) \right]$ |
| N_y | $H_{kl} x_{mk} \cos \alpha_0 \left[F_9(\xi) + \frac{2F_4}{F_1} F_7(\xi) - \frac{F_2}{F_1} F_{10}(\xi) \right]$ | $2H_{ik} x_{mk} \cos \alpha_0 \left[\frac{F_9}{F_1} F_7(\xi) + \frac{F_8}{F_1} F_{10}(\xi) \right]$ |
| M_x | $H_{kl} \frac{\sin \alpha_0}{2k} \left[F_{10}(\xi) - \frac{2F_4}{F_1} F_8(\xi) + \frac{F_2}{F_1} F_9(\xi) \right]$ | $H_{ik} \frac{\sin \alpha_0}{k} \left[\frac{F_9}{F_1} F_8(\xi) - \frac{F_8}{F_1} F_9(\xi) \right]$ |
| Q_x | $-H_{kl} \sin \alpha_0 \left[F_7(\xi) - \frac{F_4}{F_1} F_{10}(\xi) + \frac{F_2}{F_1} F_8(\xi) \right]$ | $H_{ik} \sin \alpha_0 \left[-\frac{F_9}{F_1} F_{10}(\xi) + \frac{2F_8}{F_1} F_8(\xi) \right]$ |
| Δr | $H_{kl} \frac{\sin^2 \alpha_0}{4D_{xk}^3} \left[F_9(\xi) + \frac{2F_4}{F_1} F_7(\xi) - \frac{F_2}{F_1} F_{10}(\xi) \right]$ | $H_{ik} \frac{\sin^2 \alpha_0}{2D_{xk}^3} \left[\frac{F_9}{F_1} F_7(\xi) + \frac{F_8}{F_1} F_{10}(\xi) \right]$ |
| β | $H_{kl} \frac{\sin \alpha_0}{2D_{xk}^2} \left[-F_8(\xi) + \frac{F_4}{F_1} F_9(\xi) + \frac{F_2}{F_1} F_7(\xi) \right]$ | $-H_{ik} \frac{\sin \alpha_0}{2D_{xk}^2} \left[\frac{F_9}{F_1} F_9(\xi) + \frac{2F_8}{F_1} F_7(\xi) \right]$ |
| |  $x_{tm} = \frac{\sqrt{3} (1 - \mu_x \mu_\theta)}{\sqrt{6} x_{mk} \cot \alpha_0}$ | $D_x = \frac{E_x t^3}{12 (1 - \mu_x \mu_\theta)}$ |

¹See Table 2.33-g.

For F factors, see paragraph 2.42.6

Cylindrical Shell. All formulas given in Tables 2.33-11 and 2.33-12 and Tables 2.33-14 through 2.33-17 can be modified if the following replacement is made:

$$k = \frac{L}{\sqrt{Rt}} \sqrt[4]{3(1 - \mu^2)} \Rightarrow \frac{L}{\sqrt{Rt}} \sqrt[4]{3(1 - \mu'_1 \mu'_2)}$$

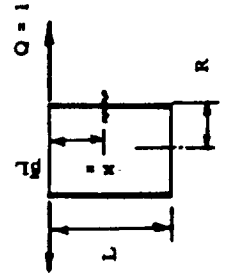
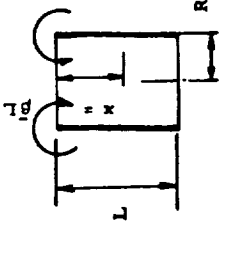
$$D = \frac{Et^3}{12(1 - \mu^2)} \Rightarrow \frac{Et^3}{12(1 - \mu'_1 \mu'_2)}$$

$$Et \Rightarrow B_\theta(1 - \mu'_1 \mu'_2)$$

$$D = B \frac{t^2}{12}$$

Table 2.64-4 is a correspondent modification of that previously given for the orthotropic case Table 2.33-11.

TABLE 2.64-4. LONG ORTHOTROPIC CYLINDER - UNIT EDGE LOADING SOLUTIONS ¹

| |  $Q = 1$ $D_x = \frac{E_x t^3}{12(1 - \nu_x^2 \mu_0)}$ $k = \frac{L \sqrt[3]{3(1 - \nu_x^2 \mu_0)}}{\sqrt{Rt}}$ |  $M = 1$ $D_x \text{ and } k$ $D_x = \frac{E_x t^3}{12(1 - \nu_x^2 \mu_0)}$ $k = \frac{L \sqrt[3]{3(1 - \nu_x^2 \mu_0)}}{\sqrt{Rt}}$ |
|-----------------------------------|---|---|
| N_x | 0 | 0 |
| N_0 | $-\frac{2Rk}{L} e^{-k\beta} \cos k\beta$ | $\frac{2\sqrt{2}Rk^2}{L^2} e^{-k\beta} \cos(k\beta + \frac{\pi}{4})$ |
| M_x | $\frac{L}{k} e^{-k\beta} \sin k\beta$ | $-\sqrt{2} \cdot e^{-k\beta} \sin(k\beta + \frac{\pi}{4})$ |
| M_0 | $\mu_x M_x$ | $\mu_x M_x$ |
| Q | $\sqrt{2} \cdot e^{-k\beta} \cos(k\beta + \frac{\pi}{4})$ | $\frac{2k}{L} e^{-k\beta} \sin k\beta$ |
| β | $\frac{L^2}{\sqrt{2k^2 D_x}} e^{-k\beta} \sin(k\beta + \frac{\pi}{4})$ | $-\frac{L}{D_x k} e^{-k\beta} \cos k\beta$ |
| Δr | $\frac{L^3}{2D_x k^3} e^{-k\beta} \cos k\beta$ | $-\left(\frac{L^2}{\sqrt{2} D_x k^2} e^{-k\beta} \cos(k\beta + \frac{\pi}{4})\right)$ |
| For $\beta = 0$ | | |
| ρ | $L^2 / 2k^2 D_x$ | $-L / D_x k$ |
| Δr | $L^3 / 2k^3 D_x$ | $-L^2 / D_x k^2$ |

¹See Table 2.33-11.

2.64.5 Orthotropic Analysis, If Shear Distortions are Included

For this more complicated case, the solution may be found in Ref. 2-12, which was considered as the basis for the Paragraphs 2.64.5 and 2.64.6. Cylinders and spheres only are considered herein.

A. Cylindrical Shell

In the case of a cylinder constructed from a sandwich with a relatively low traverse shear rigidity, the shear distortion may not be negligible; therefore, an analysis is presented which includes shear distortion for a symmetrically loaded orthotropic sandwich cylinder.

The following nomenclature is used:

D_x, D_y = Beam flexural stiffnesses per inch of width of orthotropic shell in axial and circumferential directions, respectively, in-lb.

D_{Q_x} = Shear stiffness in xz plane per inch of width, lb/in.

B_x, B_y = Extensional stiffnesses of orthotropic shell in axial and circumferential directions, respectively, lb/in.

G_c = Core shear modulus in xz plane, psi.

M_x = Moment acting in the x direction, in-lb/in.

Q_x = Transverse shear force acting in xz plane, lb/in.

μ_x, μ_y = Poisson's ratio associated with bending in x and y directions, respectively.

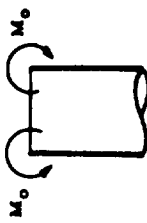
μ'_x, μ'_y = Poisson's ratio associated with extension in x and y directions, respectively.

The derived solutions are tabulated in Tables 2.64-5 and 2.64-6.

B. Half-Spheres

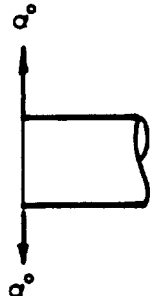
Based on Beckler's assumption for the half-sphere, all formulas derived for cylinders can be adapted for the spherical shell, too.

TABLE 2.64-5. INFLUENCE COEFFICIENTS DUE TO EDGE LOADING M_0 IN ORTHOTROPIC CYLINDERS, SHEAR DISTORTIONS CONSIDERED

|  | | Constante | | |
|---|-------------|--|--|-------------------------------------|
| | | $\sigma^2 = \frac{B_y}{4D_0 R^2}$ | $\beta^4 = \frac{B_y (1 - \nu_x \nu_y)}{4D_x R^2}$ | $D = \frac{D_x}{(1 - \nu_x \nu_y)}$ |
| | | $e^4 - \beta^4 > 0$ | $e^4 - \beta^4 = 0$ | $e^4 - \beta^4 < 0$ |
| | N_0° | N_0° | N_0° | N_0° |
| w | 1 | $\left[\frac{e^{mx}}{2e^2} + \frac{x e^{mx}}{m} \right] \left(-\frac{M_0}{D} \right)$ | | 4 |
| M_x | 2 | $M_0 \left(\frac{A_2 e^{-A_1 x} - A_1 e^{-A_2 x}}{A_2 - A_1} \right)$ | $e^{mx} M_0 (1 - mx)$ | 5 |
| Q_x | 3 | $M_0 \left(\frac{-A_1 A_2 e^{-A_1 x} + A_1 A_2 e^{-A_2 x}}{A_2 - A_1} \right)$ | $-2e^2 e^{mx} x M_0$ | 6 |
| Constants: | | $A_1 = \left[2e^2 + 2(e^4 - \beta^4)^{\frac{1}{2}} \right]^{\frac{1}{2}}$ $A_2 = \left[2e^2 - 2(e^4 - \beta^4)^{\frac{1}{2}} \right]^{\frac{1}{2}}$ | $m = - (2)^{\frac{1}{2}} e$ | 7 8 9 |
| Influence Coefficients for the displacements and rotation at the edge of the shell | | | | |
| $w_{x=0}$ | | $V = (\beta^2 + e^2)^{\frac{1}{2}}$ $P = (\beta^2 - e^2)^{\frac{1}{2}}$ | | |
| $\left[\frac{dw}{dx} \right]_{x=0}$ | | $-M_0/2\beta^2 D$ $(M_0/D\beta^2) (e^2 + \beta^2)^{\frac{1}{2}}$ | | |
| | 10 | | | |
| | 11 | | | |

*Formula modifications are presented in Table 2.64-7.

TABLE 2.64-6. INFLUENCE COEFFICIENTS DUE TO EDGE LOADING Q_0 IN ORTHOTROPIC CYLINDERS

| | |  | | Constants $\sigma^2 = \frac{B}{4D_x R^2}; \beta^2 = \frac{B_y(1-\mu_x\mu_y)}{4D_x R^2}; D = \frac{D_x}{(1-\mu_x\mu_y)}$ | |
|--|--|--|--|--|-----|
| | | $\sigma^4 - \beta^4 > 0$ | $\sigma^4 - \beta^4 = 0$ | $\sigma^4 - \beta^4 < 0$ | No* |
| w | | $\frac{Q_0}{D(A_2 - A_1)} \left[\frac{e^{-Ax}}{4\sigma^2 - A_1} + \frac{e^{-Ax}}{A_2 - A_1} \right]$ | $\frac{Q_0}{D\sigma^2} \left[\frac{mx}{m} + \frac{x\sigma^{mx}}{2} \right]$ | $\frac{e^{-Vx}}{2D\beta^4} Q_0 \left(\frac{\sigma^2}{P} \sin Px - V \cos Px \right)$ | 18 |
| M_x | | $Q_0 \left[\frac{-Ax}{e^x - e^{-x}} \right]$ | $e^{mx} x Q_0$ | $\frac{e^{-Vx} Q_0}{P} \sin Px$ | 19 |
| Q_x | | $Q_0 \left[\frac{-A_1 e^{-A_1 x} + A_2 e^{-A_2 x}}{A_2 - A_1} \right]$ | $e^{mx} Q_0 [1 + mx]$ | $\frac{e^{-Vx} Q_0}{P} \left[P \cos Px - V \sin Px \right]$ | 20 |
| Constants | | $A_1 = \left[2\sigma^2 + 2(\sigma^4 - \beta^4) \right]^{\frac{1}{2}}$ $A_2 = \left[2\sigma^2 - 2(\sigma^4 - \beta^4) \right]^{\frac{1}{2}}$ | $m = -(2)^{\frac{1}{2}} \sigma$ | $V = (\beta^2 + \sigma^2)^{\frac{1}{2}}$ $P = (\beta^2 - \sigma^2)^{\frac{1}{2}}$ | |
| Influence coefficients for the displacements and rotation at the edge of the shell | | | | | |
| $w_{x=0}$ | | | | | 21 |
| $\left[\frac{dw}{dx} \right]_{x=0}$ | | | | | 22 |

*Formula modifications are presented in Table 2.64-7.

2.64.6 Influence of Axial Forces on Bending in Cylinder

Usually it is assumed that the contribution of the axial force N_o to the bending deflection is negligible; however, for a cylinder with a relatively large radius, the axial force may significantly contribute to the bending deflection. Therefore, the preceding analysis was extended by the same author (Ref. 2-12) to include the effect of the axial force on the deflections. This leads to the modification of the formulas (Tables 2.64-5 and 2.64-6) in the manner as shown in

Table 2.64-7. The constants are slightly modified:

$$\alpha^2 = \frac{\left[\frac{B_y}{D_{Q_x} R^2} + \frac{1 - \mu_x \mu_y}{D_x} N_o \right]}{4 \left[1 + \frac{N_o}{D_{Q_x}} \right]}$$

$$\beta^4 = \frac{B_y (1 - \mu_x \mu_y)}{4 D_x R^2 \left[1 + \frac{N_o}{D_{Q_x}} \right]}$$

$$\gamma^2 = \frac{B_y}{4 D_{Q_x} R^2} \quad ; \quad V = 4\gamma^4 - 4\gamma^2\alpha^2 + \beta^4$$

$$S = (\beta^2 + \alpha^2)^{1/2}$$

TABLE 2.64-7. MODIFICATION OF TABLES 2.64-5 AND -6 TO INCLUDE THE EFFECTS OF AXIAL FORCES ON BENDING (REF. 6-12)

| Formula | Quantities: (Formulas in tables 6.64-5 and -6) | Substitute |
|---------|---|--|
| 1 | $(4\alpha^2 - A_1^2)$ $(A_2^2 - 4\alpha^2)$ | $(4\gamma^2 - A_1^2)$ $(A_2^2 - 4\gamma^2)$ |
| 4 | Whole formula | $w = \frac{e^{mx} M_o}{D (m^2 - 4\gamma^2)^2} \left[(4\gamma^2 - 3m^2) + (m^2 - 4\gamma^2) mx \right]$ |
| 6 | $2\alpha^2 M_o x$ | $m^2 M_o$ |
| 7 | Whole formula | $w = \frac{M_o e^{-sx}}{2VD} \left[(S^2 + \gamma^2) \cos Px + \frac{S}{P} (\gamma^2 + P^2) \sin Px \right]$ |
| 8 | V | S |
| 9 | V | S |
| 10 | Whole formula | $w_{x=0} = (-M_o / 2VD) (2\alpha^2 + \beta^2 - 2\gamma^2)$ |
| 11 | Whole formula | $\left[\frac{dw}{dx} \right]_{x=0} = (M_o \beta^2 / VD) (\alpha^2 + \beta^2)^{\frac{1}{2}}$ |
| 12 | $(4\alpha^2 - A_1^2)$ $(A_2^2 - 4\alpha^2)$ | $(4\gamma^2 - A_1^2)$ $(A_2^2 - 4\gamma^2)$ |
| 15 | Whole formula | $w = \frac{e^{mx} Q_o}{D (m^2 - 4\gamma^2)^2} \left[2m - (m^2 - 4\gamma^2)x \right]$ |
| 18 | Whole formula | $w = \frac{Q_o e^{-sx}}{2VD} \left[\frac{\gamma^2}{P} \sin Px - S \cos Px \right]$ |
| 19 | V | S |
| 20 | V | S |
| 21 | Whole formula | $(-Q_o / 2VD) (\alpha^2 + \beta^2)^{\frac{1}{2}}$ |
| 22 | Whole formula | $\left(\frac{dw}{dx} \right)_{x=0} = \frac{Q_o}{2\gamma D} (\beta^2 + 2\gamma^2)$ |

2.65 CONCLUSION

In this section the necessary methods and formulas were presented for the analysis of stiffened and sandwich shells. Such shells are analyzed in the same manner as the monocoque shells with minor modifications of previously given formulas, except if shear distortions must be considered. For this case, the additional formulas are given. Actually, more often, the stiffened and sandwich shells must be analyzed in respect to stability. Chapter 3:00 describes the methods for the stability analysis of shells. Also in Chapter 3:00 D_i , B_i , and μ_i and μ'_i values are given for the most common types of sandwich section, and this information is useful for stress design also. (See Section 3.32.)

2.70 UNSYMMETRICALLY LOADED SHELLS

2.71 INTRODUCTION

Until now, the axisymmetrical cases have been treated in respect to the geometry, material, and loading. The "unit load method" was exclusively used for the solution. In Chapter 1:00, the most commonly used procedures for solving different shell systems have been discussed. It was shown that the most complex solutions are applied to the shells without symmetry, loaded unsymmetrically. The first level of simplification of the complex procedures would be the usage of axisymmetric shell loaded unsymmetrically.

The scope of this manual does not permit presentation of the actual derivations, but solutions for the most commonly appearing cases in engineering will be presented in the following tables.

The shells are assumed to be thin enough in order to use the membrane theory. The following tables of solutions also provide the necessary information about the loading and geometry.

2.72 SHELLS OF REVOLUTION

The first level of simplification of the complex procedures would be axisymmetric shells loaded unsymmetrically. Similarly, symmetrical shells may have unsymmetrical boundaries, which will make the symmetrical loading not be symmetrical any more.

Table 2.72-1 presents some solutions for certain loadings for spherical, conical, and cylindrical shells loaded unsymmetrically.

Table 2.72-2 presents the solutions for spherical shell with non-symmetrical boundaries.

TABLE 2.72-1. SPHERE, CONE, AND CYLINDER LOADED BY WIND LOADING

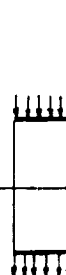






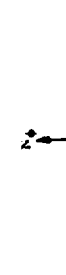



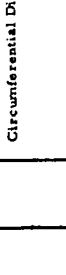


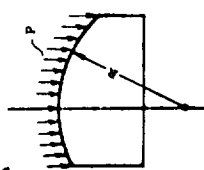
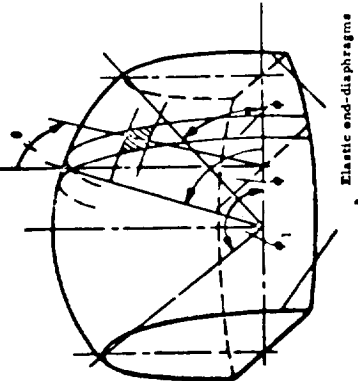
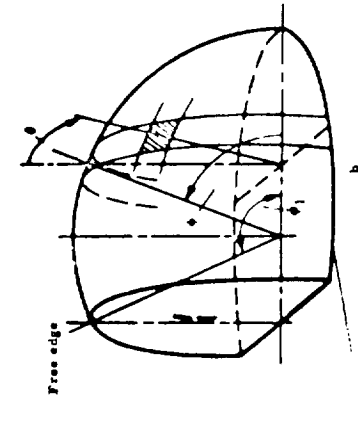
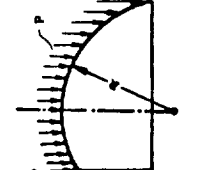
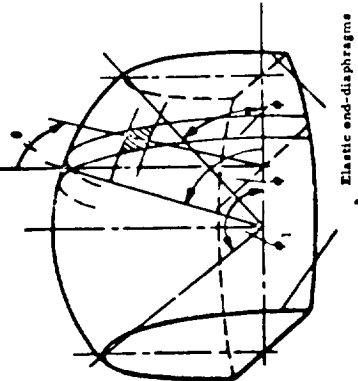
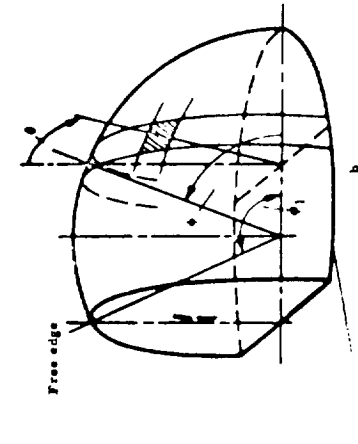
| | | | | | | |
|---|---|--|---|---|--|--|
|  <p style="text-align: center;">$Z = P_w \sin \phi \cos \theta$</p> |  <p style="text-align: center;">$Z = P_w \sin \phi \cos \theta$</p> <p style="text-align: center;">Conical shell supported at the vertex of the cone with free edge</p> |  <p style="text-align: center;">$Z = P_w \sin \phi \cos \theta$</p> |  <p style="text-align: center;">$Z = P_w \sin \phi \cos \theta$</p> | <p style="text-align: center;">Circumferential Direction</p>  <p style="text-align: center;">N_{θ}</p> |  <p style="text-align: center;">N_{θ}</p> |  <p style="text-align: center;">N_{θ}</p> |
| <p style="text-align: center;">Circumferential Direction</p>  <p style="text-align: center;">N_{θ}</p> |  <p style="text-align: center;">N_{θ}</p> |  <p style="text-align: center;">N_{θ}</p> |  <p style="text-align: center;">N_{θ}</p> |  <p style="text-align: center;">N_{θ}</p> |  <p style="text-align: center;">N_{θ}</p> |  <p style="text-align: center;">N_{θ}</p> |
| <p style="text-align: center;">N_{θ}</p> | <p style="text-align: center;">N_{θ}</p> | <p style="text-align: center;">N_{θ}</p> | <p style="text-align: center;">N_{θ}</p> | <p style="text-align: center;">N_{θ}</p> | <p style="text-align: center;">N_{θ}</p> | <p style="text-align: center;">N_{θ}</p> |
| <p style="text-align: center;">N_{θ}</p> | <p style="text-align: center;">N_{θ}</p> | <p style="text-align: center;">N_{θ}</p> | <p style="text-align: center;">N_{θ}</p> | <p style="text-align: center;">N_{θ}</p> | <p style="text-align: center;">N_{θ}</p> | <p style="text-align: center;">N_{θ}</p> |
| <p style="text-align: center;">N_{θ}</p> | <p style="text-align: center;">N_{θ}</p> | <p style="text-align: center;">N_{θ}</p> | <p style="text-align: center;">N_{θ}</p> | <p style="text-align: center;">N_{θ}</p> | <p style="text-align: center;">N_{θ}</p> | <p style="text-align: center;">N_{θ}</p> |

TABLE 2.72-2. SPHERICAL SHELLS WITH UNSYMMETRICAL BOUNDARIES

| Shell | Loading | N_θ | N_ϕ | $N_{\phi\theta}$ |
|--|---|---|--|---|
|  | <p>Free edge</p>  <p>Elastic end-diagrams</p>  | $- p R \frac{\cos \theta}{\sin^3 \phi} (\cos \phi_0 - \cos \phi)$ $- \cos \phi (\cos \phi - \cos \phi_1)$ $- p R \frac{\cos^2 \phi_1 - \cos^2 \phi}{\sin^3 \phi} \cos \theta$ | $p R \left[\frac{1}{\sin^3 \phi} (\cos \phi_0 - \cos \phi) \cdot (\cos \phi - \cos \phi_1) - \sin \phi \right] \cos \theta$ | $p R \frac{\cos \phi}{\sin^3 \phi} (1 + \sin^2 \phi) + \cos \phi_0 \cos \phi_1 - \frac{\cos \phi_0 + \cos \phi_1}{\cos \phi} \sin \theta$ |
|  | <p>Free edge</p>  <p>Elastic end-diagrams</p>  | $- p R \frac{(\cos \phi - \cos \phi_1)^2}{\sin^3 \phi} \cos \theta$ $p R \frac{\cos^2 \phi_1 - \cos^2 \phi}{\sin^3 \phi} \cos \theta$ | $p R \left[\frac{\cos^2 \phi_1 - \cos^2 \phi}{\sin^3 \phi} - \sin \phi \right] \cos \theta$ | $p R \frac{\cos \phi}{\sin^3 \phi} \left[\sin^2 \phi + \sin^2 \phi_1 \right] \sin \theta$ |
| <p>For $\phi_1 = \pi - \phi_0$ (end-diagrams in symmetrical position):</p> | | | | |
| <p>For $\phi_1 = \frac{\pi}{2}$:</p> | | | | |
| <p>$X = p \sin \theta$</p> | | | | |
| <p>$Z = p \cos \theta$</p> | | | | |
| $p R (\cos \phi - \cos \phi_1) \frac{\cos \phi}{\sin^3 \phi} - \left[(\cos \phi - \cos \phi_1) + \frac{2 \sin^2 \phi}{\cos \phi} \right] \sin \theta$ $p R (2 \cot \phi + \cot^2 \phi) \sin \theta$ | | | | |

2.73 SHELLS OF BEAM SYSTEMS

Presented herein are some solutions collected for the thin shells of different beam systems; i. e., cantilever beam, simple beam, and continuous beam. The loadings considered are the dead-weight, the equally distributed loading over the base, end-moments, concentrated loads, etc. The shells are cylindrical, conical, and curved panels (circular, elliptical, cycloidal, parabolical, catenary).

2.73.1 Cantilever Cylindrical Shell

Tabulated solutions for cantilever cylindrical shells under different loading conditions are presented herein. The only exception is the shell loaded torsionally (Table 2.73-1.) which can be regarded as a cantilever, or simple beam system. The solutions are presented in the Tables 2.73-1 and 2.73-2.

TABLE 2.73-1 CANTILEVERED AND FREE CYLINDERS LOADED IN TORSION REF. 2-9

| | <p> Loading: Dead Weight (q) $X = 0$ $Y = 0$ $Z = q \cos \phi$ </p> | <p> Loading: Concentrated Load $X = Y = Z = 0$ $V = \int_0^{2\pi} \frac{1}{R} \sin^2 \phi \cdot R d\phi \dots$ </p> | <p> Loading: Torsional $X = Y = Z = 0$ $M = \int_0^{2\pi} \frac{1}{2R^2} \cdot R d\phi \cdot R \dots$ </p> |
|--------------|---|---|--|
| N_ϕ | $-q R \cos \phi$ | 0 | 0 |
| N_{x0} | $2 q (L-x) \sin \phi = N_\phi x$ | $\frac{-\sin \phi}{R^2}$ | $-\frac{1}{2 R^2 v}$ |
| N_x | $\frac{q}{R} (L-x)^2 \cos \phi$ | $\frac{(L-x) \cos \phi}{R^2 v}$ | 0 |
| $E_{\phi u}$ | $\frac{q x}{R} (L^2 - Lx + \frac{x^2}{3} + \mu R^2) \cos \phi$ | $\frac{x (2L-x) \cos \phi}{2R^2 v}$ | 0 |
| $E_{\phi v}$ | $\frac{q x}{12R} [48(1+\mu) L R^2 + 6(L^2 - R^2(4+3\mu))x - 4 L x^2 + x^3] \sin \phi$ | $\frac{x [12(1+\mu) R^2 + 3 L x - x^2] \sin \phi}{6R^3 v}$ | $\frac{1+\mu}{R^2} \frac{L}{v} \cdot x$ |
| $E_{\phi w}$ | $-\frac{q}{12R} [12R^2 (R^2 + \mu L^2) + 24(2+\mu) R^2 L x + 6(L^2 - R^2(4+\mu))x^2 - 4 L x^3 + x^4] \cos \phi$ | $-\frac{6(2+\mu) R^2 x + x^2 (12L-x) + 6\mu R^2 L}{6R^3 v} \cos \phi$ | 0 |
| $E_{\phi p}$ | $-\frac{q}{R} [R^2 + \mu(L-x)^2] \sin \phi$ | $-\frac{\mu(L-x) \sin \phi}{R^2 v}$ | $\frac{1+\mu}{R^2} \frac{1}{v} \cdot x$ |

ORIGINAL PAGE IS OF POOR QUALITY

TABLE 2.73-2. CYLINDER LOADED BY WIND LOADING (REF. 2-9)

| Structural System and Distribution of Stresses (cantilever) | |
|---|--|
| | |
| Loading: wind pressure p | |
| $X = Y = 0; Z = \sum p \cos n\theta$, where $n = 0, 1, 2, 3, \dots$ | |
| Stresses | |
| $N_\theta = -p R \cos n\theta; \quad N_x = \frac{p n^2}{2R} (L-x)^2 \cos n\theta$ $N_{x\phi} = N_{\phi x} = p n (L-x) \sin n\theta$ | |
| Deformations | |
| $Etu = \frac{p x}{6R} \left[n^2 (3L^2 - 3Lx + x^2) + 6\mu R^2 \right] \cos n\theta$ $Etv = \frac{p nx}{24R^2} \left[48 (1 + \mu) R^2 L - 12 (2 + \mu) R^2 x + n^2 x (6L^2 - 4Lx + x^2) \right] \sin n\theta$ $Etw = \frac{-p}{24R^2} \left[24R^4 + 12R^2 n^2 \left[\mu L^2 + 2 (2 + \mu) Lx - 2x^2 \right] + n^4 x^2 (6L^2 - 4Lx + x^2) \right] \cos n\theta$ $Et\beta = \frac{p n}{24R^2} \left[-24R^4 + 48 (1 + \mu) R^2 Lx - 12 (2 + \mu) R^2 x^2 - 12R^2 n^2 \left[\mu L^2 + 2 (2 + \mu) Lx - 2x^2 \right] + n^2 (1 - n^2) x^2 (6L^2 - 4Lx + x^2) \right] \sin n\theta$ | |

2.73.2 Cantilevered Conical Shell

The configuration, geometrical data, and loading are presented in Fig. 2.73-1. A set of such thin conical shells was analyzed, and the corresponded curves, representing the solutions, were obtained.

Solutions are presented in following charts (Figs. 2.73-2 to 10). The charts should be useful for the following ranges of several parameters.

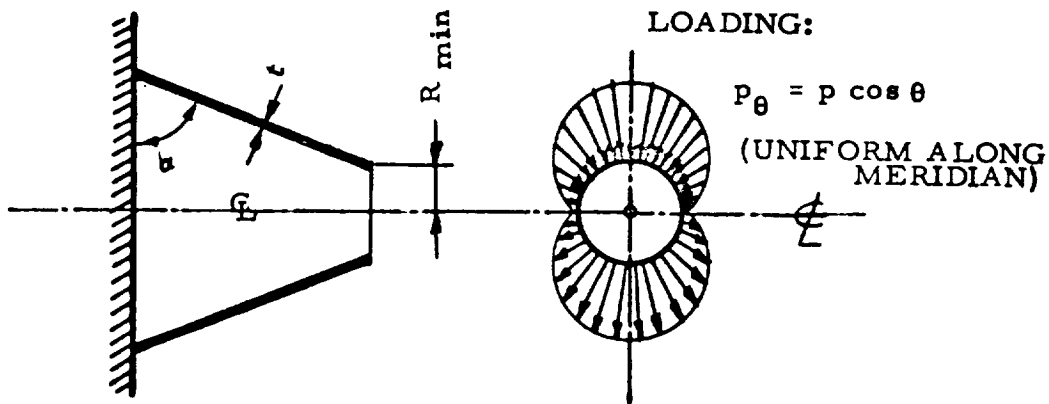


FIG. 2.73-1. Structural System and Loading

$$30^{\circ} \leq \alpha \leq 90^{\circ}$$

$$10 \text{ in.} \leq L \leq 500 \text{ in.}$$

$$\frac{1}{4} \text{ in.} \leq t \leq 2 \text{ in.}$$

$$50 \text{ in.} \leq R_{\min} \leq 200 \text{ in.}$$

Extrapolation beyond indicated ranges is not recommended. The results given in the charts are the maximum values at $\theta = 0$ degrees. If values at some other circumferential angle are desired, simply multiply the corresponding chart value by $\cos \theta$, where θ is the angle of interest.

The following is an example problem:

Suppose one wished to find an approximate value for the maximum normal deflection of a cantilevered conical shell frustum with $\alpha = 45$ degrees, $L = 300$ inches, $t = 1$ inch, and $R_{min} = 150$ inches. Suppose the loading is of the type shown in Fig. 2.73-1 with $p = 2$ psi and $E = 30 \times 10^6$ psi; then,

$$\frac{p}{Et} = 6.67 \times 10^{-8} \text{ in.}^{-1}$$

Since the case described does not correspond exactly to any given in the charts, interpolation will be necessary. The required computations are summarized in Table 2.73-3, where the approximate maximum deflection for the example problem is found as 0.073 inches. Obviously, a problem requiring fewer interpolations should yield more correct results.

TABLE 2.73-3. METHOD OF INTERPOLATION TO SOLVE
EXAMPLE PROBLEM

| Case | α (deg) | Rmin (in.) | L (in.) | w_{\max} | Comment |
|------|----------------|------------|---------|-----------------------|-----------------------------------|
| 1 | 30 | 100 | 100 | 1.6×10^{-2} | Read from Fig. 2.73-4 |
| 2 | 30 | 200 | 100 | 3.0×10^{-2} | Read from Fig. 2.73-4 |
| 3 | 30 | 150 | 100 | 2.3×10^{-2} | Interpolated from cases 1 and 2 |
| 4 | 30 | 100 | 500 | 2.2×10^{-1} | Read from Fig. 2.73-4 |
| 5 | 30 | 200 | 500 | 2.7×10^{-1} | Read from Fig. 2.73-4 |
| 6 | 30 | 150 | 500 | 2.45×10^{-1} | Interpolated from cases 4 and 5 |
| 7 | 30 | 150 | 300 | 0.134 | Interpolated from cases 3 and 6 |
| 8 | 60 | 100 | 100 | 2.3×10^{-3} | Read from Fig. 2.73-7 |
| 9 | 60 | 200 | 100 | 5.7×10^{-3} | Read from Fig. 2.73-7 |
| 10 | 60 | 150 | 100 | 4.0×10^{-3} | Interpolated from cases 8 and 9 |
| 11 | 60 | 100 | 500 | 1.57×10^{-2} | Read from Fig. 2.73-7 |
| 12 | 60 | 200 | 500 | 2.33×10^{-2} | Read from Fig. 2.73-7 |
| 13 | 60 | 150 | 500 | 1.95×10^{-2} | Interpolated from cases 11 and 12 |
| 14 | 60 | 150 | 300 | 0.0117 | Interpolated from cases 10 and 13 |
| 15 | 45 | 150 | 300 | 0.073 | Interpolated from cases 7 and 14 |

FIG. 2.73-2. MAXIMUM MERIDIONAL STRESS FOR $\alpha = 30^\circ$

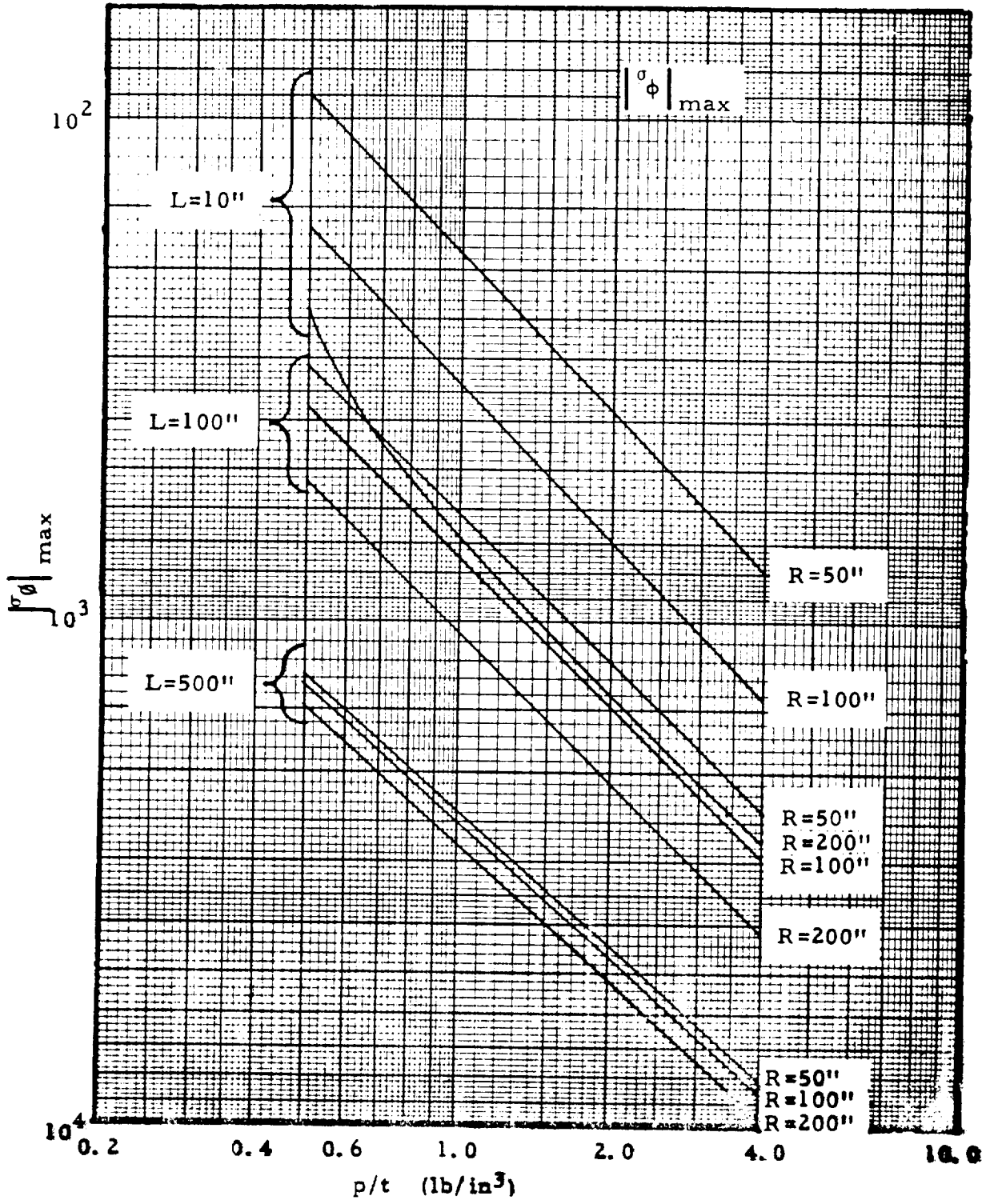


FIG. 2.73-3. MAXIMUM CIRCUMFERENTIAL STRESS FOR $\alpha = 30^\circ$

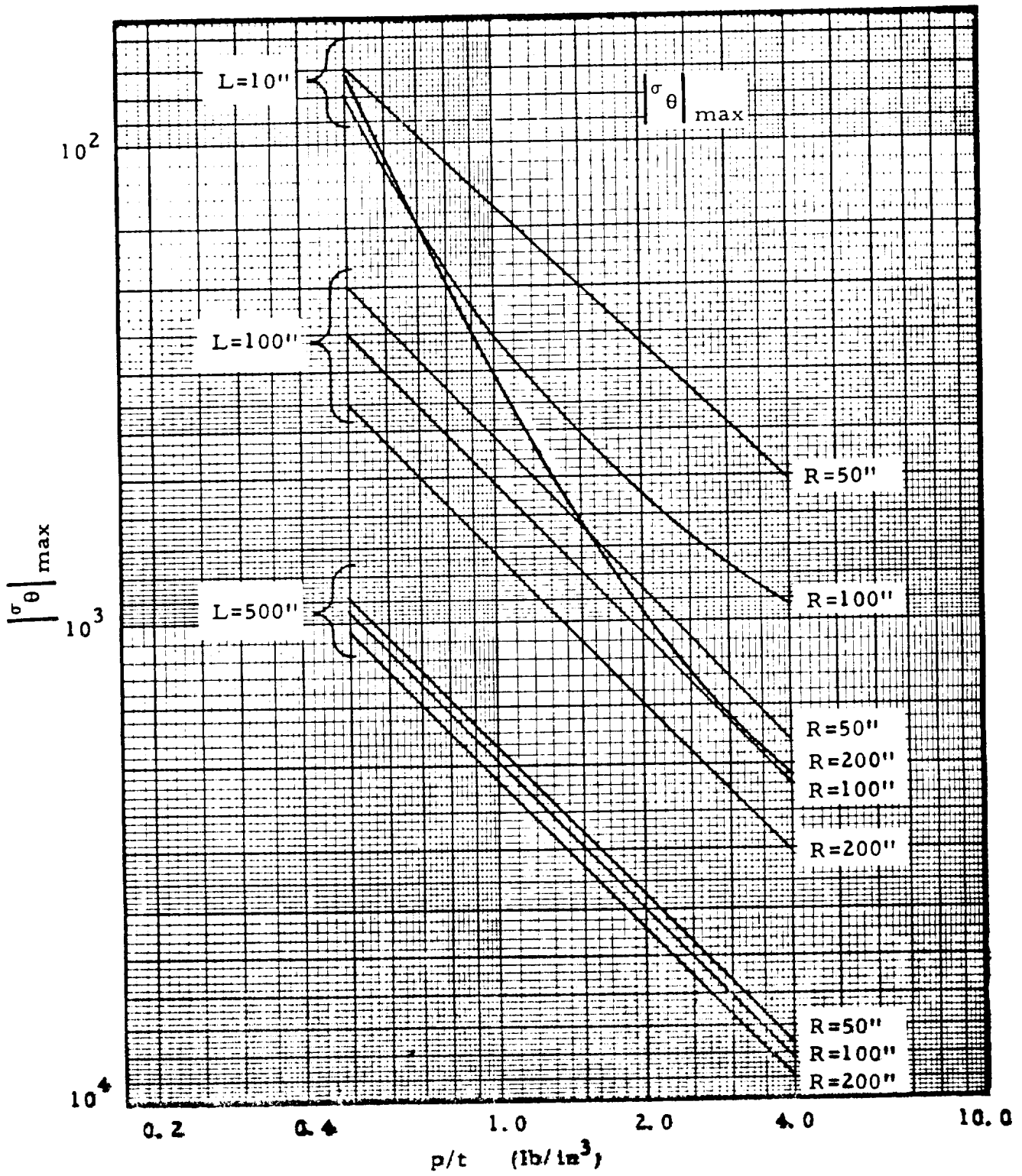


FIG. 2.73-4. MAXIMUM NORMAL DEFLECTION FOR $\alpha = 30^\circ$

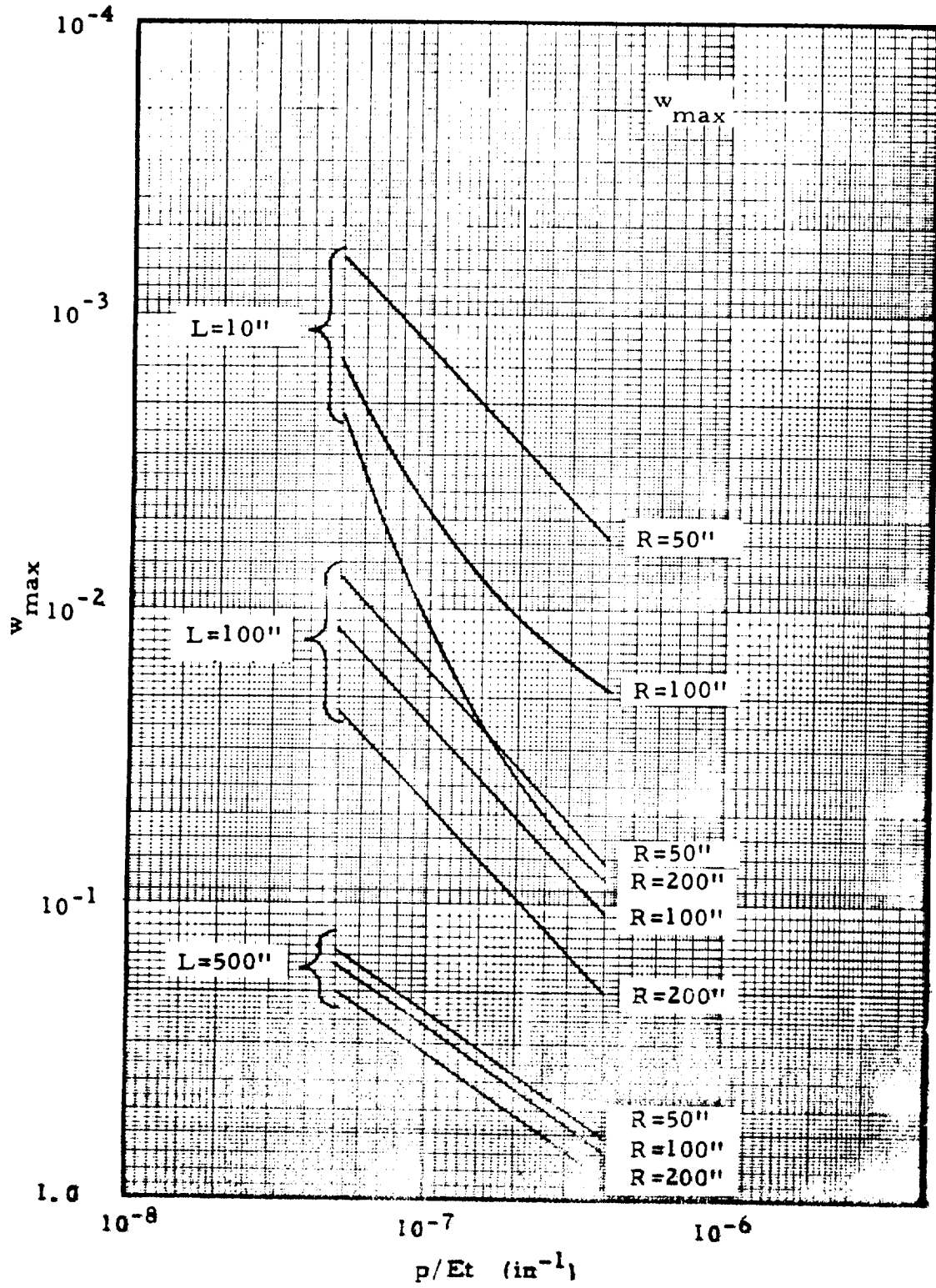


FIG. 2.73-5. MAXIMUM MERIDIONAL STRESS FOR $\alpha = 60^\circ$

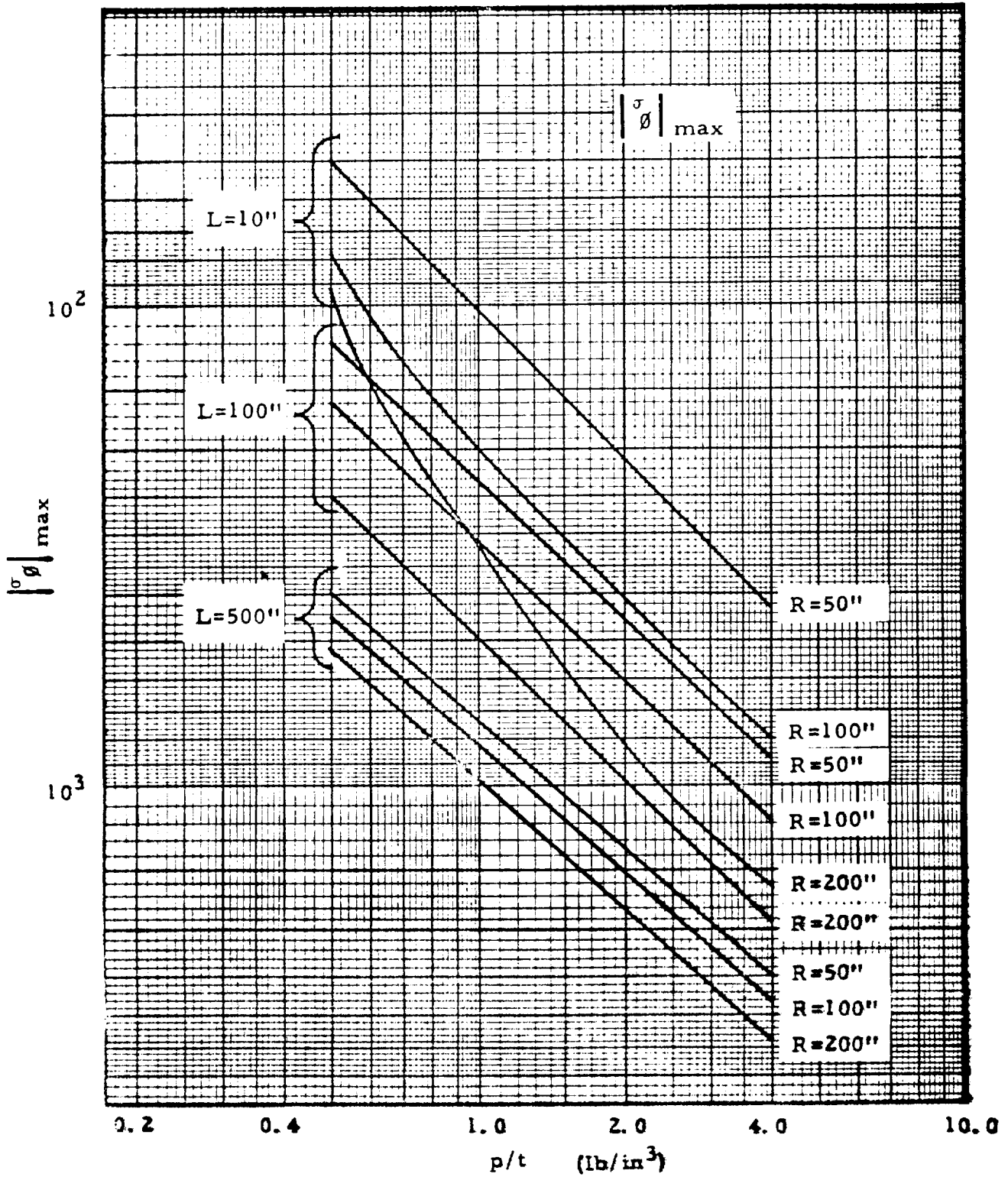


FIG. 2.73-6. MAXIMUM CIRCUMFERENTIAL STRESS FOR $\alpha = 60^\circ$

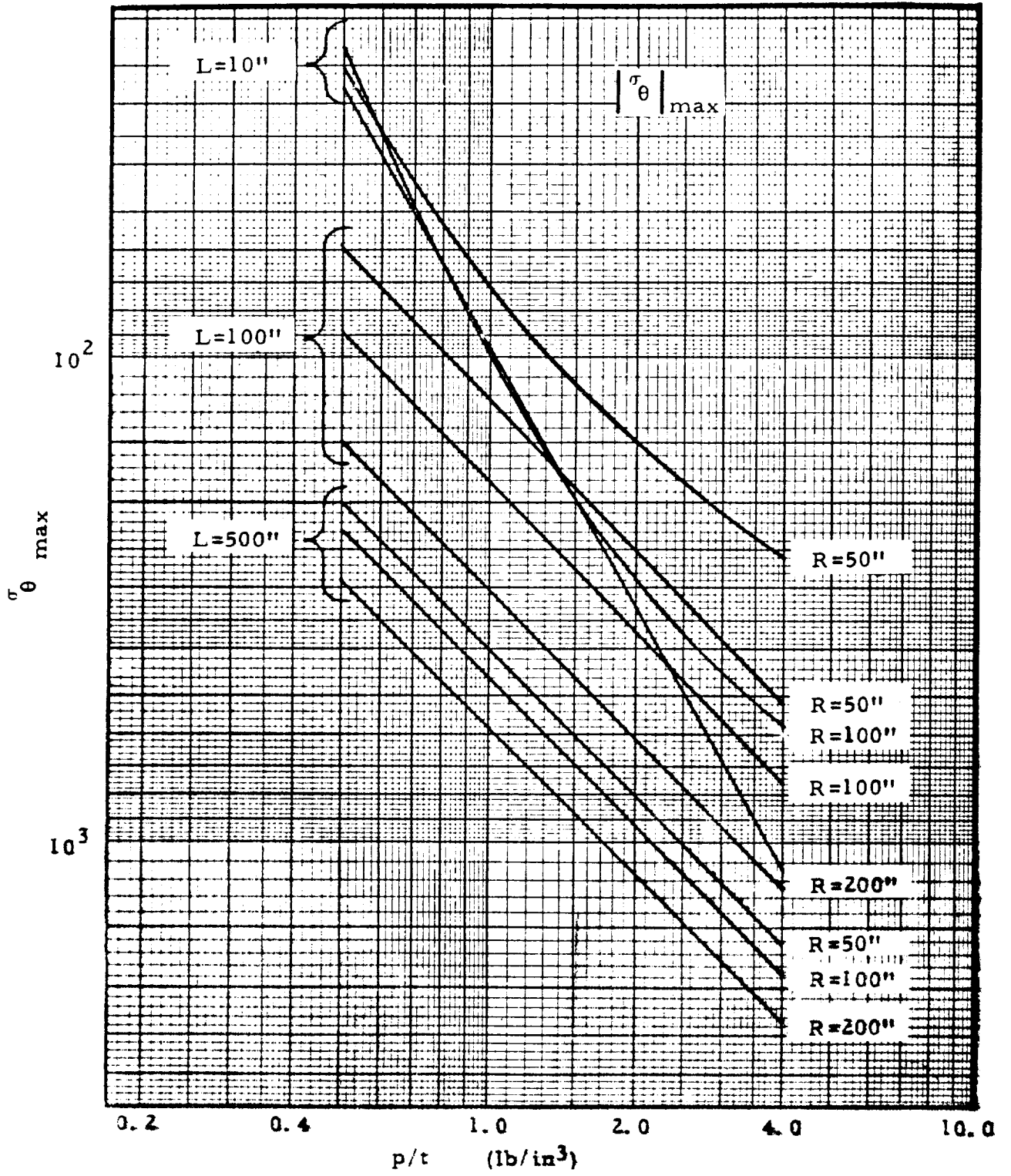


FIG. 2.73-7. MAXIMUM NORMAL DEFLECTION FOR $\alpha = 60^\circ$

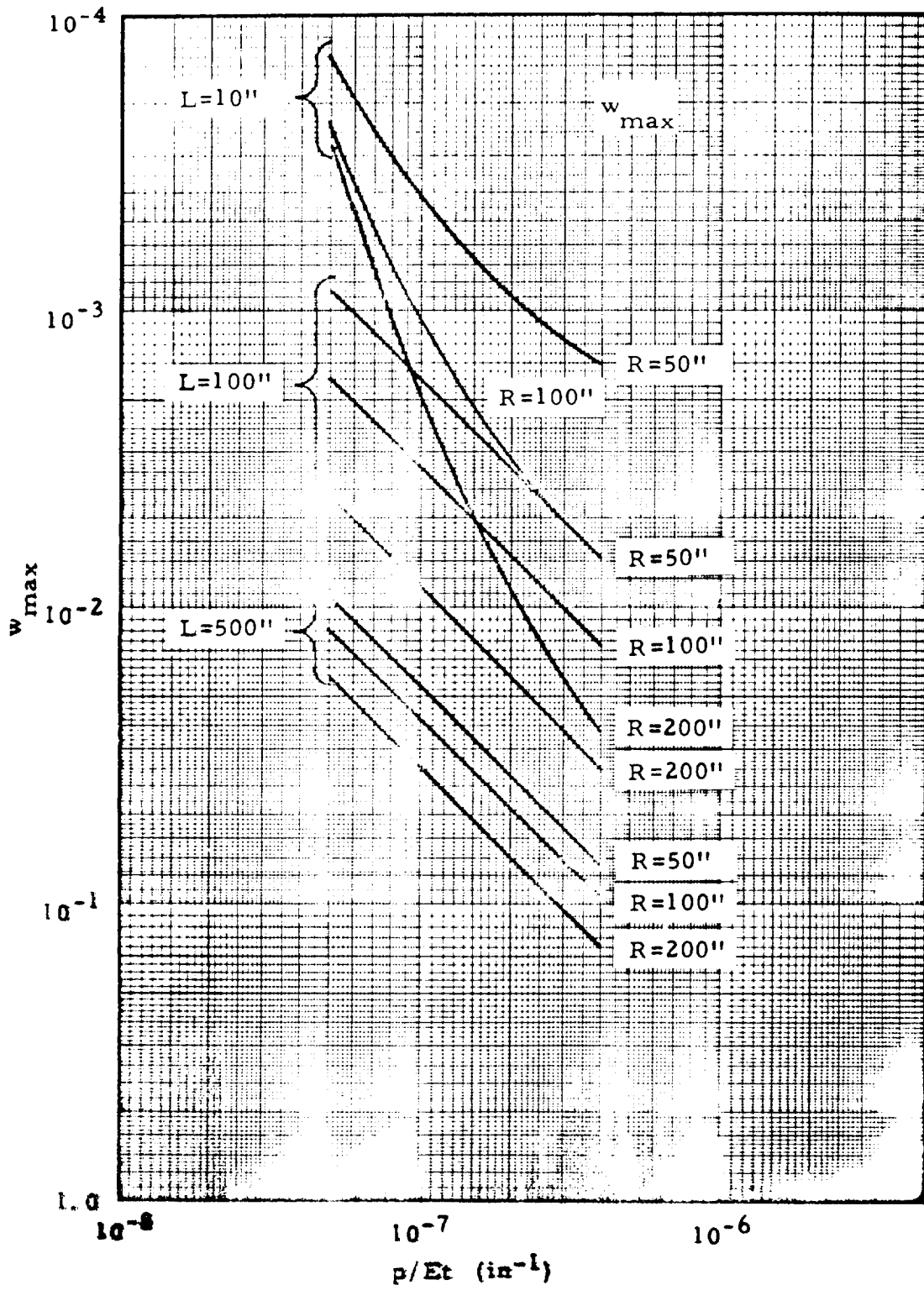


FIG. 2.73-8. MAXIMUM MERIDIONAL STRESS FOR $\alpha = 90^\circ$

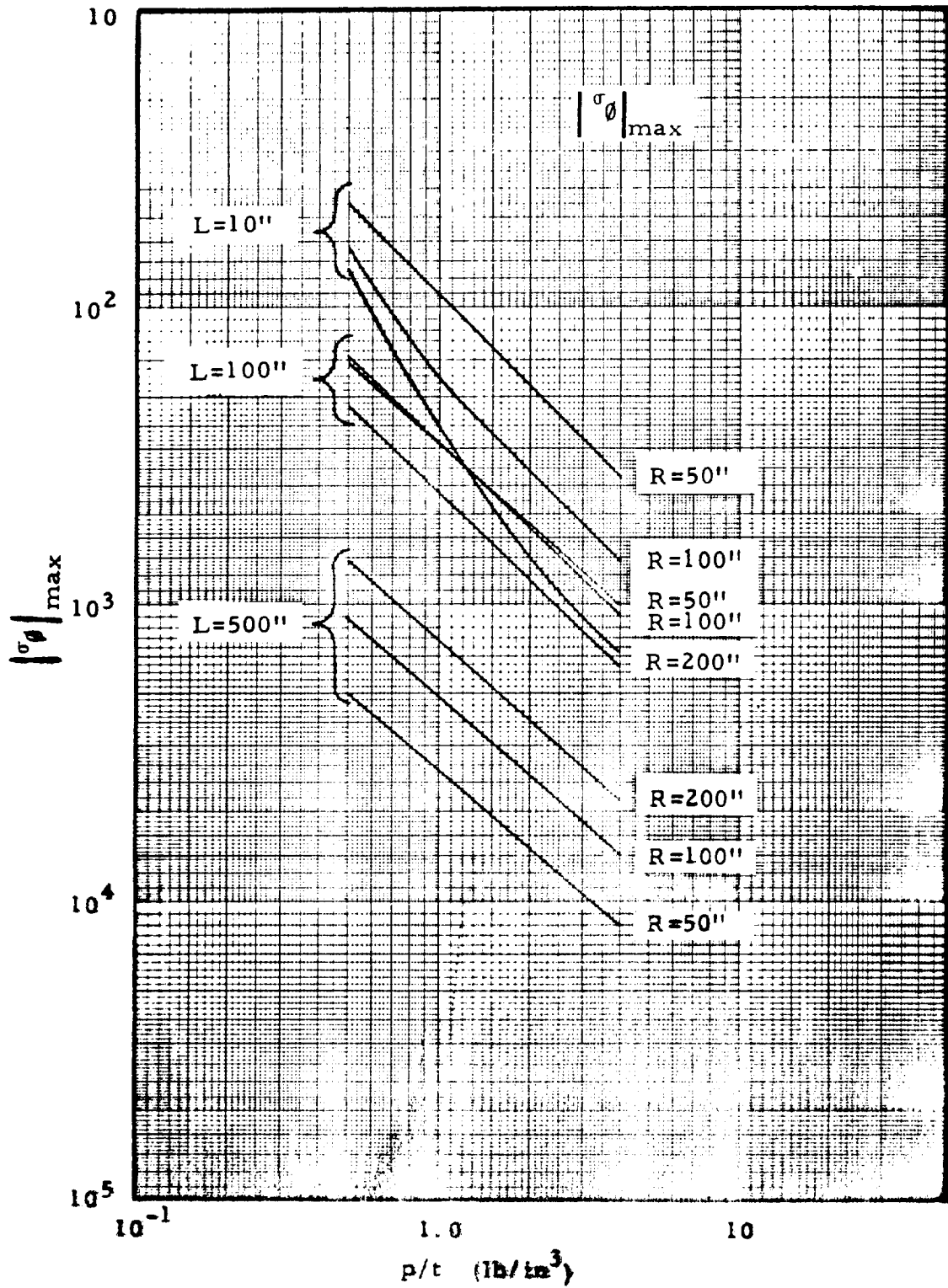


FIG. 2.73-9. MAXIMUM CIRCUMFERENTIAL STRESS FOR $\alpha = 90^\circ$

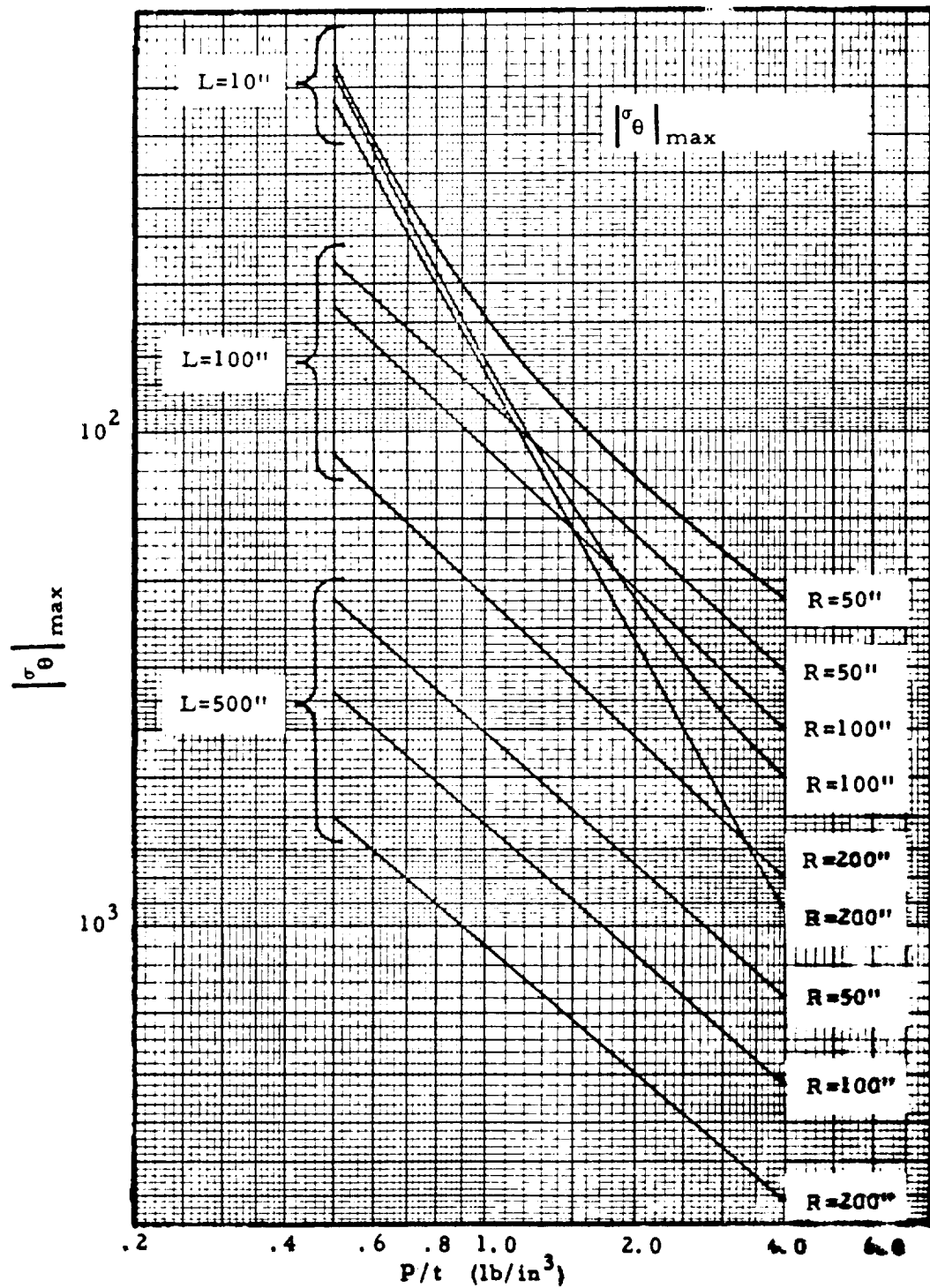
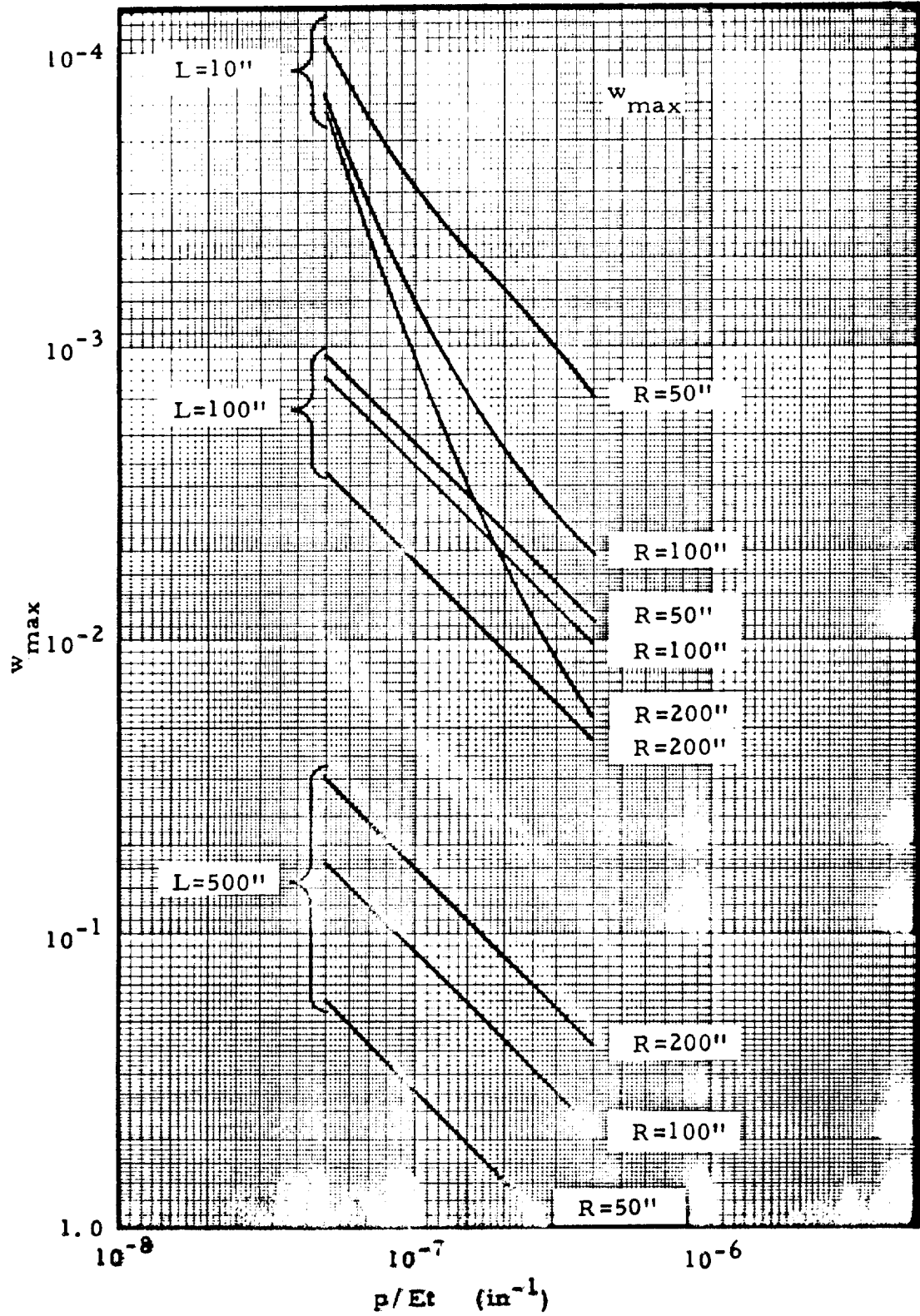


FIG. 2.73-10. MAXIMUM NORMAL DEFLECTION FOR $\alpha = 90^\circ$



2.73.3 Simple and Fixed Beam Cylindrical Shell

Table 2.73-4 presents the solutions for cylindrical shells of a simple beam and fixed beam system under different loading conditions (Ref. 2-9).

TABLE 2.73-4. CYLINDRICAL SHELL LOADED AS A BEAM (Ref. 2-9)

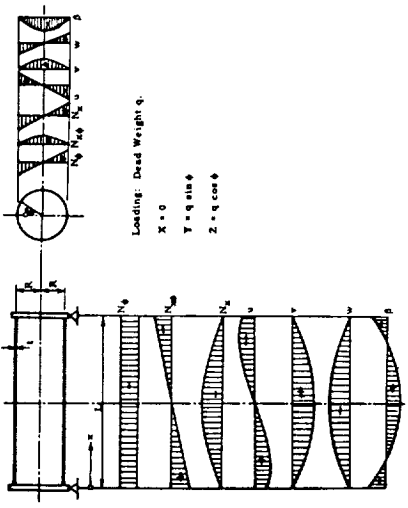
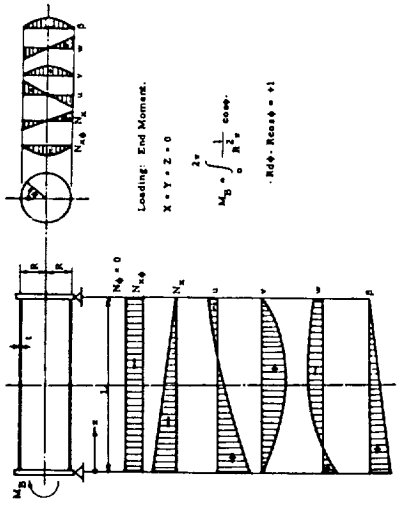
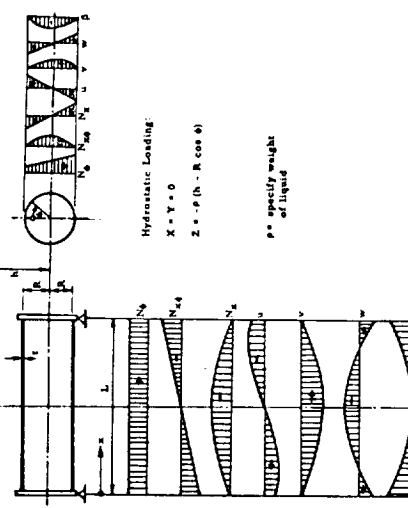
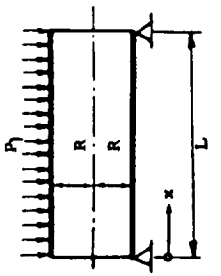

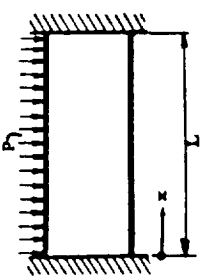
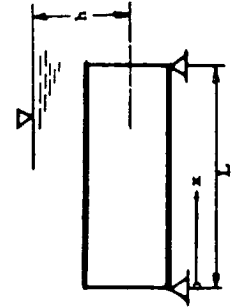
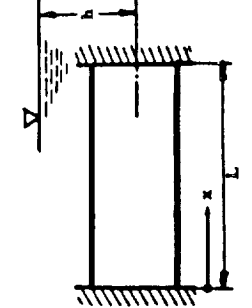
| |  <p> Loading: Dead Weight q $X = 0$ $Y = q \sin \phi$ $Z = q \cos \phi$ </p> |  <p> Loading: End Moments $X = Y = Z = 0$ $M_0 = \int_0^L \frac{1}{R^2} \cos \phi \cdot R d\phi \cdot R \cos \phi = \pi$ $M_L = -\pi$ </p> |  <p> Hydrostatic Loading: $X = Y = 0$ $Z = -p(h - R \cos \phi)$ $p = \text{specific weight of liquid}$ </p> |
|----------|--|--|--|
| M_0 | $-qR \cos \phi$ | 0 | $pR(h - R \cos \phi)$ |
| N_{x0} | $q(L - 2x) \sin \phi = N_{xL}$ | $-\frac{\sin \phi}{R} M_0 = N_{xL}$ | $\frac{pR}{2}(L - 2x) \sin \phi = N_{xL}$ |
| N_{y0} | $-\frac{q}{R}(L - x) \cos \phi$ | $-\frac{(L - x) \cos \phi}{R^2} M_0$ | $-\frac{p}{2}(L - x) \cos \phi$ |
| M_{x0} | $\frac{q(L - 2x)}{12R} \left[L^2 + 2x(L - x) - 6\mu R^2 \right] \cos \phi$ | $\frac{2L^2 + 12(1 + \mu)R^2 - 3x(2L - x)}{6R^2} \frac{\cos \phi}{L^2}$ | $\frac{p(L - 2x)}{24} \left[L^2 + 2x(L - x) - 12\mu R^2 \right] \cos \phi + 12\mu R^2 h$ |
| M_{xL} | $-\frac{q}{12R} \left[12R^2 + x(L - x) + 6(\mu + 3)R^2 \right] \sin \phi$ | $-\frac{\pi(L - x)}{6R^2} \frac{\sin \phi}{L^2}$ | $-\frac{p}{24R} (L - x) \left[L^2 + \pi(L - x) + 12(1 + \mu)R^2 \right] \sin \phi$ |
| M_{y0} | $-\frac{q}{12R} \left[12R^2 + x(L - x) + 6(\mu + 3)R^2 \right] \cos \phi$ | $-\frac{(L - x)}{6R^2} \frac{\cos \phi}{L^2} \left[\pi(2L - x) - 6R^2 \mu \right]$ | $\frac{pR^2}{24R} \left[24R^2 + \pi(L - x) \right] \left[\frac{L^2}{2} + \pi(L - x) + 24R^2 \right] \cos \phi$ |
| M_{yL} | $-\frac{q}{R} \left[R^2 - \mu \pi (L - x) \right] \sin \phi$ | $\frac{\pi(L - x) \sin \phi}{R^2 L^2}$ | $\frac{p}{2} \left[2R^2 - \mu \pi (L - x) \right] \sin \phi$ |

TABLE 2.73-4 (Ref. 2-4) (CONT)

| Shell | Loading | N_x | N_ϕ | $N_{x\phi}$ |
|---|--|---|---|---|
|  |  $Y = -P \cos \phi$ $Z = P \sin \phi$ | $-P \frac{x}{R} (R - x) \sin \phi$ | $-P R \sin \phi$ | $-P (L - 2x) \cos \phi$ |
|  | | $P \left[\frac{L^2}{6R} - \mu R - \frac{x}{R} (L - x) \right] \sin \phi$ $\mu = \text{Poisson's ratio}$ | $-P R \sin \phi$ | $-P (L - 2x) \cos \phi$ |
|  | $Z = -p (h - R \sin \phi)$ | $-P \frac{x}{2} (L - x) \sin \phi$ | $PR^2 \left(\frac{h}{R} - \sin \phi \right)$ | $PR \left(\frac{L}{2} - x \right) \cos \phi$ |
|  | $p = \text{specific weight of liquid}$ | $-P \left[\frac{L^2}{12} - \mu R^2 - \frac{x}{2} (L - x) \right] \sin \phi - \mu R h$ $\mu = \text{Poisson's ratio}$ | $PR^2 \left(\frac{h}{R} - \sin \phi \right)$ | $PR \left(\frac{L}{2} - x \right) \cos \phi$ |

2.73.4 Continuous Cylindrical Shell Under Dead Weight (Ref. 2-9)

Fig. 2.73-11 shows the loaded cylindrical shell.

The system is symmetrical and externally statically indeterminate. For the statically indeterminate value, select the moment X_1 above the middle support. For solution, combine the case of simple beam loaded with dead weight (call case 1) and simple beam loaded with the end moment (call case 2). For reference, see Table 2.73-4.

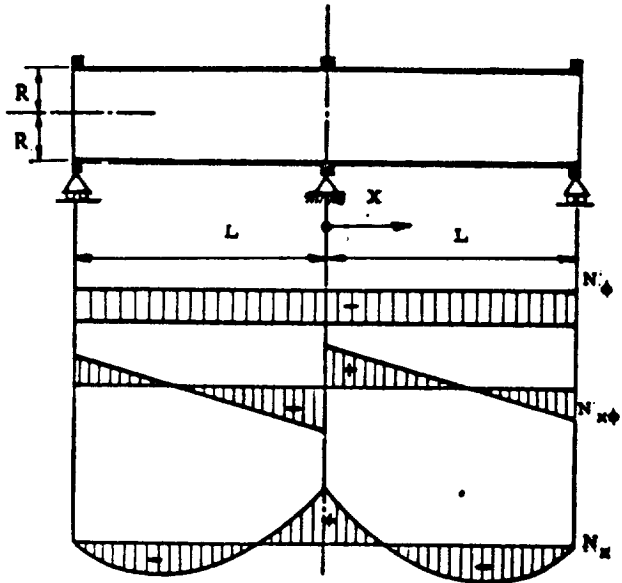


FIG. 2.73-11. Continuous Cylindrical Shell Loaded with Dead Weight

For $X_1 = 0$ (case 1), $Etu_0 = \frac{qL}{12R} (L^2 - 6\mu R^2) \cos \phi$

For $X_1 = +1$ (case 2), $Etu_1 = \frac{1}{3R^2 \pi L} [L^2 + 6(1 + \mu)R^2] \cos \phi$

where u is deflection.

Because of symmetry at $x = 0$, it follows

$$u = u_0 + X_1 u_1 = 0$$

Consequently,

$$X_1 = \frac{u_0}{u_1} = - \frac{qR \pi L^2}{4} \frac{L^2 - 6\mu R^2}{L^2 + 6(1 + \mu)R^2}$$

If $p = q 2\pi R$ = weight for 1 foot of cylinder is introduced and $\mu = 0$,

finally,

$$X_1 = - \frac{pL^2}{8} \frac{1}{1 + 6(R/L)^2}$$

for

$$R/L \rightarrow 0 \dots X_1 = - p \frac{L^2}{8}$$

and for

$$R/L \rightarrow \infty \dots X_1 = 0$$

The null-point of shear corresponds to

$$x_0 = \frac{L}{8} \frac{5L^2 + 6(4 + 3\mu)R^2}{L^2 + 6(1 + \mu)R^2}$$

For the longitudinal stress, N_x will be the null-point located at

$$x_1 = \frac{L}{4} \frac{L^2 - 6\mu R^2}{L^2 + 6(1 + \mu)R^2}$$

Other continuous systems under different loading conditions can be solved in a similar manner.

2.73.5 Curved Panels (Barrel Vaults)

This paragraph presents the collection of different solutions for curved panels of simple beam system. The geometry of curved panels is circular, elliptical, cycloidal, parabolical, catenary, and special shape. The solutions for different loadings are tabulated in Tables 2.73-5 to -7. The shells under consideration are thin, and linear theory was the basis for the derived formulas.

TABLE 2.73-5. CURVED CIRCULAR PANELS—BARREL VAULTS (REF. 2-9)

| Internal Forces | Deadweight loading | Uniform load on projected area Loading $X = 0, Y = p \sin^2 \phi$ $Z = p \cos^2 \phi$ |
|----------------------------------|--|--|
| N_ϕ $N_{x\phi}$ N_x | <p>For this case the formulas which apply to the cylindrical shell (simply supported) can be used.</p> | <p> $-p R \cos^2 \phi$ $N_{\phi x} = \frac{3}{4} p (L - 2x) \sin 2\phi$ $-\frac{3}{2} p x (L - x) \cos 2\phi$ </p> <p>At $\phi = 45^\circ$ $N_x = 0$ $N_{x\phi} = \text{max}$ </p> |

TABLE 2.73-6. CURVED ELLIPTICAL AND CYCLOIDAL PANELS—
BARREL VAULTS (REF. 2-9)

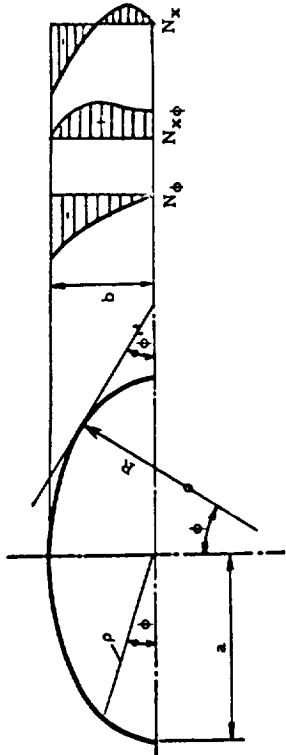
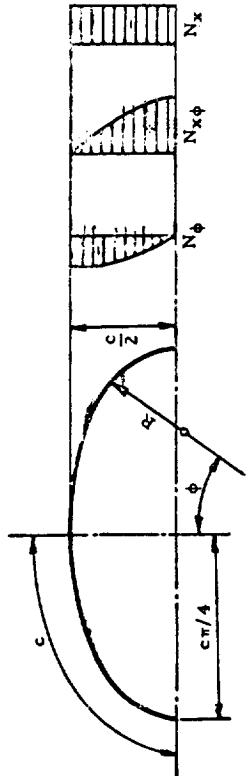
| | Cycloidal Panel, Deadweight Loading |
|---|---|
| <p style="text-align: center;">Elliptical panel, Deadweight Loading</p>  <p style="text-align: center;">The radius of curvature: $R = \frac{\rho^3}{ab}$</p> <p style="text-align: center;">where $\rho = ab / (a^2 \sin^2 \phi + b^2 \cos^2 \phi)^{1/2}$</p> <p style="text-align: center;">Loading components: $X = 0, Y = q \sin \phi, Z = q \cos \phi$ (For x and L see Table 2-73-6)</p> |  <p style="text-align: center;">The radius of curvature $R = c \cos \phi$</p> <p style="text-align: center;">Loading - components: $X = 0, Y = q \sin \phi,$ $Z = q \cos \phi$</p> |
| <p style="text-align: center;">N_ϕ</p> <p style="text-align: center;">$N_{x\phi}$</p> <p style="text-align: center;">N_x</p> | <p style="text-align: center;">$-qc \cos^2 \phi$</p> <p style="text-align: center;">$\frac{3}{2}q(L - Zx) \sin \phi$</p> <p style="text-align: center;">$-\frac{3q}{2c}x(L - x)$</p> |

TABLE 2.73-7. BARREL VAULTS (REF. 2-4) (SHEET 1 OF 4)

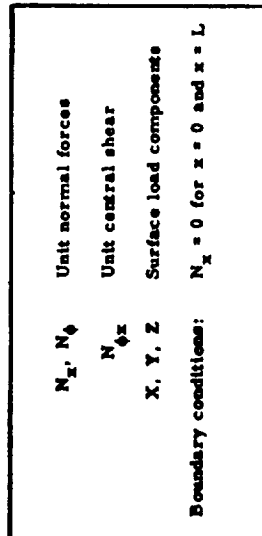
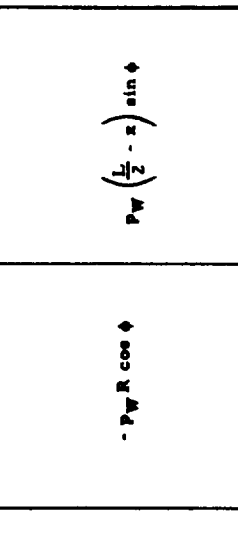
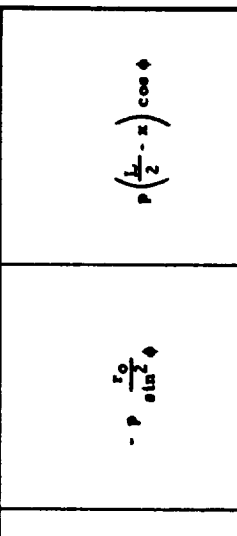
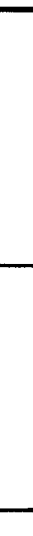
| Shell | Loading | N_x | N_ϕ | $N_{\phi x}$ |
|---|--|--|--|--|
|  | <p>Unit normal forces N_x, N_ϕ Unit central shear $N_{\phi x}$ Surface load components X, Y, Z Boundary conditions: $N_x = 0$ for $x = 0$ and $x = L$</p> | | | |
|  <p>Circle</p> | <p>$Y = -p \cos \phi$ $Z = p \sin \phi$</p> | <p>$-p \frac{L-x}{R} \sin \phi$</p> | <p>$-pR \sin \phi$</p> | <p>$-p(L-2x) \cos \phi$</p> |
|  <p>Circle</p> | <p>$Z = p_w \cos \phi$</p> | <p>$-p_w \frac{x}{2R} (L-x) \cos \phi$</p> | <p>$-p_w R \cos \phi$</p> | <p>$p_w \left(\frac{L}{2} - x \right) \sin \phi$</p> |
|  <p>Parabola</p> | <p>$Y = -p \cos \phi$ $Z = p \sin \phi$</p> | <p>$p \frac{x}{2r_0} (L-x) \sin^2 \phi$</p> | <p>$-p \frac{r_0}{\sin^2 \phi}$</p> | <p>$p \left(\frac{L}{2} - x \right) \cos \phi$</p> |

TABLE 2. 73-7 (Sheet 2 of 4)

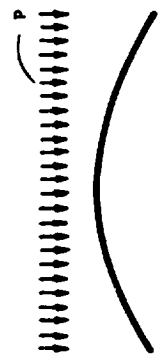

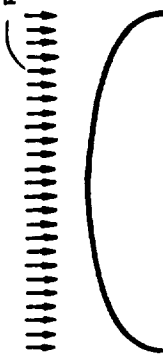

| Shell | Loading | N_x | N_ϕ | $N_{x\phi}$ |
|--|--|--|--|--|
|  <p>Parabola</p> | $Y = -p \sin \phi \cos \phi$ $Z = p \sin^2 \phi$ | 0 | $-P \frac{r_0}{\sin \phi}$ | 0 |
|  <p>Cycloid</p> | $Z = P_W \cos \phi$ | $P_W \frac{x}{2r_0} (L-x) \sin \phi \cos \phi \times$ $\times (3 + 2 \sin^2 \phi)$ | $-P_W r_0 \frac{\cos \phi}{\sin^3 \phi}$ | $P_W \left(\frac{L-x}{2} - x \right) \frac{1 + 2 \cos^2 \phi}{\sin \phi}$ |
|  <p>Cycloid</p> | $Y = -p \sin \phi \cos \phi$ $Z = p \sin^2 \phi$ | $P \frac{2x}{r_0} (L-x) \frac{1 - 2 \sin^2 \phi}{\sin \phi}$ | $-P r_0 \sin^3 \phi$ | $-P \left(\frac{L}{2} - x \right) 4 \sin \phi \cos \phi$ |
|  <p>Cycloid</p> | $Z = P_W \cos \phi$ | $-P_W \frac{x}{r_0} (L-x) \times$ $\times (1 - \cos \phi) \frac{\cos \phi}{\sin^3 \phi}$ | $-P_W r_0 \sin \phi \cos \phi$ | $-P_W \left(\frac{L}{2} - x \right) \frac{1 - 2 \sin^2 \phi}{\sin \phi}$ |

TABLE 2.73-7 (Sheet 3 of 4)

Ref (2-45)

| Shell | Loading | N_x | N_ϕ | $N_x \phi$ |
|-------|---|---|---|--|
| | $Y = -p \sin \phi \cos \phi$ $Z = p \sin^2 \phi$ | $-p \frac{x(L-x)}{2a^2 \eta} \times$ $\times \left[b^2 (a^2 \cos^2 \phi - b^2 \sin^2 \phi) + \right.$ $\left. + 2\eta (\sin^2 \phi - \cos^2 \phi) \right]$ | $-p a^2 b^2 \frac{\sin^2 \phi}{\eta^{3/2}}$ | $p \left(\frac{L}{2} - x \right) \times$ $\times \frac{3 \sin \phi \cos \phi}{\eta} (b^2 - 2\eta)$ |
| | $Z = P_w \cos \phi$ | $-P_w \frac{x}{2} \frac{(L-x) \cos \phi}{a^2 \eta^{1/2}} \left[\eta^2 + \right.$ $\left. + 3\eta (b^2 - a^2) (1 - 3 \sin^2 \phi) - \right.$ $\left. - 6 (b^2 - a^2)^2 \sin^2 \phi \cos^2 \phi \right]$ | $-P_w a^2 b^2 \frac{\cos \phi}{\eta^{3/2}}$ | $P_w \left(\frac{L}{2} - x \right) \frac{3}{\eta} \frac{b^2 - a^2}{\eta} \times$ $\times (1 + \cos^2 \phi) \sin \phi$ |
| | $Y = -p \cos \phi$ $Z = p \sin \phi$ | 0 | $-p \frac{r_0}{\sin \phi}$ | 0 |
| | $Y = -p \sin \phi \cos \phi$ $X = p \sin^2 \phi$ | $p \frac{x}{2r_0} (L-x) \sin^2 \phi \times$ $\times (1 - 2 \sin^2 \phi)$ | $-p r_0$ | $-p \left(\frac{L}{2} - x \right) \sin \phi \cos \phi$ |

TABLE 2.73-7 (Sheet 4 of 4)

| Shell | Loading | N_x | N_ϕ | $N_{x\phi}$ |
|-------|---|---|---|--|
| | $Z = P_W \cos \phi$ | $P_W \frac{x}{2r_0} (L - x) \cdot (2 + \sin^2 \phi) \cos \phi$ | $- P_W \frac{\cos \phi}{\sin^2 \phi}$ | $P_W \left(\frac{L}{2} - x \right) \frac{1 + \cos^2 \phi}{\sin \phi}$ |
| | $Y = -p \cos \phi$ $Z = p \sin \phi$ | $P \frac{x(L-x)(y+\pi/4)}{2a(y+\sin \phi)^3} \cdot \left[y(1-6\sin^2 \phi) - (2y^2+3\sin^2 \phi)\sin \phi \right]$ | $- \frac{p}{y+\pi/4} \cdot (y+\sin \phi) \sin \phi$ | $P \left(x - \frac{L}{2} \right) \frac{(2y+3\sin \phi) \cos \phi}{y+\sin \phi}$ |
| | $Y = -p \sin \phi \cos \phi$ $Z = p \sin^2 \phi$ | $P \frac{x(L-x)(y+\pi/4)}{2a(y+\sin \phi)^3} \cdot \left[y(8-15\sin^2 \phi)\sin \phi + (3y^2+4\sin^2 \phi) \cdot (1-2\sin^2 \phi) \right]$ | $\frac{p}{y+\pi/4} \cdot (y+\sin \phi) \sin^2 \phi$ | $P \left(x - \frac{L}{2} \right) \cdot \frac{(3y+4\sin \phi) \sin \phi \cos \phi}{y+\sin \phi}$ |
| | $Z = P_W \cos \phi$ | $- P_W \frac{x(L-x)(y+\pi/4)}{2a(y+\sin \phi)^3} \cdot \cos \phi (1+y^2+\sin^2 \phi + 4y \sin \phi)$ | $- P_W \frac{p}{y+\pi/4} \cdot (y+\sin \phi) \cos \phi$ | $P_W \left(x - \frac{L}{2} \right) \frac{1-2\sin^2 \phi - y \sin \phi}{y+\sin \phi}$ |

2.74 SUMMARY

This section primarily presented the individual solutions for different type of unsymmetrically loaded shells or shells with nonsymmetrical geometry. This section has a secondary significance because Chapter 2.00 mainly deals with the axisymmetrical shells of revolution located axisymmetrically. Since there were few solutions for unsymmetrical cases, it was reasonable to include them in this chapter.

2.80 MARGIN OF SAFETY

2.81 GENERAL

Methods have been shown to determine the state of stresses and deformations in different kind of shells; however, this is not the final step in shell design. It must be proven that the determined stresses and deformations can be withstood by the material from which shell is made. The following definitions are common in engineering:

Failing stress = stress under which failure occurs
(rupture, buckle)

Limit stress = stress due to the limit load (also called
actual stress)

Limit load (or applied load) = load which has to be taken by
structure

Ultimate stress = limit stress x factor of safety

$$\begin{aligned}\text{Margin of safety} &= \frac{\text{failing stress}}{\text{ultimate stress}} - 1 \\ &= \frac{\text{failing stress}}{\text{limit stress} \times \text{factor of safety}} - 1 \\ &= \frac{\text{allowable stress}}{\text{calculated stress}} - 1\end{aligned}$$

The material will fail if a certain combination of stresses reaches a certain level, which is called failing stress. The uniaxial failing stress is usually known for materials. Multiaxial failing stress cannot be determined in general at the present time because of technical difficulties. This program will be discussed later in this section. Analysis of shells is usually restricted to the elastic range or in a range where the stresses can be assumed to be elastic.

2.82 DEFINITIONS

In the uniaxial case, the allowable stress is the limiting stress, such that the maximum actual stress $\sigma_{\max} \leq \sigma_{\text{allow}}$. Instead of using allowable stress, in many instances, the analyst is operating with the margin of safety, which is related to the allowable stress as was shown above. When the allowable stress is established, the margin of safety has to be larger or equal to zero. If the margin of safety is negative, the configuration must be revised in order not to exceed prescribed limit, unless there is additional justification. The allowable stress is defined as

$$\sigma_{\text{allow}} = \frac{\sigma}{n}, \bar{\sigma} \begin{cases} = \sigma^* \text{ for ductile materials} \\ = \sigma^{**} \text{ for brittle materials} \end{cases}$$

where

σ^* = the stress which corresponds to the elastic limit of materials of plastic characteristics. However, depending on requirements and specifications which are usually different for various designs, the definition of σ^* may be modified and designated as the stress at which the plastic deformations (that do not disappear after deloading) reach

some amount, which is satisfactory to the design requirements in first time of loading, (i. e., 0.001 to 0.003 percent).

σ^{**} = the stress which corresponds to the fictitious elastic limit of materials of brittle characteristics. Such materials usually have no elastic limit; consequently, when the fictitious elastic limit is introduced, the remaining deformation will not exceed 2 percent, or thereabouts.

n = safety factor, which can be also designated with F. S.

Similarly, allowable shear stress $\tau_{allow} \geq \tau_{max}$ is introduced, where τ_{max} is the largest shear stress. As before,

$$\tau_{allow} = \frac{\bar{\tau}}{n}$$

where $\bar{\tau}$ is an artificial value accepted in the correspondence with the used material and design (Ref. 2-18).

Determination of allowable stresses or margins of safety does not present any difficulty for the uniaxial case, as was evident from the above discussion. It is wrong, however, to compare the stresses for multiaxial case against uniaxial allowables. If such a comparison is made, then not the stresses, but certain combinations of such may be compared with the uniaxial tensional allowables, as will be shown in the following paragraph.

2.83 THREE-DIMENSIONAL FIELD OF STRESSES

Considerable difficulty exists if the stress is not uniaxial, because then it is not clear what shall be used for allowable stresses. Consequently, the equivalency of multiaxial with the uniaxial state of stresses must be established so that the allowable uniaxial tensile stress can be used. Several existing theories attempted to relate the multiaxial and uniaxial stresses, but only theories that are justified by test can be considered.

2.83.1 Maximum Stress Theory

According to this theory, the two state of stresses are considered equivalent if their principal stresses are equal. Consequently, if uniaxial principal stress of system (a) is σ' and principal stress of multiaxial stress system (b) is σ_1 , for equivalency must be $\sigma' = \sigma_1$. Then $\sigma_1 \leq \sigma_{\text{allow}}$, where σ_{allow} is the allowable stress for uniaxial system (a).

2.83.2 Maximum Strain Theory (Mariotte)

According to this theory, two states of stress are equivalent if their maximum linear strains are equal:

$$\epsilon'_{\text{max}} = \epsilon_{\text{max}} .$$

For an uniaxial system, assume

$$\epsilon'_{\text{max}} = \frac{\sigma_1}{E}$$

For a multistress system,

$$\epsilon'_{\max} = \frac{1}{E} \left[\sigma_1 - \mu(\sigma_2 + \sigma_3) \right]$$

Consequently,

$$\sigma_1 - \mu(\sigma_2 + \sigma_3) \leq \sigma_{\text{allow}} \text{ for uniaxial case.}$$

2.83.3 Maximum Shear Theory (Kulon)

According to this theory, two states of stress (a) and (b) are equivalent if their maximum shear stresses are equal:

$$\left| \tau'_{\max} \right| = \left| \tau_{\max} \right|$$

Since

$$\tau_{\max} = \frac{\sigma_1 - \sigma_3}{2} ,$$

for uniaxial

$$\tau'_{\max} = \frac{\sigma'_1}{2} ,$$

then

$$\sigma'_1 = \sigma_1 - \sigma_3 .$$

Consequently,

$$\sigma_1 - \sigma_3 \leq \sigma_{\text{allow}} \text{ (for uniaxial case)}$$

2.83.4 Maximum Strain Energy Theory (Beltrami)

According to this theory, two states of stress are equivalent if the strain energies are equal: $U' = U$.

$$U' = (\sigma'_1)^2 / 2E$$

for the uniaxial case.

$$U = \frac{1}{2E} \left[\sigma_1^2 + \sigma_2^2 + \sigma_3^2 - 2\mu(\sigma_1\sigma_2 + \sigma_2\sigma_3 + \sigma_3\sigma_1) \right]$$

for the multistress field. Consequently,

$$\sqrt{\sigma_1^2 + \sigma_2^2 + \sigma_3^2 - 2\mu(\sigma_1\sigma_2 + \sigma_2\sigma_3 + \sigma_3\sigma_1)} \leq \sigma_{\text{allow}} \quad (\text{for uniaxial stress field})$$

where σ_1 , σ_2 , and σ_3 are principal stresses.

Unfortunately, the experimental data do not agree with this theory.

Consequently, Huber suggested this correction: two states of stresses are equivalent if the distortion energies are equal. After similar reasoning, this leads to the following criterion:

$$\sqrt{\sigma_1^2 + \sigma_2^2 + \sigma_3^2 - \sigma_1\sigma_2 - \sigma_2\sigma_3 - \sigma_3\sigma_1} \leq \sigma_{\text{allow}}$$

or

$$\frac{1}{\sqrt{2}} \sqrt{(\sigma_1 - \sigma_2)^2 + (\sigma_2 - \sigma_3)^2 + (\sigma_3 - \sigma_1)^2} \leq \sigma_{\text{allow}}$$

where σ_1 , σ_2 , and σ_3 are principal stresses.

This theory holds for the ductile materials only, as will be shown later.

2.83.5 Mohr's Theory

Where all previously mentioned theories may be useful for the ductile materials. Mohr provided a suitable theory for brittle materials. According to Mohr's assumption, different states of stress are equivalent if all correspondent Mohr's circles have the same envelope, as shown in Fig. 2.80-1. Only two main stresses are considered. Disregard of the third main stress introduces only a negligible difference. If the allowable stress for uniaxial compression and tension is known, two Mohr circles can be drawn as shown in Fig. 2.80-2. The first two circles in Fig. 2.80-2 represent reduced Mohr circles corresponding to the safety factor of limiting compressional and tensional stresses. Consequently, the third circle also represents the same for the biaxial stress. This leads to the following criteria:

$$\frac{\text{all } \sigma_t}{\text{all } \sigma_c} = m; \sigma_1 - m \sigma_3 \leq \text{all } \sigma_t$$

For the ductile materials, usually

$$\frac{\text{all } \sigma_t}{\text{all } \sigma_c} = 1; \sigma_1 - \sigma_3 \leq \sigma_{\text{allow.}} \text{ (for uniaxial case)}$$

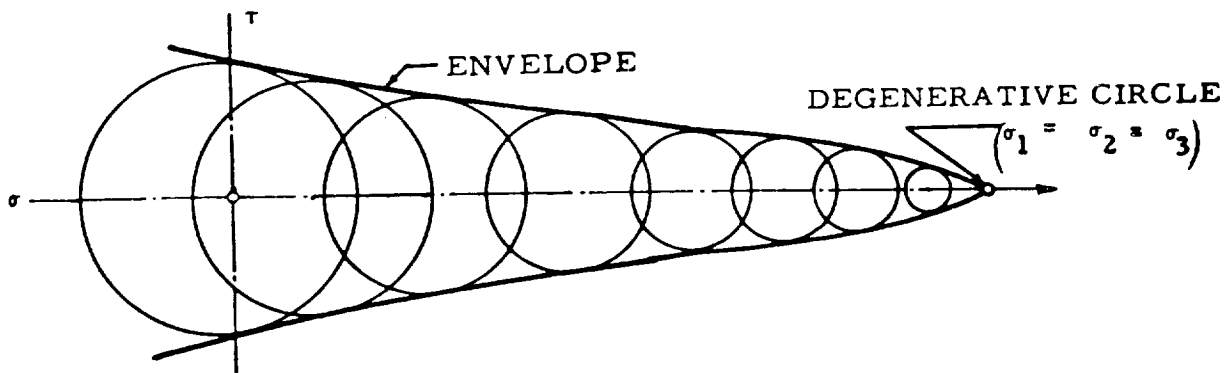


FIG. 2.80-1. Different States of Stress at the Same Point, With the Same Envelope

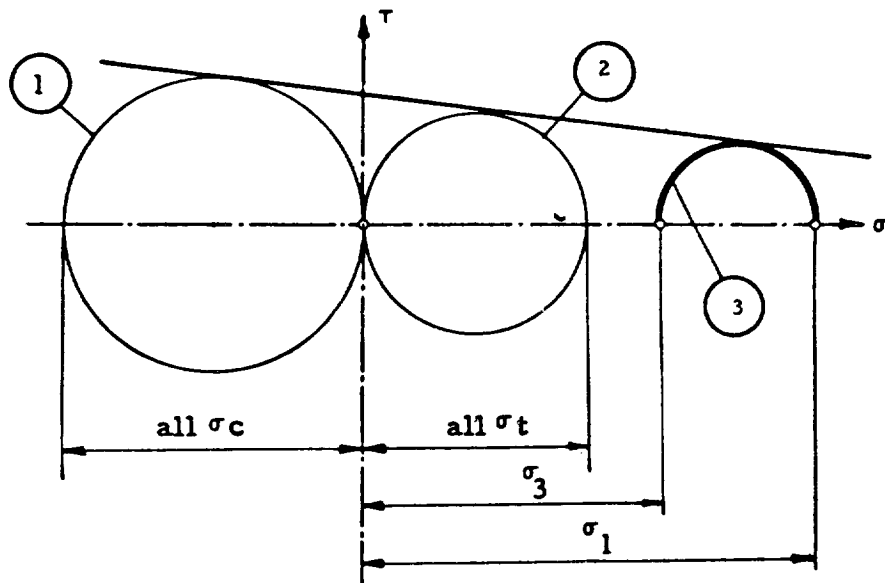


FIG. 2.80-2. Three Mohr Circles With the Mutual Tangent

2.84 CONDITIONS OF PLASTICITY (HENCKY—VON MISES, AND TRESCA)

Recently, the third and fourth theory found extensions in connection with the theory of plasticity. According to the assumption of Hencky and von Mises, the material stressed with three-dimensional field stresses behaves elastically if the intensity of stresses does not exceed the elastic limit for uniaxial stress. According to Huber (see the theory of change of geometry),

$$\frac{1}{\sqrt{2}} \sqrt{(\sigma_1 - \sigma_2)^2 + (\sigma_2 - \sigma_3)^2 + (\sigma_3 - \sigma_1)^2} = \sigma_S$$

or

$$\sqrt{2} \sqrt{\tau_{12}^2 + \tau_{23}^2 + \tau_{31}^2} = \sigma_S$$

This equation represents ellipsoid if both sides of equation are squared. If the actual state of principal stresses ($\sigma_1, \sigma_2, \sigma_3$) is within this ellipsoid, the material is still in the elastic range.

For two-dimensional state of stresses (assume $\sigma_3 = 0$),

$$(\sigma_1 - \sigma_2)^2 + \sigma_2^2 + \sigma_1^2 = 2 \sigma_S^2$$

This represents an ellipse inclined to 45 degrees to the axis σ_1 and σ_2 as shown in Fig. 2.80-3 and is called the ellipse of Hencky-von Mises, or von Mises yield surface.

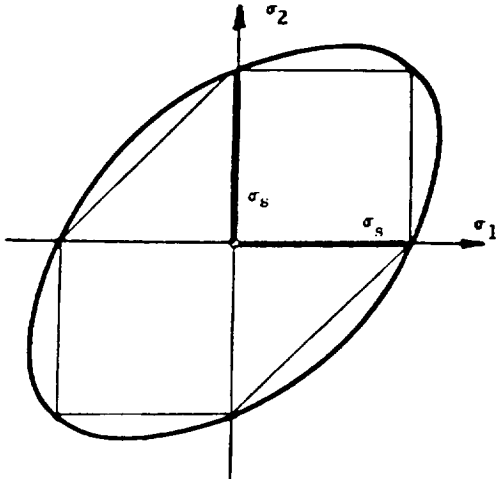


FIG. 2.80-3. Ellipse of Hencky-von Mises

It is important to note that the intersection points of the ellipse with σ_1 and σ_2 -axis are located from the origin of coordinates with σ_S . Every two-dimensional state of stresses (σ_1, σ_2) can be interpreted as a point. If this is within the area of ellipse, the state of stresses is elastic.

According to the assumption of Kulon (See Paragraph 2.83.3) and later San-Venant, the plastic stage begins when maximum shear is equal to some constant value τ_S . For three-dimensional state of stress, maximum stress is the largest of the following:

$$\tau_{12} = \frac{\sigma_1 - \sigma_2}{2}; \quad \tau_{23} = \frac{\sigma_2 - \sigma_3}{2}; \quad \tau_{31} = \frac{\sigma_3 - \sigma_1}{2}$$

For two-dimensional state of stress (assume $\sigma_3 = 0$) τ_{maximum} will be the largest of the following values:

$$\frac{\sigma_1 - \sigma_2}{2}; \quad \frac{\sigma_1}{2}; \quad \frac{\sigma_2}{2}$$

If σ_1 and σ_2 have the same sign, the $\max \tau = \frac{\sigma_1}{2}$ or $\frac{\sigma_2}{2}$. This corresponds to uniaxial tension or compression. Consequently, in

the first or third quadrant of the ellipse, the condition $\tau_{\max} = \tau_s$ will be represented with two lines:

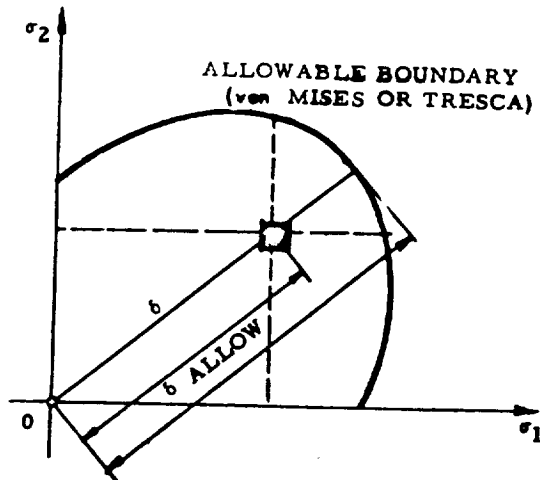
$$\sigma_1 = \pm \sigma_s; \sigma_2 = \pm \sigma_s$$

In the second and fourth quadrant $\tau_{\max} = \frac{\sigma_1 - \sigma_2}{2}$, and the condition $\tau_{\max} = \tau_s$ will be represented with the straight lines, that are parallel to the bisectrix between σ_1 and σ_2 . These lines can be found in Fig. 2.80-3. The hexagon inscribed into von Mises' ellipse is known as Tresca yield surface. For the two-dimensional surface,

$$\sigma_{1,2} = \frac{\sigma_x + \sigma_y}{2} \pm \sqrt{\frac{(\sigma_x - \sigma_y)^2}{2} + \tau_{xy}^2}$$

These approaches help to determine whether or not the certain state of stresses (σ_1, σ_2) is still in elastic range.

Fig. 2.80-4 shows a point (square) representing a (σ_1, σ_2) stress



condition that is considerably less than the allowable value. If σ_1 and σ_2 are known to be proportional, the true margin of safety is found by projecting from the original through the point (σ_1, σ_2) to intersect the allowable boundary. Then, in accordance with Fig. 2.80-4,

$$M. S. = \frac{\delta_{\text{allow}}}{\delta} - 1 \geq 0$$

FIG. 2.80-4. Margin of Safety (Ref. 2-20).

2.85 TWO-DIMENSIONAL FIELD OF STRESSES

Shells usually are stressed by two-dimensional fields of stress.

Consequently, assuming $\sigma_2 = 0$, the results of previously listed theories can be simplified as follows:

| | |
|------------------------------|---|
| Maximum Stress Theory | $\sigma_1 \leq \sigma_{\text{allow}}$ |
| Maximum Strain Theory | $\sigma_1 - \mu \sigma_3 \leq \sigma_{\text{allow}}$ |
| Maximum Shear Theory | $\sigma_1 - \sigma_3 \leq \sigma_{\text{allow}}$ |
| Maximum Strain Energy Theory | $\sqrt{\sigma_1^2 + \sigma_3^2 - \sigma_1 \sigma_3} \leq \sigma_{\text{allow}}$ |
| Mohr's Theory | $\sigma_1 - m \sigma_3 \leq \sigma_{\text{allow}} \text{ (tens.)}$ |

where the principal stresses are:

$$\sigma_{1,3} = \frac{\sigma_z + \sigma_y}{2} \pm \sqrt{(\sigma_z - \sigma_y)^2 + 4\tau_{zy}^2}$$

$$\tau_{1,3} = \frac{1}{2} \sqrt{(\sigma_z - \sigma_y)^2 + 4\tau_{zy}^2}$$

With consideration of these two formulas, the previous theories lead to the following formulas:

Maximum Stress Theory: $\frac{\sigma_z + \sigma_y}{2} + \frac{1}{2} \sqrt{(\sigma_z - \sigma_y)^2 + 4\tau_{zy}^2} \leq \sigma_{\text{all.}}$

Maximum Strain Theory: $\frac{1 - \mu}{2} (\sigma_z + \sigma_y) +$

$$\frac{1 + \mu}{2} \sqrt{(\sigma_z - \sigma_y)^2 + 4\tau_{zy}^2} \leq \sigma_{\text{all.}}$$

Maximum Shear Theory:

$$\sqrt{(\sigma_z - \sigma_y)^2 + 4\tau_{zy}^2} \leq \sigma \text{ all}$$

Maximum Strain Energy Theory:

$$\sqrt{\sigma_z^2 + \sigma_y^2 - 4\sigma_z \sigma_y + 3\tau_{zy}^2} \leq \sigma \text{ all tens}$$

Mohr's Theory:

$$\frac{1 - m}{2} (\sigma_z + \sigma_y) +$$

$$\frac{1 + m}{2} \sqrt{(\sigma_z - \sigma_y)^2 + 4\tau_{zy}^2} \leq \sigma \text{ allow tension.}$$

where $(\sigma_y, \sigma_z, \tau_{zy}, \tau_{yz})$ is a two-dimensional field of stress, related to the (z, y) system of coordinates.

2.86 COMPARISON OF RESULTS

The results can be easily compared if a one-dimensional element (bar) will be considered under uniaxial loading or bending. All theories for the middle of the cross-section ($\tau = 0$) leads to the same result:

$$\sigma \leq \sigma_{\text{allow.}}$$

However, if the bar is loaded with pure shear (torsional loading), then $\sigma = 0$. Shear τ , however, will differ according to the theory used:

Maximum Stress Theory: $\tau \leq \sigma_{\text{allow}}$

Maximum Strain Theory: $1.3\tau \leq \sigma_{\text{allow}}$

Maximum Shear Theory: $2\tau \leq \sigma_{\text{allow}}$

Maximum Strain Energy Theory: $\sqrt{3}\tau \leq \sigma_{\text{allow}}$

Mohr's Theory: $(1 + m)\tau \leq \sigma_{\text{allow}}$

The first two theories do not lead to results that tests can justify. The third theory leads to the satisfactory result ($\tau = 0.5\sigma_{\text{allow}}$). The fourth theory leads to $\tau \approx 0.6\sigma_{\text{allow}}$, which is excellent according to the tests. The fifth theory gives the following satisfactory result:

$$\tau = \frac{(\text{allow. } \sigma_t) \cdot (\text{allow } \sigma_c)}{\text{allow } \sigma_t + \text{allow } \sigma_c}$$

Consequently, the distortion energy theory is recommended for ductile materials; and Mohr's theory is recommended for brittle materials.

2.87 FAILURE

If design is limited by the established allowable stresses (and corresponding margin of safety), the structure is safe and will not fail. However, in reality, the structure can be loaded even further beyond the elastic limit. If this is permitted, it is important to find the ultimate condition for the multiaxial state of stresses.

The theory of shells as presented in this chapter is based on the theory of elasticity. Consequently, the stress-strain relation must be linear, which is what would actually exist if $\sigma_{\text{allowable}}$ is based on elastic limit.

In some cases, design can be still carried without difficulty in the plastic range. This is the case of all pressurized membranes. Since the membrane is a statically determinate system, there are no material constants involved; consequently, derived theories may still be used. Otherwise, the stress-strain diagram will be needed for the multiaxial case to determine what relation between stresses and strains exists.

Numerous tests proved that the stress-strain curves $\sigma' \sim \epsilon'$ and $\sigma_i \sim \epsilon_i$ for uniaxial and multiaxial case are identical in elastic range and

only slightly different in the plastic range. The meaning of these symbols is as follows:

σ' = uniaxial tensile stress

ϵ' = uniaxial strain in direction of σ'

$$\sigma_i = \frac{1}{\sqrt{2}} \sqrt{(\sigma_x - \sigma_y)^2 + (\sigma_y - \sigma_z)^2 + (\sigma_z - \sigma_x)^2 + 6(\tau_{yz}^2 + \tau_{zx}^2 + \tau_{xy}^2)}$$

$$\epsilon_i = \frac{\sqrt{2}}{3} \sqrt{(\epsilon_x - \epsilon_y)^2 + (\epsilon_y - \epsilon_z)^2 + (\epsilon_z - \epsilon_x)^2 + 6(\epsilon_{yz}^2 + \epsilon_{zx}^2 + \epsilon_{xy}^2)}$$

where $(\sigma_x, \sigma_y, \sigma_z, \tau_{yz}, \tau_{zx}, \tau_{xy})$ is state of stresses.

$(\epsilon_x, \epsilon_y, \epsilon_z, \epsilon_{yz}, \epsilon_{zx}, \epsilon_{xy})$ is state of deformations.

Consequently, if the uniaxial stress-strain diagram is known, the multiaxial stress-strain diagram is also known. This is correct if the corresponding strain is needed for certain combinations of stresses. However, this relation is not valid for determination of the ultimate stress for multiaxial state of stresses.

Certainly on diagram $\epsilon' \sim \sigma'$, the point which corresponds to the failure can be found. Assume that the failure is occurring at certain stress σ_u . This does not mean that the same stress will be stress of failure for multiaxial case on diagram $\epsilon_i \sim \sigma_i$. For example, assume the element which is stressed with the uniform tension in all three directions:

$$\sigma_1 = \sigma_2 = \sigma_3 = \sigma$$

then

$$\sigma_i = 0$$

At some level $\sigma = \sigma_f$ will occur failure; however, σ_i will remain zero, and the point of failure on $\epsilon_i \sim \sigma_i$ diagram will correspond to the origin of system of coordinates.

The problem of determining ultimate stresses in multiaxial case has not yet been solved (Ref. 2-19).

At present, critical combinations (several) that correspond to the points of failure (several) can be discussed. The test shows that the failure predominantly occurs due to normal or tangential stresses. Further study of plastic range is not covered in this chapter.

2.88 CONCLUSION

The distortion energy theory (or von Mises-Tresca method) is recommended for ductile materials and Mohr's theory for brittle materials.

For ductile materials:

$$\sigma_p = \sqrt{\frac{2}{3}(\sigma_z^2 + \sigma_y^2 - \sigma_z\sigma_y + 3\tau_{zy}^2)} \leq \sigma_{\text{allow}} \text{ (uniaxial)}$$

For brittle materials:

$$\sigma_b = \frac{1-m}{2}(\sigma_z + \sigma_y) + \frac{1+m}{2}\sqrt{(\sigma_z - \sigma_y)^2 + 4\tau_{zy}^2} \leq \sigma_{\text{allow}} \text{ (tensile)}$$

Margin of Safety:

$$\text{M. S.} = \frac{\text{allowable stress}}{\text{calculated stress}} - 1 \geq 0$$

where:

for ductile materials: $\sigma = \sigma_p$,

for brittle materials: $\sigma = \sigma_b$.

If the ellipse of von Mises or hexagon of Tresca are to be used, then the point (σ_1, σ_2) must be within the areas limited by ellipse or hexagon.

The corresponding margin of safety will be determined as described in the Section 2.84.

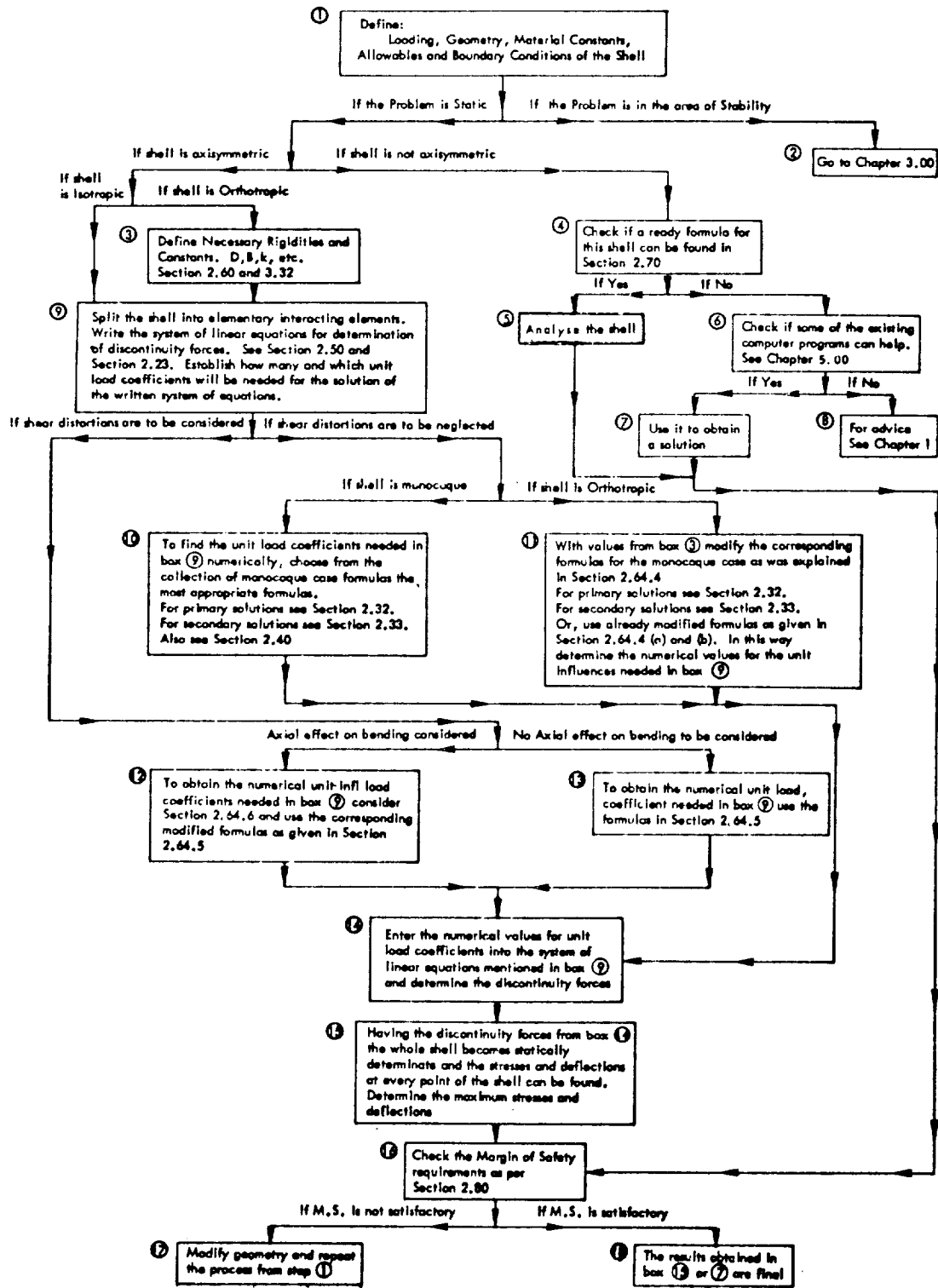
The use of presented theory of thin shells would be incorrect in plastic range, except for pressurized membranes. If the state of stress in plastic range is known, the correspondent deformation can be determined from similarity of $\sigma_i \sim \epsilon_i$ and $\sigma' \sim \epsilon'$ diagrams. At present, ultimate stresses in multiaxial case cannot be determined.

For more detailed study of this subject Refs. 2-17 to 2-21 are recommended.

2.90 SUMMARY AND CONCLUSION

In this chapter a method was outlined for the analysis of shells and multishells of revolution exposed to axisymmetrical loading, of isotropic and nonisotropic characteristics. To make the analysis simple for usage, numerous formulas for stresses and deflections for different elementary shells subjected to different loadings were collected and systematically presented in the form of formulas, charts, and tables. At the end of the chapter the collection of known formulas for other kinds of shells (nonsymmetrical loading, nonsymmetrical geometry) was presented. The suggested procedure is generalized and presented in the form of a flow diagram (Table 2.90-1) to make the application of the described procedures as simple as possible. This concludes the discussion on the statics of shells.

TABLE 2.90-1. FLOW DIAGRAM FOR STATIC ANALYSIS OF SHELLS



REFERENCES

- 2-1. Novozhilov, V. V. Theory of Thin Shells. (In Russian):
State Federal Publishing of Navy Industry (1962)
- 2-2. Hampe, E. Statik Rotationssymmetrischer Flachentragwerke,
(In German) Band 1, 2, 3, and 4. Berlin: Bauwesen (1964).
- 2-3. Föppl, L, and G. Sonntag, Tafeln und Tabellen Zur Festigkeitlehre,
(In German) Munich (1951).
- 2-4. Pflüger, A., Elementare Schalenstatik, 3 Auflage. (In German)
Berlin/Göttingen/Heidelberg: Springer-Verlag (1960).
- 2-5. Flügge, W., Stresses in Shells. Berlin/Göttingen/Heidelberg:
Springer (1960).
- 2-6. Salvadori, M. G., "Live Load and Temperature Moments in Shell
of Rotation Built into Cylinders", published by Journal of American
Concrete Institute (October 1955).
- 2-7. Worch, G., "Elastische Schalen", Beton-Kalender. (In German)
Berlin: Wilhelm Ernst & Sohn (1941).
- 2-8. Worch, G., "Elastische Platten", (In German) Beton-Kalender
Berlin: Wilhelm Ernst & Sohn (1943).
- 2-9. Worch, G., "Elastische Schalen", (In German) Beton-Kalender
Berlin: Wilhelm Ernst & Sohn (1958).

- 2-10. Marcus, H., Die Theorie Elastischer Gewebe. (In German) Berlin (1932).
- 2-11. Harris, Dr. L. A., and R. V. Spencer, "Design and Analysis of Sandwich Structures" (to be published).
- 2-12. Baker, E. H., "Analysis of Symmetrically Loaded Sandwich Cylinder", published by American Institute of Aeronautics and Astronautics.
- 2-13. Föppl, A.; and L. Föppl, Drang and Zwang, I and II. (In German) Munich: R. Oldenburg (1941).
- Föppl, L., Drang und Zwang, III. (In German) Munich: Leibniz Verlag (1947).
- 2-14. Kovalevsky, L., T. Furuike, L. A. Nelson, and F. L. Rish. "Analysis of Webs of Partial Tension Field Beams Subject to Lateral Pressure Loadings". Published by NAA, S&ID, 1966
- 2-15. Timoshenko, S., Theory of Plates and Shells. New York: McGraw-Hill (1940).
- 2-16. Hill, R., The Mathematical Theory of Plasticity. Oxford: Clarendon Press (1950).
- 2-17. Hodge, P. G., Jr., "The Rigid-Plastic Analysis of Symmetrically Loaded Cylindrical Shells", Journal of Applied Mechanics, Vol. 21, (1954), pp. 336-342.

- 2-18. Levshin, V. A. , Strength of Materials. (In Russian)
ROSTEHIZDAT (1961).
- 2-19. Iljushin, A. A. , and V. S. Lenskij, Strength of Materials.
(In Russian) FIZMATGIZ (1959).
- 2-20. Shanley, F. R. , Strength of Materials. New York: McGraw-
Hill (1957).
- 2-21. Verette, R. , "Elasto-Plastic Analysis of Shells of Revolution",
NAA S&ID STR 150.

3.00 PROCEDURES FOR STABILITY ANALYSIS

3.10 GENERAL

If a shell structure is subjected to a given compressive load and an infinitesimal increase in the load results in a large change in the equilibrium configuration of the shell, the applied load is defined as the buckling load. The change in equilibrium configuration is usually a large increase in the deflections of the shell, which may or may not be accompanied by a change in the basic shape of the shell from the pre-buckled shape. Occasionally, the given definition of buckling is difficult to apply to an actual structure. The change in the configuration of the shell may be gradual, and the actual buckling point is rather arbitrary. However, for most types of shells and loading conditions, the buckling load is quite pronounced and easy to identify.

The load carrying capability of the shell may or may not decrease after buckling. This depends on the type of loading, the geometry of the shell, the stress levels of the buckled shell, etc. Only the buckling load will be discussed in this chapter because the information available on collapse loads is quite limited. In general, the buckling load and collapse load are nearly the same and, if they are different, the deformations prior to collapse are often very large.

For columns and flat plates, the classical small deflection theory predicts the buckling load quite well and, in general, the theoretical buckling load is used as the design allowable buckling load. Therefore, the structure will usually buckle at approximately the design buckling load. In general, this method of design analysis cannot be used for shell structures. The buckling load for some types of shells and loadings may be much less than the load predicted by classical small deflection theory and, in addition, the scatter of the test data may be quite large. For example, if a set of ten nominally identical thin-walled cylinders of the same geometry were fabricated from a particular metal, none of the cylinders would fail at the same axial compressive load. In fact, the scatter of results may range to 500 percent at a given time, and the average buckling load may be one eighth of the theoretical buckling load. An explanation for this discrepancy is presented in Chapter 1.00. When sufficient data exist, a statistical reduction of the test data may be useful in determining a design allowable buckling load. This method has been used to determine most of the design curves for unstiffened curved panels and cylinders presented in this chapter. A discussion of the statistical methods used is given in Refs. 3-1 and 3-2.

A best fit curve is determined for a given set of data, and the standard deviation of the test data is established. Using this information and small sample theory, a design curve is obtained at a certain probability level. The probability level used for the statistical design allowable curves presented in this chapter is 90 percent; that is, if a shell is subjected to the design allowable buckling load, the chances are nine out of ten that the shell will not buckle. The load at which the shell may be expected to buckle is the load which corresponds to the best fit curve. Best fit curves have not been presented in this chapter because, in design analysis, the load at which the shell will not buckle is the primary interest, and approximately half of the shells would buckle at loads less than the load corresponding to the best fit curve.

One of the primary shortcomings of this method of obtaining design curves is that the test specimens and boundary conditions used to obtain the design curves may not be typical of the particular structure which the design curves are being used to analysis. However, until additional information on shell stability is obtained, a statistical analysis has been used whenever possible to obtain design curves.

Whenever sufficient data do not exist to obtain a statistical design allowable buckling load, design recommendations have been made on

available information. In general, this involved recommending correction factors to reduce the theoretical buckling loads. Due to the lack of data for some types of shells and loading as well as the question of over what range the theory is applicable, the recommendation may be too conservative for some cases. Further theoretical and experimental investigations are necessary to justify raising the design curves.

Most analysis procedures presented in this chapter are for shells with simply supported edges. For most applications, simply supported edges should be assumed unless test results are obtained which indicate the effects of the actual boundary condition of the design. An attempt was made to indicate over what range of the parameters clamped edges give approximately the same buckling load as simply supported edges. In this chapter, the edge of a shell is assumed to be simply supported if at the edge the radial and circumferential displacements are zero and there is no restraint against translation or rotation in the axial direction. For clamped edges, the rotation of the edge is zero.

An attempt has been made to simplify the analysis procedure so that the design allowable buckling loads may be obtained from hand computations and graphs. The analyses which have been presented are sometimes quite long (orthotropic cylinders, for instance) but, in

general, results can be obtained quickly with a few simple computations. In many cases more sophisticated approaches are available, but computer programs are necessary to obtain results. It is not in the scope of this chapter to present an analysis method which requires a computer solution. The references that discuss the more complicated analysis procedure should be obtained if a more detailed investigation is warranted.

As more information on shell buckling becomes available, this chapter will be revised. However, the analyst should attempt to keep abreast with changes in the state of the art because significant changes may result from recent theoretical and experimental investigations.

3.20 UNSTIFFENED SHELLS

3.21 GENERAL

Design allowable buckling stresses for shells have been established only for the more common loading and edge support conditions. The design curves that have been presented in this section for unstiffened homogeneous isotropic curved plates and cylinders (Ref. 3-4) have, in most cases, been obtained statistically from test data. The method of statistically reducing test data to design information is discussed briefly in Section 3.10.

Ref. 3-3 presents a bibliography of the theoretical and experimental investigations available on the general instability of cones. In general, the design information on unstiffened cones which is presented in this section uses the equivalent cylinder approach. The buckling load of the cone is obtained from the buckling stress or load of an equivalent cylinder. The definition of the length and radius of the equivalent cylinders depends on the types of loading. The available test data for cones verify this method of obtaining design curves.

Design information is also presented in this section for spherical caps subjected to external pressure. The analysis procedure is primarily based on test results of shallow spherical caps. Although a method is presented for analyzing deep spherical caps, more information is needed in this area.

3.22 CURVED PANELS

3.22.1 Axial Compression, Curved Panels

A. Unpressurized

The design allowable buckling stress for unpressurized curved panels subjected to axial compression is given by

$$\frac{\sigma_{cr}}{\eta} = K_c \frac{\pi^2 E}{12(1 - \mu^2)} \left(\frac{t}{b}\right)^2$$

in which b is the width of the panel in the circumferential direction.

Design values of the buckling-stress coefficient K_c are given in

Fig. 3.22-1. For simply supported curved panels having a curvature parameter $Z > 30$ and for fixed-edge curved panels having a $Z > 50$,

Fig. 3.22-2 may be used instead in Fig. 3.22-1 to compute the critical stress. The design allowable buckling stress is then given by

$$\frac{\sigma_{cr}}{\eta} = C_c \frac{Et}{R}$$

in which design values of C_c are given in Fig. 3.22-2. For elastic

buckling, $\eta = 1.0$. For inelastic buckling, the critical stress, σ_{cr} , may be found by using curves E_1 in Section 3.62 on plasticity correction.

Note that the design curves in Fig. 3.22-1 or 3.22-2 are valid only for $a/b > 0.5$.

B. Pressurized

The design allowable buckling stress of curved panels under internal pressure and axial compression may be determined by using Fig. 3.22-3 in conjunction with Figs. 3.22-1 or 3.22-2. A curve is presented in Fig. 3.22-3 that allows the calculation of the increase in buckling stress as a function of pressure and geometry only. To calculate the axial-compressive buckling stress of a pressurized curved panel, the unpressurized critical stress must first be computed from the design curves in Fig. 3.22-1 or 3.22-2. Then, the incremental buckling stress caused by internal pressure is computed by using Fig. 3.22-3, and this stress is added to the unpressurized value.

The pressurized curved panel is capable of resisting a total axial-compressive load which is the sum of the unpressurized buckling load, the incremental buckling load caused by internal pressure, and an external load sufficient to balance the longitudinal internal-pressure tensile load in the skin. Note that the design curves in Fig. 3.22-3 are valid only for $a/b > 0.5$. In addition, the curved panels must fall in the domain defined by the straight-line portion of the design curves shown in Fig. 3.22-1. For inelastic buckling, the critical stress may be found by using curves E_1 of Section 3.62. The total stress field should be considered when the plasticity correction is determined.

FIG. 3.22-1. BUCKLING-STRESS COEFFICIENT, K_c , FOR UNPRESSURIZED CURVED PANELS SUBJECTED TO AXIAL COMPRESSION

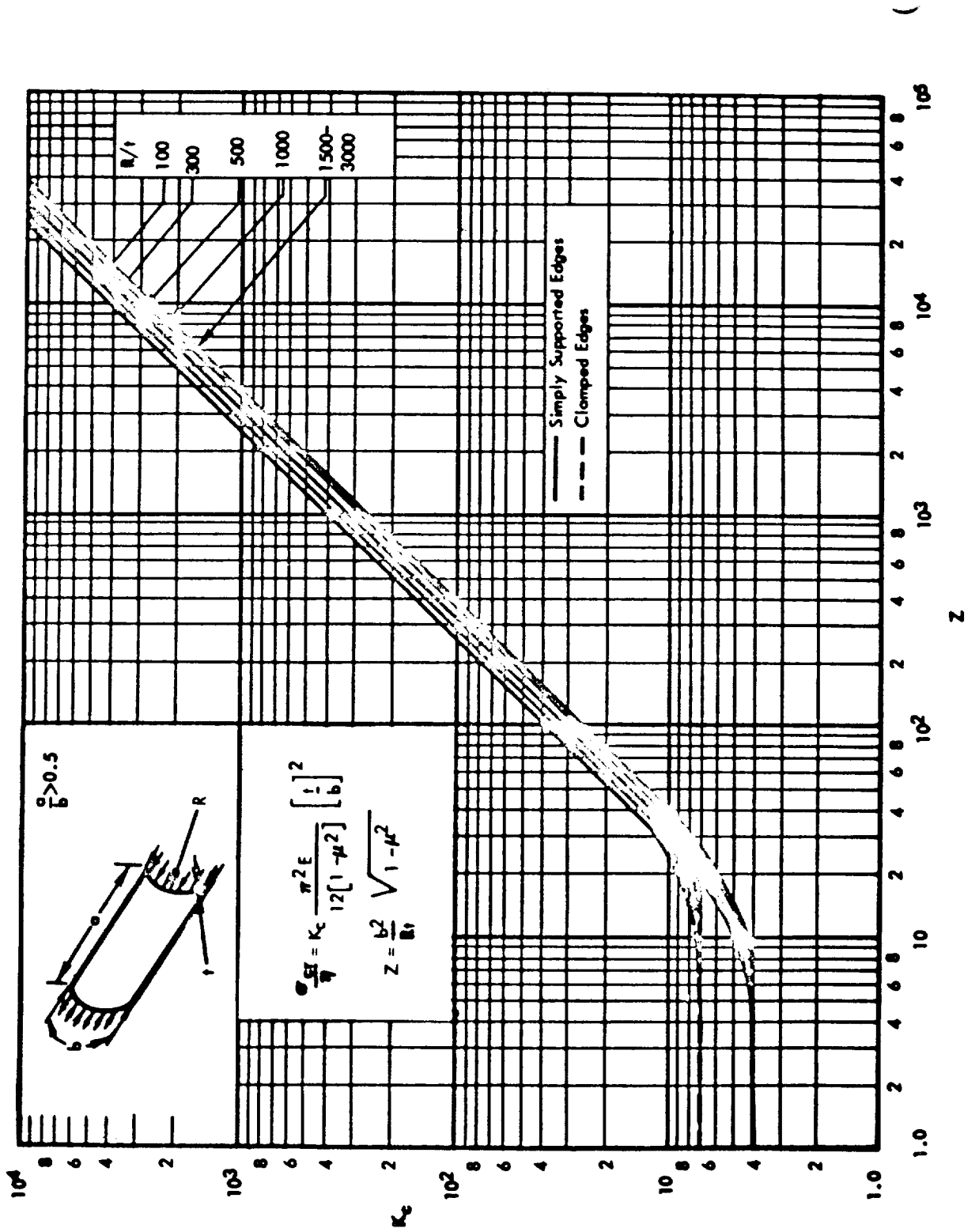


FIG. 3.22-2. BUCKLING-STRESS COEFFICIENT, C_c , FOR UNPRESSURIZED CURVED PANELS SUBJECTED TO AXIAL COMPRESSION

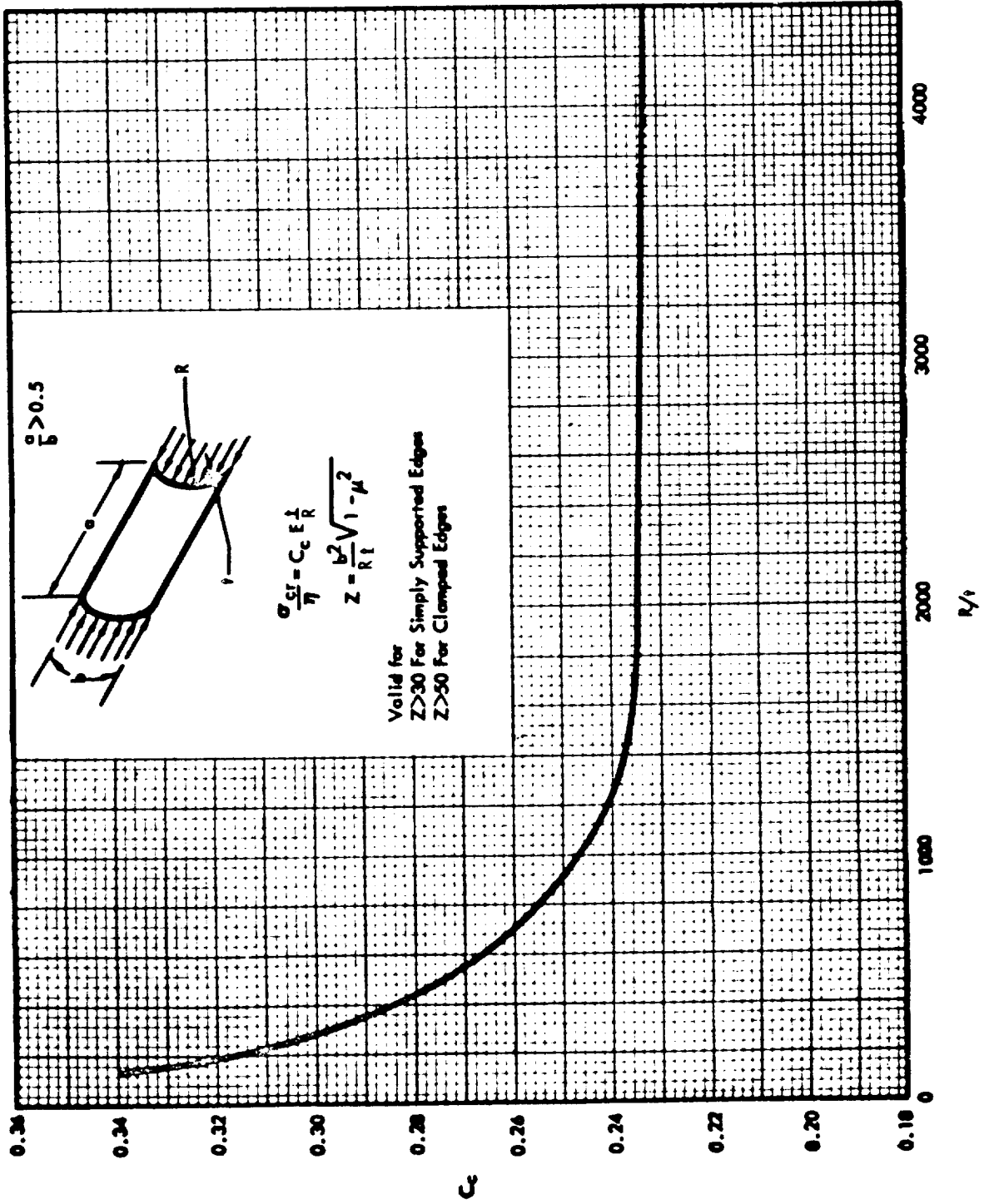
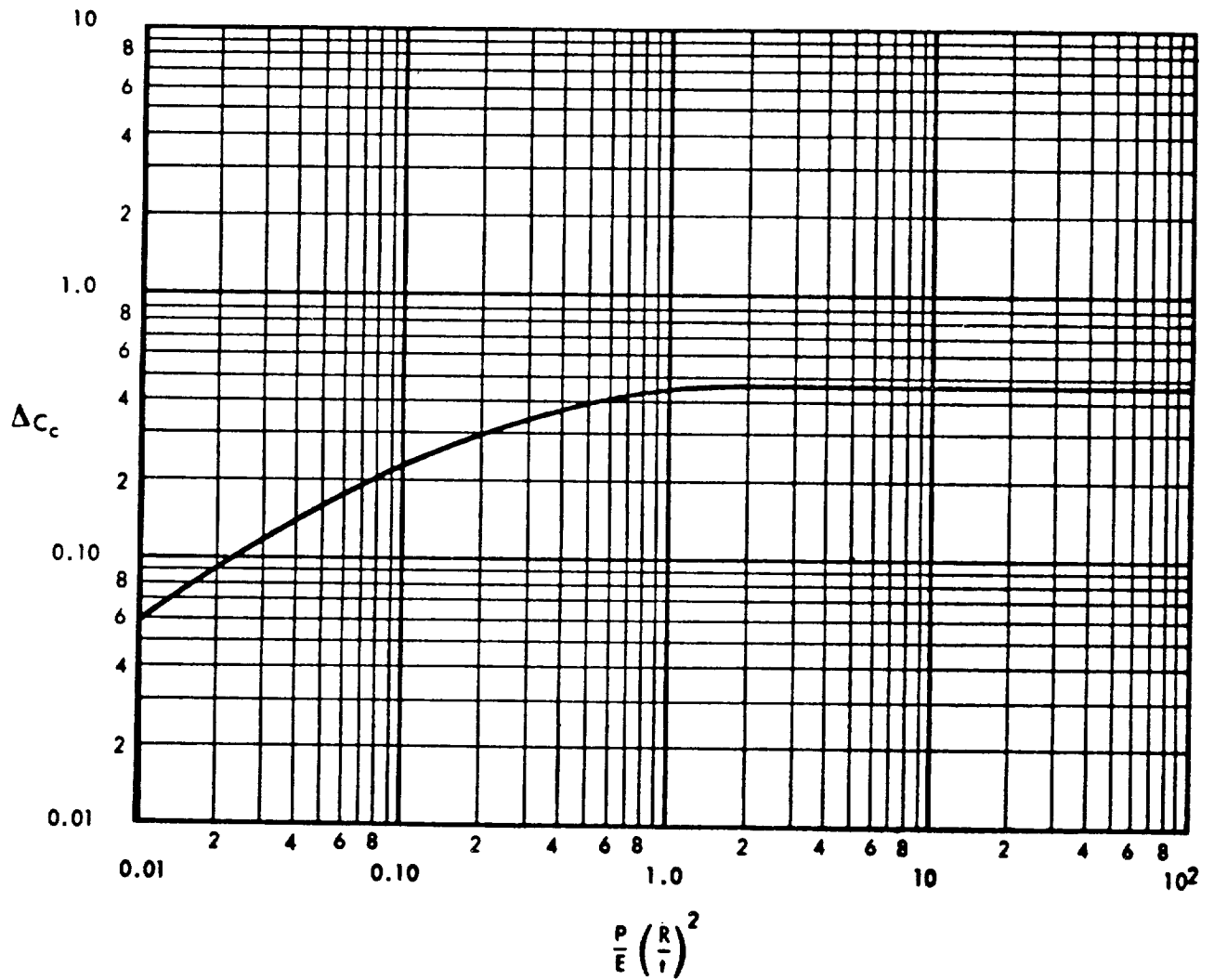


FIG. 3.22-3. INCREASE IN AXIAL-COMPRESSIVE BUCKLING-STRESS
 COEFFICIENT OF CURVED PANELS DUE TO
 INTERNAL PRESSURE



3.22.2 Shear, Curved Panels

A. Unpressurized

The design allowable buckling stress for unpressurized, rectangular curved plates subjected to shear is

$$\frac{\tau_{cr}}{\eta} = K_s \frac{\pi^2 E}{12(1 - \mu^2)} \left[\frac{t}{b} \right]^2$$

in which the buckling-stress coefficient K_s is given in Figs. 3.22-4 and 3.22-5. For elastic buckling, $\eta = 1$. For inelastic buckling, the relation between τ_{cr}/η and τ_{cr} may be determined from the σ_{cr}/η versus σ_{cr} curves in Section 3.62 on plasticity corrections by using one of the theories for failure of materials. There is evidence that the shearing stress at which inelastic action occurs in pure shear in ductile materials is related to the analogous tensile stress in pure tension by the equation

$$\tau_{xy} = \frac{1}{\sqrt{3}} \sigma_y$$

The calculated τ_{cr}/η may then be converted to the corresponding σ_{cr}/η by multiplying by $\sqrt{3}$; σ_{cr} may be read from the σ_{cr}/η versus σ_{cr} curve; and σ_{cr} may be converted back to τ_{cr} by dividing $\sqrt{3}$. For curved plates in shear, curve A in Section 3.62 is suggested.

B. Pressurized

The design allowable buckling shear stress for pressurized curved panels may be determined by using Fig. 3.22-6 with Fig. 3.22-4 or 3.22-5. The curves in Fig. 3.22-6 allow the calculation of the increase in shear buckling stress as a function of pressure and geometry only. To calculate the shear buckling stress of a pressurized curved panel, two quantities must be computed. The unpressurized buckling stress must first be computed from the design curves in Fig. 3.22-4 or 3.22-5. Then, the incremental buckling stress caused by internal pressure is computed and added to the unpressurized value.

The design curves should be used for the loading condition in which the axial tensile load caused by internal pressure is not balanced. For inelastic buckling, the critical stress may be found by the procedure recommended for unpressurized curved panels subjected to shear. The total stress field should be considered when the plasticity correction is determined.

FIG. 3.22-4. BUCKLING STRESS COEFFICIENT, K_B , FOR UNPRESSURIZED CURVED PANELS SUBJECTED TO SHEAR

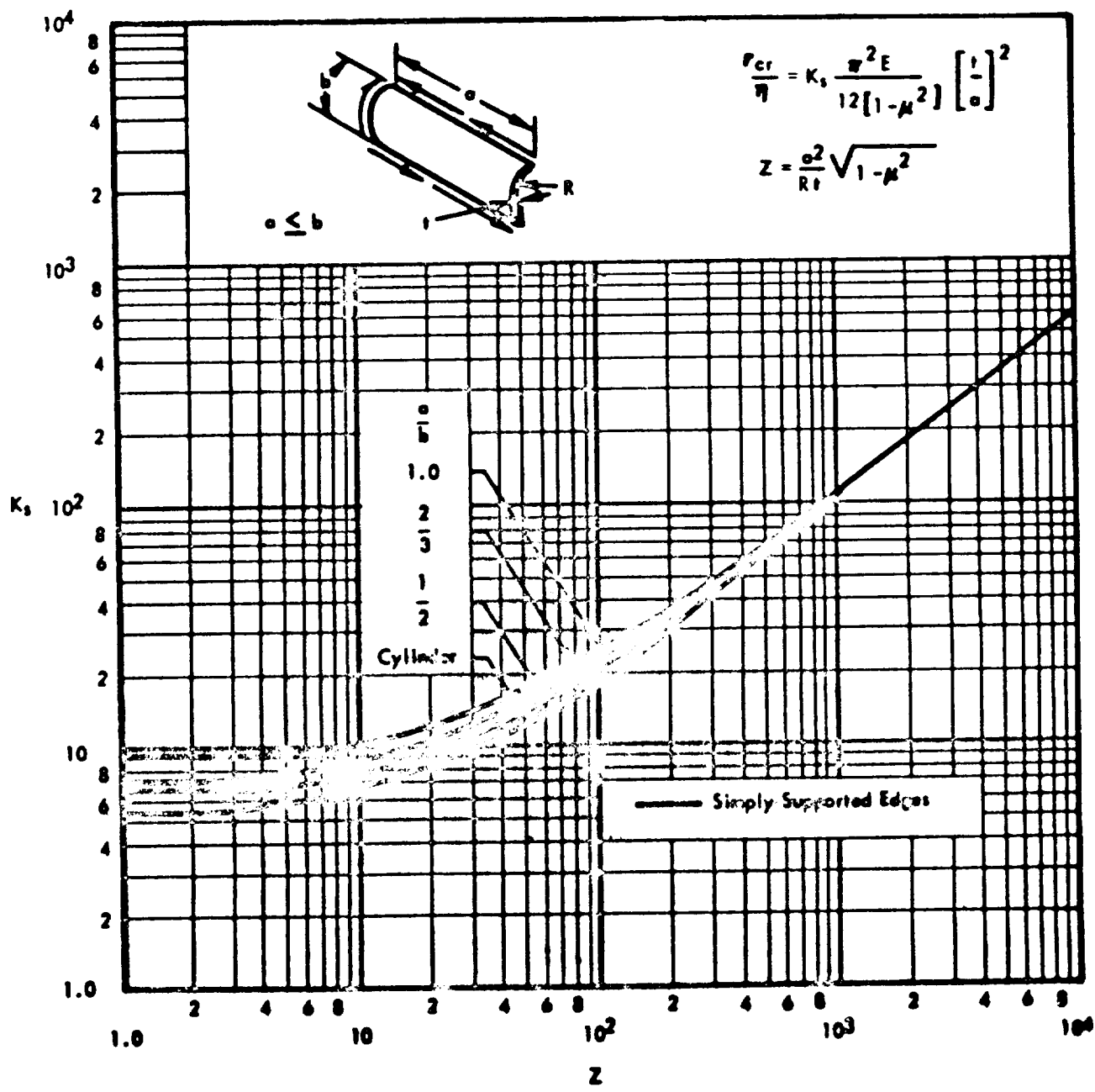


FIG. 3.22-5. BUCKLING STRESS COEFFICIENT, K_s , FOR UNPRESSURIZED CURVED PANELS SUBJECTED TO SHEAR

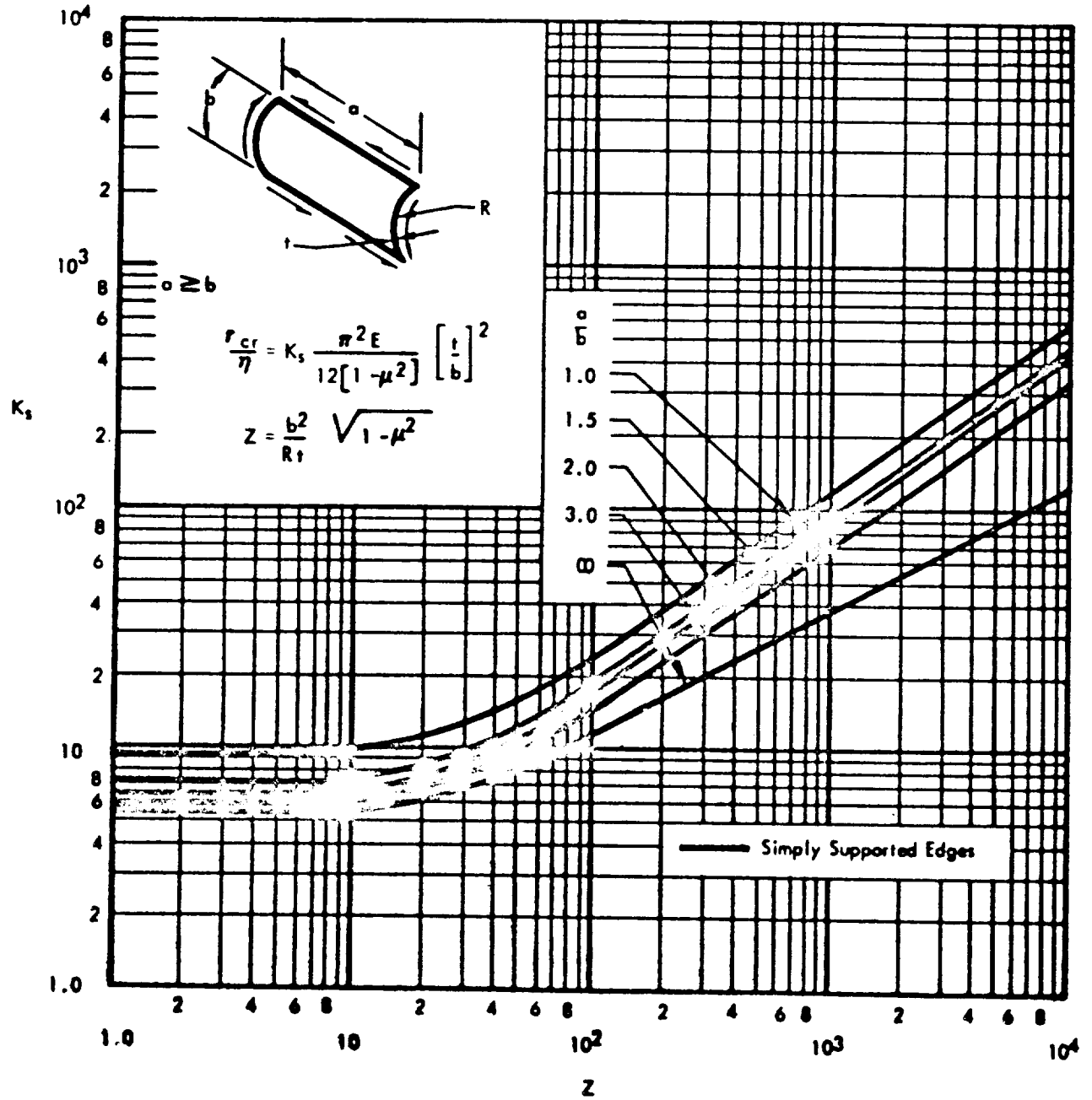
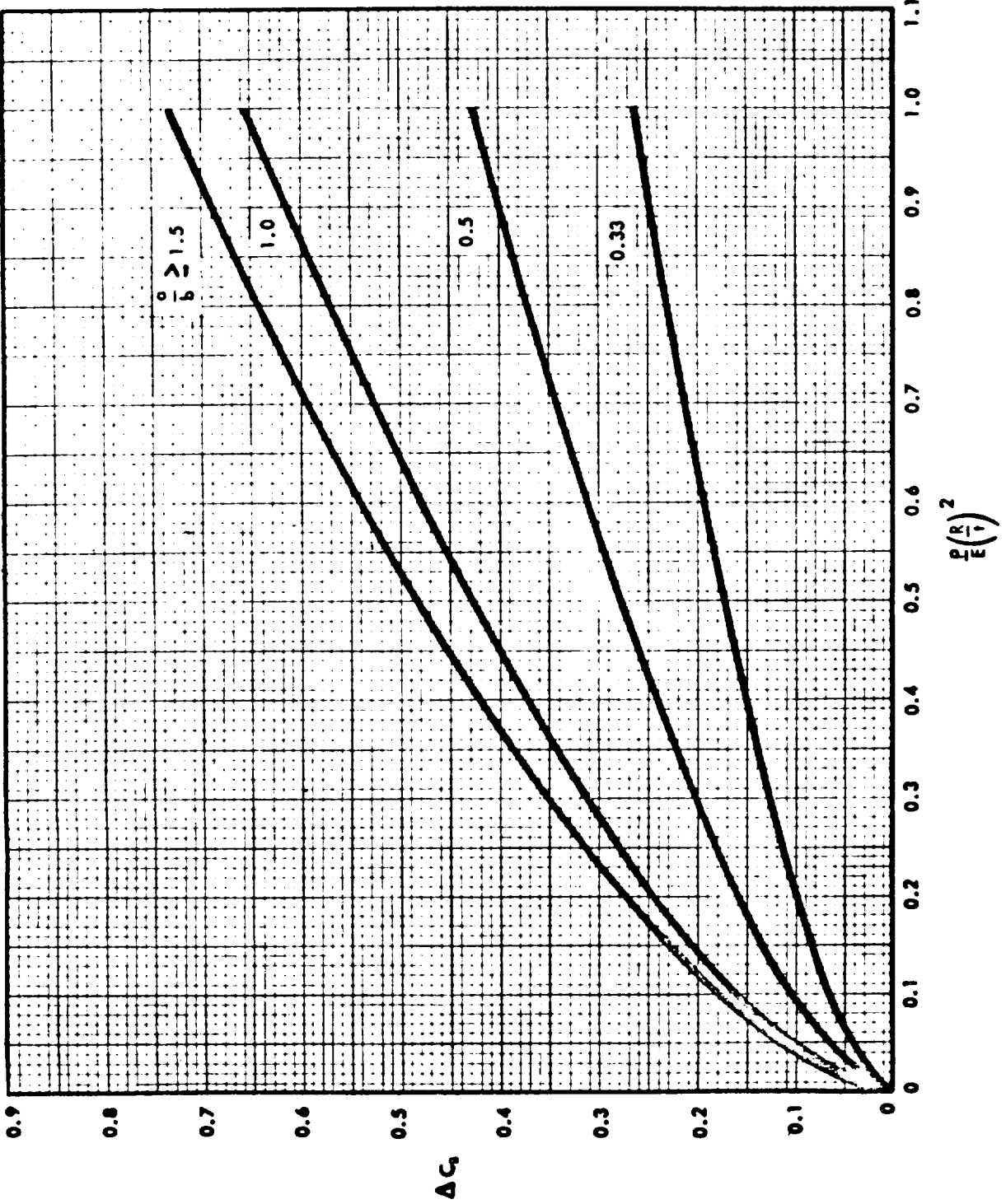


FIG. 3.22-6. INCREASE IN TORSIONAL BUCKLING STRESS COEFFICIENT OF CURVED PANELS DUE TO INTERNAL PRESSURE



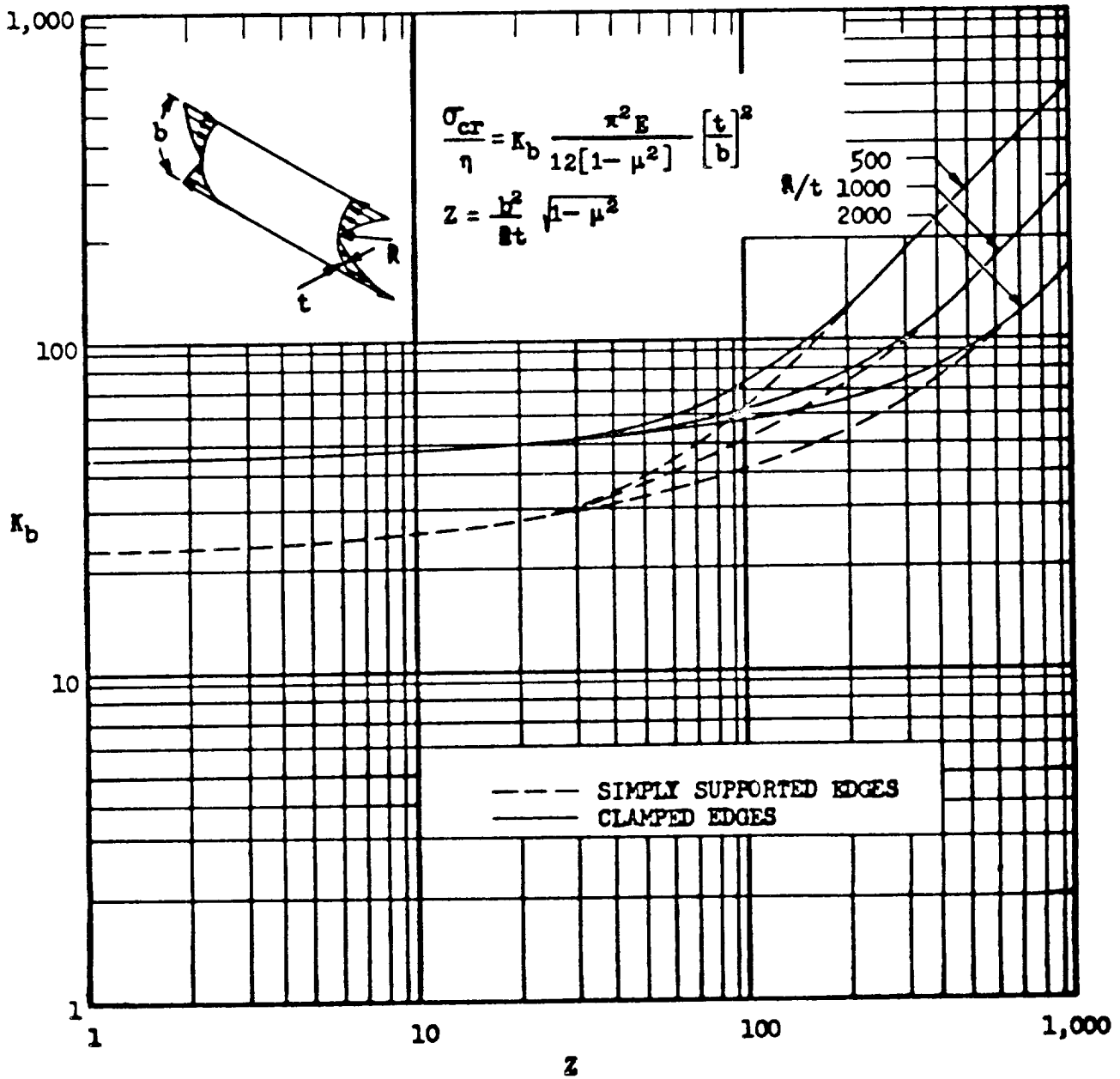
3.22.3 Bending, Curved Panels

Test data are not available on the allowable buckling stress of curved plates in bending. However, at low values of the curvature parameter, Z , the buckling coefficient for a long, curved plate should approach that for a long, flat plate in bending and, at high values of Z , it should approach that for a long cylinder in bending (Section 3.23). These extremes are plotted in Fig. 3.22-7 with smooth curves faired between. The coefficients are to be used with the equation

$$\frac{\sigma_{cr}}{\eta} = K_b \frac{\pi^2 E}{12(1 - \mu^2)} \left(\frac{t}{b}\right)^2$$

For elastic buckling, $\eta = 1$. For inelastic stresses, use the correction suggested for curved panels subjected to axial compression.

FIG. 3.22-7. CRITICAL BUCKLING STRESS COEFFICIENTS FOR LONG CURVED PANELS SUBJECTED TO BENDING



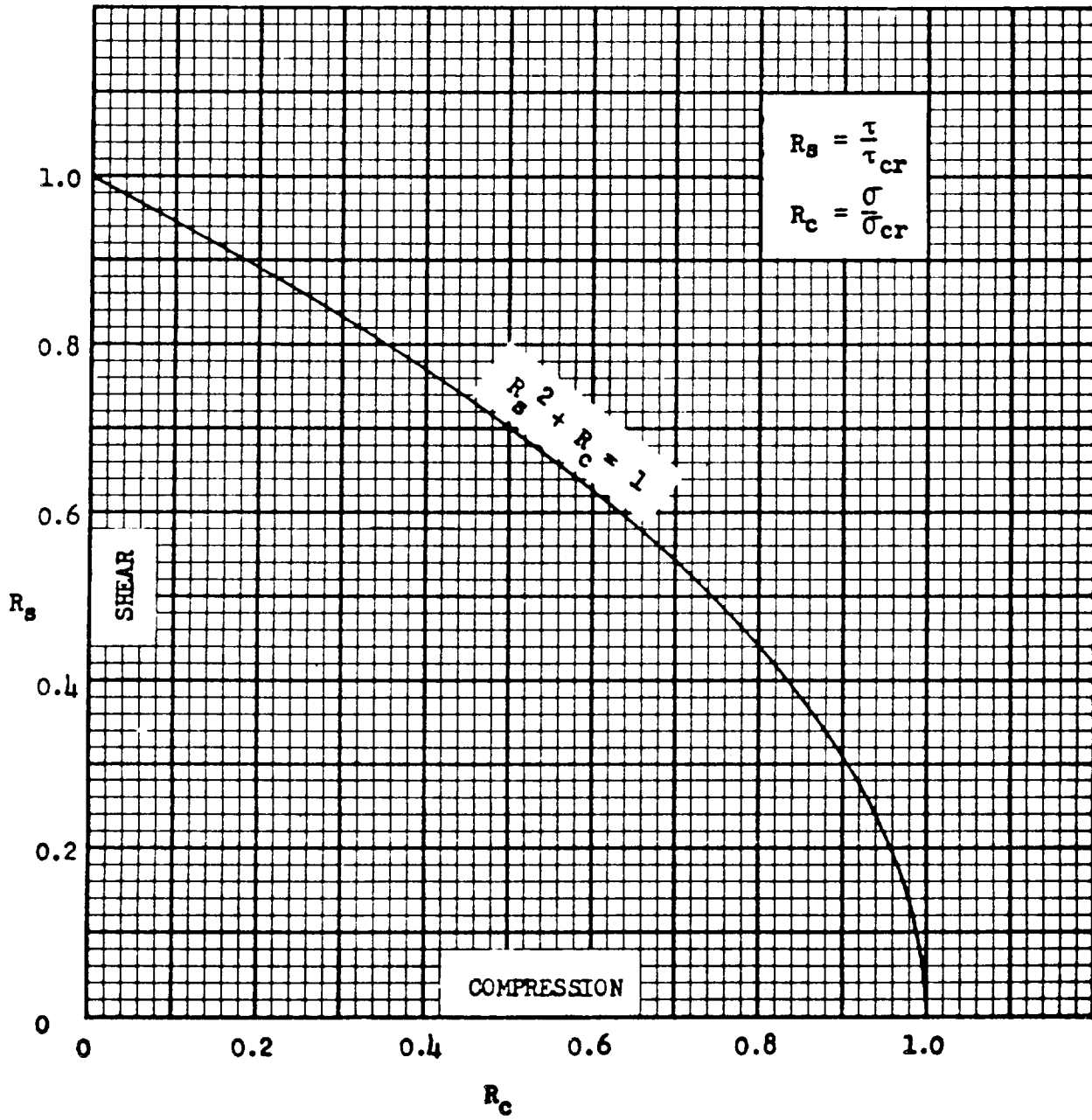
3. 22. 4 External Pressure, Curved Panels

There is little information available on the buckling of rectangular plates with single curvature subjected to external pressure. In thin-walled cylinders, external lateral pressure causes buckling by producing a circumferential compressive stress. It is probable that a curved panel which is not shallow may be designed by assuming that it will buckle at a circumferential compressive stress equal to the critical circumferential stress of a thin-walled cylinder of the same proportions. The design-allowable buckling pressure for cylinders subjected to only lateral pressure is given in Section 3. 23. While edge stiffeners will have generally a stabilizing effect, the panel may be less stable than a geometrically similar cylinder if the stiffeners are torsionally weak and the circumferential load in the skin is not applied to the stiffeners near their shear center.

3. 22. 5 Combined Loading, Curved Panels

An interaction curve for buckling of rectangular curved plates under combined compression and shear is shown in Fig. 3. 22-8. σ_{cr} is found from Paragraph 3. 22. 1 and τ_{cr} from Paragraph 3. 22. 2. To use the curve given in Fig. 3. 22-8, a straight line is drawn through the origin with slope R_s/R_c , and R_s or R_c is read at the intersection of this line with the given curve.

FIG. 3.22-8. BUCKLING STRESS INTERACTION CURVE FOR
RECTANGULAR CURVED PLATES UNDER COMBINED
SHEAR AND COMPRESSION



3.23 CYLINDERS

3.23.1 Axial Compression, Unstiffened Cylinders

A. Unpressurized

The design-allowable buckling stress for a circular cylinder subjected to axial compression is given by

$$\frac{\sigma_{cr}}{\eta} = C_c \frac{Et}{R}$$

For simply supported cylinders with the curvature parameter $Z > 25$ and for clamped-edge cylinders with $Z > 80$ (i. e., in the long-cylinder domain), the design curve of Fig. 3.23-1 presents the buckling-stress coefficient, C_c , for an unpressurized cylinder in axial compression as a function of the radius-to-thickness ratio, R/t . For elastic buckling, $\eta = 1$ is used. In the inelastic range, the critical stress, σ_{cr} , may be found by using curves E_1 in Section 3.62. Very long cylinders must be checked for Euler-column buckling.

B. Pressurized

The buckling stress of long cylinders under internal pressure and axial compression may be determined by using Fig. 3.23-2 in conjunction with Fig. 3.23-1. Fig. 3.23-2 presents a curve that allows the calculation of the increase in buckling stress as a function of pressure and geometry only.

The design allowable buckling stress is

$$\frac{\sigma_{cr}}{\eta} = (C_c + \Delta C_c) \frac{Et}{R}$$

where C_c is obtained from Fig. 3.23-1, and ΔC_c is obtained from Fig. 3.23-2. For inelastic buckling, the critical stress may be found by using curves E_1 of Section 3.62. The total stress field should be considered when determining the plasticity correction. The pressurized cylinder is capable of resisting a total compressive load, P_{cr} , which may be obtained from the equation

$$P_{cr} = 2\pi R \sigma_{cr} t + \pi R^2 p$$

It should be noted that the pressurized design curve in Fig. 3.23-2 is valid only for long cylinders. Very long cylinders must be checked for buckling as Euler columns.

FIG. 3.23-1. BUCKLING-STRESS COEFFICIENT, C_c , FOR UNSTIFFENED UNPRESSURIZED CIRCULAR CYLINDERS SUBJECTED TO AXIAL COMPRESSION

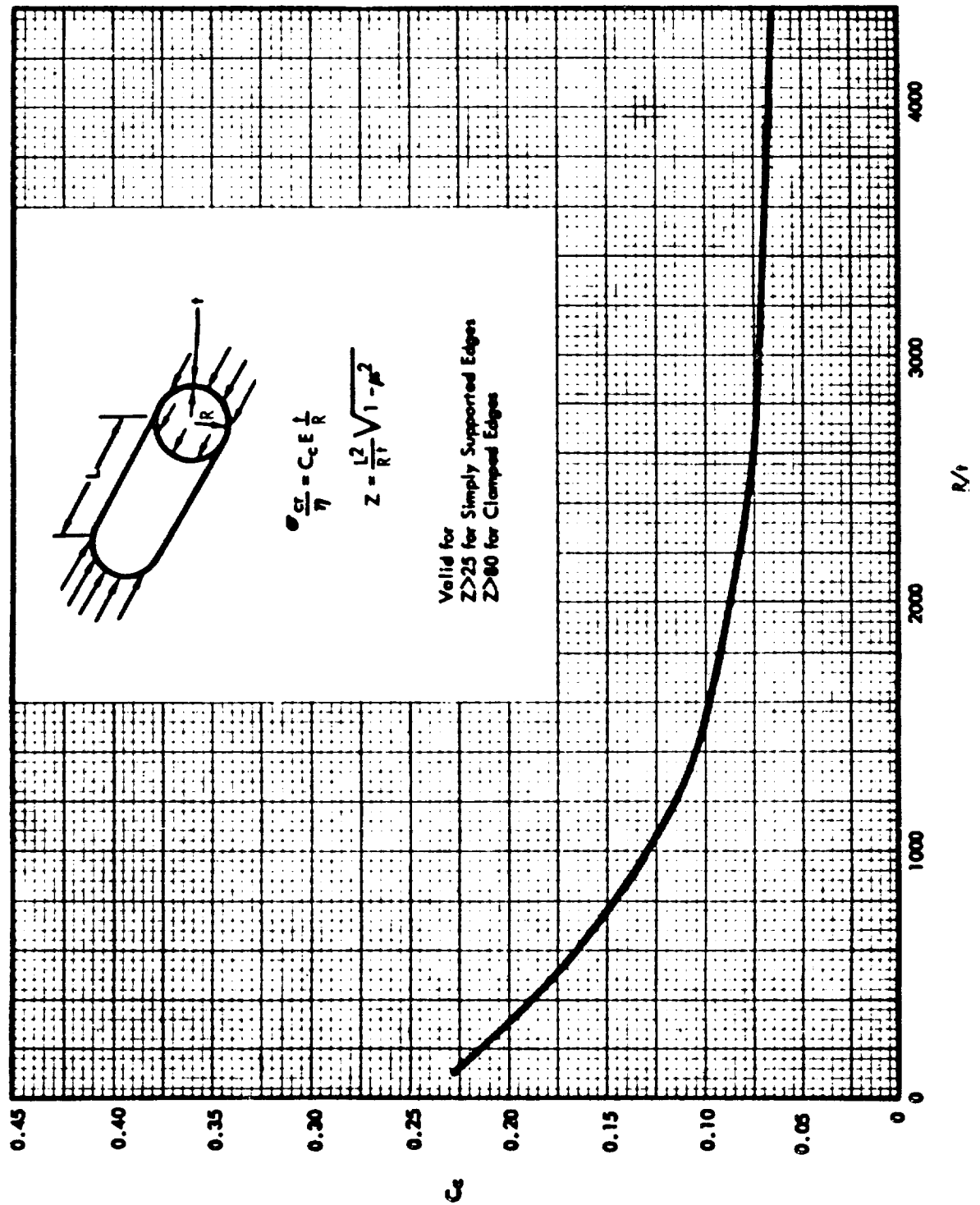
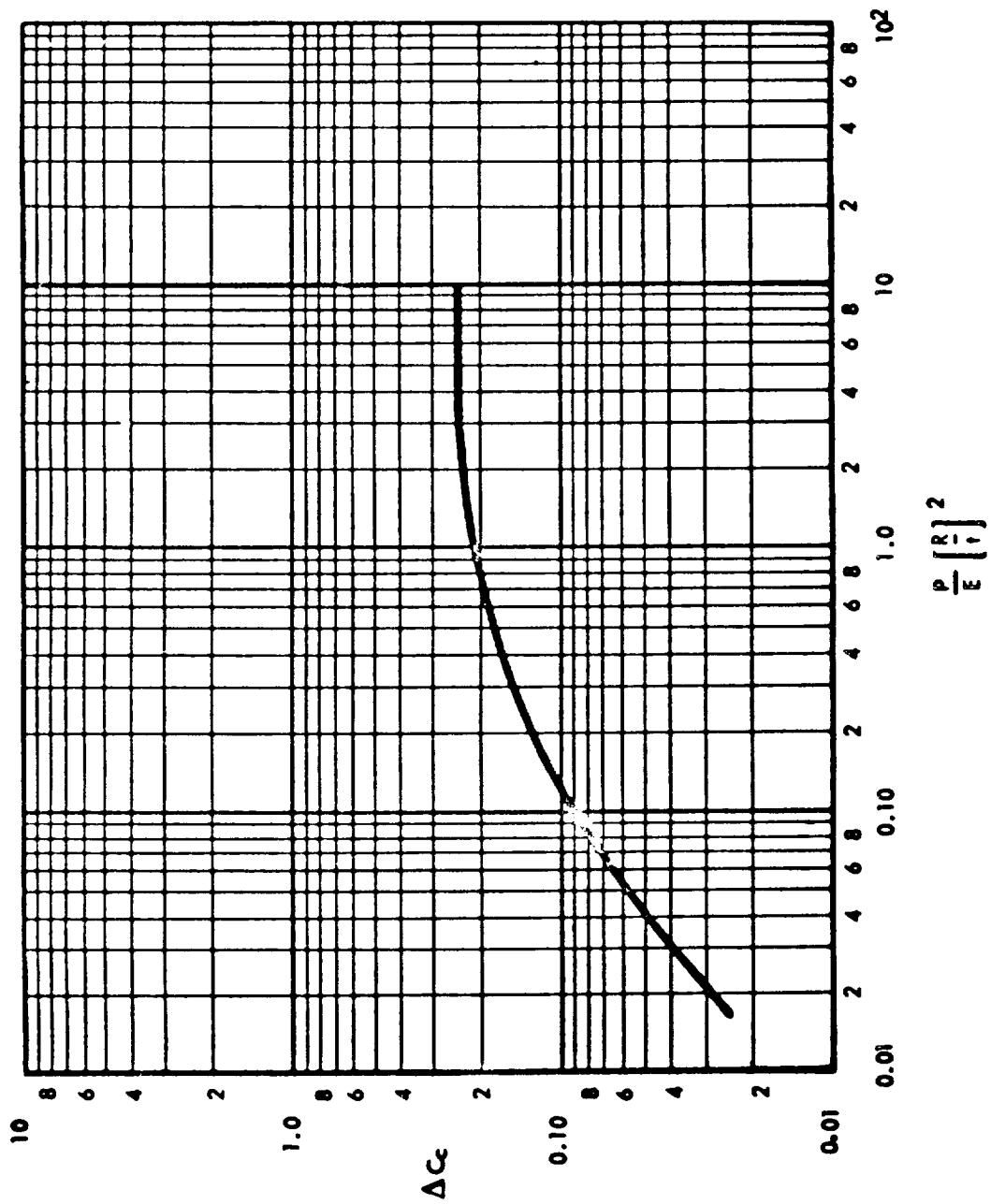


FIG. 3.23-2. INCREASE IN AXIAL-COMPRESSIVE BUCKLING-STRESS
 COEFFICIENT OF CYLINDERS DUE TO INTERNAL PRESSURE



3.23.2 Shear of Torsion, Unstiffened Cylinders

A. Unpressurized

The design-allowable shear buckling stress of thin-walled circular cylinders subjected to torsion is given by

$$\frac{\tau_{cr}}{\eta} = C_s \frac{Et}{R Z^{1/4}}$$

in which the shear buckling-stress coefficient, C_s , is given in Fig. 3.23-3 for simply supported and fixed-edge cylinders with a curvature parameter $Z > 100$. For elastic buckling, the plasticity correction term $\eta = 1.0$ is used. For inelastic buckling, the critical shear stress, τ_{cr} , may be found by the procedure outlined in Paragraph 3.22.2.

B. Pressurized

The shear buckling stress of long thin-walled cylinders subjected to internal pressure and torsion may be determined by using Fig. 3.23-4 in conjunction with Fig. 3.23-3. Fig. 3.23-4 presents curves that allow the calculation of the increase in buckling stress as a function of pressure and geometry only.

The design-allowable shear buckling stress is given by

$$\frac{\tau_{cr}}{\eta} = (C_s + \Delta C_s) \frac{Et}{R Z^{1/4}}$$

where C_s is obtained from Fig. 3.23-3 and ΔC_s is obtained from Fig. 3.23-4.

Two curves are presented in Fig. 3.23-4 for calculating the increment in critical stress caused by pressurization. One curve, labeled "No External Axial Load," should be used for calculating the critical stress of a cylinder subjected to torsion and internal pressure only. The second curve, labeled "External Axial Load Balances Longitudinal Pressure Load," should be used to calculate the critical stress of a cylinder subjected to torsion and internal pressure plus an external axial compression load equal to the internal pressure load $\pi R^2 p$, acting on the heads of the cylinder. It should be noted that the pressurized design curves of Fig. 3.23-4 are valid only for long cylinders. For inelastic buckling, the critical shear stress may be obtained by following the procedure outlined in Paragraph 3.22.2. The total stress field should be taken into consideration when the plasticity correction is determined.

FIG. 3.23-3. BUCKLING-STRESS COEFFICIENT, C_B , FOR UNSTIFFENED UNPRESSURIZED CIRCULAR CYLINDERS SUBJECTED TO TORSION

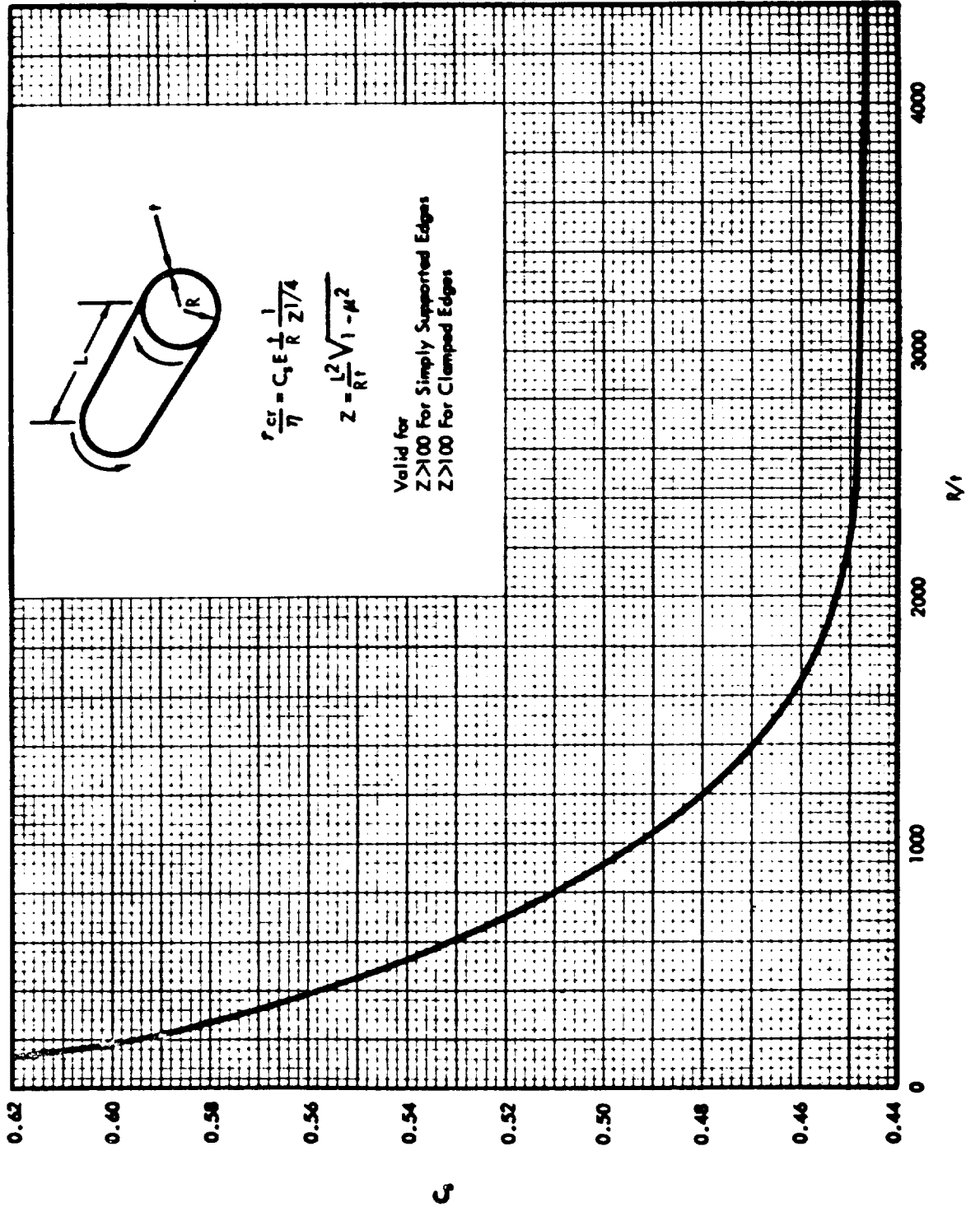
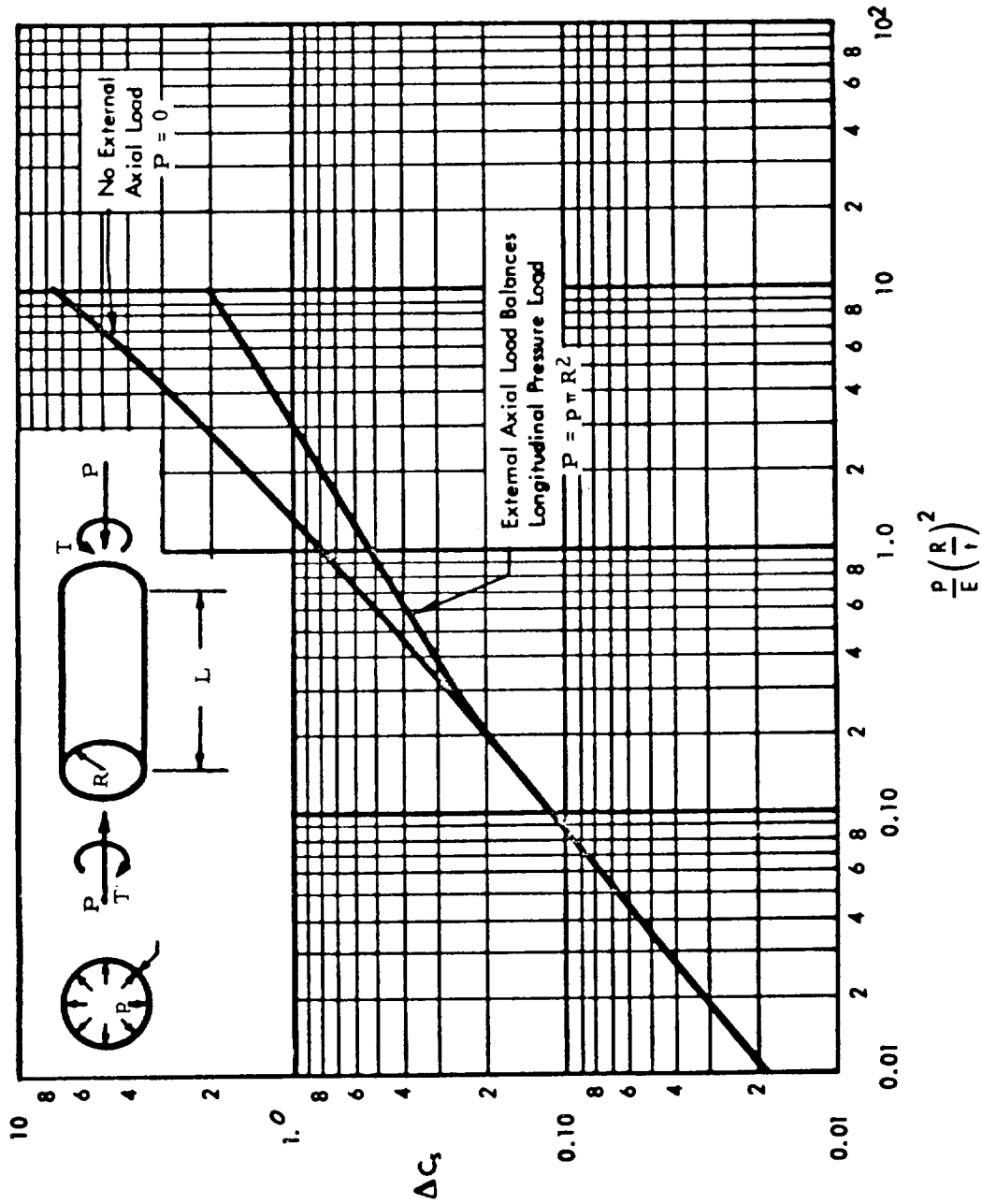


FIG. 3.23-4. INCREASE IN TORSIONAL BUCKLING-STRESS COEFFICIENT OF CYLINDERS DUE TO INTERNAL PRESSURE



3.23.3 Bending, Unstiffened Cylinders

A. Unpressurized

The design-allowable buckling stress for a thin-walled circular cylinder subjected to bending is given by

$$\frac{\sigma_{cr}}{\eta} = C_b \frac{Et}{R}$$

where the buckling-stress coefficient, C_b , is given in Fig. 3.23-5 for simply supported cylinders having a curvature parameter $Z > 20$ and for clamped edge cylinders with $Z > 80$. σ_{cr} is the maximum stress due to the bending moment (e. g. , the outer fiber stress). For elastic buckling, the plasticity correction term $\eta = 1.0$ is used. For inelastic buckling, the critical stress, σ_{cr} , may be found by using curves E_1 in Section 3.62. If the stresses are elastic, the allowable moment is

$$M_{cr} = \pi R^2 \sigma_{cr} t$$

B. Pressurized

The buckling stress of long cylinders subjected to internal pressure and bending may be determined by using Fig. 3.23-6 in conjunction with Fig. 3.23-5. Fig. 3.23-6 presents curves that allow the calculation of the increase in critical stress as a function of pressure and geometry only. The design-allowable buckling stress is

$$\frac{\sigma}{\eta} = (C_b + \Delta C_b) \frac{Et}{R}$$

where C_b is obtained from Fig. 3.23-5 and ΔC_b is obtained from Fig. 3.23-6.

Two curves for calculating the increment in critical stress caused by pressurization are presented in Fig. 3.23-6. The curve labeled "No External Axial Load" should be used to calculate the critical stress of a cylinder subjected to bending and internal pressure only. The curve labeled "External Axial Load Balances Longitudinal Pressure Load" should be used to calculate the critical stress of a cylinder subjected to bending and internal pressure plus an external axial compression load equal to the internal pressure load, $\pi R^2 p$, acting on the heads of the cylinder.

If the curve for no axial load is used and the stresses are elastic, the design-allowable moment is

$$M_{cr} = \pi R^2 \left[\sigma_{cr} t + \frac{pr}{2} \right]$$

It should be noted that the pressurized design curves in Fig. 3.23-6 are valid only for long cylinders. For inelastic buckling, the critical stress, σ_{cr} , may be found by using curves E_1 in Section 3.62. The total stress field should be taken into consideration when determining the plasticity correction.

FIG. 3.23-5. BUCKLING-STRESS COEFFICIENT, C_b , FOR UNSTIFFENED UNPRESSURIZED CIRCULAR CYLINDERS SUBJECTED TO BENDING

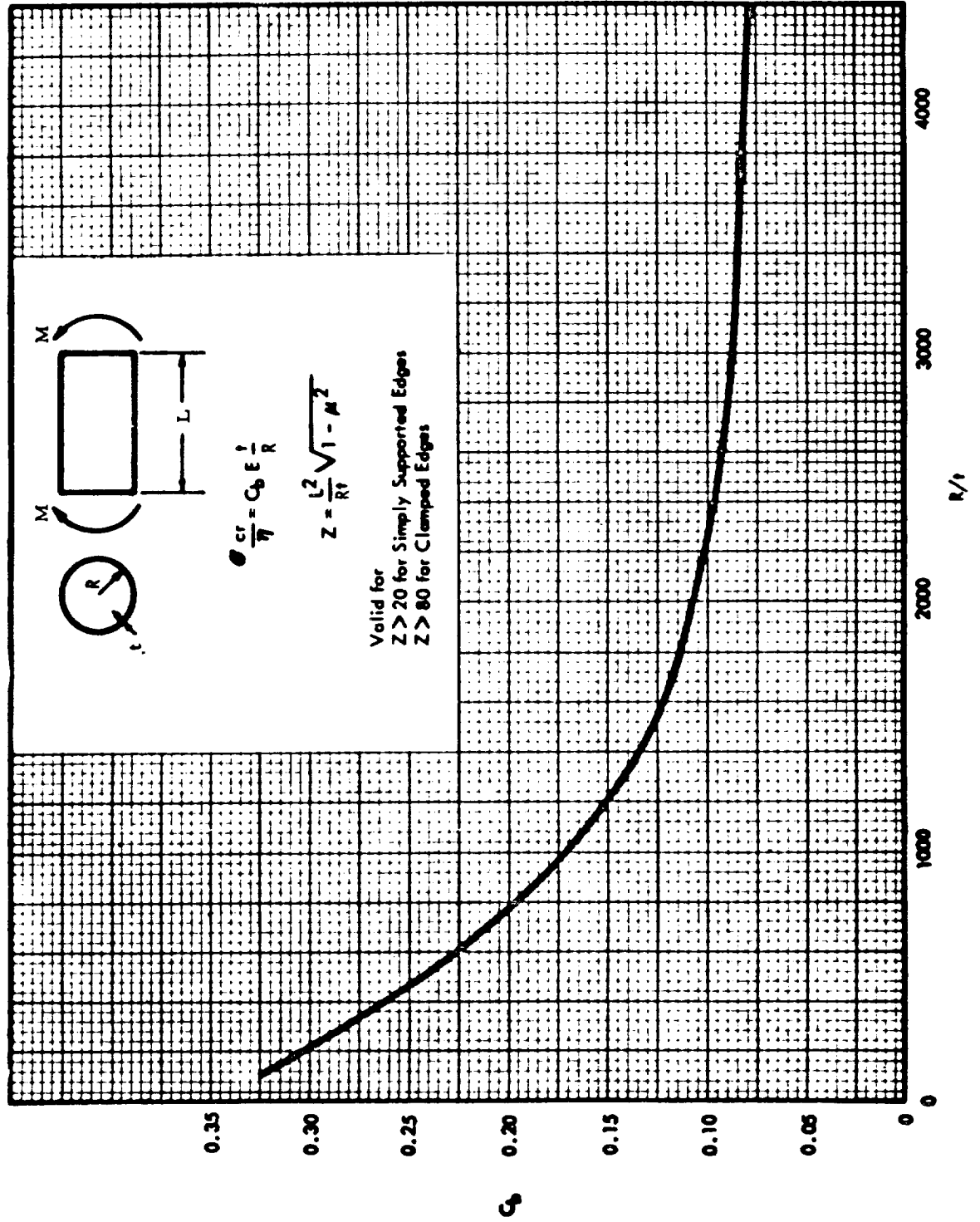
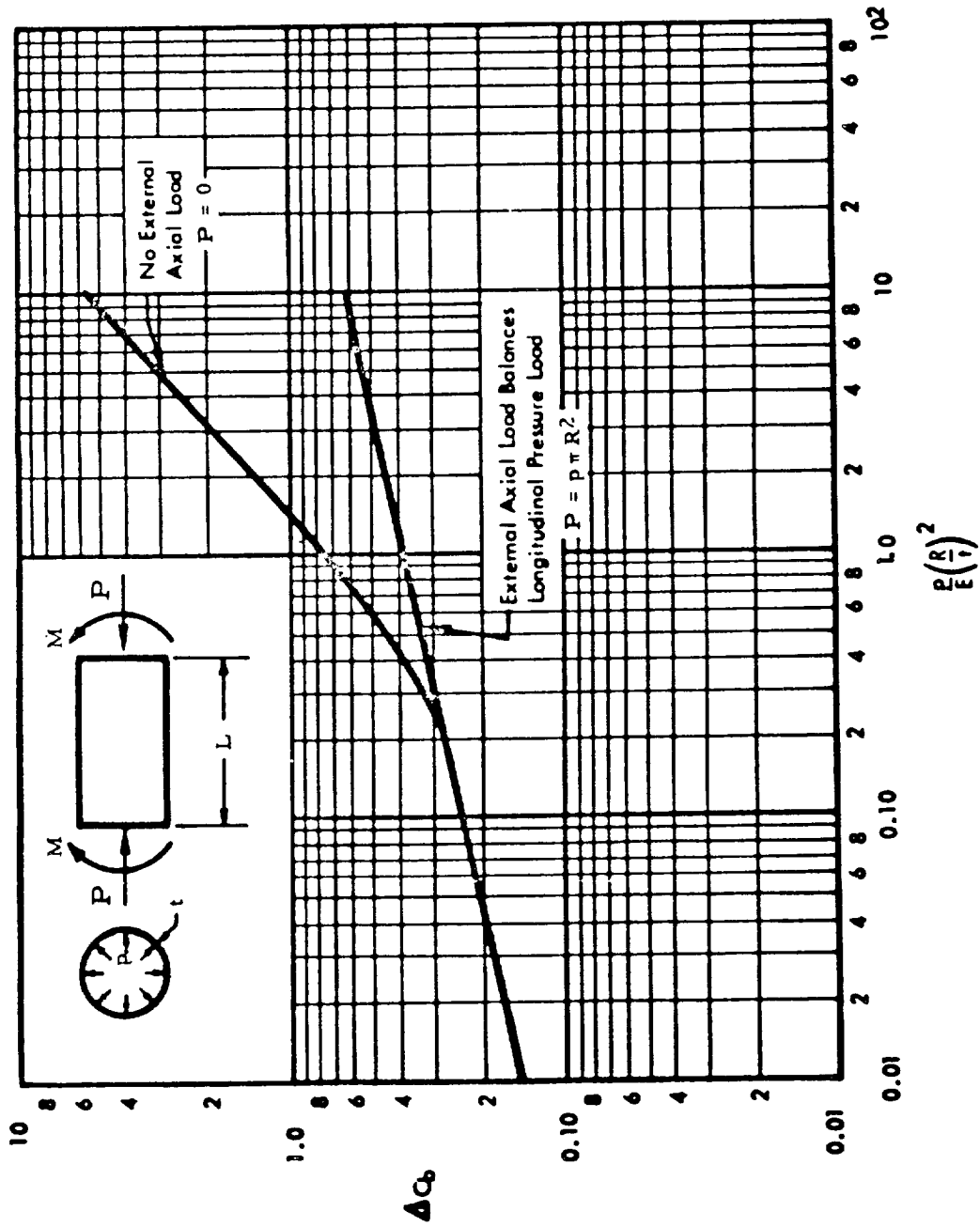


FIG. 3.23-6. INCREASE IN BENDING BUCKLING-STRESS COEFFICIENT OF CYLINDERS DUE TO INTERNAL PRESSURE



3.23.4 External Pressure, Unstiffened Cylinders

If a cylindrical shell with simply supported edges is subjected to uniform-external pressure, p , the design-allowable buckling stress in the circumferential direction is

$$\frac{\sigma_{cr}}{\eta} = K_p \frac{\pi^2 E}{12(1-\mu^2)} \left(\frac{t}{L}\right)^2$$

The buckling coefficient, K_p , and a definition of the geometrical parameters is given in Fig. 3.23-7. For elastic buckling, $\eta = 1$ is used. For moderate length cylinders ($100 < Z < 11 R^2/t^2$) in the inelastic range, Ref. 3-6 recommends

$$\eta = \frac{E_s}{E} \sqrt{\left(\frac{E_t}{E_s}\right)^{1/2} \left(\frac{1}{4} + \frac{3}{4} \frac{E_t}{E_s}\right)}$$

where

E_s = secant modulus

E_t = tangent modulus

For inelastic stresses, σ_{cr} may be obtained for the E_1 curves of Section 3.62 because, for most materials, the value of η for the E_1 curves does not vary appreciably from the value obtained from the preceding formula. For short cylinders ($Z < 10$), the C curves of Section 3.62 should be used. For $10 < Z < 100$, a linear interpolation between the E_1 and C curves with the Z parameter is probably

sufficiently accurate. For long cylinders, (e. g., $L^2/R^2 > 11 R/t$) the design-allowable buckling stress is

$$\frac{\sigma_{cr}}{\eta} = \frac{\gamma E}{4(1-\mu^2)} \left(\frac{t}{R}\right)^2$$

The factor, γ , was introduced to reduce the theory to a design value. Ref. 3-6 recommends $\gamma = 0.9$. For inelastic buckling, Ref. 3-7 recommends

$$\eta = \frac{E_s}{E} \left(\frac{1}{4} + \frac{3}{4} \frac{E_t}{E_s} \right)$$

Sufficiently accurate values of σ_{cr} may be obtained by using the E curves of Section 3.62.

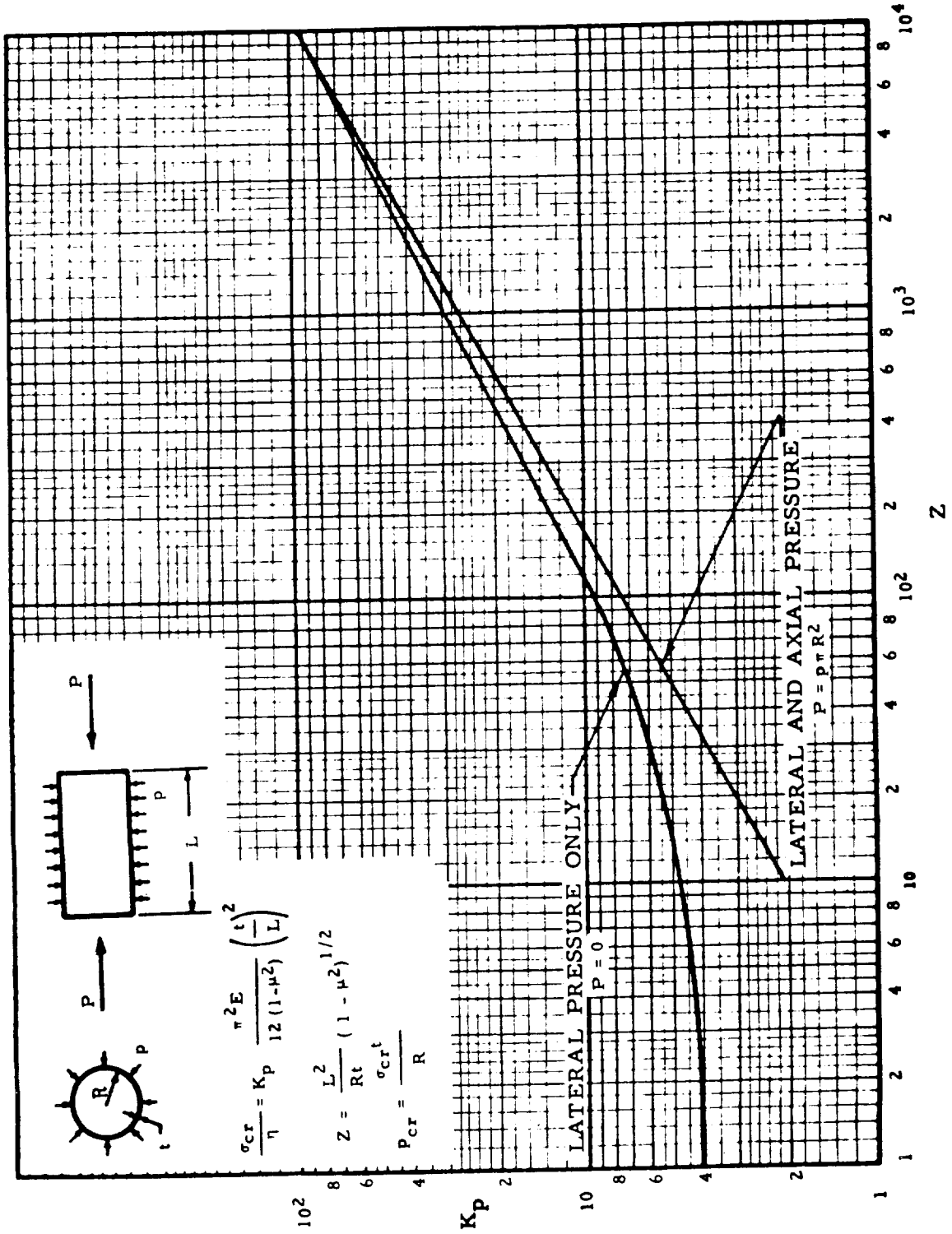
The design-allowable pressure may be obtained from the formula

$$p_{cr} = \frac{\sigma_{cr} t}{R}$$

The pressure, p_{cr} , is the design-allowable pressure for complete buckling of the shell (e. g., when buckles have formed all the way around the cylinder). For some values of the parameters (large R/t and/or large initial imperfections), single buckles will occur at pressures less than p_{cr} , but complete buckling will occur at higher pressures. Therefore, for some applications these results should be used with caution.

The plasticity correction factors recommended in this section were obtained primarily for the case of lateral pressure, but they are probably sufficiently accurate for the case of lateral and axial pressure.

FIG. 3.23-7. BUCKLING COEFFICIENTS FOR CIRCULAR CYLINDERS
SUBJECTED TO EXTERNAL PRESSURE



3.23.5 Combined Loading, Unstiffened Cylinders

The criterion for structural failure of a member under combined loading is frequently expressed in terms of a stress-ratio equation, $R_1^x + R_2^y + R_3^z = 1$. The subscripts denote the stress due to a particular kind of loading (compression, shear, etc.), and the exponents (usually empirical) express the general relationship of the quantities for failure of the member. The stress-ratio, R , is most easily understood if it is defined first for a particular loading condition. In combined compression and torsion loading ($R_c^x + R_s^z = 1$), the stress-ratio, R_c , is defined as the ratio of compressive stress at which buckling occurs under the combined loading to the compressive stress at which buckling occurs under compression alone. In general, the stress-ratio is the ratio of the allowable value of the stress caused by a particular kind of load in a combined loading condition to the allowable stress for the same kind of load when it is acting alone. A curve drawn from such a stress-ratio equation is termed a stress-ratio interaction curve. In simple loadings, the term "stress-ratio" is used to denote the ratio of applied to allowable stress.

A. Combined Torsion and Axial Loading

A semi-empirical interaction curve for circular cylinders under combined torsion and axial loading is given in Fig. 3.23-8. σ_{CR} is found

from Paragraph 3.23.1 and τ_{CR} from Paragraph 3.23.2. In Fig. 3.23-8, the curves for R/t ratios of 600, 800, and 1000 were determined by test data in Ref. 3-8. Curves for R/t of 1500 and 2000 were drawn by extrapolation.

B. Bending and Torsion

Test results shown in Ref. 3-7 indicate that a conservative estimate of the interaction for cylinders under combined bending and torsion may be obtained from Fig. 3.23-9; σ_{CR} is found from Paragraph 3.23.3 and τ_{CR} from Paragraph 3.23.2.

C. Axial Compression and Bending

The test data presented in Ref. 3-7 and 3-9 indicate that the linear interaction for the case of cylinders under combined axial compression and bending, shown in Fig. 3.23-10, may be used. The buckling stress due to bending alone may be found from Paragraph 3.23.3, and the buckling stress under axial compression alone may be found in Paragraph 3.23.1.

D. Axial Compression and External Pressure

The limited test data from Ref. 3-9 for cylinders subjected to axial compression and external lateral and axial pressure indicate that the linear interaction curve presented in Fig. 3.23-11 may be used for design. σ_{CR} is found from Paragraph 3.23.1 and p_{CR} from Paragraph 3.23.4.

FIG. 3.23-8. BUCKLING STRESS INTERACTION CURVE FOR UNSTIFFENED CIRCULAR CYLINDERS UNDER COMBINED TORSION AND AXIAL LOADING

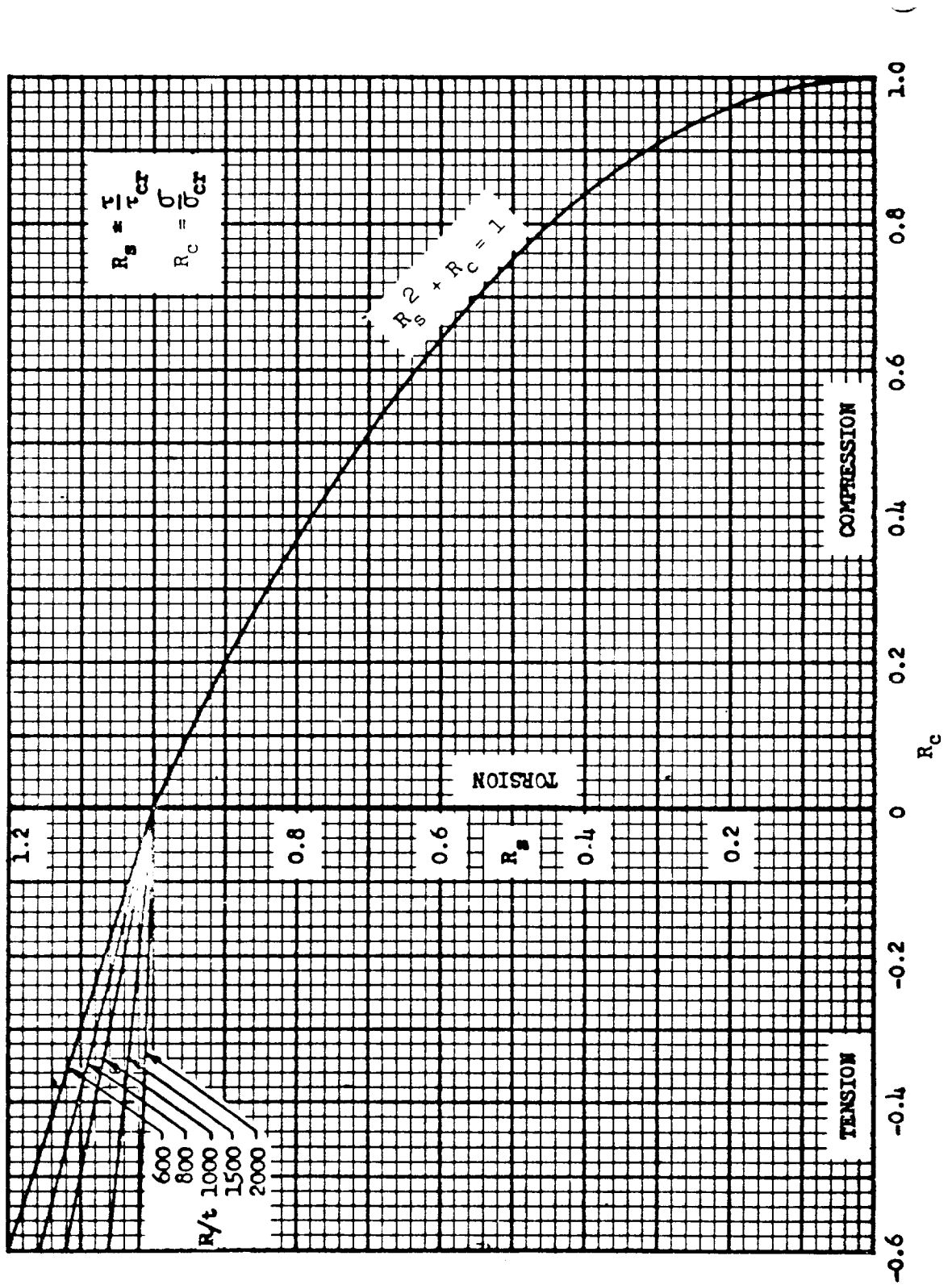


FIG. 3.23-9. BUCKLING STRESS INTERACTION CURVE FOR UNSTIFFENED CIRCULAR CYLINDERS UNDER COMBINED BENDING AND TORSION

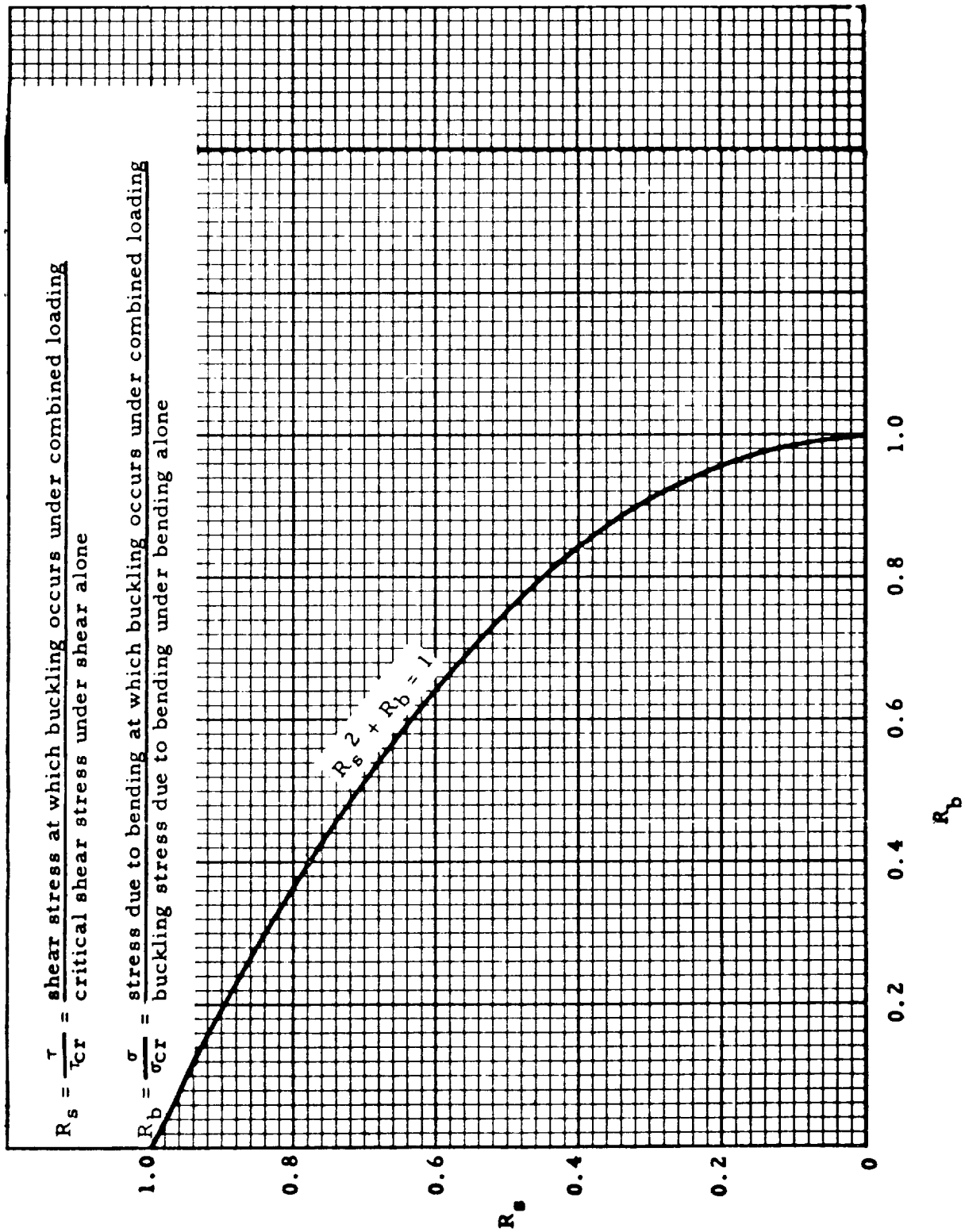


FIG. 3.23-10. BUCKLING STRESS INTERACTION CURVE FOR UNSTIFFENED CIRCULAR CYLINDERS UNDER COMBINED AXIAL COMPRESSION AND BENDING

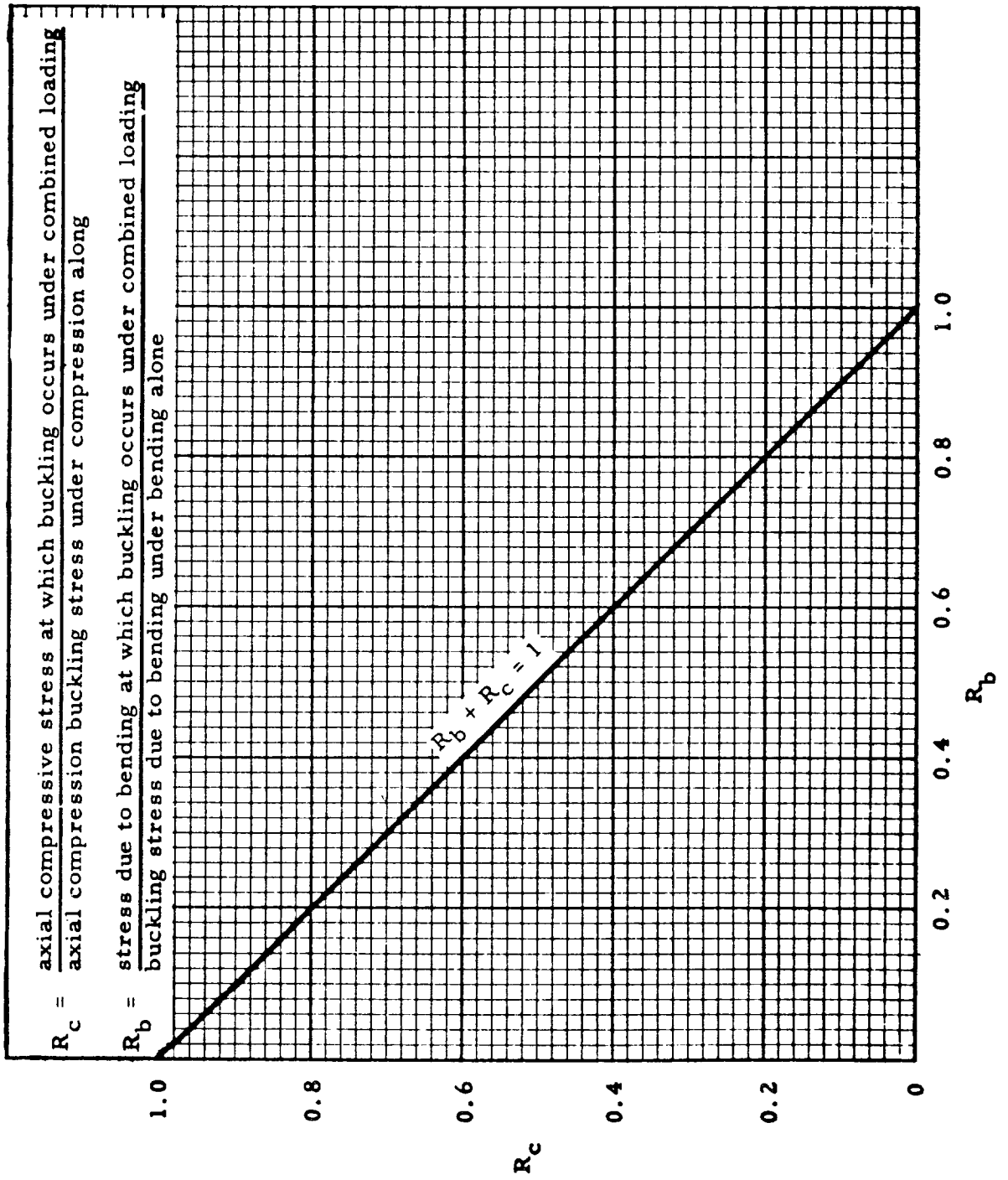
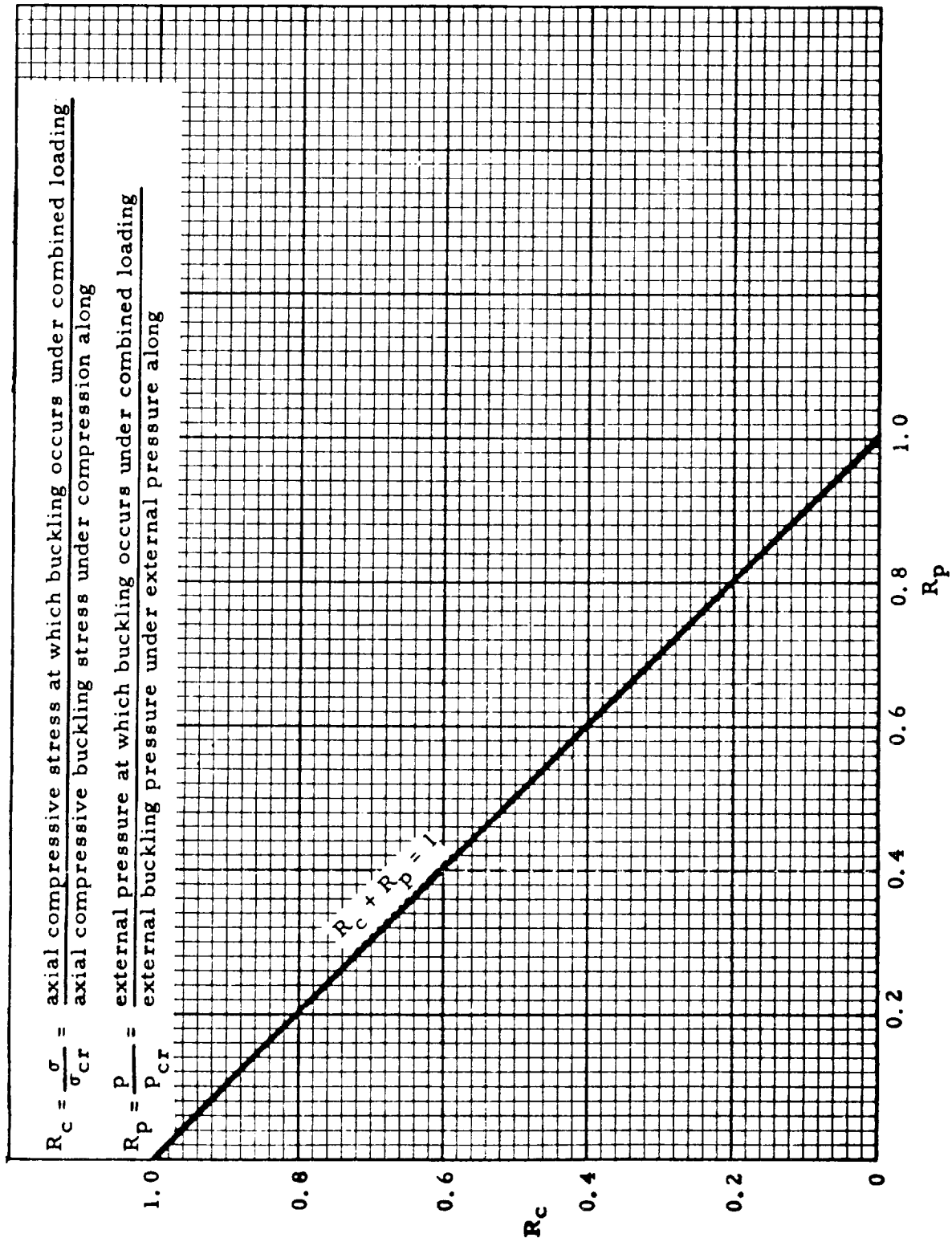


FIG. 3.23-11. BUCKLING STRESS INTERACTION CURVE FOR UNSTIFFENED CIRCULAR CYLINDERS UNDER COMBINED EXTERNAL PRESSURE AND AXIAL COMPRESSION



3.24 CONES

3.24.1 Axial Compression, Unstiffened Cones

A. Unpressurized

The equivalent cylinder approach recommended in Ref. 3-9 will be used for determining the buckling stress for a circular right cone subjected to axial compression. The statistical reduction of experimental cone data presented in Ref. 3-10 indicates that the equivalent cylinder approach may be conservative for large radius-to-thickness ratios, but the results of Ref. 3-10 would be unconservative for small cone angles (e. g., cones that are almost cylinders). The design-allowable buckling stress may be obtained from the formula

$$\frac{\sigma_{cr}}{\eta} = C_c \frac{Et}{R_e}$$

σ_{cr} is the stress at the small end of the cone. The buckling stress coefficient, C_c , and a definition of the geometrical parameters is given in Fig. 3.24-1 as are the limitations of the buckling equation. The curve of C_c versus R_e/t given in Fig. 3.24-1 for cones is the same curve given in Fig. 3.23-1 for cylinders. For elastic buckling, $\eta = 1$ is used. In the inelastic range, the critical stress σ_{cr} may be found by using curves E_1 in Section 3.62. The design-allowable total compressive load, P_{cr} , may be obtained from the equation

$$P_{cr} = 2\pi R_e \sigma_{cr} t \cos^2 \alpha$$

B. Pressurized

The design-allowable buckling stress for cones under internal pressure and axial compression may be determined by using Fig. 3.24-1 in conjunction with Fig. 3.24-2. Fig. 3.24-2 presents a curve that allows the calculation of the increase in buckling stress as a function of pressure and geometry only. The design-allowable buckling stress may be obtained from the formula

$$\frac{\sigma_{cr}}{\eta} = (C_c + \Delta C_c) \frac{Et}{R_e}$$

where C_c is obtained from Fig. 3.24-1, and ΔC_c is obtained from Fig. 3.24-2. For elastic buckling, $\eta = 1$ is used. In the inelastic range, the critical stress, σ_{cr} , may be found by using curves E_1 in Section 3.62. The total stress field should be taken into consideration when determining the plasticity correction. The pressurized cone is capable of resisting a total compressive load, P_{cr} , which may be obtained from the equation

$$P_{cr} = 2\pi R_e \sigma_{cr} t \cos^2 \alpha + \pi R_e^2 p \cos^2 \alpha$$

The P_{cr} found for pressurized cones subjected to axial compression may be conservative for certain values of the parameters because it has been shown both theoretically and experimentally that internal pressure increases the buckling load of cones more than it increases

the buckling load of cylinders. However, test data for pressurized cones is too limited to determine an empirical design curve based on parameters from the theoretical buckling analysis of pressurized cones.

FIG. 3.24-1. BUCKLING-STRESS COEFFICIENT, C_c , FOR UNSTIFFENED UNPRESSURIZED CIRCULAR CONES SUBJECTED TO AXIAL COMPRESSION

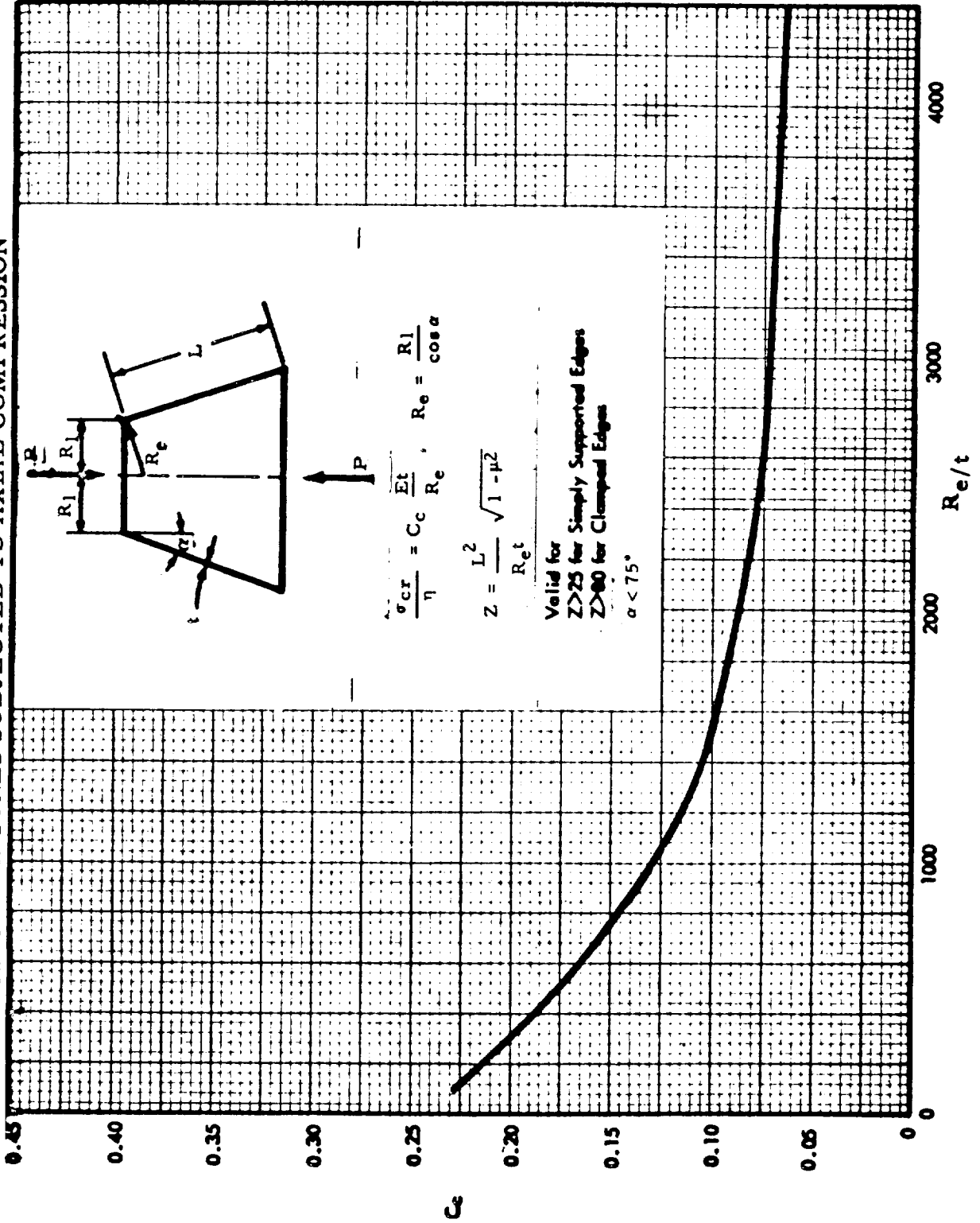
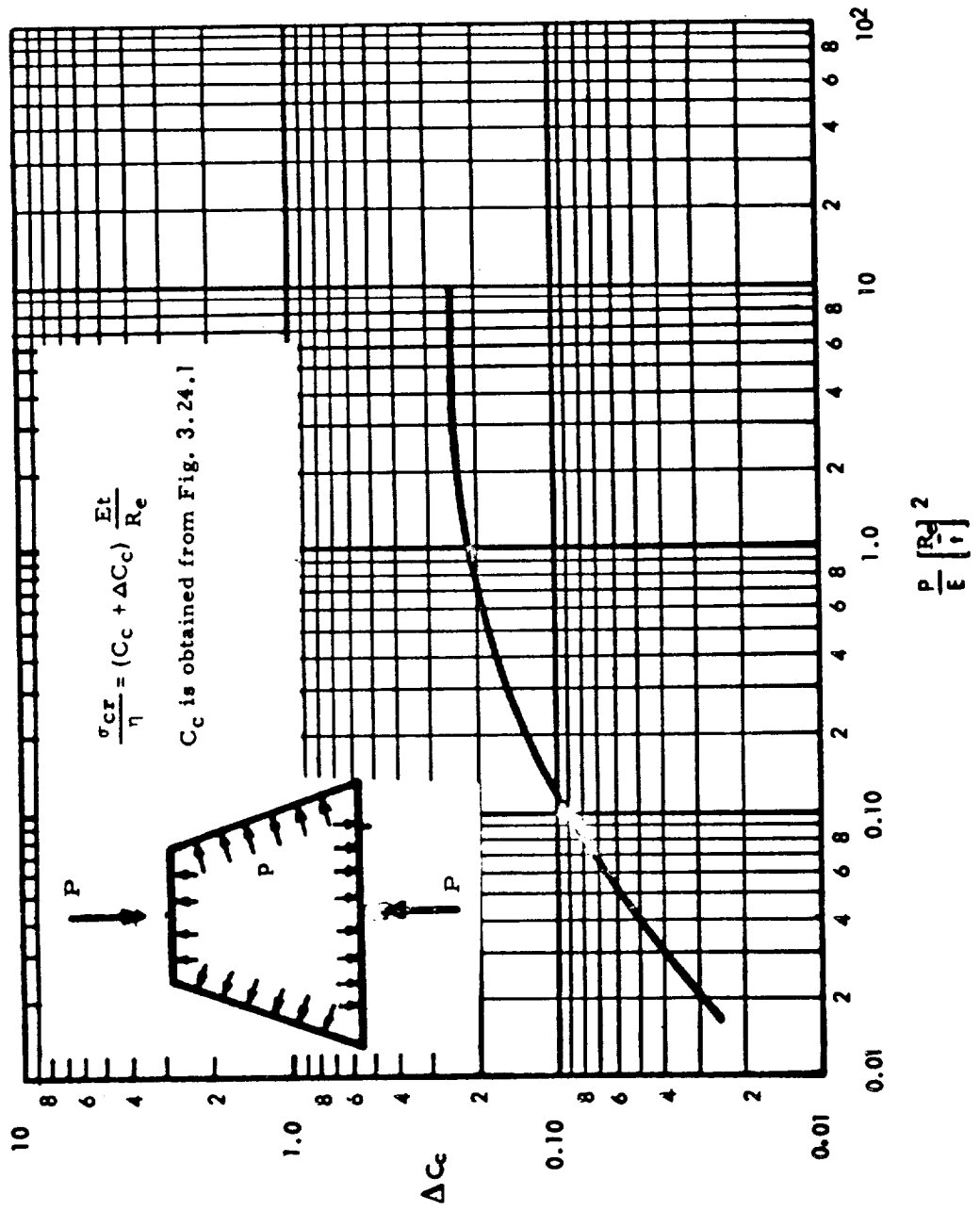


FIG. 3.24-2. INCREASE IN AXIAL-COMPRESSIVE BUCKLING-STRESS COEFFICIENT OF CONES DUE TO INTERNAL PRESSURE



3.24.2 Shear or Torsion, Unstiffened Cones

A. Unpressurized

The equivalent cylinder approach recommended in Ref. 3-11 will be used to determine the buckling stress for a circular right cone subjected to torsion. The design-allowable buckling stress is

$$\frac{\tau_{cr}}{\eta} = \frac{R_e^2}{R_l^2} C_s \frac{Et}{R_e Z^{1/4}}$$

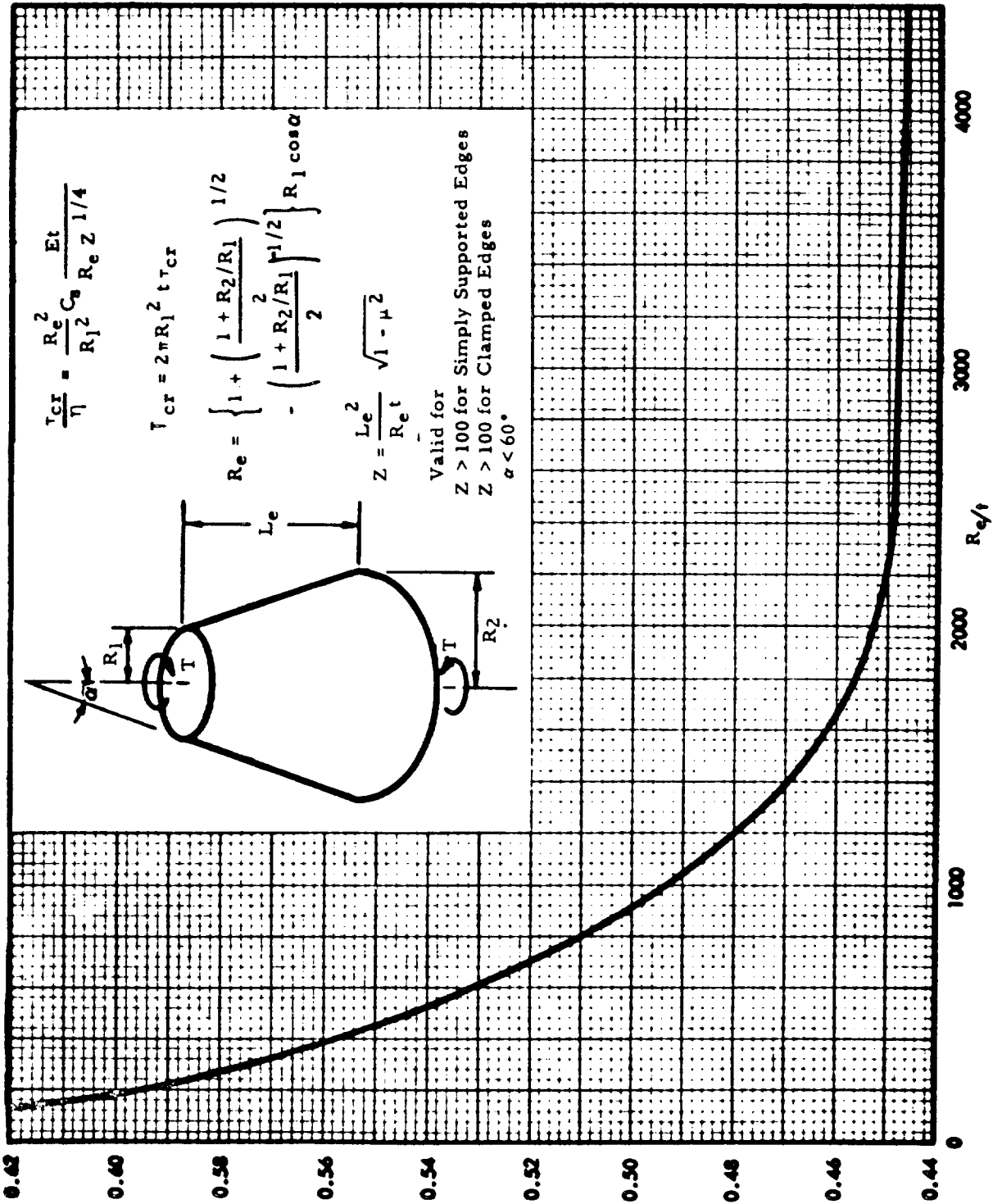
τ_{cr} is the shear stress at the small end of the cone. The buckling stress coefficient, C_s , and a definition of the geometrical parameters are given in Fig. 3.24-3, as are the limitations of the buckling equation. The curves of C_s versus R_e/t given in Fig. 3.24-3 for cones is the same curve given in Fig. 3.23-3 for cylinders. For elastic buckling, the plasticity correction term $\eta = 1.0$ is used. For inelastic buckling, the critical shear stress, τ_{cr} , may be found by using the procedure recommended in Paragraph 3.22.2. The design allowable torque, T_{cr} , may be obtained from the equation

$$T_{cr} = 2\pi R_l^2 t \tau_{cr}$$

B. Pressurized

The theoretical results and the test results of Ref. 3-12 show that internal pressure will increase the torsional buckling load of cones, but simple design formulas for computing this increase are not available.

FIG. 3.24-3. BUCKLING-STRESS COEFFICIENT, C_B , FOR UNSTIFFENED UNPRESSURIZED CIRCULAR CONES SUBJECTED TO TORSION



3.24.3 Bending, Unstiffened Cones

A. Unpressurized

The equivalent cylinder approach recommended in Ref. 3-9 will be used to determine the buckling stress of a circular right cone subjected to bending. The design-allowable buckling stress is

$$\frac{\sigma_{cr}}{\eta} = C_b \frac{Et}{R_e}$$

where σ_{cr} is the maximum stress at the small end of the cone. The buckling coefficient, C_b , and a definition of the geometrical parameters are given in Fig. 3.24-4. The curve of C_b versus R/t given in Fig. 3.24-4 for cones is the same curve as that given in Fig. 3.23-5 for cylinders. For elastic buckling, $\eta = 1$ is used. In the inelastic range, the critical stress, σ_{cr} , may be found by using curves E_1 in Section 3.62. If the stresses are elastic, the allowable moment may be obtained from the formula

$$M_{cr} = \pi R_1^2 \sigma_{cr} t \cos \alpha$$

B. Pressurized

An estimate of the design-allowable buckling stress for a cone under internal pressure and axial compression may be determined by using Fig. 3.24-4 in conjunction with Fig. 3.24-5. Fig. 3.24-5 presents a curve that allows the calculation of the increase in buckling

stress as a function of pressure and geometry only. The design-allowable buckling stress may be obtained from the formula

$$\frac{\sigma_{cr}}{\eta} = (C_b + \Delta C_b) \frac{Et}{R_e}$$

where C_b is obtained from Fig. 3.24-4 and ΔC_b is obtained from Fig. 3.24-5. For elastic buckling, $\eta = 1$ is used. In the inelastic range, the critical stress, σ_{cr} , may be found by using curves E_1 in Section 3.62. The total stress field should be taken into consideration when the plasticity correction is determined. If the stresses are elastic and no external axial load is applied, the allowable moment may be obtained from the formula

$$M = \pi R_1^2 t \sigma_{cr} \cos \alpha + \pi p \frac{R_1^3}{2}$$

FIG. 3.24-4. BUCKLING-STRESS COEFFICIENT C_b FOR UNSTIFFENED UNPRESSURIZED CIRCULAR CONES SUBJECTED TO BENDING

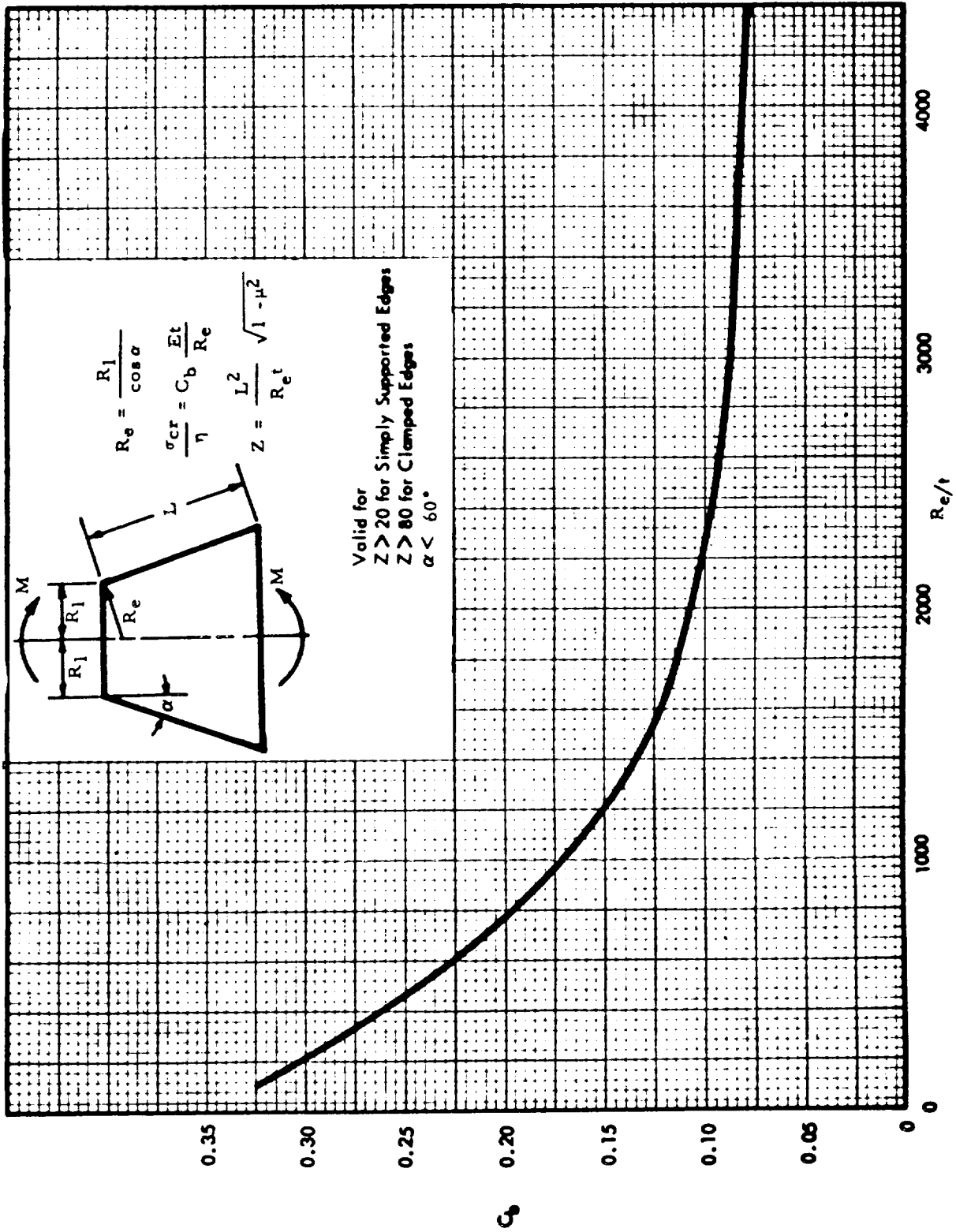
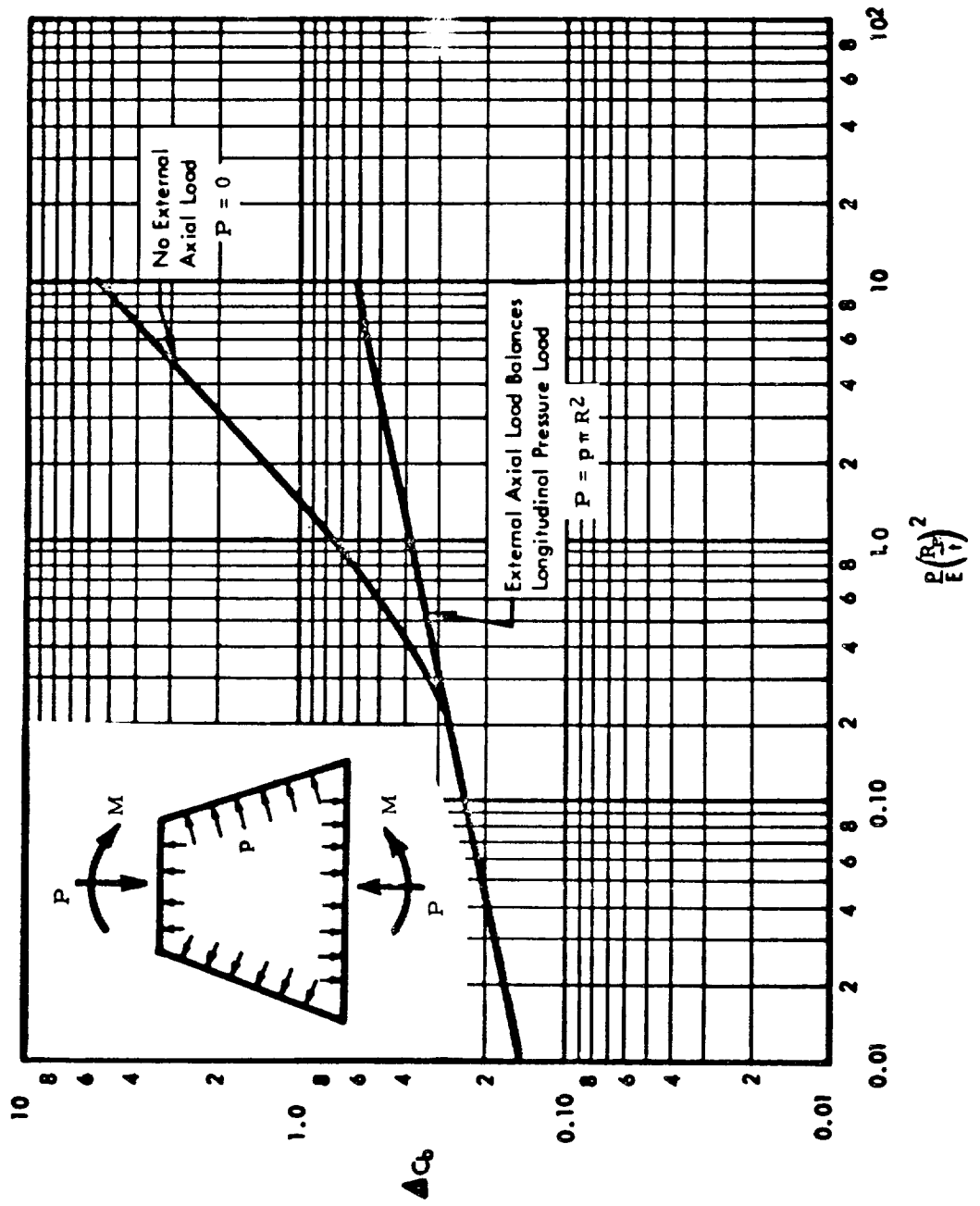


FIG. 3.24-5. INCREASE IN BENDING BUCKLING-STRESS COEFFICIENT OF CONES DUE TO INTERNAL PRESSURE



3.24.4 Lateral and Axial External Pressure, Unstiffened Cones

The equivalent cylinder recommended in Ref. 3-9 will be used to determine the design-allowable buckling stress for a circular right cone subjected to lateral and axial external pressure. The design-allowable buckling stress may be obtained from the formula

$$\frac{\sigma_{cr}}{\eta} = K_p \frac{\pi^2 E}{12(1 - \mu^2)} \left(\frac{t}{L_e} \right)^2 \frac{R_2}{R_e \cos \alpha}$$

σ_{cr} is the circumferential membrane stress at the large end of the cone due to an external pressure, p_{cr} . The buckling stress coefficient, K_p , and a definition of the geometrical parameters are given in Fig. 3.24-6. Fig. 3.24-6 is for simply supported edges and will be conservative for fixed edges. For elastic buckling, $\eta = 1$ is used. In the inelastic range, the critical stress, σ_{cr} , may be found by using the method discussed in Paragraph 3.23.4. The design-allowable external pressure may be obtained from the formula

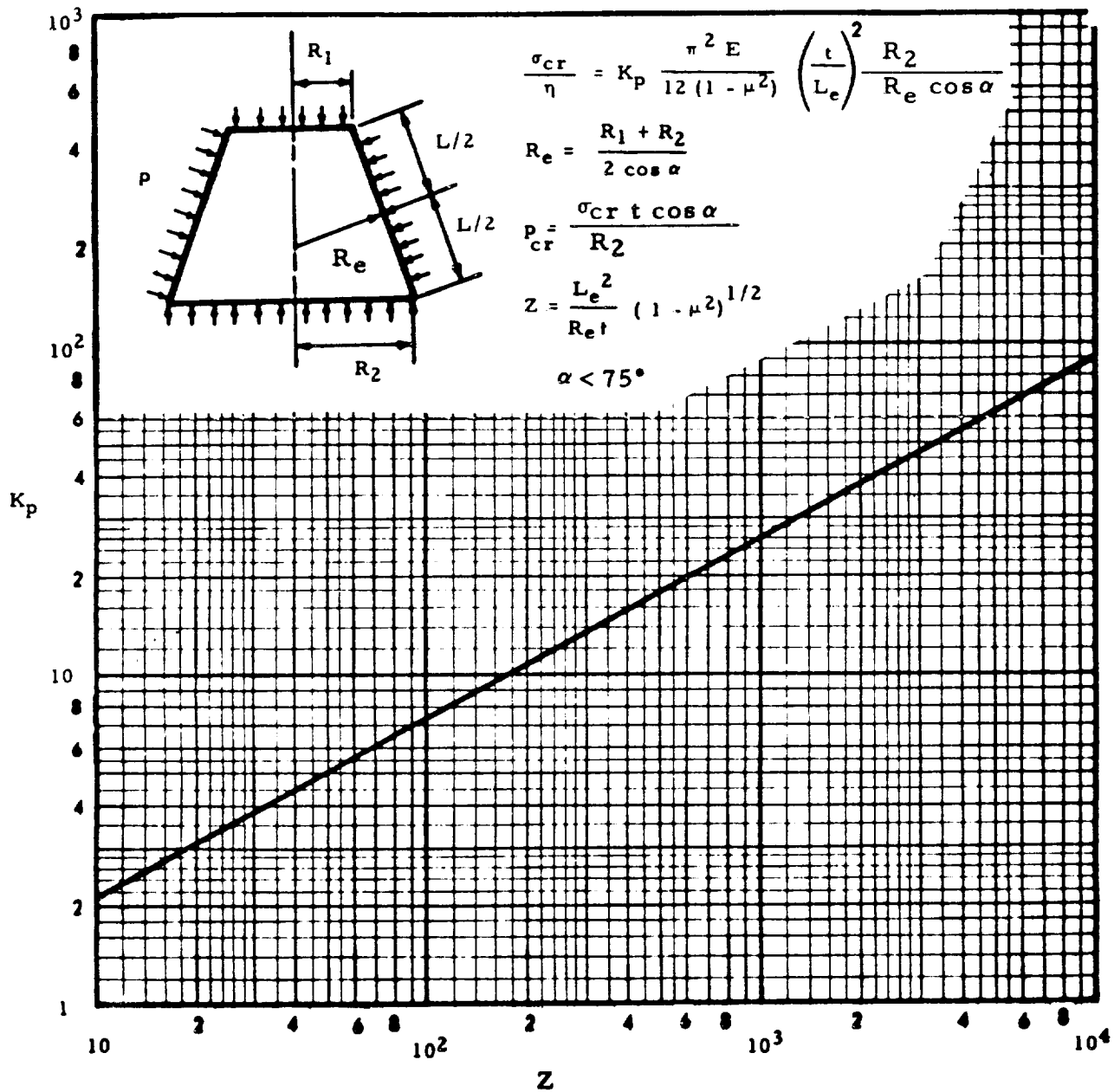
$$p_{cr} = \frac{\sigma_{cr} t \cos \alpha}{R_2}$$

The pressure, p_{cr} , is the design-allowable pressure for complete buckling of the shell (e. g., when buckles have formed all the way around the cone). For some values of the parameters (such as large $\frac{R}{t}$ or large initial

imperfections), single buckles will occur at pressures less than p_{cr} , but complete buckling will occur at higher pressures. Therefore, for some applications, these results should be used with caution.

It has been shown in the literature that the critical pressure is a function of the quantity $(1-R_1/R_2)$, but the effect is generally small and the available information has not been reduced for design purposes.

FIG. 3.24-6. BUCKLING PRESSURE COEFFICIENTS FOR CIRCULAR CONES SUBJECTED TO EXTERNAL RADIAL AND AXIAL PRESSURE



3.24.5 Combined Loading, Unstiffened Cones

The concept of stress-ratio interaction curves as described for cylinders in Paragraph 3.23.5 will also be used for cones.

A. Axial Compression and Torsion

Ref. 3-13 has shown that for unstiffened right conical shells, the curve given in Fig. 3.23-8 may be used for predicting the interaction between axial compression and torsion. σ_{cr} is found from Paragraph 3.24.1 and τ_{cr} from Paragraph 3.24.2.

B. Axial Compression and Bending

The very limited test data in Ref. 3-9 indicate that the linear interaction equation shown in Fig. 3.23-10 may be used for right circular cones subjected to combined axial compression and bending. The buckling stress due to bending alone may be found from Paragraph 3.24.3, and the buckling stress under axial compression alone may be found in Paragraph 3.24.1.

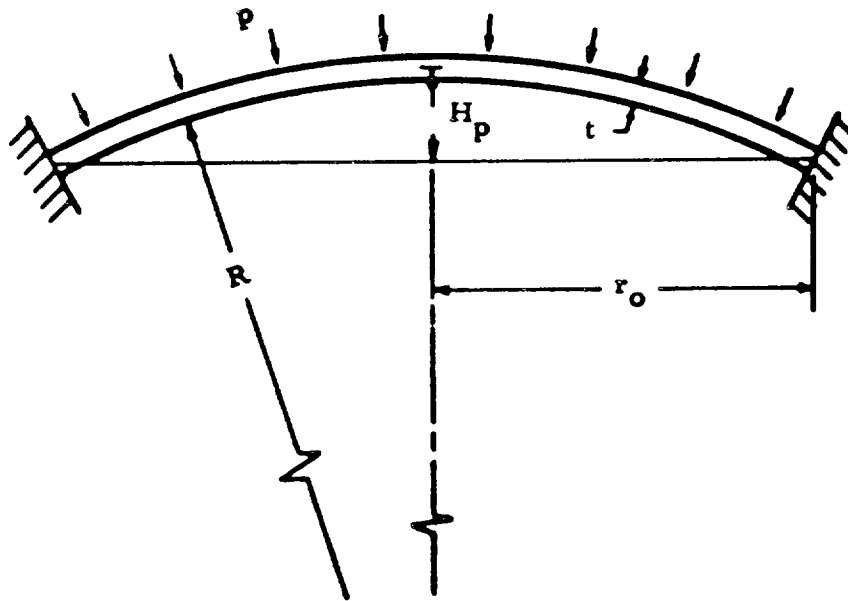
C. Axial Compression and External Pressure

The limited test data from Ref 3-9 indicated that the curve given in Fig. 3.23-11 may be used for right circular cones subjected to axial compression and external lateral and axial pressure. σ_{cr} may be obtained from Paragraph 3.24.1 and p_{cr} from Paragraph 3.24.4.

3.25 SPHERICAL CAPS

3.25.1 External Pressure, Shallow Spherical Caps

The following figure shows the type of shell and load that will be considered in this section:



The shell is spherical, and the ratio of $H_p/2r_o$ should be small, say, $H_p/2r_o < 1/8$. The design-allowable buckling stress may be obtained from the following formula:

$$\frac{\sigma_{cr}}{\eta} = C_p \frac{Et}{R} \text{ for } 4 < \lambda < 24$$

$$C_p = 0.175$$

where

$$\lambda = \left[12 (1-\mu^2) \right]^{\frac{1}{4}} r_o / \left[Rt \right]^{\frac{1}{2}}$$

For elastic buckling, $\eta = 1$ is used. For inelastic buckling, the critical stress, σ_{cr} , may be found, using curves E_1 in Section 3.62.

The design-allowable buckling pressure is

$$p_{cr} = \sigma_{cr} \frac{2t}{R}$$

The coefficient, C_c , should be a function of λ . However, it was shown in Ref. 3-14 that for $6 < \lambda < 24$, the increase in the theoretical value of C_p is very small as λ increases, provided the shell is free of initial imperfections. In addition, test data for $4 < \lambda < 6$ indicate a value of C_p that is approximately the same as the value of C_p for $6 < \lambda < 8$. Therefore, it was assumed that C_p was independent of λ for $4 < \lambda < 24$. The quantity $C_p = 0.175$ was obtained by a statistical reduction of the test data from Refs. 3-15, 3-16, 3-17, and 3-18. The test specimens in Refs. 3-15, 3-16, 3-17 and 3-18 failed considerably below the theoretical curve given in Ref. 3-14. One of the primary reasons for these low buckling loads is probably initial imperfections in the test specimens.

The lower bound of the values of C_p obtained in tests of spherical caps with very small imperfections, as reported in Refs. 3-19 and 3-20,

was approximately $C_p = 0.39$, which indicates that the buckling stress is much greater if the initial imperfections are small. However, it is not felt that the shells tested in Refs. 3-19 and 3-20 are typical of a production part.

3.25.2 External Pressure, Spherical Caps

Spherical caps for which $H_p/2r_o > 1/8$ (see Section 3.25.1) have not been discussed in the literature as often as spherical caps for which $H_p/2r_o < 1/8$ due to the added complexity of the problem. Theoretical investigations of shells free of initial imperfections indicate that the buckling pressure for deep spherical caps would be greater than for shallow spherical caps of the same radius and thickness, but this has not been verified experimentally. The test data for deep spherical caps subjected to external pressure show that the buckle is usually confined to a small area of the shell. Therefore, the area of the shell that participates in the buckle could be thought of as a shallow spherical cap. Until additional information is available, it is recommended that the information contained in Paragraph 3.25.1 be used to obtain the design-allowable buckling stress for spherical caps with $\lambda > 24$ and $H_p/2r_o > 1/8$ which are subjected to external pressure. The limited results of test data for hemispherical shells subjected to external pressure, such as Refs. 3-21 and 3-22, indicate that this is an adequate procedure.

The test data from Ref. 3-21 indicate that the inelastic properties of the material influences the buckling load even though the nominal membrane stress may be below the inelastic limits; but a method of accounting for this effect was not presented.

An empirical analysis procedure is presented in Ref. 3-23 which may be useful if the initial imperfections of a shell are known. However, it is difficult to use for a shell which is to be built because an estimate of the initial imperfection is necessary.

At the present time, the effects of various boundary conditions for partial spheres are unknown. Until additional information is obtained, the analysis which has been presented may be used for hemispherical caps with fixed or simply supported boundaries. Ref. 3-24 presents test results for spherical caps with various boundary conditions and may be of some use in estimating the effects of boundary conditions other than clamped.

3.30 ORTHOTROPIC SHELLS

3.31 GENERAL

This section deals with shells with stiffness properties different in the circumferential and meridional directions. The stiffness properties of the shell wall in the two directions may be completely independent (i. e., the bending stiffnesses, extensional stiffnesses, in-plane shear stiffness, and twisting stiffness of the walls of the shell are not necessarily interrelated as they are in a homogeneous isotropic shell or a homogeneous orthotropic shell). An example of this type of shell is a multilayered filament wound cylinder. Other types of construction, such as integrally stiffened waffle with closely spaced stiffeners, can be idealized as orthotropic by assuming that discrete stiffening elements are evenly distributed per unit width of wall. It is difficult to determine how close the stiffeners must be to treat the shell as an orthotropic shell. For the case of buckling, a buckle must include several stiffeners before orthotropic shell theory would be a useful tool in predicting the buckling load.

Definitions of the stiffness properties (elastic constants) for an orthotropic shell wall are given in Section 3.32, and approximate formulas are given for computing the stiffness properties for several types of construction.

The buckling formulas presented in this section are based on the classical small deflection theory of orthotropic shells. Experimental and theoretical studies indicate that the discrepancy between test and theory as well as the scatter of the test data may be much smaller for certain types of orthotropic cylinders than it was for homogeneous isotropic cylinders. However, the number of tests conducted to date on orthotropic shells typical of large production parts is limited and covers only a small range of possible parameters. Therefore, the results of homogeneous isotropic cylinder tests are used to modify the orthotropic theory until more information is available.

The analysis presented assumes that the centroid planes of the orthotropic wall in the axial direction coincide with the centroid planes of the wall in the circumferential direction. This assumption eliminates coupling between many of the internal stress resultants and simplifies the analysis. Although the effects of coupling can be large for some types of construction, they are usually small for the types of construction presented in this section (multilayered, integrally stiffened, homogeneous orthotropic).

The effects of Poisson's ratio have been included in the analysis procedures that are presented. However, the analysis may be simplified by neglecting Poisson's ratio. For many types of orthotropic construction, the effect of Poisson's ratio is very small.

3.32 ELASTIC CONSTANTS

3.32.1 Definitions

The elastic constants are defined in this section, and approximate formulas are given for computing the elastic constants for several types of construction that may be idealized as orthotropic construction. These constants can be used in Chapter 2.00 for stress analysis or in this chapter (Chapter 3.00) for stability analysis. The formulas for the constants have been derived for flat orthotropic plates but are sufficiently accurate for thin orthotropic shells.

The x direction is the axial direction for cylinders and cones and the meridional direction for spheres. The θ direction is the circumferential direction. The elastic constants are defined as follows:

- B_x, B_θ = The extension stiffnesses of the shell wall in the x and θ directions, respectively, (lb/in.)
- D_x, D_θ = The bending stiffnesses of the shell wall in the x and θ directions, respectively, (in.-lb)
- $D_{x\theta}$ = The twisting stiffness of the shell wall (in.-lb)
- D_{Q_x}, D_{Q_θ} = The transverse shear stiffnesses of the shell wall in the x and θ directions, respectively (lb/in.)

μ_x, μ_θ = Poisson's ratios associated with bending in the x and θ directions, respectively

μ'_x, μ'_θ = Poisson's ratios associated with extension in the x and θ directions, respectively

$G_{x\theta}$ = Shear stiffness of the shell wall in the $x\theta$ plane
(lb/in.)

From the reciprocity theorem, it has been shown that the following useful relationships exist:

$$D_x \mu_\theta = D_\theta \mu_x$$

$$B_x \mu'_\theta = B_\theta \mu'_x$$

The elastic constants required for Chapter 2.00 are $B_\theta, D_x, \mu_x, \mu_\theta, \mu'_x, \mu'_\theta$ and D_{Q_x} . All of the elastic constants with the exception of D_{Q_x} and D_{Q_θ} are required in Section 3.33. The constants, D_{Q_x} and D_{Q_θ} , are not needed in Section 3.33 because transverse shear deflections have been neglected in the basic analysis. Sandwich-type construction is the only orthotropic construction in which shear deflections are likely to be important. In general, the data of Section 3.50 should be used for the stability analysis of sandwich shells. However, if Section 3.50 does not include a particular type of sandwich (for instance, facings made from a different material), and if the core is very stiff in transverse shear (Section 3.50 can be used to estimate if the transverse

shear stiffness is large), the design buckling load can be estimated using the formulas from Section 3.33 and the elastic constants given in this section.

3.32.2 Orthotropic Layered Shells

The elastic constants for orthotropic layered shells were obtained from Ref. 3-25. A typical multilayered cross section is shown in Fig. 3.32-1. It can be seen that there are m layers. The inner layer is δ_1 thick, the next layer is $(\delta_2 - \delta_1)$ thick, etc., and the total thickness of the shell is δ_m . It is assumed that each layer is homogeneous and orthotropic.

The material properties of a layer are:

E_{x_i}, E_{θ_i} = Moduli of elasticity in the x and θ directions,
respectively

$\mu_{x_i}, \mu_{\theta_i}$ = Poisson's ratios associated with stretching in the
 x and θ directions, respectively

$G_{x\theta_i}$ = In-plane shear modulus

Subscript i represents the layer to which the material property corresponds ($i = 1, 2, \dots, m$). Refer to Paragraph 3.32.1 for a definition of the x and θ direction.

Let

$$C_{x_i} = \frac{E_{x_i}}{1 - \mu_{x_i} \mu_{\theta_i}}$$

$$C_{\theta_i} = \frac{E_{\theta_i}}{1 - \mu_{x_i} \mu_{\theta_i}}$$

$$C_{\mu_i} = \frac{\mu_{x_i} E_{\theta_i}}{1 - \mu_{x_i} \mu_{\theta_i}}$$

$$\delta_0 = 0$$

Then

$$\Delta_x = \frac{\sum_{i=1}^m C_{x_i} (\delta_i^2 - \delta_{i-1}^2)}{2 \sum_{i=1}^m C_{x_i} (\delta_i - \delta_{i-1})}$$

$$\Delta_{\theta} = \frac{\sum_{i=1}^m C_{\theta_i} (\delta_i^2 - \delta_{i-1}^2)}{2 \sum_{i=1}^m C_{\theta_i} (\delta_i - \delta_{i-1})}$$

$$\Delta_{\mu} = \frac{\sum_{i=1}^m C_{\mu_i} (\delta_i^2 - \delta_{i-1}^2)}{2 \sum_{i=1}^m C_{\mu_i} (\delta_i - \delta_{i-1})}$$

$$\Delta_{x\theta} = \frac{\sum_{i=1}^m G_{x\theta_i} (\delta_i^2 - \delta_{i-1}^2)}{2 \sum_{i=1}^m G_{x\theta_i} (\delta_i - \delta_{i-1})}$$

$$B_x = \sum_{i=1}^m C_{x_i} (\delta_i - \delta_{i-1})$$

$$B_\theta = \sum_{i=1}^m C_{\theta_i} (\delta_i - \delta_{i-1})$$

$$D_x = \frac{1}{3} \sum_{i=1}^m C_{x_i} \left[(\delta_i^3 - \delta_{i-1}^3) - 3 \Delta_x (\delta_i^2 - \delta_{i-1}^2) + 3 \Delta_x^2 (\delta_i - \delta_{i-1}) \right]$$

$$D_\theta = \frac{1}{3} \sum_{i=1}^m C_{\theta_i} \left[(\delta_i^3 - \delta_{i-1}^3) - 3 \Delta_\theta (\delta_i^2 - \delta_{i-1}^2) + 3 \Delta_\theta^2 (\delta_i - \delta_{i-1}) \right]$$

$$D_{x\theta} = \frac{1}{3} \sum_{i=1}^m G_{x\theta_i} \left[(\delta_i^3 - \delta_{i-1}^3) - 3 \Delta_{x\theta} (\delta_i^2 - \delta_{i-1}^2) + 3 \Delta_{x\theta}^2 (\delta_i - \delta_{i-1}) \right]$$

$$G_{x\theta} = \sum_{i=1}^m G_{x\theta_i} (\delta_i - \delta_{i-1})$$

$$\mu_x = \frac{1}{3D_\theta} \sum_{i=1}^m C_{\mu_i} \left[(\delta_i^3 - \delta_{i-1}^3) - 3 \Delta_\mu (\delta_i^2 - \delta_{i-1}^2) + 3 \Delta_\mu^2 (\delta_i - \delta_{i-1}) \right]$$

$$\mu_\theta = \frac{\mu_x D_\theta}{D_x}$$

$$\mu_x' = \frac{1}{B_\theta} \sum_{i=1}^m C_{\mu_i} (\delta_i - \delta_{i-1})$$

$$\mu_\theta' = \frac{\mu_x' B_\theta}{B_x}$$

D_{Q_x} and D_{Q_θ} are effectively infinite for most layered shells (if the shell is sandwich construction, see Paragraph 3.32.3).

For simplicity, μ_x could be assumed to equal μ_x' , which would save the computation of Δ_μ and μ_x .

For a single layer t thick ($\delta_1 = t$), the formulas reduce to

$$B_x = C_{x_1} t$$

$$B_\theta = C_{\theta_1} t$$

$$D_x = \frac{C_{x_1} t^3}{12}$$

$$D_\theta = \frac{C_{\theta_1} t^3}{12}$$

$$D_{x\theta} = \frac{G_{x\theta_1} t^3}{12}$$

$$G_{x\theta} = G_{x\theta_1} t$$

$$\mu_x = \mu'_{x_1} = \mu_{x_1}$$

$$\mu_\theta = \mu'_{\theta_1} = \mu_{\theta_1}$$

If the layer is isotropic with a Young's modulus of E , Poisson's ratio of μ , and shear modulus of G , the constants are

$$B_x = B_\theta = \frac{Et}{1 - \mu^2}$$

$$D_x = D_\theta = \frac{Et^3}{1 - \mu^2}$$

$$D_{x\theta} = \frac{Gt^3}{12}$$

$$G_{x\theta} = Gt$$

$$\mu = \mu_x = \mu_\theta = \mu'_{x_1} = \mu'_{\theta_1}$$

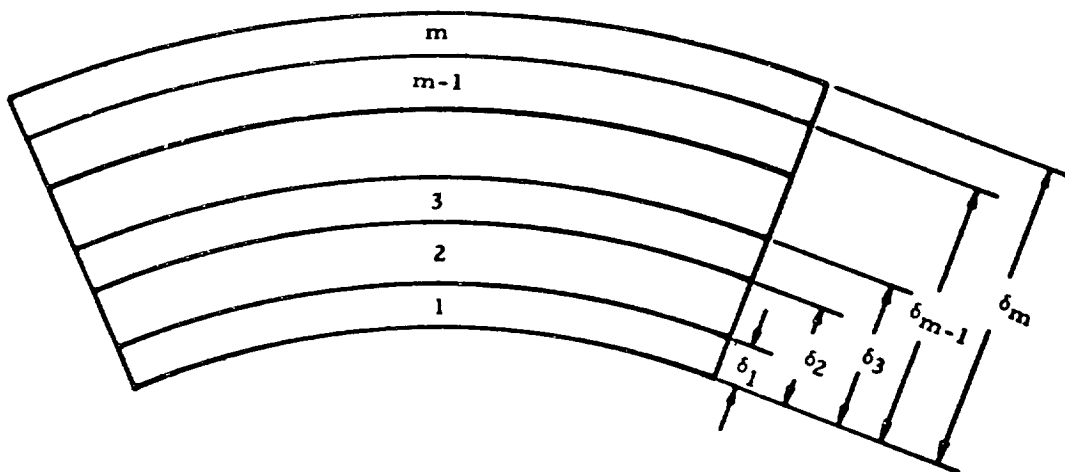


FIG. 3.32-1. Layered Construction

3.32.3 Sandwich Shells

The elastic constants presented in this section are for a sandwich construction with a core that resists very little bending or stretching (such as honeycomb core) and thin facing sheets relative to the overall thickness of the sandwich. A typical sandwich element and a definition of the geometrical parameters are given in Fig. 3.32-2.

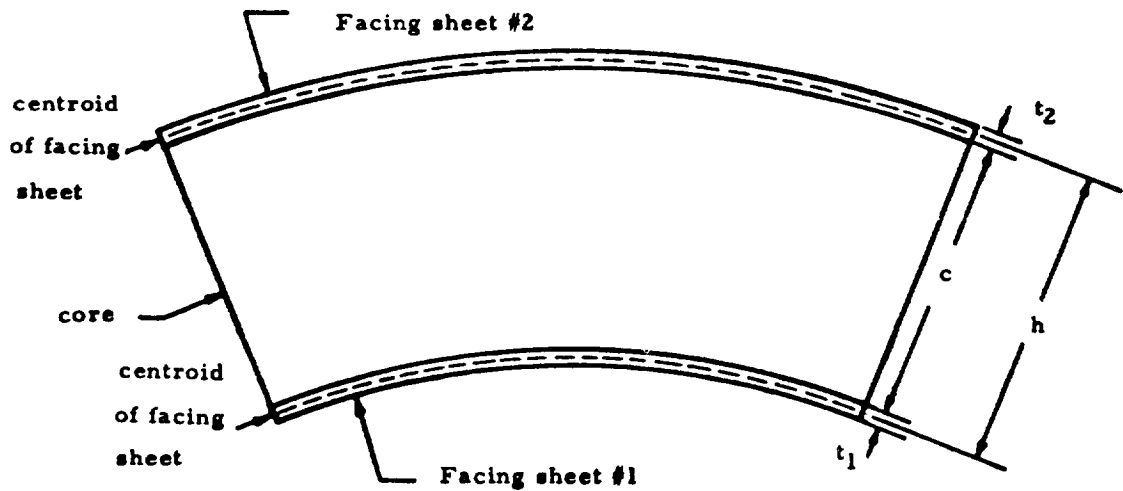


FIG. 3.32-2. Sandwich Construction

The material properties of a facing sheet are:

E_{x_i}, E_{θ_i} = Moduli of elasticity in the x and θ directions, respectively

$\mu_{x_i}, \mu_{\theta_i}$ = Poisson's ratios associated with stretching in the x and θ directions respectively

$G_{x\theta_i}$ = In-plane shear modulus

Sub-subscript i represents the facing sheet to which the material corresponds ($i = 1, 2$). Refer to Paragraph 3.32.1 for a definition of the x and θ directions.

The only property required for the type of core considered is G_{xz} and $G_{\theta z}$, which are the transverse shear moduli of the core in the x and θ directions, respectively. The formulas for the elastic constants are approximate but sufficiently accurate for engineering purposes.

A. Sandwich with Orthotropic Facings

$$C_{x_i} = \frac{E_{x_i}}{1 - \mu_{x_i} \mu_{\theta_i}}$$

$$C_{\theta_i} = \frac{E_{\theta_i}}{1 - \mu_{x_i} \mu_{\theta_i}}$$

$$C_{\mu_i} = \frac{\mu_{x_i} E_{\theta_i}}{1 - \mu_{x_i} \mu_{\theta_i}}$$

$$B_x = C_{x_1} t_1 + C_{x_2} t_2$$

$$B_{\theta} = C_{\theta_1} t_1 + C_{\theta_2} t_2$$

$$G_{x\theta} = G_{x\theta_1} t_1 + G_{x\theta_2} t_2$$

$$D_{x\theta} = \frac{G_{x\theta_1} G_{x\theta_2} t_1 t_2 h^2}{G_{x\theta_1} t_1 + G_{x\theta_2} t_2}$$

$$D_x = \frac{C_{x_1} C_{x_2} t_1 t_2 h^2}{C_{x_1} t_1 + C_{x_2} t_2}$$

$$D_\theta = \frac{C_{\theta_1} C_{\theta_2} t_1 t_2 h^2}{C_{\theta_1} t_1 + C_{\theta_2} t_2}$$

$$\mu'_x = \frac{1}{B_\theta} (C_{\mu_1} t_1 + C_{\mu_2} t_2)$$

$$\mu'_\theta = \frac{\mu'_x B_\theta}{B_x}$$

$$\mu_x = \frac{C_{\mu_1} C_{\mu_2} t_1 t_2 h^2}{C_{\mu_1} t_1 + C_{\mu_2} t_2}$$

$$\mu_\theta = \frac{\mu_x D_\theta}{D_x}$$

$$D_{Q_x} = \frac{G_{xz} h^2}{c}$$

$$D_{Q_\theta} = \frac{G_{\theta z} h^2}{c}$$

B. Sandwich with Isotropic Facings

$$B_x = B_\theta = \frac{E}{(1 - \mu^2)} (t_1 + t_2)$$

$$D_x = D_\theta = \frac{E t_1 t_2 h^2}{(1 - \mu^2) (t_1 + t_2)}$$

$$G_{x\theta} = G(t_1 + t_2)$$

$$D_{x\theta} = G \frac{t_1 t_2 h^2}{t_1 + t_2}$$

$$\mu_x = \mu_\theta = \mu'_x = \mu'_\theta = \mu$$

$$D_{Q_x} = \frac{G_{xz} h^2}{c}$$

$$D_{Q_\theta} = \frac{G_{\theta z} h^2}{c}$$

3.32.4 Integrally Stiffened Waffle Shells

The approximate elastic constants for shells with closely spaced integral ribs running in a waffle-like pattern were obtained from Ref. 3-26. Fig. 3.32-3 shows the type of construction being considered and also defines the geometrical parameters.

The definitions of the material properties are:

E = Young's modulus

G = Shear modulus

μ = Poisson's ratio

Refer to Section 3.32.1 for a definition of the x and θ directions.

The elastic constants for integrally stiffened waffle construction are

$$B_x = \frac{EH}{(1 - \mu'_x \mu'_y)} \left(\frac{\bar{A}_s^2}{A_y} \right)$$

$$B_y = \frac{EH}{(1 - \mu'_x \mu'_y)} \left(\frac{\bar{A}_s^2}{A_x} \right)$$

$$D_x = EH^3 \left[I_x - \frac{A_s^2 A_x}{\bar{A}_s^2} (\bar{k}_x - \bar{k}_s)^2 \right]$$

$$D_\theta = EH^3 \left[I_\theta - \frac{A_s^2 A_\theta}{\bar{A}_s^2} (\bar{k}_\theta - \bar{k}_s)^2 \right]$$

$$D_{x\theta} = EH^3 \left(\frac{I_{x\theta}}{2} \right)$$

$$D_{Q_x} = \infty$$

$$D_{Q_\theta} = \infty$$

$$G_{x\theta} = EH(A_{x\theta})$$

$$\mu_x = \frac{\bar{I}_s^{-2}}{I_\theta \bar{A}_s^{-2} - A_s^2 A_\theta (\bar{k}_\theta - \bar{k}_s)^2}$$

$$\mu_y = \frac{\bar{I}_s^{-2}}{I_x \bar{A}_s^{-2} - A_s^2 A_x (\bar{k}_x - \bar{k}_s)^2}$$

$$\mu_x' = \frac{A_s}{A_\theta}$$

$$\mu_y' = \frac{A_s}{A_x}$$

where

$$\bar{A}_s^{-2} = A_x A_\theta - A_s^2$$

$$\bar{I}_s^{-2} = I_s \bar{A}_s^{-2} + A_s A_x A_\theta (\bar{k}_x - \bar{k}_s)(\bar{k}_\theta - \bar{k}_s)$$

$$A_x = \frac{1}{1 - \mu} \frac{t_s}{H} + \frac{A_{ws}/b_s}{H} \cos^4 \Gamma$$

$$A_\theta = \frac{1}{1 - \mu} \frac{t_s}{H} + \frac{A_{ws}/b_s}{H} \sin^4 \Gamma$$

$$A_s = \frac{\mu}{1 - \mu} \frac{t_s}{H} + \frac{A_{ws}/b_s}{H} \sin^2 \Gamma \cos^2 \Gamma$$

$$A_{x\theta} = \frac{1}{2(1+\mu)} \frac{t_s}{H} + \frac{A_{w_s}/b_s}{H} \sin^2 \Gamma \cos^2 \Gamma$$

$$\bar{k}_x = \frac{1}{A_x} \frac{A_{w_s}/b_s}{H} \bar{k}_{w_s} \cos^4 \Gamma$$

$$\bar{k}_\theta = \frac{1}{A_\theta} \frac{A_{w_s}/b_s}{H} \bar{k}_{w_s} \sin^4 \Gamma$$

$$\bar{k}_s = \frac{1}{A_s} \frac{A_{w_s}/b_s}{H} \bar{k}_{w_s} \sin^2 \Gamma \cos^2 \Gamma$$

$$\bar{k}_{x\theta} = \frac{1}{A_{x\theta}} \frac{A_{w_s}/b_s}{H} \bar{k}_{w_s} \sin^2 \Gamma \cos^2 \Gamma$$

$$I_x = \frac{1}{12(1-\mu^2)} \left(\frac{t_s}{H}\right)^3 + \frac{I_{w_s}/b_s}{H^3} \cos^4 \Gamma + \frac{1}{1-\mu} \frac{t_s}{2H} (\bar{k}_x)^2$$

$$+ \frac{A_{w_s}/b_s}{H} \left[\left(\bar{k}_{w_s} - \bar{k}_x \right)^2 \cos^4 \Gamma \right]$$

$$I_\theta = \frac{1}{12(1-\mu^2)} \left(\frac{t_s}{H}\right)^3 + \frac{I_{w_s}/b_s}{H^3} \sin^4 \Gamma + \frac{1}{1-\mu} \frac{t_s}{2H} (\bar{k}_\theta)^2$$

$$+ \frac{A_{w_s}/b_s}{H} \left(\bar{k}_{w_s} - \bar{k}_y \right)^2 \sin^4 \Gamma$$

$$I_s = \frac{\mu}{12(1-\mu)^2} \left(\frac{t_s}{H}\right)^3 + \frac{I_{w_s}/b_s}{H^3} \sin^2 \tau \cos^2 \tau + \frac{\mu}{1-\mu} \frac{t_s}{2H} (\bar{k}_s)^2$$

$$+ \frac{A_{w_s}/b_s}{H} \left(\bar{k}_{w_s} - \bar{k}_s\right)^2 \sin^2 \tau \cos^2 \tau$$

$$I_{x\theta} = \frac{1}{6(1+\mu)} \left(\frac{t_s}{H}\right)^3 + 4 \frac{I_{w_s}/b_s}{H^3} \sin^2 \tau \cos^2 \tau + \frac{2}{1+\mu} \frac{t_s}{H} (\bar{k}_{x\theta})^2$$

$$+ 4 \frac{A_{w_s}/b_s}{H} \left(\bar{k}_{w_s} - \bar{k}_{x\theta}\right)^2 \sin^2 \tau \cos^2 \tau$$

$$\frac{A_{w_s}/b_s}{H} = 2 \left\{ 1 - \left[1 - 0.43 \left(\frac{r_{w_s}}{t_s}\right)^2 \left(\frac{t_s}{t_{w_s}}\right) \right] \frac{t_s}{H} \right\} \frac{t_{w_s}}{t_s} \frac{t_s}{b_s}$$

$$\bar{k}_{w_s} = \frac{2}{\frac{A_{w_s}/b_s}{H}} \left[\frac{1}{2} \left(1 - \frac{t_s}{H}\right)^2 + 0.14 \left(\frac{r_{w_s}}{t_s}\right)^3 \left(\frac{t_s}{t_{w_s}}\right) \left(\frac{t_s}{H}\right)^2 \right] \frac{t_{w_s}}{t_s} \frac{t_s}{b_s} + \frac{1}{2} \frac{t_s}{H}$$

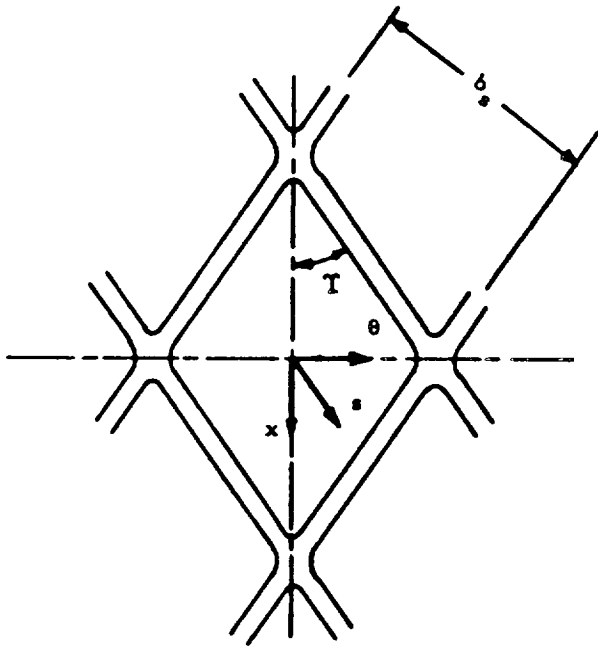
$$\frac{I_{w_s}/b_s}{H^3} = 2 \left\{ \frac{1}{12} \left(1 - \frac{t_s}{H}\right)^3 + \left(1 - \frac{t_s}{H}\right) \left(\frac{1}{2} - \bar{k}_{w_s}\right)^2 + 0.01 \left(\frac{r_{w_s}}{t_s}\right)^4 \left(\frac{t_s}{t_{w_s}}\right) \left(\frac{t_s}{H}\right)^3 \right.$$

$$\left. + 0.43 \left(\frac{r_{w_s}}{t_s}\right)^2 \left(\frac{t_s}{t_{w_s}}\right) \left(\frac{t_s}{H}\right) \left[\bar{k}_{w_s} - \frac{1}{2} \frac{t_s}{H} - 0.218 \left(\frac{r_{w_s}}{t_s}\right) \left(\frac{t_s}{H}\right) \right]^2 \right\} \frac{t_{w_s}}{t_s} \frac{t_s}{b_s}$$

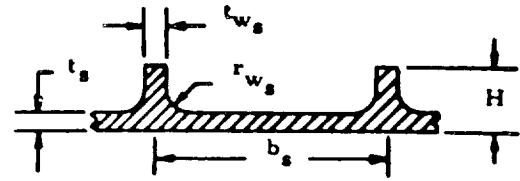
The special case of $T = 90$ degrees corresponds to a shell with circumferential stiffeners $2t_{w_s}$ wide and b_s apart. The case of $T = 0$ corresponds to a shell with longitudinal or meridional stiffeners only, depending on the type of shells considered, $2t_{w_s}$ wide and b_s apart.

For more exact formulas of the elastic constants for this type of construction, or if a more complex type of construction is used which contains stiffeners in the x and θ directions as well as skewed stiffeners, Ref. 3-26 may be used.

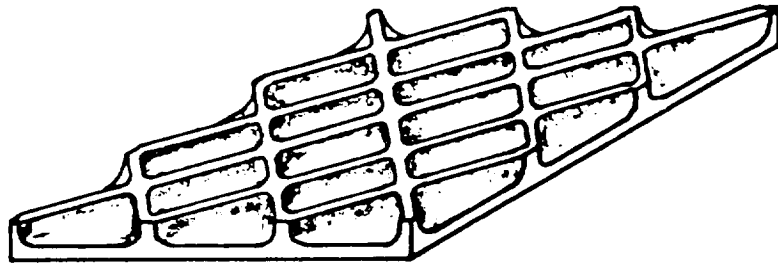
FIG. 3.32-3. WAFFLE CONSTRUCTION



(a) Coordinate System



(b) Waffle Section



(c) Typical Pattern

3.33 CYLINDERS

3.33.1 Axial Compression, Orthotropic Cylinders

The following stability analysis for orthotropic cylinders subjected to axial compression is based primarily on the theory from Refs. 3-27 and 3-28. This analysis may be used for layered construction (such as filament wound) and for stiffened construction (such as integrally stiffened waffle construction) if the stiffeners are very close together. The definition of the elastic constants used in this section and the formulas for computing the elastic constants for typical types of construction are given in Section 3.32. The design allowable buckling load per unit width, N_x , for moderate length orthotropic cylinders is

$$N_x = \gamma \frac{2}{R} \left[B_\theta D_x (1 - \mu'_x \mu'_\theta) \right]^{1/2} U$$

and the allowable compressive load for the cylinder is

$$P_{cr} = N_x 2\pi R$$

R and L are the cylinder radius and length, respectively.

The following parameters are defined in terms of the elastic constants

$$\bar{G} = \frac{B_\theta (1 - \mu'_x \mu'_\theta)}{2 G_{x\theta}} - \mu'_\theta$$

$$\bar{D} = \frac{D_{x\theta}}{D_x} + \mu'_\theta$$

$$\omega_1 = \frac{B_\theta}{B_x \bar{G}^2}$$

$$\omega_2 = \frac{B_x D_\theta}{B_\theta D_x}$$

$$\omega_3 = \frac{\bar{D}}{\bar{G}}$$

For $\omega_2 \geq 1$, $\omega_3 \geq 1$, $U = 1$.

For $\omega_2 \geq \omega_3$, $\omega_3 < 1$, $U = U_1$.

For $\omega_2 < \omega_3$, $\omega_2 < 1$, $U = 1$ if $U_2 \geq 1$; $U = U_2$ if $U_2 < 1$.

The parameter U_1 can be obtained from the formula

$$U_1 = \left[\frac{1 + 2 \bar{D} \psi^2 + (D_\theta / D_x) \psi^4}{1 + 2 \bar{G} \psi^2 + (B_\theta / B_x) \psi^4} \right]^{1/2}$$

for

$$\psi^2 = S_1 \pm \sqrt{S_1^2 + S_2}$$

$$S_1 = \frac{1}{2\bar{G}} \left[\frac{(1 - \omega_2)}{(\omega_2 - \omega_3)} \right]$$

$$S_2 = \frac{B_x}{B_\theta} \left[\frac{(1 - \omega_3)}{(\omega_2 - \omega_3)} \right]$$

Only values of $\psi^2 > 0$ may be used to compute U_1 . If both values of ψ^2 are greater than zero, then U_1 must be computed for each ψ^2 and the smallest U_1 must be used to compute N_x .

The parameter U_2 can be obtained from the formula

$$U_2 = \frac{\pi^2}{4 \sqrt{3} Z} \left[1 + 2 \bar{D} \psi^2 + \frac{D_\theta}{D_x} \psi^4 + \frac{12 Z^2 / \pi^4}{(1 + 2 \bar{G} \psi^2 + (B_\theta / B_x) \psi^4)} \right]$$

where

$$\psi = \frac{L}{2\pi R} n, \quad Z^2 = \frac{B_\theta (1 - \mu'_x \mu'_\theta)}{12 D_x R^2} L^4$$

The value of n must be varied until the minimum value of U_2 is found. The quantity n is the number of half waves of the buckles in the circumferential direction. Therefore, n is restricted to even positive integers greater than 4.

The quantity γ can be computed from the formula

$$\gamma = (\gamma_2 + 0.044/\gamma_2) \gamma_1 / 0.49$$

where γ_2 is obtained from Fig. 3.33-1 through 3.33-5; γ_1 is obtained from Fig. 3.33-6, where ρ is the radius of gyration of the cylinder wall. For radii of gyration which differ in the axial and circumferential direction, Ref. 3-29 recommends using the geometric mean of the two radii of gyrations; therefore,

$$\rho = \sqrt[4]{\frac{D_x D_\theta}{B_x B_\theta}}$$

The parameter γ was introduced to allow for the discrepancy between test data and the buckling theory.

The term $\gamma_1/0.49$ was introduced to make γ a function of ratio R/ρ as suggested in Ref. 3-29. The curve given in Fig. 3.33-6 for γ_1 was obtained by replotting the curve given in Fig. 3.23-1 as a function of R/ρ and normalizing C_c with respect to the theoretical small deflection theory coefficient, $C_c \approx 0.606$. Therefore, Fig. 3.33-6 is consistent with this chapter and is not the same as in Ref. 3-29. The term $(\gamma_2 + 0.044/\gamma_2)$ was introduced as an attempt to account for the fact that the ratio of the postbuckling load to the classical buckling load for orthotropic cylinders is different than for isotropic cylinders (Ref. 3-30). If the results of this section are reduced to the special case of a homogeneous isotropic cylinder, $\gamma = \gamma_1$ and the design buckling load would be the same as obtained from Paragraph 3.23.1.

The method of obtaining γ for orthotropic cylinders has been verified by only a limited amount of test data and caution should be used in applying it to a design. Some test results, such as the tests described in Ref. 3-28 and 3-31, indicate that this method may be conservative but the specimens tested were not typical of large production parts.

The preceding analysis is good only for moderate length cylinders; therefore, for simply supported edges, $Z > 25U_3$; for clamped edges, $Z > 80U_3$. Where, if $U = 1$ or $U = U_2$, then $U_3 = 1$, and, if $U < 1$, then

$$U_3 = \left[1 + 2\bar{D}\psi^2 + \frac{D_\theta}{D_x} \psi^4 \right]^{1/2} \left[1 + 2\bar{G}\psi^2 + \frac{B_\theta}{B_x} \psi^4 \right]^{1/2}$$

The parameter Z is as previously defined

$$Z^2 = \frac{B_\theta}{12D_x} \frac{(1 - \mu'_x \mu'_\theta)}{R^2} L^4$$

For axial-stiffened cylinders ($D_x > 300 D_\theta$) in the short cylinder range, the following formula is recommended in Ref. 3-32:

$$N_x = \frac{c\pi^2 D_x}{L^2} + \frac{2\gamma_1}{R} \sqrt{B_x D_\theta}$$

Coefficient c is equivalent to the column fixity coefficient in Euler's column formula. It is recommended that this formula be restricted to geometry where $\gamma_1 \sqrt{B_x D_\theta}/R < c\pi^2 D_x/L^2$. Verification of this formula has been limited and the range of validity is not well defined; therefore, it should be used with caution. The factor γ_1 is consistent with this section and is not the same as in Ref. 3-32.

If a cylinder is stiffened with stringers and frames, it is recommended that Section 3.42 be used unless the stringers and frames are very close together. The test results of Ref. 3-33 for cylinders with light frames and heavy stringers indicate that the analysis presented in this section may be unconservative for cylinders with large frame spacing.

Plasticity may be considered by modifying Young's modulus in the stiffness constants (Ref. 3-27) or may be accounted for with a plasticity factor as in Paragraph 3.23.1.

FIG. 3.33-1. CORRECTION COEFFICIENTS FOR ORTHOTROPIC CYLINDERS SUBJECTED TO COMPRESSION

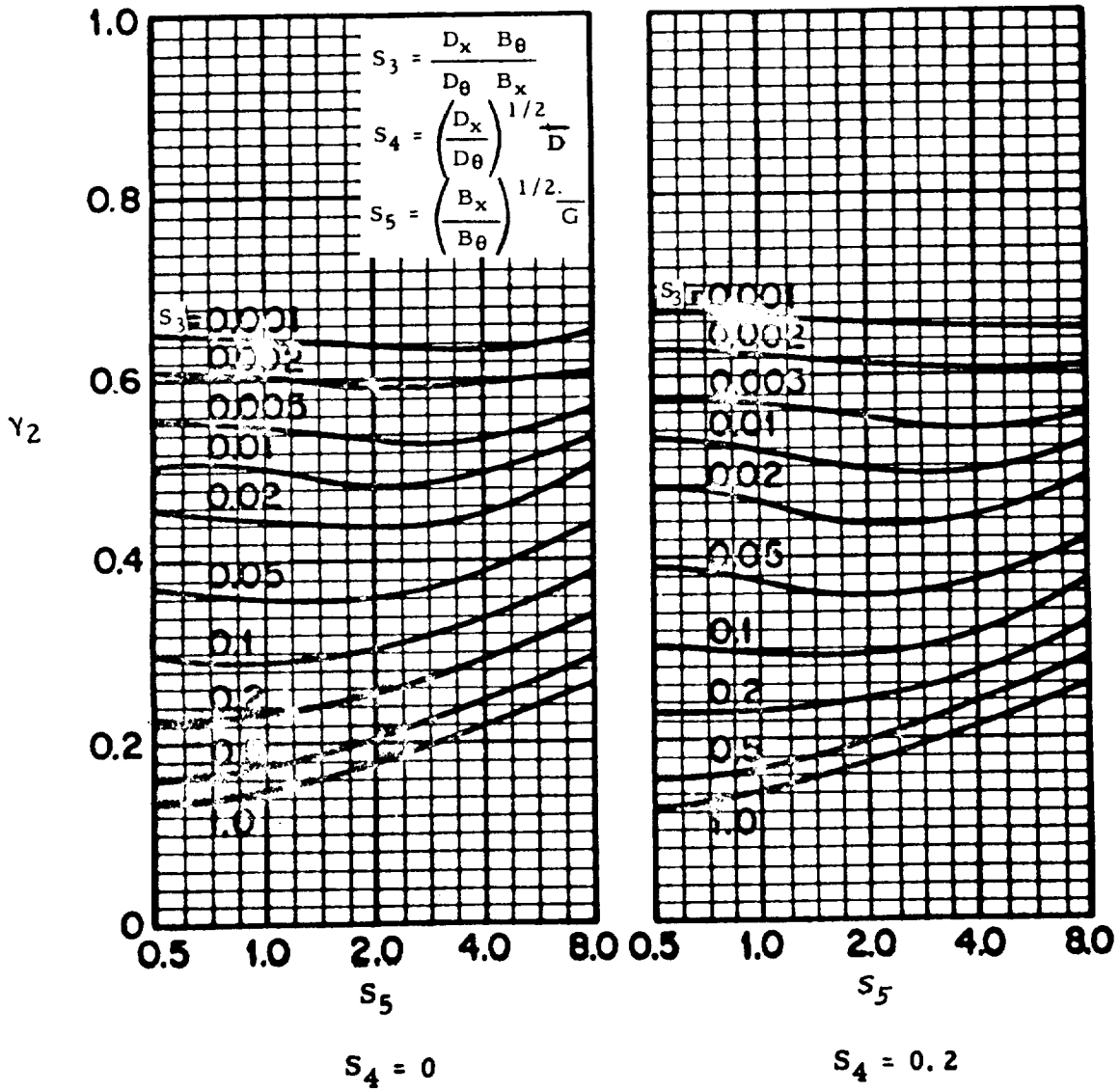


FIG. 3.33-2. CORRECTION COEFFICIENTS FOR ORTHOTROPIC CYLINDERS SUBJECTED TO COMPRESSION

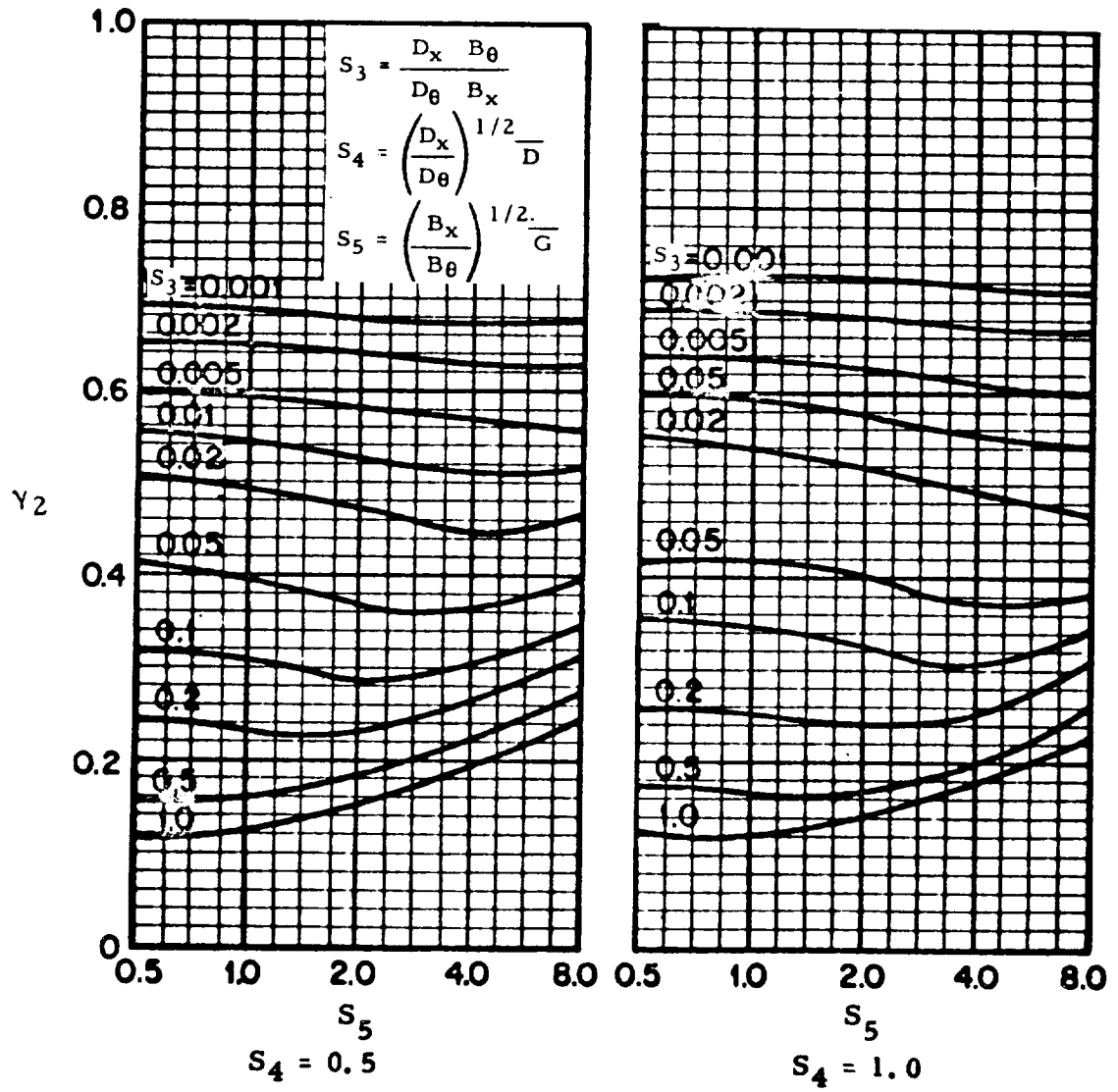


FIG. 3.33-3. CORRECTION COEFFICIENTS FOR ORTHOTROPIC CYLINDERS SUBJECTED TO COMPRESSION

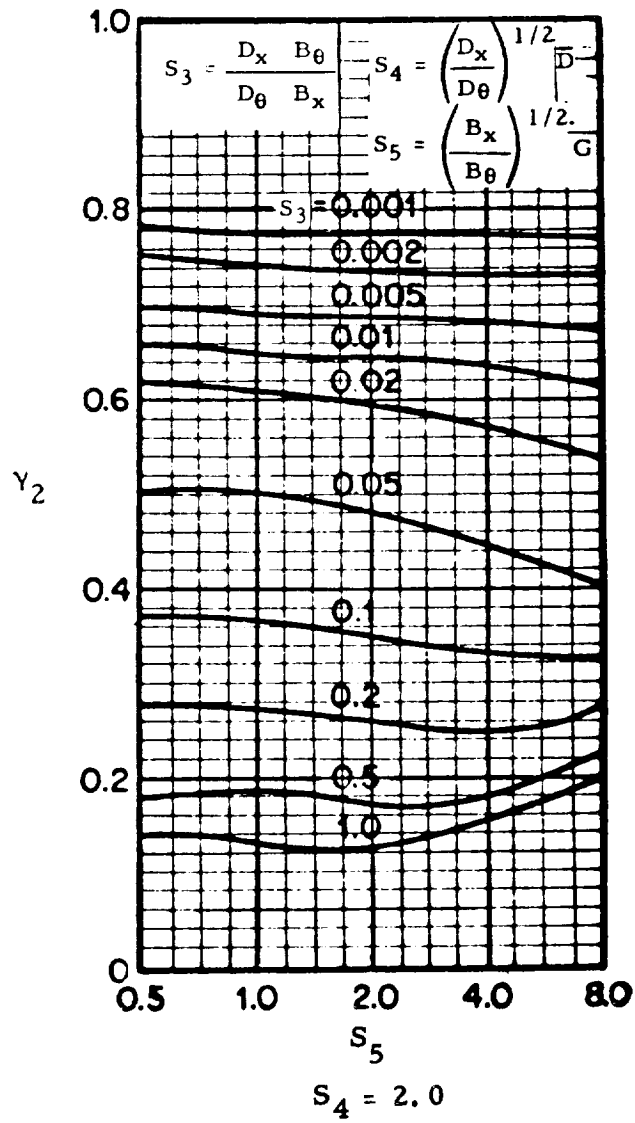
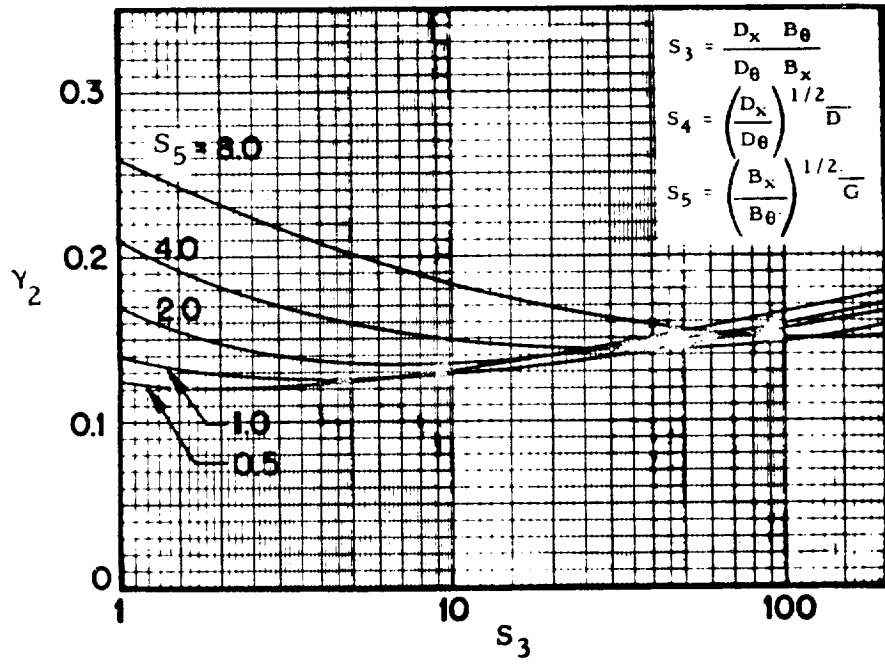
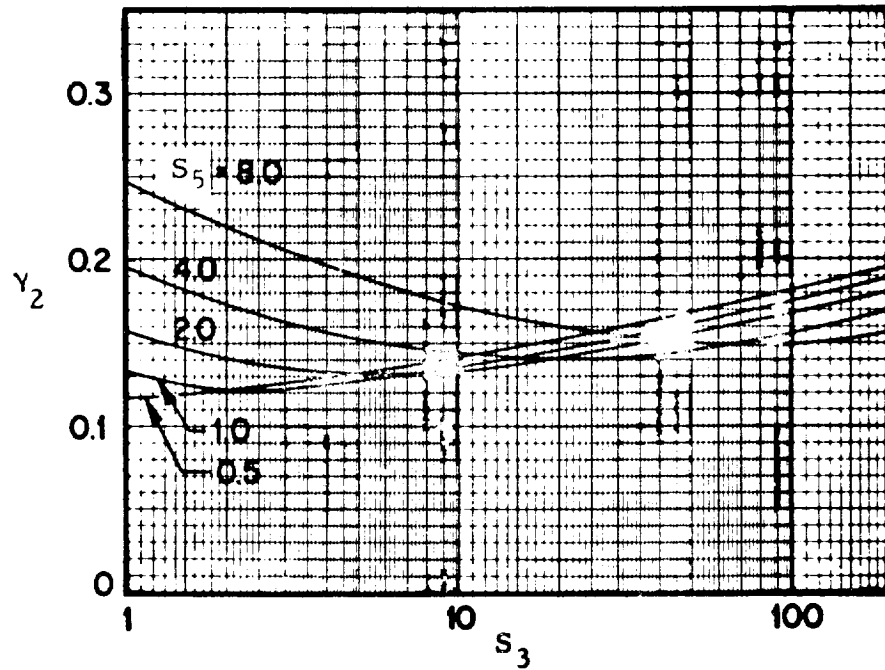


FIG. 3.33-4. CORRECTION COEFFICIENTS FOR ORTHOTROPIC CYLINDERS SUBJECTED TO COMPRESSION

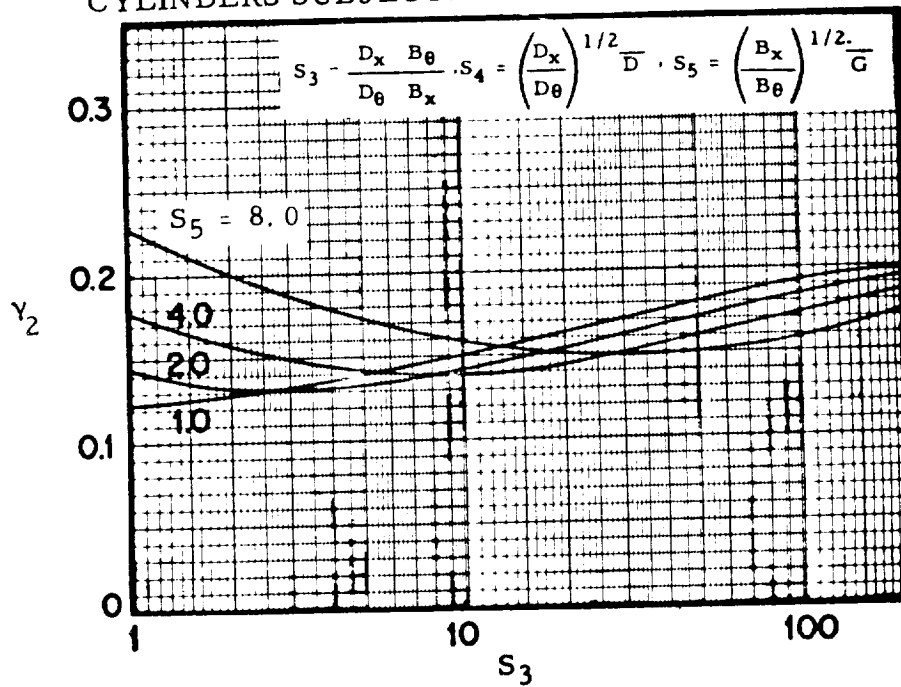


$S_4 = 0.2$

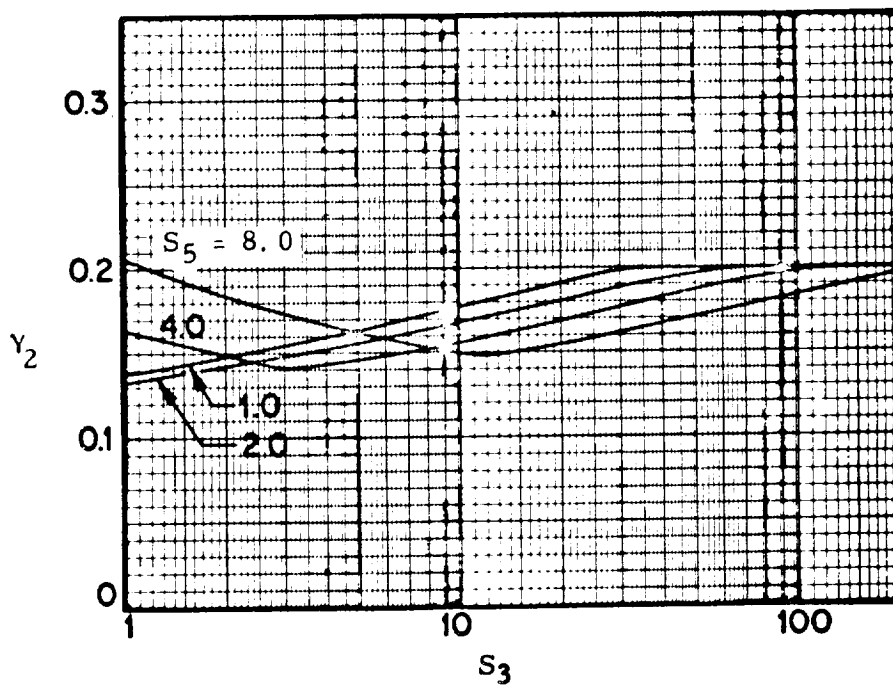


$S_4 = 0.5$

FIG. 3.33-5. CORRECTION COEFFICIENTS FOR ORTHOTROPIC CYLINDERS SUBJECTED TO COMPRESSION

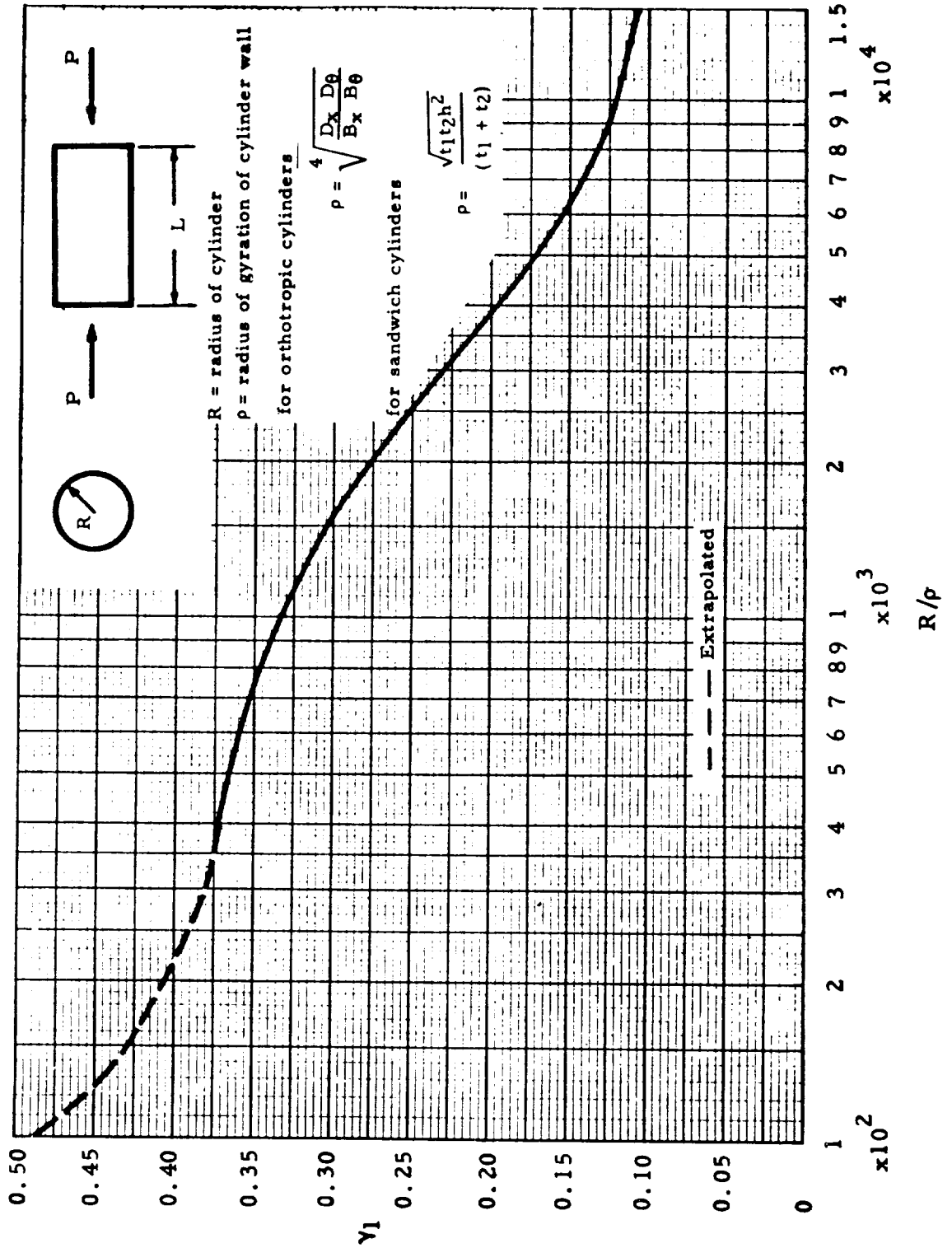


$S_4 = 1.0$



$S_4 = 2.0$

FIG. 3.33-6. DESIGN CORRECTION COEFFICIENT FOR CYLINDERS
SUBJECTED TO AXIAL COMPRESSION



3.33.2 Torsion, Orthotropic Cylinders

The curves in Ref. 3-34 will be used to determine the buckling load for orthotropic cylinders subjected to torsion. The design allowable shear load per unit length of circumference is

$$N_{x\theta} = \frac{\gamma K_s \pi^2 D_x}{L^2}$$

and the design allowable torque for the cylinder is

$$T_{cr} = N_{x\theta} 2 \pi R^2$$

The buckling coefficient, K_s , may be obtained from Fig. 3.33-7 for the elastic constants as given in Table 3.33-1, and γ may be obtained from Fig. 3.33-8. The definition of the elastic constants used in this section and formulas for computing the elastic constants for typical types of construction are given in Section 3.32.

The coefficient γ reduces the theory presented in Ref. 3-34 by the same percentage as the theory for homogeneous isotropic cylinders was reduced to obtain the curve presented in Fig. 3.23-3.

The method of analysis presented may be used for cylinders with simply supported edges, although a small rotational restraint at the edge of the shell is included in the results presented in Fig. 3.33-7. It can be seen from Fig. 3.33-7 that for large values of Z_s , all curves merge into one line. The equation of this line as given in Ref. 3-34, is

$$K_s = 0.89 Z_s^{3/4}$$

where

$$Z_s = (D_\theta / D_x)^{5/6} (B_x / B_\theta)^{1/2} Z$$

$$Z^2 = \frac{B_\theta (1 - \mu'_x \mu'_y) L^4}{12 D_x R^2}$$

If the value of Z_s is large enough, this formula can be used to estimate the critical torque for geometries other than the ones given in Table 3.33-1.

This section should not be used for any type of cylinder with skin that buckles between stiffeners prior to general instability failure. The test data presented in Ref. 3-33 indicate that the results may be unconservative for this case.

TABLE 3.33-1 CYLINDER PARAMETERS USED FOR K-Z PLOTS

| Curve Number | $\frac{D_{xy}}{D_x} + \mu_\theta$ | $\frac{D_\theta}{D_x}$ | $\frac{B_x}{B_\theta}$ | $\frac{B_\theta (1 - \mu'_x \mu'_\theta)}{2G_{xy}} - \mu'_\theta$ |
|--------------|-----------------------------------|------------------------|------------------------|---|
| 1 | 0 | 1/8 | 4 | 1 |
| 2 | 0 | 1/2 | 1 | 1 |
| 3 | 0 | 2 | 1/4 | 1 |
| 4 | 1 | 1/8 | 4 | 4 |
| 5 | 1 | 1/2 | 1 | 4 |
| 6 | 1 | 2 | 1/4 | 4 |
| 7 | 1 | 4 | 1/8 | 4 |
| 8 | 1 | 8 | 1/16 | 4 |

FIG. 3.33-7. BUCKLING COEFFICIENT FOR ORTHOTROPIC CYLINDERS
SUBJECTED TO TORSION

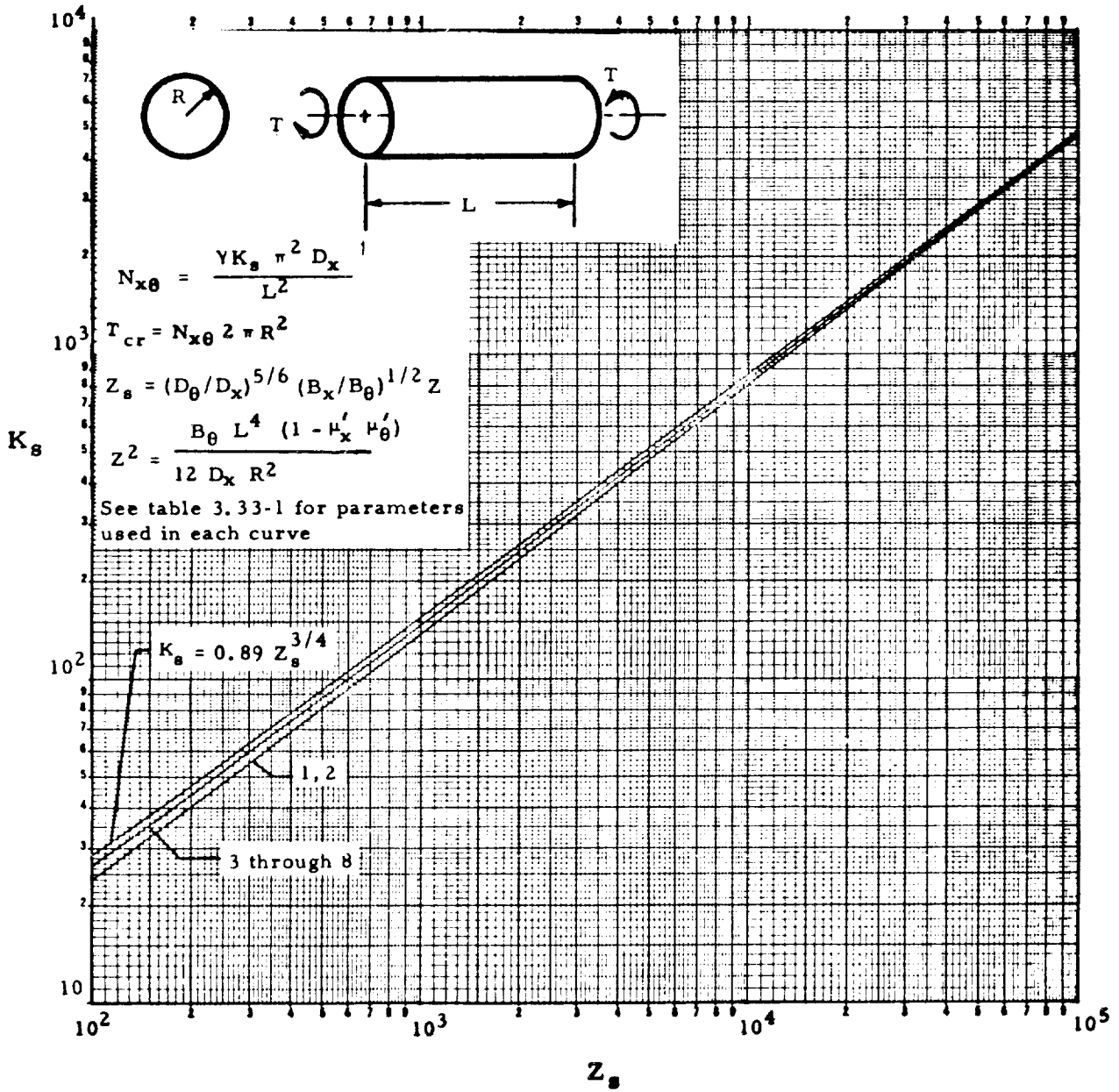
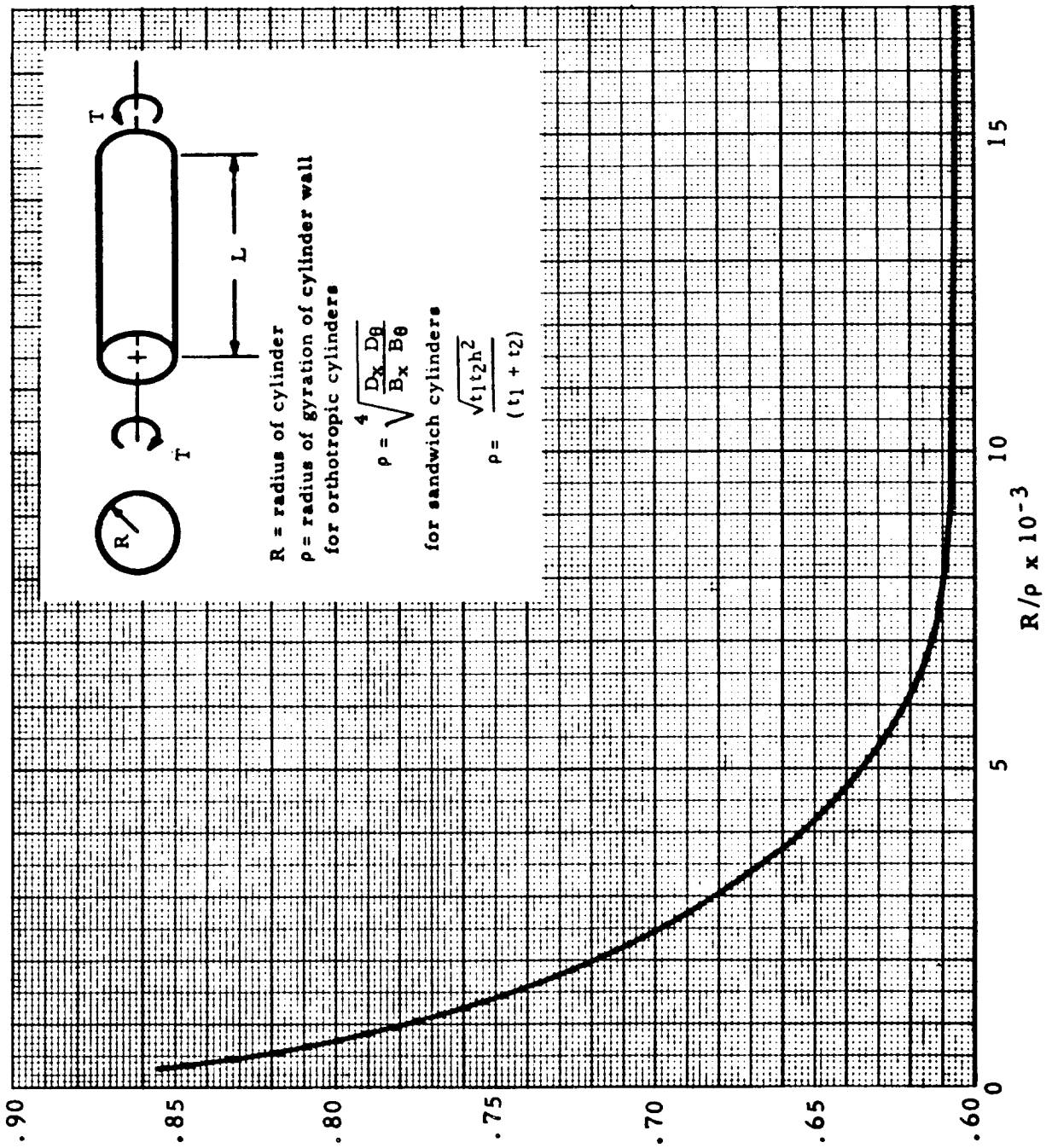


FIG. 3.33-8. DESIGN CORRECTION COEFFICIENT FOR CYLINDERS
SUBJECTED TO TORSION



3.33.3 Bending, Orthotropic Cylinders

The formulas presented in Paragraph 3.33.1 may be used to determine the design allowable buckling stress for orthotropic cylinders subjected to bending if the following formula is used to compute γ :

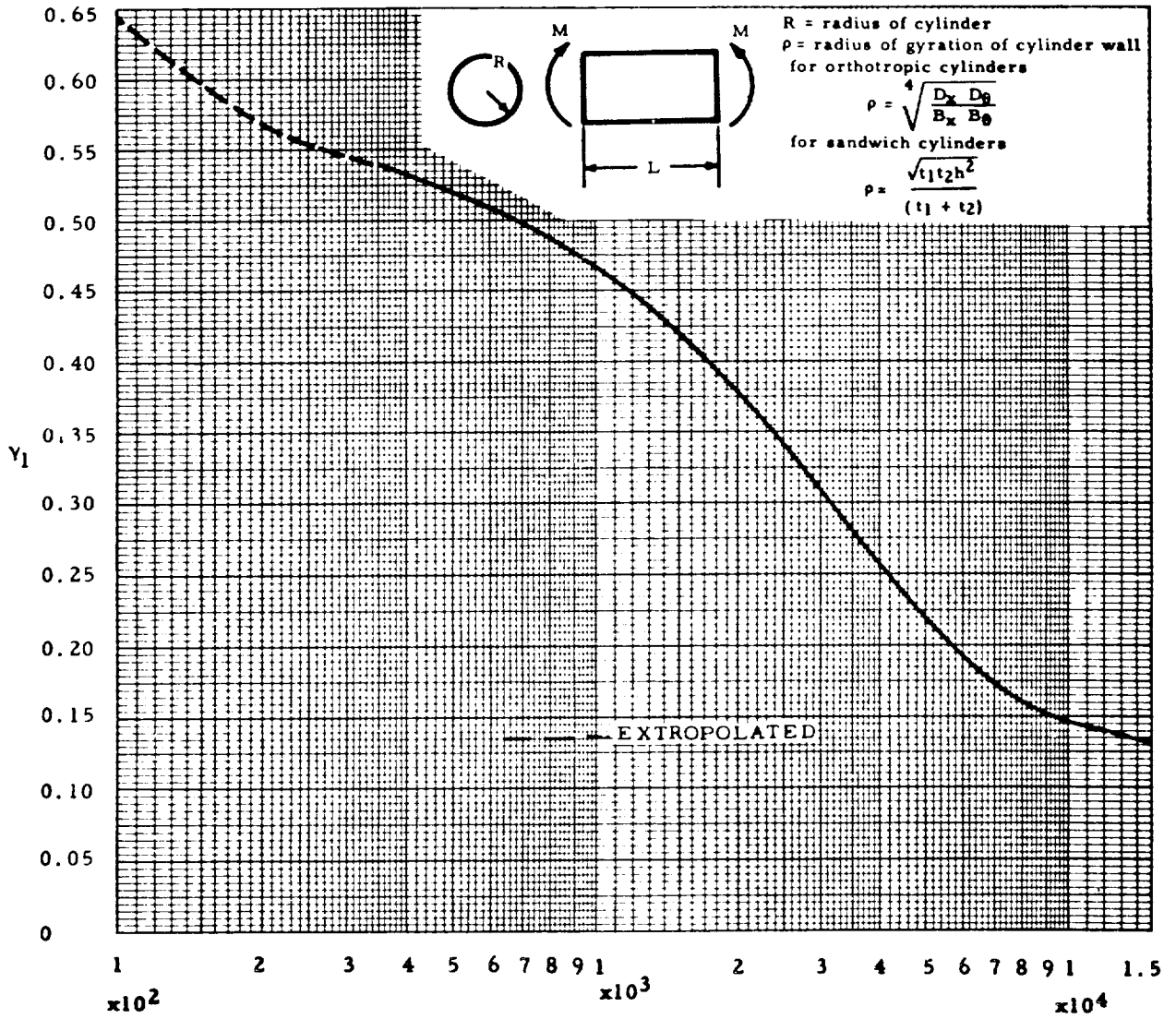
$$\gamma = \left(\gamma_2 + \frac{0.062}{\gamma_2} \right) \frac{\gamma_1}{0.64}$$

where γ_2 is obtained from Figs. 3.33-1 through 3.33-5 and γ_1 is obtained from Fig. 3.33-9. Fig. 3.33-9 was obtained from Fig. 3.22-5 as described in Paragraph 3.33.1.

For bending, N_x is the maximum compressive load per unit length due to the bending moment (e.g., outer fiber load). If the stresses are elastic, the design allowable bending moment may be obtained from

$$M_{cr} = N_x \pi R^2$$

FIG. 3.33-9. DESIGN CORRECTION COEFFICIENT FOR CYLINDERS
SUBJECT TO BENDING



3.33.4 Lateral External Pressure, Orthotropic Cylinders

The curves presented in Ref. 3-34 will be used to determine the buckling pressure of orthotropic cylinders with simply supported edges subjected to lateral external pressure. The design allowable pressure is

$$p_{cr} = \frac{\gamma K_p \pi^2 D_x}{RL^2}$$

The buckling coefficient, K_p , may be obtained from Fig. 3.33-10 or 3.33-11 for several ratios of the elastic constants. The definition of the elastic constants and formulas for computing the elastic constants for typical types of construction are given in Section 3.32.

The coefficient γ was introduced to reduce the theory presented in Ref. 3-34 by the same percentage as the theory for homogeneous isotropic cylinders was reduced to obtain the curve presented in Fig. 3.23-7.

Therefore,

$$Z_p > 10^2, \gamma = 0.9;$$

$$Z_p < 10^2, \gamma = 1.0 - Z_p \times 10^{-3}$$

It can be seen from Fig. 3.33-11 that for large values of Z_p all curves merge into one line. The equation of this line is $K_p = 1.039Z_p^{1/2}$

and the design allowable pressure is

$$P_{cr} = \frac{5.5 D_{\theta}^{3/4} \gamma \left[B_x (1 - \mu'_x \mu'_{\theta}) \right]^{1/4}}{LR^{3/2}}$$

If the value of Z_p is large enough, this formula can be used to estimate the critical pressure of geometries other than the ones given in Table 3.33-1.

If the stiffness parameters are not in the range given in Table 3.33-1 and Z_p is not large, K_p may be determined from

$$K_p = \frac{1}{\psi^2} \left[1 + 2 \bar{D} \psi^2 + \frac{D_{\theta}}{D_x} \psi^4 \right] + \frac{12Z^2}{\pi^4} \left[\frac{1}{1 + 2 \bar{G} \psi^2 + (B_{\theta}/B_x) \psi^4} \right]$$

where \bar{G} and \bar{D} are defined in Paragraph 3.33.1.

$$\psi = \frac{nL}{2 \pi R}$$

$$Z^2 = \frac{B_{\theta} (1 - \mu'_x \mu'_y) L^4}{12 D_x R^2}$$

The value of n must be varied until the minimum value of K_p is found. The quantity n is restricted to even positive integers greater than or equal to 4.

For very long cylinders, the buckling pressure becomes independent of length and may be computed from

$$P_{cr} = \frac{3\gamma D_{\theta}}{R^3}$$

The point at which the buckling pressure becomes independent of length is difficult to determine. One indication is the point at which the minimum value of K_p is found for $n = 4$.

The design allowable pressure is for complete buckling of the shell (e. g., when buckles have formed all the way around the cylinder). If single buckles are not allowable for a particular design, the pressure computed by the preceding formulas may be unconservative.

Shells that are relatively stiff in the circumferential direction and relatively free of initial imperfection will be less likely to have single isolated buckles at pressures less than the design allowable pressures which have been given.

If the stresses are in the plastic range, a reduced modulus must be included in the stiffness constants (Ref. 3-32) or a plasticity correction factor such as that given in Paragraph 3.23.4 should be used.

FIG. 3.33-10. BUCKLING COEFFICIENT FOR SHORT ORTHOTROPIC CYLINDERS SUBJECTED TO LATERAL EXTERNAL PRESSURE

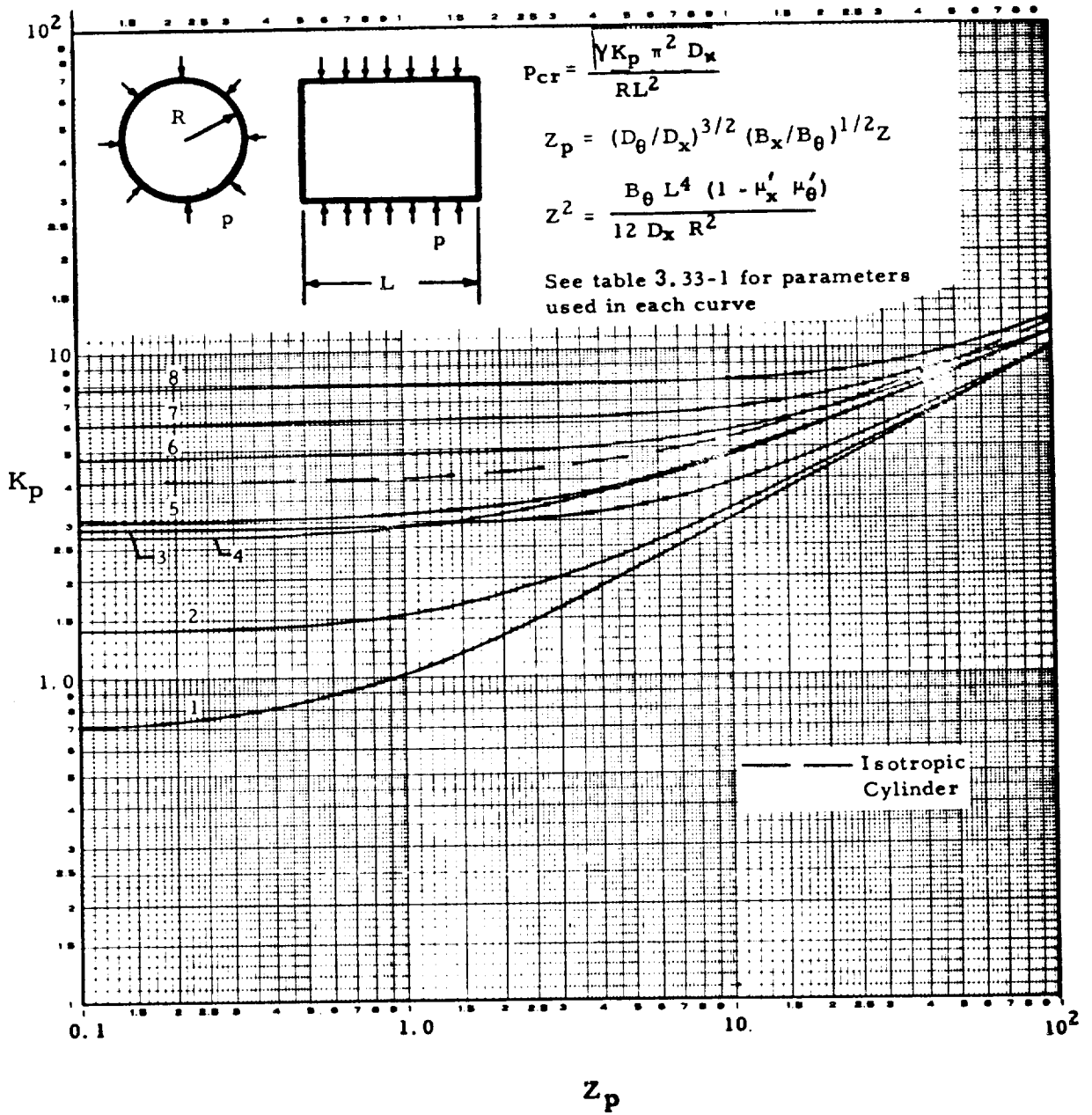
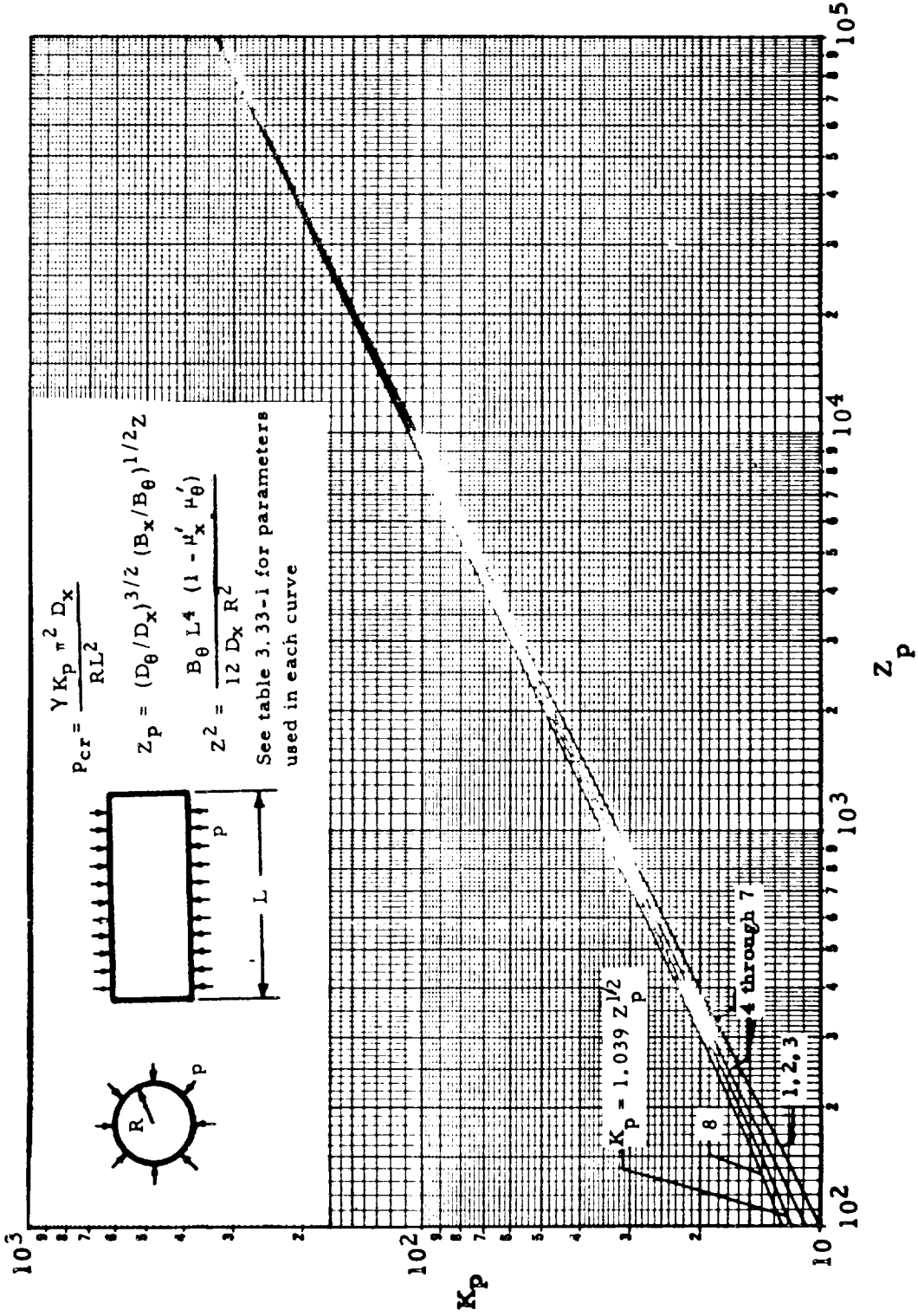


FIG. 3.33-11. BUCKLING COEFFICIENT FOR LONG ORTHOTROPIC CYLINDERS SUBJECTED TO LATERAL EXTERNAL PRESSURE



3.34 CONES

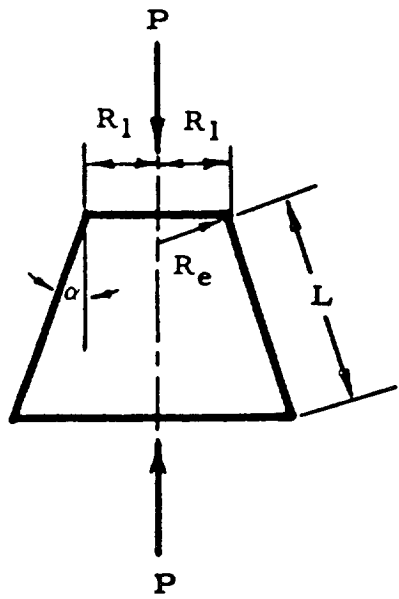
3.34.1 Axial Compression, Orthotropic Cones

The limited amount of information available on orthotropic cones is not in a form suitable for design analysis until additional information is available. The equivalent cylinder approach recommended in Paragraph 3.24.1 should be used. The cone shown in Fig. 3.34-1a can be analyzed as a cylinder with a radius $R_e = R_1 / \cos \alpha$ and length L . The design allowable load per inch, N_x , for the equivalent cylinder can be obtained from Paragraph 3.33.1. The design allowable total compressive load for the cone can be obtained from

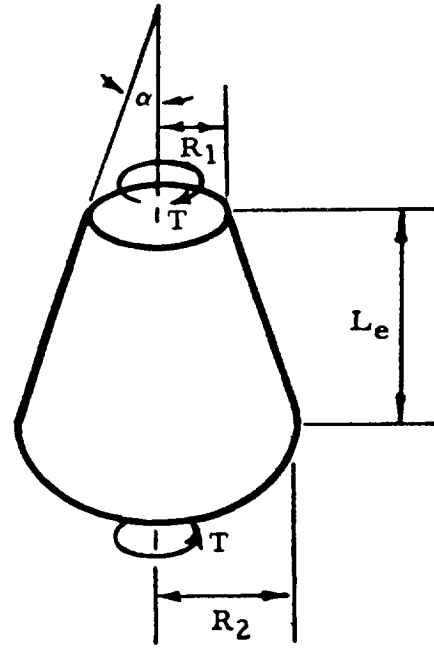
$$P_{cr} = 2 \pi R_e N_x \cos^2 \alpha$$

This method of analysis should be used with caution and should be limited to cones with $\alpha < 30$ degrees.

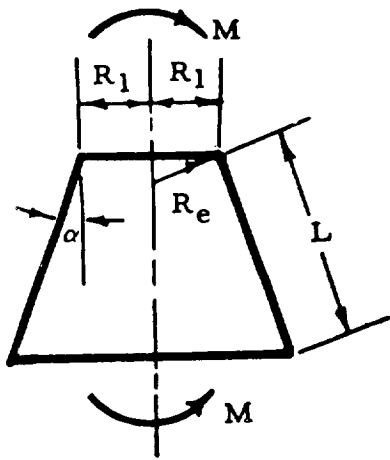
FIG. 3.34-1. CONES SUBJECTED TO VARIOUS LOADINGS



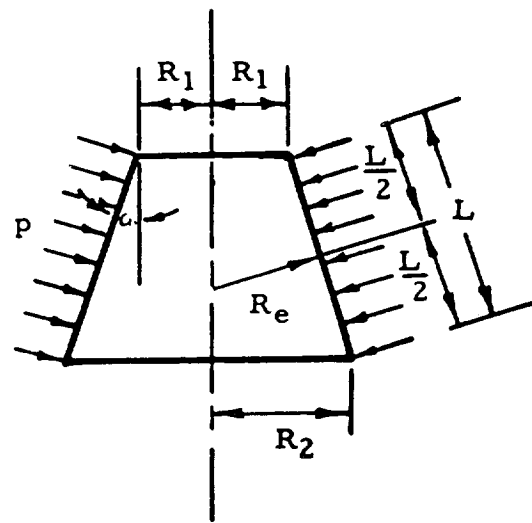
(a)



(b)



(c)



(d)

3.34.2 Torsion, Orthotropic Cones

Until additional information is available, the equivalent cylinder approach recommended in Paragraph 3.24.2 should be used for orthotropic cones subjected to torsion. The cone shown in Fig. 3.34-1b can be analyzed as a cylinder with a radius

$$R_e = \left\{ 1 + \left[\frac{1 + R_2/R_1}{2} \right]^{1/2} - \left[\frac{1 + R_2/R_1}{2} \right]^{-1/2} \right\} R_1 \cos \alpha$$

and length $L_e = L/\cos \alpha$.

The design allowable shear per unit length, $N_{x\theta}$, for the equivalent cylinder can be obtained from Paragraph 3.33.2. The design allowable torque for the cone can be obtained from

$$T_{cr} = 2 \pi R_e^2 N_{x\theta}$$

The design allowable shear stress for the cone should be based on T_{cr} .

This method should be used with caution and should be limited to cones with $\alpha < 30$ degrees.

3.34.3 Bending, Orthotropic Cones

Until additional information is available, the equivalent cylinder approach recommended in Paragraph 3.24.3 should be used for orthotropic cones subjected to bending. The cone shown in Fig. 3.34-1c can be analyzed as a cylinder with a radius $R_e = R_1/\cos \alpha$ and length L .

The design allowable load per inch, N_x , for the equivalent cylinder can

be obtained from Paragraph 3.33.3. If the stresses are elastic, the design allowable moment for the cone can be obtained from

$$M_{cr} = \pi R_1^2 N_x \cos \alpha$$

This method of analysis should be used with caution and should be limited to cones with $\alpha < 30$ degrees.

3.34.4 Lateral External Pressure, Orthotropic Cones

Until additional information is available, the equivalent cylinder approach recommended in Paragraph 3.24.4 should be used for an orthotropic cone subjected to lateral pressure as shown in Fig. 3.34-1d. The cone can be analyzed as a cylinder with a radius

$$R_e = \frac{R_1 + R_2}{2 \cos \alpha}$$

and length L. The design allowable pressure can be obtained from Paragraph 3.33.4. This method of analysis should be used with caution and should be limited to cones with $\alpha < 30$ degrees.

3.40 STIFFENED SHELLS

3.41 GENERAL

The stiffened shells which are discussed in the following sections are cylinders which consist of a thin metal sheet stiffened by frames (circumferential stiffening elements) and stringers (longitudinal stiffening elements). In general, this type of shell should be analyzed for three modes of failure: (1) material failure, (2) buckling between frames, and (3) general instability failure.

If the frames and stiffeners are close together, the procedures presented in Section 3.30 may be useful for the general instability analysis, but the range of applicability of the method is not well defined. In this section, a different method of analysis is presented for frame and stringer stiffened cylinders subjected to compressive loads in the axial direction as well as for frame stiffened cylinders subjected to lateral and axial external pressure. In general, it is easier to obtain the buckling loads using the methods presented in this section.

3. 42 FRAME AND STRINGER STIFFENED CYLINDERS

3. 42. 1 Axial Compression, Frame and Stringer Stiffened Cylinders

Very little test data are available on the general instability of cylindrical shells that have both frames (circumferential stiffeners) and stringers (longitudinal stiffeners) subjected to axial compression. Until additional data are available, Paragraph 3. 42. 2 may be utilized for stiffened cylinders subjected to axial compression if $C = 3. 2$ is used for computing the general instability stress. The reduction in C for axial compression was introduced because of the lower buckling strength of other types of cylinders subjected to axial compression.

3. 42. 2 Bending, Frame and Stringer Stiffened Cylinders

If a cylindrical shell having both frames (circumferential stiffeners) and stringers (longitudinal stiffeners) is subjected to bending, it may fail in one of three distinct ways. The types of failure are classified as (1) material failure, (2) buckling between frames, and (3) general instability.

A. Material Failure

For purposes of analysis, the bending-stress distribution is assumed to be in accord with the elementary beam theory. When buckling of the sheet occurs or the stresses exceed the proportional limit, appropriate modifications must be made in calculating section

properties. The stress caused by the applied moment should be compared against the materials allowable stress.

B. Buckling Between Frames

Buckling between frames will occur in a cylinder that has relatively heavy frames and light stringers; the cylinder tends to act as a number of isolated axially stiffened cylinders each of which is one frame spacing long. Failure will occur by some form of instability of the stringers, modified by the effect of the attached sheet. The frames will remain circular in cross-section. The only function of the frames in this case will be to determine the end fixity coefficient of the stringers. The four forms of instability which must be investigated for this type of failure are as follows:

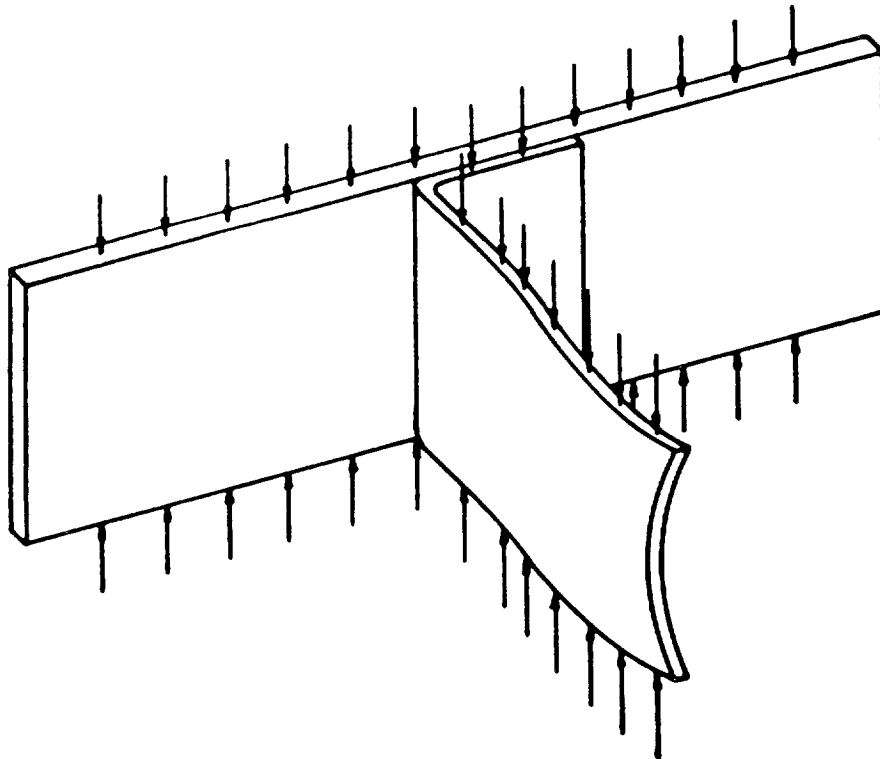
1. Buckling of the sheet between stringers and frames
2. Crippling of the stringers
3. Torsional instability of the stringers
4. Lateral buckling of the sheet stringer panel between frames

Although there are four distinct instability modes, the ultimate buckling failure between frames of a stiffened cylinder subjected to bending is usually a combination of these modes.

Buckling of the sheet between the stringers and frames does not necessarily constitute an ultimate failure of the structure; however, the

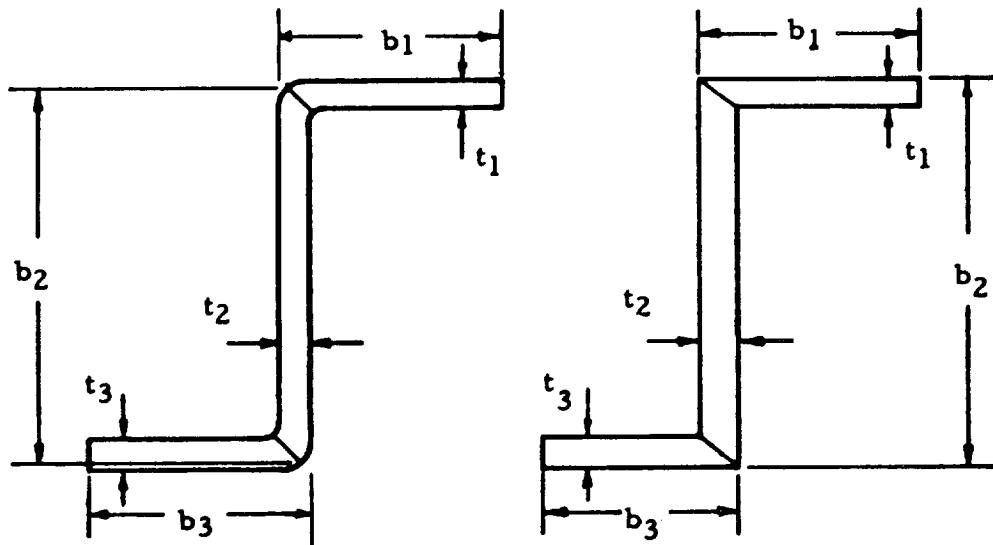
buckling stresses, σ_{CS} , of the sheet must be known to determine the stress distribution in the cylinder. The buckling stresses for this mode may be calculated by the methods presented in Paragraph 3.22.1 on curved panels.

Crippling is a local instability failure of the elements of the stringers and is defined as any type of failure in which the cross-sections of the stringers are distorted in their own plane but not translated or rotated. The length of the buckle involved in a crippling failure is of the same order of magnitude as its cross-sectional dimensions. A typical crippling failure is shown in the following figure.



Crippling generally occurs in stringers having wide thin flanges. The crippling stress is defined as σ_{cc} and may be determined by the usual methods of analysis of columns.

One of the procedures for computing the allowable crippling stress of stringers with simple cross-sections will be presented. This method is primarily from Ref. 3-35. The stringer is broken up into parts as shown in the following figure:



The allowable crippling stress for the total stringer is

$$\sigma_{cc} = \left(\sum_{i=1}^m \sigma_{cc_i} A_i \right) / \sum_{i=1}^m A_i$$

$$\sigma_{cc_i} = C_{ei} \sqrt{\sigma_{cy_i} E_i} \eta_i (t_i/b_i)^{3/4}$$

m = Number of parts the stringer is cut in

i = Subscript referring to part number

C_e = Material and shape parameter constant derived from test specimens (see Table 3.40-1)

$C_e = C_{e_1}$ = If one edge is free such as parts 1 and 3 of preceding figure

$C_e = C_{e_2}$ = If both edges are attached to adjacent parts such as part 2 in preceding figure

σ_{cy} = Compressive yield stress of material

E = Compressive modulus of elasticity of material

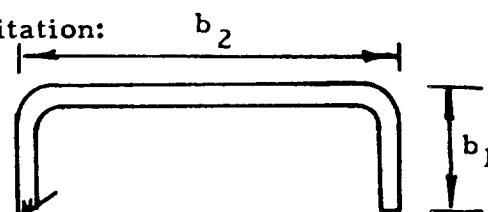
A_i = Area of part

η = Plasticity correction given by curve A if C_{e_1} is used and curve C if C_{e_2} is used (see Section 3.60)

If σ_{cc_i} is below the proportional limit then $\eta_i = 1$. At higher stresses, η_i must be compatible with σ_{cc_i} . σ_{cc_i} must be less than or equal to σ_{cy_i} . The amount of sheet to include with the part of the stringer attached to the skin depends on the method of attachment.

TABLE 3.40-1

Return Flange Limitation:



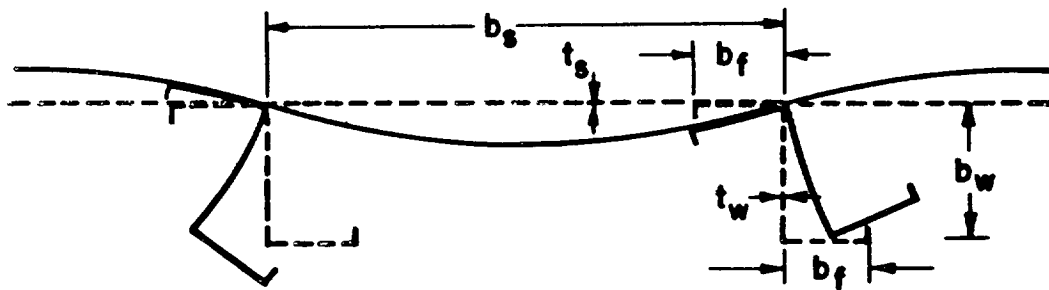
b_1 must be $\geq 1/3 b_2$ to consider the b_2 leg as continuous at both ends.

| Material | C_{e_1} | C_{e_2} | Maximum Element Stress (σ_{cy}) | Modulus ($E \times 10^{-6}$) |
|--|-----------|-----------|--|--------------------------------|
| 24S-T4 Bare, Extruded | 0.312 | 0.590 | 40,000 | 10.5 |
| 24S-T4 | 0.312 | 0.590 | 36,000 | 10.5 |
| 75S-T6 Bare | 0.312 | 0.590 | 71,000 | 10.5 |
| 75S-T6 Clad | 0.312 | 0.590 | 66,000 | 10.5 |
| 75S-T6 Extruded | 0.312 | 0.590 | 70,000 | 10.5 |
| Ti 6AL-4V Annealed (Formed) | 0.304 | 0.771 | 126,000 | 15.8 |
| Ti 6AL-4V Annealed (Extruded) | 0.304 | 0.771 | 120,000 | 15.8 |
| Ti 6AL-4V Heat Treated (Formed and Extruded) | 0.304 | 0.771 | 150,000 | 17.0 |
| 4130 Formed, 4340 Extruded | 0.312 | 0.735 | 175,000 | 29.0 |
| 1/2 Heat (301 Formed) (303 Extruded) | 0.365 | 0.800 | 85,000 | 26.0 |
| 17-7PH Formed | 0.333 | 0.631 | 158,000 | 30.0 |
| 17-7PH Extruded | 0.333 | 0.631 | 176,000 | 30.0 |
| AM350 Formed, AM355 Extruded | 0.333 | 0.631 | 165,000 | 28.6 |

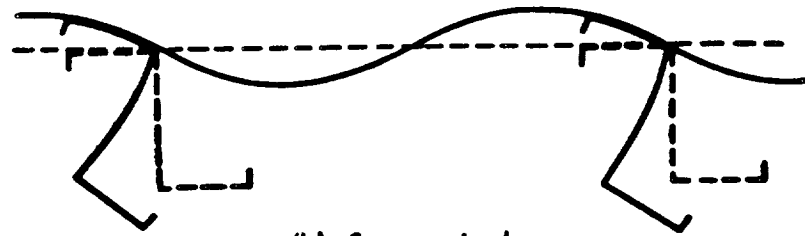
TABLE 3.40-1 (CONT)

| Material | C_{e1} | C_{e2} | Maximum Element Stress (σ_{cy}) | Modulus ($E \times 10^{-6}$) |
|-------------------------------------|----------|----------|--|--------------------------------|
| Inconel X Formed | 0.300 | 0.750 | 105,000 | 31.0 |
| H-11 Formed and Extruded | 0.296 | 0.704 | 280,000 | 30.9 |
| PH15-7Mo (cres) Formed and Extruded | 0.300 | 0.700 | 220,000 | 30.0 |
| Rene'41 Formed | 0.300 | 0.700 | 130,000 | 31.0 |
| Ti 4AL-3Mo-IV Formed | 0.304 | 0.771 | 160,000 | 16.0 |
| Ti 5AL-2.5 (Formed and Extruded) | 0.304 | 0.771 | 115,000 | 15.5 |

Torsional instability occurs when the cross-section of the stringer rotates but does not distort or translate in its own plane. Typical torsional modes of instability are shown in the following figure:



(a) Antisymmetric



(b) Symmetrical

The methods of analysis of torsional instability of stiffeners attached to sheets, as suggested in Ref. 3-36, will be described. For the case of cylinders with typical ring spacing, $[d > \pi (E \eta_G \Gamma/k)^{1/4}]$, the allowable torsional instability stress, σ_{ct} , for the mode shown in the preceding figure is

$$\sigma_{ct} = G \eta_A \left[\frac{J}{I_p} \right] + 2 \left[\frac{\sqrt{\Gamma}}{I_p} \right] \sqrt{E \eta_G k}$$

where

G = Elastic shear modulus for stringer material

η_A = Plasticity correction given by curve A in Section 3.62

E = Young's modulus for stringer material

η_G = Plasticity correction given by curve G in Section 3.62

I_p = Polar moment of inertia of section about center of rotation (in. ⁴)

$\frac{J}{I_p}$ and $\frac{\sqrt{\Gamma}}{I_p}$ = May be obtained from Fig. 3.42-1 and 3.42-2 for two commonly used types of stringers

J = Torsion constant of the stringer

$$\left(GJ = \frac{\text{torque}}{\text{twist per unit length}} \right)$$

Γ = Torsional-bending constant (in.⁶)

k = Rotational spring constant

b, d = Stringer and frame spacing, respectively

$$\frac{1}{k} = \frac{1}{k_{\text{web}}} + \frac{1}{k_{\text{sheet}}}$$

$$k_{\text{web}} = \frac{Et_w^3}{4 b_w + 6 b_f}$$

$$k_{\text{sheet}} = \lambda_1 \frac{Et_s^3}{b}$$

$\lambda_1 = 1$ for the symmetric mode

$$\lambda_1 = 1/3 \left[1 + 0.6 \frac{(\sigma_{\text{ct}} - \sigma_{\text{cs}})}{\sigma_{\text{cs}}} \right] \text{ for the antisymmetric mode}$$

σ_{cs} = Compressive buckling stress of the sheet

(see Section 3.22)

If $\sigma_{\text{ct}} < 4.33 \sigma_{\text{cs}}$, the antisymmetric mode is critical. If $\sigma_{\text{ct}} > 4.33 \sigma_{\text{cs}}$, the symmetric mode of failure is critical. Since λ_1 , η_A , and η_G depend on σ_{ct} , the solution for σ_{ct} is in general a trial and error procedure. Start with the assumption that $\lambda_1 = 1$, $\eta_A = \eta_G = 1$, calculate σ_{ct} , and correct for plasticity if required.

Correct λ_1 if required, and repeat procedure until desired convergence is obtained. Then check to see if $d > \pi \left(\frac{E \eta_G \Gamma}{k} \right)^{1/4}$.

If $d < \pi \left(\frac{E \eta_G \Gamma}{k} \right)^{1/4}$ the allowable torsional instability stress

is

$$\sigma_{ct} = G \eta_A \left(\frac{J}{I_p} \right) + \frac{E \eta_G \Gamma}{I_p} \left(\frac{\pi}{d} \right)^2 + \frac{k (d/\pi)^2}{I_p}$$

where

$$\Gamma = \left(\frac{\sqrt{\Gamma}}{I_p} \right)^2 I_p^2$$

and J/I_p and $\sqrt{\Gamma}/I_p$ may be obtained from Figs. 3.42-1 or 3.42-2.

The formulas which have been presented may be used for stringers with sections other than those shown in Figs. 3.42-1 and 3.42-2 if the values of I_p , J and Γ are known.

Lateral buckling of the sheet stringer panel between frames is essentially a column instability in which the cross-section of the stringer translates. It is customary to idealize the sheet-stringer as a column with length equal to the frame spacing, d . The lateral buckling stress of the sheet-stringer panel is defined as σ_{cp} . If no restraint exists normal to the sheet stringer panel, it is free to buckle

FIG. 3.42-1. TORSIONAL SECTION PROPERTIES FOR LIPPED Z STRINGER - SHEET PANELS

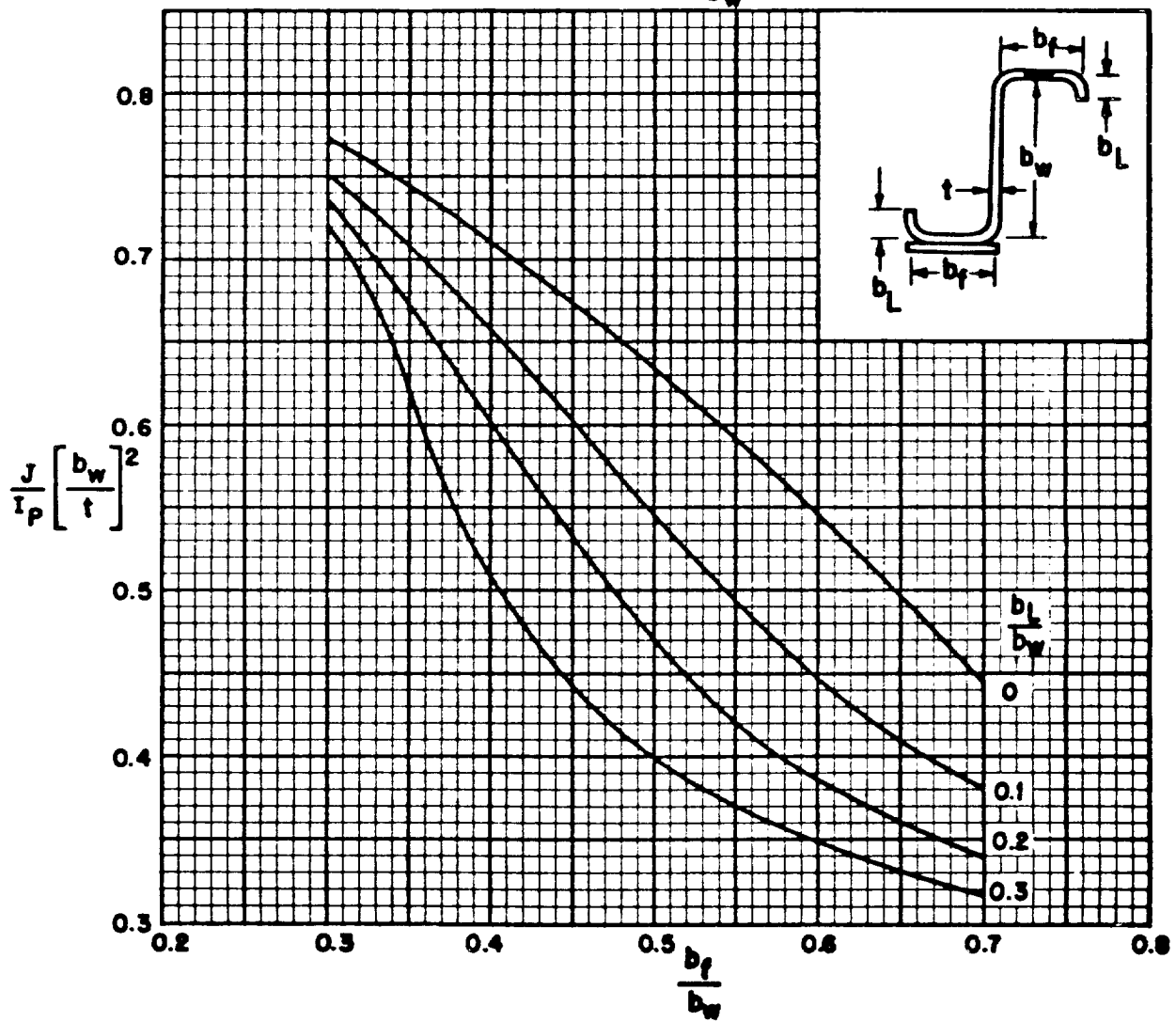
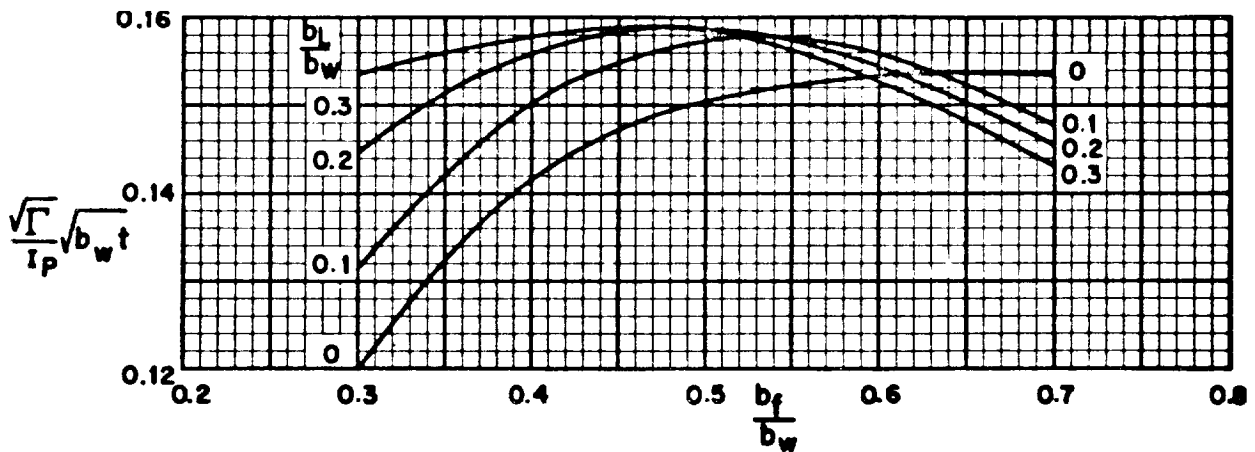
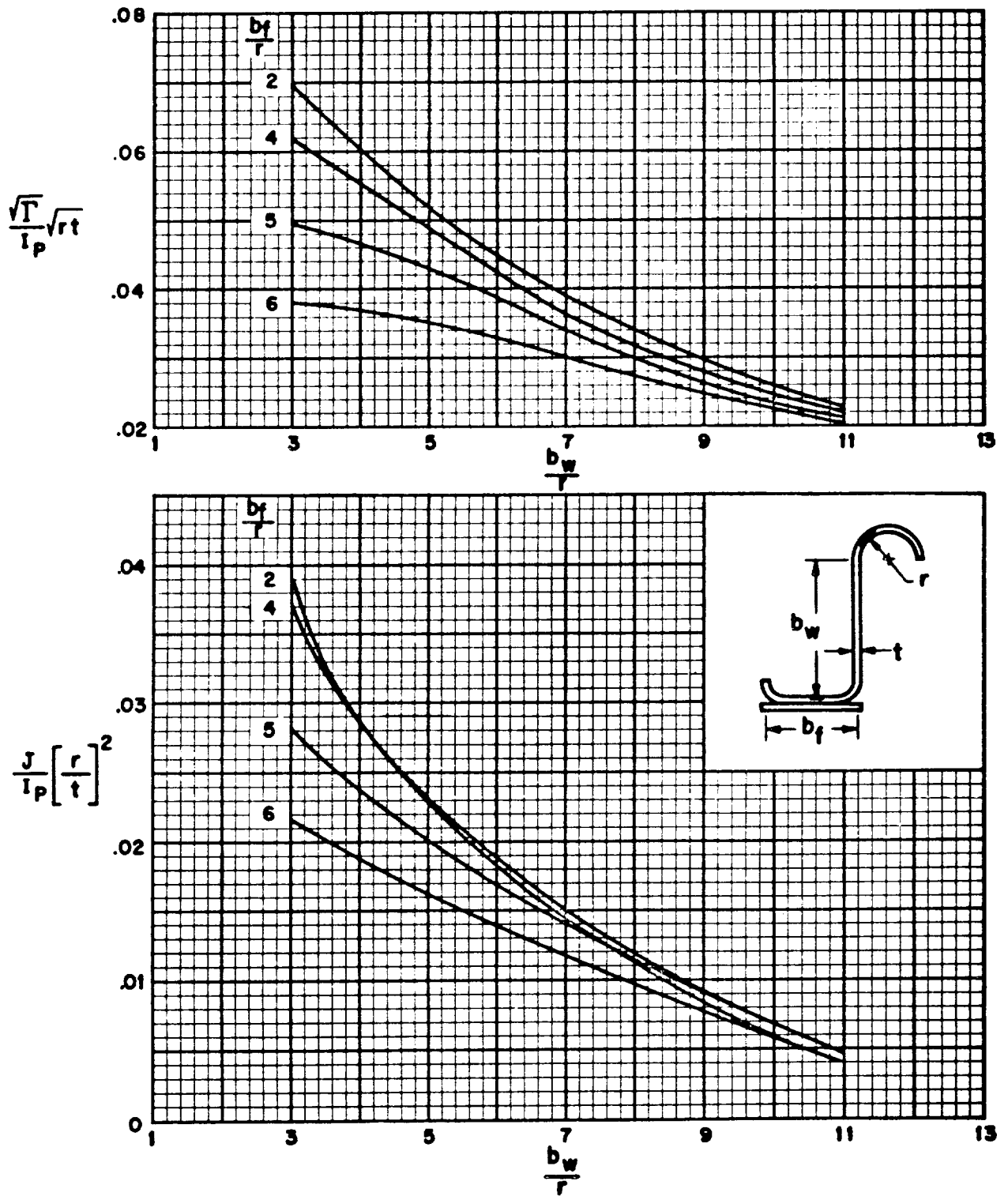


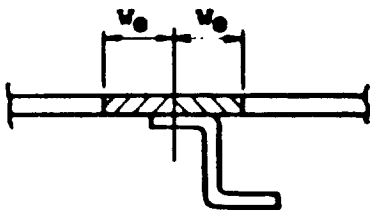
FIG. 3.42-2. TORSIONAL SECTION PROPERTIES FOR J STRINGER-SHEET PANELS



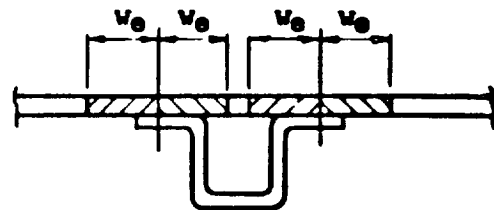
in alternate in-and-out waves in which the frames are nodes. In such case, the panel will act as a pinned end column and the effective end fixity, c , is equal to 1.0. Because of the curvature of the shell, a certain restraint to the outward buckle mode will exist because that deflection mode will involve some stretching of the sheet in the hoop direction. This restraint as well as the torsional restraint of the frame will tend, in general, to provide an effective end fixity coefficient in the sheet-stringer column that is somewhat greater than 1.0.

A satisfactory means of determining c is not available at the present time and the use of fixity coefficients greater than 1.0 must be substantiated by tests.

The buckling stress of the sheet-stringer panel depends on the effective width of skin, w_e , which is acting with the stringer. Two common examples of effective width of sheet are shown in the following illustrations:



(a) Single Line Attachment



(b) Double Line Attachment

For calculating the effective width of sheet acting with a stiffener, the following equation has been found to give results consistent with tests:

$$w_e = .85 t_s \sqrt{\frac{E}{\sigma_{cr}/\eta}}$$

where

$$\sigma_{cr} = \sigma_{cp}$$

σ_{cp} = Lateral buckling stress of sheet stringer panel

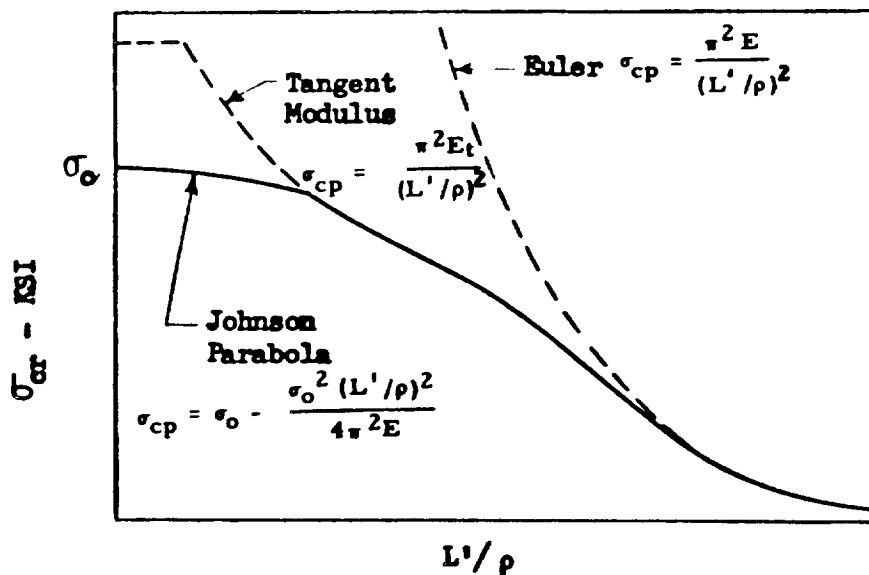
When σ_{cr} is known, σ_{cr}/η may be found using curves C in Section 3.62.

Other methods of obtaining w_e are available (Ref. 3-32) but, in general, the difference will be small if the skin does not carry a large percentage of the load. σ_{cp} depends on the radius of gyration, ρ , of the sheet stringer column which, in turn, depends on w_e ; therefore, an iteration procedure is needed to determine σ_{cp} . In addition, there may be an interaction between the lateral buckling of the panel and the torsional buckling or crippling of the stringer. The following procedure is recommended for determination of the allowable stress for the sheet stringer panel.

1. Determine the radius of gyration of the stiffener cross-section about the centroidal axis
2. Determine the effective slenderness ratio L'/ρ of the stiffener alone

$$\frac{L'}{\rho} = \frac{d}{\sqrt{c}} \rho$$

3. Determine the crippling stress, σ_{cc} , and the torsional instability stress, σ_{ct} . The lower of these two stresses, σ_o , determines the intercept ($L'/\rho = 0$) of a modified Johnson parabola and defines a complete column curve, as can be seen in the following illustration.

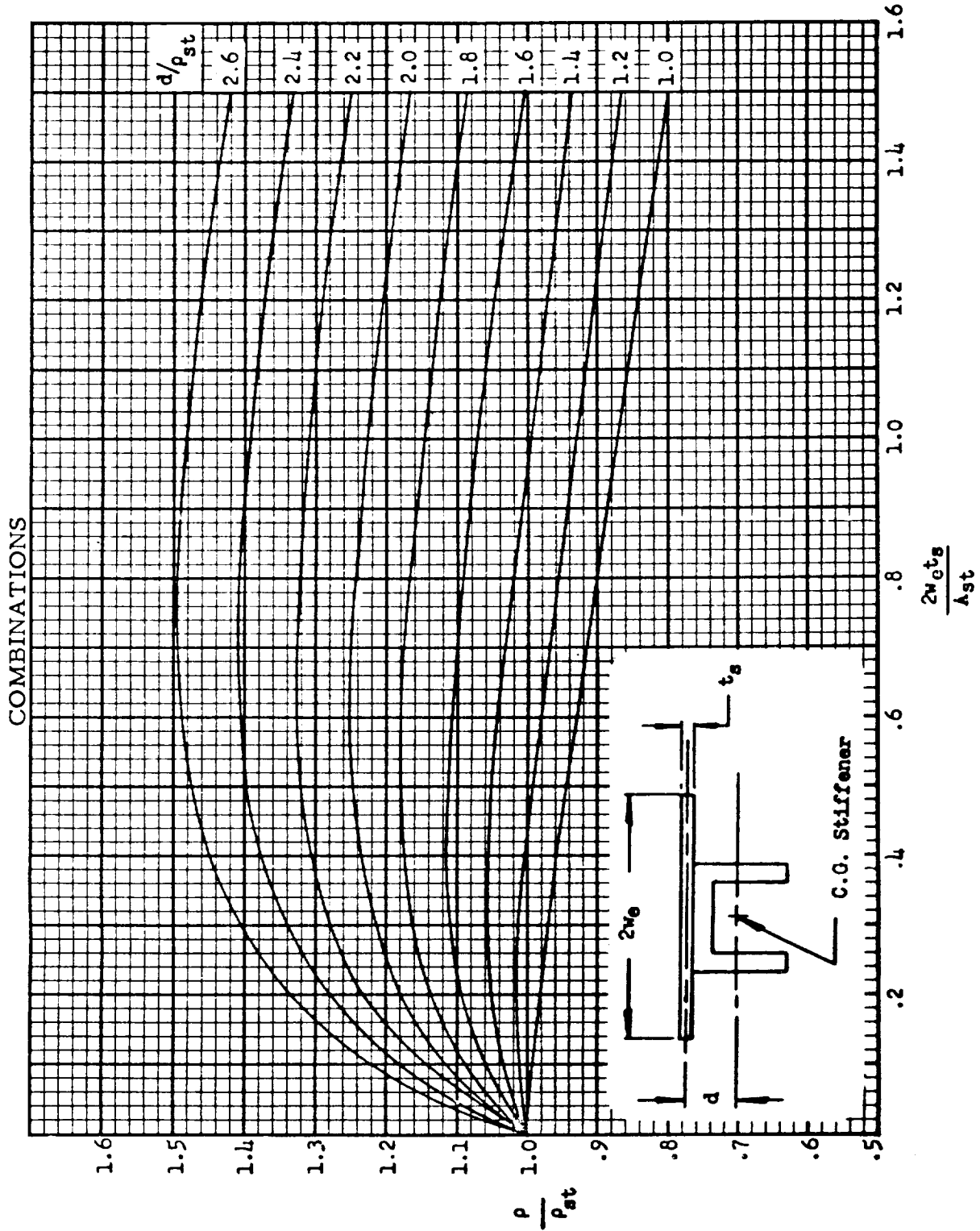


4. Using the column curve and the slenderness ratio determined in steps 1, 2, and 3, record the value of σ_{cp} .
5. Compute the effective width of sheet acting with the stiffener.
6. Use the curves in Fig. 3.42-3 to compute ρ of the stiffener plus effective sheet. A_{st} and ρ_{st} are the area and radius of gyration of the stringer, respectively.
7. Compute L'/ρ for the new value of ρ .
8. Enter the column curve a second time with the new L'/ρ and record the corrected value of σ_{cp} .
9. Repeat steps 5, 6, and 7 until satisfactory convergence to a final stress, σ_{cp} , is obtained. Convergence generally occurs after two or three iterations.
10. The allowable load, P_{cr} , for the skin stringer combination with single line attachment is

$$P_{cr} = \sigma_{cp} (A_{st} + 2 w_e t_s) + \sigma_{cs} (b - 2 w_e) t_s$$

The preceding analysis assumes that the skin stringer panel between the frames buckles as a column and neglects the stiffening effect of the curvature. If the stiffeners are close together, the formula given in Paragraph 3.33.1 for axially stiffened cylinders may

FIG. 3.42-3. VARIATION OF RADIUS OF GYRATION FOR SHEET-STIFFENER COMBINATIONS



be used to account for the effects of curvature. If $c \pi^2 / (d/\rho)^2$ is equal to $\frac{3t_s}{R} \left[t_s b / (A_{st} + 2 w_e) \right]^{1/2}$ the effects of curvature is less than approximately 5 percent. As $\frac{2t_s}{R} \left[t_s b / (A_{st} + 2 w_e) \right]^{1/2}$ becomes greater than $c \pi^2 / (d/\rho)^2$, the effect of curvature becomes more important.

C. General Instability

The general instability type of failure will occur in a structure which has frames and stringers that fail simultaneously under the critical load; that is, collapse takes place in a manner so as to destroy the load-carrying properties of all three structural elements—sheet, frames, and stringers.

Of the two possible types of general instability failures for cylinders subjected to bending, one is characterized by a general flattening of the cylinder. Both theory and experiments indicate that for general flattening to occur, the length-diameter ratio of the cylinder must be so large that it is completely out of the range of most aerospace structures. (See Ref. 3-37.)

The second class of general instability failure is one in which the wave form of the buckle is multilobed and has, in general, an axial wavelength less than the length of the cylinder but greater than the

frame spacing. The buckle form corresponds to the usual "diamond-shaped" wave pattern which is observed in the failure of unstiffened cylinders under compressive loads.

Two different methods of general instability analysis are frequently considered for stiffened shells subjected to compressive loads. One method of analysis distributes the stiffnesses of the frames and stringers over the entire cylinder and then uses orthotropic shell theory to analyze the cylinder. This method, which is useful if the stringers and frames are relatively close together, is presented in Section 3.30; however, the test results of Ref. 3-33 show that this method may be unconservative for large stiffener and frame spacings.

The second method is the semi-empirical approach presented in Ref. 3-33 which was done when there was little in the way of theory to serve as a guide. By means of a dimensional analysis in conjunction with the behavior of unstiffened circular cylinders, a nondimensional parameter, Q_b , was derived to correlate test data. It is believed that this method should be used for the analysis of frame stringer stiffened shells subjected to bending until the range of application of the first method is established.

The design-allowable general instability stress, σ_{cr} , for a frame stringer stiffened cylindrical shell subjected to bending may be obtained from the following formula which was given in Ref. 3-33.

$$\frac{\sigma_{cr}}{\eta} = CEQ_b$$

$$Q_b = \frac{1}{R} \sqrt[4]{\frac{\rho_s^3 \rho_f^3}{bd}}$$

where

$$C = 4.2$$

ρ_f = Radius of gyration of the frame sheet combination

ρ_s = Radius of gyration of the stringer sheet combination

E = Young's elastic modulus of the material

b, d = Stringer and frame spacing, respectively

σ_{cr} = Maximum stress due to bending moment (e. g., out fiber stress)

The value of $C = 4.2$ is based on the test data for 67 cylinders as reported in Ref. 3-33. This value of C agrees well with three of six tests reported more recently in Ref. 3-38 and was conservative for the other three tests.

The effective sheet to use with the stringers to determine ρ_s may be obtained from

$$\frac{w_e}{b} = 0.447 \sqrt{\frac{\sigma_{cs}}{\sigma_{cr}}}$$

while for the frames, the total width, d , should be used. Fig. 3.42-3 will aid in the computation of ρ_s and ρ_f . An iterative procedure is

necessary if the full width of skin cannot be used to compute ρ_s . For elastic buckling, $\eta = 1$ is used. In the inelastic range, the critical stress σ_{cr} can be found using curves A of Section 3.62.

The frames must be attached to the skin between stiffeners and the frames and stringers must be continuous if $C = 4.2$ is used. It can be seen that the preceding analysis does not depend on whether the stiffeners are inside or outside. Experimental and theoretical investigations (Refs. 3-39 and 3-40) have shown that there can be an appreciable difference between the buckling load of a cylinder with the stiffeners on the inside and the buckling load for the same cylinder with the same stiffeners on the outside. The theoretical equations are complicated, and a computer program is required to determine the buckling loads. There is no simple procedure available at the present for predicting the difference in buckling load due to locating the stiffeners on different sides of the sheet.

It can also be noted that the formula for σ_{cr} is independent of length and boundary conditions. It is difficult to determine how long the cylinder must be to be independent of length and edge effects. An estimate of whether the buckling load is independent of length for a given edge fixity can be obtained from Paragraph 3.33.1.

If the primary loading of a stiffened cylinder is bending, the frame stiffness necessary to ensure a general instability failure

rather than panel instability can be estimated from the following formula

$$EI_f = C_f \frac{M (2R)^2}{d}$$

where

$$C_f = 6.84 \times 10^{-5}$$

EI_f = flexural stiffness frame requirement

M = applied bending moment

Several values of C_f have been suggested in the literature but $C_f = 6.84 \times 10^{-5}$, as suggested in Ref. 3-41, is recommended because it is slightly more conservative and does have some theoretical justification. For frames with flexural stiffnesses greater than EI_f , the increase in the strength of the cylinder when subjected to bending is a relatively small increase in the effective edge fixity of the panel. The value of frame stiffness found in this manner is only approximate, and each mode of failure should be investigated separately to determine a final frame stiffness.

3.43 FRAME-STIFFENED CYLINDERS

3.43.1 Lateral and Axial External Pressure, Frame-Stiffened Cylinders

If a cylindrical shell with frames (circumferential stiffeners) is subjected to lateral and axial external pressure, it may fail in three distinct ways. The types of failure will be classified as material failure, buckling between frames, and general instability. A brief discussion of these failure modes is presented in this manual. A more detailed discussion of frame-stiffened cylinders subjected to external pressure is presented in Ref. 3-42.

A. Material Failure

For purposes of analysis, the stress deflection distribution of a cylinder prior to buckling can be assumed to be axisymmetric. Therefore, the analysis methods of Chapter 2.00 can be used to determine the stresses in the cylinder. A more detailed procedure is discussed in Ref. 3-43. The actual stresses must be compared against the material allowable stresses. In addition, the compressive stress in the frame must be compared against the local buckling stresses of the frame.

B. Buckling Between Frames

This failure will occur in a cylinder having relatively heavy frames. The sheet will buckle between frames and the frames will

remain circular in cross-section. The allowable buckling stress for this mode of failure can be obtained from Paragraph 3.22.4, using a cylinder length equal to the frame spacing. A more detailed method of analyzing this mode of failure is presented in Ref. 3-44.

C. General Instability

General instability of failure will occur when the frame buckles with the sheet at the critical load. The design allowable general instability pressure, p_{cr} , for a frame-stiffened cylinder subjected to lateral and axial external pressure can be obtained from

$$p_{cr} = \frac{\gamma E}{30 \times 10^6} [p_s + p_f]$$

where

E = Young's modulus of the material (the frame and sheet must be made from the same material)

p_s Can be obtained from Fig. 3.43-1 if $\frac{I_e}{dR^3} \times 10^6 < 10$ and from Fig. 3.43-2 if $\frac{I_e}{dR^3} \times 10^6 \geq 10$

p_f Can be obtained from Fig. 3.43-3 or 3.43-4

The quantity, p_{cr} , must be computed for $n = 2, 3, 4,$ and 5 ; its lowest value is the critical allowable buckling pressure. This graphical method for determining p_s and p_f was obtained from Refs. 3-45 and 3-46, which are based on Ref. 3-47. Reference 3-47

analyzes simply supported cylinders. The test results of Ref. 3-48 indicate an appreciable increase in buckling pressure due to edge fixity, but a method of including these effects for design purposes has not been developed.

The parameter, γ , is introduced to reduce the theoretical results of Ref. 3-47 to a value which may be used for design purposes. It is a function of many variables such as initial out-of-roundness of the cylinder. For the test data given in Refs. 3-48 and 3-49, $\gamma = 1$ is adequate. However, the cylinders in Refs. 3-48 and 3-49 were machined to very close tolerances. Presently, it is not known what value of γ to use, but for $\left(\frac{12I_e}{dt_s}\right)^{3/2} \frac{L^2}{t_s^4 R} > 4 \times 10^3$, $\gamma = 0.9$ is probably reasonable.

The value of I_e required in Figs. 3.43-3 or 3.43-4 can be calculated from

$$I_e = \frac{A_f e^2}{1 + \frac{A_f}{d t_s}} + I_f + \frac{d t_s^3}{12}$$

where

A_f, I_f = area of the frame and moment of inertia of the frame about its own neutral axis, respectively

e = distance from the middle surface of the sheet to the centroid of the frame

$$d_e = (d - t_w) F_1 + t_w$$

t_w = frame web thickness

The value of F_1 can be obtained from Fig. 3.43-5. Parameter λ_2 in Fig. 3.43-5 is a function of p_{cr} , which is unknown. A good approximation can be obtained by using $\lambda_2 = 0$. For cases in which $\lambda_3 < 2$, this approximation gives results within 5-percent accuracy.

For the loading case of external pressure, Ref. 3-50 states that a cylinder with frames on the inside will be stronger than a cylinder with frames on the outside if $Z > 500$, where $Z = (1 - \mu^2)^{1/2} L^2 / R t_s$. If the frames are on the inside and $Z > 500$, the results will be slightly conservative because the curves presented are for external frames. Therefore, the curves presented will probably be conservative if the frames are located on the outside because most stiffened cylinders fall in the range $Z > 500$.

If the parameters for a particular design do not fall in the range of parameters presented in Figs. 3.43-3 and 3.43-4, the following formula (given in Ref. 3-37) can be used to estimate the design allowable external pressure

$$p_{cr} = \frac{5.5 \gamma E \left(\frac{I_e}{d}\right)^{3/4} t_s^{1/4}}{LR^{3/2}}$$

if

$$\left(\frac{12 I_e}{d t_s}\right)^{3/2} \frac{1}{t_s^4} \frac{L^2}{R} > 4 \times 10^3$$

The theoretical results of Ref. 3-47 were reduced 10 percent for design purposes, and it has been found that the theory of Ref. 3-47 predicts buckling pressures that are, in some cases, 80 percent of the theoretical results given in Ref. 3-37; therefore, $\gamma = 0.8 \times 0.9 = 0.72$ can be used in the preceding formula to obtain the design allowable buckling pressure.

A simple method of including plasticity in the preceding formulas is not available, but an estimate can be obtained by using the plasticity correction factor suggested in Paragraph 3.23.4. A more detailed procedure is presented in Ref. 3-51.

FIG. 3.43-1. SHELL PRESSURE FACTOR (p_s) AS A FUNCTION OF BULKHEAD SPACING (L/R) FOR $\frac{I_e}{dR^3} \times 10^6 < 10$

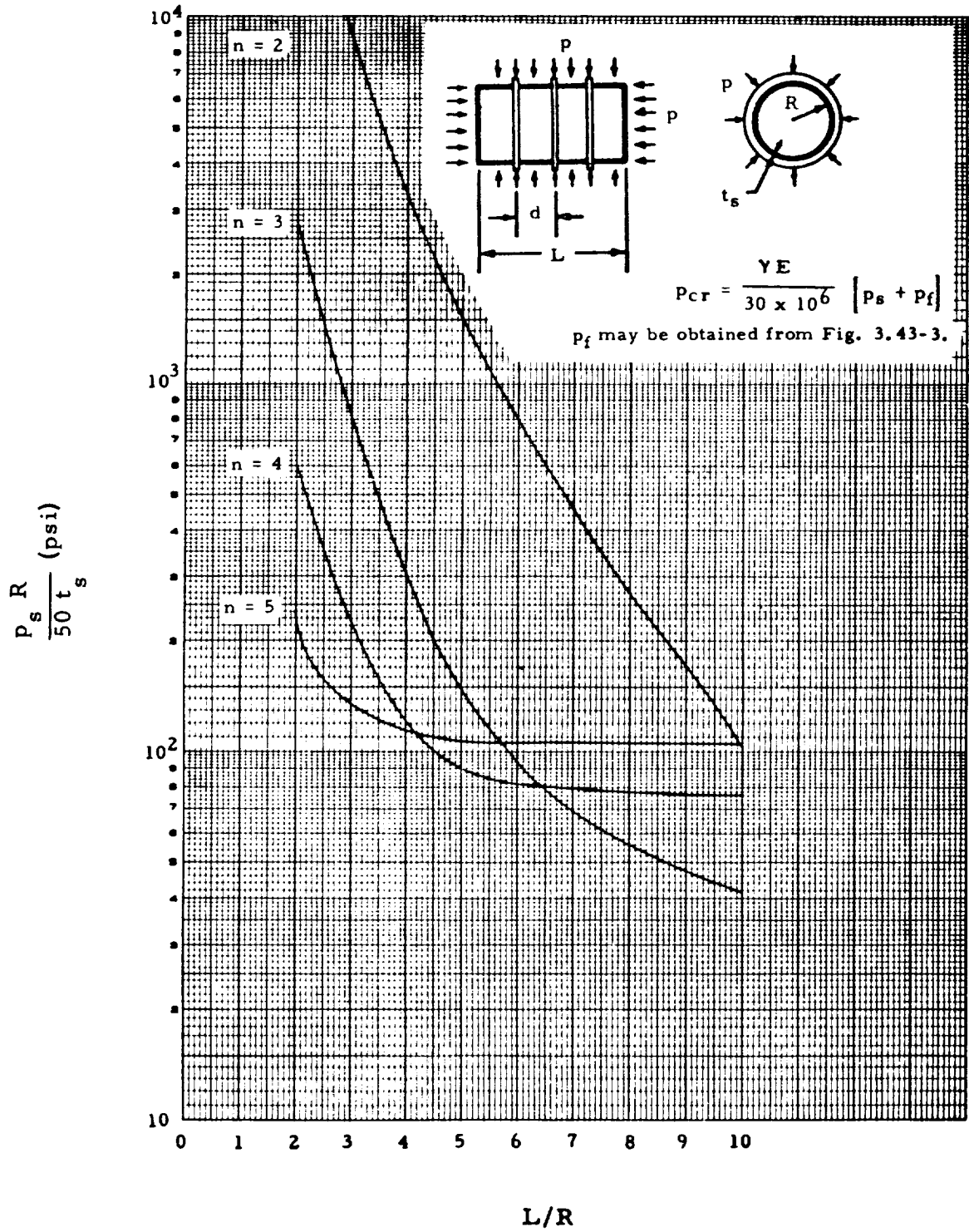


FIG. 3.43-2. SHELL PRESSURE FACTOR (p_s) AS A FUNCTION OF BULKHEAD SPACING (L/R) FOR $\frac{l_e}{dR^3} \times 10^6 \geq 10$

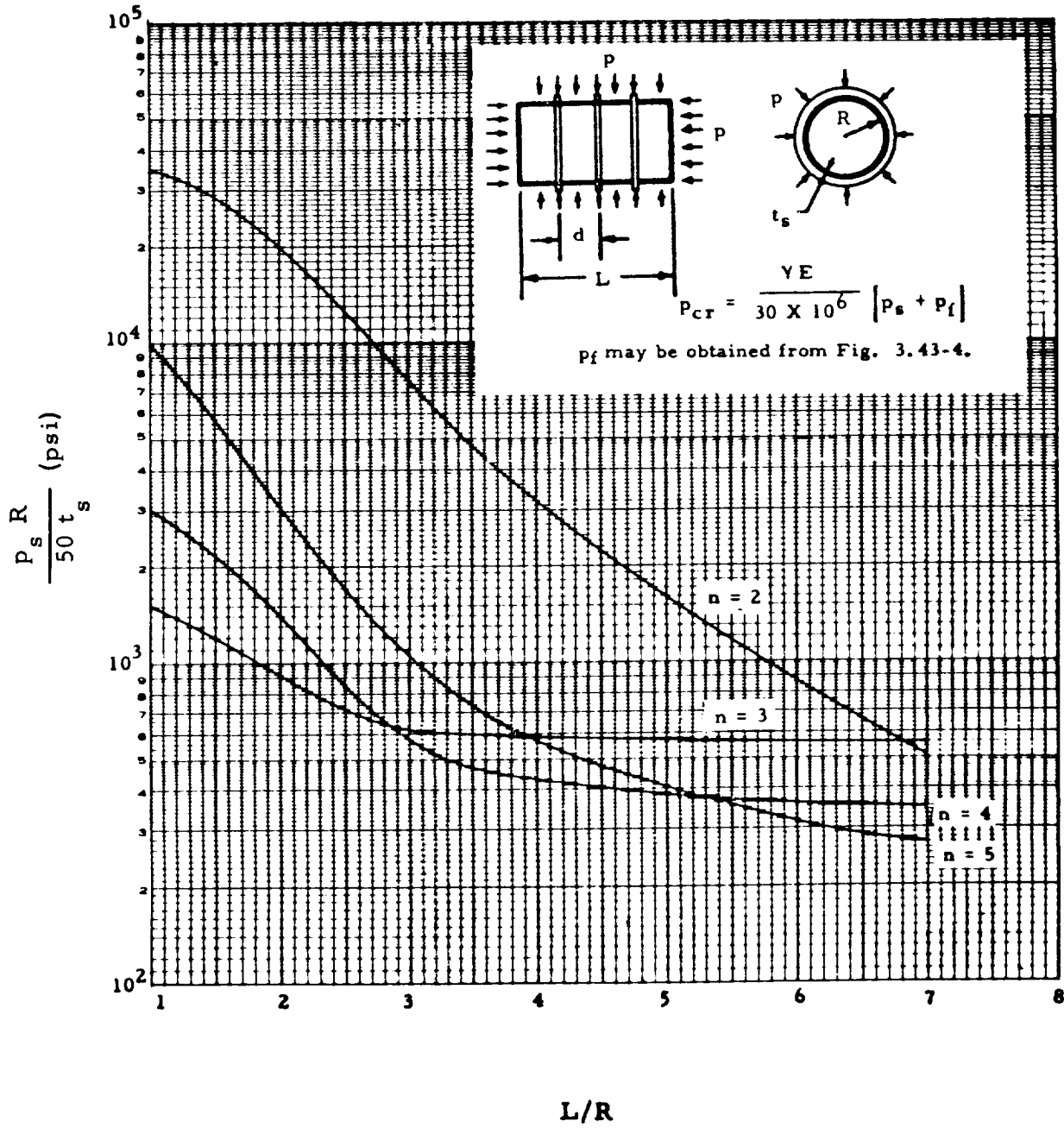


FIG. 3.43-3. FRAME PRESSURE FACTOR (p_f) AS A FUNCTION OF FRAME STIFFNESS (I_e/dR^3)

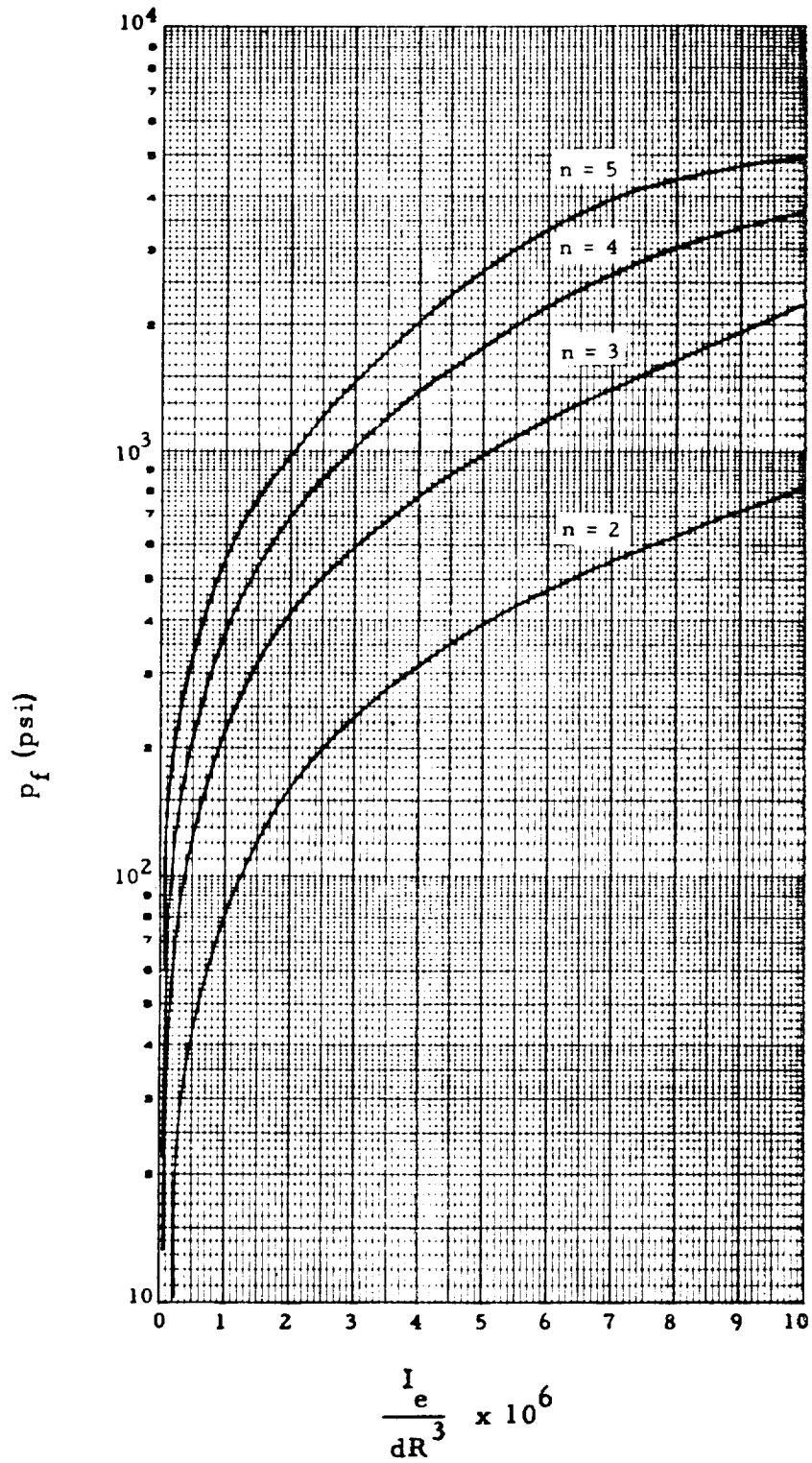


FIG. 3.43-4. FRAME PRESSURE FACTOR (p_f) AS A FUNCTION OF FRAME STIFFNESS (I_e/dR^3)

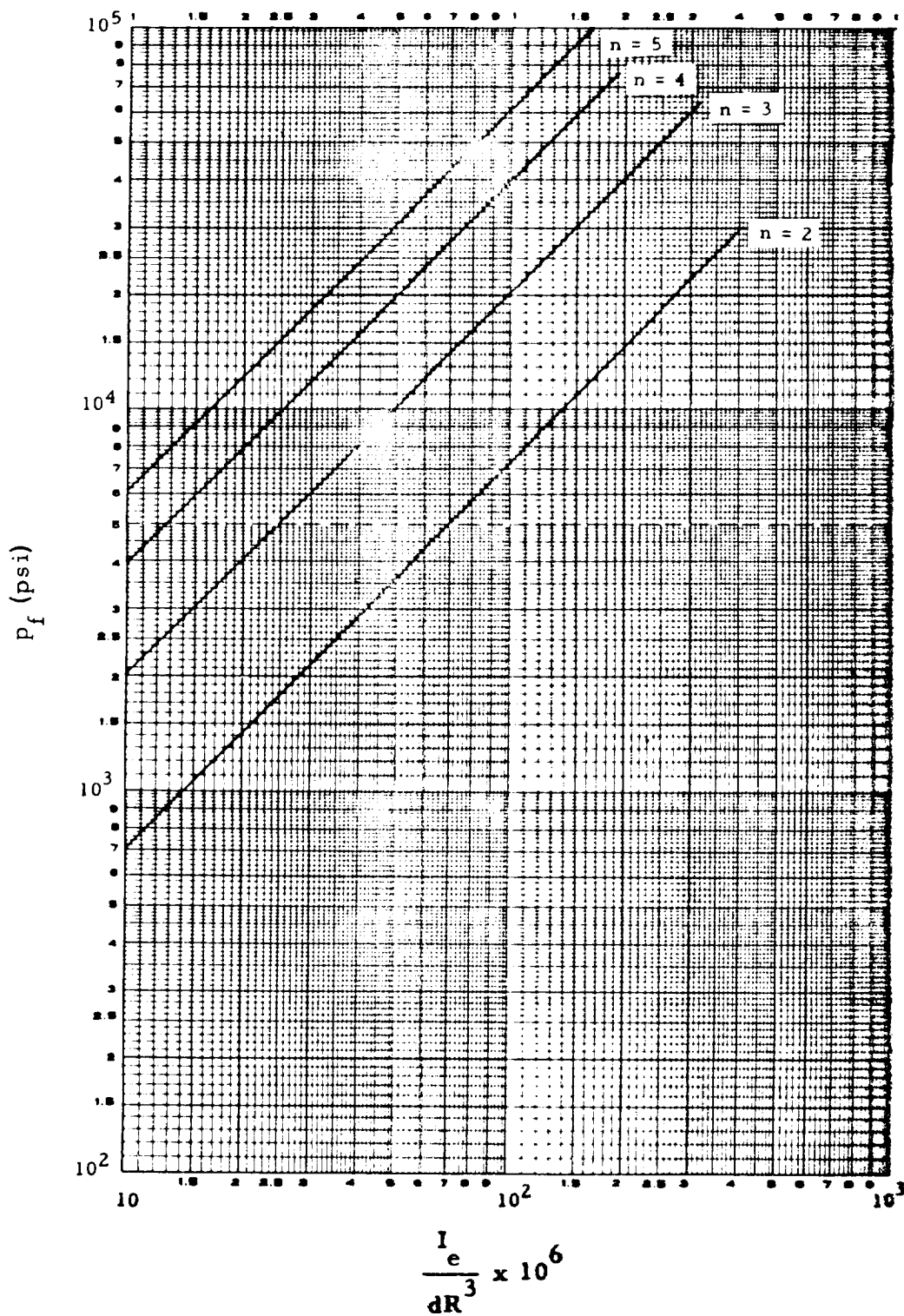
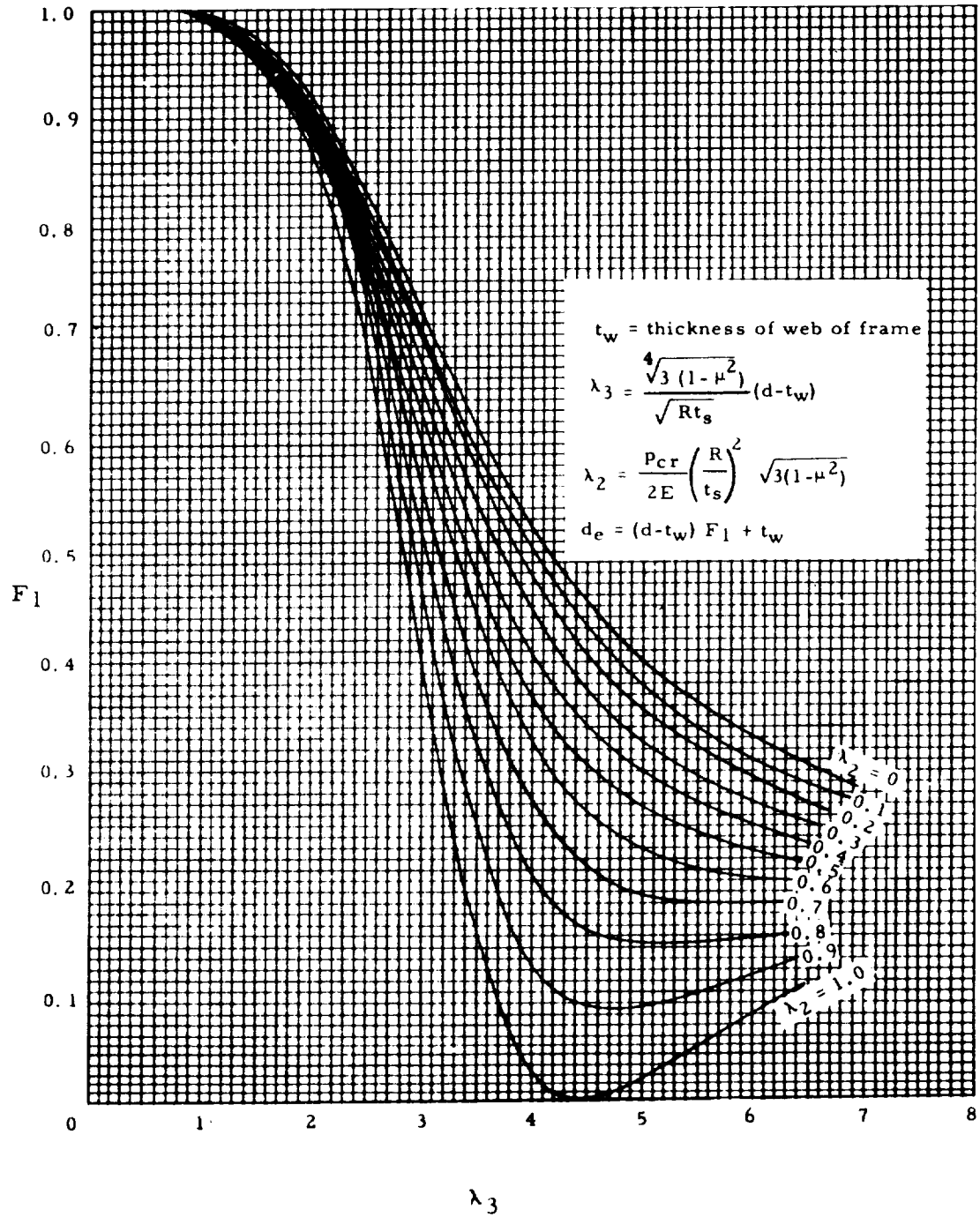


FIG. 3.43-5. STRESS FUNCTION FOR DETERMINING EFFECTIVE LENGTH



3.50 SANDWICH SHELLS

3.51 GENERAL

Sandwich-type construction is a composite construction consisting of three layers bonded together. The middle layer of the sandwich is the core; the outer two layers are the facing sheets. Generally, the facing sheets are very thin relative to the overall thickness of the sandwich and the elastic modulus of the facing sheet material is much larger than the corresponding effective modulus of the core. The primary difference between sandwich shells and orthotropic or isotropic shells is the relatively low transverse shear stiffness of the sandwich construction; therefore, the transverse shear stiffness must be included in the analysis.

Generally, sandwich construction should be analyzed for three modes of failure: (1) material failure, in which the applied stresses exceed the material allowable stresses; (2) general instability failure, in which the whole shell fails with the core and facings acting together; and (3) local instability failure, in which the facing sheet fails because it is not sufficiently stabilized by the core. (The forms of local instability for sandwich construction with honeycomb core are intracell buckling and wrinkling. Design formulas for these two modes of local instability are given in Section 3.52.)

Although a considerable amount of theoretical information is available concerning the general instability of sandwich shells, there is not enough test data available to obtain design curves directly. Therefore, the design curves for homogeneous isotropic shells are used to reduce the theoretical buckling loads for sandwich shells to design allowable buckling loads.

3.52 LOCAL INSTABILITY

3.52.1 Intracell Buckling

If the core of a sandwich is constructed of cellular (honeycomb) material, it is possible for the facings to buckle or dimple into the spaces between core walls. Dimpling of the facings may not lead to failure unless the amplitude of the dimples becomes large and causes the dimples to grow across the core cell walls, resulting in wrinkling of the facings. Dimpling that does not cause total structural failure may be sufficiently severe that permanent dimples remain after removal of the load.

The design allowable uniaxial intracell buckling failure stress, σ_{cr} , can be obtained from the formulas given in Ref. 3-4:

$$\frac{\sigma_{cr}}{\eta} = \frac{K_L E}{1 - \mu^2}$$

where

E = Young's compression modulus of elasticity of the facing sheet

μ = Poisson's ratio of the facing sheet

The coefficient, K_L , can be obtained from Fig. 3.52-1.

For elastic buckling, the plasticity correction term $\eta = 1$ is used.

In the inelastic range, Ref. 3-52 recommends

$$\eta = \frac{2E_t}{E + E_t}$$

For most materials, curves E_1 of Section 3.62 are a sufficiently accurate representation of this plasticity correction.

It should be noted that the formula for obtaining σ_{cr} is based primarily on test data from brazed flat honeycomb sandwich panels with PH 15-7 Mo core and facings. Limited test results indicate that the formula may be used for other types of materials and bonding methods.

It can be seen that the formula for computing σ_{cr} is independent of the foil thickness of the core and does not include any interaction between a wrinkling failure and an intercell buckling failure. Until an adequate method of analysis is developed which includes all the important variables, it is recommended that a limited number of compression tests be conducted to verify a design that may be critical in intercell buckling.

If an element of a sandwich shell is subjected to in-plane shear or combined loadings, the maximum principal compressive stress in the facing sheet should be compared against σ_{cr} to determine if intracell buckling may occur. If the stress normal to the maximum principal compressive stress is a tensile stress, the preceding formulas for σ_{cr} is probably adequate. If this stress is a compressive stress, Ref. 3-52 indicates that the following reduction of σ_{cr} is necessary:

$$\frac{\sigma_{cr}}{\eta} = \frac{K_L}{\sqrt[3]{1+S^3}} \cdot \frac{E}{(1-\mu^2)}$$

where

$$S = \frac{\text{minimum principal compressive stress in facing}}{\text{maximum principal compressive stress in facing}}$$

Dimples may occur at stress levels less than σ_{cr} , but the sandwich will carry more load. An estimate of the stress, σ_0 , at which initial dimpling may occur is given in Ref. 3-53 as

$$\frac{\sigma_0}{\eta} = \frac{E}{1-\mu^2} 2 \left(\frac{t}{s} \right)^2$$

t = thickness of facing sheet

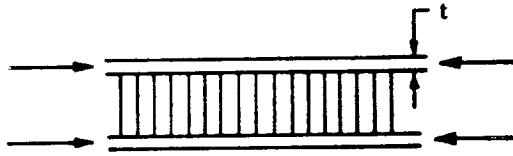
s = cell size of core

For elastic buckling, the plasticity correction term, $\eta = 1$, is used. In the inelastic range, the stress, σ_0 , can be found by using curves G in Section 3.62.

It should be mentioned, however, that for sandwich construction with very thin facing sheets, dimples in the facings can sometimes be observed before the sandwich is loaded. These dimples are the result of the manufacturing procedure.

Although the intracell buckling formulas are based on data for flat panels, they are adequate for curved panels because the cell size is usually much less than the radius of curvature.

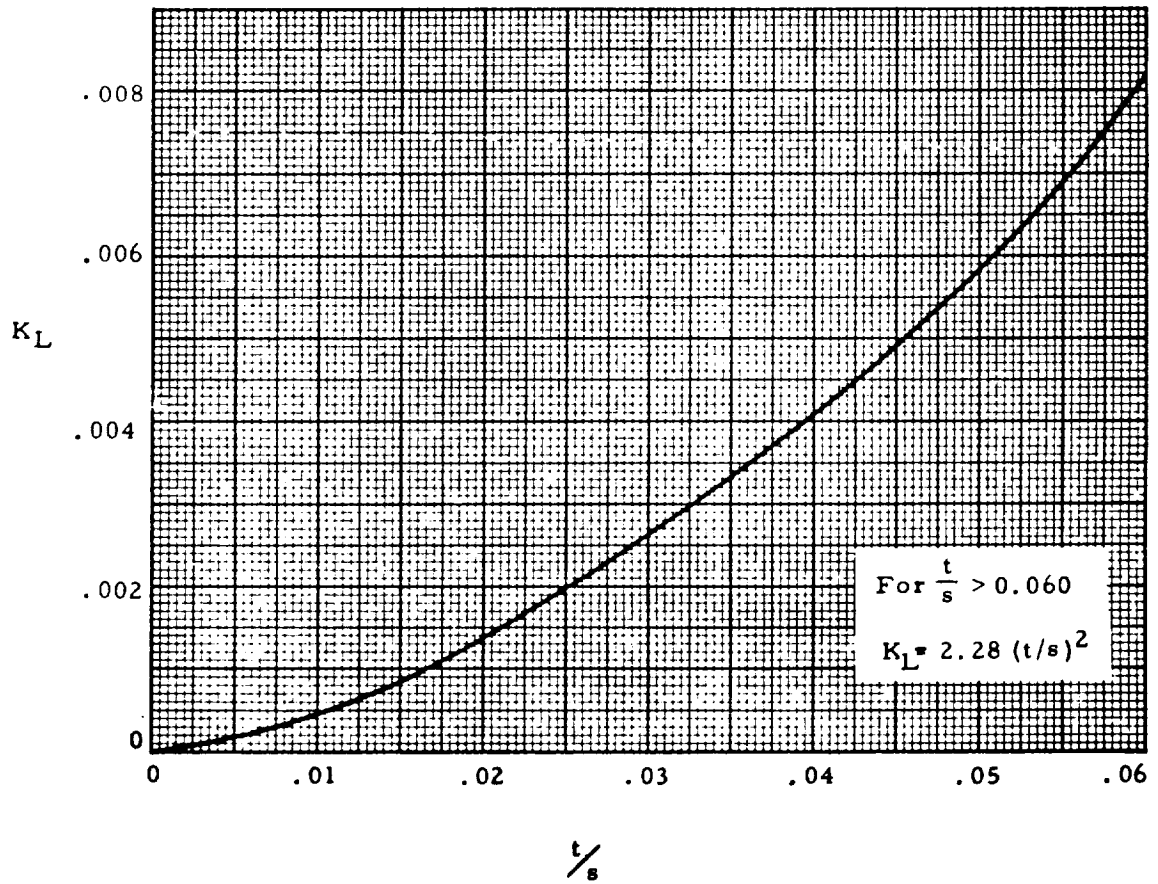
FIG. 3.52-1. INTRACELL BUCKLING COEFFICIENT



SANDWICH WITH
HONEYCOMB CORE

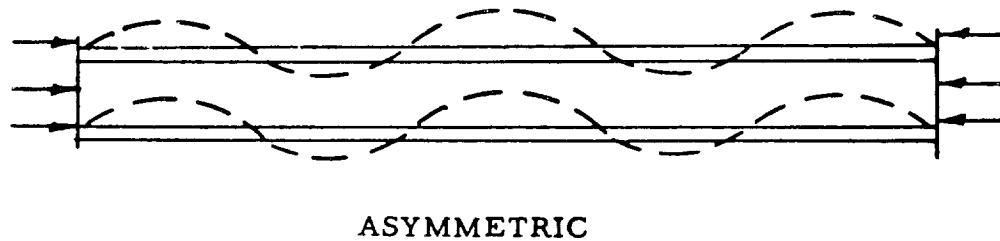
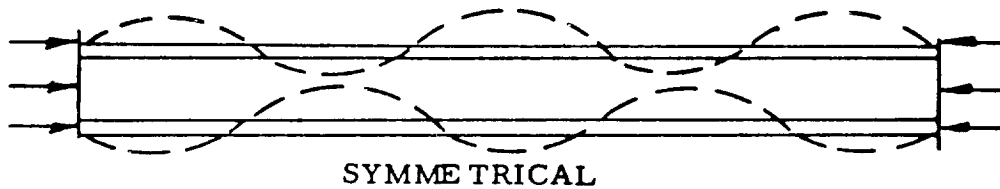
$$\frac{\sigma_{cr}}{\eta} = \frac{K_L E}{1 - \mu^2}$$

s = core cell size (diameter of inscribed circle)

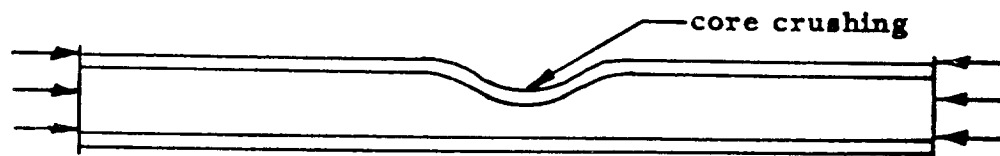
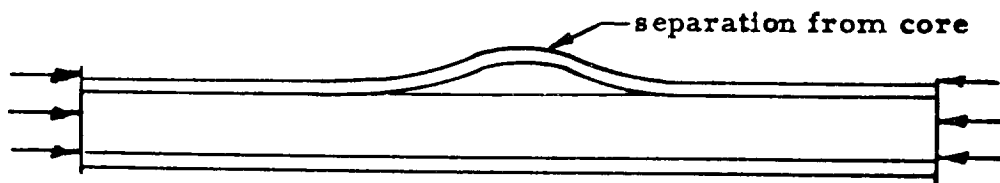


3.52.2 Face Sheet Wrinkling

When a facing sheet of a sandwich element is subjected to axial compression, face sheet wrinkling may occur. This failure is similar to buckling of a plate on an elastic foundation. Typical buckling modes for wrinkling are shown below.



The resulting failure mode will depend on the flatwise compressive strength of the core relative to the flatwise tensile strength of the bond between the facing core. Typical wrinkling failures are shown below.



If the bond between the facing and the core is strong, the facing can still wrinkle outward by causing tension failure of the core.

It can be seen that the wrinkling load depends on the stiffness and strength of the foundation system. Since the facing is never flat, the wrinkling load will also depend on the initial facing eccentricity or original waviness. A method of analysis which includes these variables is given in Ref. 3-54. One method of determining the initial waviness parameter needed in Ref. 3-54 is presented in Ref. 3-55. However, until the analysis in Ref. 3-54 is developed, for design purposes, the following wrinkling analysis from Ref. 3-52 is recommended. A limited number of tests should be conducted to verify the analysis procedure for a particular sandwich configuration.

The information on wrinkling of sandwich facings pertains primarily to flat panels. However, it is adequate for shells because the wavelength of the buckle is small relative to the radius of curvature.

The design allowable uniaxial compressive wrinkling stress, σ_{cr} , can be obtained from

$$\frac{\sigma_{cr}}{\eta} = K_L \sqrt[3]{E E_c G_c}$$

where

$$K_L = 0.43$$

- E = Young's compressive modulus of elasticity of the facing sheet
- E_c = flatwise compression modulus of the core (in a direction normal to the surface of the shell)
- G_c = transverse shear modulus of the core in the direction of the maximum compressive stress

For elastic buckling, the plasticity correction term, $\eta = 1$, is used. In the inelastic range, Ref. 3-52 recommends

$$\eta = \sqrt[3]{\frac{3E_t + E_s}{4E}}$$

For most materials, curves C of Section 3.62 are sufficiently accurate representations of this plasticity correction coefficient.

If an element of a sandwich shell is subjected to in-plane shear or combined loadings, the maximum principal compressive stress in the facing sheet should be compared against σ_{cr} to determine whether wrinkling will occur. Theoretically, it has been shown that the wrinkling stress is unaffected by the stresses normal to the maximum compressive principal stress. However, Ref. 3-52 has indicated that if the principal stresses are both compression, the following reduction in K is necessary:

$$K_L = \frac{.43}{\sqrt[3]{1 + S^3}}$$

where

$$S = \frac{\text{minimum principal compressive stress in facing}}{\text{maximum principal compressive stress in facing}}$$

For a sandwich with orthotropic core, wrinkling should also be checked in the direction in which the shear modulus of the core is lowest.

3. 53 CYLINDERS

3. 53. 1 Axial Compression, Sandwich Cylinders

The curve presented in Ref. 3-56 will be used to determine the buckling stress for sandwich cylinders subjected to axial compression. The results are applicable to a sandwich with homogeneous isotropic unequal facing sheets with orthotropic core that does not carry in-plane loads. The design allowable buckling stress is

$$\frac{\sigma_{cr}}{\eta} = \gamma_1 C_c E \frac{h}{R} \frac{2\sqrt{t_1 t_2}}{\sqrt{1 - \mu^2} (t_1 + t_2)}$$

where

E = Young's modulus of the facing sheet material

μ = Poisson's ratio of the facing sheet material

$G_{xz}, G_{\theta z}$ = transverse shear moduli of the core in the longitudinal and circumferential directions, respectively

The buckling coefficient, C_c , and a definition of the geometrical parameters are given in Fig. 3. 53-1. The correction factor, γ , was introduced to reduce the theoretical results of Ref. 3-56 to values that can be used for design purposes. The factor γ_1 can be obtained from Fig. 3. 33-6 where

$$\rho = \sqrt{t_1 t_2 h^2 / (t_1 + t_2)}$$

Existing test data show that the value of γ_1 may be conservative for some values of the parameters, but a sufficient number of tests have not been conducted to justify increasing the value of γ_1 .

The method for obtaining γ_1 is discussed in Paragraph 3.33.1 for orthotropic cylinders. This method would be consistent if the shear stiffness of the core is large (i. e. , when V_c is small). Due to manufacturing limitation and local instability problems, V_c is usually small. However, if V_c is large (i. e. , when $V_c > 0.5$), γ_1 would approach 1. There is not enough information available to obtain γ_1 as a function of V_c ; therefore, Fig. 3.33-6 should be used to obtain γ_1 for all values of $V_c < 0.5$.

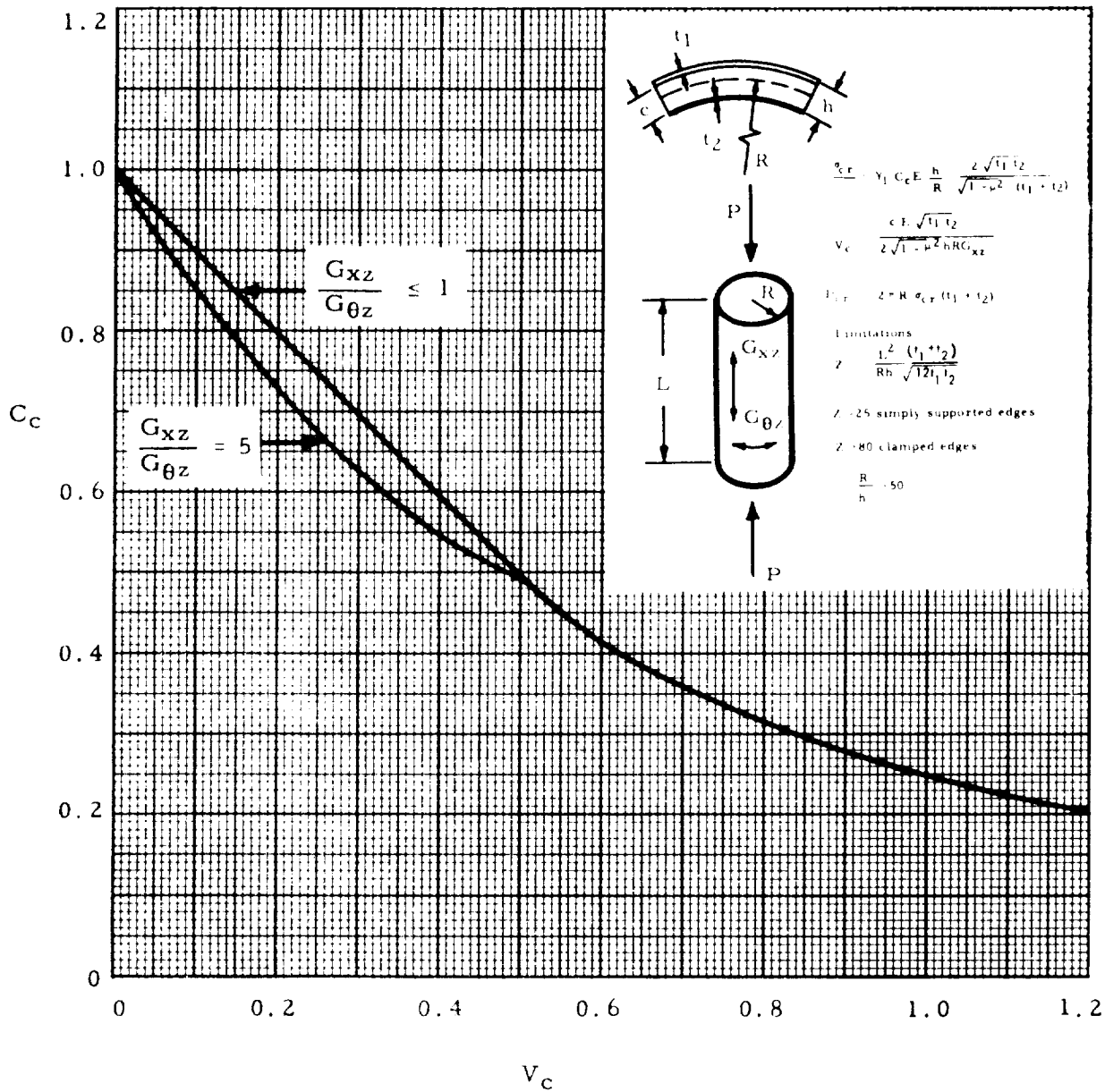
The curve presented in Fig. 3.53-1 is for a sandwich with very thin facing sheets ($c/h \approx 1$). For small values of c/h , the results of Fig. 3.53-1 may yield excessive error for certain values of the parameters. For values of $c/h > 0.9$, Fig. 3.53-1 should be adequate for $V_c > 0.5$. Sandwich cylinders subjected to axial compression must be analyzed for local instability as discussed in Section 3.52.

For elastic buckling, the plasticity correction term, $\eta = 1$, is used. In the inelastic range, an estimate of the stress, σ_{CR} , can be found by using curves E_1 in Section 3.62. The parameter V_c is a function of the stress level for stresses above the proportional limit.

By assuming V_s is independent of the stress level, the results will be conservative. For most practical designs, the difference will be very small.

References 3-62 and 3-63 may be used to obtain buckling loads for sandwich cylinders with corrugated core subjected to axial compression.

FIG. 3.53-1. CLASSICAL BUCKLING COEFFICIENT FOR SANDWICH CYLINDERS SUBJECTED TO AXIAL COMPRESSION



3.53.2 Torsion of Shear, Sandwich Cylinders

The curves presented in Ref. 3-57 will be used to determine the buckling stress for sandwich cylinders subjected to torsion. The results are applicable to a sandwich with homogeneous isotropic unequal facing sheets and an orthotropic core which does not carry in-plane loads. The design allowable shear buckling stress is

$$\frac{\tau_{cr}}{\eta} = \gamma C_s E \frac{h_1}{R}$$

where

E = Youngs' modulus of the facing sheet material

G_{xz} , $G_{\theta z}$ = transverse shear modulus of the core in the longitudinal and circumferential directions, respectively

A definition of the geometrical parameters and C_s can be obtained from Figs. 3.53-2 through 3.52-7. The correction factor, γ , was introduced to reduce the theoretical results of Ref. 3-57 to values that can be used for design. γ can be obtained from Fig. 3.33-8.

where

$$\rho = \sqrt{t_1 t_2 h^2} / (t_1 + t_2)$$

The method for obtaining Fig. 3.33-8 is discussed in Paragraph 3.33.2 for orthotropic cylinders. The correction factor used in Paragraph 3.33.2 and this section would be consistent if V_s is small (i.e.,

a core with relatively large shear stiffness). Due to manufacturing limitations and local instability considerations, V_g is usually small. However, if V_g is large, γ will approach 1 for all values of R/ρ . There is no information available to obtain γ as a function of V_g .

Figure 3.53-3 predicts results that are, at most, about 6-percent higher than the results of Ref. 3-58 for isotropic sandwich cylinders with simple supports. Therefore, the results presented in Figs. 3.53-2 through 3.53-7 are probably sufficiently accurate for cylinders with simply supported edges.

Sandwich cylinders subjected to torsion must be analyzed for local instability, as discussed in Section 3.52. For elastic buckling, the plasticity correction term, $\eta = 1$, is used. If the stresses are above the proportional limit, the procedure discussed in Paragraph 3.22.2 can be used. The parameter, V_g , is also a function of the stress level for stresses above the proportional limit. By assuming that V_g is independent of the stress level, the results will be conservative. For most practical designs, the differences will be small.

References 3-62 and 3-63 can be used to obtain the buckling load for sandwich cylinders with corrugated core subjected to torsion.

FIG. 3.53-2. BUCKLING COEFFICIENTS FOR CYLINDERS HAVING ISOTROPIC FACINGS $\frac{c}{h} = 1.0$, $G_{xz}/G_{\theta z} = 0.4$

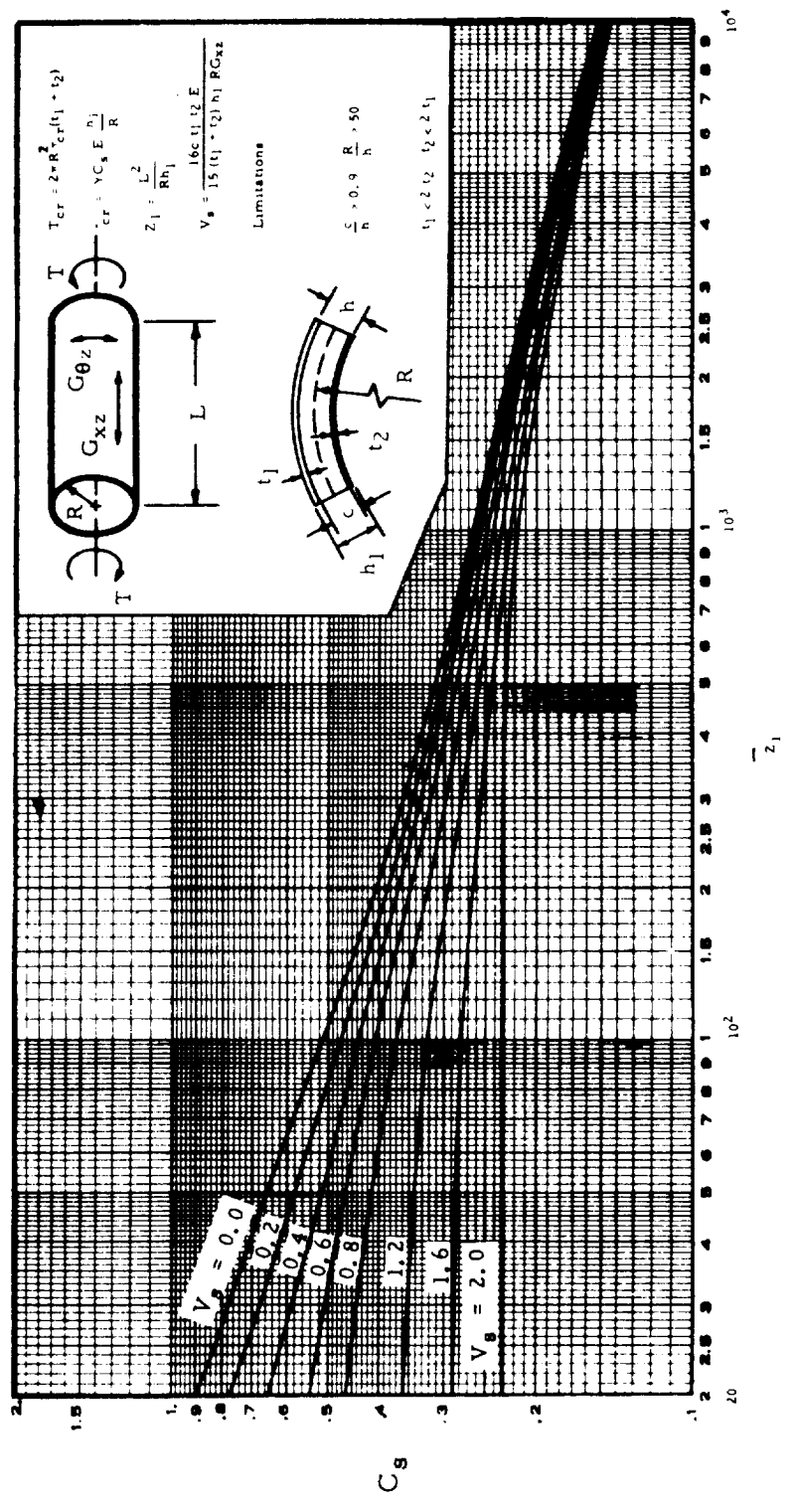


FIG. 3.53-3. BUCKLING COEFFICIENTS FOR CYLINDERS HAVING ISOTROPIC FACINGS $\frac{c}{h} = 1.0$, $G_{xz}/G_{\theta z} = 1.0$

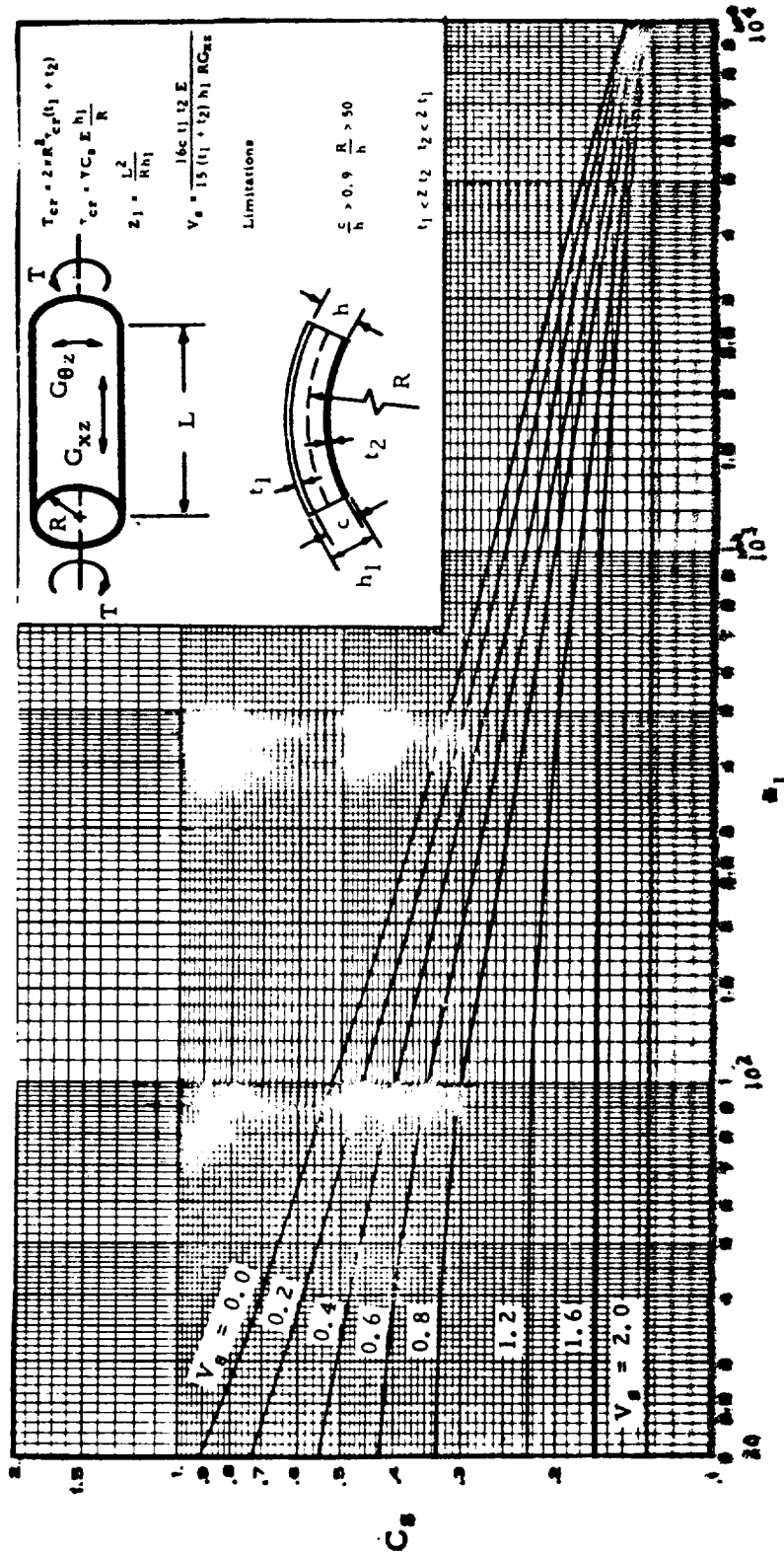


FIG. 3.53-4. BUCKLING COEFFICIENTS FOR CYLINDERS HAVING ISOTROPIC FACINGS $\frac{C}{h} = 1.0$, $G_{xz}/G_{\theta z} = 2.5$

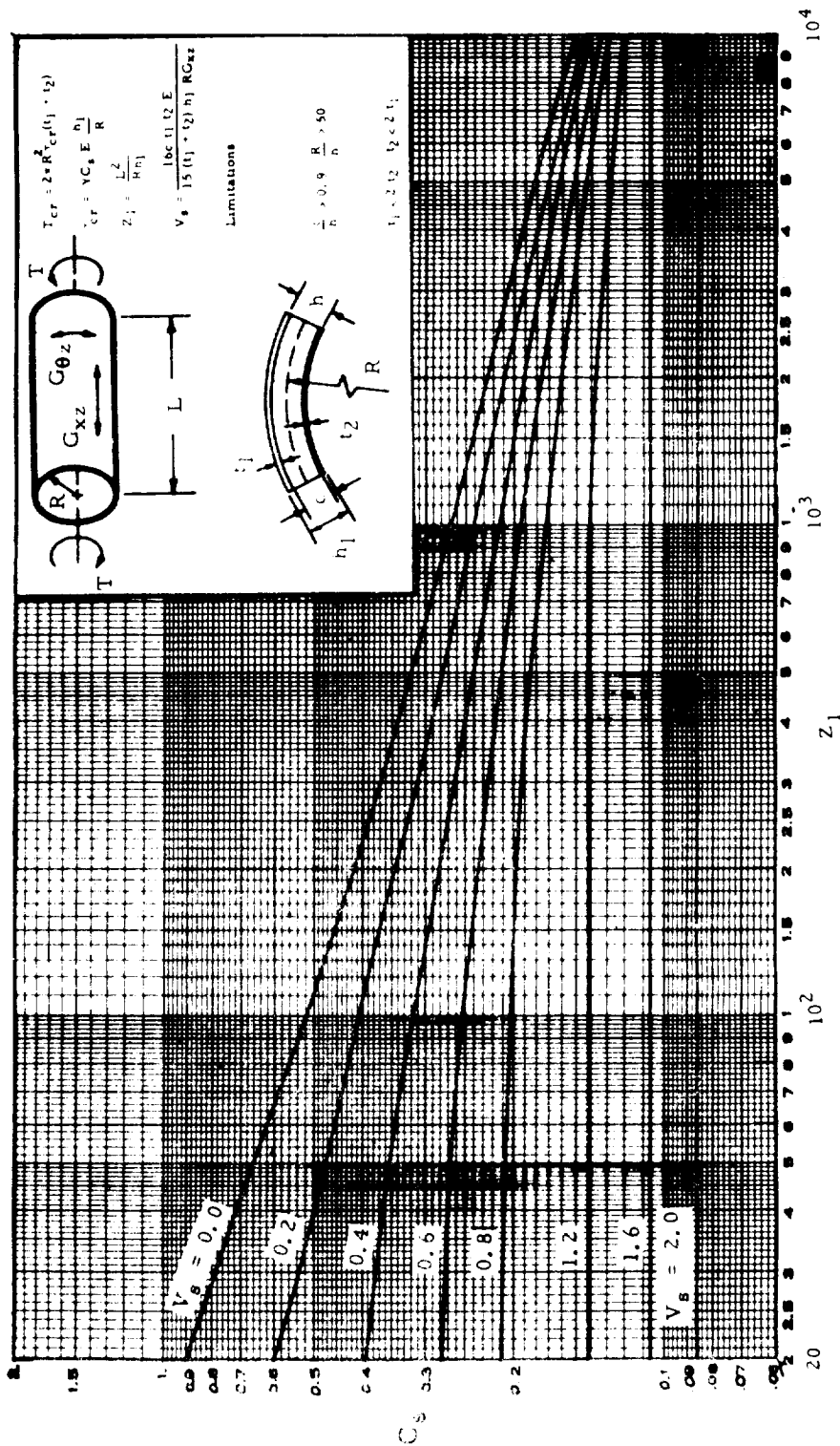


FIG. 3.53-5. BUCKLING COEFFICIENTS FOR CYLINDERS HAVING ISOTROPIC FACINGS $\frac{c}{h} = .82$, $C_{xz}/G\theta_z = 0.4$

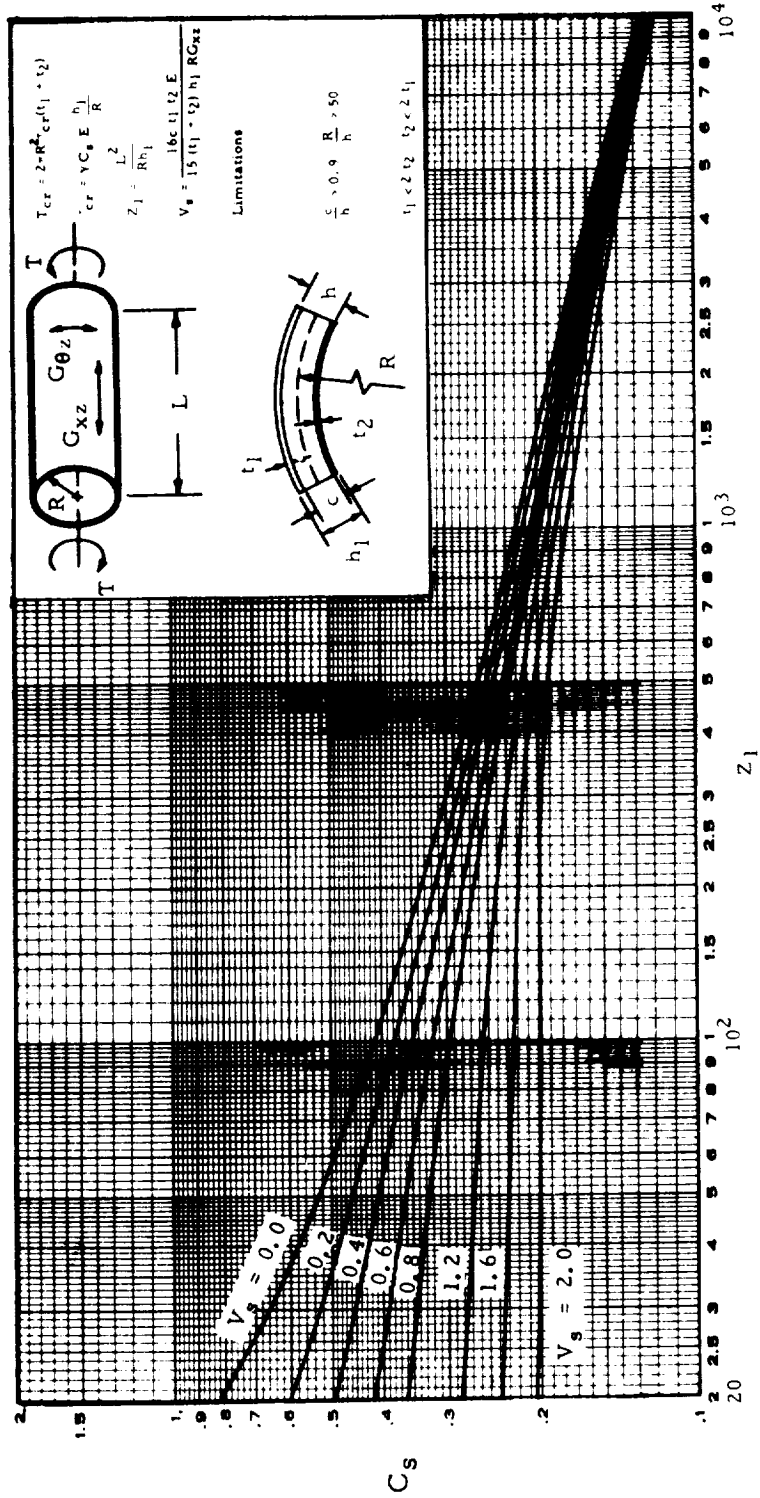


FIG. 3.53-6. BUCKLING COEFFICIENTS FOR CYLINDERS HAVING
ISOTROPIC FACINGS $\frac{c}{h} = .82$, $G_{xz}/G_{\theta z} = 1.0$

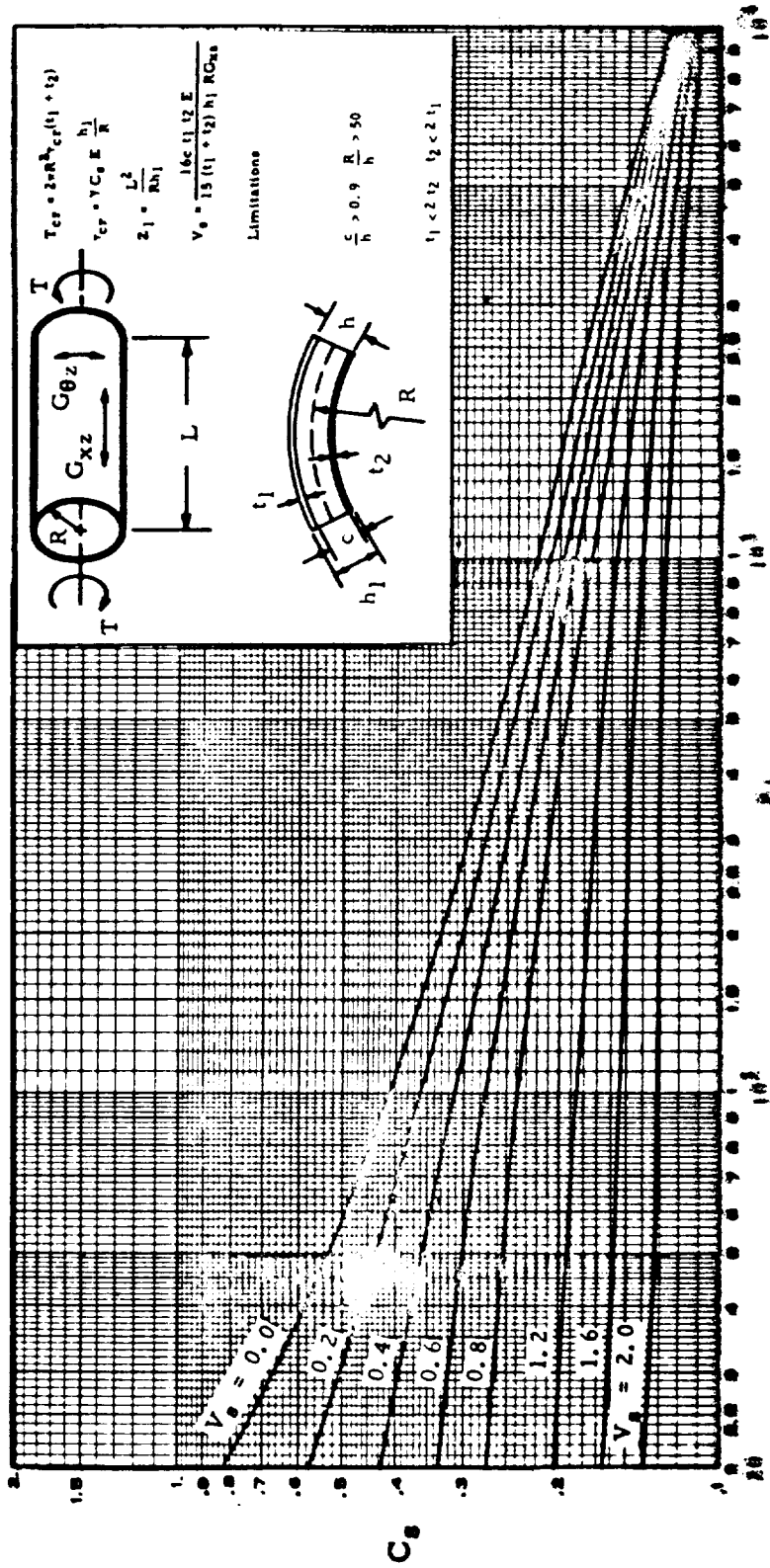
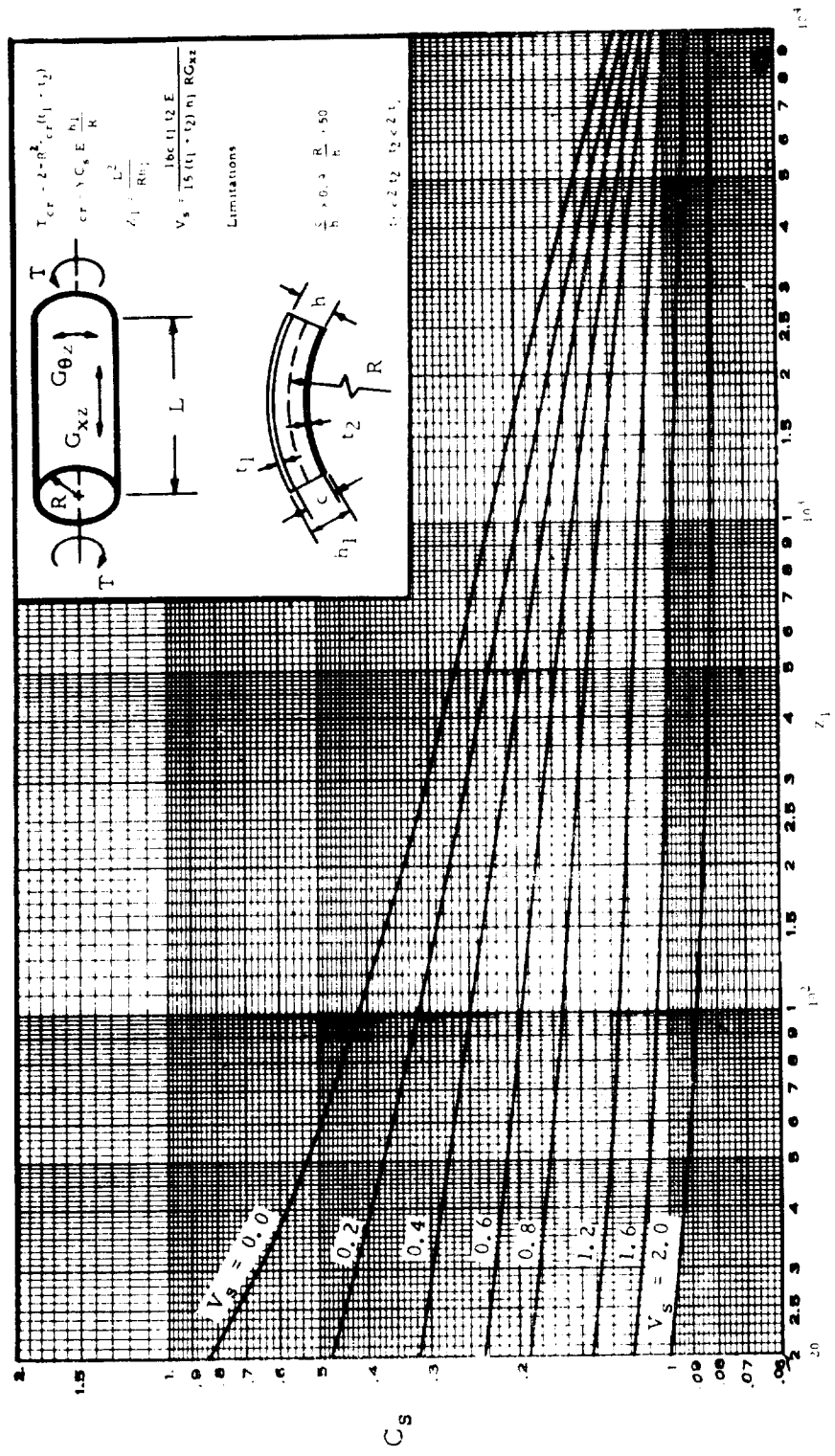


FIG. 3.53-7. BUCKLING COEFFICIENTS FOR CYLINDERS HAVING ISOTROPIC FACINGS $\frac{c}{h} = .82$, $G_{xz}/G_{\theta z} = 2.5$



3.53.3 Bending, Sandwich Cylinders

The formula presented in Paragraph 3.53.1 can be used to determine the design allowable buckling stress for unpressurized sandwich cylinders subjected to bending if γ_1 is obtained from Fig. 3.33-9.

$$\rho = \sqrt{t_1 t_2 h^2} / (t_1 + t_2)$$

For bending, σ_{cr} is the maximum compressive stress due to the bending moment (outer fiber stress). Figure 3.33-9 is based on the correction factors used to modify the small deflection theoretical results for homogeneous isotropic cylinders subjected to bending.

Existing test data show that the value of γ_1 may be conservative for some values of the parameters, but there has not been a sufficient number of tests conducted to justify increasing the value of γ_1 .

3.53.4 Lateral External Pressure, Sandwich Cylinders

The curves presented in Ref. 3-59 will be used to determine the buckling stress for sandwich cylinders with simply supported edges subjected to lateral external pressure. The results are applicable for a sandwich with isotropic facings of equal or unequal thickness and of the same or different materials. The core material may be orthotropic or isotropic but may not carry in-plane loads. The design allowable

buckling pressure is

$$P_{cr} = \frac{\gamma C_p}{(1 - \mu^2)} \frac{(E_1 t_1 + E_2 t_2)}{R}$$

where

E_1, E_2 = Young's moduli of the outer and inner facing sheets,
respectively

$G_{xz}, G_{\theta z}$ = transverse shear moduli of the core in the longitudinal
and circumferential directions, respectively

$$\mu = (\mu_1 E_1 t_1 + \mu_2 E_2 t_2) / (E_1 t_1 + E_2 t_2)$$

μ_1, μ_2 = Poisson's ratios of the outer and inner facing sheets,
respectively

The buckling coefficient, C_p , and a definition of the geometrical parameters may be obtained from Figs. 3.53-8 through 3.53-23. The coefficient γ was introduced to reduce the theory presented in Ref. 3-59 by the same percentage as the theory for homogeneous isotropic cylinders was reduced to obtain the curve presented in Fig. 3.23-7. Therefore, if

$$Z_p = \frac{(E_1 t_1 + E_2 t_2)}{\sqrt{12 E_1 t_1 E_2 t_2}} \frac{L^2}{Rh} (1 - \mu^2)^{1/2}$$

$$\gamma = 0.9 \text{ for } Z_p > 10^2$$

$$\gamma = 1 - Z_p \times 10^{-3} \text{ for } Z_p < 10^2$$

For large values of L/R , it can be seen that C_p becomes independent of $\frac{L}{R}$.

The design allowable buckling pressure can then be obtained from

$$P_{cr} = \frac{3\gamma D_{\theta}}{R^3 \left[1 + 4D_{\theta} / (R^2 G_{\theta z} h) \right]}$$

where

$$D_{\theta} = \frac{E_1 t_1 E_2 t_2 h^2}{(1 - \mu^2) (E_1 t_1 + E_2 t_2)}$$

The pressure, p_{cr} , is the design allowable pressure for complete buckling of the cylinder (e. g., when buckles have formed all the way around the cylinder). For some values of the parameters, single buckles will occur at pressure less than p_{cr} ; therefore, if single buckles are not allowable for a particular design, the results of this section may be unconservative. In addition, if single buckles occur at pressures less than p_{cr} , the resulting stresses may fail the core, causing a complete collapse of the cylinders. However, sandwich shells are generally relatively stiff with only small initial imperfection; therefore, for most cases, sandwich shells will be considerably less likely to have single isolated buckles at pressures less than the design allowable pressures which have been given.

The curves presented in Figs. 3.53-8 through 3.53-23 are for a sandwich construction with very thin facing sheets ($\frac{c}{h} \approx 1$). For small values of $\frac{c}{h}$, the results of Figs. 3.53-8 through 3.53-23 may yield excessive errors for certain values of the parameters. For values of $\frac{c}{h} > 0.9$, the curves should be adequate.

Sandwich cylinders subjected to lateral pressure must be analyzed for local instability as described in Section 3.52. If the stresses are above the proportional limit and both facing sheets are made of the same material, the procedure discussed in Paragraph 3.23.4 can be used. The parameter, V_p , is also a function of the stress level for stresses above the proportional limit. By assuming that V_g is independent of the stress level, the results will be conservative. For most practical designs, the difference will be small.

References 3-62 and 3-63 may be used to obtain buckling loads for sandwich cylinders with corrugated core subjected to external pressure.

FIG. 3.53 -8. VALUES OF C_p FOR $V_p = 0$, AND FOR $\frac{E_1 t_1}{E_2 t_2} = 1$

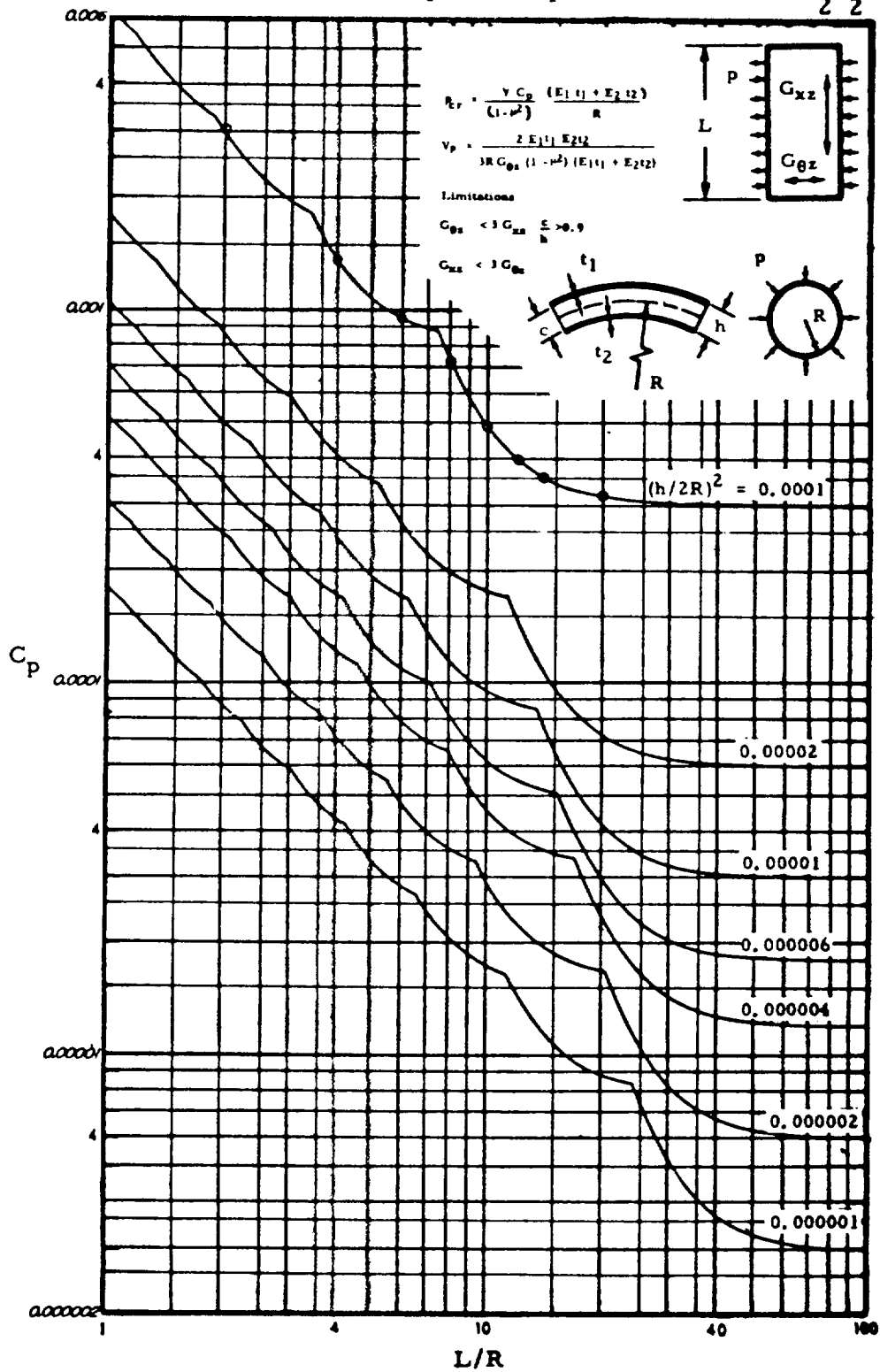


FIG. 3.53-9. VALUES OF C_p FOR $\nu_p = 0$, AND FOR $\frac{E_1 t_1}{E_2 t_2} = 2$

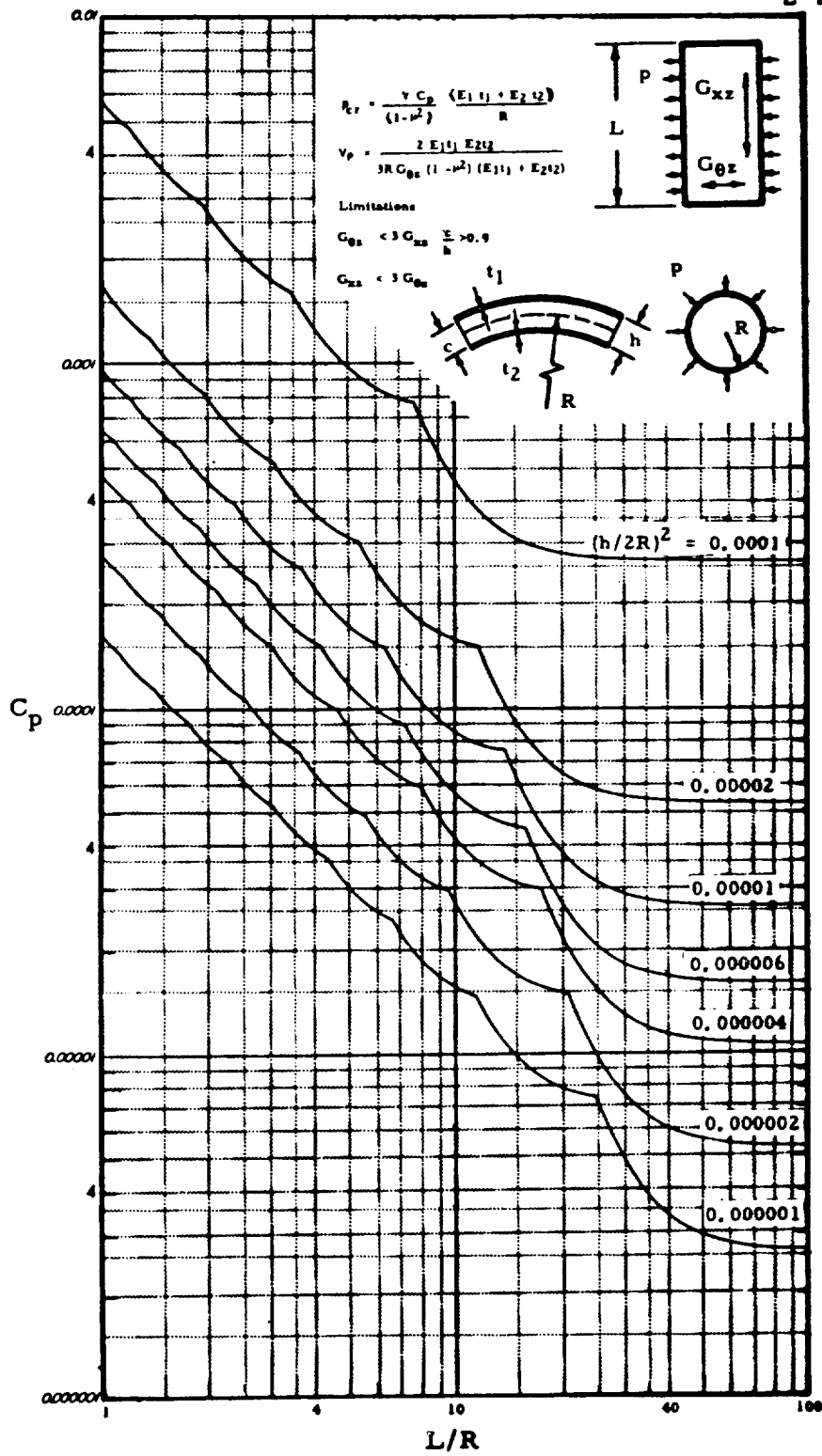


FIG. 3.53-10. VALUES OF C_p FOR $V_p = 0$, AND FOR $\frac{E_1 t_1}{E_2 t_2} = 3$

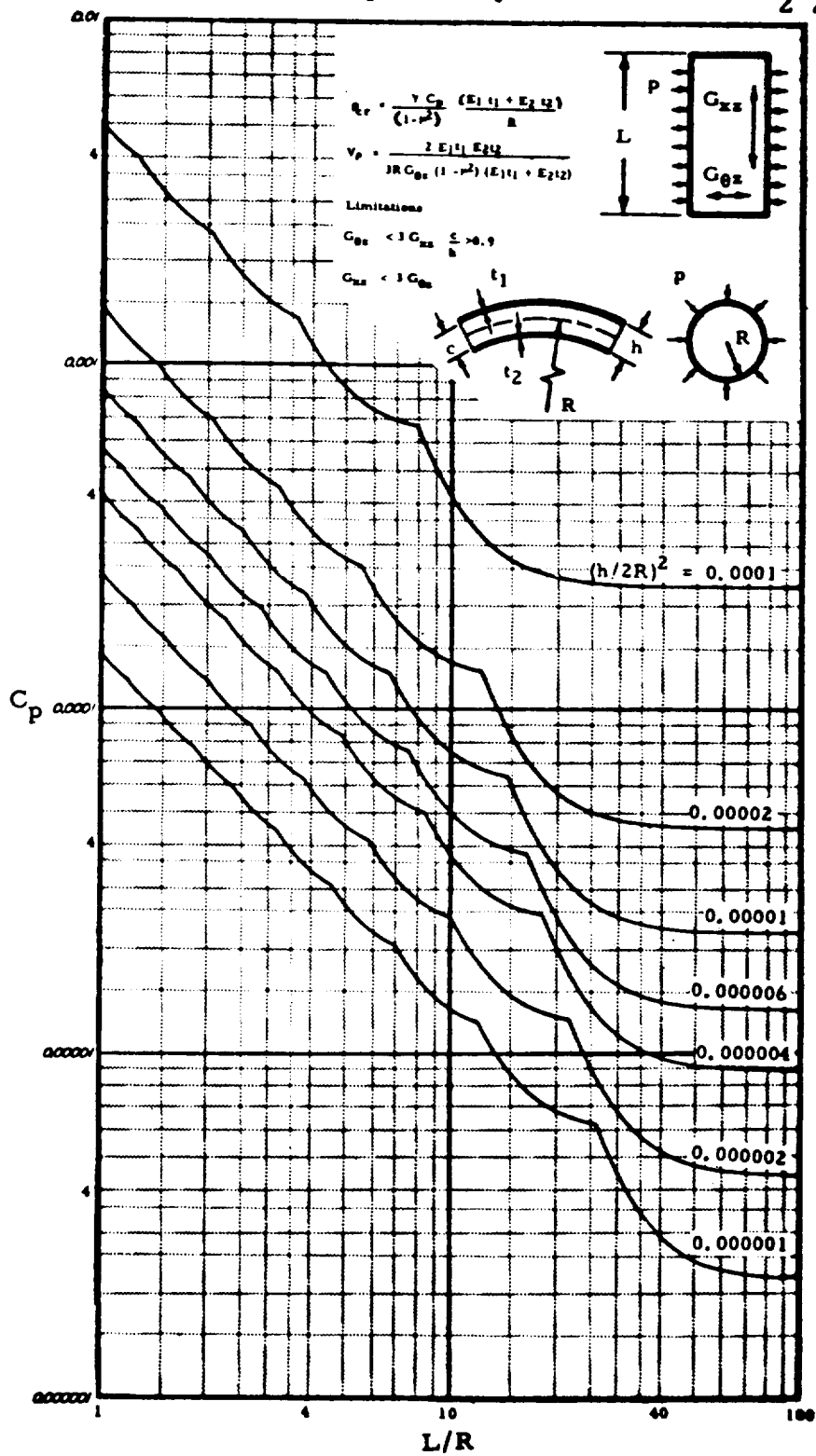


FIG. 3.53-11. VALUES OF C_p FOR $V_p = 0$, AND FOR $\frac{E_1 t_1}{E_2 t_2} = 4$

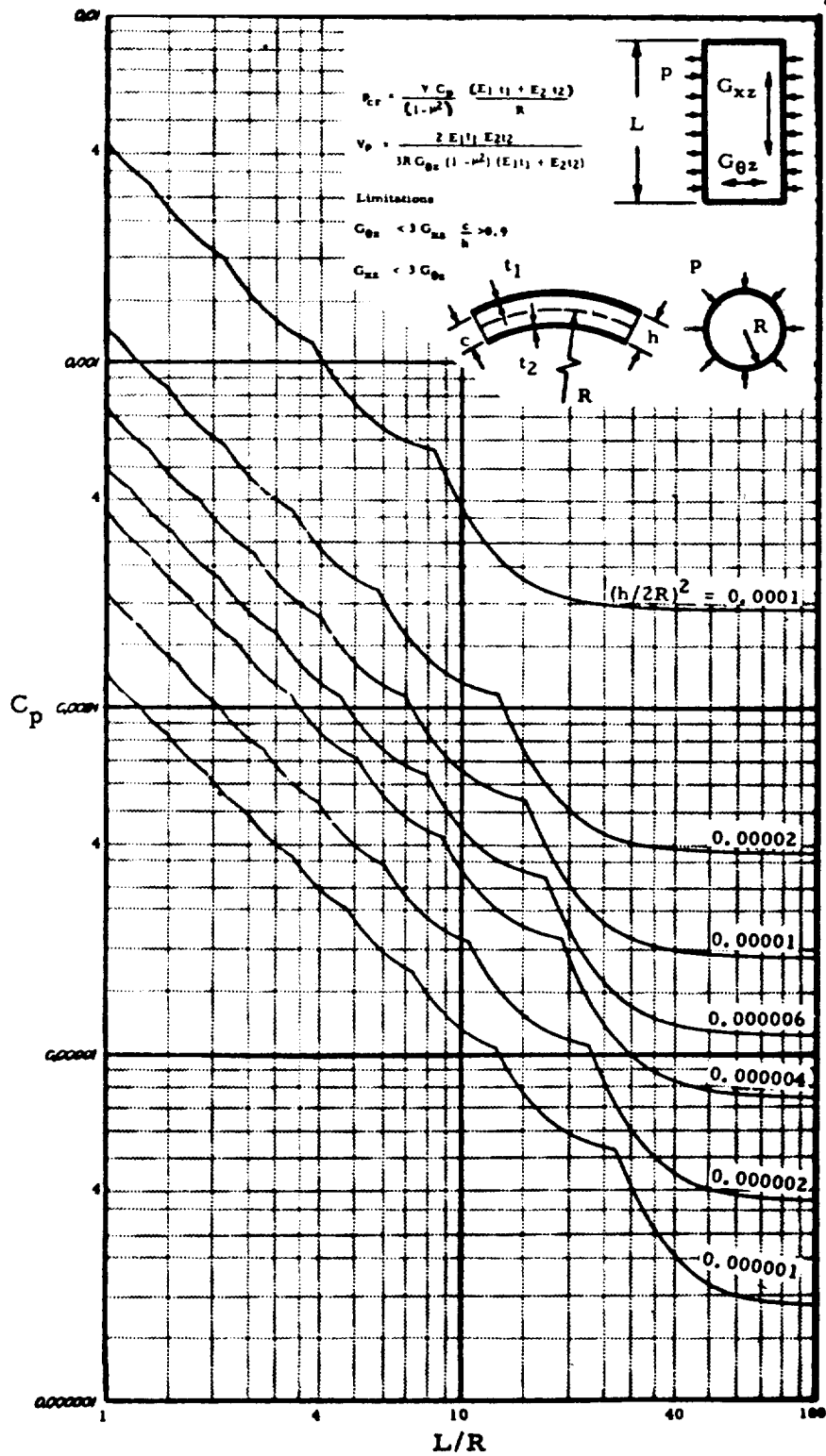


FIG. 3.53-12. VALUES OF C_p FOR $V_p = 0.5$, AND FOR $\frac{E_1 t_1}{E_2 t_2} = 1$

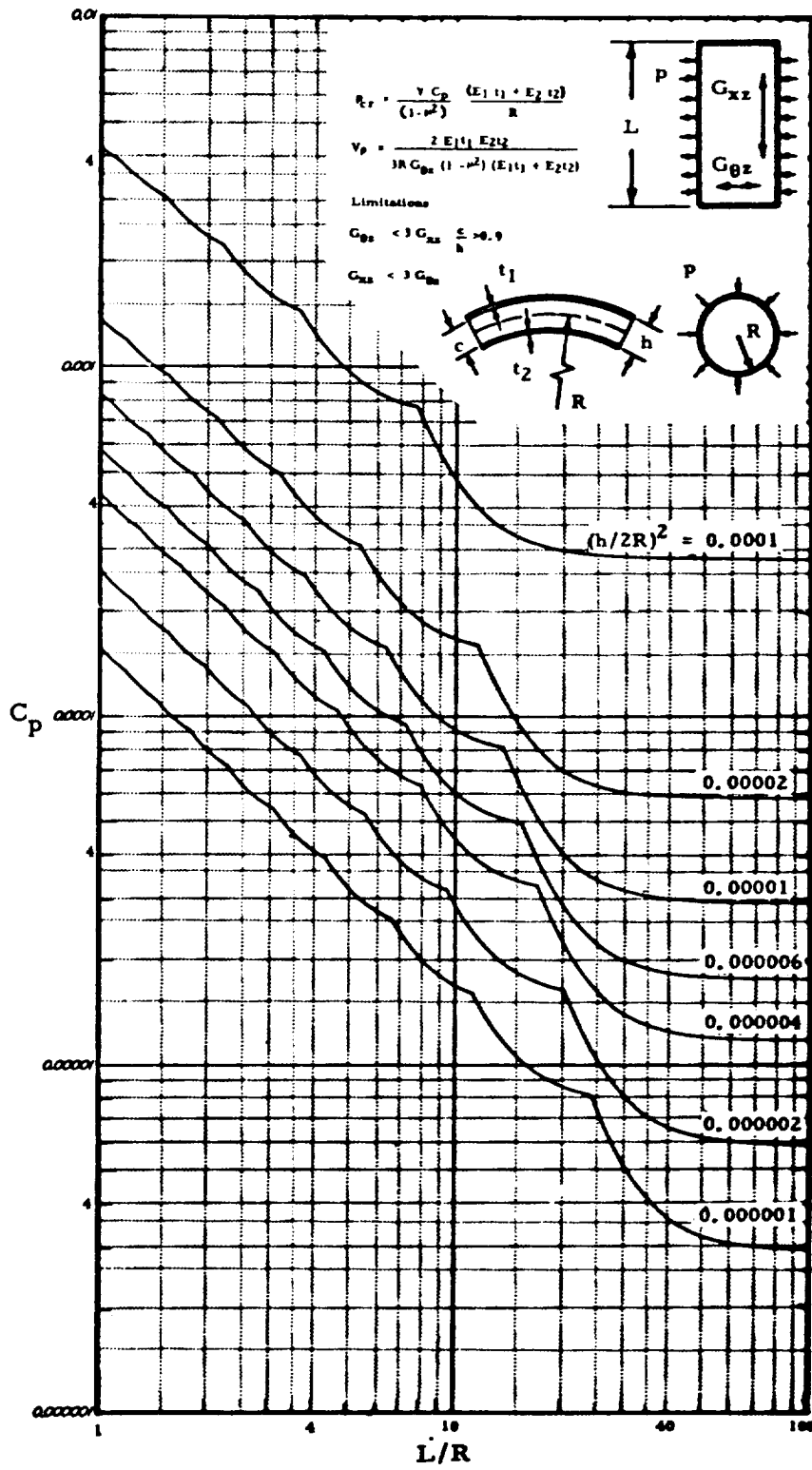


FIG. 3.53-13. VALUES OF C_p FOR $V_p = 0.5$ AND FOR $\frac{E_1 t_1}{E_2 t_2} = 2$

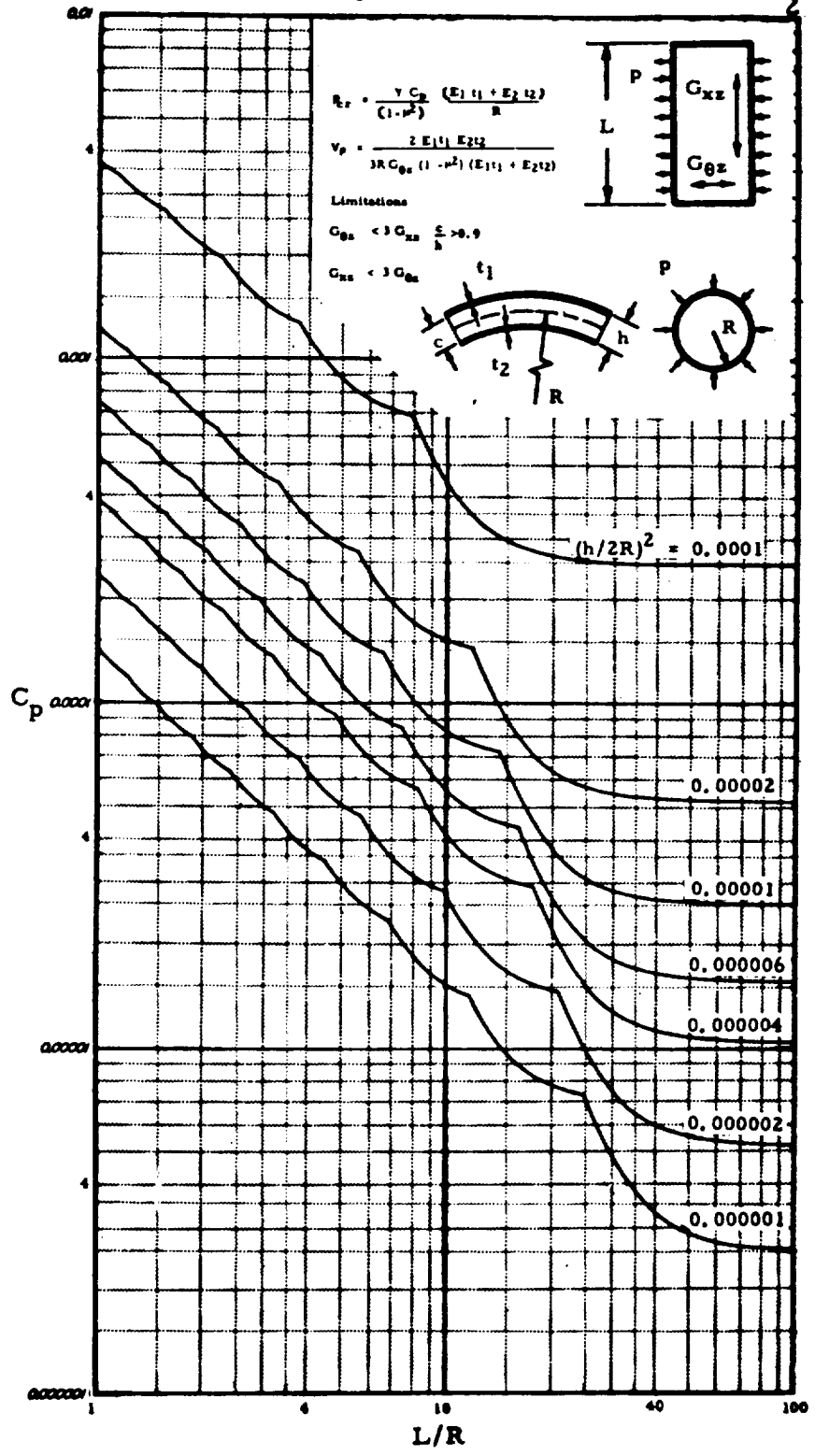


FIG. 3.53-14. VALUES OF C_p FOR $\nu_p = 0.5$, AND FOR $\frac{E_1 t_1}{E_2 t_2} = 3$.

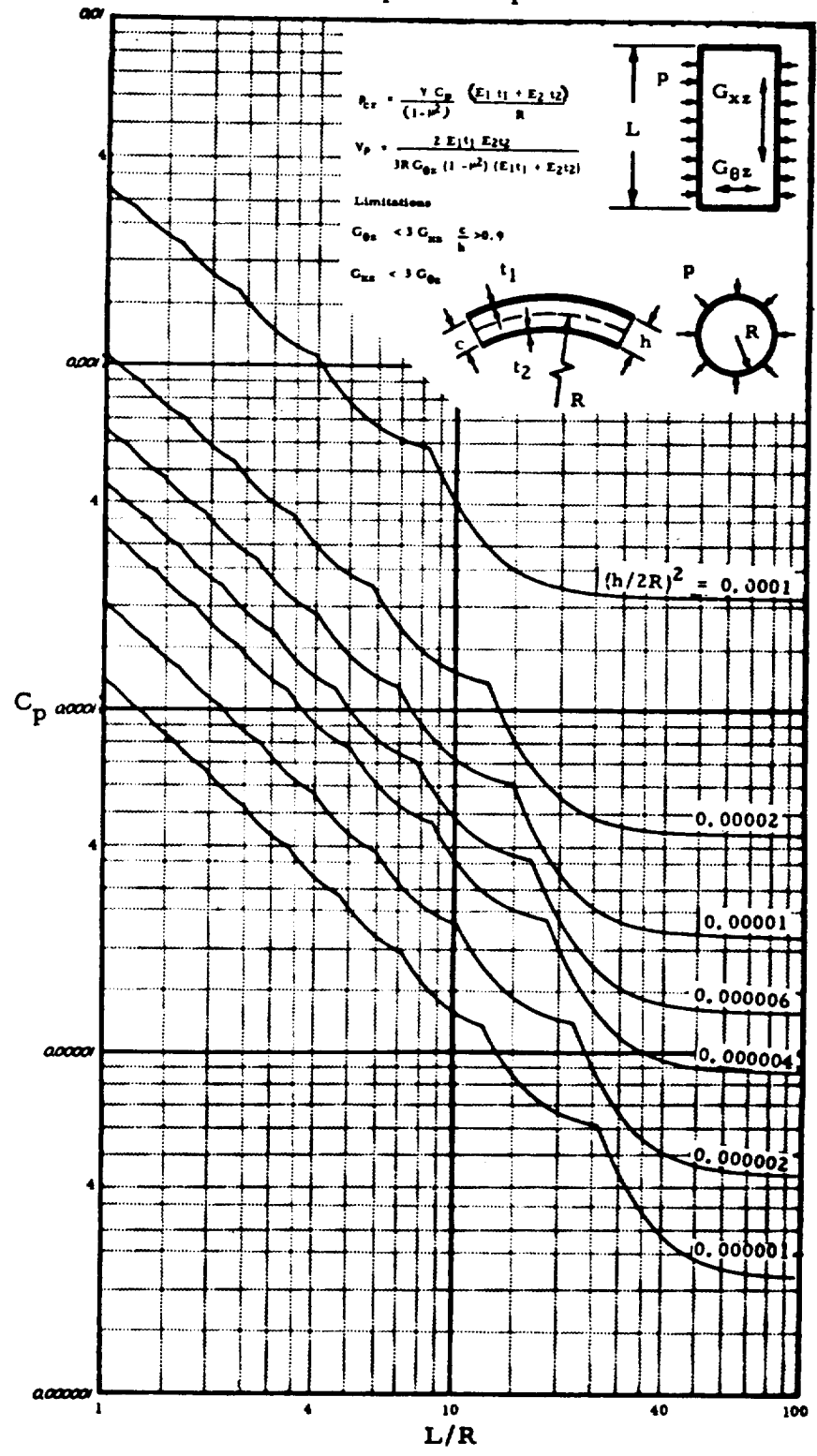


FIG. 3.53-15. VALUES OF C_p FOR $V_p = 0.5$, AND FOR $\frac{E_1 t_1}{E_2 t_2} = 4$

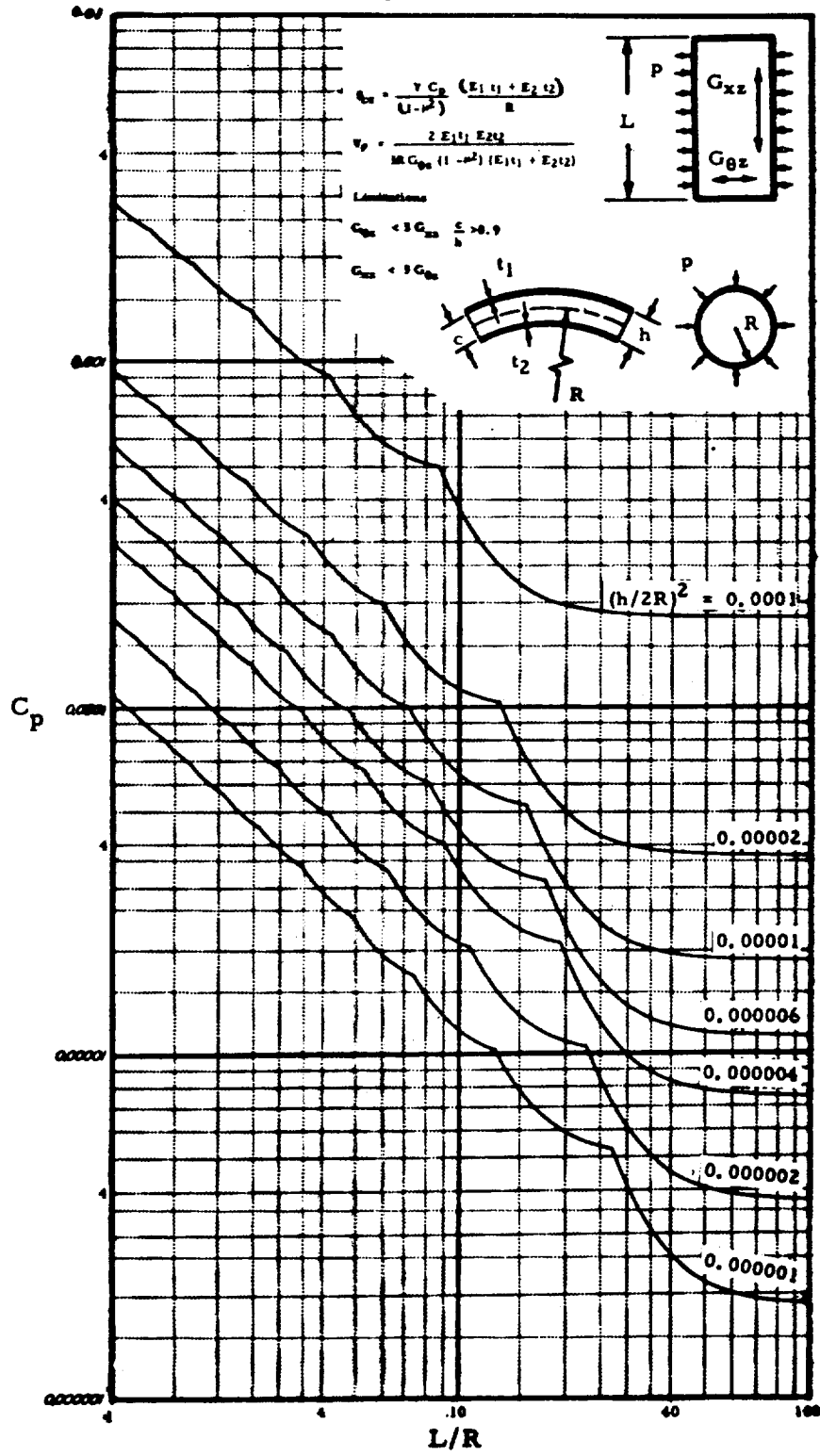


FIG. 3.53-16. VALUES OF C_p FOR $V_p = 1$, AND FOR $\frac{E_1 t_1}{E_2 t_2} = 1$

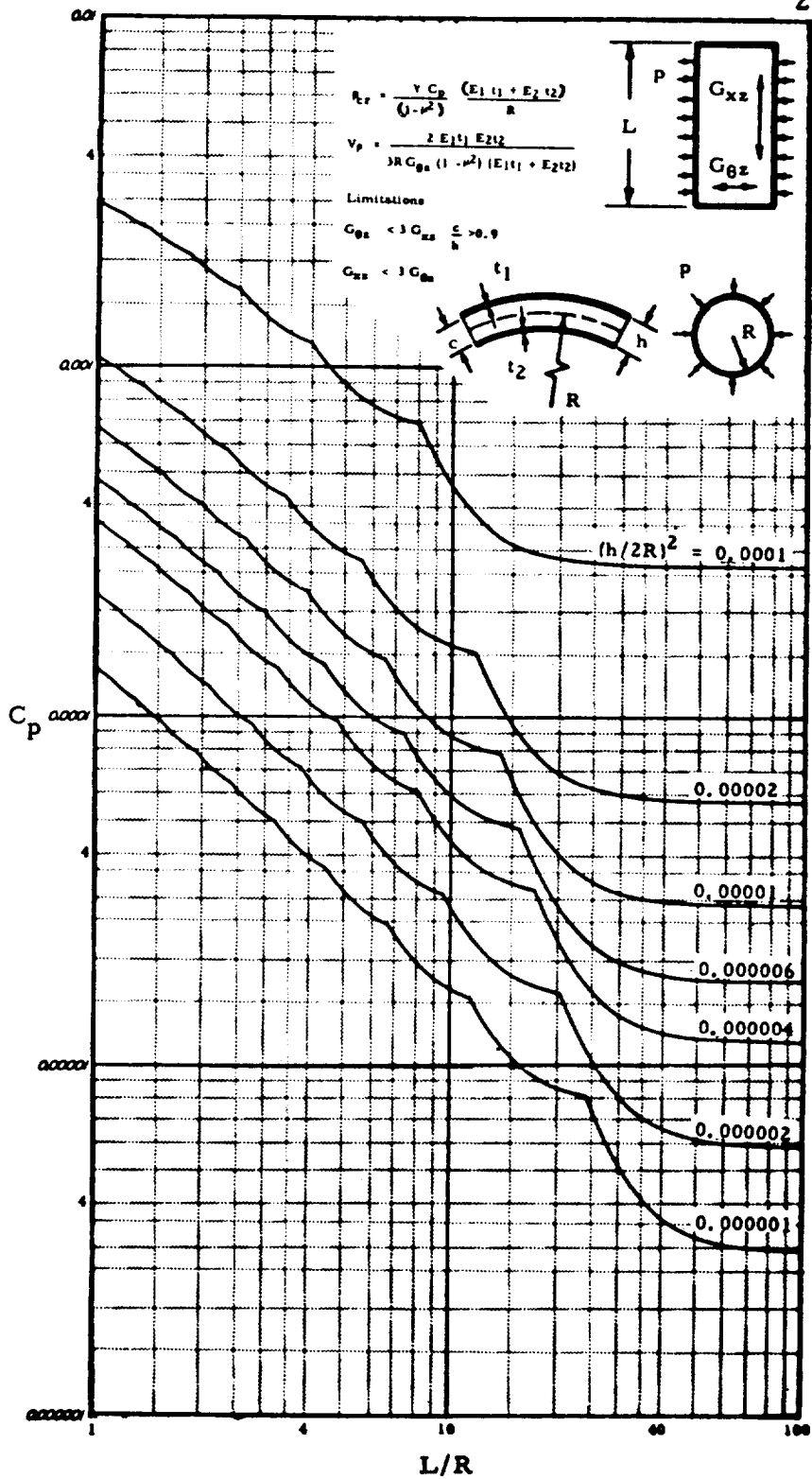


FIG. 3.53-17. VALUES OF C_p FOR $V_p = 1$, AND FOR $\frac{E_1 t_1}{E_2 t_2} = 2$

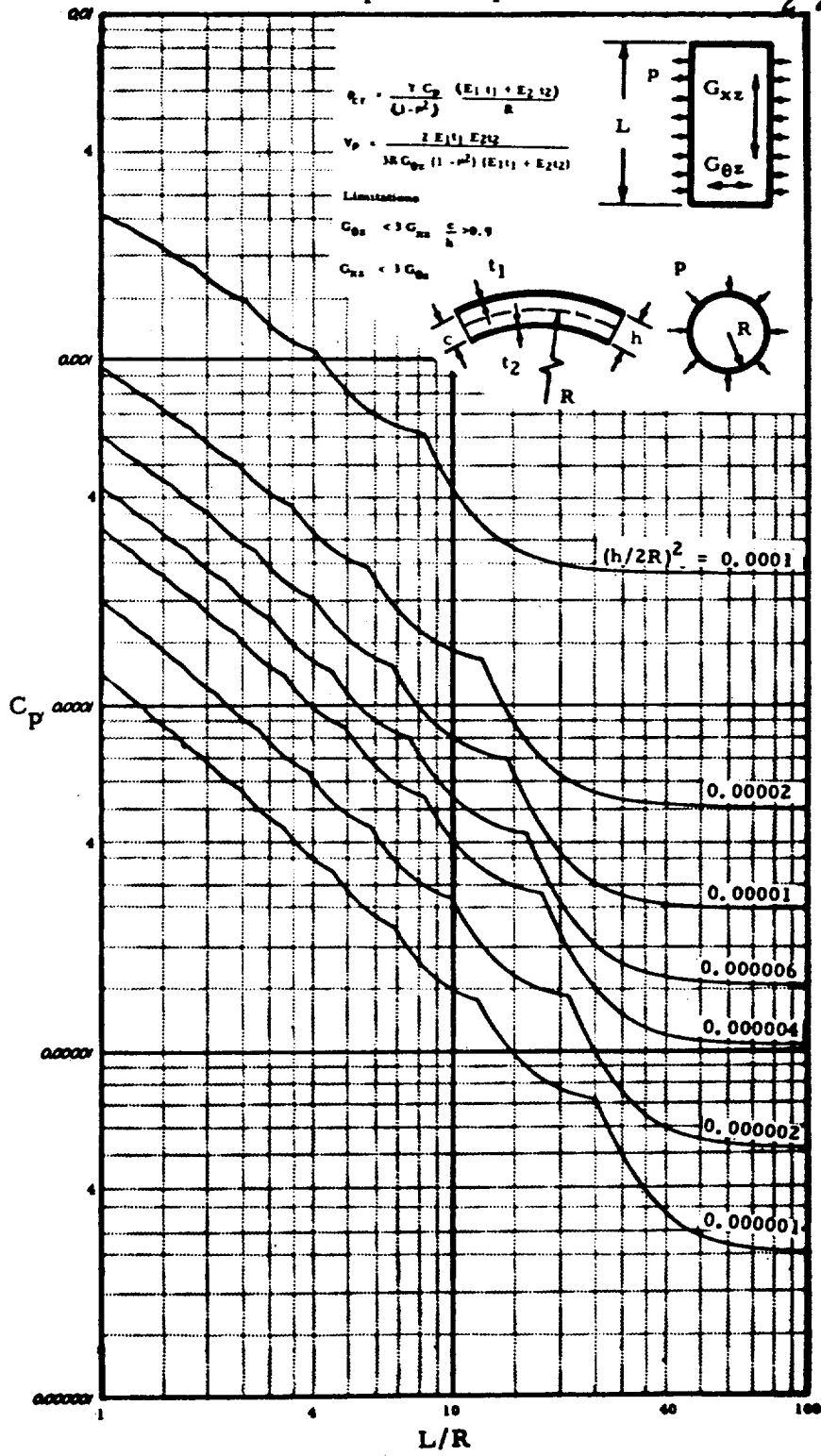


FIG. 3.53-18. VALUES OF C_p FOR $V_p = 1$, AND FOR $\frac{E_1 t_1}{E_2 t_2} = 3$

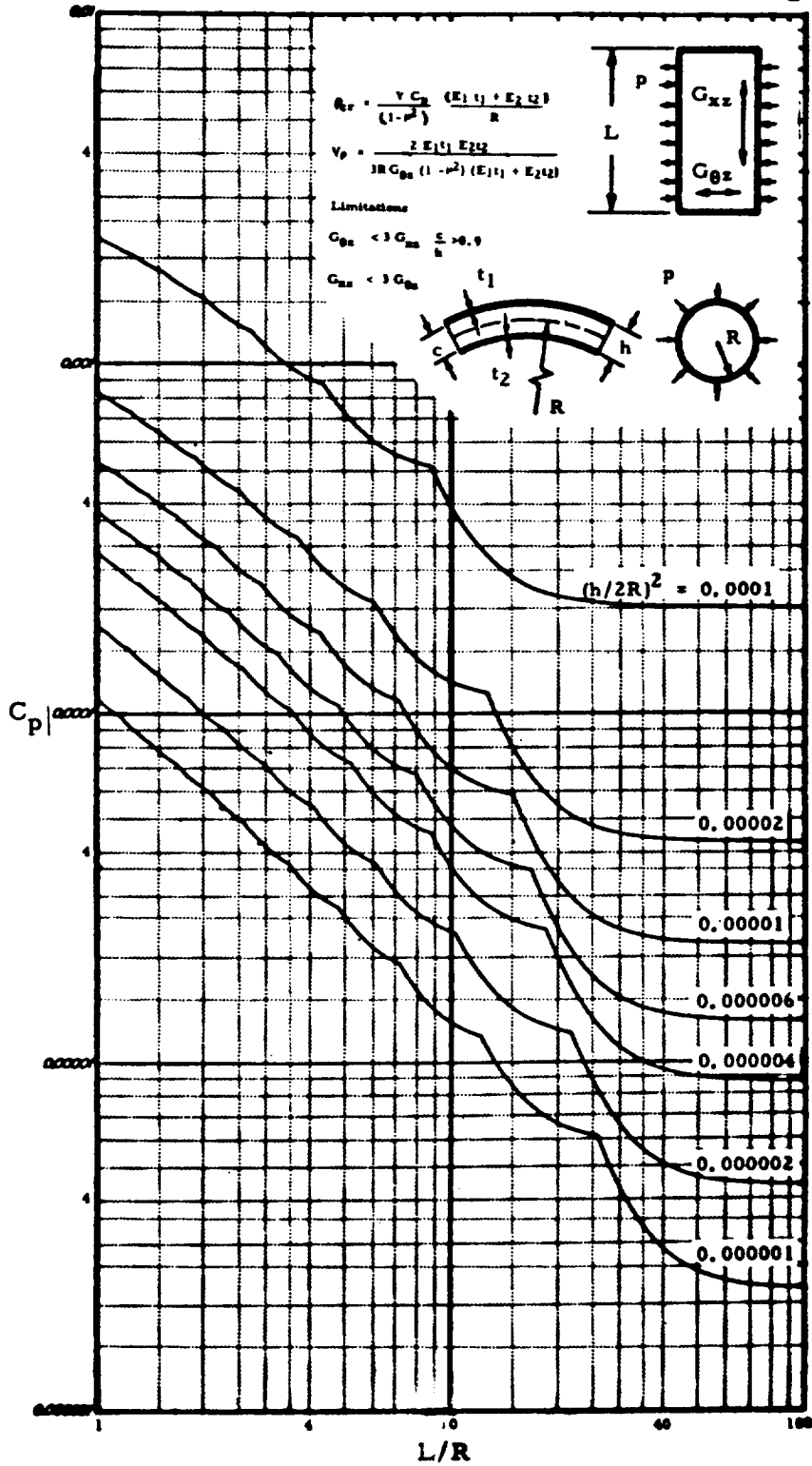


FIG. 3.53-19. VALUES OF C_p FOR $V_p = 1$, AND FOR $\frac{E_1 t_1}{E_2 t_2} = 4$

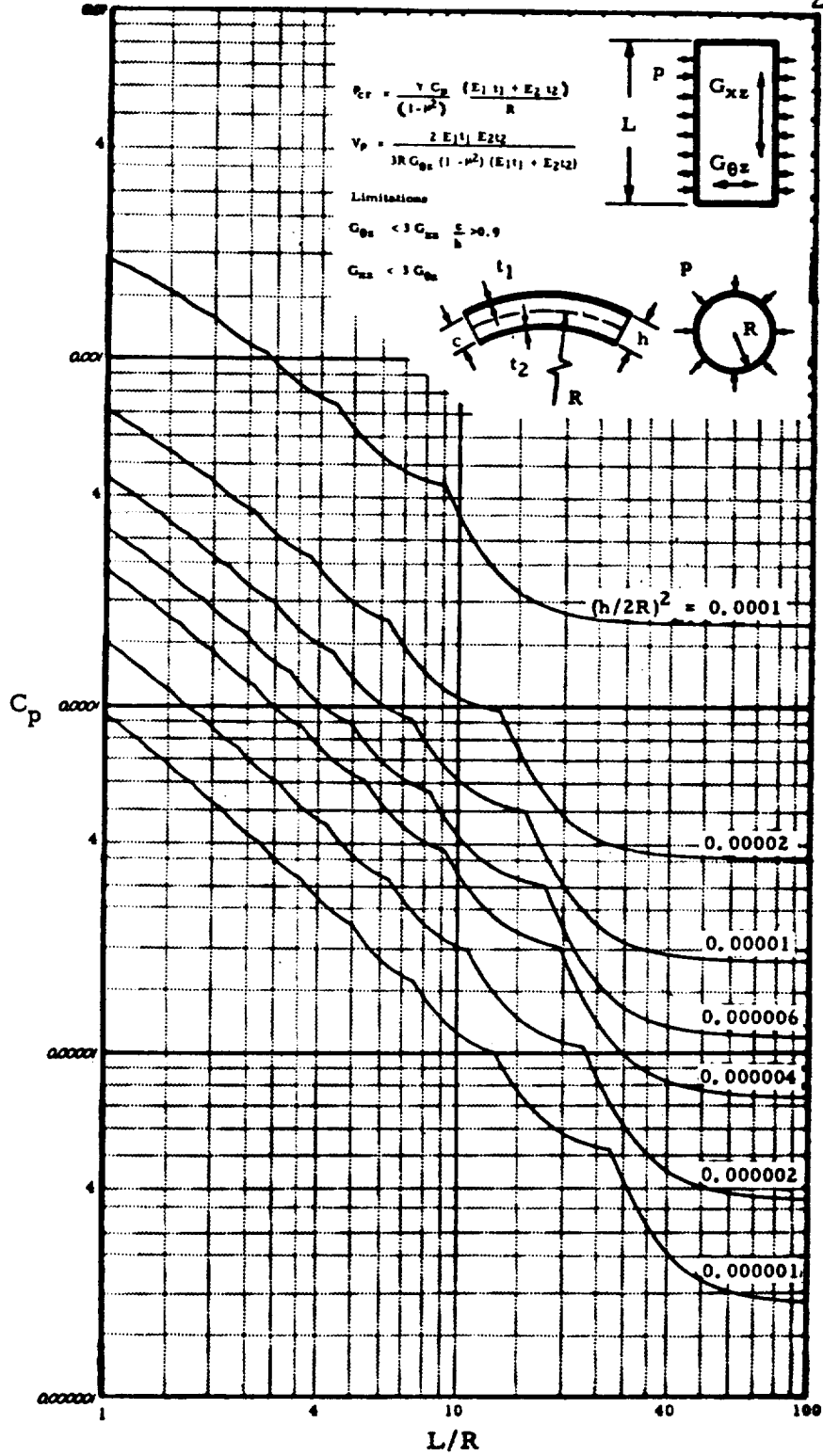


FIG. 3.53-20. VALUES OF C_p FOR $V_p = 1.5$, AND FOR $\frac{E_1 t_1}{E_2 t_2} = 1$

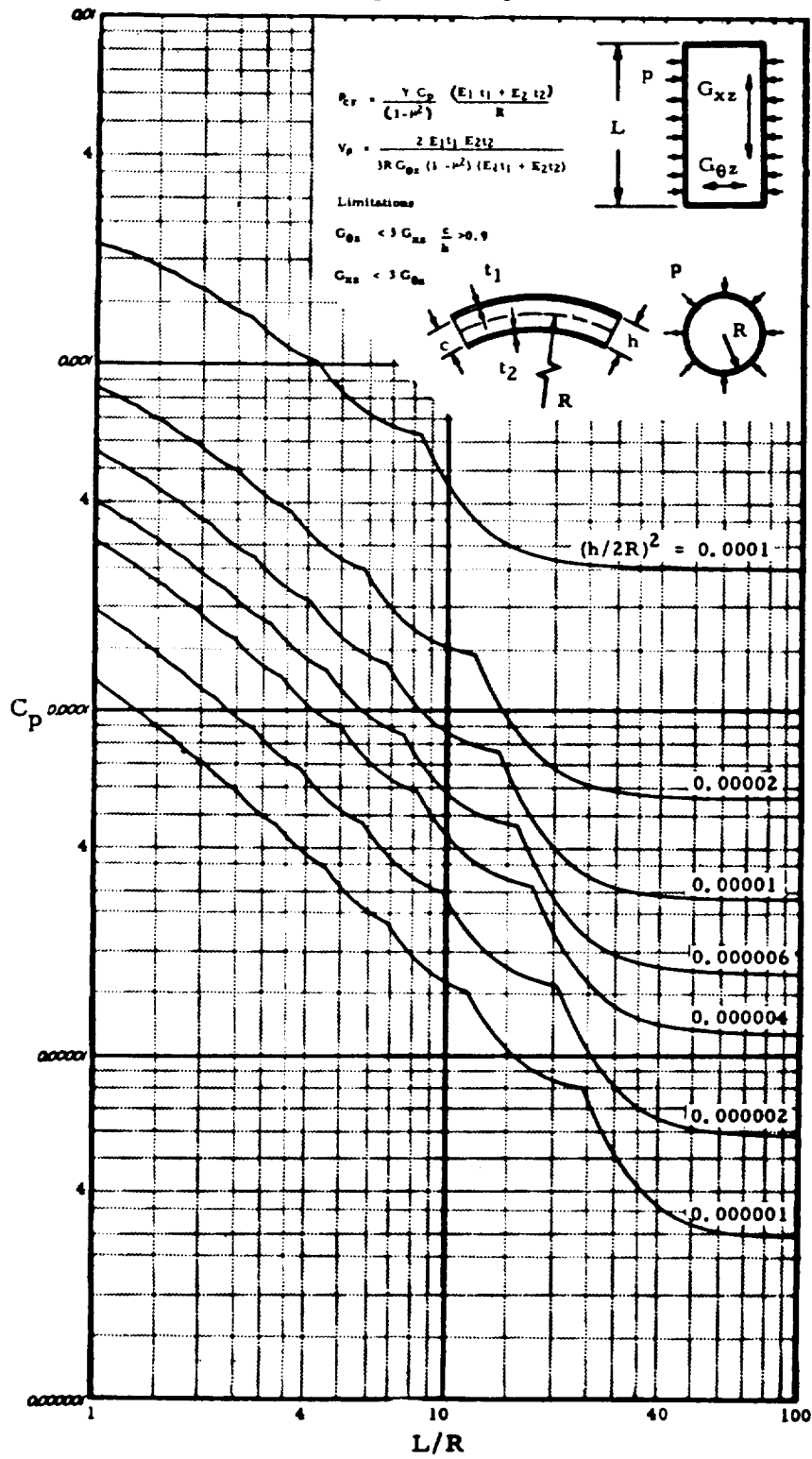


FIG. 3.53-21. VALUES OF C_p FOR $V_p = 1.5$, AND FOR $\frac{E_1 t_1}{E_2 t_2} = 2$

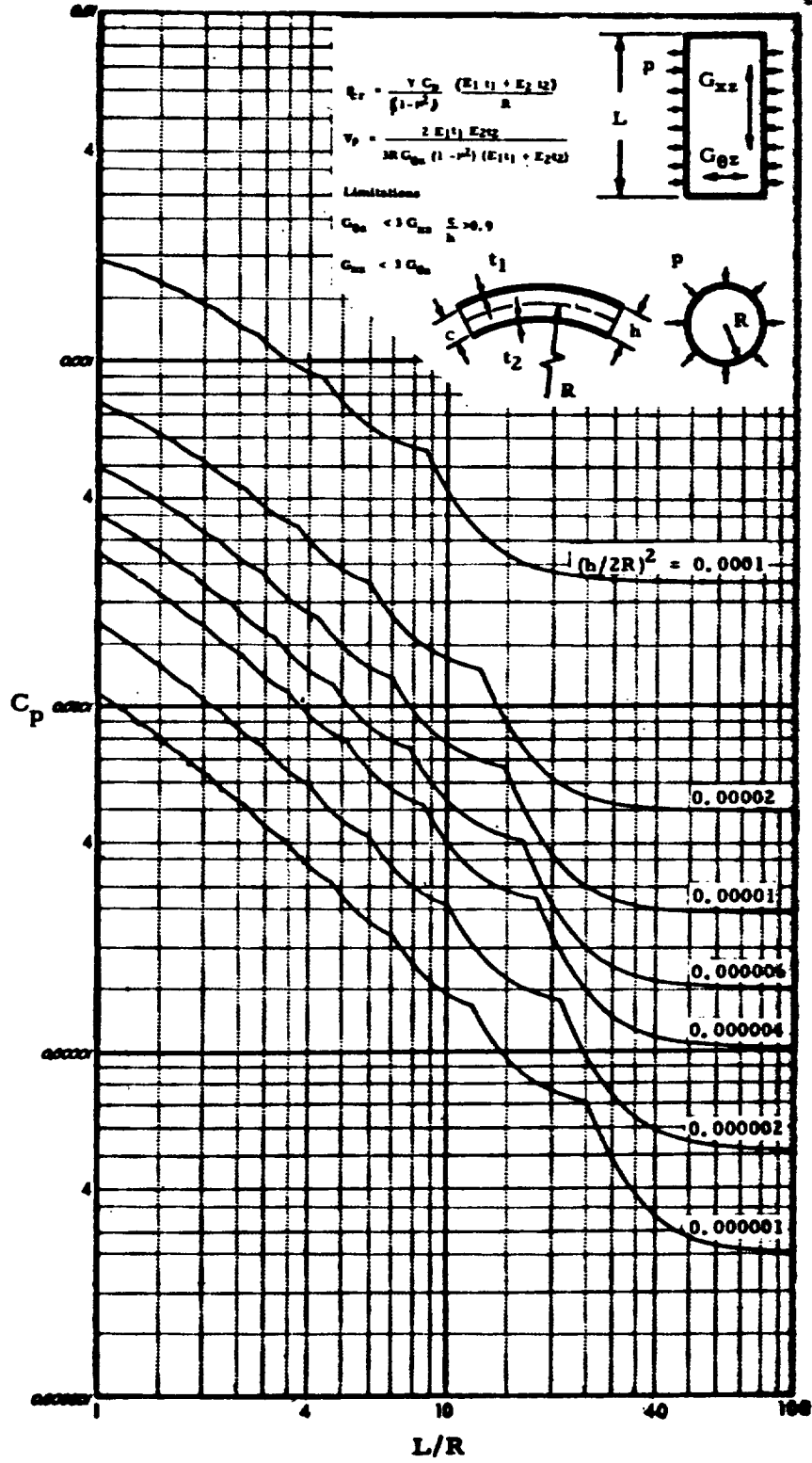


FIG. 3.53-22. VALUES OF C_p FOR $V_p = 1.5$, AND FOR $\frac{E_1 t_1}{E_2 t_2} = 3$

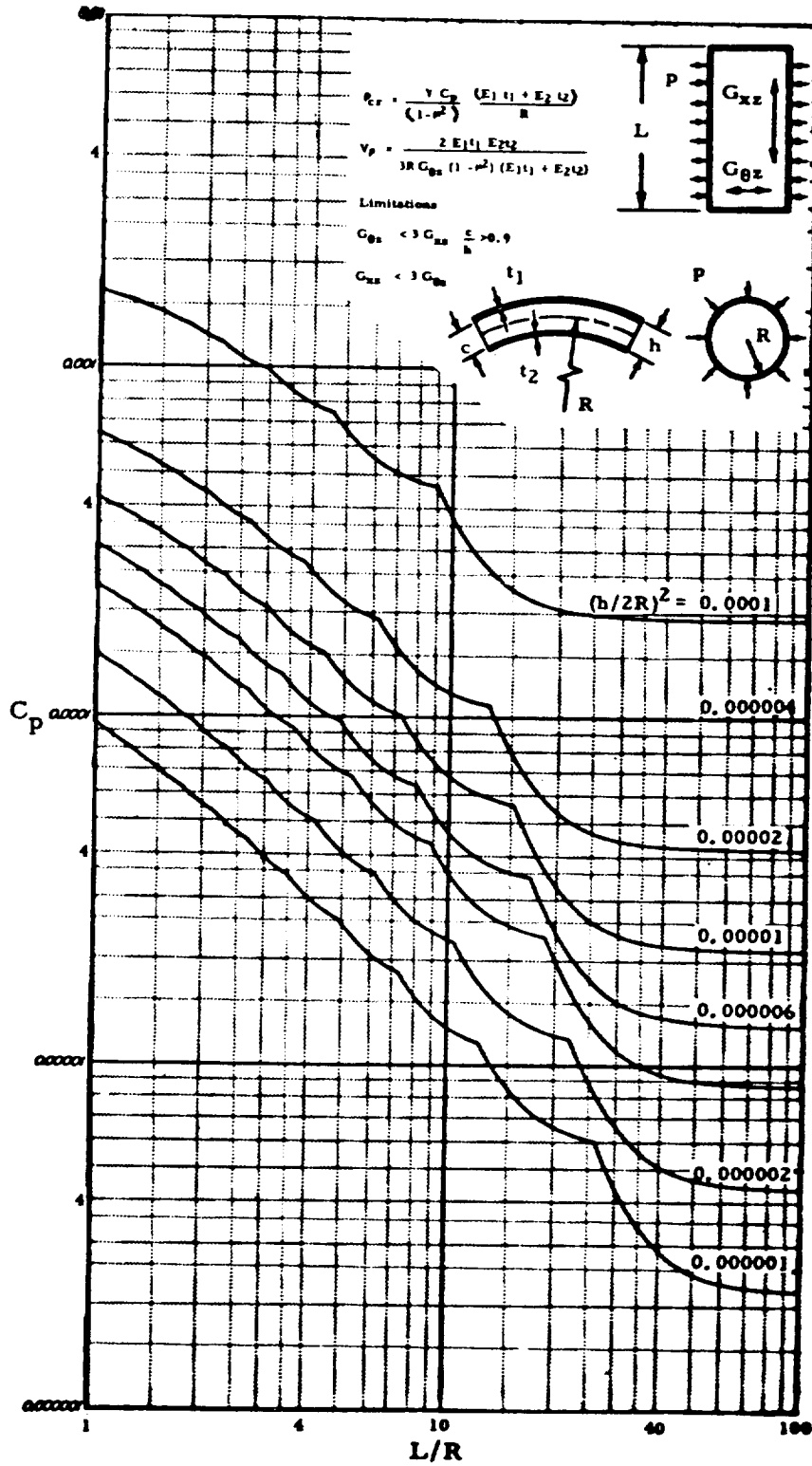
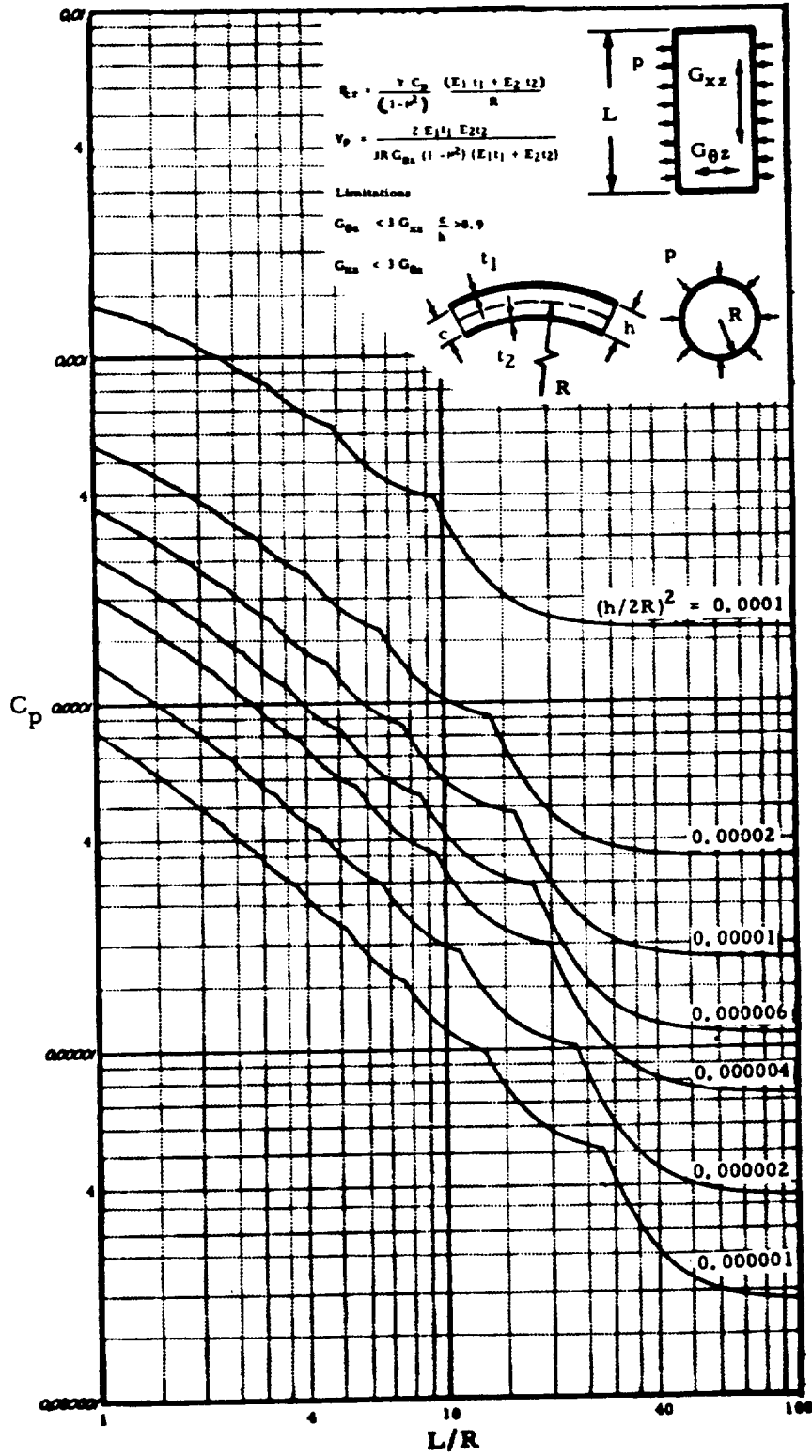


FIG. 3.53-23. VALUES OF C_p FOR $V_p = 1.5$, AND FOR $\frac{E_1 t_1}{E_2 t_2} = 4$



3.54 CONES

3.54.1 Axial Compression, Sandwich Cones

Until additional information is available, the equivalent cylinder approach recommended in Paragraph 3.24.1 may be used. The cone shown in Fig. 3.34-1a can be analyzed as a cylinder with a radius $R_e = R_1 / \cos \alpha$ and length L . The design allowable stress, σ_{cr} , for the equivalent cylinder can be obtained from Paragraph 3.53.1. The design allowable total compressive load for the cone may be obtained from

$$P_{cr} = 2\pi R_e \sigma_{cr} (t_1 + t_2) \cos^2 \alpha$$

This method of analysis should be used with caution and should be limited to cones with $\alpha < 30$ degrees.

3.54.2 Torsion, Sandwich Cones

Until additional information is available, the equivalent cylinder approach recommended in Paragraph 3.24.2 can be used for sandwich cones subjected to torsion. The cone shown in Fig. 3.34-1b can be analyzed as a cylinder with a radius

$$R_e = \left\{ 1 + \left[\frac{1 + R_2/R_1}{2} \right]^{1/2} - \left[\frac{1 + R_2/R_1}{2} \right]^{-1/2} \right\} R_1 \cos \alpha$$

and length $L_e = L / \cos \alpha$.

The design allowable shear stress, τ_{cr} , for the equivalent cylinder can be obtained from Paragraph 3.53.2. The design allowable

torque for the cone can be obtained from the equation

$$T_{cr} = 2\pi R_e^2 \tau_{cr} (t_1 + t_2)$$

The design allowable shear stress for the cone should be based on τ_{cr} .

This method of analysis should be used with caution and should be limited to cones with $\alpha < 30$ degrees. For inelastic stresses, the reduction of τ_{cr} due to plasticity should be based on the stresses at the smaller end of the cone and not on the stress of the equivalent cylinder.

3. 54. 3 Bending, Sandwich Cones

Until additional information is available, the equivalent cylinder approach recommended in Paragraph 3. 24. 3 can be used for sandwich cones subjected to bending. The cone shown in Fig. 3-34-1c can be analyzed as a cylinder with a radius $R_e = R_1 / \cos \alpha$ and length L . The design allowable stress, σ_{cr} , can be obtained from Paragraph 3. 53. 3. If the stresses are elastic, the design allowable moment for the cone can be obtained from

$$M = \pi R_1^2 \sigma_{cr} (t_1 + t_2) \cos^2 \alpha$$

This method of analysis should be used with caution and should be limited to cones with $\alpha < 30$ degrees.

3. 54. 4 Lateral External Pressure, Sandwich Cones

Until additional information is available, the equivalent cylinder approach recommended in Paragraph 3. 24. 4 can be used for sandwich cones subjected to lateral pressure as shown in Fig. 3. 34-1d. The cone can be analyzed as a cylinder with radius $R_e = (R_1 + R_2)/(2 \cos \alpha)$ and length L. The design allowable buckling pressure, p_{cr} , can be obtained from Paragraph 3. 53. 4.

For inelastic stresses, the reduction of p_{cr} due to plasticity should be based on the stresses at the larger end of the cone and not on the stress of the equivalent cylinder. This method of analysis should be used with caution and should be limited to cone with $\alpha < 30$ degrees.

3.60 INELASTIC BUCKLING

3.61 GENERAL

The formulas presented to determine the allowable buckling load are based primarily on theoretical results which have assumed that the compressive modulus of the material is a constant. If the buckling stress is below the proportional limit, this is a reasonable assumption; if the stresses are in the inelastic range, however, the modulus of the material becomes a function of the stresses. The modulus of the material decreases at inelastic stresses; therefore, there is a decrease in the stiffness of the shell and a corresponding decrease in the buckling load.

The Euler formula, which was derived for an elastic column, is used for the case of inelastic buckling of a column. However, the elastic modulus in the formula is replaced by the tangent modulus of the material. The agreement between the predicted buckling stress and test data has been quite good. It is considerably more difficult to include the effects of plasticity for shells. Methods have been developed but, in general, they are quite complicated, and computer programs are needed to obtain results. Plasticity correction factors derived for some types of loadings and shells are briefly discussed in the next section. Until additional information is available this method is recommended as a simple way to account for the effects of plasticity on the buckling load.

3. 62 PLASTICITY CORRECTION FACTOR

The effect of plasticity on the buckling of shells can be accounted for by the use of the plasticity coefficient, η . This coefficient is defined by the ratio

$$\eta = \frac{\sigma_{cr}}{\sigma_e}$$

where

σ_{cr} = the actual buckling stress

σ_e = the elastic buckling stress (the stress at which buckling would occur if the material remained elastic at any stress level)

The elastic buckling stress, therefore, is given by the equation

$$\sigma_e = \frac{\sigma_{cr}}{\eta}$$

The definition of η depends on σ_{cr}/σ_e , which is a function of the loading, the type of shell, the boundary conditions, and the type of construction. For example, the η recommended in Ref. 3-7 for homogeneous isotropic cylindrical shells with simply supported edges subjected to axial compression is

$$\eta = \frac{\sqrt{E_t E_s}}{E} \left[\frac{(1 - \mu_e^2)}{(1 - \mu^2)} \right]^{1/2}$$

where E_t , E_s , and μ are the tangent modulus, secant modulus and Poisson's ratio, respectively, at the actual buckling stress, and μ_e is the elastic Poisson's ratio.

For a given material, temperature, and η , a chart may be prepared for σ_{cr}/η versus σ_{cr} . By first calculating the elastic buckling stress, σ_{cr}/η , the actual buckling stress σ_{cr} can be read from the chart of σ_{cr}/η versus σ_{cr} . This method eliminates an iterative procedure which would otherwise be necessary.

The formulas for η are, in general, determined theoretically and the testing performed to evaluate the theoretical η provides only qualitative agreement. In addition, the number of charts of σ_{cr}/η versus σ_{cr} necessary to cover all combinations of materials, temperatures, loadings, shells, boundary conditions, and types of construction would be excessively large and, in many cases, the curves would be very close to each other.

To reduce the number of σ_{cr}/η versus σ_{cr} curves, only the η 's defined in Refs. 3-7 and 3-60 will be presented because these curves have already been computed and, in general, cover the range of possible η within the accuracy of which the actual η is known. The curve that gives the best agreement with experimental and theoretical results of shell structures will be recommended whenever possible.

Figs. 3.62-1 through 3.62-27 present curves of σ_{cr}/η versus σ_{cr} for materials and temperatures commonly encountered in the aerospace industry. In many cases, the curves are so close together that they are drawn as one curve.

The η 's used to determine each curve are defined as follows:

| Curve | η |
|----------------|---|
| A | $\frac{E_s}{E}$ |
| B | $\frac{E_s}{E} \left[0.330 + 0.670 \sqrt{\mu^2 + (1 - \mu^2) \frac{E_t}{E_s}} \right]$ |
| C | $\frac{E_s}{E} \left[\frac{1}{2} + \frac{1}{2} \sqrt{\mu^2 + (1 - \mu^2) \frac{E_t}{E_s}} \right]$ |
| D | $\frac{E_s}{E} \left[0.352 + 0.648 \sqrt{\mu^2 + (1 - \mu^2) \frac{E_t}{E_s}} \right]$ |
| E | $\mu^2 \frac{E_s}{E} + (1 - \mu^2) \frac{E_t}{E}$ |
| F | $0.046 \frac{E_s}{E} + 0.954 \frac{E_t}{E} \quad \mu = 0.33$ |
| G | $\frac{E_t}{E}$ |
| E ₁ | $\frac{\sqrt{E_t E_s}}{E} \left[\frac{1 - \mu_e^2}{1 - \mu^2} \right]^{1/2}$ |

The formulas for η for curves A through G were obtained from Ref. 3-60, which is based on Ref. 3-61. However, Ref. 3-61 assumes $\mu = 1/2$. The constants outside of the radical for curve B differ from Ref. 3-61 due to a correction that was made. Although the value of μ is a function of the stresses for stresses in excess of the proportional limit, the plasticity curves were obtained assuming the conservative value of $\mu = 1/3$. The difference between using the value of $\mu = 1/3$ and $\mu = 1/2$ is small except for curves E and F.

It is worth noting that for curve A, $\eta = E_s/E$; for curve G, $\eta = E_t/E$ and, on the remaining curves, η is a function of both E_t and E_s . It can be seen that curve A and curve G bound the range of η . Curve G is the most conservative while curve A results in the smallest possible reduction in the buckling load due to plasticity.

FIG. 3.62-1. 2014-T6, -T651 ALUMINUM ALLOY SHEET AND PLATE
 SPECIFICATION MB0170-002

PLASTICITY CORRECTION CURVES (-423 F, -300 F)

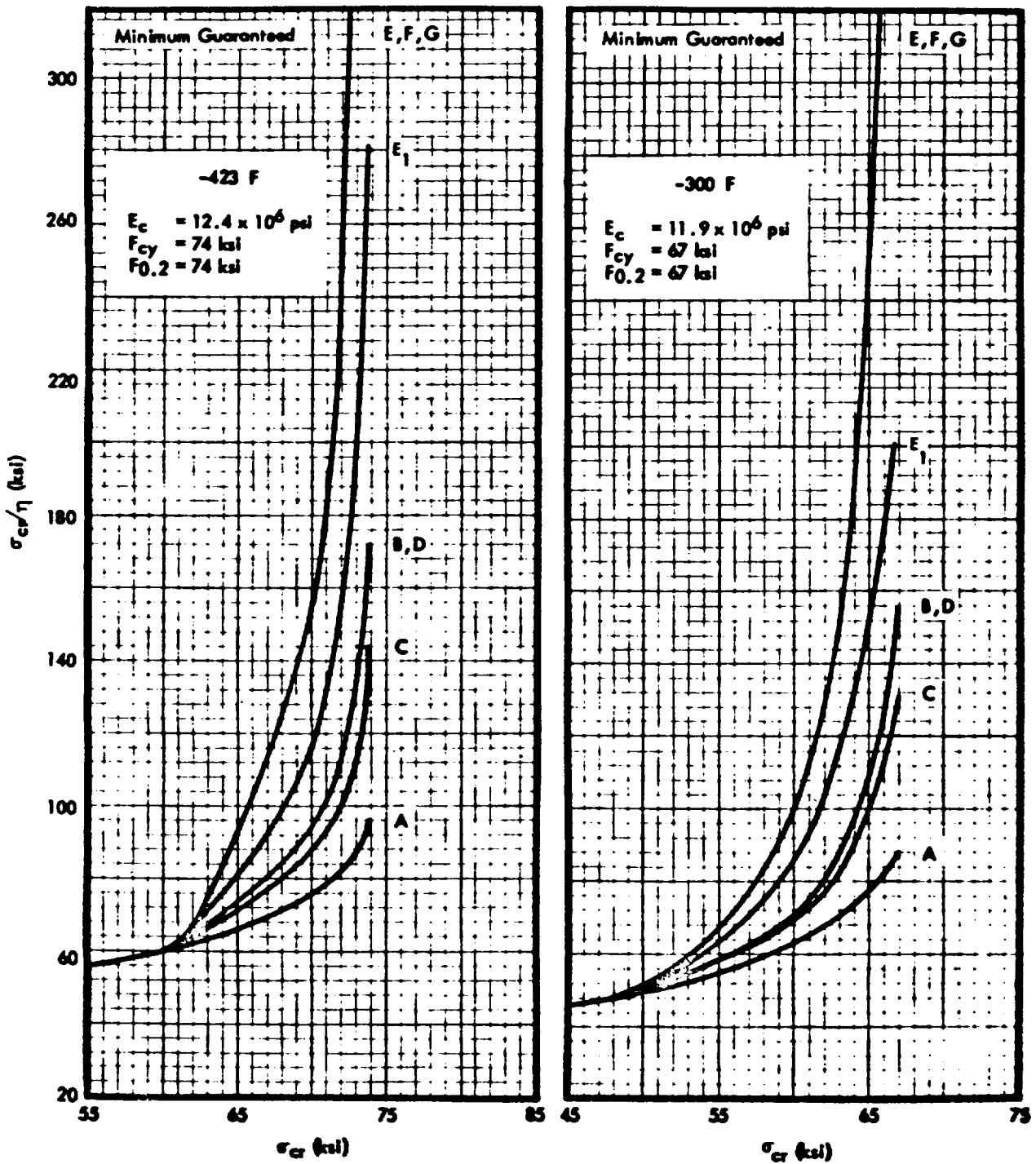


FIG. 3.62-2. 2014-T6, -T651 ALUMINUM ALLOY SHEET AND PLATE SPECIFICATION MB0170-002

PLASTICITY CORRECTION CURVES (-200 F, -100 F)

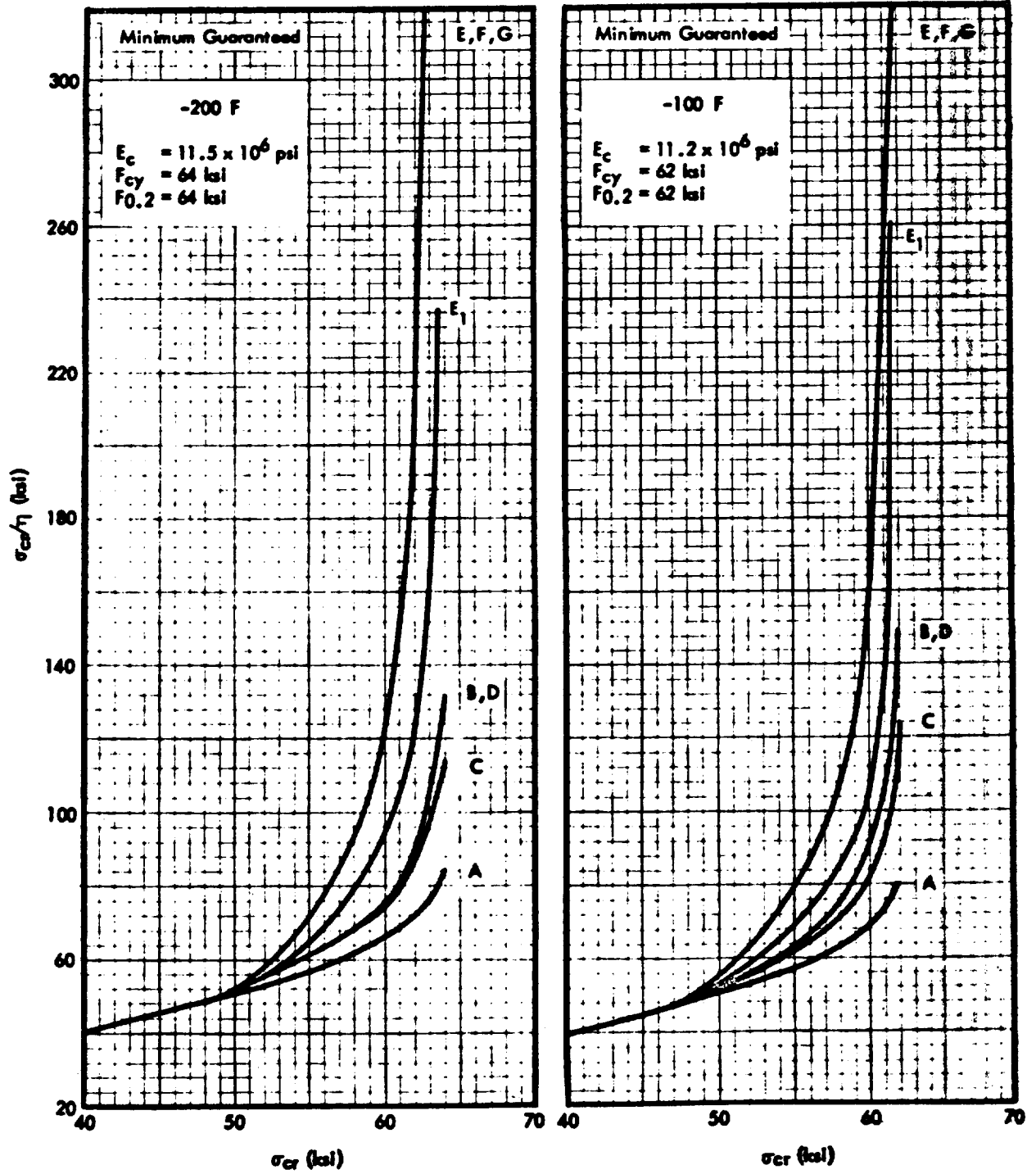


FIG. 3.62-3. 2014-T6, -T651 ALUMINUM ALLOY SHEET AND PLATE SPECIFICATION MB0170-002

PLASTICITY CORRECTION CURVES (R.T.; 200 F, 1/2 HOUR)

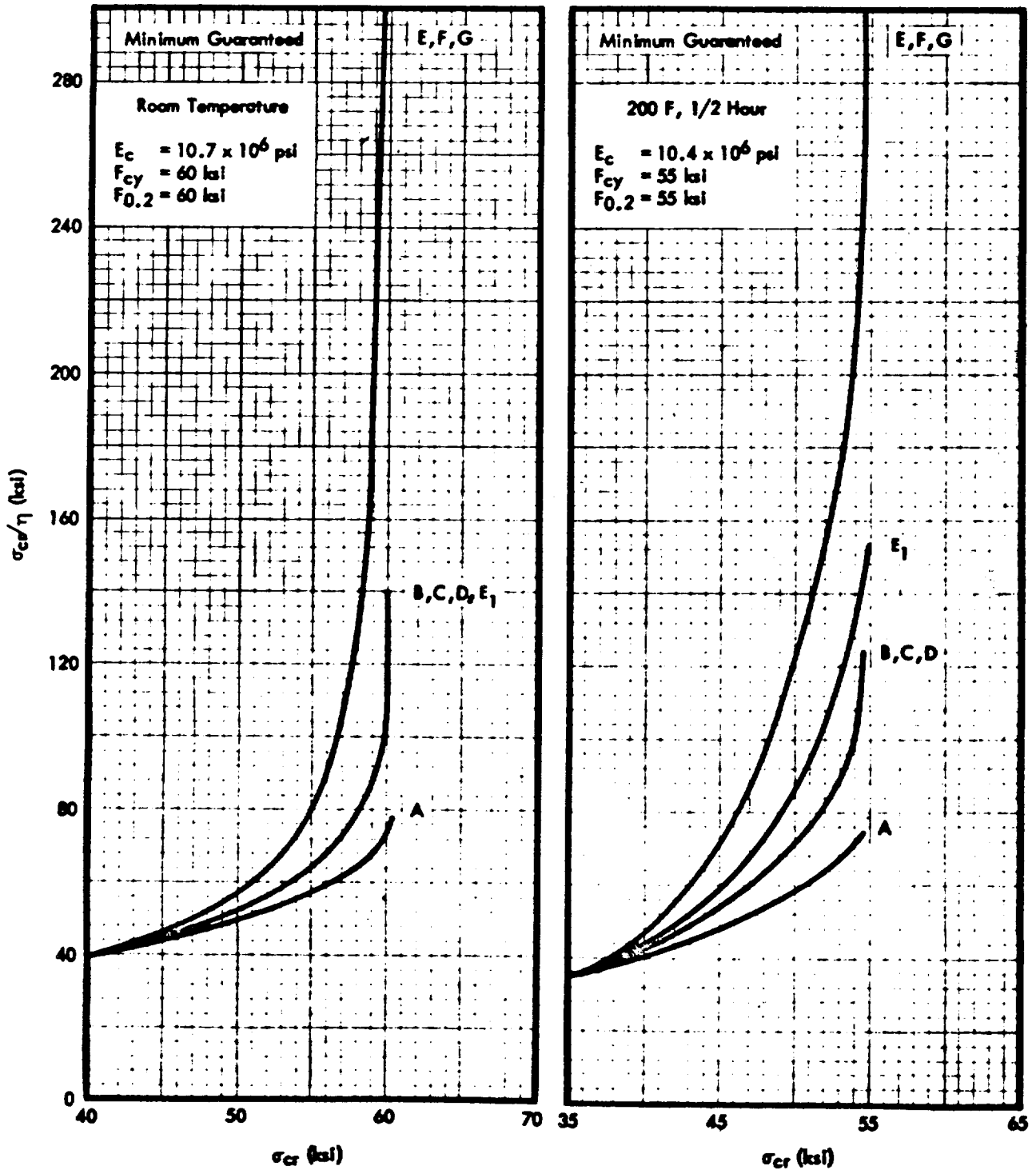


FIG. 3.62-4. 2014-T6, -T651 ALUMINUM ALLOY SHEET AND PLATE SPECIFICATION MB0170-002

PLASTICITY CORRECTION CURVES (300 F, 1/2 HOUR; 400 F, 1/2 HOUR)

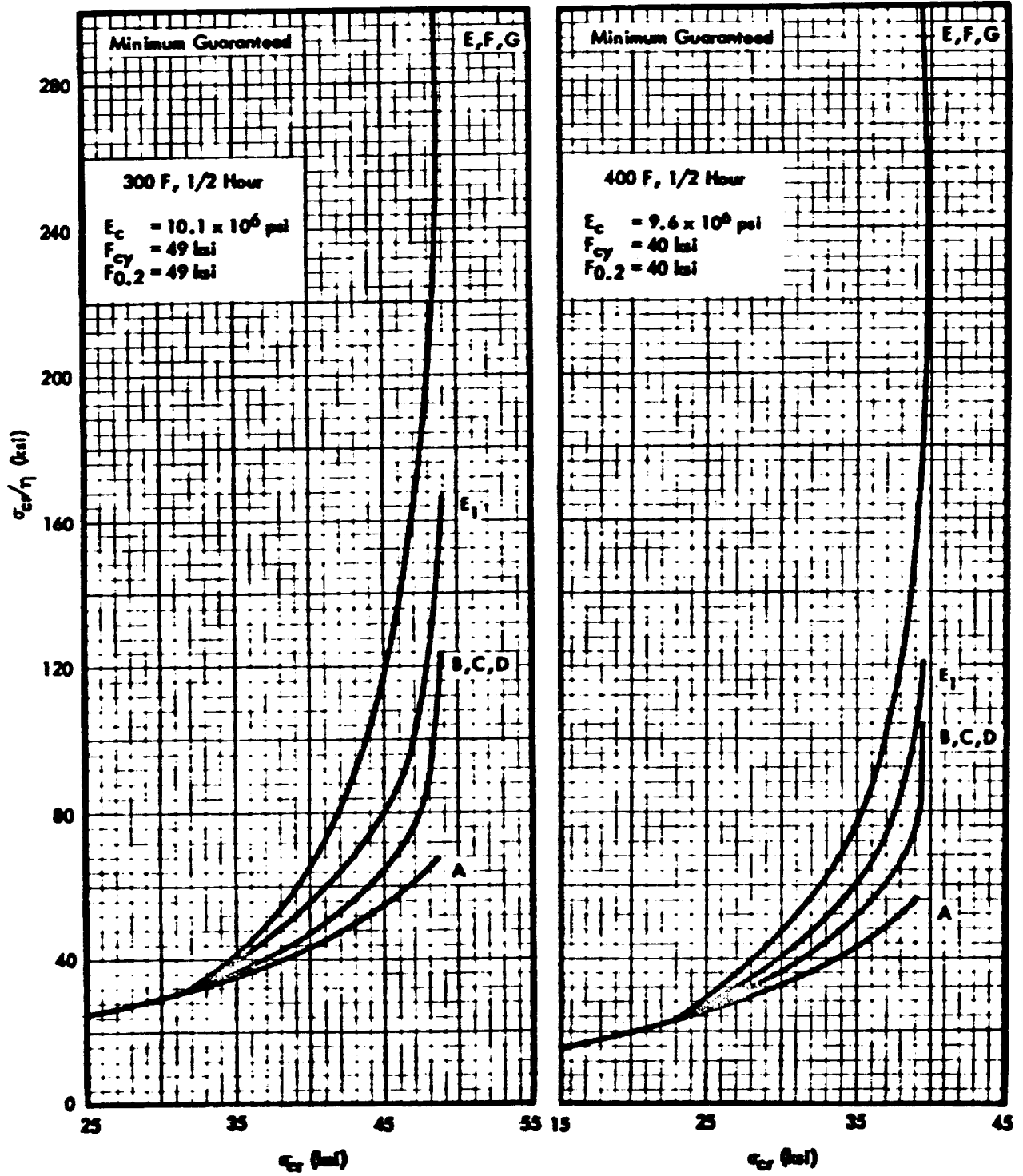


FIG. 3.62-5. 2014-T6, -T651 ALUMINUM ALLOY SHEET AND PLATE
 SPECIFICATION MB0170-002
 PLASTICITY CORRECTION CURVES (500 F, 1/2 HOUR; 600 F, 1/2 HOUR)

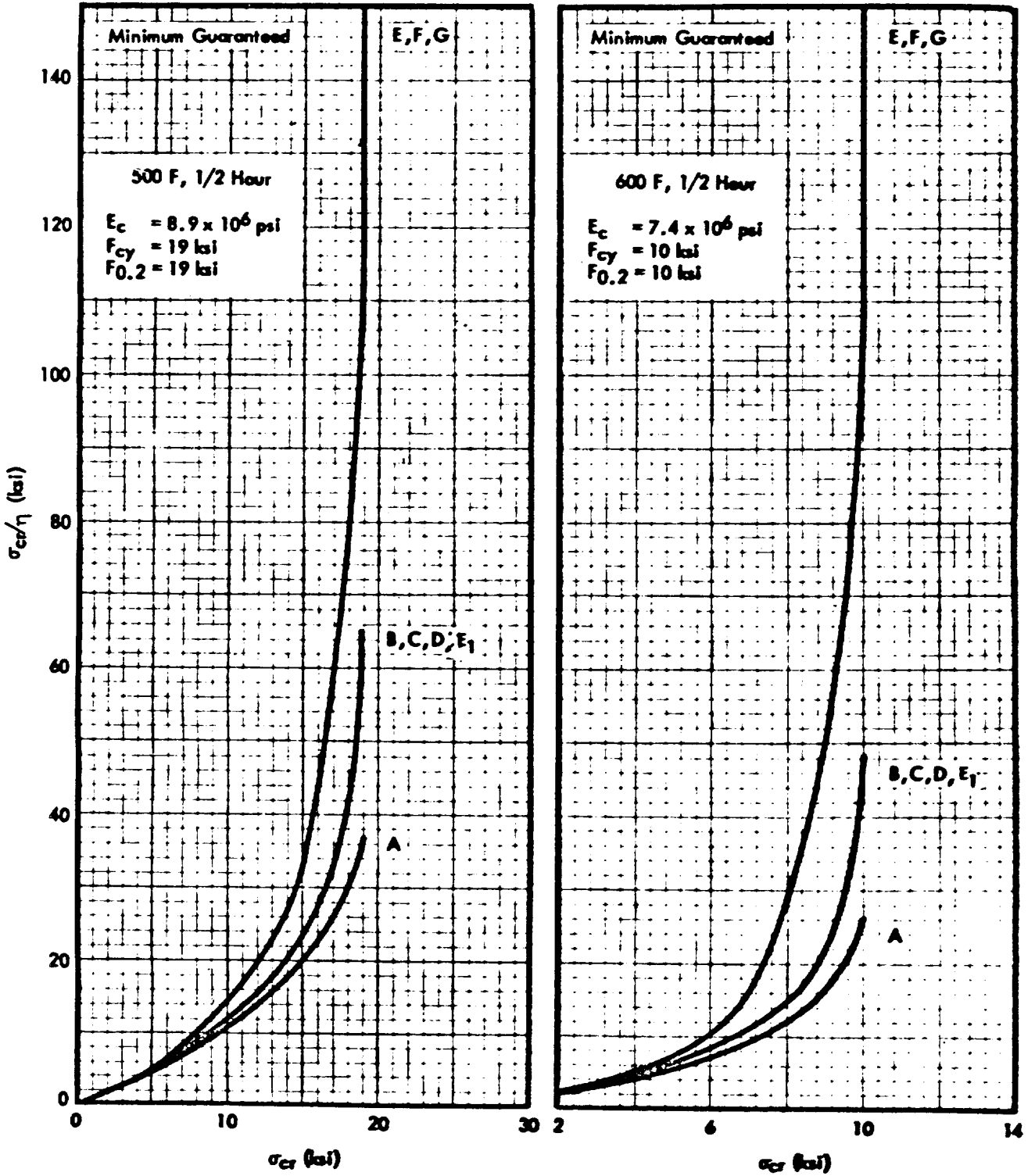


FIG. 3.62-6. PLASTICITY CORRECTION BARE 7075-T6 ALUMINUM ALLOY SHEET

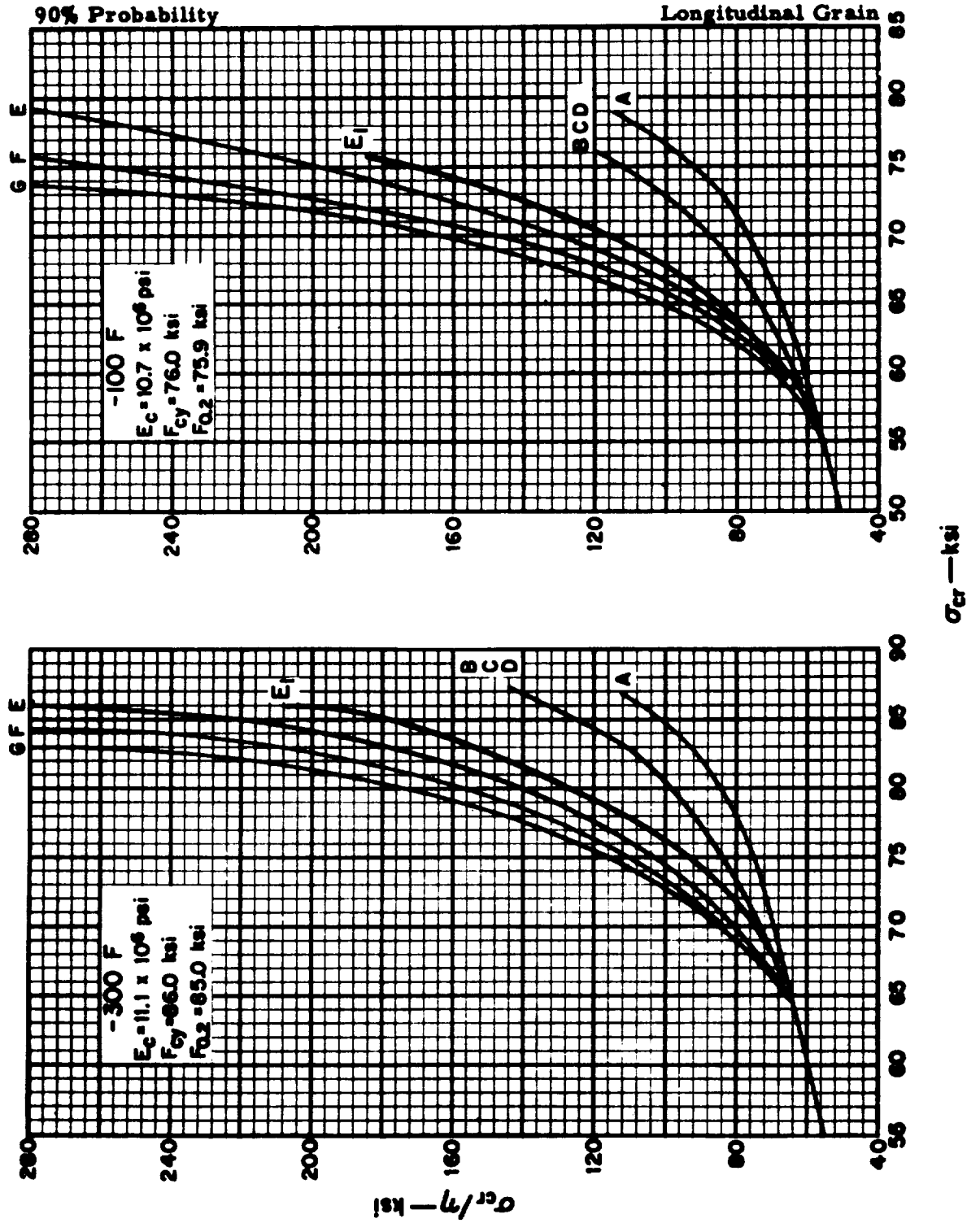


FIG. 3.62-7. PLASTICITY CORRECTION BARE 7075-T6 ALUMINUM ALLOY SHEET

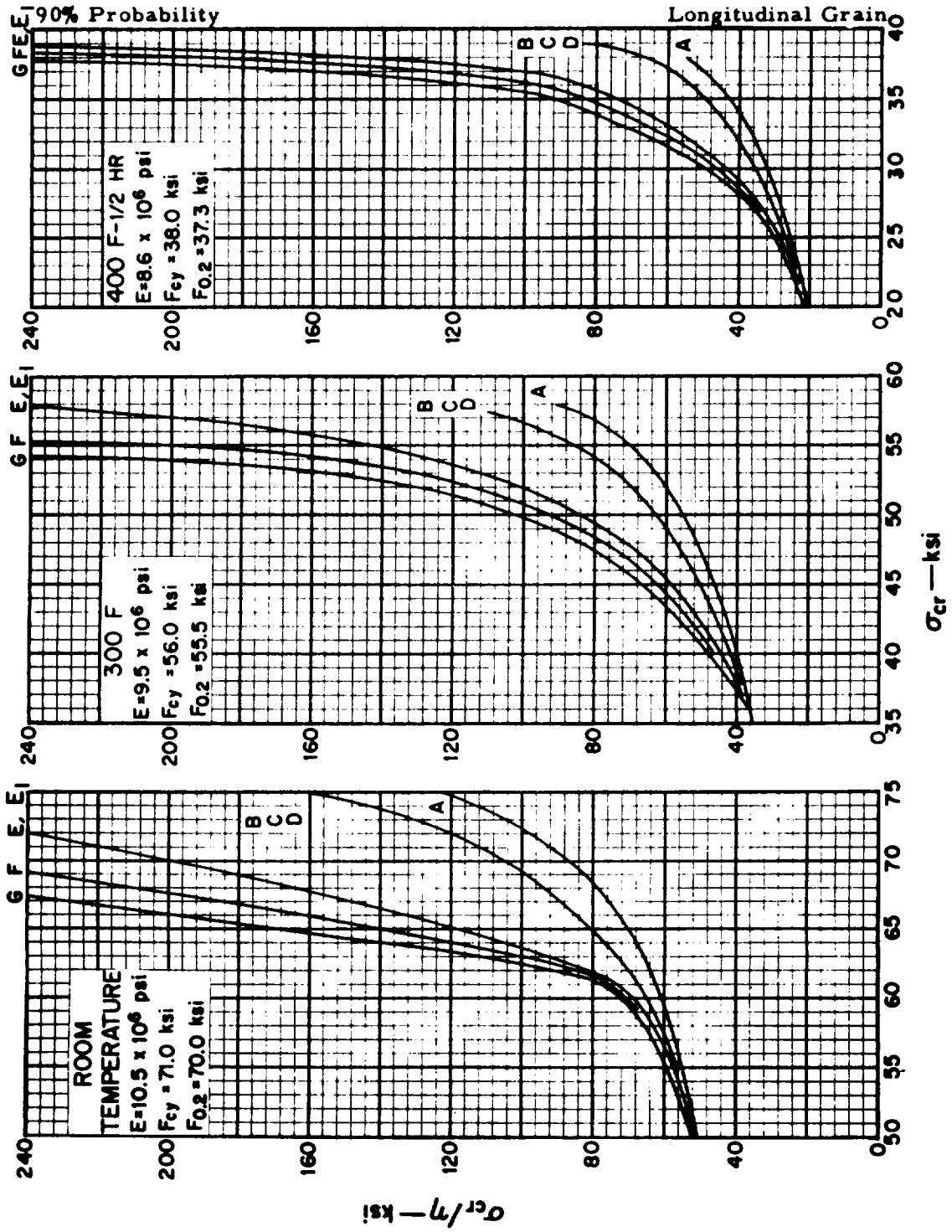


FIG. 3.62-8. PLASTICITY CORRECTION ALLOY STEEL 4130, 4140,
4340 - H. T. 180,000

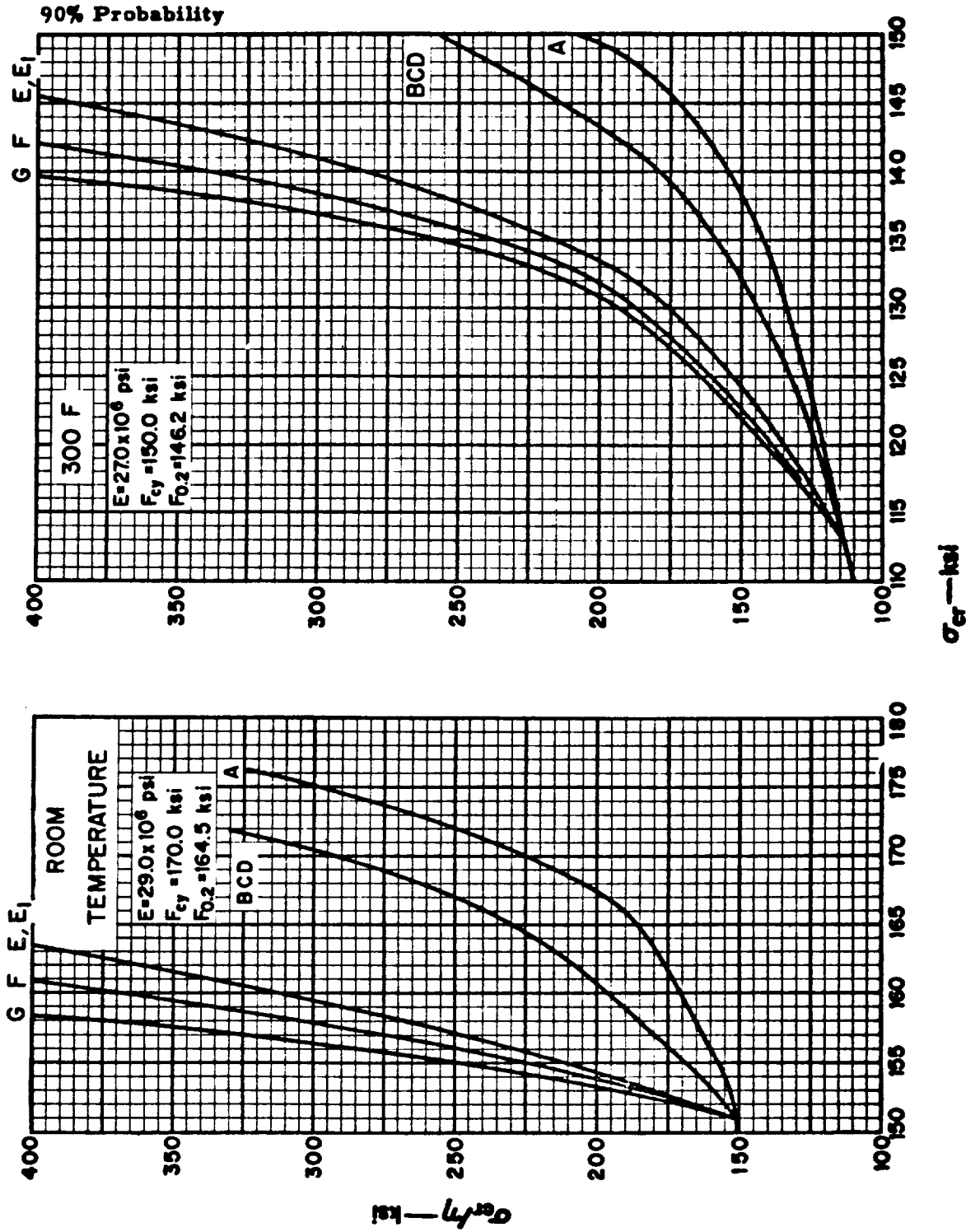


FIG. 3.62-9. PLASTICITY CORRECTION ALLOY STEEL 4130, 4140,
4340 - H. T. 180,000

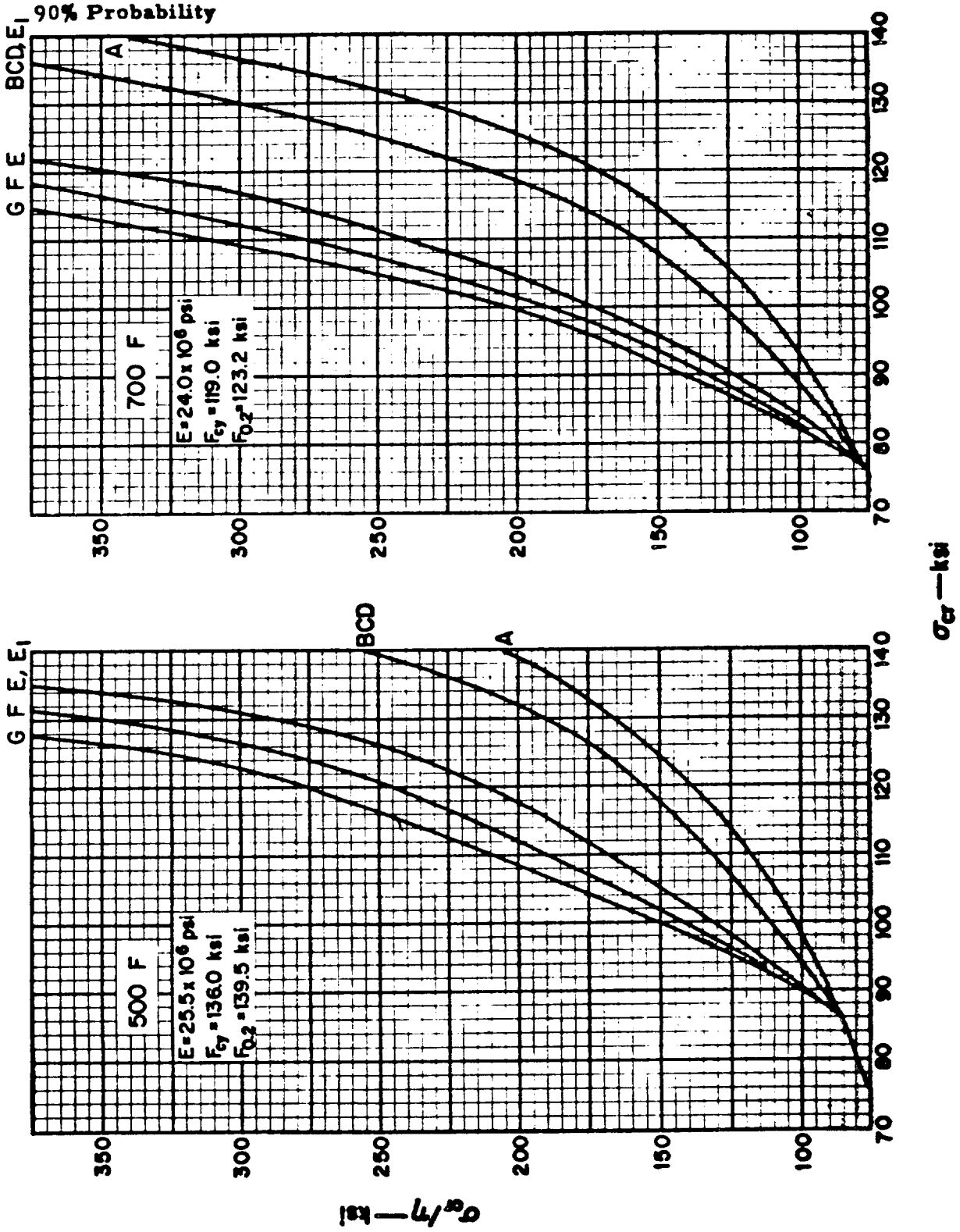


FIG. 3.62-10. PLASTICITY CORRECTION ALLOY STEEL 4140, 4340 -
 H. T. 180,000

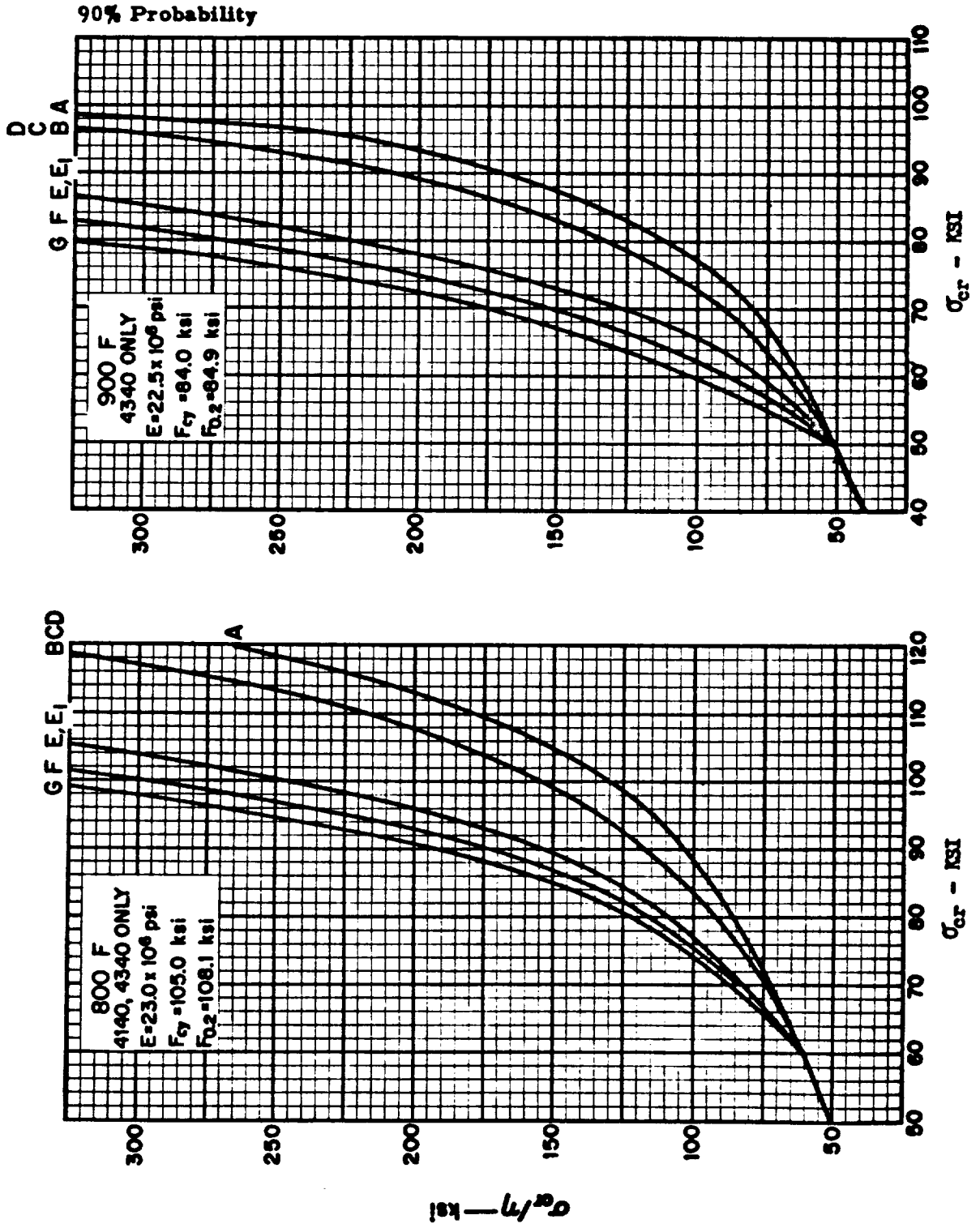


FIG. 3.62-11. PH 15-7 Mo STAINLESS STEEL SHEET AND PLATE -
 RH 1050, RH 1075 - SPECIFICATIONS LB0160-100, LB0160-129,
 LB0160-130, HB0160-010. LA0111-022, MA0107-023

PLASTICITY CORRECTION CURVES (-200 F)

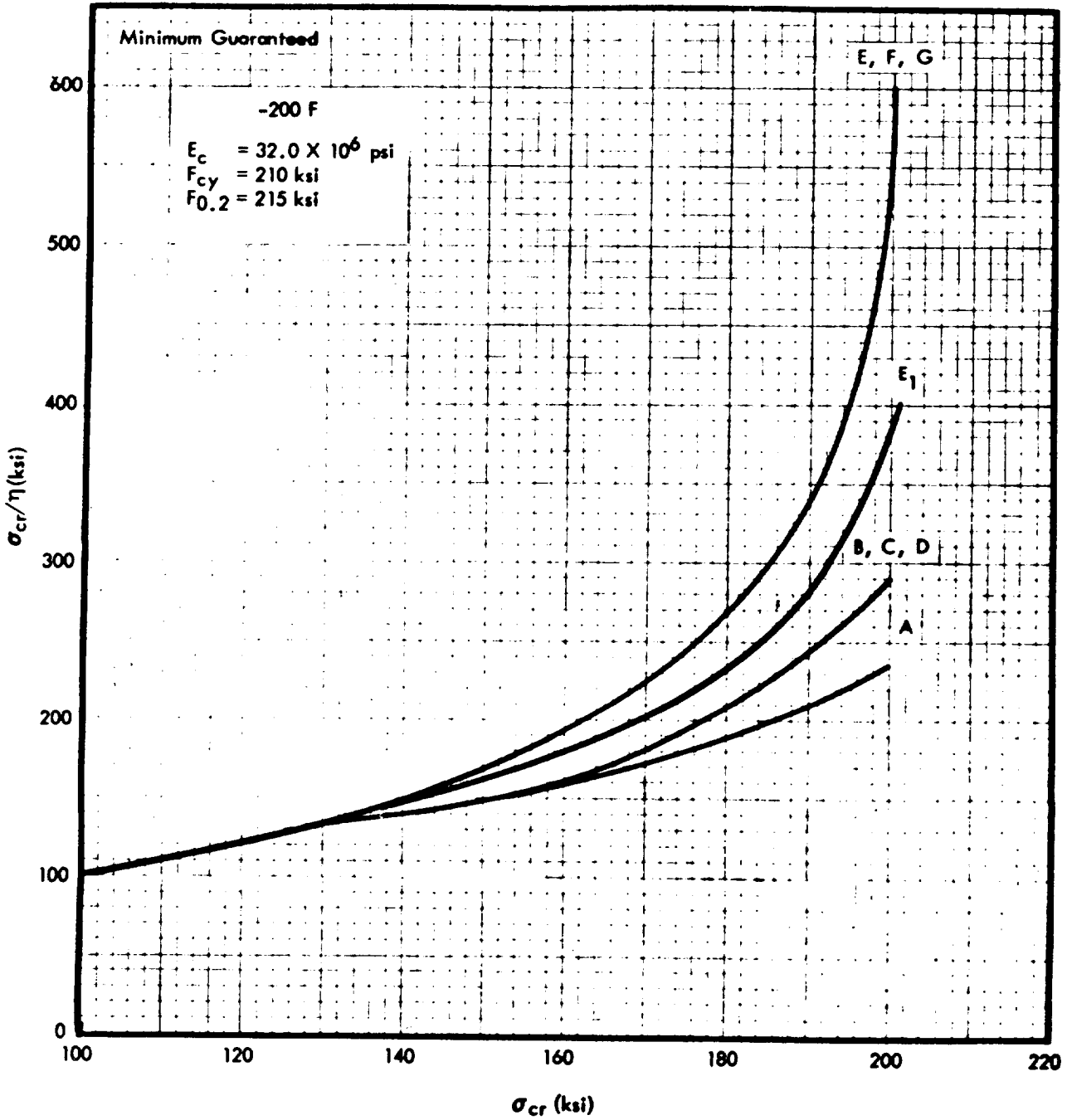


FIG. 3.62-12. PH 15-7 Mo STAINLESS STEEL SHEET AND PLATE
 RH 1050, RH 1075 - SPECIFICATIONS LB0160-100, LB0160-129,
 LB0160-130, HB0160-010, LA0111-022, MA0107-023
 PLASTICITY CORRECTION CURVES (-100 F)

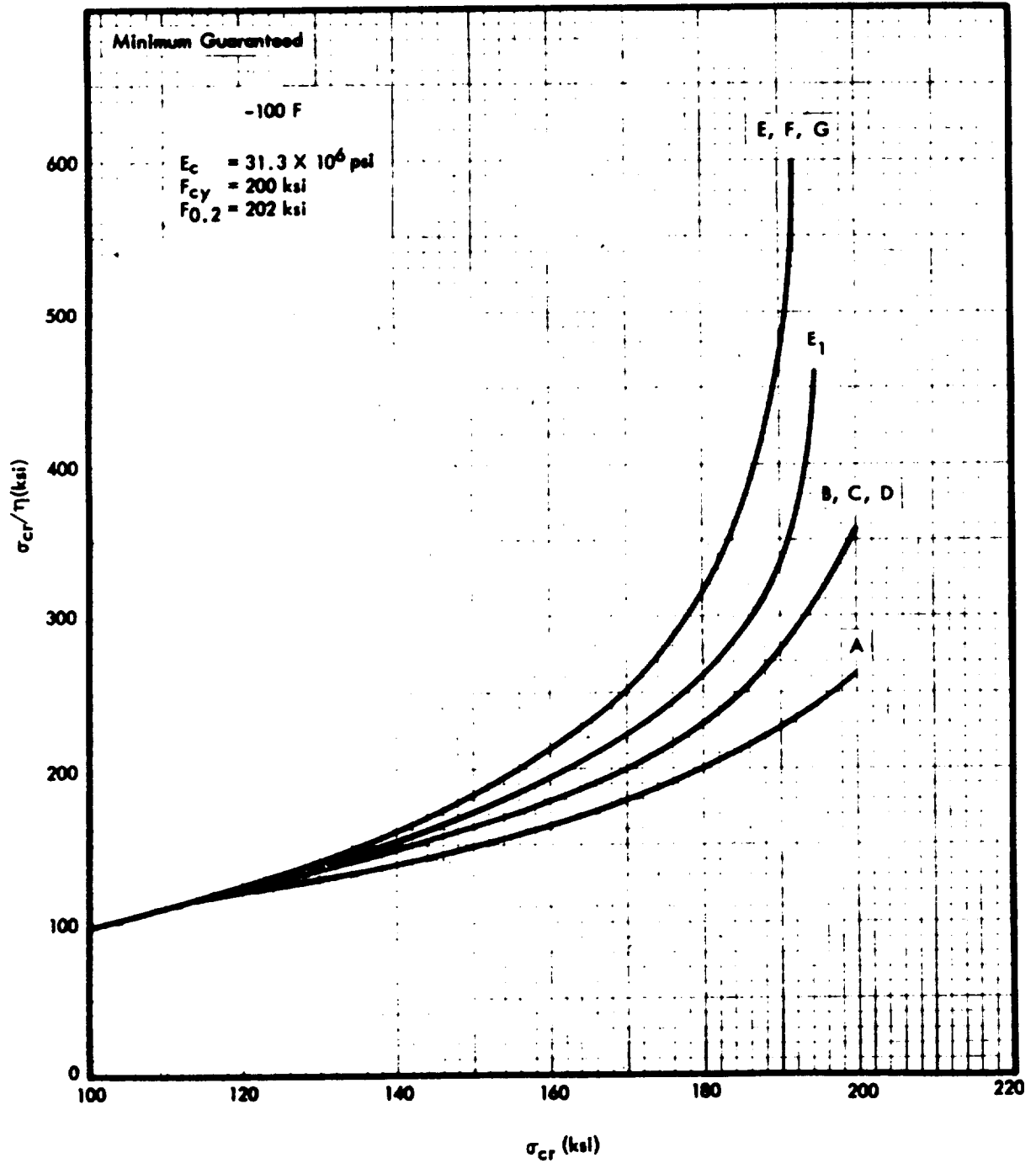


FIG. 3.62-13. PH 15-7 Mo STAINLESS STEEL SHEET AND PLATE -
 RH 1050, RH 1075 - SPECIFICATIONS LB0160-100, LB0160-129,
 LB0160-130, HB0160-010, LA0111-022, MA0107-023

PLASTICITY CORRECTION CURVES (R.T.)

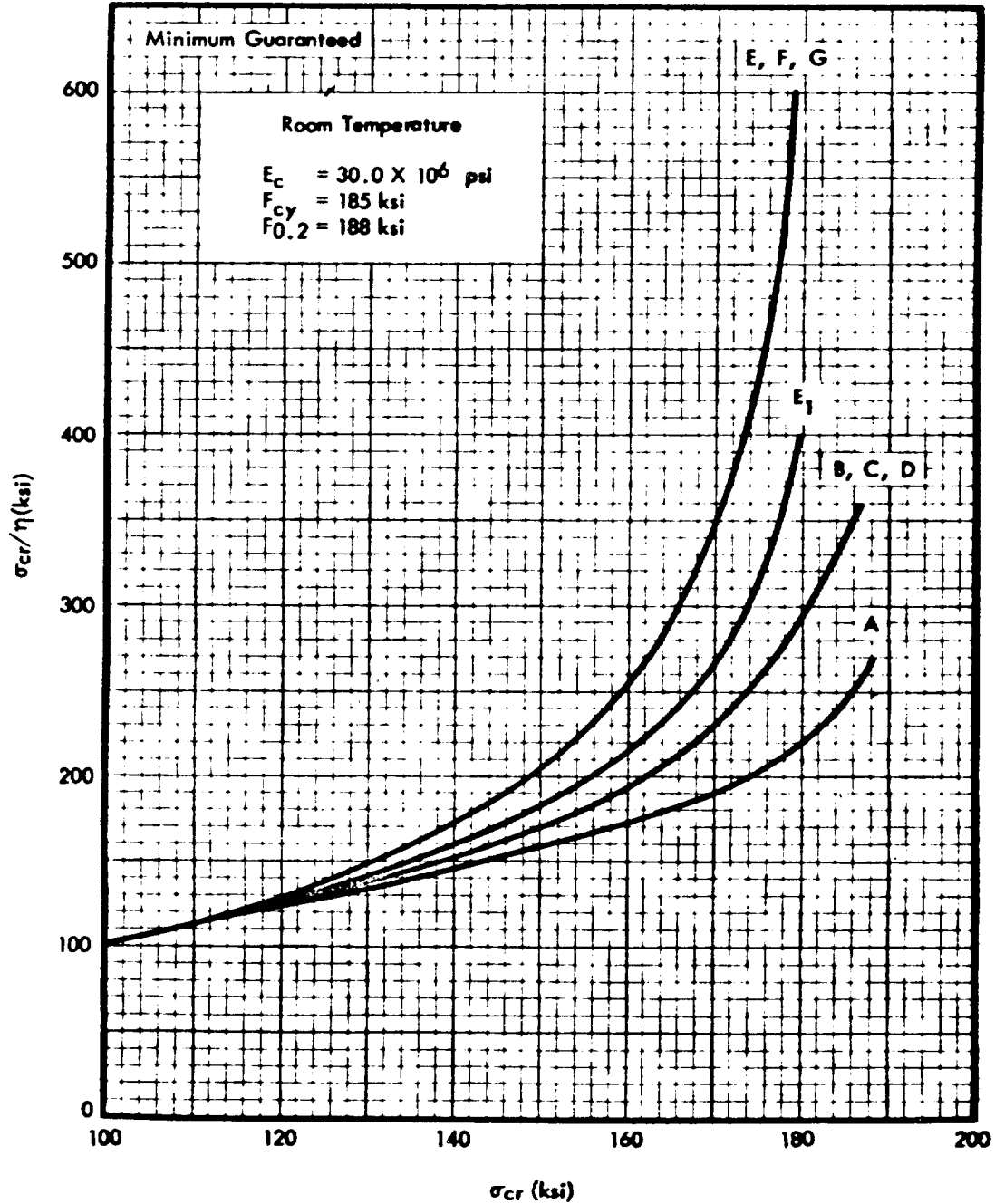


FIG. 3.62-14. PH 15-7 Mo STAINLESS STEEL SHEET AND PLATE -
 RH 1050, RH 1075 - SPECIFICATIONS LB0160-100, LB0160-129,
 LB0160-130, HB0160-010, LA0111-022, MA0107-023

PLASTICITY CORRECTION CURVES (200 F)

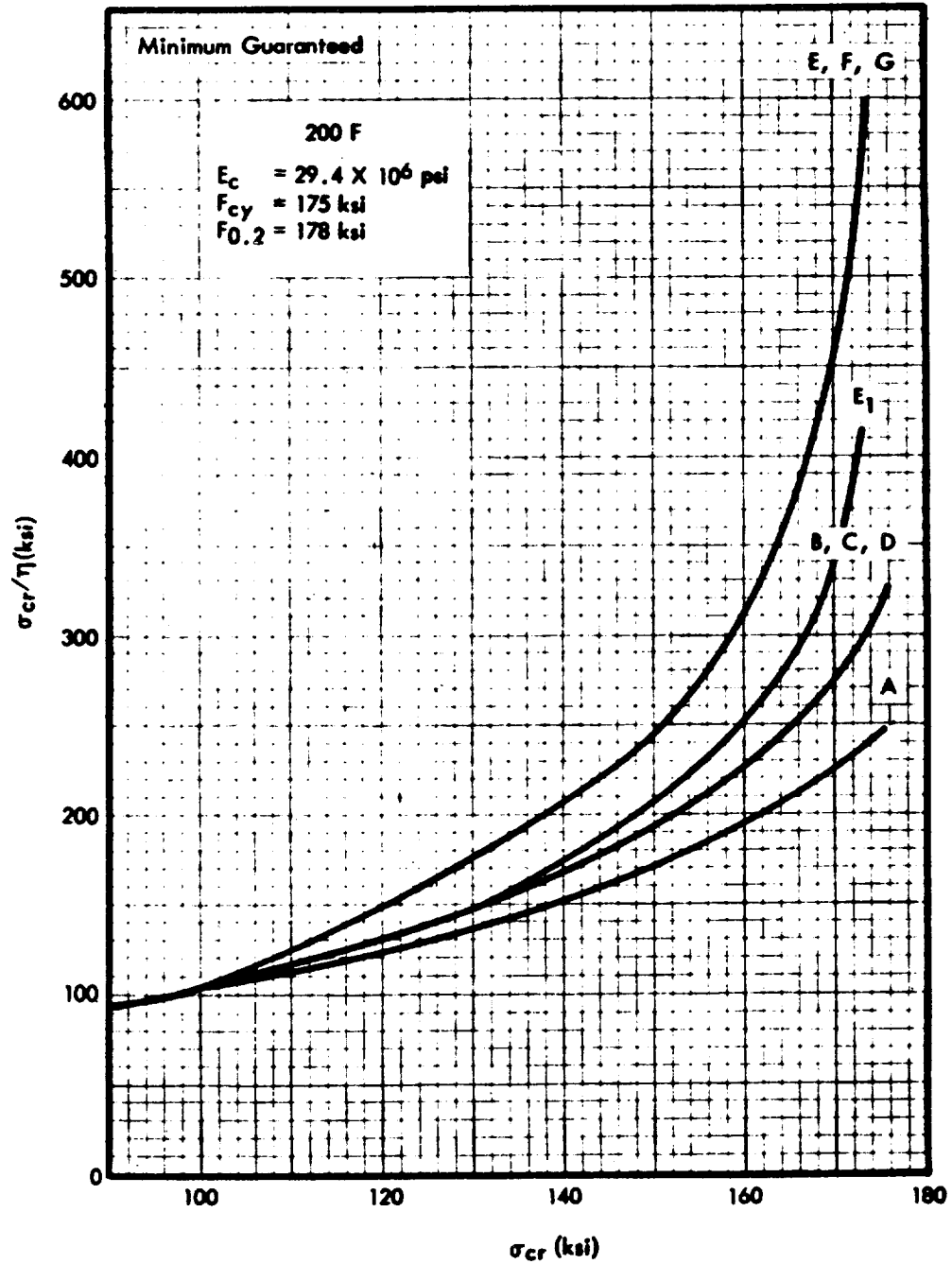


FIG. 3.62-15. PH 15-7 Mo STAINLESS STEEL SHEET AND PLATE -
 RH 1050, RH 1075 - SPECIFICATIONS LB0160-100, LB0160-129,
 LB0160-130, HB0160-010, LA0111-022, MA0107-023
 PLASTICITY CORRECTION CURVES (300 F)

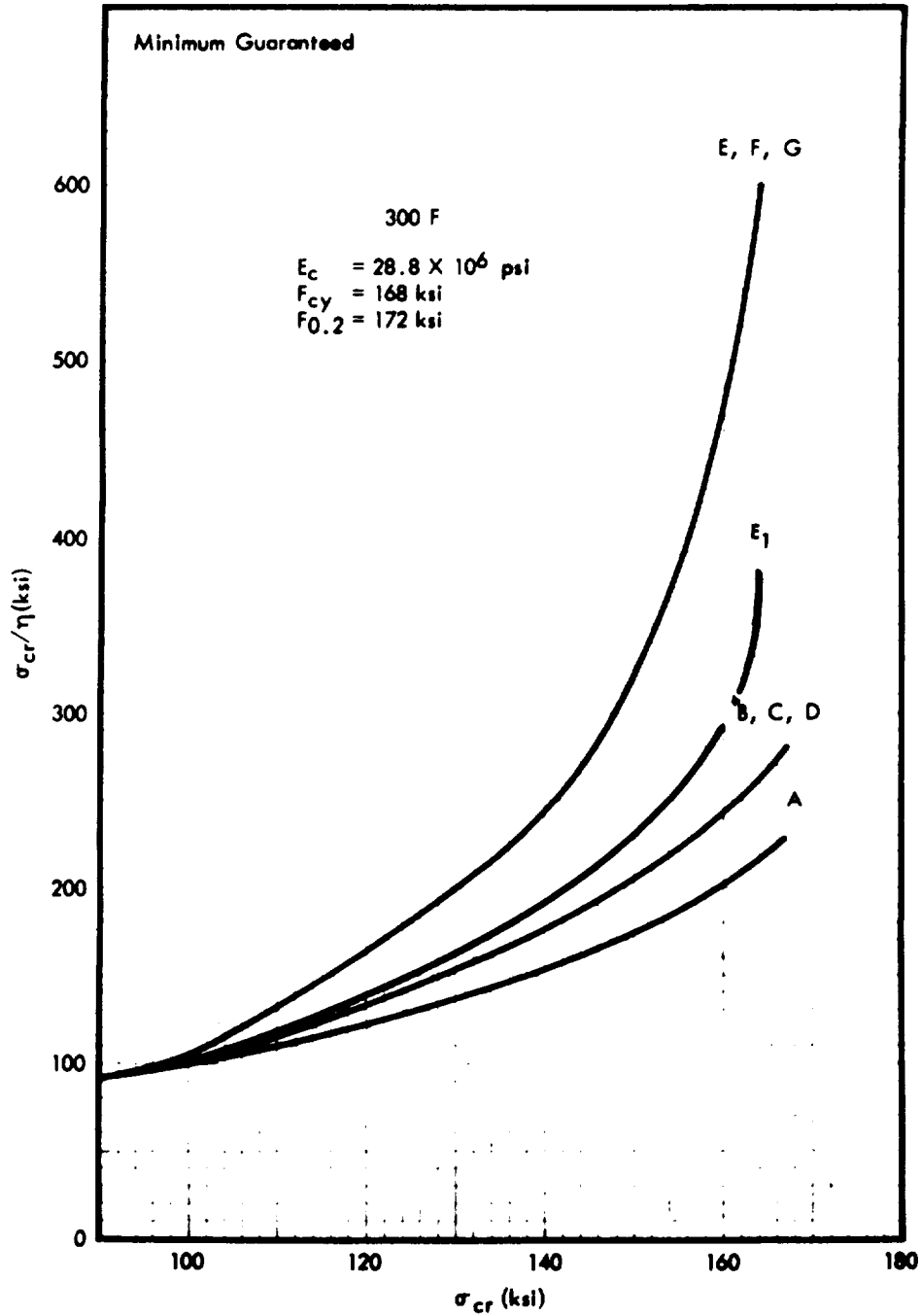


FIG. 3.62-16. PH 15-7 Mo STAINLESS STEEL SHEET AND PLATE -
 RH 1050, RH 1075 - SPECIFICATIONS LB0160-100, LB0160-129,
 LB0160-130, HB0160-010, LA0111,022, MA0107-023
 PLASTICITY CORRECTION CURVES (400 F)

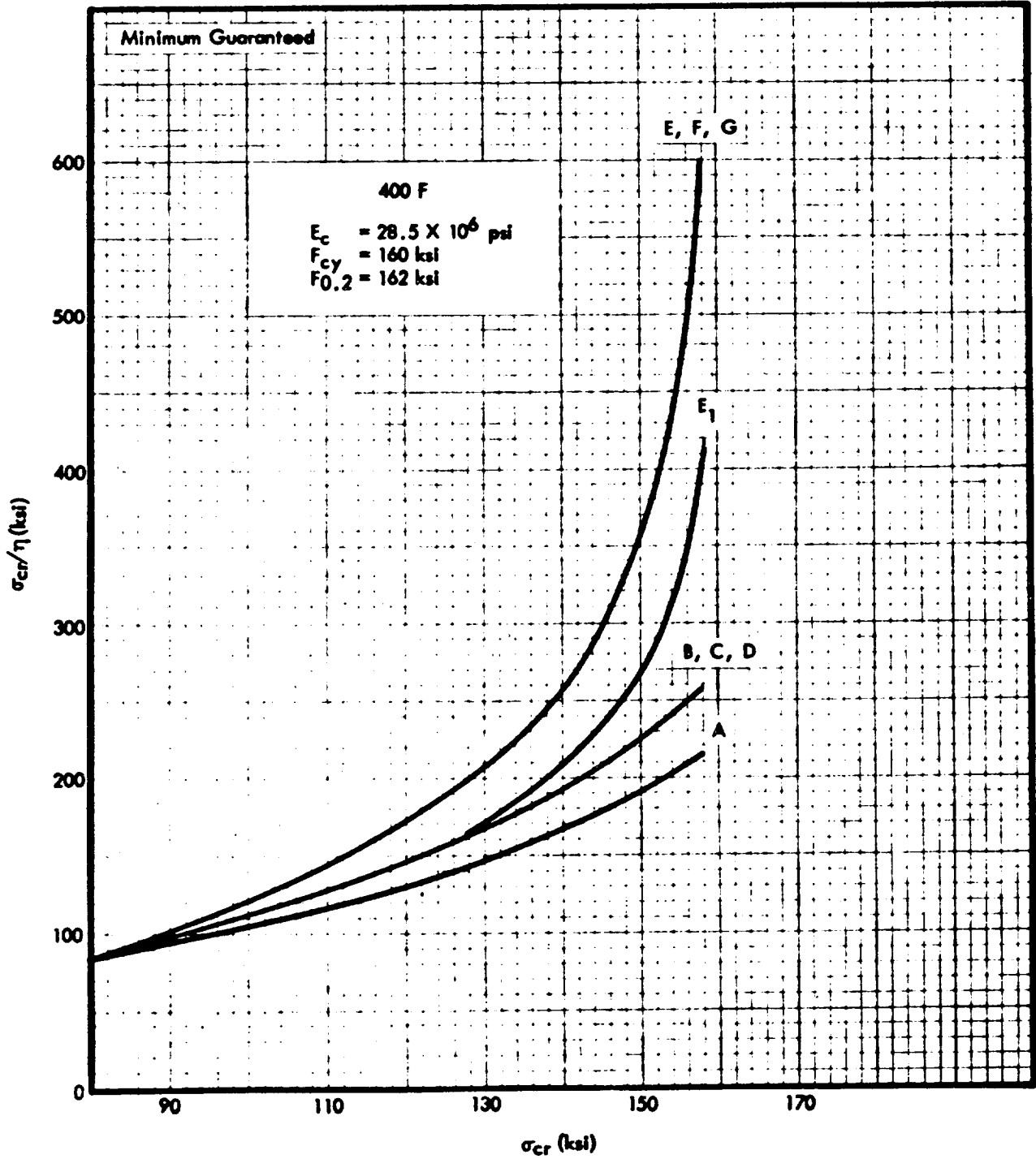


FIG. 3.62-17. PH 15-7 Mo STAINLESS STEEL SHEET AND PLATE -
 RH 1050, RH 1075 - SPECIFICATIONS LB0160-100, LB0160-129,
 LB0160-130, HB0160-010, LA0111-022, MA0107-023
 PLASTICITY CORRECTION CURVES (500 F)

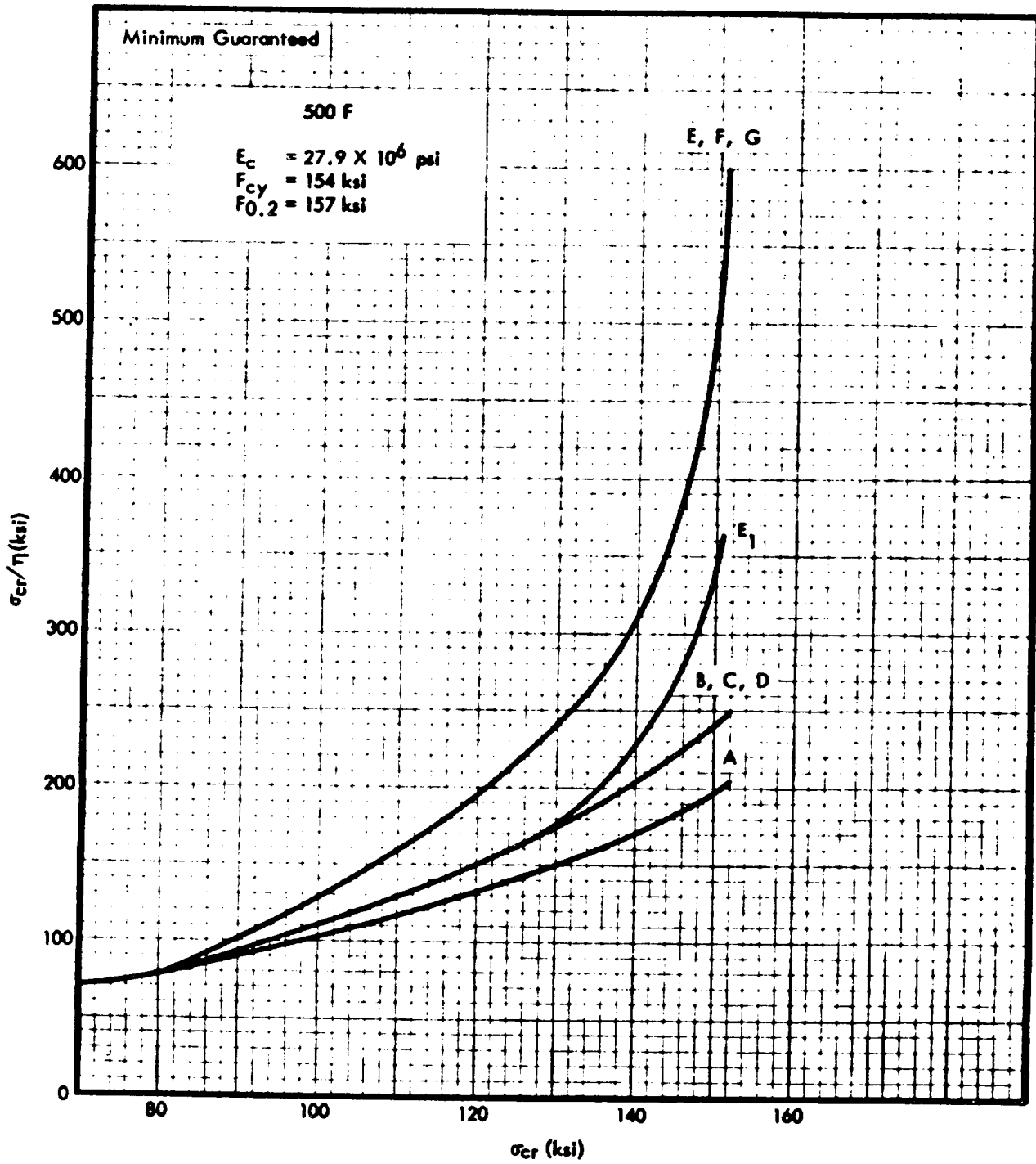


FIG. 3.62-18. PH 15-7 Mo STAINLESS STEEL SHEET AND PLATE -
 RH 1050, RH 1075 - SPECIFICATIONS LB0160-100, LB0160-129,
 LB0160-130, HB0160-010, LA0111-022, MA0107-023
 PLASTICITY CORRECTION CURVES (600 F)

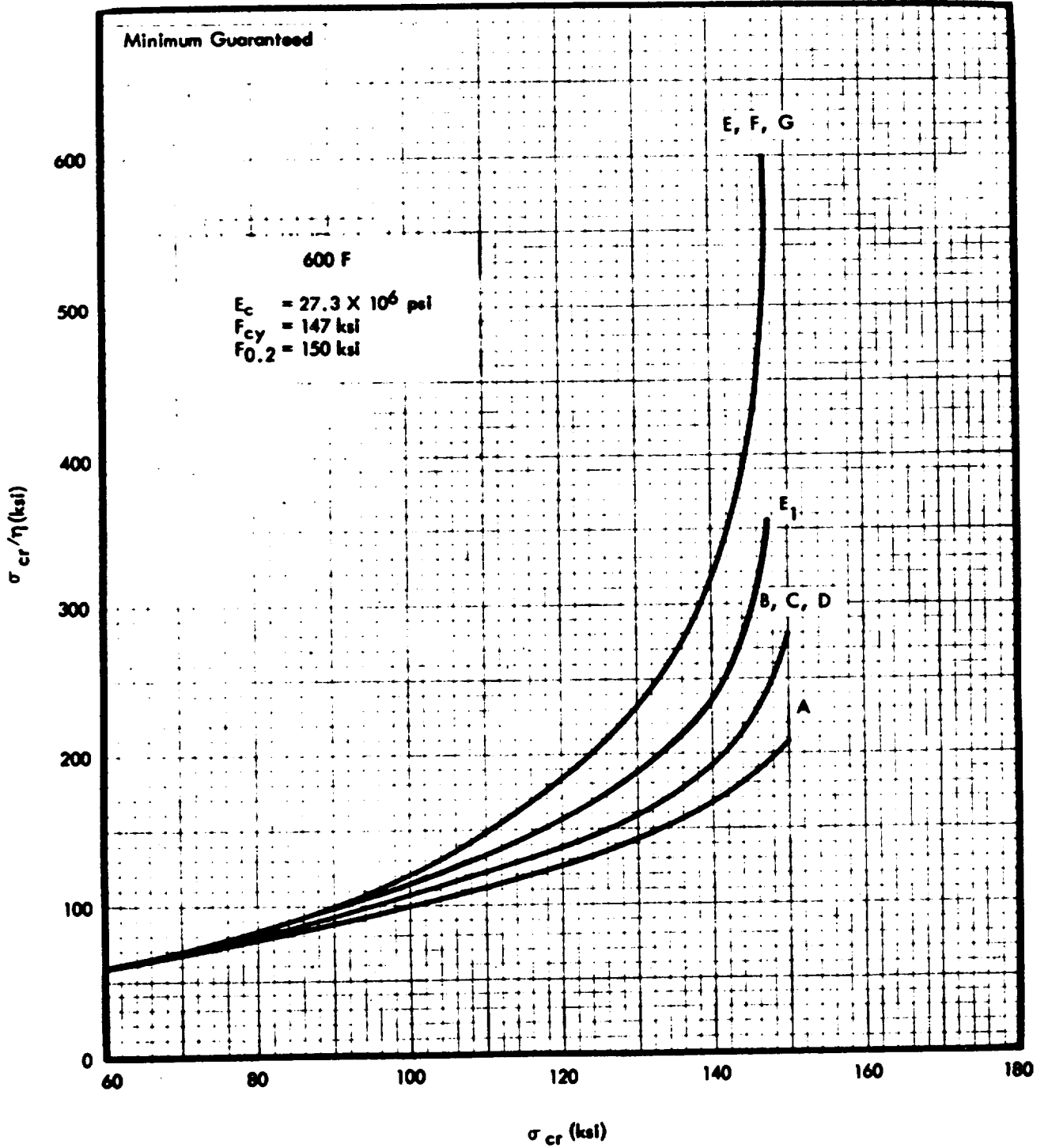


FIG. 3.62-19. PH 15-7 Mo STAINLESS STEEL SHEET AND PLATE -
 RH 1050, RH 1075 - SPECIFICATIONS LB0160-100, LB0160-129,
 LB0160-130, HB0160-010, LA0111-022, MA0107-023
 PLASTICITY CORRECTION CURVES (700 F)

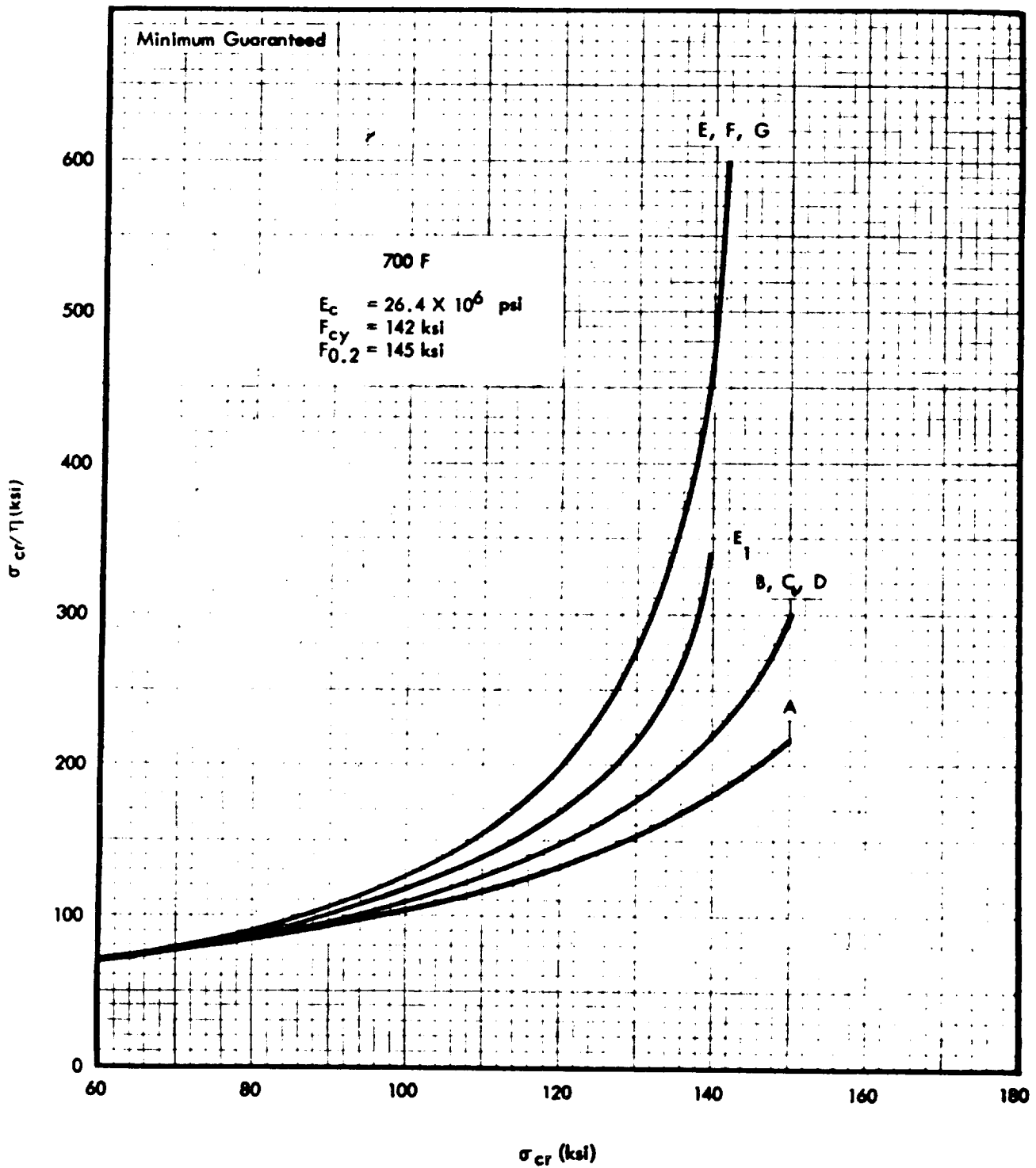


FIG. 3.62-20. PH 15-7 Mo STAINLESS STEEL SHEET AND PLATE -
 RH 1050, RH 1075 - SPECIFICATIONS LB0160-100, LB0160-129,
 LB0160-130, HB0160-010, LA0111-022, MA0107-023
 PLASTICITY CORRECTION CURVES (800 F, 900 F)

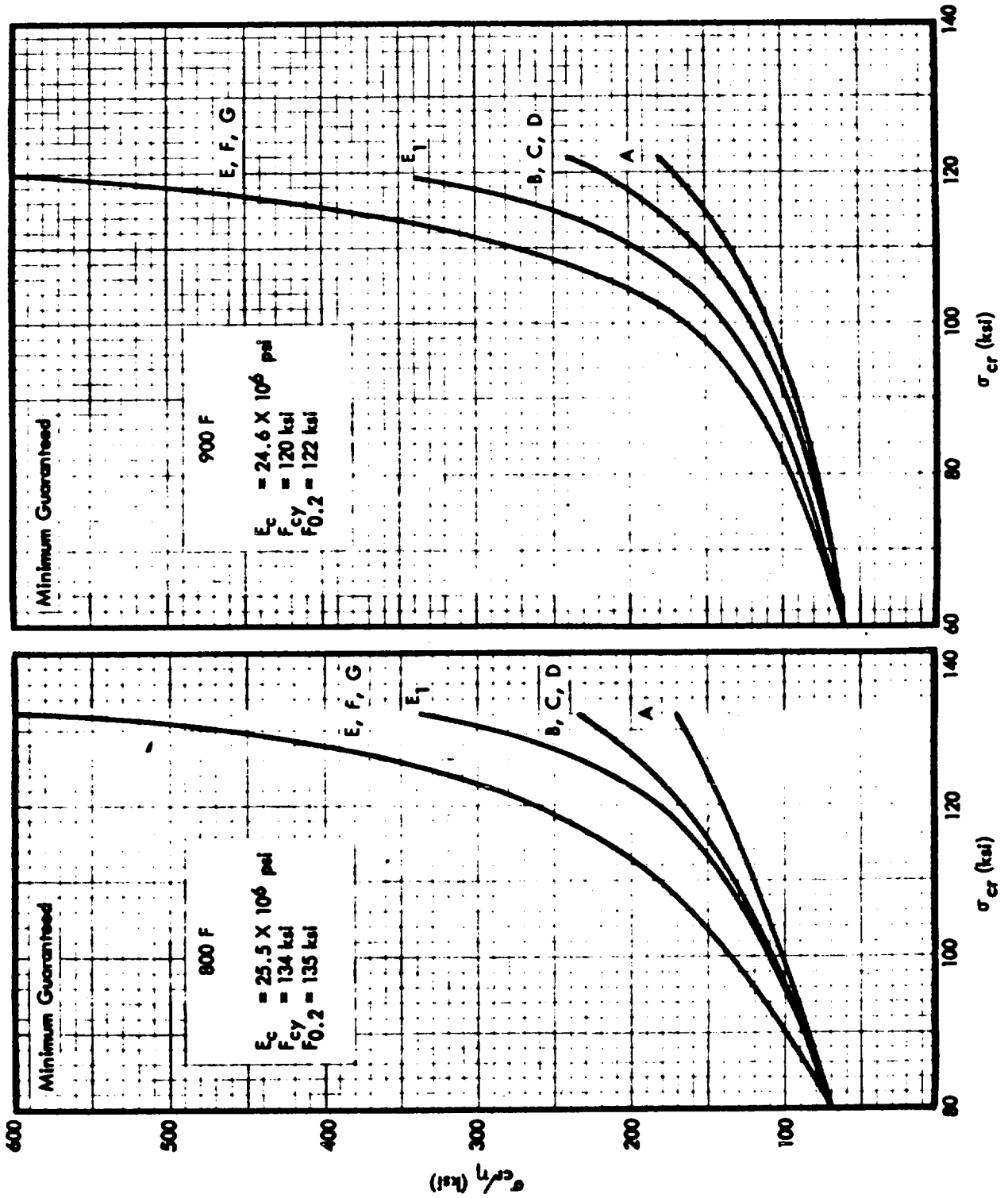


FIG. 3.62-21. PLASTICITY CORRECTION TITANIUM ALLOY SHEET <.25
6AL-4V ANNEALED LB0170-113

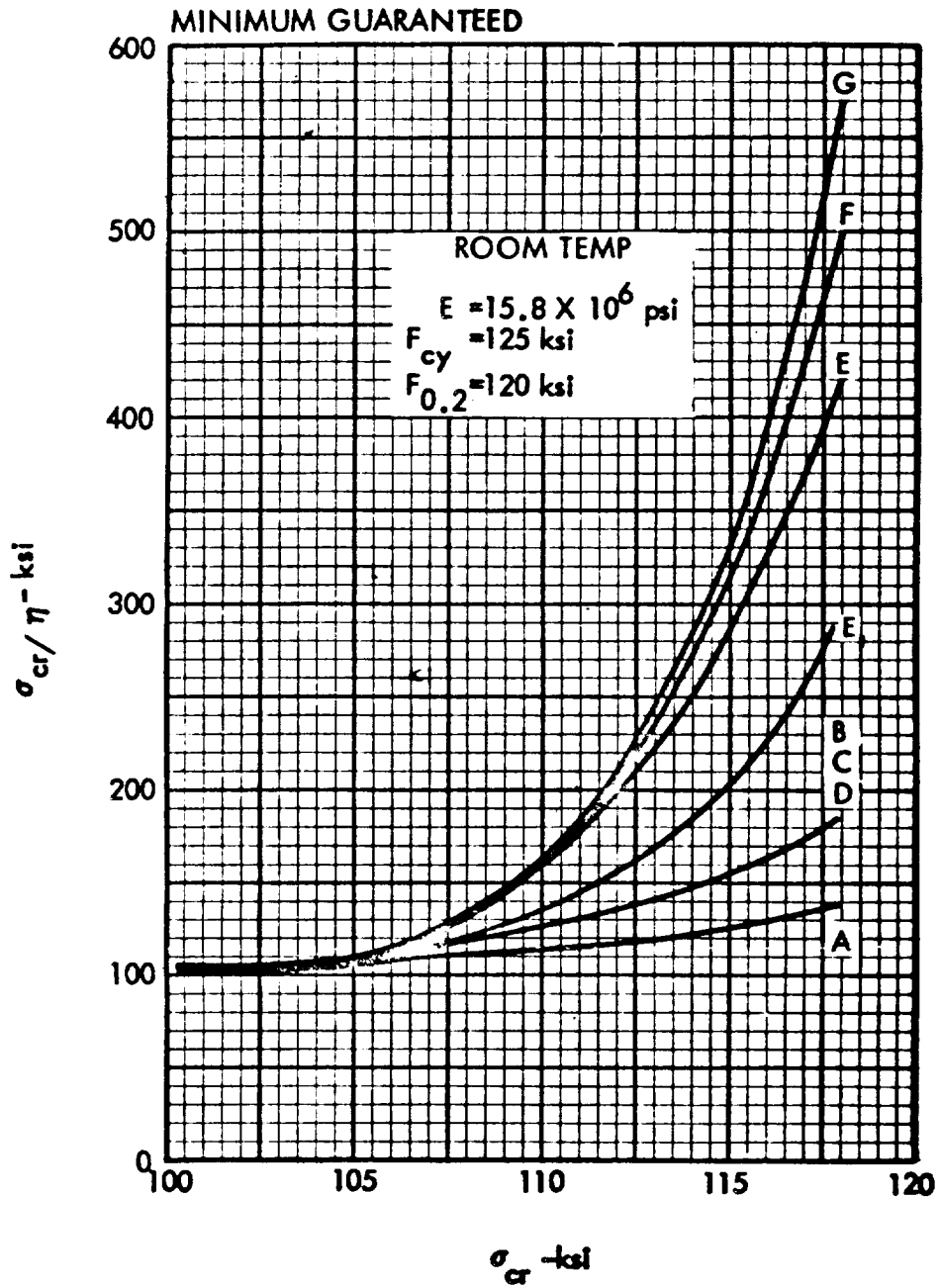


FIG. 3.62-22. PLASTICITY CORRECTION TITANIUM ALLOY SHEET <.25
6AL-4V ANNEALED LB0170-113

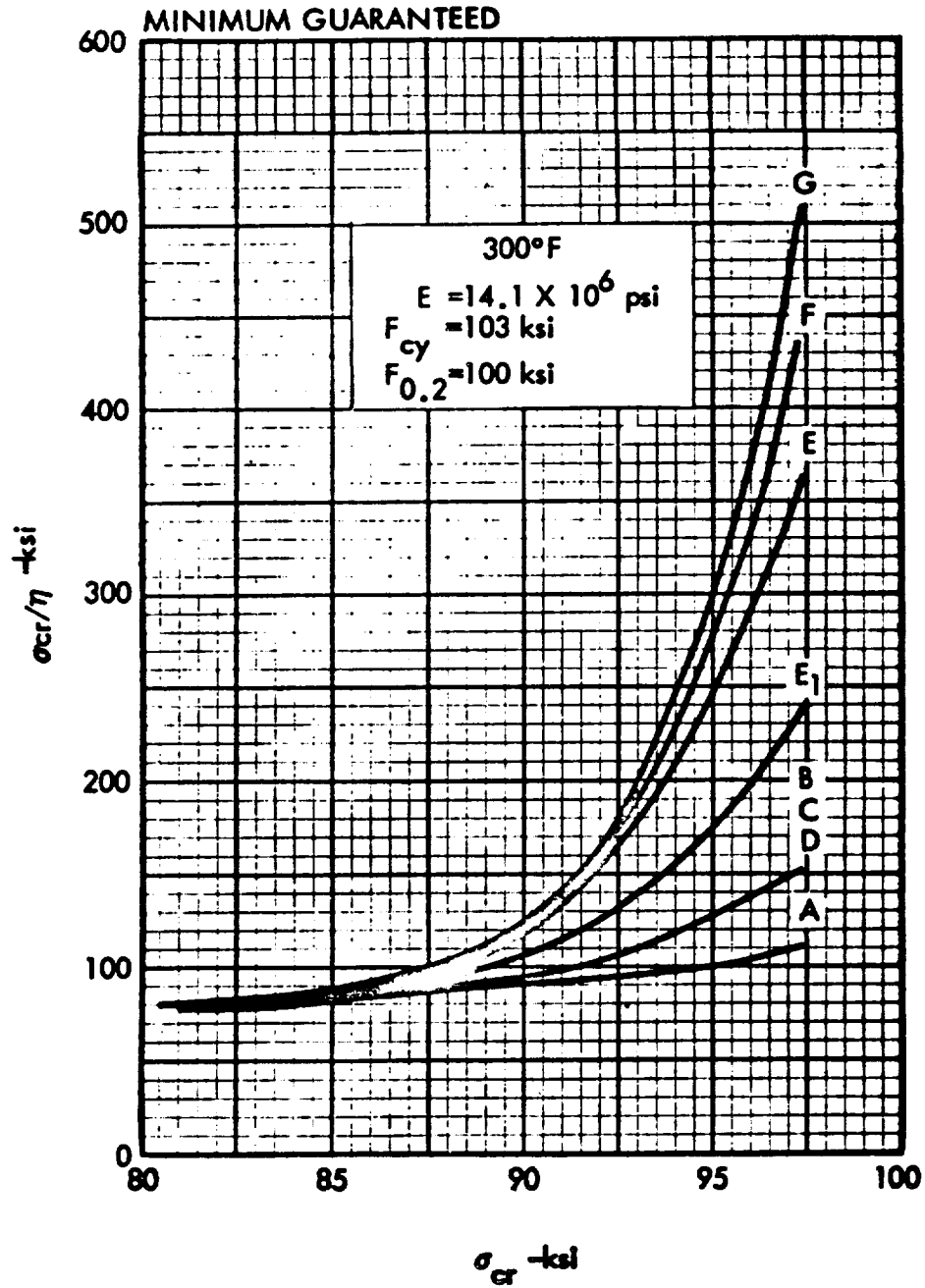


FIG. 3.62-23. PLASTICITY CORRECTION TITANIUM ALLOY SHEET < .25
6AL-4V ANNEALED

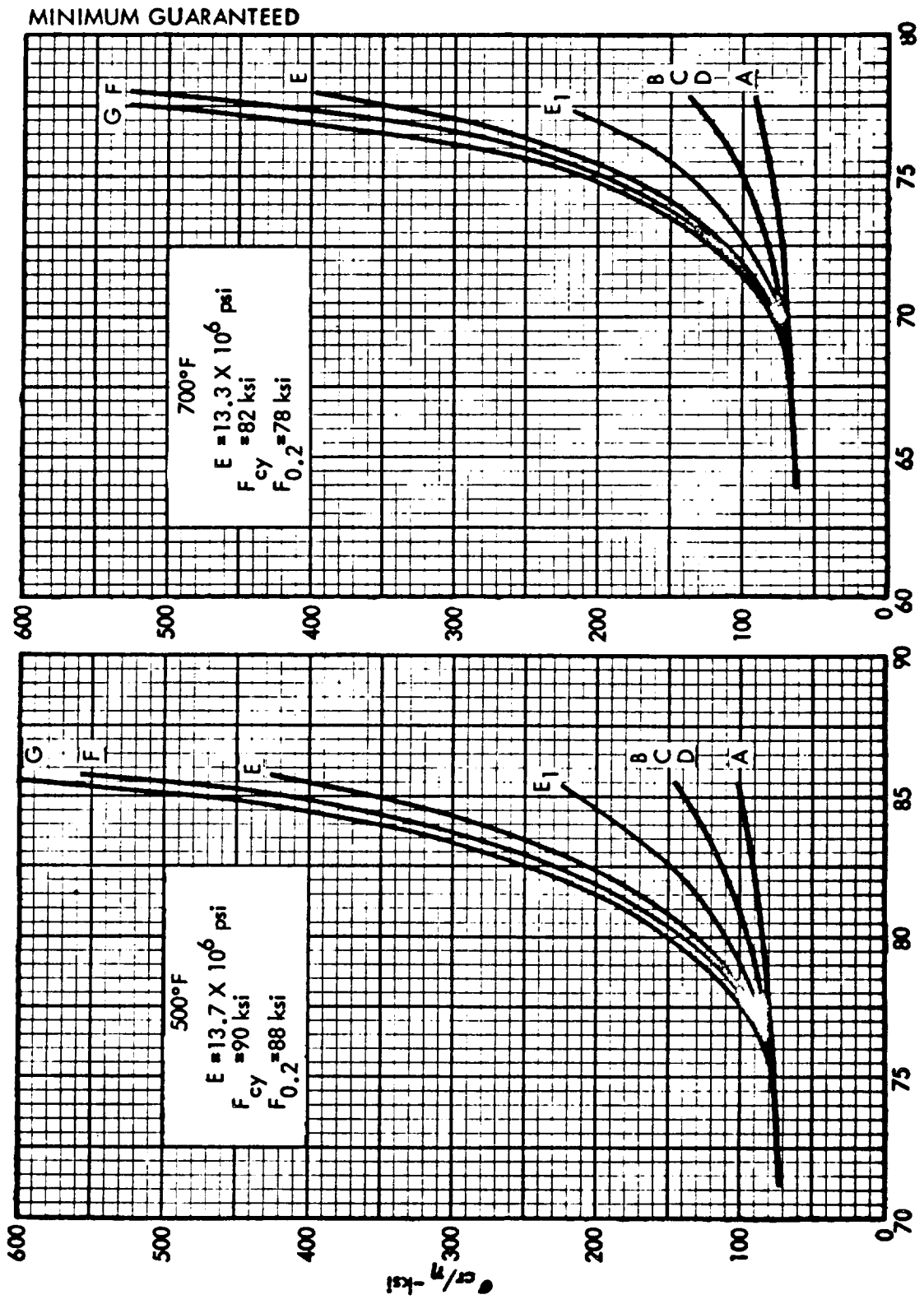


FIG. 3.62-24. PLASTICITY CORRECTION TITANIUM ALLOY SHEET <.25
6AL-4V ANNEALED LB0170-113

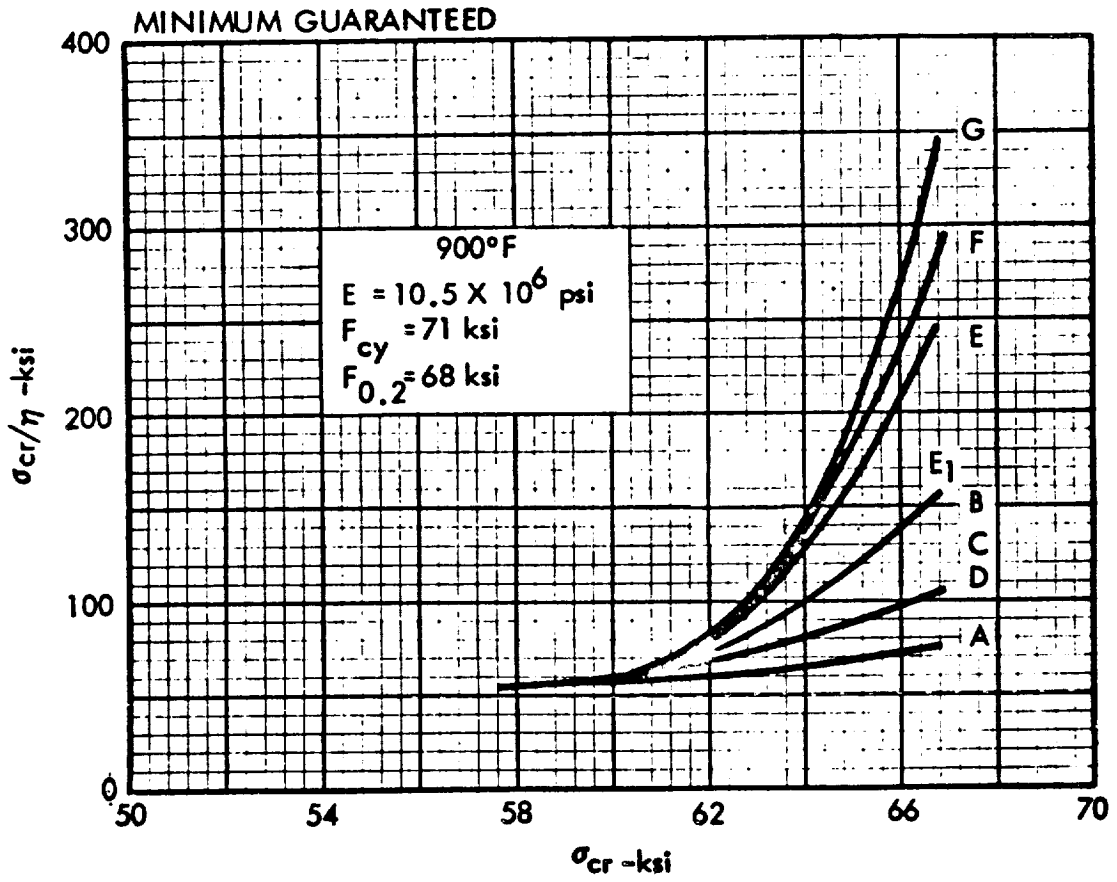


FIG. 3.62-25. PLASTICITY CORRECTION TITANIUM ALLOY SHEET <.25
6AL-4V CONDITION S. T. A.

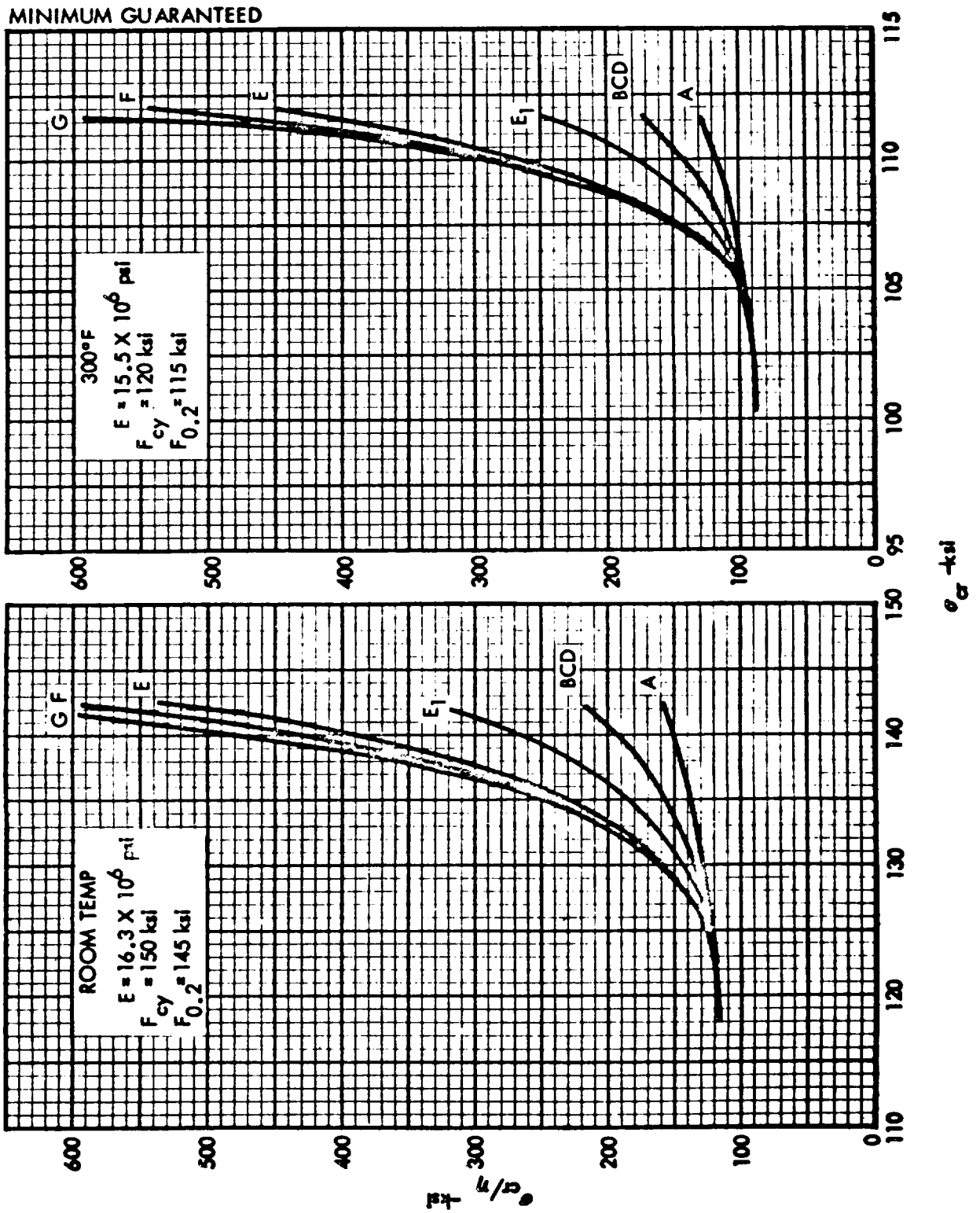


FIG. 3.62-26. PLASTICITY CORRECTION TITANIUM ALLOY SHEET <.25
6AL-4V CONDITION S. T. A.

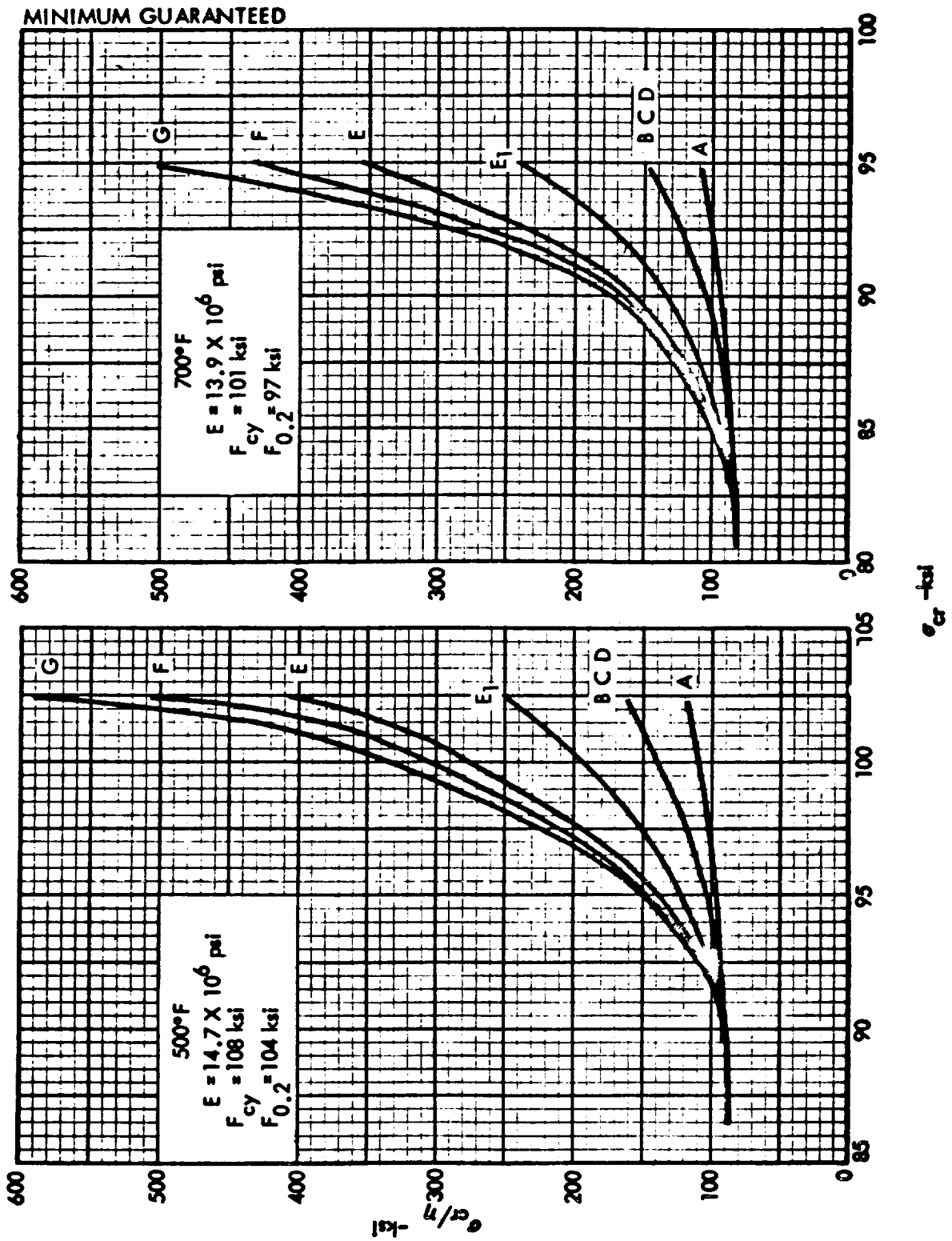
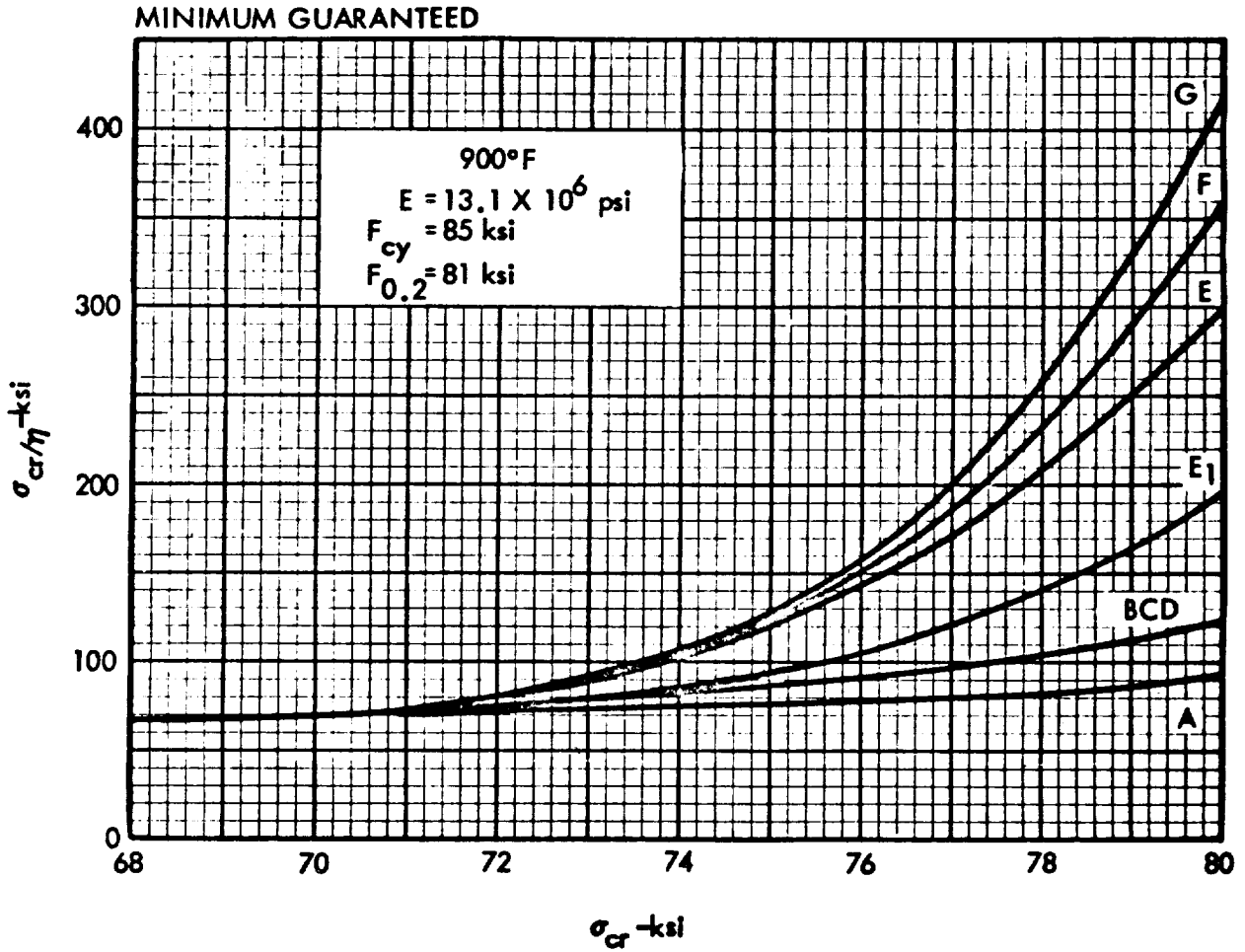


FIG. 3.62-27. PLASTICITY CORRECTION TITANIUM ALLOY SHEET <.25
6AL-4V CONDITION S. T. A. LB0170-113



3.63 COMBINED LOADINGS

The information on the inelastic stability analyses of shell structures subjected to combined loadings is limited. Very little theoretical work has been done in this field due to the complexity of the problem and, in general, plasticity correction factors are not available.

Methods of determining whether the stresses are in the inelastic range are discussed in Section 2.80. The method that can be used for ductile materials will be described.

The stress intensity σ_i and strain intensity e_i are obtained from the formulas

$$\sigma_i = \sqrt{\sigma_\phi^2 + \sigma_\theta^2 - \sigma_\phi \sigma_\theta + 3\tau^2}$$
$$e_i = \frac{2}{\sqrt{3}} \sqrt{\epsilon_\phi^2 + \epsilon_\theta^2 + \epsilon_\phi \epsilon_\theta + \frac{\gamma_{\phi\theta}^2}{4}}$$

where

$\sigma_\phi, \sigma_\theta$ = the stresses in the ϕ and θ directions, respectively
(for a cylinder or cone, the ϕ direction is the x direction)

τ = in-plane shear stress

$\epsilon_\phi, \epsilon_\theta$ = the strains in the ϕ and θ directions, respectively

$\gamma_{\phi\theta}$ = shear strain

For a ductile material, the σ_i versus e_i curve for a biaxial stress field is very close to the σ versus ϵ curve in a uniaxial stress field.

Therefore, if σ_i is greater than the uniaxial proportional limits of the material, the stress field is in the inelastic range.

It can be seen from the formula for σ_i that each of the individual stresses may be less than the proportional limits of the material, but σ_i may be in the inelastic range.

If the stress is in the inelastic range for a shell subjected to combined loads, an estimate of the inelastic buckling load can be obtained by using the plasticity correction factor associated with σ_i to modify the elastic buckling load. This method is useful if the plasticity correction factor of each of the pure loading cases is approximately the same.

A cylinder subjected to external lateral and axial pressure will be investigated as an example. The stress in the circumferential direction σ_θ is twice as large as the stress in the axial direction, σ_x ; therefore,

$$\begin{aligned}\sigma_i &= \sqrt{\left(\frac{\sigma_\theta}{2}\right)^2 + \sigma_\theta^2} - \frac{\sigma_\theta}{2} \sigma_\theta \\ &= \frac{\sqrt{3}}{2} \sigma_\theta\end{aligned}$$

The elastic critical circumferential buckling stress σ_{cr}/η may be obtained from Paragraph 3.23.4. The elastic stress intensity σ_i/η is therefore

$$\frac{\sigma_i}{\eta} = \frac{\sqrt{3}}{2} \frac{\sigma_{cr}}{\eta}$$

If σ_i/η is less than the proportional limit, $\eta = 1$. If the stresses are inelastic, σ_i may be obtained from Section 3.62 using σ_i/η and curves E. Then $\sigma_{cr} = 2\sigma_i/\sqrt{3}$ and the design allowable pressure is $p_{cr} = \sigma_{cr}t/R$.

REFERENCES

- 3-1 Kovalevsky, L., and R. Verette. Statistical Applicability of Data and Selection of Best Fit Curve. NAA S&ID, Downey, Calif., STR 112 (1965).
- 3-2 Harris, L. A., H. S. Suer, W. T. Skene, and R. J. Benjamin. "The Stability of Thin Walled Unstiffened Cylinders Under Axial Compression Including the Effects of Internal Pressure," Journal of Aerospace Sciences (Aug. 1957).
- 3-3 Stocker, J. A Review of the Literature on the Buckling Characteristics of Conical Shells. Boeing Co., Seattle, Wash., D2-23835-1, (1965).
- 3-4 S&ID Structures Manual. NAA S&ID, 543-G-11 (1964).
- 3-5 Gerard, G. Handbook of Structural Stability, Supplement to Part III—Buckling of Curved Plates and Shells. NASA TN D-163 (Sept. 1959).
- 3-6 Buckling of Thin-Walled Circular Cylinders. NASA, SP 8007 (1966).
- 3-7 Gerard, G., and H. Becker. Handbook of Structural Stability, Part III—Buckling of Curved Plates and Shells. NACA TN 3783 (1957).

- 3-8 Batdorf, Stein, and Schildcrout. Critical Combinations of Torsion and Direct Axial Stress for Thin-Walled Cylinders. NACA TN 1345 (June 1947).
- 3-9 Weingarten, V., E. Morgan, and P. Seide. Final Report on Development of Design Criteria for Elastic Stability of Thin Shell Structures. Space Technology Laboratories, Inc., STL/TR-60-0000-19425 (1960).
- 3-10 Hausrath, A., and F. Dittoe. Development of Design Strength Levels for the Elastic Stability of Monocoque Cones Under Axial Compression. NASA TN D-1510 (1962).
- 3-11 Seide, P. "On Buckling of Truncated Conical Shells in Torsion," Journal of Applied Mechanics, Vol. 29 (1962), pp. 320-238.
- 3-12 Weingarten, V. "Experimental Investigation of the Stability of Internally Pressurized Conical Shells Under Torsion," AIAA Journal, Vol. 2, No. 10 (1964).
- 3-13 Singer, J., et al Buckling of Isotropic, Orthotropic, and Ring Stiffened Conical Shells. TAE report No. 30, Israel Institute of Technology, AD 434845 (Sept. 1963).
- 3-14 Haung, Nai-Chien, "Unsymmetrical Buckling of Shallow Spherical Shells," AIAA Journal, Vol. 1, No. 4 (1963), p. 945.

- 3-15 Kaplan, A. and Y. C. Fung. A Nonlinear Theory of the Bending and Buckling of Thin Elastic Shallow Spherical Shells. NACA TN 3212 (1954).
- 3-16 Homewood, R., A. Brine, and A. Johnson. Experimental Investigation of the Buckling Instability of Monocoque Shells. SESA Paper No. 547, Vol. 18, No. 1 (1961), pp. 88-96.
- 3-17 Bellinfante, R. "Buckling of Spherical Caps Under Uniform External Pressure. Douglas Aircraft Co., Report No. SM-38938, (1962).
- 3-18 Tsien, Hsue-Shen, "A Theory for the Buckling of Thin Shells," Journal of Aero. Sci., Vol. 9, No. 10 (Aug. 1942), pp 373-384.
- 3-19 Parmenter, R. The Buckling of Clamped Shallow Spherical Shells Under Uniform Pressure. AFOSR 5362, AD No. 429764, (1963).
- 3-20 Krenzke, M., and T. Kiernan. "Elastic Stability of Near-Perfect Shallow Spherical Shells," AIAA Journal, Vol. 1, No. 12 (1963).
- 3-21 Tong, K. Buckling and Creep Buckling of Spherical Shells Under Uniform External Pressure. Syracuse University Research Institute, M. E. Dept., SURI Report No. ME992-764S (July 1964).

- 3-22 Modeer, J. Buckling Coefficients for Hemispheres and Oblate Hemispheroids. NAA S&ID, Downey, Calif., STR 92 (May 1963).
- 3-23 Krenzke, M., and T. Kiernan. The Effect of Initial Imperfections on the Collapse Strength of Deep Spherical Shells. DTMB Report No. 1757 (1965).
- 3-24 Wang, L. Buckling of a Spherical Shell With Various Boundary Conditions. Sc. D. Thesis, Civil Engineering Dept., Massachusetts Institute of Technology (June 1965).
- 3-25 Ambartsumyan, S. A. Theory of Anisotropic Shells. NASA F-118 (May 1964).
- 3-26 Dow, N., C. Libove, and R. E. Hubka. Formulas for the Elastic Constants of Plates with Integral Waffle-Like Stiffening. NACA RM L53 E13a (1953).
- 3-27 Gerard, G. "Compressive Stability of Orthotropic Cylinders," Journal of Aerospace Sciences (Oct. 1962).
- 3-28 Milligan, R., G. Gerard, and Lakshminantham. General Instability of Orthotropically Stiffened Cylinders Under Axial Compression. AIAA Paper No. 66-139, 3rd Aerospace Sciences meeting (Jan 1966).
- 3-29 Peterson, J. Weight-Strength Studies of Structures Representative of Fuselage Construction. NACA TN 4114, (1957).

- 3-30 Almroth, B. "Postbuckling Behavior of Orthotropic Cylinders Under Axial Compression," AIAA Journal Vol 2, No. 10 (Oct 1964).
- 3-31 Tasi, J., A. Feldman, and D. Stang. The Buckling Strength of Filament-Wound Cylinders Under Axial Compression. NASA CR-266 (July 1965).
- 3-32 Peterson, J., R. Whitley, and J. Deaton. Structural Behavior and Compressive Strength of Circular Cylinders With Longitudinal Stiffening. NASA TN D-1251 (1962).
- 3-33 Dunn, L. Some Investigations of the General Instability of Stiffened Metal Cylinders. IX Criteria for the Design of Stiffened Metal Cylinders Subjected to General Instability Failures. NACA TN 1198 (1947).
- 3-34 Becker, H. and G. Gerard. "Elastic Stability of Orthotropic Shells," Journal of Aerospace Sciences, Vol. 29, No. 5 (May 1962).
- 3-35 Structures Manual. NAA Los Angeles Division, NA-52-400.
- 3-36 Argyris, J. "Flexure-Torsion Failure of Panels," Aircraft Engineering, June-July 1954.
- 3-37 Becker, H. Handbook of Structural Stability Part VI—Strength of Stiffened Curved Plates and Shells. NASA TN 3786 (1956).

- 3-38 Card, M. F. Bending Tests of Large Diameter Stiffened Cylinders Susceptible to General Instability. NASA TN D-2200.
- 3-39 Dickson, J. and R. Brollear. The General Instability of Ring-Stiffened Corrugated Cylinders Under Axial Compression. NASA TN D3089 (Jan. 1966).
- 3-40 Block, D., M. Card, and M. Mikulas. Buckling of Eccentrically Stiffened Orthotropic Cylinders. NASA TN D-2960 (Aug. 1965).
- 3-41 Gerard, G. Minimum Weight Analysis of Compression Structure. New York: New York University Press (1956).
- 3-42 Pulos, J. Structural Analysis and Design Considerations for Cylindrical Pressure Hulls. David Taylor Model Basin Report 1639 (April 1963).
- 3-43 Pulos, J., and V. Salerno. Axisymmetric Elastic Deformations and Stresses in Ring-Stiffened Perfectly Circular Cylindrical Shell Under External Hydrostatic Pressure. David Taylor Model Basin Report 1497 (Sept. 1961).
- 3-44 Reynolds, T. E. Elastic Lobar Buckling of Ring-Supported Cylindrical Shells Under Hydrostatic Pressure. David Taylor Model Basin Report 1614 (Sept. 1962).
- 3-45 Reynolds, T. E. A Graphical Method for Determining the General-Instability Strength of Stiffened Cylindrical Shells. David Taylor Model Basin Report 1106 (Sept. 1957).

- 3-46 Ball, W. Formulas and Curves for Determining the Elastic General-Instability Pressures of Ring-Stiffened Cylinders.
David Taylor Model Basin Report 1570 (Jan. 1962).
- 3-47 Kendrick, S. The Buckling Under External Pressure of Circular Cylindrical Shells With Evenly-Spaced, Equal Strength Circular Ring-Frames—Part III. Naval Construction Research Establishment Report R-244 (1953).
- 3-48 Reynolds, T., and W. Blumenberg. General Instability of Ring-Stiffened Cylindrical Shells Subjected to External Hydrostatic Pressure. David Taylor Model Basin Report 1324 (June 1959).
- 3-49 Galletly, G., et al. "General Instability of Ring-Stiffened Cylindrical Shells Subjected to External Hydrostatic Pressure—A Comparison of Theory and Experiment." Journal of Applied Mechanics, Vol. 25, Trans. ASME, Vol. 80 (June 1958).
- 3-50 Singer, J., M. Baruch, and O. Harari. Further Remarks on the Effects of Eccentricity of Stiffeners on the General Instability of Stiffened Cylindrical Shells. Technion-Israel Institute of Technology, TAE Report No. 42 (Aug. 1965).
- 3-51 Lunchick, M. Plastic General-Instability Pressure of Ring-Stiffened Cylindrical Shells. David Taylor Model Basin Report 1587.

- 3-52 Konishi, D. et al, Honeycomb Sandwich Structures Manual. NAA
Los Angeles Division, Report NA58-899.
- 3-53 Norris, C. Short-Column Compressive Strength of Sandwich
Constructions as Affected by Size of Cells of Honeycomb Core
Materials. Forest Products Laboratory, FPL-026 (Jan. 1964).
- 3-54 Yusuff, S. "Face Wrinkling and Core Strength in Sandwich
Construction." Journal of Royal Aeronautical Society, Vol. 64
(March 1960).
- 3-55 Harris, B., and W. Crisman. "Face-Wrinkling Mode of
Buckling of Sandwich Panels," ASCE Journal of Engineering
Mechanics Division, EM3 (June 1965).
- 3-56 Zahn, J., and E. Kuenzi. Classical Buckling of Cylinders
for Sandwich Construction in Axial Compression—Orthotropic
Cores. Forest Products Laboratory, FPL-018 (1963).
- 3-57 March, H. W., and E. W. Kuenzi. Buckling of Sandwich
Cylinders in Torsion. Forest Products Report No. 184
(Jan. 1958).
- 3-58 Kiciman, M. O., and D. Y. Konishi. Stability of Honeycomb
Sandwich Cylinders. ASME Paper No. 61-AV-36 (1961).

- 3-59 Kuenzi, E., B. Bohannon, and G. Stevens. Buckling Coefficients for Sandwich Cylinders of Finite Length Under Uniform External Lateral Pressure. Forest Product Laboratory, Research Note FPL-0104, (Sept. 1965).
- 3-60 Silver, P. The Effects of Poisson's Ratio on Plasticity Corrections. NAA S&ID, STR55 (April 1957).
- 3-61 Stowell, E. A Unified Theory of Plastic Buckling of Columns and Plates. NACA TN 1556 (April 1943).
- 3-62 Baker, E. "Stability of Circumferentially Corrugated Sandwich Cylinders Subjected to Combined Loads," AIAA Journal, Vol. 2, No. 12 (Dec. 1964).
- 3-63 Harris, L., and E. Baker. Elastic Stability of Simply Supported Corrugated Core Sandwich Cylinders. NASA D-1510 (1962).

4.00 MINIMUM WEIGHT SHELL DESIGN

4.10 INTRODUCTION

To obtain the best possible performance in spacecraft design, one of the main objectives is to achieve a minimum-weight structure that meets the requirements of structural integrity. This chapter presents a review of the literature and methods of analysis for use in preliminary design to determine the lightest shell wall for various constructions subjected to specific loading conditions. It is intended that Chapter 4.00 supplements the solutions presented in Chapters 2.00 and 3.00.

Chapter 2.00 presents deflection and internal load distribution solutions for a number of shell geometries and loading conditions. Chapter 3.00 presents general and local instability solutions for shells. Whereas use of these chapters will achieve designs which will preclude failure, Chapter 4.00 presents methods to achieve minimum weight, also.

In most of the published work concerning minimum-weight analysis and the design of elements subjected to buckling, it is generally accepted as axiomatic that minimum weight is attained when the possible buckling modes occur simultaneously. Limited proofs of this statement have been presented (Refs. 4-1 and 4-2). An additional assumption is that the margins of safety are zero for all buckling modes.

Some of the existing minimum-weight analyses are based on approximate methods which, however, are adequate for preliminary analysis. It is important to realize that the minimum weight construction theoretically derived may not be practical for actual construction because of material gage limitations, etc. Since it is theoretically possible to arrive at impractical designs, various minimum weight analyses should be used with caution unless the proportions are examined to ensure that they are realistic. The weight of the final design can be established by summing the weight of the individual components.

4.20 STIFFENED SHELLS

4.21 GENERAL

Stiffened cylinders under bending are representative of aircraft fuselages whereas launch vehicles and some spacecraft can be treated as stiffened cylinders under compression. Hence, there is considerable literature on the optimum design of stiffened cylindrical shells. The following is a summary of the literature from Ref. 4-3.

For unstiffened cylinders under bending, Clayton (Ref. 4-4) established that the appropriate design index is (M/R^3) or (N/R) . Becker (Ref. 4-5) treated the unstiffened cylinder diameter as an open dimension and found the ideal value of the optimum stress as well as the diameter of the lightest weight cylindrical cross section under bending. Shanley (Refs. 4-6 and 4-7) also considered this problem by a numerical procedure and concluded that for typical values of the design index for aircraft fuselages, the diameter was far beyond the optimum for an unstiffened shell.

Joyce and Mitchell (Refs. 4-8 and 4-9) determined stiffener and frame spacings for minimum weight stiffened cylinders. By neglecting the frame weight, Shanley (Refs. 4-6 and 4-7) also investigated numerically the minimum-weight design of stiffened panel-frame cylinder construction for various frame spacings. Micks (Ref. 4-10)

extended this analysis by a numerical procedure which included the frame weight, and he was able to determine optimum frame spacings for longitudinally stiffened cylinders. Gerard (Refs. 4-1 and 4-11) analyzed the frame stiffness requirements for general instability in terms of a transverse stiffener criterion and determined optimum frame spacings for longitudinally stiffened cylinders in bending.

Because of its importance in the design of submarine pressure hulls and underwater launched missiles, the efficient design of stiffened cylinders under external pressure has received some recent attention. Wenk (Refs. 4-12 and 4-13) has established the pressure (p) as the design index and has presented a series of minimum weight design charts for aluminum and steel ring-stiffened cylinders. Gerard (Ref. 4-14) treated the minimum-weight design of ring-stiffened cylinders based on orthotropic shell theory and obtained results for the optimum configuration of I-ring stiffeners.

Stiffened cylinders under compression are of interest in missile, launch vehicle, and spacecraft applications and, therefore, recent minimum-weight studies have been concerned with such structures. Crawford and Burns (Refs. 4-15 and 4-16) treated integral ring-stiffened cylinders under hydrostatic pressure. Gerard and Papirno (Ref. 4-17) have considered the minimum-weight design of ring-stiffened and

longitudinal ring-stiffened cylinders under compression based on orthotropic cylinder theory. The optimum design of cylinders utilizing unflanged and flanged stiffener shapes was investigated to determine their effect upon the cylinder efficiency.

The advent of thin aircraft wing and tail structures in the late 1940's has resulted in investigations to define the regions of efficient application of composite structures. Stiffened panel and multicell box construction were compared by Gerard (Ref. 4-18) for typical ranges of parameters and also by Kolom (Ref. 4-19). Hubka et al., (Ref. 4-20) in a similar study compared stiffened panel and sandwich box construction. In a further attempt to define the ranges of efficient application of various types of wing and fuselage construction. Gerard (Refs. 4-1 and 4-11) conducted a comprehensive comparative efficiency analysis of stiffened panel-rib, multicell and post-stiffened, sandwich plate and full-depth sandwich box beams of high-strength aluminum alloy.

In order to improve the structural efficiency of multicell construction, various types of compression cover and web elements were investigated. Anderson (Ref. 4-21) studied the comparative efficiencies of multicell boxes with steel sandwich covers and channel and corrugated webs as well as full-depth sandwich boxes. Semonian and Crawford (Ref. 4-22) made comparisons with the efficiencies of multicells of

flat, integrally stiffened and sandwich cover plates employing plate and corrugated webs. They also treated multiweb boxes of wide-column and Z-stiffened panels employing corrugated ribs, in addition to full-depth sandwich boxes.

The comparative efficiency of longitudinal, transverse, and waffle grid stiffening systems for plates used as compression covers for multicells were investigated by Gerard (Ref. 4-23) by use of orthotropic plate theory. Lampert and Younger (Ref. 4-24) treated, in rather great detail, the comparative structural efficiency of various truss-core configurations for sandwich plates. Crawford and Burns (Refs. 4-15 and 4-16) conducted comparative efficiency studies of integrally stiffened, Z-stiffened, and corrugated core sandwich plates under compression. They also treated multicell boxes with flat and corrugated core sandwich plates as covers and employing flat, integrally stiffened, Z-stiffened and corrugated core sandwich webs to establish the comparative efficiencies of the various combinations. Gerard (Ref. 4-25) investigated the comparative efficiencies of various types of box beams.

Aircraft fuselages and later missile, launch vehicle, and spacecraft structures have encouraged comparative efficiency studies of stiffened cylinders. Shanley (Refs. 4-6 and 4-7) compared unstiffened

and longitudinally stiffened cylinders of the same length under bending. Gerard (Refs. 4-1 and 4-11) conducted a comparative efficiency analysis of unstiffened, longitudinally-stiffened frame and sandwich cylinders all of optimum design under bending. Peterson (Ref. 4-26) presented weight-strength charts on ring, longitudinally and waffle stiffened, and sandwich cylinders in bending. The effect of shear loads on bending strength was also considered.

For cylinders under compression, Gerard (Refs. 4-27 and 4-28) presented comparative efficiency results for unstiffened, ring-stiffened, longitudinally stiffened-ring, and sandwich shells of optimum design. An analysis of pressure stabilized cylinders was also included. Crawford and Burns (Refs. 4-15 and 4-16) compared unstiffened and corrugated core sandwich cylinders of optimum design for compression, torsion, and hydrostatic pressure. Based on orthotropic cylinder theory, Gerard and Papirno (Ref. 4-17) compared ring and longitudinal-ring stiffened cylinders under compression and also established the influence of unflanged and flanged stiffeners upon the cylinder efficiency.

4.22 STIFFENED CYLINDRICAL SHELLS IN PURE BENDING

Based on the design axiom that minimum weight is attained when the possible buckling loads occur simultaneously, it is possible to present a necessary condition for minimum weight of stiffened cylindrical shells. A stiffened cylindrical shell has two primary modes of failure: (1) buckling of the panel between frames, and (2) general instability. If the rings are sufficiently stiff to resist buckling, the stiffened shell will buckle between the frames. Buckling of the skin-stringer column between frames may occur as a result of material failure, stringer crippling, or primary bending or torsional instability.

The ultimate strength of the plate-stringer combination is found by assuming an effective width of curved sheet to act at the critical buckling stress of the column in the manner presented in Section 3.00. If, however, the calculated buckling stress of the sheet is higher than that of the stringer plus its effective width sheet, the entire width is assumed to act at the column buckling stress (Ref. 4-29). If the frames are not sufficiently stiff to resist buckling, the stiffened cylindrical shell may fail in a general instability mode.

A necessary condition for minimum weight dictates that both panel and general instability modes of failure should occur simultaneously. The frame stiffness for which panel instability and general instability

are equally critical may be estimated from the following formula from Ref. 4-1.

$$(EI)_f = C_f \frac{M(2R)^2}{d} \quad (4.22-1)$$

where

$(EI)_f$ = flexural stiffness requirement for frame

M = applied bending moment

d = frame spacing

If the frame stiffness is greater than $(EI)_f$, the cylinder will fail in panel instability, and if the frame stiffness is less than $(EI)_f$ the cylinder will fail in general instability. Several values of C_f have been suggested in the literature; $C_f = 6.84 \times 10^{-5}$ as suggested in Ref. 4-1 is recommended because it has some theoretical and experimental justification. For frames with flexural stiffness greater than $(EI)_f$ the increase in the strength of the cylinder when subjected to bending is relatively small. The minimum weight design in practice can be obtained by an iterative procedure.

4.30 SANDWICH SHELLS

4.31 GENERAL

The main purpose of the sandwich construction is to achieve a high bending rigidity-to-weight ratio. Sandwich construction consists essentially of two high strength-to-weight ratio facing sheets. These sheets are joined and separated by a relatively thick low-density core that transmits shear between the facing sheets. The facings are designed to take all compressive or bending loads, while the core is supposed to transfer shear between the facings and allow the facings to bend about a common neutral axis. For most cases of interest for space vehicles, the facing sheets are so thin that their flexural rigidities about their respective neutral axes can be neglected. The facings, therefore, behave essentially as membranes and withstand bending stresses directly except in the vicinity of concentrated loads or rapid changes in cross section.

The sandwich core may consist of any of a number of types. The most common cores are the open cell, honeycomb configurations, the corrugated core, and the closed-cell foam cores. The honeycomb cores are, currently, the most widely used in space vehicle construction, particularly in boosters. To use the core of the lightest type is

desirable, yet in reality its weight is a substantial part of the total weight of the sandwich.

The third element, as far as weight is concerned, is the bonding medium, which can be either adhesive or braze material. All three elements of the sandwich structure must be considered in a minimum weight analysis: the facings, the core, and the bonding medium.

Some of the earliest studies were conducted on sandwich cylinders. Leggett and Hopkins (Ref. 4-30) concluded that sandwich construction becomes increasingly more efficient than stiffened panel construction as the curvature is increased. Wittrick (Ref. 4-31) investigated the optimum design of sandwich cylinders under compression, considered various face materials and core densities, and concluded that there is a definite optimum core rigidity for each face material and design index (N/R).

Crawford and Burns (Refs. 4-15 and 4-16) presented a detailed optimum design analysis of corrugated core sandwich cylinders under compression, torsion, and hydrostatic pressure. For the latter, integral ring-stiffened cylinders were also treated.

Switzky and Cary (Ref. 4-32) presented nondimensional, minimum-weight design charts for unstiffened and corrugated core sandwich cylinders under compression, torsion, and external pressure.

The nondimensional feature accounts for material properties at various temperatures.

Kuenzi (Ref. 4-33) presented an analysis to determine the minimum weight of sandwich considering stiffness, edge load capacity, bending moment capacity, and buckling of cylindrical shells.

A number of designs, involving various thicknesses of facing and core, may meet a given stiffness or strength requirement. This concept suggests possibilities of determining constructions so proportioned that minimum weight for a given stiffness or strength is achieved. The minimum weight construction, theoretically derived, may not be practical because of unusually thin facings, which are not available, or unusually lightweight core. Since it is theoretically possible to arrive at impractical designs, various minimum weight analyses should be used with caution for comparing sandwich with other constructions, unless the sandwich proportions are examined to ensure that they are realistic.

4. 32 BUCKLING OF SANDWICH CYLINDERS UNDER AXIAL COMPRESSION

The design allowable buckling stress for general instability of a sandwich cylinder under axial compression is given by the formula from Section 3. 52.

$$\sigma_{cr} = C_c \gamma E \frac{h}{R} \frac{2\sqrt{t_1 t_2}}{\sqrt{1 - \mu^2} (t_1 + t_2)} \quad (4. 32-1)$$

for equal facings

$$\sigma_{cr} = \frac{C_c \gamma}{\sqrt{1 - \mu^2}} E \frac{h}{R} \quad (4. 32-2)$$

where

$$C_c = (1 - k_2 V_c) \text{ for } V < 0. 5 \text{ (approximately)}$$

$$k_2 = 1 \text{ for isotropic core}$$

k_2 (for orthotropic core) is the negative slope of the C_c versus V_c curve in Fig. 3. 52-1

$$V_c = \frac{Et}{2R G_{xz}} \quad (\text{approximately})$$

G_{xz} is the transverse shear modulus of the core in the axial direction and the factor γ is obtained from Fig. 3. 33-6.

Minimizing the sandwich weight with respect to the facing thickness (Ref. 4-33) and excluding local failures (wrinkling, dimpling, etc.) leads to the equation for the weight of the core to the sandwich weight minus bond weight ratio as follows:

$$\frac{W_c}{(W - W_b)} = \frac{1 - k_2 V}{2 - 3 k_2 V} \quad (4.32-3)$$

where

W_c = weight of core

W_b = weight of bond

W = total weight of sandwich

Thus, the weight of the core, W_c , is about one-half the sandwich weight for a minimum weight sandwich cylinder subjected to axial compression.

REFERENCES

- 4-1. Gerard, G. Minimum Weight Analysis of Compression Structures. New York: New York University Press (1956).
- 4-2. Cohen, G. A. "Optimum Design of Truss-Core Sandwich Cylinder Under Axial Compression," AIAA Journal, Vol. 1, No. 7 (July 1963), pp. 1626-1630.
- 4-3. Gerard, G. Optimum Structural Design Concepts for Aerospace Vehicles: Bibliography and Assessment. Air Force Flight Dynamics Laboratory Research and Technology Division, Technical Report No. AFFDL-TR-65-9.
- 4-4. Clayton, W. C. "Design Charts for Tubes Subject to Bending." Aviation, Vol. 41, No. 4 (April 1942).
- 4-5. Becker, H. "The Optimum Proportions of a Long Unstiffened Circular Cylinder in Pure Bending," Journal Aeronautical Sciences, Vol. 15, No. 10 (Oct. 1948), pp. 616-624.
- 4-6. Shanley, F. R. "Principles of Structural Design for Minimum Weight," Journal Aeronautical Sciences, Vol. 16, No. 3 188 (March 1949), pp. 133-149.
- 4-7. Shanley, F. R. Weight-Strength Analysis of Aircraft Structures. New York: McGraw-Hill Book Co., Inc., (1952), pp. 1-260.

- 4-8. Joyce, N. B. and L. H. Mitchell. Panel Shape for Least Weight Design of Stiffened Cylinders in Pure Bending. Council for Scientific and Industrial Research (Australia), Div. of Aero. SM 106 (Dec. 1947).
- 4-9. Mitchell, L. H. Minimum Weight Semi-Monocoque Cylinders Subjected to Pure Bending. Council for Scientific and Industrial Research (Australia), Div. of Aero. SM 118 (Sept. 1948).
- 4-10. Micks, W. R. "Minimum Weight of Stiffened Cylindrical Shells in Pure Bending," Journal Aeronautical Sciences, Vol. 17, No. 4 (April 1950), pp. 211-216.
- 4-11. Gerard, G. Comparative Efficiency in Bending of Structural Elements of Various Designs and Solidity. New York University Report to Office of Naval Research (April 1952).
- 4-12. Wenk, E., Jr. "Pressure Vessel Analysis of Submarine Hulls," Welding Journal, Res. Suppl. Vol. 40, No. 6 (June 1961), pp. 272S-288S.
- 4-13. Wenk, E., Jr. "Feasibility of Pressure Hulls for Ultradeep Running Submarines," Journal of Engineering for Industry, Vol. 84, No. 3 (Trans. ASME, Series B), (Aug 1962), pp. 373-393.
- 4-14. Gerard, G. "Minimum Weight Design of Ring Stiffened Cylinders Under External Pressure," Journal Ship Research, Vol. 5, No. 2 (Sept. 1961), pp. 44-49.

- 4-15. Crawford, R. F. and A. B. Burns. Strength, Efficiency and Design Data for Beryllium Structures. ASD TR 61-692 (Feb 1962).
- 4-16. Crawford, R. F. and A. B. Burns. "Minimum Weight Potentials for Stiffened Plates and Shells," AIAA Journal, Vol. 1, No. 4 (April 1963), pp. 879-886.
- 4-17. Gerard, G. and R. Papirno. Minimum Weight Design of Stiffened Cylinders for Launch Vehicle Applications. NASA CR-53316 (March 1964).
- 4-18. Gerard, G. "Efficient Applications of Stringer Panel and Multicell Wing Construction," Journal Aeronautical Sciences, Vol. 16, No. 1 (Jan. 1949), pp. 35-40.
- 4-19. Kolom, A. L. "Optimum Design Considerations for Aircraft Wing Structures," Aeronautical Engineering Review, Vol. 12, No. 10 (Oct. 1953), pp. 31-41.
- 4-20. Hubka, R. E., N. F. Dow, and P. Seide. Relative Structural Efficiencies of Flat Balsa-Core Sandwich and Stiffened Panel Construction. NACA TN 2514 (Oct. 1951).
- 4-21. Anderson, R. A. "Weight-Efficiency Analysis of Thin-Wing Construction," Symposium on Structures for Thermal Flight, ASME (March, 1956); also, ASME Transactions, Vol. 79, No. 5 (July 1957), pp. 974-979.

- 4-22. Semonian, J. W., and R. F. Crawford. "Some Methods for the Structural Design of Wings for Application Either at Ambient or Elevated Temperatures," ASME Transactions, Vol. 80, No. 2 (Feb. 1958), pp. 419-426.
- 4-23. Gerard, G. "Minimum Weight Analysis of Orthotropic Plates Under Compressive Loading," Journal Aero/Space Sciences, Vol. 27, No. 1 Jan. 1960, pp. 21-26, 64.
- 4-24. Lampert, S. and D.G. Younger. Multiwall Structures for Space Vehicles. WADD TR 60-503 (May 1960).
- 4-25. Gerard, G. Introduction to Structural Stability Theory. New York: McGraw-Hill Book Co. (1962), pp. 73-118.
- 4-26. Peterson, J. P. Weight-Strength Studies of Structures Representative of Fuselage Construction. NACA TN 4114 (Oct. 1957).
- 4-27. Gerard, G. Some Structural Aspects of Orbital Flight. American Rocket Society, Preprint 728-58, (Nov. 1958).
- 4-28. Williams, M. L., G. Gerard, and G.A. Hoffman. "Selected Areas of Structural Research in Rocket Vehicles." XI International Astronautical Congress, Stockholm, Vol. 1 (Aug. 1960), pp. 146-166.
- 4-29. Perry, D. J. Aircraft Structures. McGraw-Hill (1950).

- 4-30. Leggett, D.M.A., and H.G. Hopkins. Sandwich Panels and Cylinders Under Compressive End Loads. Aeronautical Research Council, R. and M. No. 2262 (Aug. 1949). (Note: although this paper was published in 1949, it was apparently first issued as an RAE report in 1942.)
- 4-31. Wittrick, W.H. A Theoretical Analysis of the Efficiency of Sandwich Construction Under Compressive End Load. Aeronautical Research Council, R. and M. No. 2016 (April 1945).
- 4-32. Switzky, H. and J. W. Cary. "Minimum Weight Design of Cylindrical Structures," ALAA Journal, Vol. 1, No. 10 (Oct. 1963), pp 2330-2337.
- 4-33. Kuenzi, E. W. Minimum Weight Structural Sandwich. U. S. Department of Agriculture, Forest Service, Research Note FPL-086 (Oct. 1965).

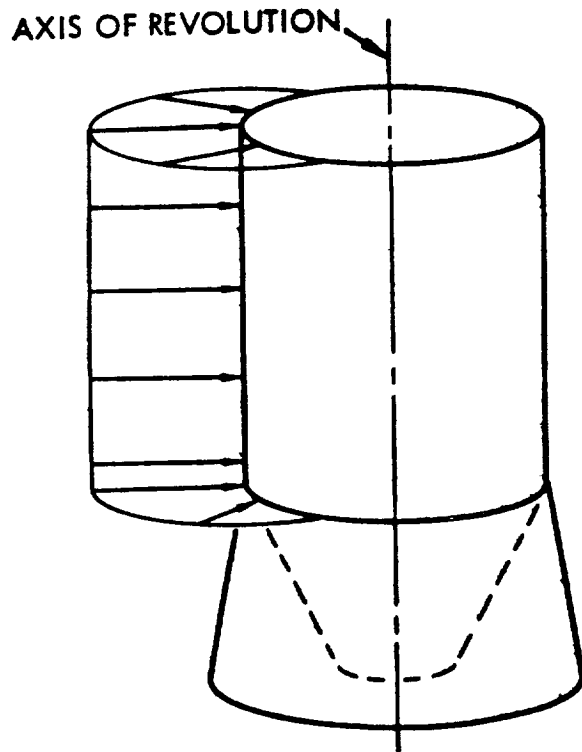
5.00 OPTIMUM USE OF COMPUTER PROGRAMS

5.10 INTRODUCTION

Previous chapters of this manual have dealt with various aspects of the analysis of shells. An introduction to shell theory was presented in Chapter 1.00, procedures for the static analysis of shells were given in Chapter 2.00, and procedures for the stability analysis of shells were given in Chapter 3.00. Although a myriad of solutions have been presented, either in explicit or graphical form, it is entirely conceivable that an analyst may encounter a problem not considered in any of the previous discussions. In such cases, a solution satisfactory for engineering purposes can often be obtained by using a digital computer.

As a typical example, consider a composite shell of revolution loaded unsymmetrically and possessing a branch configuration as shown in Fig. 5.10-1. Although procedures were developed in Chapter 2.00 for treating this configuration under axisymmetric load, the analysis under unsymmetric load is best accomplished using a digital computer (e. g., see Ref. 5-1). Many other examples could be cited to illustrate problems that can be effectively solved with the computer.

The widespread use of the computer is based on the extremely rapid and accurate manner in which it performs simple operations. In particular, it can perform addition, subtraction, multiplication



and division functions in minute fractions of a second. As a result, evaluation of series, parametric studies, and solution of simultaneous algebraic equations can be efficiently performed on the digital computer.

Fig. 5.10-1. Shell of Revolution

5.20 FUNDAMENTALS OF COMPUTER UTILIZATION

To utilize the capabilities of a digital computer, an engineer must become acquainted with some of the basic mechanics of computer operation. Even though the services of a professional programmer may be available, it is advantageous that the engineer become as acquainted as possible with computers.

Basically, a computer is a sophisticated form of desk calculator. Some small computers are not much larger than an engineer's desk, whereas the latest large computers possess over a dozen units and occupy an entire room. All computers used today are superior to desk calculators in three respects: they operate faster, possess memories, and make decisions. Just as an engineer cannot expect to obtain useful results from a slide rule or desk calculator unless he observes the governing rules of operation, successful utilization of a digital computer depends on understanding and using the basic rules governing the computer being used. The engineer is aware that he can perform operations and obtain accuracy with some slide rules that cannot be obtained using other (usually smaller) slide rules. In the case of computers, not only do some possess greater capabilities than others (e. g. , inversion or large matrixes, retention of many significant figures) but some are also capable of working several orders of magnitude faster than others.

To harness the capabilities of the computer and effectively utilize it to solve a particular problem, a set of instructions (a computer program), must be written. For example, if an engineer desires to find the roots of a quadratic equation on the computer, he must frame the quadratic formula in a manner acceptable and meaningful to the computer (i. e., he must "speak the computer's language.") Generally, two types of languages are in use: source (or user's) language and object (or machine) language. In the case of object language, the program is written in a manner so that the machine can act on it; a source program is very similar to typical analytical manipulations familiar to the engineer. In the source program, the machine uses part of its memory to translate from the source language to object language. The translator is called a compiler. Common examples of source languages are IT and FORTRAN. Since the source languages are more familiar to engineers, they are recommended over object languages. In either case, the engineer should be aware that all computers are very exacting in accepting or rejecting a set of instructions corresponding to a given physical problem. A computer program cannot possess unclear, imprecise statements.

A source program has several different types of statements that are necessary in nearly every case. Briefly, these statements are (1) control statements, which set up formats, size matrixes, etc.; (2) executable

statements, which tell the machine to add A to B, for example; and (3) input - output statements, which tell the machine to read in data, plot curves, write tapes, etc.

Often, when dealing with the larger computer systems, the engineer rarely, if ever, sees the computer itself. Instead, he deals with the input - output receiving station that may be located several miles from the computer he intends to use. Also, for reasons of efficiency, the input provided by the engineer may be given to a subordinate machine (e. g. , the IBM 1401) for reduction to a form which the main computer can more readily accept. Types of input to computers presently include paper tape (some UNIVAC machines) and cards (IBM and CDC). If it is not desired to produce the tape or cards themselves, coding sheets can be prepared from which the input (either cards or tape) can be produced.

In using the computer to analyze shell problems, it has been advantageous that the computer is capable of subscripting variables, and thus collecting similar quantities into arrays and dealing with entire arrays rather than with the individual elements of the arrays. This capability leads to a consideration of matrix algebra which is presented in the following section.

5.30 INTRODUCTION TO MATRIX ALGEBRA

The basic ideas of matrix algebra necessary for computer programming of shell problems are presented below.

Consider a set of n linear algebraic equations in the unknowns x_1, x_2, \dots, x_n ,

$$a_{11}x_1 + a_{12}x_2 + \dots + a_{1n}x_n = y_1$$

$$a_{21}x_1 + a_{22}x_2 + \dots + a_{2n}x_n = y_2$$

$$\cdot \qquad \qquad \qquad \cdot \qquad \cdot$$

$$\cdot \qquad \qquad \qquad \cdot \qquad \cdot$$

$$\cdot \qquad \qquad \qquad \cdot \qquad \cdot$$

$$\cdot \qquad \qquad \qquad \cdot \qquad \cdot$$

$$a_{n1}x_1 + a_{n2}x_2 + \dots + a_{nn}x_n = y_n$$

(5.30-1)

In summation form, these equations are,

$$\sum_{i=1}^n a_{1i}x_i = y_1$$

$$\sum_{i=1}^n a_{2i}x_i = y_2$$

$$\cdot \qquad \qquad \cdot$$

$$\cdot \qquad \qquad \cdot$$

$$\sum_{i=1}^n a_{ni}x_i = y_n$$

(5.30-2)

Consider the following representation of these equations

$$\begin{bmatrix} a_{11} & a_{12} & \dots & a_{1n} \\ a_{21} & a_{22} & \dots & a_{2n} \\ \cdot & \cdot & & \cdot \\ \cdot & \cdot & & \cdot \\ \cdot & \cdot & & \cdot \\ \cdot & \cdot & & \cdot \\ a_{n1} & a_{n2} & \dots & a_{nn} \end{bmatrix} \begin{bmatrix} x_1 \\ x_2 \\ \cdot \\ \cdot \\ \cdot \\ \cdot \\ x_n \end{bmatrix} = \begin{bmatrix} y_1 \\ y_2 \\ \cdot \\ \cdot \\ \cdot \\ \cdot \\ y_n \end{bmatrix} \quad (5.30-3)$$

The k^{th} equation of Eq. 5.30-1 is obtained by multiplying the k^{th} row of the rectangular array of coefficients a_{ij} by the corresponding terms of the x column and setting it equal to y_k . For example, the second equation is obtained by multiplying the second row of the a_{ij} rectangular array by the x column, term by term, and adding, then setting the resulting equation equal to y_2 :

$$a_{21} \cdot x_1 + a_{22} \cdot x_2 + \dots + a_{2n} \cdot x_n = y_2$$

Eq. 5.30-3 is a matrix equation that represents the set of linear algebraic Eq. 5.30-1. The $[n \times n]$ a_{ij} rectangular array and the $[n \times 1]$ x_i and y_i rectangular arrays are called $[n \times n]$ matrixes and $[n \times 1]$ matrixes, respectively. An $[n \times 1]$ matrix is also called a column vector. The

members of a matrix are called the matrix coefficients. Eq. 5.30-3 can be written in an even more concise form as

$$[A] \{x\} = \{y\} \quad (5.30-4)$$

Some matrixes are given special names. For example, the $n \times 1$ matrix (i. e., the matrix consisting of n rows and 1 column) is called a column vector. The $1 \times n$ matrix which consists of 1 row and n columns (e. g., Z_1, Z_2, \dots, Z_n) is called a row vector. A matrix containing n rows and n columns is called a square matrix. The matrix coefficient in the i^{th} row and j^{th} column of a matrix A is denoted by a_{ij} . A square matrix in which all its diagonal terms, a_{ii} , are equal to 1, while all other coefficients are

equal to zero is called an identity matrix. For example, $\begin{bmatrix} 1 & 0 \\ 0 & 1 \end{bmatrix}$ and $\begin{bmatrix} 1 & 0 & 0 \\ 0 & 1 & 0 \\ 0 & 0 & 1 \end{bmatrix}$

are identity matrixes. A matrix with coefficients related by $a_{ij} = a_{ji}$ is

called a symmetric matrix. For example, $\begin{bmatrix} 1 & 2 & 3 \\ 2 & 7 & 4 \\ 3 & 4 & -2 \end{bmatrix}$ is a symmetric matrix,

since $a_{12} = 2 = a_{21}$, $a_{13} = a_{31} = 3$, $a_{23} = a_{32} = 4$. A square matrix with all its coefficients equal to zero is called a null matrix. Identity and null matrixes are special examples of symmetric matrixes.

If $n \times m$ matrix B has each i^{th} row equal to each i^{th} column of an $m \times n$ matrix A , matrix B is called the transpose matrix of A and is

denoted by $[A]^T$. For example, consider the 2×3 matrix $A = \begin{bmatrix} 2 & 1 & -3 \\ 1 & 7 & 4 \end{bmatrix}$

The transpose of this matrix is the 3×2 matrix $[A]^T = \begin{bmatrix} 2 & 1 \\ 1 & 7 \\ -3 & 4 \end{bmatrix}$, since the 1st column of $[A]^T$ is the same as the first row of matrix A, and its 2nd column is equal to the second row of matrix A.

Matrixes may be operated upon, as with numbers; however, the operations may or may not be possible to perform. This is best illustrated by demonstration. Two matrixes, A and B, are equal if coefficient a_{ij} of matrix A is equal to coefficient b_{ij} of matrix B. It should be noted that two matrixes can only be equal if they are of the same order (i. e., if they both have m rows and n columns).

The operation of multiplying every coefficient a_{ij} in the matrix A by a number, c, is denoted by $c [A]$ and is called scalar multiplication. It can be seen that if $B = c [A]$, then $b_{ij} = c a_{ij}$.

Multiplication of two matrixes is called matrix multiplication and is defined as follows: If $C = A B$, the coefficients of C are given by

$$c_{ij} = \sum_{R=1}^n a_{iR} b_{Rj}$$

To make this operation possible, the number of columns of matrix A must be equal to number of rows of matrix B. If matrix A is $m \times n$ matrix and matrix B is $n \times p$ matrix, then matrix C is $m \times p$ matrix. In general

$[A] [B]$ is not equal to $[B] [A]$. In fact, if matrix A is a $m \times n$ matrix and B is a $n \times p$ matrix, then since matrix B has p columns and matrix A has m rows, the multiplication is not even defined (if $p \neq m$). For example, consider the matrixes

$$A = \begin{bmatrix} 1 & 3 \\ 4 & 2 \\ 1 & 2 \end{bmatrix} \quad \text{and} \quad B = \begin{bmatrix} 1 & 1 \\ 0 & 1 \end{bmatrix}$$

then

$$[A] [B] = \begin{bmatrix} 1 & 3 \\ 4 & 2 \\ 1 & 2 \end{bmatrix} \begin{bmatrix} 1 & 1 \\ 0 & 1 \end{bmatrix} = \begin{bmatrix} 1 & 4 \\ 4 & 6 \\ 1 & 3 \end{bmatrix} = C$$

where the coefficients of C are given by $c_{ij} = \sum_{R=1}^n a_{iR} b_{Rj}$ (i. e.,

$$c_{11} = a_{11}b_{11} + a_{12}b_{21} = (1)(1) + (3)(0) = 1, \quad c_{12} = a_{11}b_{12} + a_{12}b_{22} =$$

$(1)(1) + (3)(1) = 4$ etc.). In the preceding example, the premultiplication

of matrix B by matrix A is defined, however, the premultiplication of

matrix A by matrix B, denoted $[B] [A]$, is not defined since the number of

columns of matrix B is not equal to the number of rows of matrix A.

Multiplication of any matrix A by the identity matrix I is commutative,

and results in the matrix A (i. e., $[A] [I] = [I] [A] = A$). Suppose a

square matrix A is either premultiplied or postmultiplied by another square

matrix B, and the result in either case is the identity matrix I. Then

matrix B is called the inverse matrix of A, and is denoted by $[A]^{-1}$. For example, consider the following case:

$$[A] = \begin{bmatrix} 2 & 1 \\ 1 & 3 \end{bmatrix}, [B] = \begin{bmatrix} 3/5 & -1/5 \\ -1/5 & 2/5 \end{bmatrix}$$

$$[B][A] = \begin{bmatrix} 3/5 & -1/5 \\ -1/5 & 2/5 \end{bmatrix} \begin{bmatrix} 2 & 1 \\ 1 & 3 \end{bmatrix} = \begin{bmatrix} 1 & 0 \\ 0 & 1 \end{bmatrix}$$

$$[A][B] = \begin{bmatrix} 2 & 1 \\ 1 & 3 \end{bmatrix} \begin{bmatrix} 3/5 & -1/5 \\ -1/5 & 2/5 \end{bmatrix} = \begin{bmatrix} 1 & 0 \\ 0 & 1 \end{bmatrix}$$

then B ($= [A]^{-1}$) is the inverse of A, and A ($= [B]^{-1}$) is the inverse of B.

By virtue of the matrix operations indicated, it should be clear that Eq. 5.30-4 can be solved for x by premultiplying both sides by $[A]^{-1}$

The result is

$$\{x\} = [A]^{-1} \{y\} \quad (5.30-5)$$

As a simple example, suppose Eq. (5.30-1) is

$$2x_1 + x_2 = 10$$

$$x_1 + 3x_2 = 5 \quad (5.30-6)$$

In matrix form, Eq. 5.30-6 can be written as

$$\begin{bmatrix} 2 & 1 \\ 1 & 3 \end{bmatrix} \{x\} = \begin{bmatrix} 10 \\ 5 \end{bmatrix}$$

Applying Eq. 5.30-5

$$\{x\} = \begin{bmatrix} 2 & 1 \\ 1 & 3 \end{bmatrix}^{-1} \begin{bmatrix} 10 \\ 5 \end{bmatrix}$$

Since it has been shown that

$$\begin{bmatrix} 2 & 1 \\ 1 & 3 \end{bmatrix}^{-1} = \begin{bmatrix} 3/5 & -1/5 \\ -1/5 & 2/5 \end{bmatrix}$$

we have

$$\{x\} = \begin{bmatrix} 3/5 & -1/5 \\ -1/5 & 2/5 \end{bmatrix} \begin{bmatrix} 10 \\ 5 \end{bmatrix} = \begin{bmatrix} 5 \\ 0 \end{bmatrix}$$

so

$$x_1 = 5 \text{ and } x_2 = 0 \tag{5.30-7}$$

The validity of the results of Eq. 5.30-7 can easily be verified by conventionally solving Eq. 5.30-6.

Matrix inversion becomes increasingly more time consuming as the order of the matrix n increases. For large matrixes, a significant improvement over a straightforward inversion of the type indicated in Eq. 5.30-5 is to use, where possible, a Gaussian elimination procedure. For banded matrixes (i. e., matrixes having nonzero elements only within a band running along the principal diagonal as shown in Fig. 5.30-1, the inversion indicated in Eq. 5.30-5 can be replaced by inversions of sub-matrixes and application of a recursion relationship. The increase in

efficiency over the inversion of the entire A matrix makes problems tractable that were previously expensive to solve.

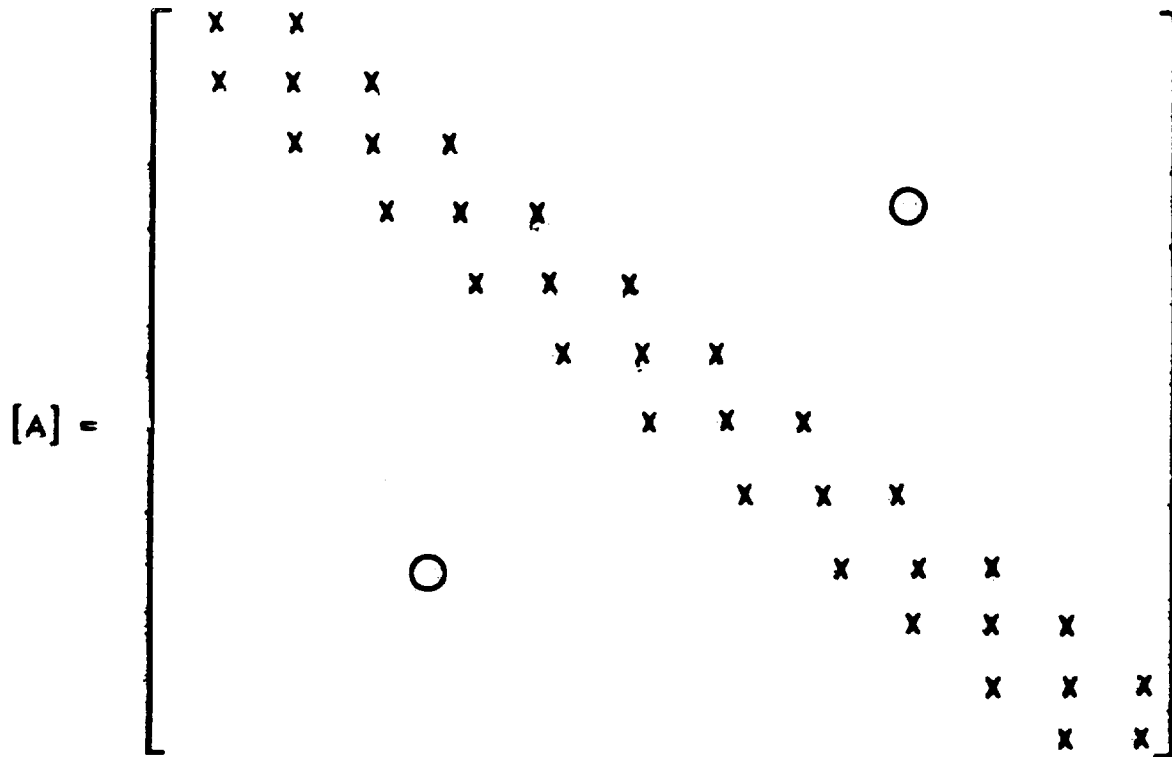


FIG. 5.30-1. Banded Matrix Upon Which Gaussian Elimination can be Performed

5.40 TECHNIQUES FOR SOLVING SHELL PROBLEMS AND THE USE OF THE COMPUTER IN THESE TECHNIQUES

In Chapter 2.00 of this manual, many closed form solutions were presented for the static analysis of shells. The computer could be used as a labor saving device to evaluate these solutions. For example, it might be feasible to use a computer if a parametric study is to be performed, or if a series solution is to be evaluated. However, the reason for the central importance of the computer in the present day analysis of shells is not because of its ability to evaluate existing solutions but as an essential ingredient in obtaining the desired solution. Several methods of solving shell problems are in use today that utilize the computer in this central capacity. These analyses all share the property that the continuous shell is replaced by a shell with a finite number of points on it, and the computer is then used to assist in the solution of this approximate problem composed of discrete points. A detailed description of the several methods follows:

5.41 THE FINITE DIFFERENCE METHOD

In Chapter 1.00, it was shown that partial differential equations are the governing differential equations for shell behavior.

In the finite difference method of analysis, the shell partial differential equations are replaced by a set of linear algebraic equations that have a readily obtainable solution. The basis for this method is the replacement of exact differentials df by approximate differences Δf . For example, consider the continuous function, $w(x)$, as shown in Fig. 5.40-1.

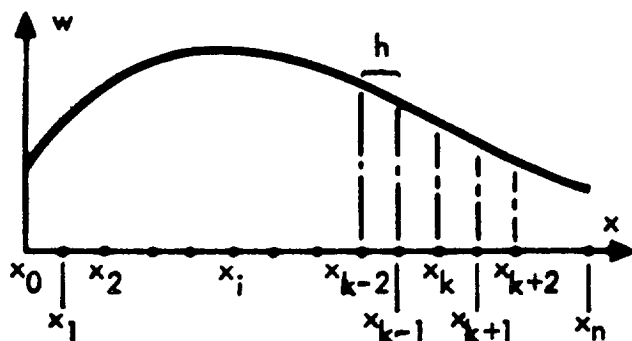


FIG. 5.40-1. Finite Difference Intervals

The independent continuous variable, x , is partitioned into n segments. The value of the dependent variable, $w(x)$, at x_k is denoted w_k . Using calculus,

$$\lim_{\Delta x \rightarrow 0} \frac{\Delta w}{\Delta x} \Big|_{x=x_k} = \frac{dw}{dx} \Big|_{x_k} \cong \frac{\Delta w}{\Delta x} \Big|_{x_k}$$

The expression for $\Delta w / \Delta x$ at $x = x_k$ can be obtained in various

ways. Consider the forward difference given by

$$\frac{\Delta w}{\Delta x} \Big|_{x_k} = \frac{w_{k+1} - w_k}{h} \quad (5.40-1)$$

and the backward difference

$$\left. \frac{\Delta w}{\Delta x} \right|_{x_k} = \frac{w_k - w_{k-1}}{h} \quad (5.40-2)$$

Usually, however, the central difference expression

$$\left. \frac{\Delta w}{\Delta x} \right|_{x_k} = \frac{w_{k+1} - w_{k-1}}{2h} \quad (5.40-3)$$

is used since it involves values of w on both sides of x_k , and it results that the error introduced in approximating the derivative by Eq. 5.40-3 is of the order of h^2 , whereas, the errors in Eqs. 5.40-1 and 5.40-2 are of the order h . Higher-order derivatives are easily obtained by continuing in this manner. For instance, the central finite difference expression for d^2w/dx^2 at $x = x_k$ is given by

$$\left. \frac{d^2 w}{dx^2} \right|_{x_k} \equiv \left. \frac{\Delta^2 w}{\Delta x^2} \right|_{x_k} = \frac{w_{k+1} - 2w_k + w_{k-1}}{h^2} \quad (5.40-4)$$

Finite difference expressions for all orders of derivatives are easily derived or may be found in any textbook on finite differences. In the case of partial derivatives, finite difference expressions are similarly defined. Consider now a partial differential equation. At each point, k , along the independent variable, x_1 , the partial differential equation can be replaced by an algebraic equation with the derivatives of the partial differential equations replaced by the corresponding finite difference expressions. Together with the boundary

conditions, the set of finite difference equations form a set of n linear algebraic equations in n unknowns. The problem is especially adaptable to matrix form and the solution easily follows. It is seen that the exact continuous solution, e. g., $w(x, y)$, for a plane problem, is replaced by the approximate discrete solution, $w_k(x_k, y_k)$. In theory, the approximate discrete solution may be made to approach the exact continuous solution, $w(x, y)$, as closely as desired by allowing the distance, h , between x_k and x_{k+1} to approach zero. In an actual case the process of allowing h to approach zero introduces a machine capacity problem which leads to w_k diverging from w . That is, in an actual problem, the number of points at which the solution is desired may be restricted by the number of simultaneous equations the computer can accurately solve. This is an important point of the method and will be discussed further. An example of the finite difference technique will illustrate the method.

Consider the partial differential equation

$$\frac{\partial^2 f}{\partial x^2} + \frac{\partial^2 f}{\partial y^2} = -2 \quad (5.40-5)$$

with boundary conditions, $f = 0$, on the boundary of the object shown in Fig. 5.40-2.

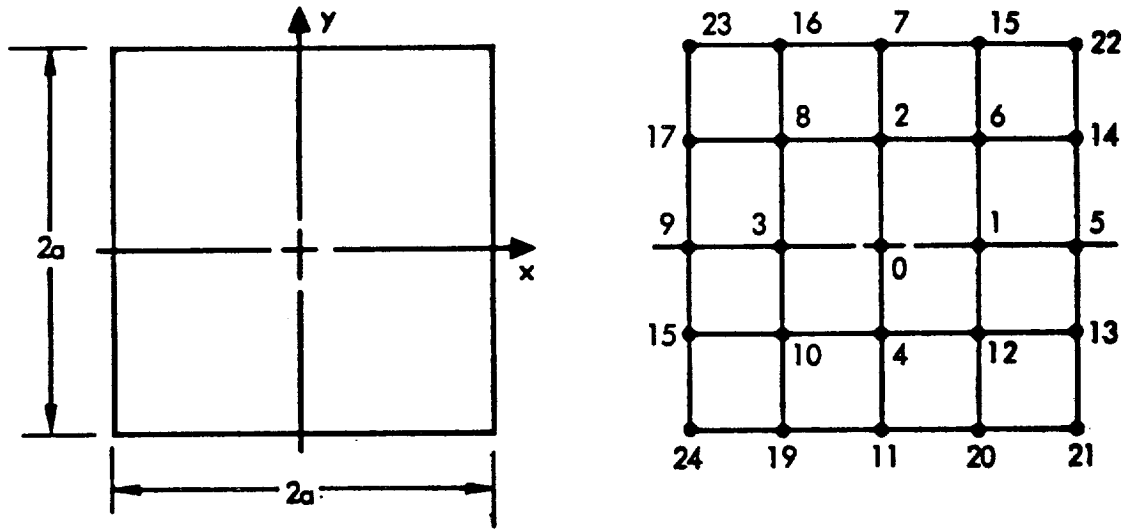


FIG. 5.40-2. Finite Difference Grid for Plate

The square plate is partitioned into 16 segments as shown. That is, the continuous variables, x and y , are partitioned into four intervals each.

The partial derivatives in terms of central finite differences are given as follows:

$$\left. \frac{\partial^2 f}{\partial x^2} \right|_{x_0, y_0} \cong \frac{\Delta_x^2 f}{h^2} = \frac{1}{h^2} (f_1 - 2f_0 + f_3)$$

$$\left. \frac{\partial^2 f}{\partial y^2} \right|_{x_0, y_0} \cong \frac{\Delta_y^2 f}{h^2} = \frac{1}{h^2} (f_2 - 2f_0 + f_4) \quad (5.40-6)$$

Then at Point 0 the partial differential equation $\frac{\partial^2 f}{\partial x^2} + \frac{\partial^2 f}{\partial y^2} = -2$ is

replaced by the following algebraic equation

$$\frac{1}{h^2} (f_1 + f_2 + f_3 + f_4 - 4 f_0) = -2 \quad (5.40-7)$$

At each interior point of the body, a similar algebraic equation may be written. The boundary condition equation, $f = 0$, is replaced by the equations, $f_i = 0$, where i is any point on the boundary. Since there are 9 interior points and 16 boundary points, there are 9 equations of type (5.40-7) and 16 equations for $f_i = 0$. The set of linear algebraic equations may be put in matrix form

$$[A] \{f\} = \{C\}$$

where $[A]$ is the 25 x 25 coefficient matrix, and $\{f\}$ is the solution column vector. If the matrix $[A]$ has an inverse, the $\{f\}$ may be obtained by $\{f\} = [A]^{-1} C$. The inversion of a 25 x 25 matrix is beyond human capacity and a machine definitely would be needed.

It can be seen from Fig. 5.40-2 that the method of finite differences replaces the continuous plate with a gridwork of discrete points. When this method is applied to shells, grid systems of the type shown in Fig. 5.40-3 occur.

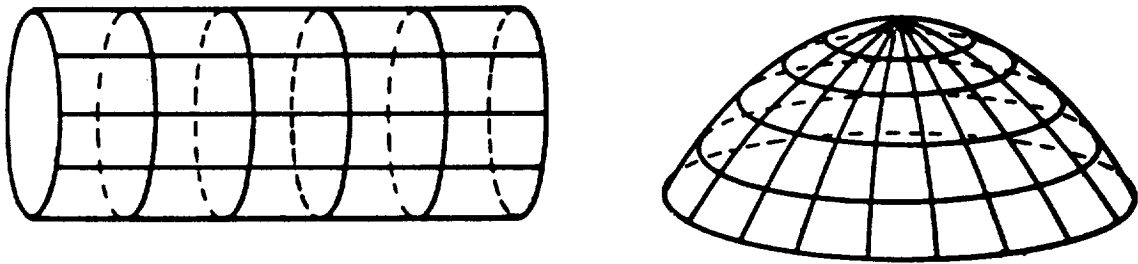


FIG. 5.40-3. Finite Difference for Shells

In general, the equilibrium, stress-strain, and strain-displacement relations can be reduced to three partial differential equations in the displacements u , v , and w . Applying finite difference approximations in both surface directions, the matrix equations are obtained as follows:

$$\begin{aligned}
 [A] \{u\} + [B] \{v\} + [C] \{w\} &= \{a\} \\
 [D] \{u\} + [E] \{v\} + [F] \{w\} &= \{b\} \\
 [G] \{u\} + [H] \{v\} + [J] \{w\} &= \{d\}
 \end{aligned}
 \tag{5.40-8}$$

By suitably inverting matrixes and performing other manipulations, Eq. 5.40-8 could be solved for the displacement matrixes u , v , and w . These three vectors will have as many elements as there are grid points on the shell.

For the general case of unsymmetrical shells loaded unsymmetrically, the two-dimensional finite difference approach will yield valid results. However, inversion of large matrixes, with accompanying long execution times on the computer and loss in accuracy, will result. For the case of shells of revolution loaded arbitrarily, a method has been devised that results in economical runs. This method will be discussed in Section 5.43.

5.42 THE NUMERICAL INTEGRATION METHOD

An alternative to the procedure described in Section 5.41, using finite differences in both directions, is the numerical integration method, described in this article. Using this procedure, the governing partial differential equations are first reduced to a set of ordinary differential equations by expanding in finite differences in one direction. The numerical integration is then performed on this set of ordinary differential equations.

To illustrate the method, consider again the partial differential equation

$$\frac{\partial^2 f}{\partial x^2} + \frac{\partial^2 f}{\partial y^2} = -2 \quad (5.42-1)$$

valid in the interior of the square shown in Fig. 5.42-1. On the boundary, $f = 0$.

To reduce the given partial differential equation to a set of ordinary linear differential equations, the operator $\partial^2 f / \partial y^2$ is approximated using finite differences. Along any $y = \text{constant}$ line, say $y = y_k$, the following holds true:

$$\left. \frac{\partial^2 f}{\partial y^2} \right|_{y=k} = \frac{1}{h^2} \left[f_{k+1}(x) - 2f_k(x) + f_{k-1}(x) \right] \quad (5.42-2)$$

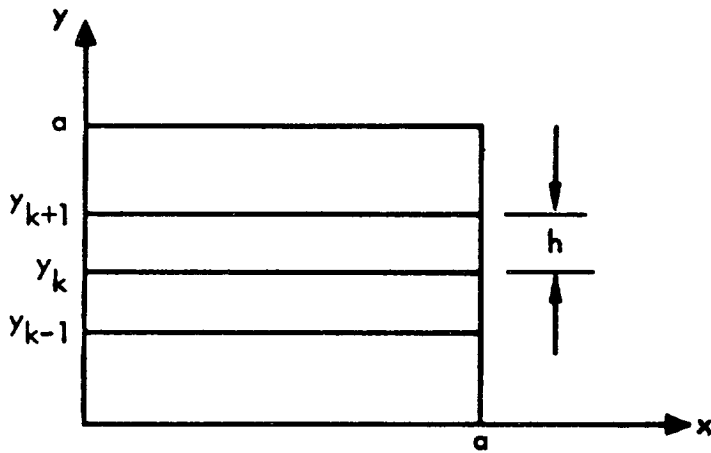


FIG. 5.42-1. Numerical Integration Locations for Plate

Substituting Eq. 5.42-2 into Eq. 5.42-1, the following is obtained:

$$\frac{d^2 f_k}{dx^2} + \frac{1}{h^2} x \left[f_{k+1}(x) - 2f_k(x) + f_{k-1}(x) \right] = -2 \quad (5.42-3)$$

where $f_k(x)$ is the value of f on the $y = y_k$ line for variable x .

If the interval $0 \leq y \leq a$ is partitioned into n equal segments of length h so that $nh = a$, the above equations are

$$\frac{d^2}{dx^2} \begin{Bmatrix} f_1 \\ f_2 \\ \vdots \\ f_{k-1} \\ f_k \\ f_{k+1} \\ \vdots \\ f_{n-1} \end{Bmatrix} + \frac{1}{h^2} \begin{bmatrix} -2 & 1 & 0 & \cdot & \cdot & \cdot & \cdot & 0 \\ 1 & -2 & 1 & 0 & \cdot & \cdot & \cdot & 0 \\ 0 & 1 & -2 & 1 & 0 & \cdot & \cdot & 0 \\ \cdot & \cdot & \cdot & \cdot & \cdot & \cdot & \cdot & \cdot \\ \cdot & \cdot & \cdot & \cdot & \cdot & \cdot & \cdot & \cdot \\ \cdot & \cdot & \cdot & \cdot & \cdot & \cdot & \cdot & \cdot \\ \cdot & \cdot & \cdot & \cdot & \cdot & \cdot & \cdot & \cdot \\ \cdot & \cdot & \cdot & \cdot & \cdot & \cdot & \cdot & \cdot \\ 0 & 0 & 0 & 0 & \cdot & 1 & -2 & 1 \\ & & & & & 0 & 1 & -2 \end{bmatrix} \begin{Bmatrix} f_1 \\ f_2 \\ \cdot \\ \cdot \\ f_{k-1} \\ f_k \\ f_{k+1} \\ \cdot \\ \cdot \\ f_{n-1} \end{Bmatrix} = \begin{Bmatrix} -2 \\ -2 \\ -2 \\ \cdot \\ \cdot \\ \cdot \\ \cdot \\ \cdot \\ \cdot \\ -2 \end{Bmatrix} \quad (5.42-4)$$

with boundary conditions $f_k = 0$ at $x = 0, a$ (where f_k is equal to f along $y = y_k$) and $f_0 = f_n = 0$ all along x . In matrix form, Eq. 5.42-4, is

$$\frac{d^2}{dx^2} \begin{bmatrix} F \end{bmatrix} + \frac{1}{h^2} \begin{bmatrix} A \end{bmatrix} \begin{bmatrix} F \end{bmatrix} = \begin{bmatrix} C \end{bmatrix} \quad (5.42-5)$$

Recognize that Eq. 5.42-5 represents a set of $(n-1)$ second-order ordinary differential equations. A common technique in numerical analysis is to reduce the order of all pertinent equations to the first order. This can be done by introducing the variable, g , defined by

$$g_k = \frac{df_k}{dx} \quad (5.42-6)$$

Then the equation can be written:

$$\frac{dg_k}{dx} + \frac{1}{h^2} \left[f_{k+1}(x) - 2f_k(x) + f_{k-1}(x) \right] = -2 \quad (5.42-7)$$

In matrix form, Eq. 5.42-6 and 5.42-7 can be written

$$\frac{d}{dx} \begin{Bmatrix} g_1 \\ g_2 \\ \cdot \\ \cdot \\ \cdot \\ g_k \\ g_{n-1} \\ \hline f_1 \\ f_2 \\ \cdot \\ \cdot \\ f_k \\ \cdot \\ \cdot \\ f_{n-1} \end{Bmatrix} + \begin{bmatrix} & & & & & & \\ & & & & & & \\ & & & & & & \\ & & & & & & \\ & 0 & & & & & \\ & \hline & & & & & & \\ & & & & & & \\ & & & & & & \\ -[I] & & & & & & \\ & & & & & & \\ & & & & 0 & & \\ & & & & & & \end{bmatrix} \begin{Bmatrix} g_1 \\ g_2 \\ \cdot \\ \cdot \\ \cdot \\ g_{n-1} \\ \hline f_1 \\ f_2 \\ \cdot \\ \cdot \\ f_{n-1} \end{Bmatrix} = \begin{Bmatrix} -2 \\ -2 \\ \cdot \\ \cdot \\ \cdot \\ -2 \\ \hline 0 \\ \cdot \\ \cdot \\ \cdot \\ 0 \end{Bmatrix} \quad (5.42-8)$$

Eq. 5.42-8 can be written more compactly if the following symbols are used:

$$\begin{Bmatrix} g_1 \\ \cdot \\ \cdot \\ \cdot \\ \cdot \\ \cdot \\ g_{n-1} \end{Bmatrix} = [G] ; \quad \begin{Bmatrix} [G] \\ \hline [F] \end{Bmatrix} = [H] ; \quad (5.42-9)$$

$$[J] = \begin{bmatrix} [O] & \frac{1}{h^2} [A] \\ -[I] & [O] \end{bmatrix} ; \quad \{K\} = \begin{Bmatrix} \{C\} \\ \text{---} \\ \{O\} \end{Bmatrix}$$

With Eq. 5.42-9, Eq. 5.42-8 becomes

$$\frac{d}{dx} \{H\} + [J] \{H\} = \{K\} \quad (5.42-10)$$

Note that Eq. 5.42-10 represents a set of $(2n - 2)$ first-order ordinary differential equations. Eq. 5.42-10 is in the form most amenable to numerical analysis. A typical numerical integration procedure, originally proposed by Euler, is to assume H_1 (see Fig. 5.42-2) is given by

$$H_1 = H_0 + h f_0(x, H)$$

where

$$h = x_1 - x_0$$

$$H_0 = H \text{ matrix at } x = x_0$$

$$H_1 = H \text{ matrix at } x = x_1$$

and

$$f_0(x, H) = K - JH_0$$

$$= \text{slope at } x = x_0$$

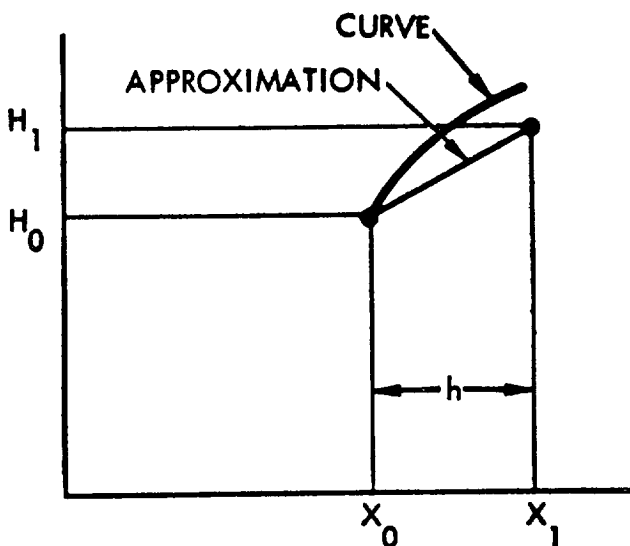


FIG. 5.42-2. Numerical Integration Procedure

It can be seen that this procedure merely assumes that the first derivative is constant throughout the interval, h . As h approaches zero, the error introduced approaches zero. Having H_1 , H_2 is obtained from

$$H_2 = H_1 + h f_1(x, H)$$

This procedure is continued until the boundary is reached.

More sophisticated procedures for numerical integration are available. One of the most popular is the Runge-Kutta method. Because of its widespread use, computer groups usually have prepared routines or programs available. As in the Euler method, the interval size may be changed as desired without any complication.

All numerical integration procedures are best suited for solving initial value problems. Thus, the Euler procedure yields the results, H_1, H_2, \dots, H_n , if H_0 is known. Thus, referring to Fig. 5.42-1, a successful numerical integration requires an a priori knowledge of the function, f , and its first derivative at $x = 0$ for all y_k . However, the problem originally stated did not specify the derivatives df/dx at $x = 0$; rather it specified that $f = 0$ at $x = 0$ and $x = a$. The given problem was a boundary value problem (as are all shell problems). To use numerical integration procedures to solve boundary value problems, sufficient initial information must be assumed (in this case, slopes) to

start the process. When the boundary, $x = a$, is reached, the values, $f(a, y)$, are compared to the given boundary conditions. The assumed slopes are then adjusted and the numerical integration performed again. After a series of trials, the boundary values from the numerical integration should compare favorably with the given boundary conditions, and hence the initial assumed slopes are acceptable and the interior results are valid.

The solution of shell problems by numerical integration is complicated not only by the necessity of having to convert a boundary value problem to an initial value problem, but more importantly, by the fact that the governing differential equations possess three dependent variables (in general). The coupling between the three equations is considerable, and hence, the numerical integrations are interconnected. For these reasons, numerical integration has not been as popular a method for solving shell problems as the other methods in this section.

5.43 THE BUDIANSKY - RADKOWSKI METHOD

In this article, an efficient method for the solution of problems involving shells of revolution is discussed. This method treats arbitrary shells of revolution subjected to arbitrary loading conditions and possessing a variety of possible end conditions. The procedure involves expanding the forces, moments, shears, rotations, temperatures, loads, strains, and displacements into Fourier series. For example, the meridional stress resultant, N_{ξ} , is expressed in series form as

$$N_{\xi} = \sigma_0 h_0 \sum_{n=0}^{\infty} t_{\xi}^{(n)} \cos n \theta \quad (5.43-1)$$

where

σ_0 = a reference stress level

h_0 = a reference thickness

θ = the circumferential coordinate

$t_{\xi}^{(n)}$ = the Fourier coefficient in the series expansion for N_{ξ} , is a function of ξ , the meridional coordinate, only

With the Fourier series expansions just described, the governing differential equations can be reduced to ordinary differential equations, where ξ is the independent variable and the Fourier coefficients for the stresses, moments, loads, and shears are the dependent variables.

Using Hooke's law and the conventional strain-displacement relations, the governing equations can be written as

$$E z'' + Fz' + Gz = e \quad (5.43-2)$$

$$' = \frac{d}{d\xi}$$

where E, F, and G are (4 x 4) matrixes which reflect the geometric and elastic properties of the shell in question, e is a (4 x 1) matrix composed of mechanical and thermal loads, and z is a (4 x 1) solution matrix composed of the Fourier coefficients for the three displacements and the meridional bending moment. Boundary and discontinuity conditions can also be written in matrix form.

Finite differences are now used for approximations to the derivatives in the meridional direction. A set of algebraic equations for z_i is obtained:

$$A_0 z_1 + B_0 z_0 = g_0$$

$$A_i z_{i+1} + B_i z_i + C_i z_{i-1} = g_i \quad (i = 1, 2, \dots, N-1)$$

$$B_n z_n + C_n z_{n-1} = g_n$$

The A, B, C, and g matrixes reflect the geometric, discontinuity, elastic, and boundary conditions of the problem. The z matrixes are obtained by

the Gaussian elimination procedure. In this case, it is necessary to invert (4 x 4) matrixes, so the process is well suited for rapid machine calculation. In practice, the procedure amounts to solving for z_i in terms of z_{i+1} , z_{i+1} in terms of z_{i+2} , etc., until the boundary is reached. Then z_N can be explicitly obtained because the boundary conditions supply the necessary additional information. Having z_N , all other z 's are systematically obtained by using the recursion relationship established on the way down the principal diagonal. Once the z matrix is known, all other quantities of interest can be obtained by differentiation.

The Budiansky - Radkowski procedure is an efficient procedure for the solution of shell problems. Experience has shown that complicated problems can be solved in a matter of seconds using this technique. In addition, the method has been extended slightly to treat shells in which shear distortion effects are significant, three-layered shells, branched, and eccentrically discontinuous shells, etc. Also, investigations are currently underway to apply the method to elastic-plastic shells, shell dynamics, and unsymmetrical shells.

Because of the efficient running times resulting from the use of the Gaussian elimination procedure, this method is recommended for cases in which it is applicable.

5.44 THE FINITE ELEMENT METHOD

In the finite element approach to analysis of shells, the shell under consideration is replaced by a set of finite elements that approximate the given shell. For example, to find the stresses and deflections existing in the hemispherical shell with an axisymmetric cutout shown in Fig. 5.44-1,



(a) Spherical Shell with Axisymmetric Hole



(b) Finite Element Approximation to Spherical Shell

FIG. 5.44-1 Spherical Shell and Finite Element Approximation

the shell under consideration could be idealized by a set of conical shell frusta as shown in Fig. 5.44-1b. Then the conical shell model could be analyzed and, as the lengths l of the conical elements approach zero, the solution obtained should approach the solution for the given shell. Thus in the finite element method, the behavior of a typical element is studied and the elements are then tied together to produce the required shell.

Two methods are commonly used when dealing with finite elements. These methods are compatibility (or force) and equilibrium (or displacement).

In the compatibility method, the requirement of geometric compatibility is used to tie the finite elements together. That is, the redundant forces and moments which exist at the interfaces of the several elements are obtained by imposing compatibility. For a structure with n redundant forces, there are n compatibility equations that must be satisfied. Suppose F_1, F_2, \dots, F_k are the applied forces (known) on the k degree of freedom coordinates of the shell. These F 's may be either forces or moments and any of them may be zero, if desired. Suppose, in addition, that $F_{k+1}, F_{k+2}, \dots, F_{k+n}$ are n redundant forces at the n coordinates $k+1, k+2, \dots, k+n$. To solve for the n redundant forces, it is noted that the displacement u_k at any location k can be related to the forces existing (both applied external forces and redundant forces) by the following equations:

$$\begin{aligned}
 u_1 &= a_{11} F_1 + a_{12} F_2 + \dots + a_{1k} F_k + \dots + a_{1, k+n} F_{k+n} \\
 u_2 &= a_{21} F_1 + a_{22} F_2 + \dots + a_{2k} F_k + \dots + a_{2, k+n} F_{k+n} \\
 &\vdots \\
 &\vdots \\
 &\vdots \\
 u_k &= a_{k1} F_1 + a_{k2} F_2 + \dots + a_{kk} F_k + \dots + a_{k, k+n} F_{k+n} \\
 &\vdots \\
 &\vdots \\
 u_{k+n} &= a_{k+n, 1} F_1 + a_{k+n, 2} F_2 + \dots + a_{k+n, k+n} F_{k+n}
 \end{aligned}
 \tag{5.44-1}$$

In matrix form these equations are

$$\{u\} = [A] \{F\}$$

where

u = the displacement vector,

F = the force vector, and

A = the flexibility matrix of the structure.

The matrixes may be partitioned as follows: those quantities associated with coordinates 1, 2, . . . , k are denoted by the quantity symbol with an asterisk superscript, and the quantities at the redundant coordinates $k+1$, . . . , $k+n$ are denoted by the quantity symbol with a zero superscript.

Then this matrix equation becomes

$$\begin{Bmatrix} u^* \\ \hline u^0 \end{Bmatrix} = \begin{bmatrix} a^{**} & a^{*0} \\ \hline a^{0*} & a^{00} \end{bmatrix} \begin{Bmatrix} F^* \\ \hline F^0 \end{Bmatrix}$$

At the redundant coordinates the relative displacements are zero, i. e.,

$\{u^0\} = 0$. Hence, the above matrix equation yields the matrix equations

$$\{0\} = [a^{0*}]\{F^*\} + [a^{00}]\{F^0\}$$

and

$$\{u^*\} = [a^{**}]\{F^*\} + [a^{*0}]\{F^0\}$$

Solving the first of these equations for the redundant forces $\{F^o\}$ yields

$$\{F^o\} = -[a^{oo}]^{-1} [a^{o*}]\{F^*\} \quad (5.44-2)$$

and substitution into the second equation yields

$$\{u^*\} = \left\{ [a^{**}] - [a^{*o}][a^{oo}]^{-1} [a^{o*}] \right\} \{F^*\} \quad (5.44-3)$$

Thus, the redundant forces $\{F^o\}$ and the displacements at the k coordinates $\{u^*\}$ are obtained using Eqs. 5.44-2 and 5.44-3. The only matrix inversion required is $[a^{oo}]^{-1}$.

Once the redundant forces are known the forces on each element are obtained from the equilibrium equations

$$\{P\} = [C] \{F\} = [C^* \mid C^o] \left\{ \begin{array}{c} F^* \\ F^o \end{array} \right\}$$

In this discussion, nothing has been said about the determination of the shell flexibility matrix A . It can easily be shown that this matrix may be obtained from the individual element flexibility matrixes $[a]_i$ by the equation

$$[A] = [\beta]^T [a] [\beta]$$

where

$$[a] = \begin{bmatrix} [a]_1 & & & \\ & [a]_2 & & \\ & & \ddots & \\ & & & [a]_m \end{bmatrix}$$

and $[a]_i$ is the flexibility matrix of the i^{th} element which is known. β is the matrix which relates element displacements to the shell displacements by the relationship

$$\{\delta\} = [\beta]\{u\}$$

The β matrix is a rectangular one in which every row consists of zeroes except for a single term of unity, the position of which identifies that element of $\{\delta\}$ which corresponds to the particular element of u . In other words, the function of the matrix β is to select the appropriate displacement from u and then place it in the required order, element by element, in the element displacement matrix δ .

The element flexibility matrixes are a function of the type of finite element chosen. For example, for the conical shell frusta elements mentioned above, the flexibility matrix is easily obtained. From what has been mentioned in Section 5.30, it is apparent that the computer can be used to good advantage in the finite element method. The matrix

manipulations and inversions required can be handled quite efficiently on the computer.

Consider the equilibrium (or displacement) method. In this method, unknown displacements and rotations are dealt with. The unknown displacements and rotations ensure equilibrium at the m degree of freedom coordinates of the structure. In this method, the idea of redundancy does not enter. In matrix form the equilibrium equations are

$$\{F\} = [K] \{u\}$$

where $[\kappa]$ is the stiffness matrix of the shell and is given by

$$[K] = [\beta]^T [\kappa] [\beta] \quad (5.44-4)$$

The matrix $[\kappa]$ is the matrix of the r element stiffness matrixes,

$$[\kappa] = \begin{bmatrix} [\kappa]_1 & & & \\ & [\kappa]_2 & & \\ & & \ddots & \\ & & & [\kappa]_i \end{bmatrix}$$

and since the force-displacement behavior of the elements is known, the individual matrixes $[\kappa]_i$ are easily obtained. The matrix equilibrium equation $\{F\} = [K] \{u\}$ can be solved for $\{u\}$ as follows:

$$\{u\} = [K]^{-1} \{F\}$$

Once the shell displacements are known, the internal forces in the elements are derived from the expression

$$\{P\} = [\kappa] [\beta] [K]^{-1} \{F\}$$

The β matrix in Eq. 5.44-4 is the same as was used in the compatibility method. The element stiffness matrixes can be obtained from the strain energy in an element, as shown in Ref. 5-2. Refs. 5-3 and 5-4 use the conical shell element discussed in conjunction with the equilibrium method. In Ref. 5-3, the equilibrium method is used to solve a problem similar to the one shown in Fig. 5.44-1. The results agree well with a closed form solution.

In finite element procedures, the matrixes to be inverted are generally not strictly banded; hence, it is generally not possible to use Gaussian elimination procedures. Thus, large matrixes may have to be inverted, resulting in long computer runs.

5. 50 ASSOCIATED PROBLEMS AND FEATURES
RELATED TO COMPUTER USAGE

Although the existence of high-speed computers has made many heretofore untractable problems solvable on a routine basis, limitations and shortcomings of the computer should not be overlooked. In this section, some of the characteristics of digital computers will be discussed.

5. 51 ACCURACY

The computer performs its operations using a different number system than ordinarily used in analytical work. Because of this, it is possible to encounter overflow or underflow problems. This means that, in the course of manipulating numbers, the permissible range of the computer can be exceeded by using a number too large or too small for the machine. Besides being bounded at the extremes, it should be recognized that the number system used is discrete; that is, finite gaps exist between the smallest consecutive numbers available on the machine.

A recent improvement is the ability of the machine to perform "double precision arithmetic." This allows twice the number of significant figures (about 16) to be retained than is done conventionally.

5. 52 TIME

Since the computer demands that a problem be given to it in a very specific fashion, considerable time is often required to transfer an analytical formulation of a problem to a form acceptable for the computer. This aspect of the work, which involves filling out coding sheets, punching cards, etc., is called programming time. After the given problem has been programmed, it is ordinarily necessary to check out the problem against known results. Depending on the complexity of the program, the time required for this phase may vary from several days to a month or more. After the program has been completely checked out, the compiled deck is entered into production status.

A compiled deck is ready, when supplied with sufficient data, to execute problems of interest. Execution time varies with the complexity of the program, the sophistication of the computer facility, and the number of cases to be run. When possible, it is advisable to stack as many cases as are of interest on one run, as opposed to having several runs with a smaller number of cases each. In the former case, a smaller amount of time per case will be required. This increase in efficiency presupposes an errorless program and data deck.

5.53 COMPATIBILITY PROBLEMS

At present, it is generally impossible to take a program written for a specific machine (e.g., Universal 1234 at Company ABC) and run it successfully on another machine (e.g., National 4567 at Company XYZ) without making some changes in the program. Nevertheless, successes are being recorded in improving the compatibility between the various machines and systems. Compatibility has increased to the extent that, with relatively minor changes in the program, SHARE, an IBM collection of existing programs, can be beneficially used. A SHARE catalogue is consulted to determine what is available, and decks of interest are then ordered. Program descriptions of some types are available for most SHARE decks. The extent of program documentation ranges from two-page short writings to complete and formal program descriptions. A typical listing in a SHARE catalogue is as follows:

Cylinder Analysis

Calculates the stresses in cylindrical geometries caused by imposed loads. It solves the system of restraints by using the short cylinder coefficients developed in the theory of beams on elastic foundation. Deflections, rotations, and three principal stresses are calculated at a number of points throughout the geometry. Restriction: no other routines

are required but the standard library routines from tape A.
FORTRAN program. Machine requirements: 7090 16K
3 tapes input, output, and library. No drum corr. 1380.

5.54 THE DYNAMIC NATURE OF THE COMPUTER

Since the development of computers is proceeding so rapidly, it is entirely possible that some of the statements made in this chapter will become invalid at an early future date. An example of this early obsolescence is the present implementation of FORTRAN IV, a source language destined to replace FORTRAN II. The time will come when it will no longer be possible to recompile programs written in FORTRAN II and thus conversion to FORTRAN IV will be mandatory.

Future computers will almost certainly be able to execute programs faster than those presently available, perhaps an order of magnitude faster. An area of potential improvement is in the inputting of programs. Investigations are proceeding on making the computer accept handwritten or oral instructions instead of using cards and tapes. Obviously, the engineer will benefit from the continuing improvements in computers.

5.60 A TYPICAL COMPUTER PROGRAM

This chapter concludes with an illustration of a typical program deck and its associated input and output. A schematic illustration of a deck that could conceivably be used to solve a shell problem is shown in Fig. 5.60-1. The main program contains the heart of the analysis. The subroutines may be matrix manipulations, graph plotting procedures, etc.

The data can be entered either as a deck of cards, or as data sheets for subsequent keypunching. A typical data sheet is shown in Fig. 5.60-2.

Upon successful execution of the program, the output is ordinarily received in printed form as shown in Fig. 5.60-3. However, techniques

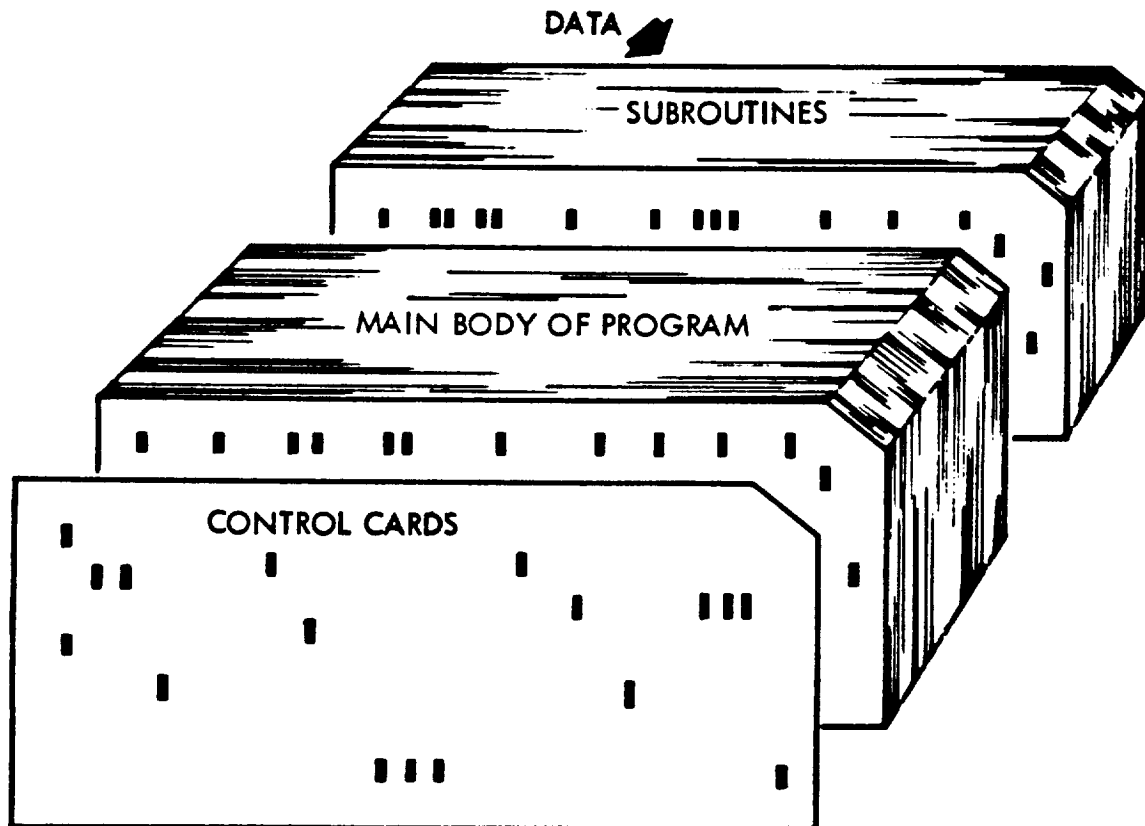


FIG. 5.60-1. Typical Program Deck

are available for obtaining the results graphically. A typical plot from the computer is shown in Fig. 5.60-4.

| FORTRAN FIXED 10 DIGIT DECIMAL DATA | | | |
|-------------------------------------|----------------|---------------------------------|-----------------------------|
| DECK NO. | PROGRAMMER | DATE | PAGE . . . of . . . JOB NO. |
| NUMBER | IDENTIFICATION | DESCRIPTION | DO NOT KEY PUNCH |
|1 | | LOCATION OF NEXT PIECE OF INPUT | |
| 30.0 | | NO. OF POINTS ALONG MERIDIAN | |
| 1 | | REFERENCE STRESS LEVEL | |
| 1 | | REFERENCE THICKNESS | |
| 1 | | REFERENCE LENGTH | |
| 1 | 1 0 | REFERENCE ELASTIC MODULUS | |
| 1 0 | | LOCATION OF NEXT PIECE OF INPUT | |
| 5 0 | | NORMAL PRESSURE IN PSI | |
|2 0 | | | |
| 2 1 0 | | LOCATION OF NEXT PIECE OF INPUT | |
| 0 3 | | SHELL THICKNESS | |
|3 0 | | | |
| 1 . | + 7 | ELASTIC MODULUS | |
|4 0 | | | |

FIG. 5.60-2. Typical FORTRAN Data Sheet

ORIGINAL PAGE IS OF POOR QUALITY

FIG. 5.60-3. UNSYMMETRICAL BENDING OF SHELLS OF REVOLUTION

INPUT DATA

EN = -3.0000E 02 A0 = 1.0000E 00 H0 = 1.0000E 00 E0 = 1.0000E 00
SIGO = 1.0000E 00 ENF = -1.0000E 00 DEL = 1.0000E 00 P01 = 3.3333E-01
THETA= 0. OMA = 1.5000E-01 RTH = 0. A = -5.0000E 01

| R(I) | D(I) | EK(I) | ENT(I) | EMT(I) | T(I) |
|---------------|---------------|---------------|--------|--------|------|
| 4.9999999E 01 | 1.0125000E 07 | 7.5940000E 04 | 0. | 0. | 0. |
| 4.9999999E 01 | 1.0125000E 07 | 7.5940000E 04 | 0. | 0. | 0. |
| 4.9999999E 01 | 1.0125000E 07 | 7.5940000E 04 | 0. | 0. | 0. |
| 4.9999999E 01 | 1.0125000E 07 | 7.5940000E 04 | 0. | 0. | 0. |
| 4.9999999E 01 | 1.0125000E 07 | 7.5940000E 04 | 0. | 0. | 0. |
| 4.9999999E 01 | 1.0125000E 07 | 7.5940000E 04 | 0. | 0. | 0. |
| 4.9999999E 01 | 1.0125000E 07 | 7.5940000E 04 | 0. | 0. | 0. |
| 4.9999999E 01 | 1.0125000E 07 | 7.5940000E 04 | 0. | 0. | 0. |
| 4.9999999E 01 | 1.0125000E 07 | 7.5940000E 04 | 0. | 0. | 0. |
| 4.9999999E 01 | 1.0125000E 07 | 7.5940000E 04 | 0. | 0. | 0. |
| 4.9999999E 01 | 1.0125000E 07 | 7.5940000E 04 | 0. | 0. | 0. |
| 4.9999999E 01 | 1.0125000E 07 | 7.5940000E 04 | 0. | 0. | 0. |
| 4.9999999E 01 | 1.0125000E 07 | 7.5940000E 04 | 0. | 0. | 0. |
| 4.9999999E 01 | 1.0125000E 07 | 7.5940000E 04 | 0. | 0. | 0. |
| 4.9999999E 01 | 1.0125000E 07 | 7.5940000E 04 | 0. | 0. | 0. |
| 4.9999999E 01 | 1.0125000E 07 | 7.5940000E 04 | 0. | 0. | 0. |
| 4.9999999E 01 | 1.0125000E 07 | 7.5940000E 04 | 0. | 0. | 0. |
| 4.9999999E 01 | 1.0125000E 07 | 7.5940000E 04 | 0. | 0. | 0. |
| 4.9999999E 01 | 1.0125000E 07 | 7.5940000E 04 | 0. | 0. | 0. |
| 4.9999999E 01 | 1.0125000E 07 | 7.5940000E 04 | 0. | 0. | 0. |
| 4.9999999E 01 | 1.0125000E 07 | 7.5940000E 04 | 0. | 0. | 0. |
| 4.9999999E 01 | 1.0125000E 07 | 7.5940000E 04 | 0. | 0. | 0. |
| 4.9999999E 01 | 1.0125000E 07 | 7.5940000E 04 | 0. | 0. | 0. |
| 4.9999999E 01 | 1.0125000E 07 | 7.5940000E 04 | 0. | 0. | 0. |
| 4.9999999E 01 | 1.0125000E 07 | 7.5940000E 04 | 0. | 0. | 0. |
| 4.9999999E 01 | 1.0125000E 07 | 7.5940000E 04 | 0. | 0. | 0. |
| 4.9999999E 01 | 1.0125000E 07 | 7.5940000E 04 | 0. | 0. | 0. |
| 4.9999999E 01 | 1.0125000E 07 | 7.5940000E 04 | 0. | 0. | 0. |
| 4.9999999E 01 | 1.0125000E 07 | 7.5940000E 04 | 0. | 0. | 0. |
| 4.9999999E 01 | 1.0125000E 07 | 7.5940000E 04 | 0. | 0. | 0. |
| 4.9999999E 01 | 1.0125000E 07 | 7.5940000E 04 | 0. | 0. | 0. |
| 4.9999999E 01 | 1.0125000E 07 | 7.5940000E 04 | 0. | 0. | 0. |
| 4.9999999E 01 | 1.0125000E 07 | 7.5940000E 04 | 0. | 0. | 0. |

FIG. 5.60-4. TYPICAL COMPUTER PLOT

0987-06
007

STATION VS. MERIDIONAL STRESS *** SIGMA(PHI) OUTER = (.), INNER = (X)



5.70 CONCLUSION

From the brief description of the computer and its use in shell analysis given in this chapter, it is obvious that the computer has a strong positive input to the efficient, successful analysis of shells. Since the future promises an increase in this role, any serious engineer must become as acquainted with the computer as possible.

REFERENCES

- 5-1 Verette, R. "On the Analysis of Branching in Shells of Revolution Loaded Arbitrarily." NAA S&ID, STR 136 (November 1965).
- 5-2 Greene, B., D. Strome, and R. Weikel. "Application of the Stiffness Method to the Analysis of Shell Structures," Am. Soc. Mech. Engrs. Paper 6-1AV-58 (1961).
- 5-3 Grafton, P., and D. Strome. "Analysis of Axisymmetrical Shells by the Direct Stiffness Method," AIAA Journal, Vol. 1, No. 10 (October 1963), pp. 2342-2347.
- 5-4 Percy, J., T. Pian, S. Klein, and D. Navaratna. "Application of Matrix Displacement Method to Linear Elastic Analysis of Shells of Revolution." AIAA Journal, Vol. 3, No. 11 (November 1965), pp. 2138-2145.